The Evolution of Male Form and Function in Nightshade Flowers

Gwendolyn Veronica Davis

Department of Plant Sciences

University of Cambridge - Wolfson College

This thesis is submitted for the degree of Doctor of Philosophy

April 2019

The Evolution of Male Form and Function in Nightshade Flowers

Gwendolyn Veronica Davis

The overall objective of this study is to investigate the diversity of anther form (male floral organs) in the genus *Solanum* to allow greater understanding of the relationship between anther form and buzz pollination. This project takes a multidisciplinary approach to investigating the anther traits found within the genus *Solanum.* We bring together both morphological and developmental genetic approaches. These constitute the two halves of this thesis.

In the morphological section (chapter 2) the epidermal cell surface of the anthers of *Solanum* is examined using scanning electron microscopy (SEM). This is the first study to examine many of these species with SEM, and the first to focus specifically on the presence, location and type of epidermal cell outgrowths on the anther surface. How anther shape varies throughout the genus is examined by measurement and analysis of anther dimensions of living and herbarium specimens. These anther dimension measurements are subjected to principal component analysis (PCA) and then analysed in a phylogenetic context using phylomorphospace approaches. The way in which anthers are arranged with respect to one another within a flower, whether separate or in a fused anther cone, is recorded and plotted onto the phylogeny to identify independent evolutions of the anther cone trait. The method of attachment between the anthers in fused anther cones is examined through SEM to better understand from a morphological perspective how this trait is created at a microscale, also shedding light on potential aspects of the trait's evolution.

The molecular section (chapter 3) of the thesis approaches the investigation of an important anther trait from a developmental genetic perspective. This trait is the fused

anther cone of *Solanum lycopersicum* (tomato), which is held together by a mesh of trichomes along the edges of the anthers. This work aims to better understand this trait by identifying genes responsible for its development. A candidate gene approach is taken, focusing on the R2R3 Myb subgroup 9 family of transcription factors. Function of the tomato members of this family is investigated through ectopic expression in tobacco and expression analysis during stages of floral development using semi qRTPCR.

This study has contributed significantly towards the understanding of the diversity of anther traits found in the genus *Solanum* from a morphological, evolutionary and developmental genetic perspective and paves the way for further studies which investigate the importance of these anther traits to the interactions of buzz-pollinating insects with these plants.

Declaration

This thesis is the result of my own work and includes nothing which is the outcome of work done in collaboration except for as declared in the preface and specified in the text.

It is not substantially the same as any that I have submitted, or, is being concurrently submitted for a degree or diploma or other qualification at the University of Cambridge or any other University or similar institution except as declared in the Preface and specified in the text. I further state that no substantial part of my dissertation has already been submitted, or, is being concurrently submitted for any such degree, diploma or other qualification at the University of Cambridge or any other University or similar institution except as declared in the Preface and specified in the text. It does not exceed the prescribed word limit..

Gwendolyn Veronica Davis, 24 October 2018

Acknowledgements

There are so many people without whom this thesis could not have come into being. First and foremost: Professor Beverley Glover, without whom the project could not have happened at all, and who went above and beyond to help me. For reading draft after draft after draft and teaching me throughout the PhD to be a better researcher, a stronger and more organized person, to be a better writer and presenter, and in general to be overall a better, more rounded scientist .

Dr Sandy Knapp: the queen of nightshade flowers, for imparting some of her expansive knowledge of the genus *Solanum* to me and teaching me how to manage the herbarium specimens with which I worked for the project.

Thank you to the entirety of the Glover Lab who have been present during my time here. But special mention should go to: Chiara: for teaching me with her vast knowledge of molecular biology and troubleshooting experiments I could have sworn were impossible. You were an amazing help from start to finish who really helped mould my laboratory work. Edwige for her also great molecular expertise and guidance. Erin for being such an excellent work companion throughout – I shall miss our lab bench banter. Róisín for being such a lab wit, Gabriela for your cheeky smiles, Chris twirling his moustache as he imparted sage wisdom, Carlos: The statistical superhero, thank you for all your help during the analysis of my morphological data. Matthew: thank you for caring for my plants throughout (and reminding me when they were flowering/dying) your expertise was essential to the production of this project. I always enjoyed our chats and you were always full of excellent advice.

Thank you especially to Hamish who not only helped me with his computer wizardry as a co-worker but who gave me a place to stay with his wonderful family (and with wonderful food!) whilst doing the last bit of my writing. I hope that when your write up comes along it is as smooth as you helped make parts of mine! Every member of the lab has created such a lovely atmosphere within which to work and I thank everyone for the help and support given throughout this process.

Thank you also to the non-lab friends and family who helped make this project possible. Special thanks to Marco for reading aloud papers to me when I was too tired to read them and to Maria for being the greatest ally from beginning to end.

Abstract

The overall objective of this study is to investigate the diversity of anther form (male floral organs) in the genus *Solanum* to allow greater understanding of the relationship between anther form and buzz pollination. This project takes a multidisciplinary approach to investigating the anther traits found within the genus *Solanum.* We bring together both morphological and developmental genetic approaches. These constitute the two halves of this thesis.

In the morphological section (chapter 2) the epidermal cell surface of the anthers of *Solanum* is examined using scanning electron microscopy (SEM). This is the first study to examine many of these species with SEM, and the first to focus specifically on the presence, location and type of epidermal cell outgrowths on the anther surface. How anther shape varies throughout the genus is examined by measurement and analysis of anther dimensions of living and herbarium specimens. These anther dimension measurements are subjected to principal component analysis (PCA) and then analysed in a phylogenetic context using phylomorphospace approaches. The way in which anthers are arranged with respect to one another within a flower, whether separate or in a fused anther cone, is recorded and plotted onto the phylogeny to identify independent evolutions of the anther cone trait. The method of attachment between the anthers in fused anther cones is examined through SEM to better understand from a morphological perspective how this trait is created at a microscale, also shedding light on potential aspects of the trait's evolution.

The molecular section (chapter 3) of the thesis approaches the investigation of an important anther trait from a developmental genetic perspective. This trait is the fused anther cone of *Solanum lycopersicum* (tomato), which is held together by a mesh of

trichomes along the edges of the anthers. This work aims to better understand this trait by identifying genes responsible for its development. A candidate gene approach is taken, focusing on the R2R3 Myb subgroup 9 family of transcription factors. Function of the tomato members of this family is investigated through ectopic expression in tobacco and expression analysis during stages of floral development using semi qRTPCR.

This study has contributed significantly towards the understanding of the diversity of anther traits found in the genus *Solanum* from a morphological, evolutionary and developmental genetic perspective and paves the way for further studies which investigate the importance of these anther traits to the interactions of buzz-pollinating insects with these plants.

Table of Contents

List of Figures

List of Abbreviations

cDNA Complementary deoxyribonucleic acid
BAP Benzyl-Amino-Purine
bHLH basic-Helix-loop-Helix
bp base pair
BSA bovine-serum-albumin
CTAB CeTylmethylAmmonium Bromide
dH2O Deionised water
DNA Deoxyribonucleic acid
dNTPs deoxyribo Nucleoside TriPhosphate
EDTA Ethylenediaminetetraacetic acid
gDNA genomic Deoxyribonucleic acid
IAA Indole-3-acetic acid
LB Luria-Betrani (medium)
MS Murashige-Skoog
mya million years ago
MYB a transcription factor family that was named for myeloblastosis
OD600 Optical density at 600nm
PCA Principal component analysis
PCR polymerase chain reaction
PVP polyvinylpyrrolidone
R2R3 repeats 2 and 3 of the MYB DNA binding domain
RNA RiboNucleic Acid
rpm rotations per minute
SDS Sodium dodecyl sulfate
SEM scanning electron microscope
sqRTPCR semi quantitative reverse transcription polymerase chain reaction
TBE Tris borate EDTA
TF transcription factor
U enzyme activity units
UV ultra violet
WT Wild type
X-gal 5-bromo-4-chloro-3-inodyl-β-D-galactopyranoside

Chapter 1: Introduction

1.1: Angiosperm diversity and plant reproduction

Plants are rooted to the spot, unable to move around to find a mate and reproduce. In order for outcrossing to occur, gametes must be exchanged between different individuals. Outcrossing increases the genetic diversity of offspring more than does sexual reproduction by selfing. Outcrossing is important for avoiding inbreeding depression and provides selective advantages (Darwin, 1876; Charlesworth. and Charlesworth, 1987). 'inbreeding depression' is where as a result of inbreeding, an increased number of deleterious mutations can be exposed due to increased homozygosity. Increased homozygosity results from inbreeding therefore recessive genes will be expressed. There are also many benefits to outcrossing; it allows opportunities to increase genetic variability as a result of meiosis and genetic recombination. This exchange of genes allows increased evolutionary potential as a greater number of genes may be exposed to selection. This then results in an increased potential opportunities for adaptation to the environment, therefore increasing chances of survival and the resulting fitness. Outcrossing also allows deleterious traits to be lost. Therefore there is a strong drive by selection to evolve mechanisms which enhance success. Many different solutions to the problem of outcrossing while rooted to the spot have evolved since the transition of plants onto land. Early evolving land plants such as the mosses and liverworts (traditionally treated as separate groups, the Bryophytes and Marchantiophytes respectively, but recently grouped together in a clade under the name 'Setaphytes' (Puttick et al, 2018), require a thin film of water through which the male gametes can swim to access the female gametes. In order for cross pollination to occur in flowering plants the pollen (the male gametophyte, containing the male gametes) must be transferred from the male parts of the flower (anthers) to the female parts (stigma at the end of a style connected to the ovary, containing the female gametes) of the flower of another plant. This transfer may be as a result of a biotic vector (such as an animal pollinator eg: a bee) or an abiotic vector such as water (Cox, 1988) or wind (Ackerman, 2000). The Angiosperms, however, the most species-rich land plant lineage (Crepet and Niklas, 2009; Fiz-Palacios et al, 2011), can use a vector such as an animal pollinator to facilitate the transfer of pollen between individuals. Increased outcrossing can promote increased genetic diversity and therefore increased chances to produce better adapted organisms, novel genetic combinations, and avoidance of inbreeding depression which can have deleterious effects (Miintzing, 1961).

This use of animal vectors for pollination, one way in which cross fertilisation can occur and outcrossing increased, was facilitated by the evolution of the flower (Kevan and Baker, 1983; Schiestl and Johnson, 2013). In biotically pollinated angiosperms the flower attracts and recruits an animal pollinator to transfer pollen from the male parts of the flower (anthers) to the female parts of the flower of another plant (Willmer, 2011). The pollen, when placed on the stigma of a sexually receptive flower, will produce a pollen tube which grows down the style into the ovary where the sperm cell will fertilise the ovule (Sanders and Lord, 1989; Lord and Russell, 2002). Flowers are themselves highly diverse and interact with equally diverse pollinators. Pollinator mediated selection is thought to result in evolutionary change to floral features (Stebbins, 1970; Bartkowska and Johnston, 2012; Mitchell et al, 1998). Such floral traits include nectar rewards (Parachnowitsch et al, 2018; Irwin et al, 2004; Perret et al, 2001; Mitchell and Waser, 1992), flower colour (Darwin, 1859; Weiss, 1991; Weiss, 1995a; Caruso et al, 2010), scent (Parachnowitsch et al, 2012; Wright and Schiestl, 2009; Dobson, 1994), the texture of floral organs/petals (Kay et al, 1981; Whitney et al, 2009; Whitney et al, 2011), flower size and shape (Spaethe et al, 2001; Parachnowitsch et al, 2010) and also breeding system evolution such as self compatability/incompatability mechanisms (Darwin, 1876; Kao and McCubbin, 1996; reviewed in Solanaceae by Kao and McCubbin, 1997). These traits can result in reproductive isolation and speciation (Grant, 1949; Baker, 1959).

The 'Pollination syndromes' concept was developed by Faegri and Van der Pijl (Faegri and Van der Pijl, 1966) to describe groups of flowers pollinated by a particular type of pollinator and sharing particular floral traits such as shapes, scents or colours specialised to the visual systems of a pollinator (Chittka, and Waser, 1997) or a reward that is tailored to attract pollination services (Perret et al, 2001). Flowers and floral organs may be specialised to many different forms of pollination, however it should be noted that this 'specialisation' is not directional, as evolution does not act with thought or directionality beyond an immediate positive or negative effect of a trait on the fitness of the plant (Stebbins, 1970). This 'specialisation' also only refers to the most effective pollinator, in reality flowers are visited by a whole host of animals that may act as pollinators to different degrees (Robertson, 1928; Waser et al, 1996), however, some floral visitors may be more effective than others at transferring pollen resulting in cross-fertilisation of the plant and therefore are most beneficial to the fitness of the plant (Stebbins, 1970; Fenster et al, 2004.)

This project focusses on the flowers of the buzz pollinated genus *Solanum* and the floral traits, specifically those of the anther, important to this form of pollination.

1.2: Buzz pollination is a highly specialised form of pollination

Buzz pollination is a specialised form of pollination in which vibrations (or sonications) are used by the pollinator to induce pollen release from the flower (Buchmann et al, 1978). It is widespread in flowering plants and found in 65 families, ~400 genera, and 15,000-20,000 species (De Luca and Vellejo-Marin 2013; Buchmann, 1983; Buchmann, 1986). Buzz pollination has evolved independently multiple times through convergent evolution (Vallejo-Marin et al, 2010). It is the pollination mechanism of a number of economically important crop species and is therefore an economically important process (Buchmann, 1983).

The buzz pollinator is usually a species of bee. Bumblebees and a number of solitary bees are able to sonicate, a notable exception being the honey bee (*Apis mellifera*) (Thorp, 2000). The pollen itself, which is produced by the plant, is used as the reward for pollination services as well as for plant reproduction (Vogel, 1978; Faegri, 1986). There is notably no nectar reward in most buzz pollinated *Solanum* flowers (Buchmann, 1986; Vallejo-Marin et al, 2009). However it should be noted that not all buzz-pollinated plants produce only pollen as a reward. Bees specifically collect pollen (Russell et al, 2017; Francis et al, 2015; Nicolson, 2011; Thorp, 2000). This pollen is used for larval nutrition by the pollinator (Buchmann, 1983; Thorp, 2000; Thorp, 1979b). Pollen is a key component of bee diet, being the primary source of both amino acids and proteins (Kevan and Baker, 1983; Nicolson and Van Wyk, 2011). Pollen tends to have a protein content of between 2.5% to 61% by dry weight (Buchmann, 1986).The pollen of buzz pollinated species appears to be especially rich in protein: ~47.8% protein by dry weight (Roulston et al, 2000) However, it was also noted that buzz pollinated species have unusually small pollen grains, and there tends to be an association between small pollen size and a high protein richness (Roulston, 2000).

In a typical buzz pollination event the pollinator will land directly onto the anthers of the flower. The pollinator grips the base of the anther firmly with its legs, especially its first pair of legs, which are connected to the thorax where vibrations are generated by the bee through contraction of the flight muscles. The bee then curls the ventral side of its body around the anther tip (King and Buchmann, 2003; King, 1993). The bee's wings are decoupled from the indirect flight muscles (King and Buchmann, 1996) so that its wings do not beat during buzzing, allowing for better grip and for a higher frequency of vibration to be transferred (King and Buchmann, 1996). These flight muscles then undergo a series of rapid contractions to produce vibrations (Michener, 1962; Buchmann and Hurly, 1978; De Luca et al, 2013; Buchmann, 1986). These vibrations transfer energy to the anther and to the pollen contained within (Buchmann and Hurley, 1978). The anthers being vibrated causes the pollen grains within to be dislodged. Energy is also transferred to the pollen grains within this

anther. The vibrations transfer kinetic energy to the pollen grains held within the anther. This causes the pollen grains to bounce around and collide with each over and against the inside of the anther walls. There is only one opening by which the pollen grains may leave the anther: the apical pore. Therefore, the pollen will eventually reach the pore and be expelled from the anther (Buchmann, 1983.) Therefore it is possible that any traits which effect the amount of kinetic energy transferred to the pollen, or effect the number of times the pollen would collide with the inside of the anther, would effect the way in which pollen is released and the vibrational energy the bee would be required to produce in order to result in pollen release. The transfer of energy from bee, to anther, to pollen, results in the ejection of pollen from the anther tip, through the anther pore, and onto the body of the pollinator (Buchmann, 1978). The bee then grooms to collect this pollen and places it into its corbiculae (Macior, 1964; Buchmann and Cane, 1989). It has been proposed that the vibrations of the anther causes collisions of the pollen grains within the anther resulting in them becoming electrostatically charged and therefore repelled by one another resulting in an explosive release. Sonications/buzzes are typically 0.1-8 seconds long in a series of varying lengths (Buchmann, 1983; King, 1993). These will be interrupted by pauses in which the bee will groom itself, whilst still hanging onto the flower by a tarsal claw (Macior, 1964; Buchmann and Cane, 1989).

Generally the first 'buzz' of a foraging event causes the majority of pollen to be released (~60% of the pollen contained within the anther). The following buzzes will then remove significantly less pollen (~10% each) (Buchmann and Hurley, 1978). However, pollen release from the flower is altered according to amplitude of sonication (De Luca et al, 2013) and other factors such as morphological adaptations (Buchmann and Hurley, 1978; Harder and Barclay, 1994; King and Buchmann, 1995) or pollen packing (Harder and Thompson, 1989). These are discussed more extensively in section **2.1.2** on potential adaptations of plants for modifying pollen release and to reduce pollen wastage. Properties of the vibrations produced by a pollinator in a sonication event include amplitude, frequency and duration, all of which may have an effect on pollen release (Buchmann and Hurley, 1978.)

Figure 1: A bee sonicating a flower of *S.dulcamara*. The bee can be seen to be gripping the anther cone of the flower and wrapping its body around the anther tip as it buzzes the flower.

Photo is a still from a video taken by Pharaoh han on Wikimedia Commons, the free media repository.

1.3 The genus *Solanum*

Solanum is a member of the family Solanaceae (commonly called the nightshade family) (Knapp, 2010), in the order Solanales, which sits within the Asterid clade (asterids 1), a section of the highly diverse angiosperms (flowering plants) (Figure 2).

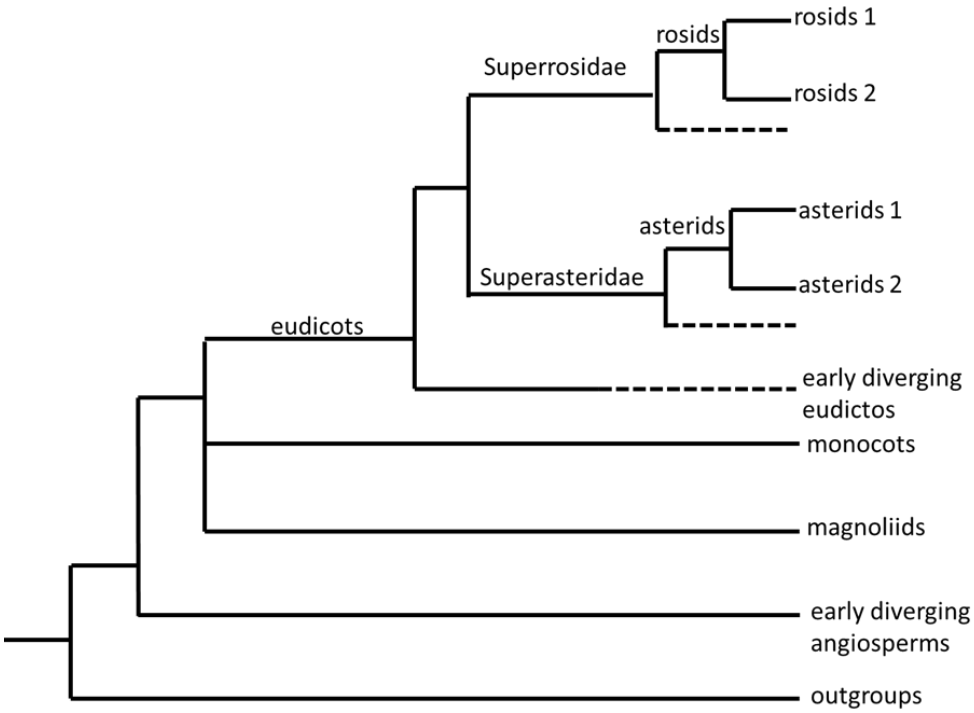

Figure 2: A cartoon of the phylogeny of the angiosperms
This cartoon shows the main divisions within the angiosperms (flowering plants). The Asterids can be seen within the Superasteridae which in turn is within the eudicots. Solanaceae is within the Asterid clade. This cartoon is based on the phylogeny of Chanderbali et al, 2016.

Solanaceae is a medium sized family containing 101 genera and approximately 3000 species (Knapp et al, 2004). The family has a great amount of variation in the habitat it occupies: from tropical rainforest to desert (Knapp et al, 2004). Species of Solanaceae are found all over the world, on every continent except for Antarctica, however most of the species diversity is to be found in Central and South America (also to a slightly lesser, but still important, degree in Australia and Africa) (Hunziker et al, 1979, Knapp et al, 2004). It is thought that Solanaceae originated in South America and then spread across the world from there (Hunziker et al, 1979; Dupin et al, 2016). Solanaceae also show great variation in morphology and habit ranging from small herbaceous species to trees to shrubs (Knapp et al, 2004).

Solanaceae is a plant family of great economic importance (Hawkes et al, 1999). Solanaceae contains a number of important genera including *Nicotiana* (Särkinen et al, 2013), which contains *Nicotiana tabacum* (tobacco), an important species for biological and scientific investigation and also of great economic importance (Hawkes et al, 1999). Solanaceae also contains the genus *Capsicum*, notable for containing many different species of chilli peppers including *C. annuum* (which comes in a wide number of varieties from 'bell pepper' to 'jalapeños') and is also of scientific, medicinal and economic importance (Särkinen et al, 2013). Solanaceae are important as food crops (Samuels, 2009; Samuels, 2012), for horticulture and ornamental plants (such as *Petunia*), medicinal plants and for scientific study as the family contains numerous model species used to study a variety of questions (reviewed by Gebhardt, 2016).

More recently the Solanaceae family has become very important for genetic studies. This has been accentuated further in recent years by a number of members of Solanaceae having fully sequenced and annotated genomes therefore facilitating research using these as model species for genetic and genomic studies. A number of noteworthy species with sequenced genomes include *Nicotiana tabacum*: tobacco (Bombarley et al, 2012), *Solanum lycopersicum*: tomato (The Tomato Genome Consortium, 2012), *Solanum tuberosum*: potato (The Potato Genome Sequencing Consortium, 2011), *Capsicum annuum*: hot pepper (Kim et al, 2014), *Petunia inflata*, *Petunia axillaris* (Bombarely et al, 2016; solgenomics.net). There is also a sequenced genome for *Solanum melongena* (aubergine/eggplant) (The Eggplant Genome Consortium, 2017) and all of the species of wild tomato relatives (The Tomato Genome Consortium, 2012; The 100 Tomato Genome Sequencing Consortium et al., 2014).

Solanaceae has long been an important family for scientific study including research into breeding system evolution (Entani et al, 1999; Ai et al, 1990; Clark et al, 1990; Ioerger, 1991; Mione and Anderson, 1992; reviewed in Kao and Tsukamoto, 2004); fruit morphology, development and diversity (reviewed in Wang et al, 2015; Knapp, 2002); floral diversity, development and morphology (Knapp, 2004); polyploidy (Leitch et al, 2008; Robertson et al, 2010); genomics (Mueller et al, 2005; Sierro et al, 2014; Gebhardt, 2016); biogeography and biodiversity (Olmstead, 2013; Knapp et al, 2004; Dupin et al, 2016); trichome development and morphology (Tominaga-Wada et al, 2013; Adedeji et al, 2007) and as model systems (Kimura and Sinha, 2008; Gerats and Vandenbussche, 2005; Goodin et al, 2008). The resource Solanacaesource.org is also available to provide phylogenetic and taxonomic frameworks for studies operating at a generic level.

This project focuses on the genus *Solanum*, which is the largest genus (in terms of number of species) within Solanaceae. The genus *Solanum* is a species-rich genus of 1500-2000 species (Bohs,

2005; Bohs, 2007). This is approximately half of the total number of species contained within the family Solanaceae (Knapp et al, 2004) and is in the top ten largest genera of the angiosperms (Frodin, 2004). The genus *Solanum* is as diverse as Solanaceae itself in terms of growth habits, global distribution and the environments within which the plants persist (Knapp et al, 2004). The *Solanum* genus is found worldwide (although most are tropical some are temperate) (Barroso et al, 1992). *Solanum* species exhibit a vast array of growth forms from shrubs to trees, woody vines, annual herbs, and some (such as the potato clade) exhibit tubers (Knapp et al, 2004). The genus *Solanum* is of importance for many reasons, including economically, scientifically and horticulturally (Weese and Bohs 2007). *Solanum* includes many crop species: *S. lycopersicum* (tomato), *S. tuberosum* (potato), *S. melongena* (aubergine/eggplant) (Bohs, 2007; Knapp, 2002,) and also lesser known crops such as pepino (*S. muricatum* Aiton) and tree tomato (*S. betaceum* cav) (Weese and Bohs, 2007). *Solanum* also contains poisonous and medicinal plants containing many useful secondary compounds (Weese and Bohs, 2007). *Solanum* is also of scientific importance. *Solanum* contains a number of important model species for scientific investigation of genetics and developmental and cell biology, notably *S. lycopersicum* (tomato) (Weese and Bohs, 2007). Seventeen *Solanum* species have sequenced genomes: *S.berthaultii, S.bulbocastanum, S.commersonii, S.dulcamara, S.incanum, S.dulcamara, S.incanum, S.melongena, S.nigrum, S.tuberosum, S.cheesmaniae, S.chilense, S.galapagense, S.habrochaites, S.lycopersicum, S.neorickii, S.penellii, S.peruvianum, S.pimpinellifolium*. *S. lycopersicum* has is a longstanding model for genetic studies (The Tomato Genome Consortium, 2012).

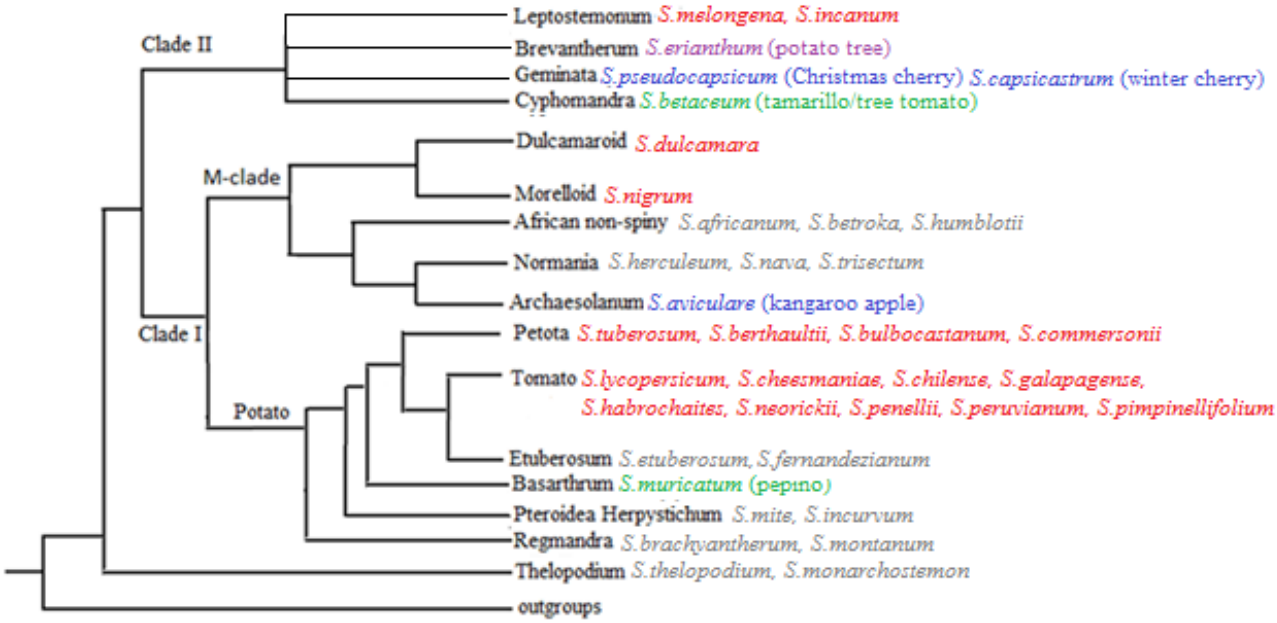

Figure 3: A cartoon of the phylogeny of the genus Solanum

This cartoon phylogeny displays the main clades within *Solanum* which may be further divided into subclades within each of these main clades. This cartoon is adapted from the phylogeny of *Solanum* in Särkinen et al, 2013. Example species are written next to each clade. Species with sequenced genomes are written in red beside the clade within which the species is found. For those clades which do not have a species with a sequenced genome, an example species of note is given in blue beside the clade. *S.aviculare, S.capsicastrum, S.pseudocapsicum a*re ornamentals that have seen wide cultivation. In green are minor crops: *S.betaceum, S.muricatum, ….*which are a significant food crop for a certain region. *S.erianthum* is a species used in traditional medicine and are written in purple.

An outline phylogeny of the genus *Solanum* can be seen in Figure 3. This Figure shows the main clades that the genus is generally divided into (Särkinen et al, 2013; Weese and Bohs, 2007). There is not yet a complete phylogenetic reconstruction of the genus containing every single species of *Solanum* due to the sheer scale of the genus, despite large scale attempts (Knapp et al, 2005). However there are studies which contain species members from almost all the main clades within *Solanum*. This study mainly relies on the phylogenetic analysis of Sarkinen et al (2013) for the structure of the genus and for mapping traits. This phylogenetic analysis contains 40% of the known species of Solanaceae and sampled all of the monotypic genera except for two and was the phylogeny which was used to form the *Solanum* phylogeny in the same paper (Sarkinen et al, 2013).

Solanum is divided into three major clades, two of which are then divided further into a number of subclades (Figure 3) (Bohs and Weese, 2007; Bohs, 2005). These three major clades are: Thelopodium, which is a sister group to the rest of *Solanum*, Clade I and Clade II. Clade I (Bohs and

Weese, 2007) contains the clades Potato (which contains the subclades Tomato, Petota, Regmandra, Etuberosum, Basarthrum and Pteroidea-Herpystrichum) (Särkinen et al, 2013), Archaesolanum and M-Clade (which contains the subclades Dulcamaroid, Morrelloid, Normania and African non-spiny) (Särkinen et al, 2013). Clade II contains the clades Leptostemonum, Cyphomandra, Brevantherum and Geminata (Bohs and Weese, 2007; Bohs, 2005; Särkinen et al, 2013).

Trichomes are an important diagnostic trait for identifying species and clades within *Solanum* due to the great variety of trichomes that can be found within the genus (Roe, 1971; Seithe, 1962; Cannon, 1909; Roe, 1967). Trichomes will be discussed in more detail in section **2.1.3.2**.

Species of the genus share a general floral form with five petals in a corolla which is radially symmetrical (Anilkumar and Murugan, 2014; Buchmann, 1983). The flowers have five poricidally dehiscing anthers arranged in a central 'cone' (discussed in detail in **2.1.3.1.3**), although the anthers may be arranged differently in relation to one another in different species, either held separately or attached to one another. There is also a great variety of anther form; dimensions of both the anther itself and the filament as well as their arrangement relative to one another can all vary, although all dehisce poricidally. The genus is mostly buzz pollinated (Buchmann, 1983), this pollination mechanism was described in section 1.2. No nectar reward is offered by *Solanum* flowers, instead pollen itself is the reward for pollination services.

Figure 4: Photos of *Solanum* flowers
From left to right: *S. dulcamara, S. lucanii* and *S. melongena.* (photos taken in Cambridge University Botanic Garden greenhouse of plants used in this study).

This project takes a multidisciplinary approach to investigating the anther traits of the genus *Solanum*. Both morphological and developmental genetic approaches are utilised creating each a half of this thesis. The results of these two approaches will then be brought together to form an overall discussion of the anthers of *Solanum* along with suggestions for future possible research into this topic.

Chapter 2 investigates the anthers of *Solanum* from a morphological perspective. It aims to identify and quantify key anther traits within the genus at both the scale of the shape of the whole anther and the epidermal cell morphology of the anther surface. The epidermal surface will be characterised through SEM and anther shape will be investigated in a phylogenetic context. This will provide a greater understanding of key anther traits. Chapter 3 meanwhile investigates a single key anther trait: the fused anther cone found in *Solanum lycopersicum* (Tomato). This utilised a candidate gene approach focussing on the R2R3 MYB Subgroup 9 family of transcription factors. All genes belonging to this family were identified and their function investigated through ectopic expression in tobacco and their expression during stages of floral development using semi quantitative RT-PCR (Semi qRT-PCR). The overall aim is a better understanding of this gene family in tomato and of potential developmental control of the trichome mesh that holds together the fused anther cone.

Chapter 2: Anther morphology in the genus *Solanum*

2.1: Overview

In buzz pollination the pollinator interacts directly with the anther of the flower. Therefore the anthers and their morphology are of great importance to this pollination syndrome as the point of interaction. This chapter poses the question; how does anther morphology vary within a buzz pollinated genus? This chapter aims to create a better understanding of the morphology of the anthers of the genus *Solanum.* The study aims to quantify variation in anther form throughout the genus. This will be done by measuring anther dimensions of herbarium and live *Solanum* specimens. The correlation between anther dimensions was examined to understand anther shape variation: does a long anther necessarily mean a thicker anther or is the relationship between the anther dimensions (and therefore the anther shapes possible) more complex? The anther dimensions measurements then underwent principle component analysis (PCA) to create an approximation of anther shape for each species of *Solanum* in the study. These principle components (PC) for each species were then plotted in morphological space so as to form a series of phylomorphospaces, First for the genus as a whole and then as separate clades. This allowed for variation in anther form to be examined with respect to the phylogeny (or relatedness). From this analysis, trends in anther form within and between clades could be identified and species which diverged from those closely related to them could also be examined examined.

The genus *Solanum* has such a large number of species that it is not possible to examine every species both from a practical perspective and from the availability of material. An initial aim was created to examine 10% of the genus, (of the possible ~1500 species). Further studies could be conducted in the future which focussed on specific clades or subclades within the genus in a greater amount of detail, however this study acts as a first look which provides a starting point for many other in-depth studies from this initial overview.

Key anther traits were be identified and plotted to the phylogeny in order to identify key evolutionary transitions. Such traits included Heteranthery (multiple anther forms on a single flower), the presence or absence of epidermal cell outgrowths on the anther surface and the arrangements of anthers in fixed or non-fixed cones: a 'pepper pot' fused anther cone or a 'salt cellar' un-fused anther cone.

The anther epidermal surface will be characterised through as much of the genus as possible so as to understand how micro-morphologies may contribute to anther form and function within the genus. Herbarium specimens and casts of live specimens will be examined using scanning electron microscopy (SEM) in order to identify and describe any epidermal cell outgrowths on the surface of the anthers such as conical cells or trichomes. This will also be used to understand key macro-morphologies such as the 'pepper-pot' anther cone: a morphology in which anthers are fused to one another creating a firm cone which a pollinator must interact with all of the anthers of the flower at once. An examination of this morphology by SEM will allow better understanding of how the anthers are fused to one another in different species and in different parts of the phylogeny therefore allowing a greater understanding of the evolution of this form.

A greater understanding of the morphologies associated with buzz pollination in a large and important genus could be a useful tool for increasing pollination rate for both yield in crop species and in conservation projects. The results of this project could also act as a starting point for many other studies into anther morphology, buzz pollination and the genus *Solanum* in general thereby acting as an excellent tool for many direction of research.

2.2: Introduction

2.2.1: Poricidal dehiscing anthers are a defining trait of the *Solanum* genus

Almost all species in the genus *Solanum* are buzz pollinated. The genus Solanum is observed to be entirely buzz pollinated from pollinator observation of species and inferred from the shared anther form. It is not currently known how many species of *Solanum* are not buzz pollinated, however all have Poricidal anthers. All species of *Solanum* share the trait of poricidal anthers such as those shown in Figure 5. This anther form is shared by many buzz pollinated species (Vogel, 1978; Faegri, 1986) although not all flowers which are/can be buzz

pollinated have poricidal anthers. There is no particular floral form 'required' for buzz pollination (De Luca and Vallejo-Marin, 2013), and many different floral morphologies have been found to be buzz pollinated (Vallejo-Marin et al, 2010; Proenca, 1992; Vogel, 1978; De Luca and Vallejo-Marin, 2013). However, there are particular floral forms which are commonly found in association with buzz pollination, and poricidal anthers is one such form (Buchmann, 1983). Poricidal anthers are shared by all species of *Solanum* and can be considered one of the defining traits of the genus (Buchmann, 1983).

In poricidal anthers the pollen is kept enclosed within the tube-like anthers. The anthers do not dehisce by the unzipping mechanism found in most angiosperms. The pollen can only be accessed through the two small pores at the anther tip (Figure 6, and labelled as 'apical pores' in Figure 5). The pollen is released from these apical pores during buzz pollination (Buchmann and Hurley 1978). Generally the filament is reduced/shorter than found in other non-buzz pollinated anther forms (http://solanaceaesource.org/content/morphology; Faegri, 1986). The anthers are often yellow coloured and of a contrasting colour to the petals in *Solanum*. The petals in *Solanum* are often white or purple (solanaceaesource.org). *Solanum* flowers also produce large quantities of pollen grains (Buchmann, 1983), as the pollen is used both for reproduction and for rewarding pollination services (Harder and Barclay, 1994). This pollen is used by pollinators as a source of larval nutrition and collected for this purpose (Buchmann, 1983).

Buzz pollination has evolved many times independently through convergent evolution (Vallejo-Marı´n et al, 2010; Buchmann, 1983; Harder and Barclay, 1994) and occurs in species from 72 families including all of Dodecatheon, (17 species) (Harder and Barclay, 1994) and Heliamphora, many species of Solanacae (including chilli pepper: Capsicum annuum, all of the genus Solanum and Melastomataceae (Renar, 1989; Berger et al, 2016; Buchmann, 1983; Cardinel et al, 2018). Buzz pollination is not evenly distributed throughout the Angiosperms: whilst there are whole genus which are buzz pollinated, other lineages contain only a few species which are buzz pollinated (Renar, 1989; Berger et al, 2016; Buchamann, 1983; Cardinel et al, 2018). Not all species which are buzz pollinated have Poricidally dehiscing anthers. Therefore Poricidal anthers are associated with buzz pollination; and the majority of buzz pollinated species do have Poricidal anthers; but not required for this method of pollination to occur.

Approximately 6% of the world's estimated number species of angiosperms have Poricidal anthers. (Buchmann, 1983; De Luca and Vallejo-Marin, 2013; Corbet and Huang, 2014.) Including species from 72 plant families and 544 genera (Buchmann, 1983; Cardinel et al, 2018). Poricidal anthers have evolved repeatedly through convergent evolution and are found throughout the angiosperms (Harder and Barclay, 1994). However there is an especially great diversity of buzz pollinated plants in tropical regions (Mesquite–Neto et al, 2018). Most species with Poricidal anthers are buzz pollinated and the trait is associated with the pollination method (Buchman, 1983.) It is thought that selection by sonicating bees is responsible for the evolution and diversification of Poricidal anthers (De Luca and Vallejo-Marin, 2013; Russell et al, 2017.)

Poricidal anthers differ from other types of anthers because of their tube-like morphology. There are within *Solanum* some species with poricidal anthers which do have unzipping pores; which form a 'tear-drop' shaped slit through which the pollen is shed, however these are still buzz pollinated (Buchmann et al. 1978; Buchmann 1985).

Whilst it is unknown why Poricidal anthers evolved where they do, it is possible that they are an adaptation to reduce pollen wastage by limiting what potential pollinators have access to the plant's pollen to only those pollinators which are able to sonicate (Harder and Thomson, 1989; Buchmann, 1974; De Luca and Vallejo-Marin, 2013; Larson and Barrett, 1999a; Michener, 1962; Harder and Barclay, 1994). The pollen is both hidden and protected inside Poricidal anthers (Arceo-Gómez et al, 2011; Buchmann and Hurley, 1978.) It is a common adaptation for plants to avoid excess pollen loss by having pollen limitation strategies (Hargreaves et al, 2009; Westerkamp and Claβen-Bockhoff, 2007; Westerkamp, 1997.) Access to the pollen being limited to only bees able to buzz pollinate also benefits the pollinator as it reduces competition with other pollinators for the resource (De Luca and Vallejo-Marin, 2013).

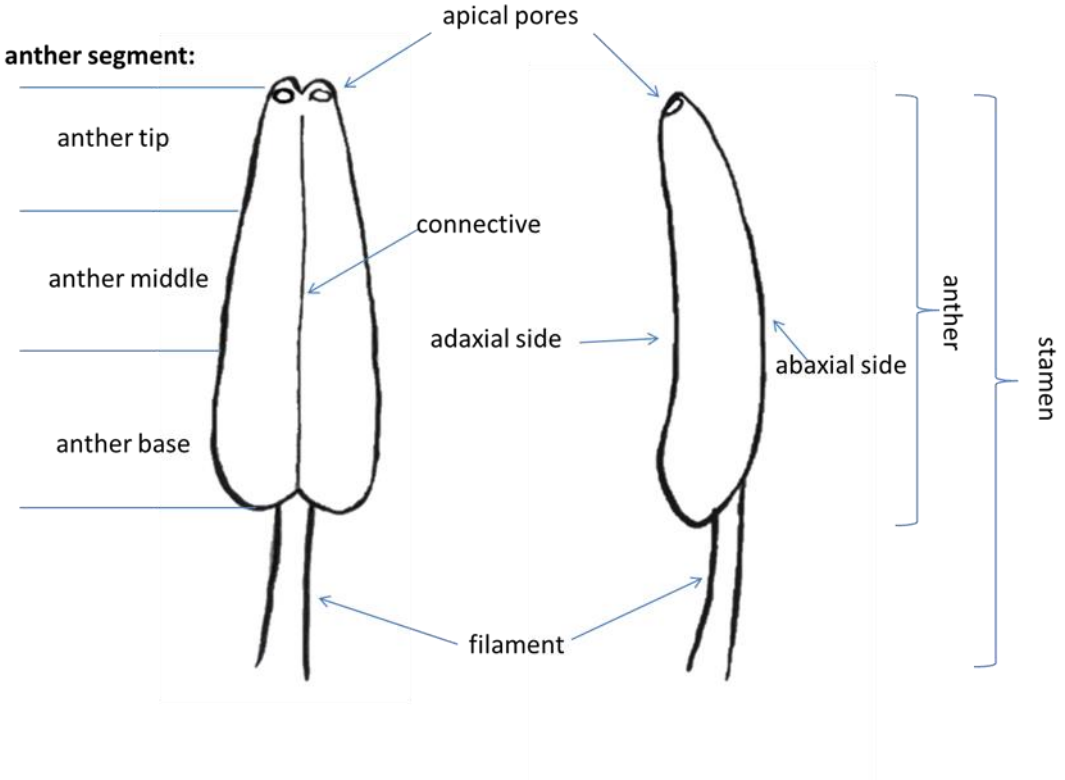

Figure 5: A diagram of a Poricidal anther

This diagram shows a generalised single anther of a typical *Solanum* flower. Key parts of the anther are labelled. The anther is divided into 'sections' along its length: anther tip, anther middle and anther base. These sections are merely for reference to provide context as to what part of the anther is being discussed in the following text. This illustration is based upon observations of *Solanum* anthers of various species.

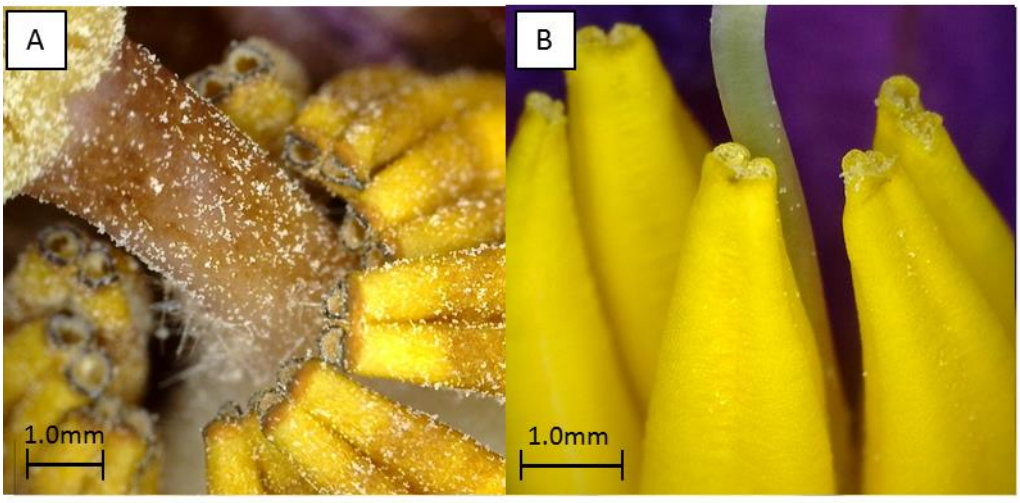

Figure 6: Photos of anther apical pores

These photos of A. *S. melongena* and B: *S. pyracanthos* show the apical pores at the tip of the poricidal anthers. It is through these pores that pollen is released during buzz pollination. (Images taken with DinoLite of study plant specimens).

2.2.2: Factors affecting pollen release by sonication during buzz pollination

There is great variation between species of *Solanum* in the amount of pollen released in response to sonication (Passarelli and Cocucci, 2006). The amount of pollen released by a sonication event can be affected by amplitude of sonication, anther dimensions, bee size, humidity/dryness, pollen packing, and flower age.

The amplitude, frequency and length of the buzzes have all been shown to affect the amount of pollen released by the flower (Buchmann and Hurley, 1978). Higher peak amplitude (and therefore energy released during a sonication) has been shown to result in greater pollen release (De Luca and Vallejo-Marin, 2013.) The vibrational transfer of energy from buzz pollination could be affected by the dimensions of the anther.

There is great variation in the shape and size of the anthers in *Solanum,* which may contribute to variation in pollen release in response to sonication. Structural properties such as anther dimensions could alter the way in which vibrations travel through the anther and consequently the amount of pollen released (Passarelli and Cocucci, 2006). This study investigates how anther dimensions vary throughout the genus.

Other anther traits, at a micro-morphological scale, may also affect pollen release during buzz pollination as well as handling efficiency and other interactions of pollinators with the anthers. Conical epidermal cells on petals have been shown to be highly important to the interactions between bees and flowers by reducing wettability (Whitney et al, 2011), enhancing petal colour intensity (Noda et al, 1994) and improving grip (Whitney et al, 2009a; Whitney et al, 2009b; Alcorn et al, 2012). This improved grip may result in a reduced handling time for bees foraging on the flower and therefore greater pollination efficiency (Whitney et al, 2009a; Whitney et al, 2009b). However in species of *Solanum* it has been noted that the conical petal epidermal cell trait has been lost repeatedly (Alcorn, 2013). For example, woody nightshade (*Solanum dulcamara)* has only flat cells on its petals (Glover et al, 2004). It was proposed that, since in buzz pollinated flowers the pollinator lands directly onto the anthers of the flower without interacting with the petals, grip provided by conical cells on the petal would be redundant (Alcorn, 2013). The observations of people examining *Solanum* anthers (such as Dr S.Knapp) raises the possibility that conical cells, or other forms of epidermal cell outgrowths, may be present on the anthers of some species of *Solanum*.

This study therefore also investigates what micromorphologies can be found on the epidermal cell surface of the anthers of *Solanum.*

2.2.3: *Solanum* anthers are highly diverse

The specificity of the pollination mechanism within this genus (all buzz pollinated, by a few specialised pollinators able to sonicate) would lead to an expectation that the anther morphology would be constrained, yet the anthers within *Solanum* are diverse (Bohs and Olmstead, 1999; Dunal, 1852; Endress, 1996; Vallejo-Marin et al, 2010; Glover et al, 2004; Whalen, 1978; Bohs and Olmstead, 1997; Vallejo-Marin et al, 2014). All species of the genus *Solanum* have poricidal anthers (as discussed in section **2.1.1**, yet within this form there is a great amount of variation both at a micro-morphological and macro-morphological level (Bohs and Olmstead, 1999; Dunal, 1852; Endress, 1996; Vallejo-Marin et al, 2010; Glover et al, 2004; Whalen, 1978; Bohs and Olmstead, 1997; Vallejo-Marin et al, 2014).

2.2.3.1: Macromorphology:

2.2.3.1.1: Anther dimensions

The size and shape of the anthers of *Solanum* are variable (Bohs and Olmstead, 1999; Dunal, 1852; Endress, 1996; Vallejo-Marin et al, 2010; Glover et al, 2004; Whalen, 1978; Bohs and Olmstead, 1997; Vallejo-Marin et al, 2014). The anthers can range from a few mm in length to a few cm. The size of the anthers allows different sized pollinators to interact with them. The anther size may also affect the way in which vibrations travel throughout the anther (Passarelli and Cocucci, 2006). The anther tip width may define the surface area of the anther in direct contact with the body of the pollinator during sonication. The width of the anther will define the amount of pollen possible to store within the anther and also the number of collisions between the pollen grains during sonication, unless the width is due to a thick anther wall which will itself influence vibration behaviour. The width of the anther base will alter the grip of the pollinator on the anther when buzzing.

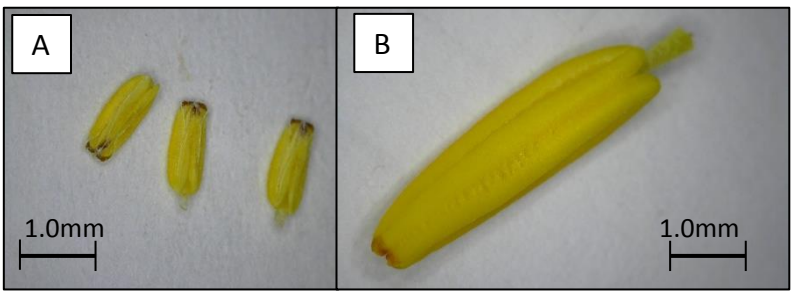

Figure 7: Photos of Solanum anthers demonstrating dimension differences.

A: *S.fraxinifolium* B: *S.Carolinense.* These photos taken at the same magnification demonstrate some of the large differences in anther size found within *Solanum*.

2.2.3.1.2: Heteranthery

Heteranthery is where more than one anther form is found in a single flower (Vallejo-Marin et al, 2009). These anther forms may be different in a number of ways, varying in filament length, anther length, overall anther size, shape and colour. It is possible that they also vary in the epidermal cell surface of the anthers, although this has not previously been investigated. One explanation for this morphology is the division of labour hypothesis (Darwin, 1899; Müller, 1882; Müller, 1883; Luo et al, 2009; Vallejo-Marın et al 2009), under which the two sets of anthers are specialised towards different functions. The smaller, but bright and attractive in colour, anthers act as 'feeding anthers', providing the pollen reward to the pollinator. They are located centrally and in an easily accessible position for visiting pollinators (Müller, 1881; Müller, 1882; Müller, 1883; Michener, 2007). Meanwhile the 'pollinating' anthers are specialised towards provision of pollen for the purpose of fertilisation/pollination (Luo et al, 2009; Vallejo-Marın et al 2009). These anthers exhibit a more cryptic appearance, are often darker in colour and less attractive to pollinators (Jesson and Barrett, 2003). These anthers deposit pollen on areas of the pollinator's body more difficult to groom (Michener, 2007).

Heteranthery is well understood in *Solanum* and its distribution has been previously examined extensively. It has been shown to be rare yet to have evolved multiple times independently through convergent evolution (Bohs et al, 2007; Vallejo-Marın et al, 2010). The morphology has also been shown to repeatedly break down (Vallejo-Marın et al , 2014). However the micomorphology of these anthers has not been previously examined.

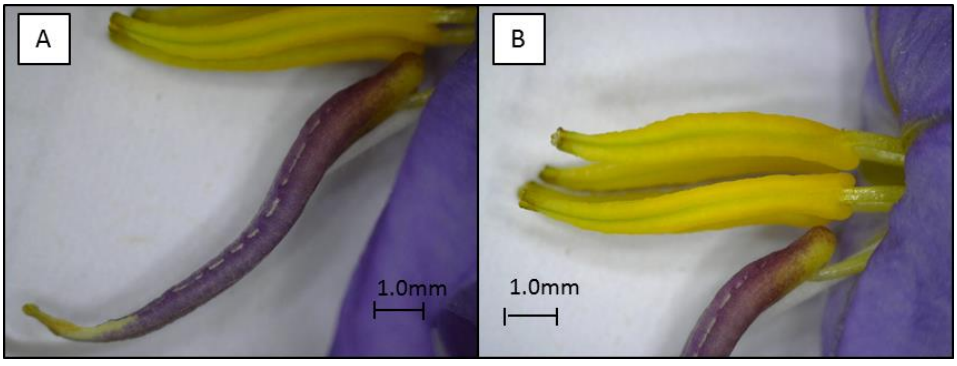

Figure 8: Photo of heteranthery in *S. citrullifolium*
This photo shows the species *S. citrullifolium* which exhibits heteranthery. A: The feeding anthers, which are smaller in size and brightly coloured yellow to attract pollinators. These provide the pollen reward. B: The pollinating anther, which is more cryptic in appearance and provides pollen for pollination. (Photos taken with DinoLite of study specimens.)

2.2.3.1.3: Anther cone type

Anthers may form different arrangements/cones within a *Solanum* flower (Glover et al, 2004). Most common is the 'salt cellar' cone (Symon 1979) which has been described as the anthers being arranged in a loose cone, separate from one another and unattached to one another. The pollen is shed onto the pollinator when sonicated and the anthers may be buzzed separately or as one unit depending on pollinator size and handling (Glover et al, 2004; Symon, 1979). A less common arrangement of anthers is the 'pepper pot' cone. In this case the anthers form a more robust cone, with the anthers fused or pressed together so they act as one unit which must be buzzed together. In pepper pot cones the filaments of the anthers are sometimes even smaller (Glover et al, 2004). The pepper pot cone may be held together by a mesh of hairs (e.g. *S. lycopersicum*) or by extracellular secretions (e.g. *S. dulcamara*), although it may also simply result from closely positioned (connivent) anthers. It is apparent from this that the characterisation of an anther cone as pepper pot or salt cellar may sometimes be subjective.

Salt Cellar cone

Pepper pot cone

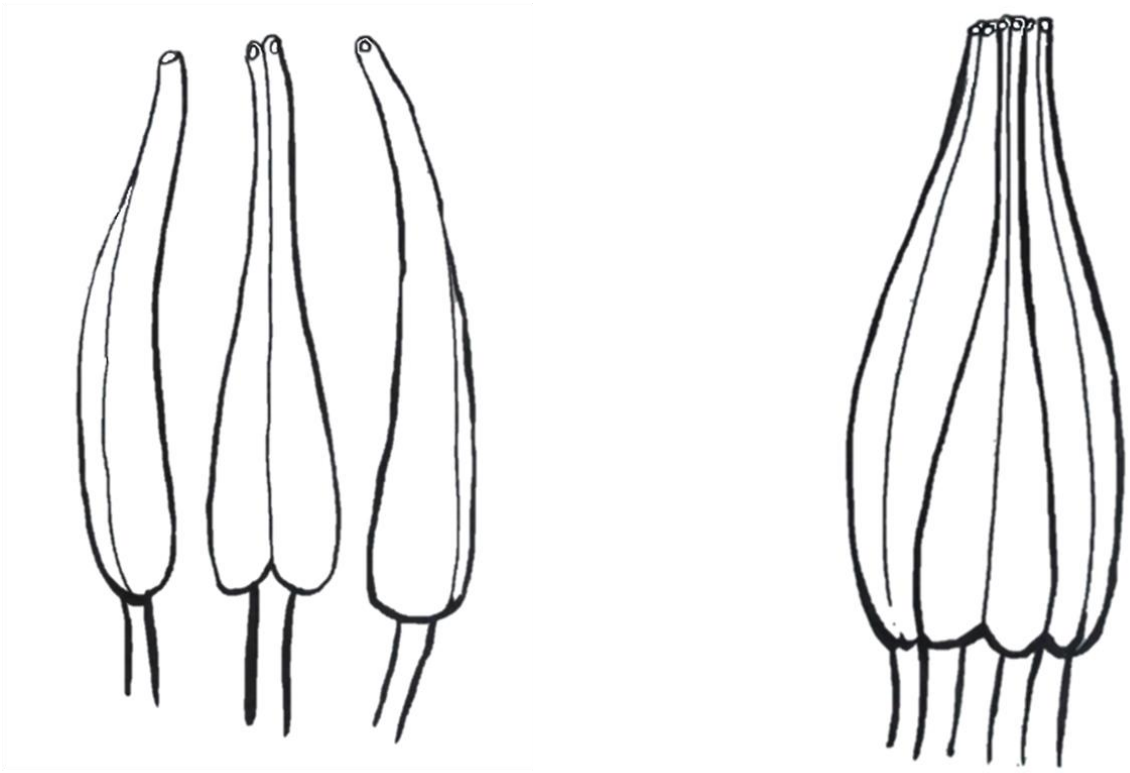

Figure 9: Illustrations of *Solanum* anther cone types

This diagram shows the two main 'cone shapes' or 'cone types' found in the genus *Solanum*: the salt cellar cone and the pepper pot cone. These diagrams are simplified for ease of interpretation, there would be five anthers in each flower, arranged together as a cone. In the salt cellar cone the anthers are not attached to one another in any way, but may be held very closely together or quite separately, and with any degree of separation of anthers between these two extremes. In the pepper pot cone the anthers are held together in some way. This may be for any portion of the anthers' length, with the most extreme pepper pot cones held together from anther base to anther tip. These simplified cartoon diagrams are based on observations of a variety of *Solanum* species.

2.2.3.2: Micromorphology

Variation in anther morphology extends also to a microscopic level. Once an insect has landed on the flower, a whole new set of traits are exposed to them as they interact with the flower at a different scale. These can be both visual and tactile. Tactile traits such as the textures of floral organs affect the way in which the pollinator handles the flower during pollination and can provide various signals to that pollinator.

Micro-morphological traits can include epidermal cell outgrowths. However little is known about their presence on the anthers of *Solanum*, what role they might play on the anther surface if present and how they might differ from those epidermal cell outgrowths found on petals. 'Papillae' have been observed on the anthers of some species of *Solanum (*D'Arcy et al, 1990; Falcão and Stehmann, 2018) but their distribution throughout the *Solanum* phylogenetic tree has not been previously examined.

Trichomes are hairs (Uphof, 1962; Esau, 1965), they can be small or large, unicellular or multicellular (Esau, 1977). Trichomes are divided into two main categories: glandular and non-glandular (Esau, 1977). Trichomes are highly morphologically diverse (Payne, 1978). They are found on most plants (Esau, 1977) and were one of the first micro-morphological traits recognised by early microscopy (Behnke, 1984). Due to the great interspecific diversity of trichome morphology they have long been used by taxonomists as key species defining traits (Roe, 1971; Seithe, 1962; Batterman and Lammes, 2004). Trichomes may be found on all organs of the plant (Levin, 1973).

Trichomes have a variety of functions (Wagner et al, 2004). They can be especially important in plant defence (Levin, 1973). Glandular trichomes have secretory roles (Uphof, 1962) and can secrete a variety of compounds including resins (Dell and McComb, 1978), secondary metabolites/poisons (Thurston, 1970), mucilage, essential oils/volatiles (Rodriguez et al, 1984; Sangwan et al, 2001; Fahn, 1988; McCaskill et al, 1992) and even nectar in nectaries (Lopes et al, 2002; Corsi and Bottega, 1999; DÍaz-Castelazo, 2005). Secretions can have a variety of functions from defence (Wagner et al, 2004) to salt secretion and removal (Dassanayake and Larkin, 2017; Esau, 1965) and scent production (Rodriguez et al, 1984; Sangwan et al, 2001; Fahn, 1988, Dudareva et al, 2004).

Non-glandular trichomes can also have functions in plant defence (Levin, 1973), by providing a mechanical barrier which may entangle, pierce or otherwise trap insect herbivores (Richardson, 1943; Johnson, 1953; Gilbert, 1971) and may also act as a feeding deterrent by making the plant less palatable (Kariyat et al, 2017; Pollard and Briggs, 1984). They may insulate leaves from heat damage (Ehleringer, 1984). They may also help protect the plant from UV-damage (Karabourniotis et al, 1995; Skaltsa et al, 1994).

Trichomes originate in the epidermal cells (Levin, 1973; Johnson, 1975), and their development will be discussed in detail in Chapter 3 It should be noted that trichome coverage on a plant is quite plastic and trichome function and or quantity may change in response to the environment and herbivore load (Upadhyaya and Furness, 1994; Ramesar-Fortner et al, 1995; Wilkens et al, 1996; Roy et al, 1999; Oney and Bingham, 2014).

Trichome morphology has been especially important in the taxonomy and systematics of Solanaceae and particularly *Solanum* (Roe, 1971; Seithe, 1962; Cannon, 1909; Roe, 1967). In *Solanum* many types of trichome varying in form, uni/multicellularity and function can be found on any one individual plant, but there is often on each individual organ of that plant only one or two trichome types present (Roe, 1971). This can be diagnostic of the species and used in identification (Roe, 1971).

2.2.4: Aims of this study

The aim of this study is to identify and quantify the diversity of anther morphology within the genus at both the macro- and microscopic level.

This diversity will be analysed in a phylogenetic context, to investigate how anther morphospace is occupied in a genus with specialised buzz-pollination. This study will test the null hypothesis that phylogeny constrains anther morphology. By considering anther morphology in a phylogenetic context this study will also consider whether *Solanum* anther traits, including macroscopic and microscopic traits, are homologous or evolve convergently across the genus. Homologous traits are defined as traits that are shared between species as a result of shared ancestry (Hubbs, 1944; Boyden, 1935; Boyden, 1943). Analogous traits are traits which are shared between two species but arise independently in each species as a result of convergent evolution (Hubbs, 1944; Boyden, 1935; Boyden, 1943).

2.3: Methods

2.3.1: Plant material

A list of all the species used in this study, with authorities, is provided as Appendix 1.

The majority of the species were examined using herbarium specimens held in Cambridge University (CGE), Natural History Museum London (BM), Royal Botanic Garden Edinburgh (E), Royal Botanic Gardens Kew (K), New York Botanical Garden (NY), Missouri Botanical Garden (MO). Full details of the source of each herbarium specimen and herbarium code for each specimen are provided in Appendix 2. Living plants were used for a number of species.

Solanum citrullifolium, S. carolinense, S. nigrum, S. lucanii, S. laciniatum, S. pseudocapsicum, S. palitans, S. riojense, S. aviculare, S. pyracanthos, S. villosum, and *S. pimpinellifolium* were all grown under controlled conditions in the Experimental glasshouses of Cambridge University Botanic Garden. Day length for plant growth was 16 hours light/8 hours dark, there was automatically-controlled supplementary lighting. Temperature was from a minimum of 15˚C day and night. Temperature varied but at 20˚C and above venting was triggered to control the temperature. Humidity was ambient. The compost used for all plants was Levington's M3 peat-based compost. Watering was performed daily by hand.

Solanum melongena, S. dulcamara, S. tuberosum and *S. fraxinifolium* were collected from the living collection of Cambridge University Botanic Garden, where they were grown outside.

2.3.2: Analysis of anther morphology

2.3.2.1: Morphological trait characterisation

Dimension measurements that were taken are listed below. Their locations on the anther are illustrated in Figure 10.

1. Anther length;

2. Filament length; This measurement was not included in the principal component analysis or phylomorphospace due to insufficient numbers of species where the measurement could

be taken. The filament was often obscured in herbarium specimens and therefore could not be measured.

3. Anther tip width;

4. Anther middle width;

5. Anther base width;

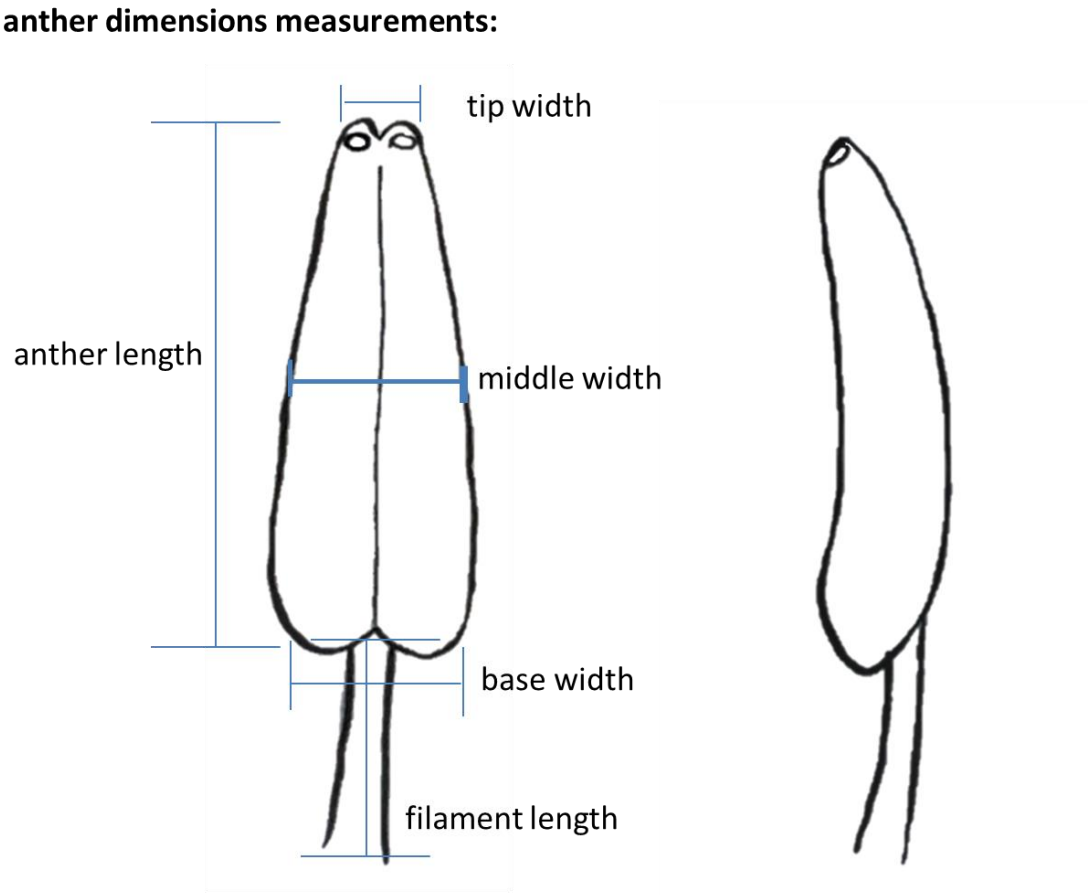

Figure 10: A diagram of a generic *Solanum* anther to indicate where dimension measurements were taken

2.3.2.2: Imaging anthers for dimension measurements

Specimens were photographed using a Dino-Lite digital microscope, Dino-lite Pro/Pro2 AM4000/AD4000 series 1.3 megapixel. Photographs were taken at 35x magnification. Three flowers were photographed per specimen where possible. Where there were fewer than three flowers on a specimen (or the anthers were not visible due to the way the specimen was preserved) then as many as possible were photographed. Where the anthers were not fully visible/obscured by petals or other parts of the plant, those traits which could be seen/measured were recorded and the remaining measurements/traits were recorded as NA (not applicable).

2.3.2.3: Analysis of anther dimension measurements

Images were measured using DinoCapture software.

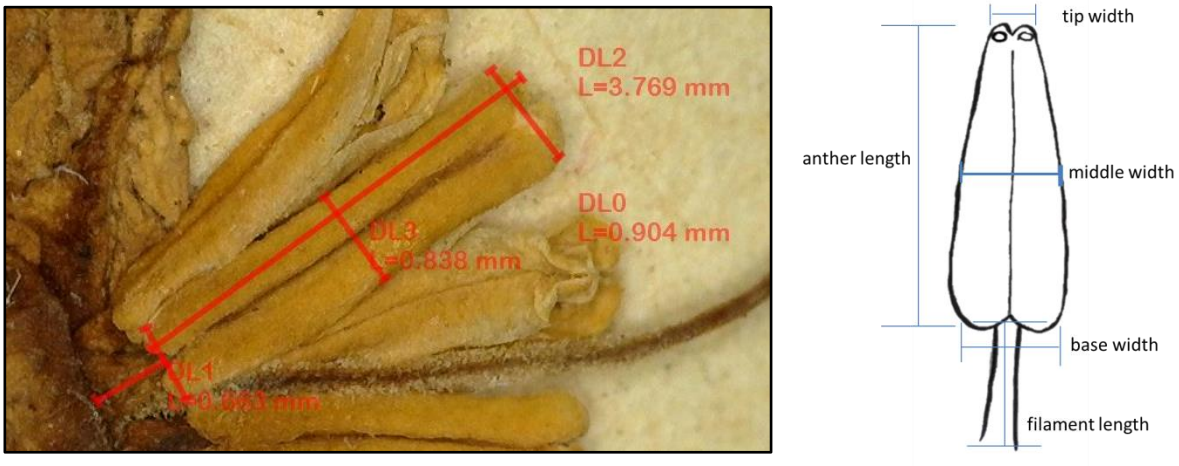

Figure 11: Anther dimension measurements in DinoCapture
This image shows a herbarium specimen being measured using the DinoCapture software. The measurements are taken from the points of the anther indicated by the illustration to the right. These measurements were all taken and recorded in mm. DL2= anther length, DL0= Tip Width, DL3= middle width, DL1=base width.

Anther dimensions were recorded in Excel (Microsoft Excel 2010). These were later transferred to R studio for analysis (R x64 3.3.0). All incomplete measurements or incomplete sets of measurements were removed prior to analysis. Filament length was removed as a trait due to insufficient data for meaningful analysis. A mean for each dimension was calculated for each species. These species means were used to calculate PCA in R studio.

Full sets of anther dimension measurements were taken from 308 *Solanum* species. Of these, 140 species were in the phylogenetic reconstruction of Särkinen et al (2013) and created a subset for further analysis. This sampling represents approximately 10-20% of the genus, depending on the estimate of the number of species. Species were sampled from across the world and from all parts of the phylogenetic tree. All clades were sampled, but the number of species of each clade sampled was naturally weighted by the size of the clade and therefore the samples available from that clade in herbaria. Sets of measurements of the anther dimensions were taken for all of the species examined. Several flowers per species were measured across multiple herbarium specimens. Where possible 3 flowers per specimen and 5 specimens per species were examined; this was rarely possible, however, due to availability of specimens and quality of specimens (or number of flowers available on a sheet to image with the anthers exposed for examination.) The mean for each anther dimension for each species was calculated.

2.3.2.4: PCA (Principal Component Analysis) and phylomorphospace

PCA (principal component analysis) (invented by Karl Pearson in 1901, reviewed by Jolliffe and Cadima, 2016) was conducted initially for all species of *Solanum* for which data had been collected, but this was later decreased to only those species which were also in the phylogenetic tree being used for trait mapping (Särkinen et al, 2013). The PCA was conducted for all clades together and then later divided by major clade, allowing for phylomorphospace to be constructed both for all species of *Solanum* for which there were data and split by major clade. PCA was conducted in R-Studio.

Phylomorphospace analyses were conducted in R-Studio, after importing the phylogenetic tree from Mesquite (based on the methodology used by Sakamoto and Ruta, 2012; Bookstein, 1985; Kimmel et al, 2017; Wilson et al, 2013).

2.3.2.5: Collection of specimens for analysis of *Solanum* anther cell morphology

2.3.2.5.1: Epoxy resin casts of living anther material for analysis of *Solanum* anther cell morphology

In order to examine the epidermal surface morphology of the anthers of live specimens of *Solanum* species, impressions were made of the anthers by imprinting them into dental wax (Zhermack®Clinical Elite ® HD +Light body A-silicone impression material). These moulds were then filled with epoxy resin (ITW Performance Polymers' Devcon® 2 Ton Epoxy High Strength S33-33345) to create casts of the anthers. This was done because living material is destroyed by the vacuum condition in the Scanning Electron Microscope.

2.3.2.5.2: Scanning Electron Microscopy (SEM) analysis

Material of two kinds was examined using SEM: casts of the anthers of living specimens of *Solanum* species and herbarium material which could be examined directly due to its dried state. Samples were mounted on metal stubs and sputter coated with gold, iridium or a combination of the two metals, depending on availability. This was done using a Quorum K756X sputter coater at the Cambridge Advanced Imaging Centre. Samples were examined using two different scanning electron microscopes, a FEI Phillips XL30 FEGSEM Scanning Electron Microscope 0.5-30KeV with Oxford Instruments INCA EDX system running at 3-mm^2 SiLi thin window pentafet EDX detector and later a FEI Verios 460 Scanning Electron Microscope with EDAX energy dispersive spectrometer running Ametek TEAM and Genesis software.

The anthers of 184 species in total were examined under SEM to investigate the presence, morphology and distribution of epidermal cell outgrowths. These species were examined from a mixture of herbarium and live specimens. Both adaxial and abaxial sides of the anther were examined and where possible the side of the anther. For full details of all the specimens used please refer to Appendix 5

Species were scored initially as 'flat' or 'non-flat'. 'Non-flat' was defined as the anthers having any kind of outgrowth of the epidermal cell surface of the anther, on any side of the anther and any part or proportion of the anther. These cell outgrowths included papillae (both small and pronounced), 'conical-like' cells, multi-lobed extensions and trichomes of all

kinds. The species were scored as ‘flat’ if the anther was entirely smooth all over, with no kind of cell outgrowth at all.

The second scoring category was ‘trichomes’ which included any species that possessed trichomes of any kind (including stellate trichomes, branched trichomes, unbranched trichomes, hairs, trichome meshes and glandular/oil secreting trichomes) but no other form of cell outgrowth on the anther surface or on the anther connective. Throughout this study the anther connective was examined as well as the anther because, although they are not the same tissue, they are likely to present to the pollinator as part of a single organ. The final category was ‘both’ which included species which contained on their anther surface both some kind of trichome and some other form of cell outgrowth.

It should be noted that the difference between trichome and non-trichome epidermal cell outgrowths is largely arbitrary and merely decided here for clarity of description of the outgrowths. The transition between non-trichome and trichome is not a clear cut one, as the two types of epidermal cell outgrowths are very closely linked. It is known that the developmental/differentiation pathways are very closely linked and so the two ‘types of cell outgrowth’ are ultimately linked and very similar to one another (Glover, 2000).

For this thesis ‘trichome’ is defined as an epidermal cell outgrowth which was longer than it was wide. If the epidermal cell outgrowth was multicellular or ‘branched’ then it was also considered a trichome, irrespective of length/width (Figure 12A).

For this thesis a non-trichome epidermal cell outgrowth/papilla is defined as a unicellular epidermal cell outgrowth that was wider than it was long (Figure 12B). If the epidermal cell outgrowth/papilla was multi-lobed it was described as a ‘glove-like’ cell outgrowth/papilla (Figure 12C). However this ‘glove-like’ cell shape was hard to identify or distinguish from herbarium specimens and could only really be discerned from casts of living specimens. So while this ‘sub-category’ is recognised where possible and discussed, it could not be properly distinguished from other epidermal cell outgrowths/papillae in most species and was generally recorded as simply a part of this category.

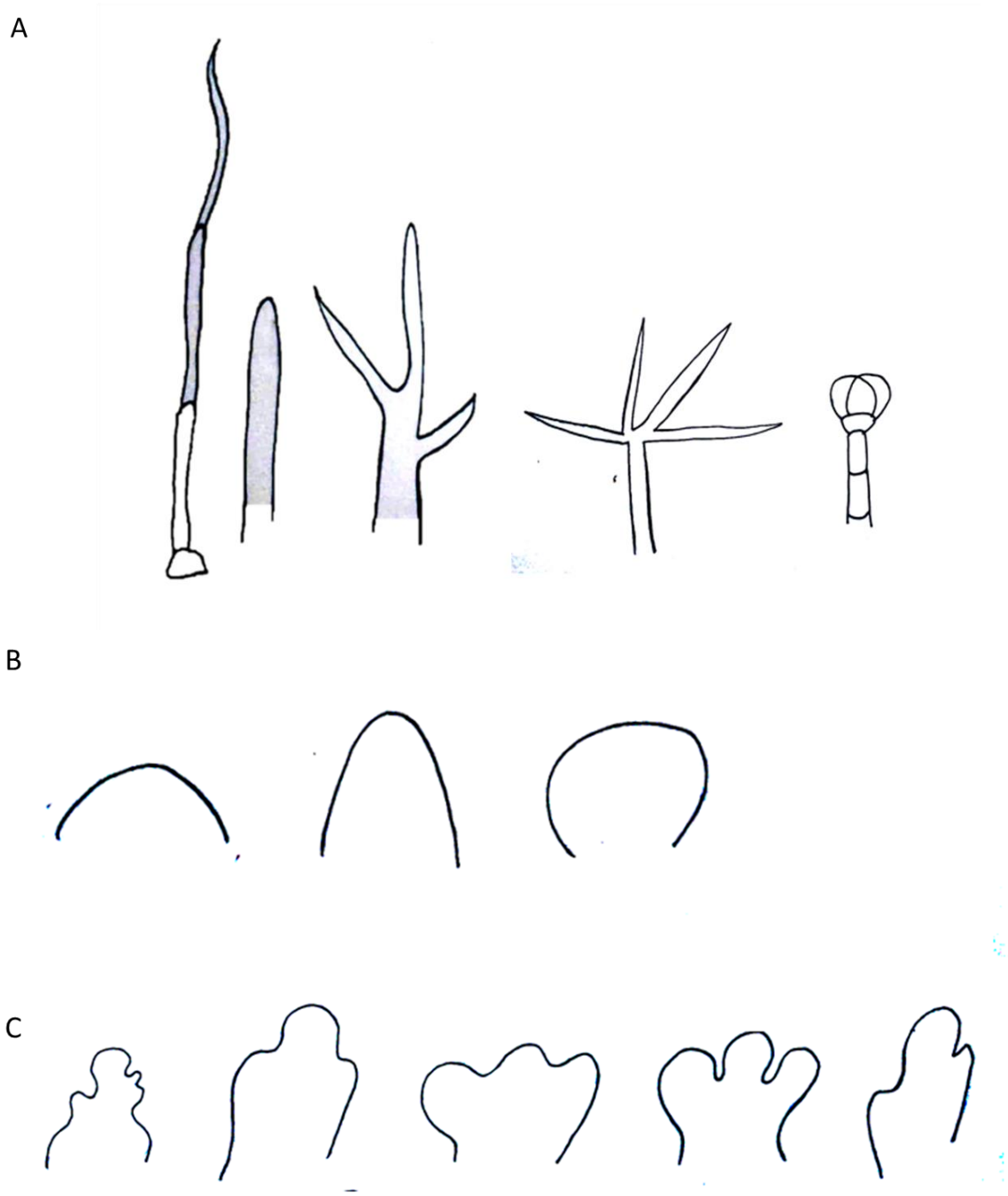

Figure 12: Illustrations to define papillae and trichomes

A: Illustrations of general trichome shapes. An epidermal cell outgrowth was considered a trichome if it was longer than it was wide, if it was multicellular or branched. B: An epidermal cell outgrowth was considered not a trichome and was defined as a papilla if it was wider than it was long and was unicellular or scale-like. C: A subcategory of the epidermal cell outgrowths/papillae was 'glove-like' papillae, the cell shape was considered this if it was multi-lobed yet still unicellular and generally wider than it was long.

The species examined represented a spread across the phylogenetic tree, sampling from the majority of clades and sub-clades. In Appendix 2 the clades and subclades are displayed alongside the species, where possible. However special care was taken to sample those subclades where the 'pepper-pot' anther cone morphology was to be found; *Bahamense,* Dulcamaroid and Potato (specifically the sub-clade Tomato within the Potato clade where effort was made to sample as many species as possible). From the Potato clade 31 species were examined, including 11 (out of 12) tomato subclade species; 16 Dulcamaroid clade species were examined; and 2 species of *Bahamense* were examined (out of 3: *S. ensifolium, S. bahamense* and *S. polyacanthos*).

2.3.2.6: Mapping of anther traits to *Solanum* phylogenetic tree

Categoric traits were mapped to the *Solanum* phylogenetic tree in Mesquite (Mesquite Project 3.0). A character matrix was created in which traits were scored as follows:

Cone type: 0= salt cellar cone. 1= pepper pot cone.

Epidermal cell outgrowths: 0= no outgrowths/flat epidermal surface. 1= any form of epidermal cell outgrowth (conical cells, trichomes etc).

Heteranthery: 0=not present, 1= present.

2.4: Results

2.4.1: Variation in anther morphology: anther dimensions showed variation within and between clades

The bar graphs shown in Figures 13 to 16 act as a visualisation of the total data set. Each Figure presents the data in two ways. Firstly the mean anther dimensions of each species measured are presented from absolute smallest to largest. Secondly, the measurements for each species are sorted by clade and presented smallest to largest species within the clade, with each clade presented sequentially. These Figures used the mean anther dimension value for each species of *Solanum* for which measurements were taken and were also in the phylogeny of Särkinen et al (2013). Using those species which were also in the phylogeny allowed for them to be sorted and colour coded by clade, to highlight any trends in anther dimension measurements between and within clades. The full data set, with the raw measurements for every specimen measured, can be seen in Appendix 2, prior to calculations of means for each dimension measurement for each species.

Anther length varied from 0.94mm (*S. brachyantherum*) at its shortest to 13.5mm at its longest (*S. lycocarpum*). There is variation in anther length within a clade (as seen in Graph A of Figure 13). The species from the phylogeny subset (the subset of the data containing only species which could be mapped to the phylogeny) with the shortest anther length was *Solanum tripartitum* with an anther length of 1.29mm. From this Figure it can also be seen that there is a gradual spread from smallest to largest value, with no clustering/grouping towards particular anther sizes or sizes of each dimension. There was instead a gradual transition along a smooth line from smallest to largest (as seen in A of Figure 13).

However it can also be seen that some clades have generally larger anther lengths than others (as seen by the limited clustering of colours in graph B of Figure 13). For instance, Leptostemonum clade has anther lengths at all areas of the graph B in Figure 13 (shown by blue bars). This shows great diversity of anther lengths. However it occupies more of the largest anther lengths than other clades do, as shown by the majority of the largest anther

lengths end of Graph B in Figure 13 being blue and therefore Leptostemonum. It can be seen from Figure 13 graph A that Leptostemonum also has the largest difference between its smallest anther length value and its largest anther length value. However there is no massive jump between the values but instead a smooth transition through anther lengths from the smallest to largest, demonstrating the amount of variation in anther length contained within this clade.

The Potato clade is also distributed in all areas of the graphs, having species with very large anther lengths and species with very short anther lengths. This can be seen in Figure 13 in both graph A and B, where potato is represented by the colour red.

Species belonging to the M-clade tend to have smaller anther lengths compared to the other clades of *Solanum.* All anther lengths measured for this clade sat in the lower half of the graph, as can be seen in Figure 13B.

Figure 13: Mean anther length displayed as a bar graph

A

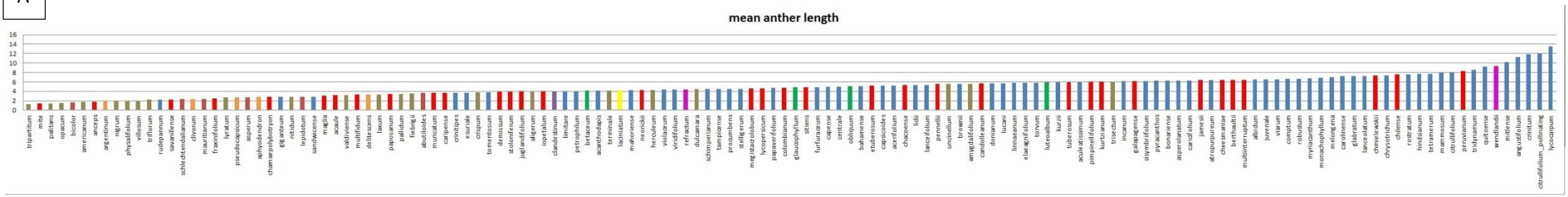

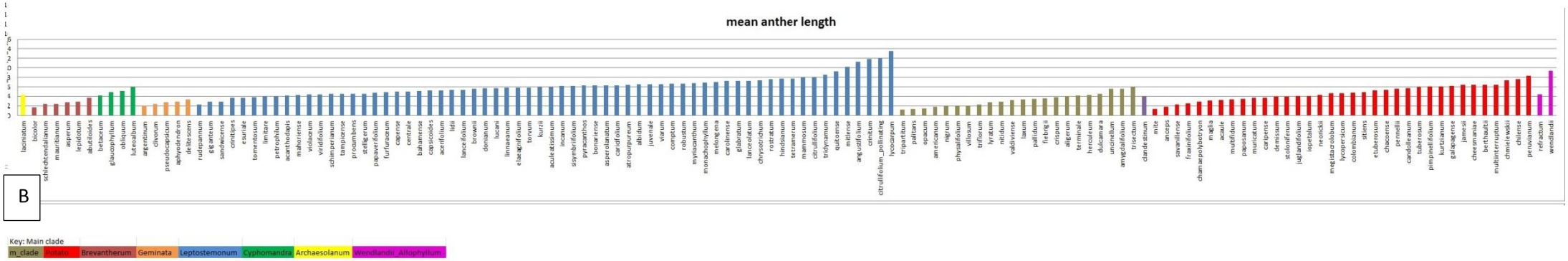

B

Figure 13: Mean anther length displayed as a bar graph

The mean anther length for each species measured (and included in the Särkinen et al (2013) phylogeny of *Solanum* and therefore identifiable to clade level) is displayed in two ways. A: from absolute smallest mean anther length to absolute largest mean anther length. B: sorted by clade and then smallest mean anther length to largest mean anther length within that clade. The clades are colour coded, the colour key is shown below the graphs. Y axis is the mean anther length in mm.

C-H shows the anther lengths measured for each species split by clade, with error bars (standard deviation) displayed for each species. Where no error bar is shown is because only a single individual was measured. It can be seen that species have different sizes of error bars, this possibly indicates that there are different levels of intraspecific variation. Unfortunately due to the low number of specimens per species that were available in this study intraspecific variation could not be investigated.

Figure 13 C

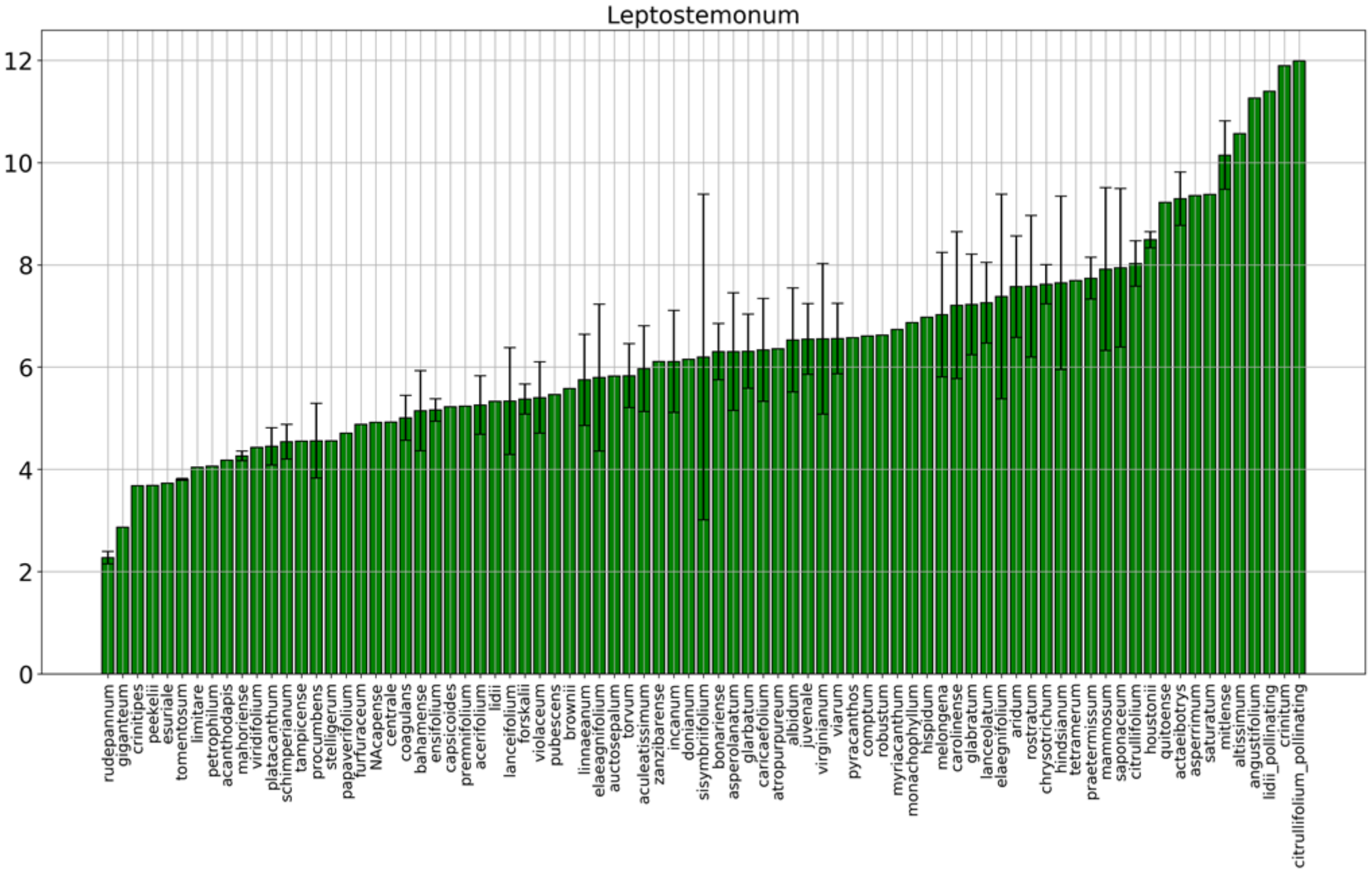
Leptostemonum
0
2
4
6
8
10
12
rudepannum
giganteum
crinitipes
peekelii
esuriale
tomentosum
limitare
petrophilum
acanthodapis
mahoriense
viridifolium
platacanthum
schimperianum
tampicense
procumbens
stelligerum
papaverifolium
furfuraceum
NAcapense
centrale
coagulans
bahamense
ensifolium
capsicoides
premnifolium
acerifolium
lidii
lanceifolium
forskalii
violaceum
pubescens
brownii
linnaeanum
elaeagnifolium
auctosepalum
torvum
aculeatissimum
zanzibarense
incanum
donianum
sisymbriifolium
bonariense
asperolanatum
glarbatum
caricaefolium
atropurpureum
albidum
juvenale
virginianum
viarum
pyracanthos
comptum
robustum
myriacanthum
monachophyllum
hispidum
melongena
carolinense
glabratum
lanceolatum
elaegnifolium
aridum
rostratum
chrysotrichum
hindsianum
tetramerum
praetermissum
mammosum
saponaceum
citrullifolium
houstonii
quitoense
actaeibotrys
asperrimum
saturatum
mitlense
altissimum
angustifolium
lidii_pollinating
crinitum
citrullifolium_pollinating

Figure 13 D

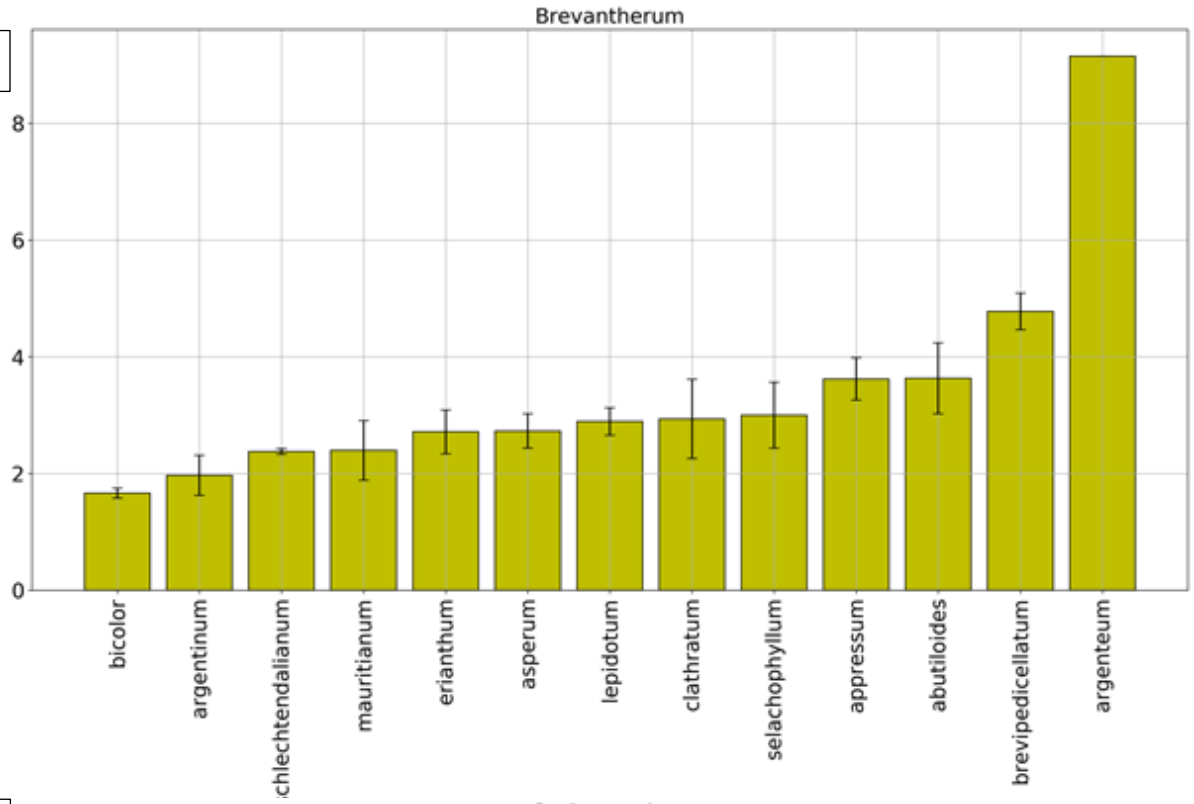

Figure 13 E

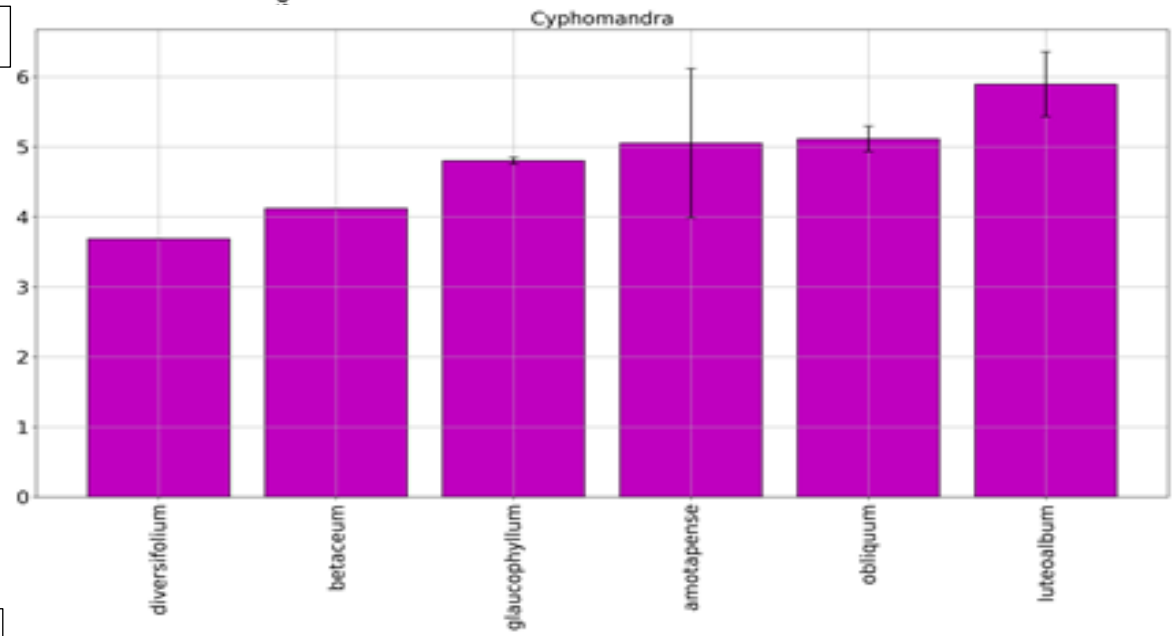

Figure 13 F

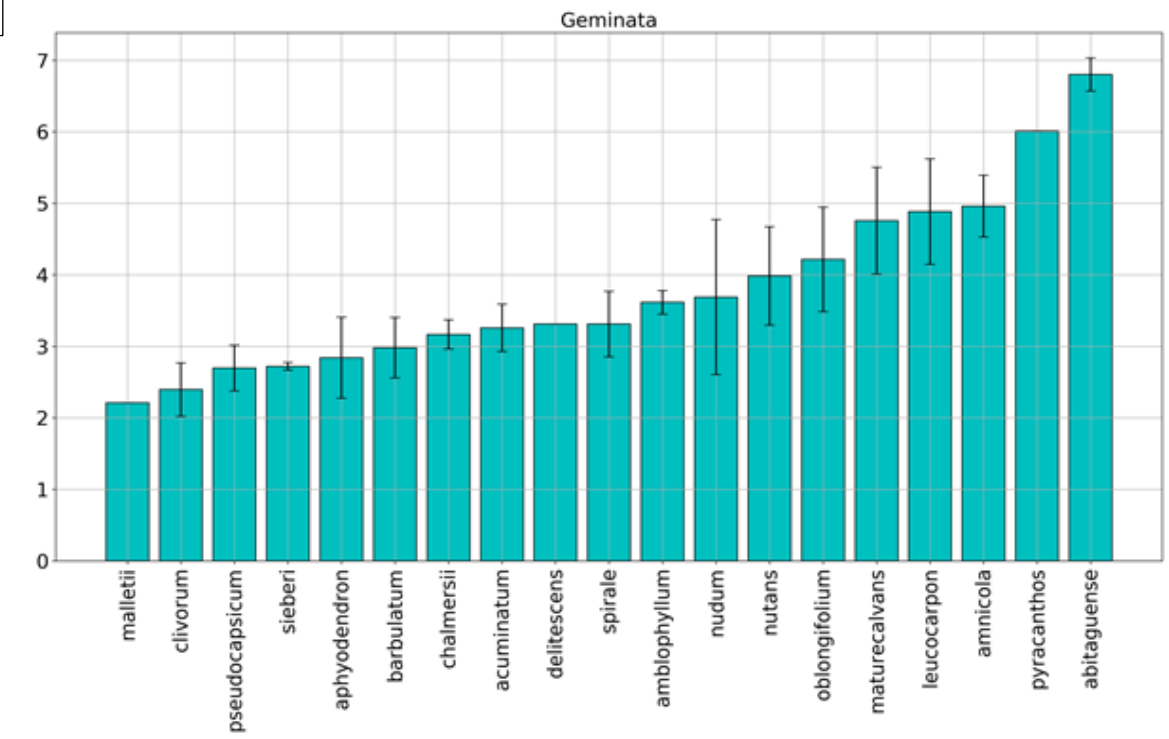

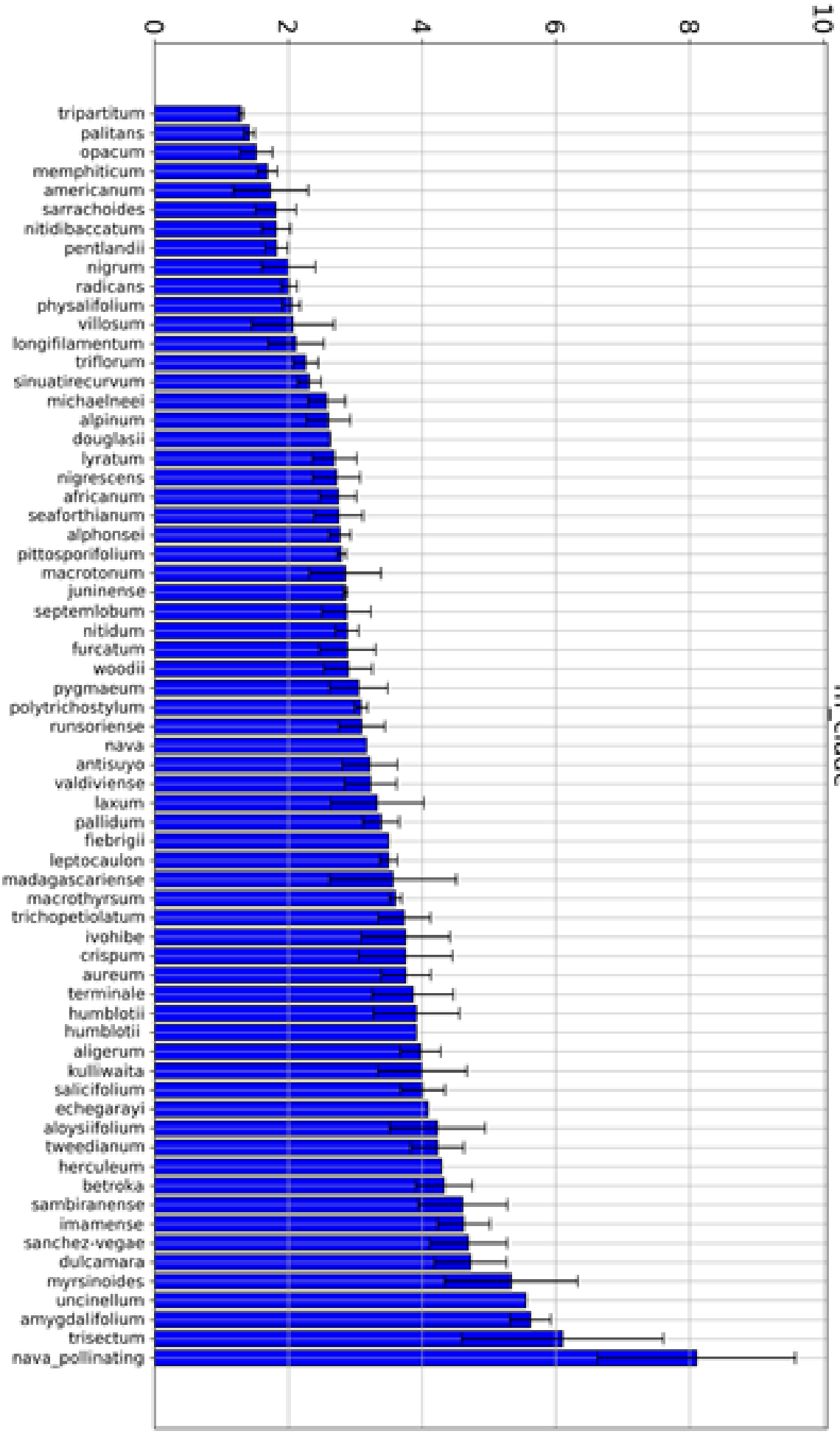
0
2
4
6
8
10
m_clade
tripartitum
palitans
opacum
memphiticum
americanum
sarrachoides
nitidibaccatum
pentlandii
nigrum
radicans
physalifolium
villosum
longifilamentum
triflorum
sinuatirecurvum
michaelneei
alpinum
douglasii
lyratum
nigrescens
africanum
seaforthianum
alphonsei
pittosporifolium
macrotonum
juninense
septemlobum
nitidum
furcatum
woodii
pygmaeum
polytrichostylum
runsoriense
nava
antisuyo
valdiviense
laxum
pallidum
fiebrigii
leptocaulon
madagascariense
macrothyrsum
trichopetiolatum
ivohibe
crispum
aureum
terminale
humblotii
humblotii
aligerum
kulliwaita
salicifolium
echegarayi
aloysiifolium
tweedianum
herculeum
betroka
sambiranense
imamense
sanchez-vegae
dulcamara
myrsinoides
uncinellum
amygdalifolium
trisectum
nava_pollinating

Figure 13 G

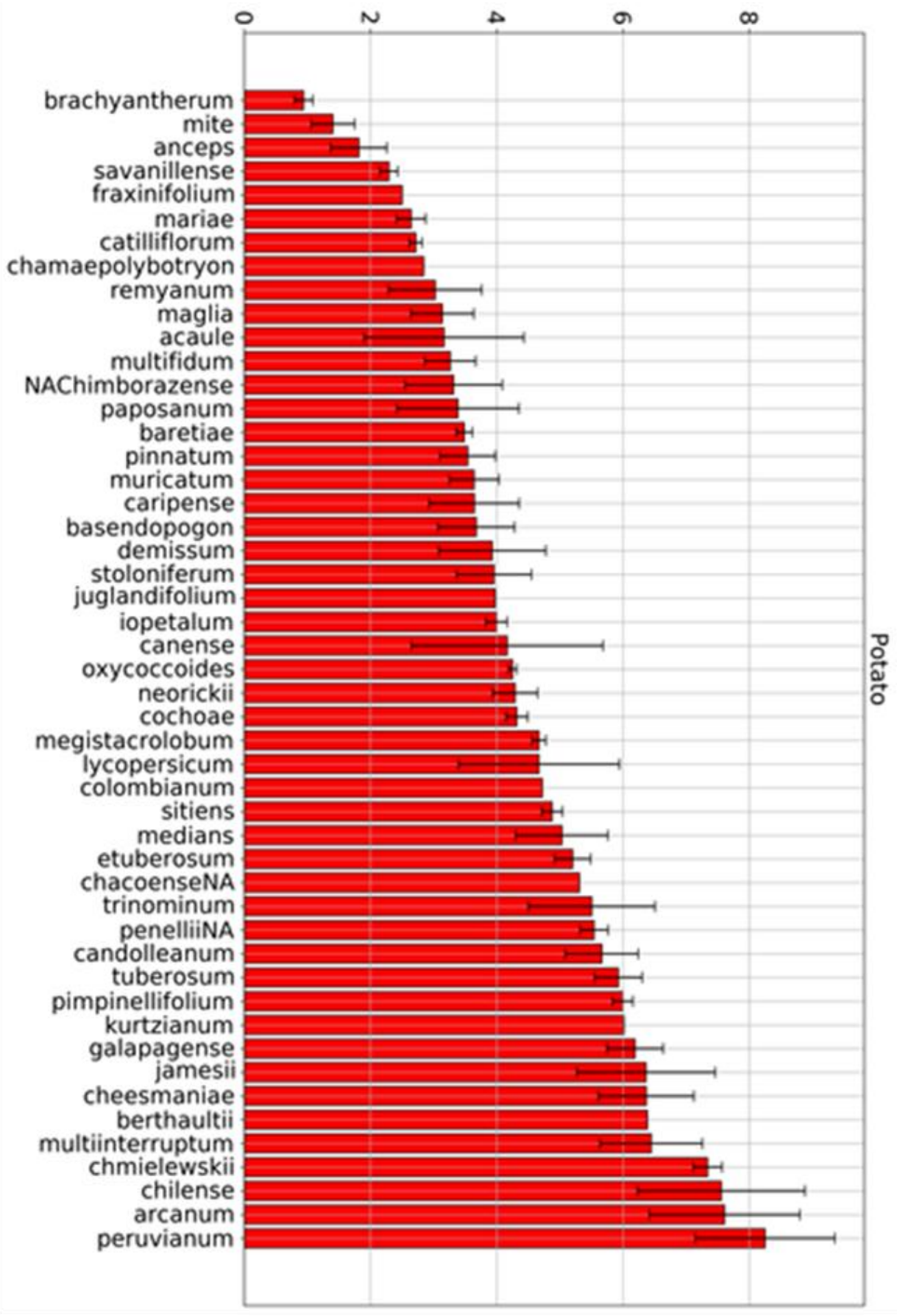
0
2
4
6
8
brachyantherum
mite
anceps
savanillense
fraxinifolium
mariae
catilliflorum
chamaepolybotryon
remyanum
maglia
acaule
multifidum
NAChimborazense
paposanum
baretiae
pinnatum
muricatum
caripense
basendopogon
demissum
stoloniferum
juglandifolium
iopetalum
canense
oxycoccoides
neorickii
cochoae
megistacrolobum
lycopersicum
colombianum
sitiens
medians
etuberosum
chacoenseNA
trinominum
penelliiNA
candolleanum
tuberosum
pimpinellifolium
kurtzianum
galapagense
jamesii
cheesmaniae
berthaultii
multiinterruptum
chmielewskii
chilense
arcanum
peruvianum
Potato

Figure 13 H

Mean anther middle width also varied in a gradual scale from smallest measurement to largest. They did not separate into group or size categories but were distributed in a smooth transition from the smallest species to the largest, as seen in Figure 14 graph B. Anther middle widths ranged from smallest at 0.43mm (*S. crinitipes*) to largest 3.31mm (*S. macrocanthum*) (and within those species measured in the phylogeny, largest was *S. uncinellum* 2.98mm).

It can be seen from Figure 14A that Potato clade species tend to have larger middle widths than the other clades. However there is still variation in the anther widths within this clade, and some Potato species appear towards both extremes of Figure 14A, showing that there are also species with anthers with very small middle widths. The variation within this clade can be seen in Figure 14B, where there is a smooth transition from the smallest anther middle width value to the largest in the Potato clade section of the graph. Leptostemonum clade has anther middle widths distributed throughout the length of Figure 14A, this shows that there is a wide variation in anther widths within this clade. This is further illustrated by Figure 14B, where a great variation can be seen between the smallest anther width of Leptostemonum clade, *S. crinitipes* (which is also the smallest anther middle width in Figure 14 overall), and the largest anther middle width of the Leptostemonum clade, *S. quitoense* (which, while not being the largest anther middle width in Figure 14, is the second largest.) From Figure 14B it can be seen that there is a smooth transition in the graph between these anther widths, with anther width measurements for Leptostemonum filling all possible lengths in between the two values. In the M clade, *S.uncinellum* has a remarkably large anther middle width compared to the rest of its clade, as can be seen in Figure 14B. *S.uncinellum* also has the largest anther width of all the species displayed in Figure 14, while the rest of M-Clade species are spaced throughout Figure 14A, with some species at the smallest anther widths end of the graph and others towards the middle and to the end of the graph representing the largest anther widths.

Figure 14: Mean anther middle width for each species displayed as a bar graph

A

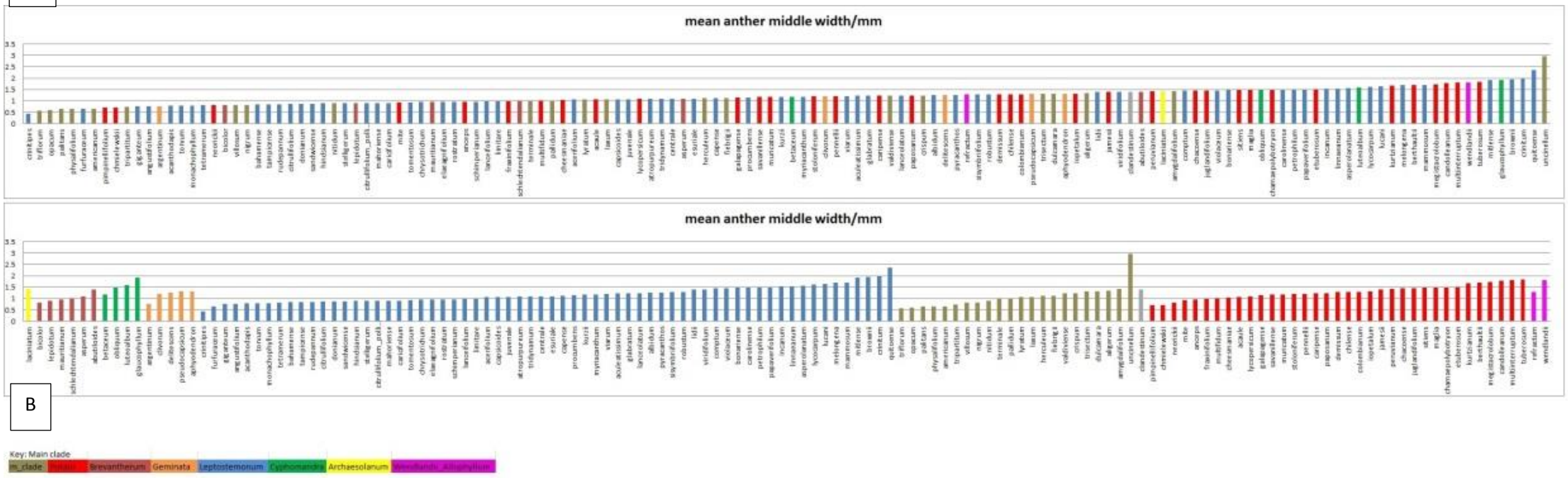

B

Figure 14: Mean anther middle width displayed as a bar graph

The mean anther middle width for each species measured (and included in the Särkinen et al (2013) phylogeny of *Solanum* and therefore identifiable to clade level,) is displayed in two ways. A: from absolute smallest mean anther middle width to absolute largest mean anther middle width. B: sorted by clade and then smallest mean anther length to largest mean anther middle width within that clade. The clades are colour coded, the colour key is shown below the graphs. Y axis is the mean anther middle width in mm.

For anther base width there was variation both within clades and between clades. Anther base width varied from 0.38mm (*S. tripartitum*) to 2.51mm (*S. uncinellum*). There was a gradual transition between the largest and smallest anther base widths, as seen in Figure 15A. The Potato clade (red) had generally larger anther base widths, as can be seen in Figure 15A by most of the clade occupying the larger anther base width end of the graph. Leptostemonum clade had species distributed throughout the entirety of Figure 15A, demonstrating the large amount of variation in anther base width within this clade.

Solanum uncinellum had a notably large anther base width when compared to the rest of M-clade, as seen in Figure 15B. The rest of M-clade has much less variation in anther base width with the exception of this species and occupy largely the smaller half of Figure 15A, having largely smaller anther base widths than the other clades. The smallest five anther base widths displayed in Figure 15A belong to M-clade.

Figure 15: Mean anther base width of each species displayed as a bar graph

A

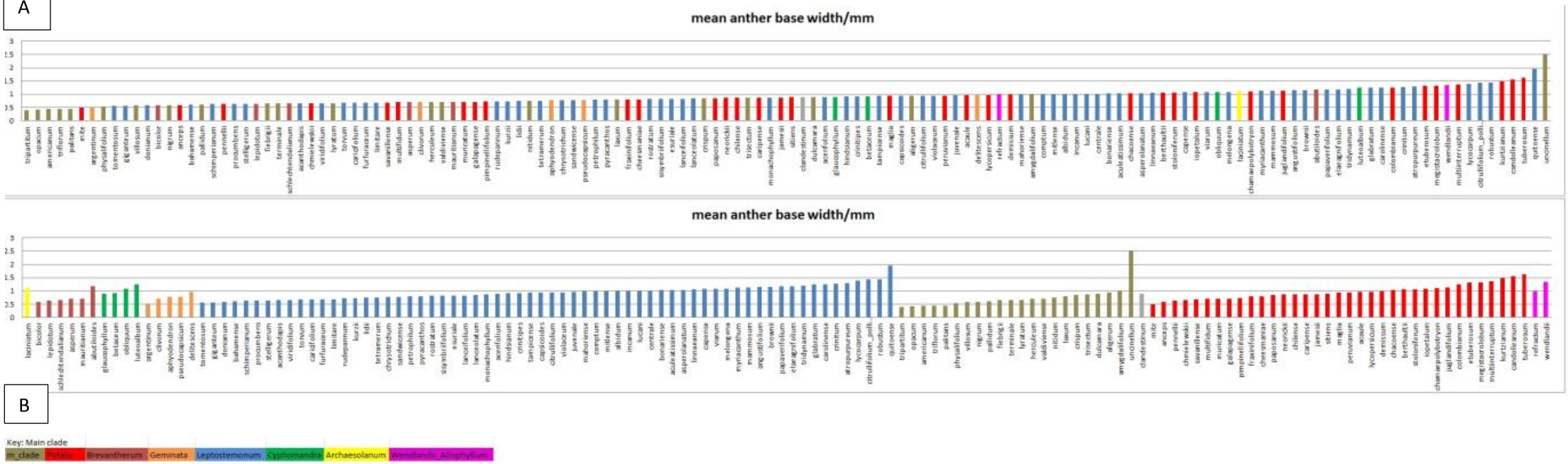

B

Key: Main clade
m_clade | Potato | Brevantherum | Geminata | Leptostemonum | Cyphomandra | Archaesolanum | Wendlandia_Allophyllum

Figure 15: Mean anther base width displayed as a bar graph

The mean anther base width for each species measured (and ncluded in the Särkinen et al (2013) phylogeny of *Solanum* and therefore identifiable to clade level) is displayed in two ways. A: from absolute smallest mean anther base width to absolute largest mean anther base width. B: sorted by clade and then smallest mean anther base width to largest mean anther base width within that clade. The clades are colour coded, the colour key is shown below the graphs. The Y axis is the mean anther base width in mm.

Anther tip width had the greatest difference between the smallest and largest anther tip width value, compared with the other dimension measurements. Anther tip width varied from 0.21mm at its smallest (*S. chmielewskii*) to 1.23mm at its largest (*S. brownii*). The greater variation in this anther tip width measurement compared with the other anther dimensions can be seen in Figure 16A, when compared with the other graphs (Figure 13 to 16) it can be seen to have the steepest curve to it from smallest to largest value.

The Potato clade (red) is spread at the two extremes of Figure 16A, species in the Potato clade can be seen at the end of the graph representing the smallest anther tip widths and also at the end of the graph representing the largest anther tip widths. There is an absence of species from the Potato clade in the middle section of Figure 16A. This can also be seen in Figure 16B where there are distinctly two groupings of anther tip widths, dividing the Potato clade effectively into two.

Leptostemonum clade (blue) has a great amount of variation in the anther tip widths of its species, spread throughout Figure 16A at all areas of the graph. There is a smooth transition from the species with the smallest anther tip width to the species with the largest anther tip width in Figure 16B, with no groupings towards particular values of anther tip width within this clade. M-Clade (brown) follows a similar pattern with species distributed throughout Figure 16A.

Figure 16: Mean anther tip width of each species displayed as a bar graph

A

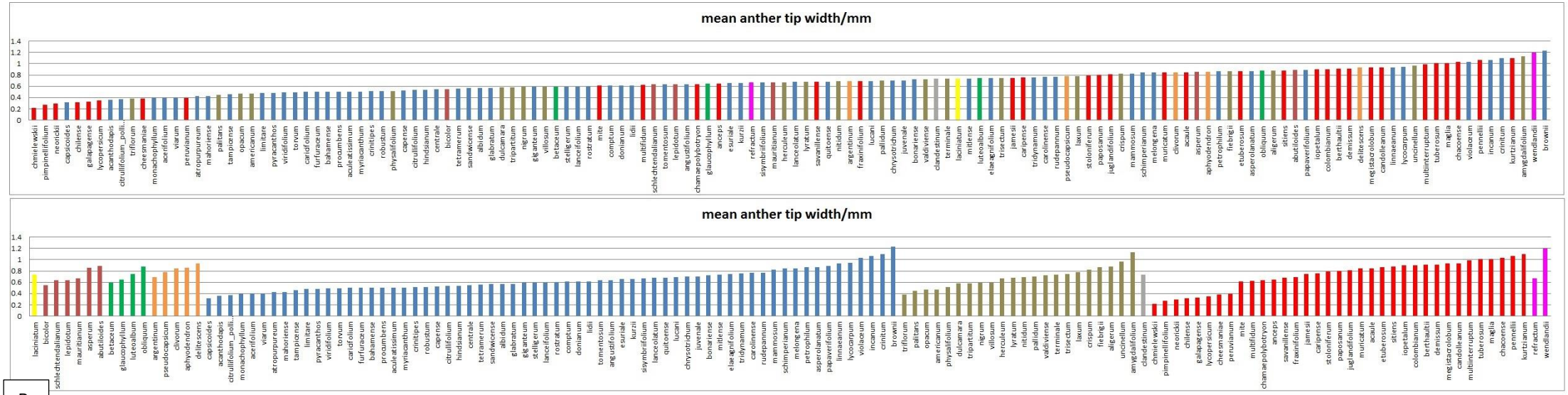

B

Figure 16: Mean anther tip width displayed as a bar graph

The mean anther tip width for each species measured (and included in the Särkinen et al (2013) phylogeny of *Solanum* and therefore identifiable to clade level) is displayed in two ways. A: from absolute smallest mean anther tip width to absolute largest mean anther tip width. B: sorted by clade and then smallest mean anther tip width to largest mean anther tip width within that clade. The clades are colour coded, the colour key is shown below the graphs. The Y axis is the mean anther tip width in mm.

Overall it can be seen from Figures 13 to 16 that, for all the anther dimension measurements taken, there is variation both within clades and between clades. It can also be seen that there is a gradual spread from smallest species to largest species in each of the anther dimension measurements, causing all the graphs A of Figures 13 to 16 to follow a smooth curve from smallest species to largest species. There is no general grouping to particular values for each anther dimension, nor separation into clear size categories.

It should also be noted that there does not appear to be a pattern of which clade generally has the largest of each anther dimension value. A large value in one anther dimension does not necessarily mean a large value in the other anther dimensions. It appears that the anther dimensions vary largely independently of one another, however this is further explored in Figure 17.

It should be noted from Figures 13 to 16 that there is a trend towards certain anther shapes for some of the clades. These trends do not describe the full diversity of each clade, as there is so much variation within clades. Potato clade anthers tend towards a shape of ‘short but fat’. Leptostemonum clade species fill all anther shape categories, showing both larger anthers, small anthers and every possible anther shape represented. This idea of anther shapes will be further explored in the section on phylomorphospace and Figures 20 to 32 where anthers will be represented in morphological space.

2.4.2: The anther dimensions varied largely independently from one another

The correlation matrix, Figure 17, displays the correlation between each of the anther dimensions.

None of the dimensions measured have a negative correlation between them, all of the values have at least a small amount of positive correlation between them (Figure 17). Colours at the red end of the key indicate dimensions with high amounts of correlation. Anther middle width and anther base width are the anther dimensions which are most correlated to one another (Figure 17, they have a correlation value of 0.8/1). The second most correlated anther dimensions were anther middle width and anther tip width (Figure 17, they have a correlation value of 0.7/1). The least correlated anther dimensions were anther tip width and anther length (Figure 17, they have a correlation value of 0.1/1).

From the perspective of anther shape, this means that knowing one anther dimension would not allow you to predict the anther shape: a long anther would not necessarily have higher values for any of the other anther dimensions. It is almost equally likely to be a long thin anther or a long thick anther. This means that the variety of anther shapes possible within *Solanum* is very large as the anther dimensions vary largely independently from one another.

Figure 17: Correlation Matrix for all anther dimensions

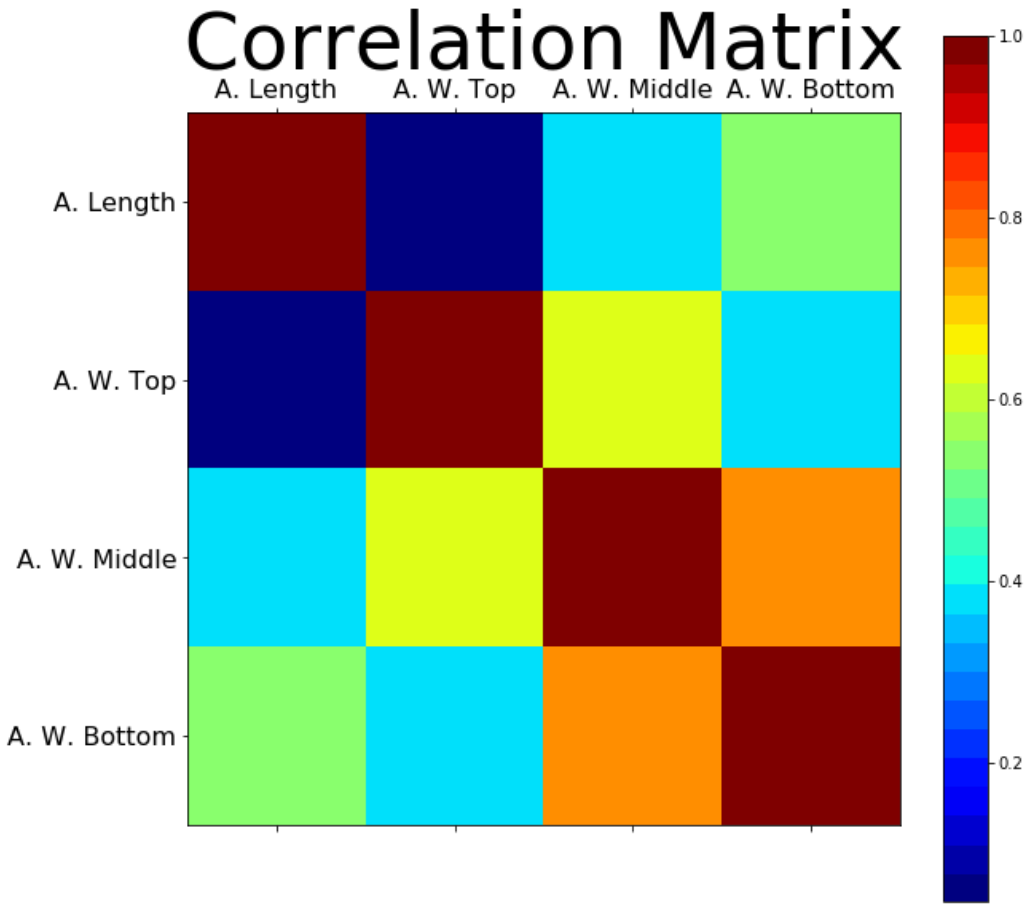

Figure 17: Correlation Matrix of all anther dimensions

This Figure displays the correlation between each of the anther dimensions. The correlation matrix uses the standardised mean values of the anther dimensions and compares them to one another. There are 6 correlates displayed in this matrix, each compares two of the anther dimensions (and their standardised values) to see if there is a correlation or not. A correlation of 0 represents no correlation at all between the two dimensions values. 1 represents a high correlation between the two values. Values between 0 and 1 represent the amount of positive correlation between the two sets of dimension values.

Figure 18: Correlation scatter-grams for anther dimensions

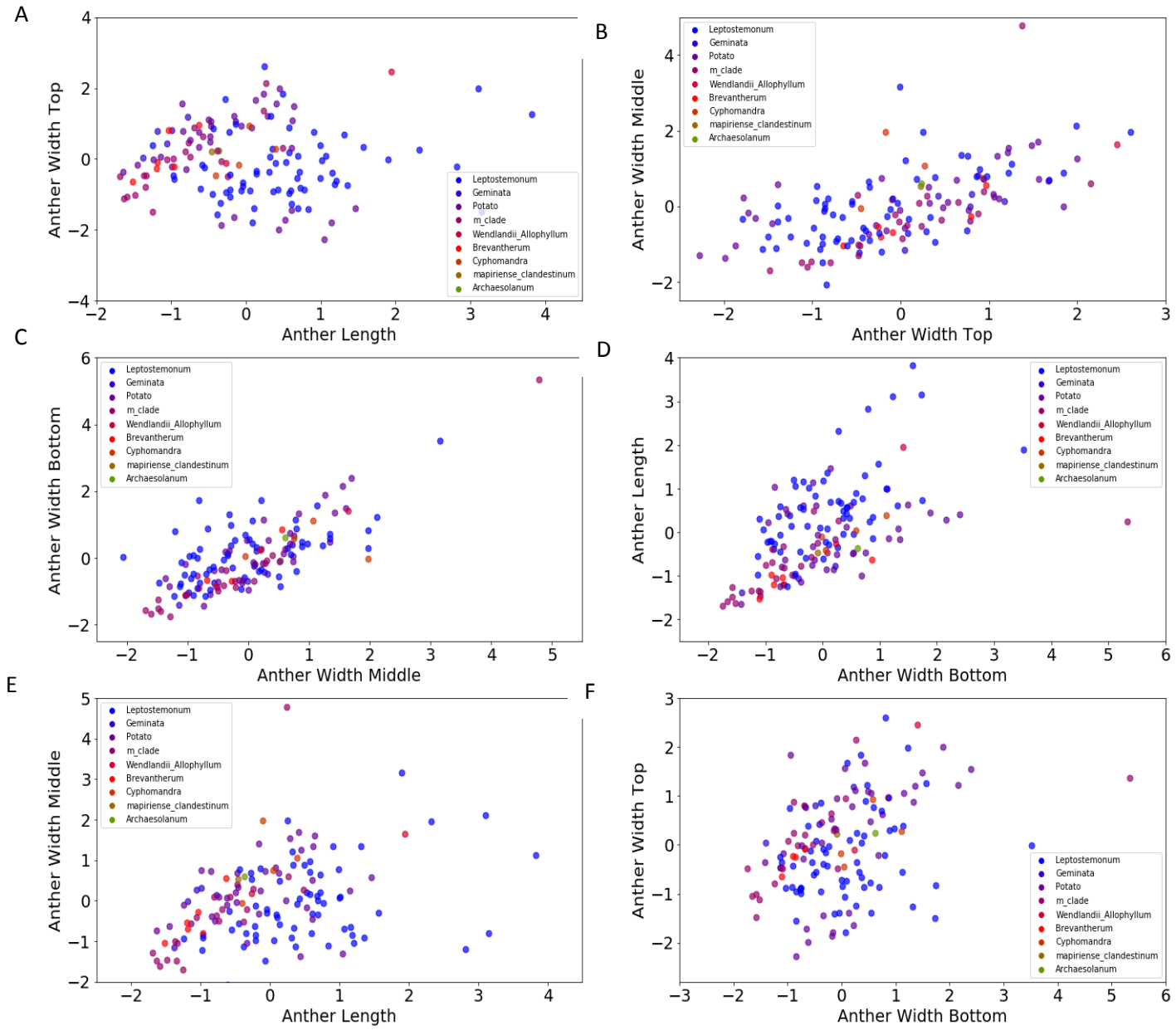

Figure 18: Correlation scatter-grams for anther dimensions.

These scattergrams (A to F) display the standardised mean anther dimension measurements plotted against one another. 0 now represents the standard theoretical mean value for each dimension, negative values being less than the overall average value for that anther dimension in *Solanum* and positive values being measurements larger than that average value for the anther dimension. As the standardised anther dimensions measurements are now ratios they no longer have units.

The scattergrams shown in Figure 18 use standardised means for each anther dimension value. Thereby the anther dimensions become ratios by which the anther dimension measurement from a single species can be seen to be larger or smaller than the average value for all of the species of *Solanum* for which there were measurements in this study. 0 on the scattergrams represents this average value for that anther dimension measurement in *Solanum:* therefore positive values on the axis represent a measurement larger than this average for the genus and negative values on the axis represent a measurement smaller than this average for the genus. These scattergrams allow us to see the general direction of variation within the genus as a whole and how the data is spread and also an initial look at the general morphological distribution of the clades.

From the scattergrams shown in Figure 18, it can be seen that there is a degree of clustering of the nodes (species) from each clade (indicated by the node colour) into the same area of morphological space (the same area of the scattergram).

The values plotted in Figure 18 are standardised dimension values. These values give a distance from a theoretical standardised overall mean value for that dimension. This is so that the disparate values can be displayed neatly and easily on one diagram as it puts them into the same scale. Here the standardised mean for the dimension value is 0. Therefore, for example, species with a standardised mean for anther length larger than 0 would be species that had a longer average anther length than the mean anther length of all the species. For less than 0 they have anthers that are shorter than the average anther length.

In Figure 18, it can be seen that each of the scattergrams A-F have different amounts of spread in the data (how distant the species nodes are from one another). All of the dimensions, when compared with one another in this way, have a small degree of positive correlation (all of the scattergrams would have a theoretical line of best fit from the bottom left hand corner of the scattergram to the top right corner of the scattergram). However the species nodes would not stay very close to this theoretical line of best fit, showing that the positive correlation between each of the anther dimensions is quite weak (as was observed from Figure 17). In Figure 18C, the species nodes cluster most closely to one another and are the least spread out, this shows that these two anther dimensions (anther middle width and anther base width) are the most correlated with one another (as was concluded from

Figure 17). Anther length and anther tip width were the least correlated, indicated by the species nodes being the most spread out in Figure 18A (and confirmed in Figure 17). The second least correlated sets of anther dimension were anther length against anther middle width and anther width base against anther width tip (Figure 18E and F).

Leptostemonum clade species spread all over the graphs with little clustering in specific parts of the morphological space (Figure 18, A-F. Blue nodes represent Leptostemonum). This indicates a wide variety of anther shapes for species contained within this clade.

We can see from Figure 18 that the anthers of M-Clade species are almost all in the below 0 zone of the graph for most of the dimension values (Figure 18 A to F), indicating that species of the M-clade tend to have smaller anthers than average for the genus.

For the Potato clade, Figure 18E shows that they are mostly located in the below 0 zone of the scattergram. This indicates that Potato clade species tend to have short anthers with thin anther middle widths. However from Figure 18A, the species nodes are mainly above 0 for the anther tip width dimension (while still below 0 for anther length), this indicates that while Potato species anthers tend to be short they have large anther tip widths compared with other clades in *Solanum.*

These trends will be further explored using phylomorphospace in section **2.3.4.**

2.4.3: Principal component analysis (PCA) of anther dimension measurements

PCA uses correlation data to generate a set of principal components, reducing the data set from sets of dimension measurements to instead a few Principal Components (PCs) which summarise the variation in the data. Here PC1 and PC2 take into account 87% of the variance within the data set (Figure 19). Because PC1 and PC2 take into account most of the variance in the data set only PC1 and PC2 will be considered for the phylomorphospace and for analysis of anther morphology. However phylomorphospace analyses utilising PC3 and PC4 (which account for the remaining 13% of the variance in the data) can be found in appendix 4.

PC1 and PC2 are composed of the variance in the data set and the general spread of the data. Most of this variance is contained within two of the anther dimensions: anther length and anther tip width (this can be seen in Figure 18A, where the scattergram shows the most spread in the points, the points are the least clustered compared with the scattergrams of the other dimension measurements. Figure 17 also concluded that anther length and anther tip width were the least correlated anther dimensions). So while PC1 and PC2 are composed of variance within all of the anther dimensions (anther length, anther tip width, anther base width and anther middle width), they are heavily weighted by the variance contained within anther length and anther tip width.

Figure 19: Covariance Matrix of the Principal Components

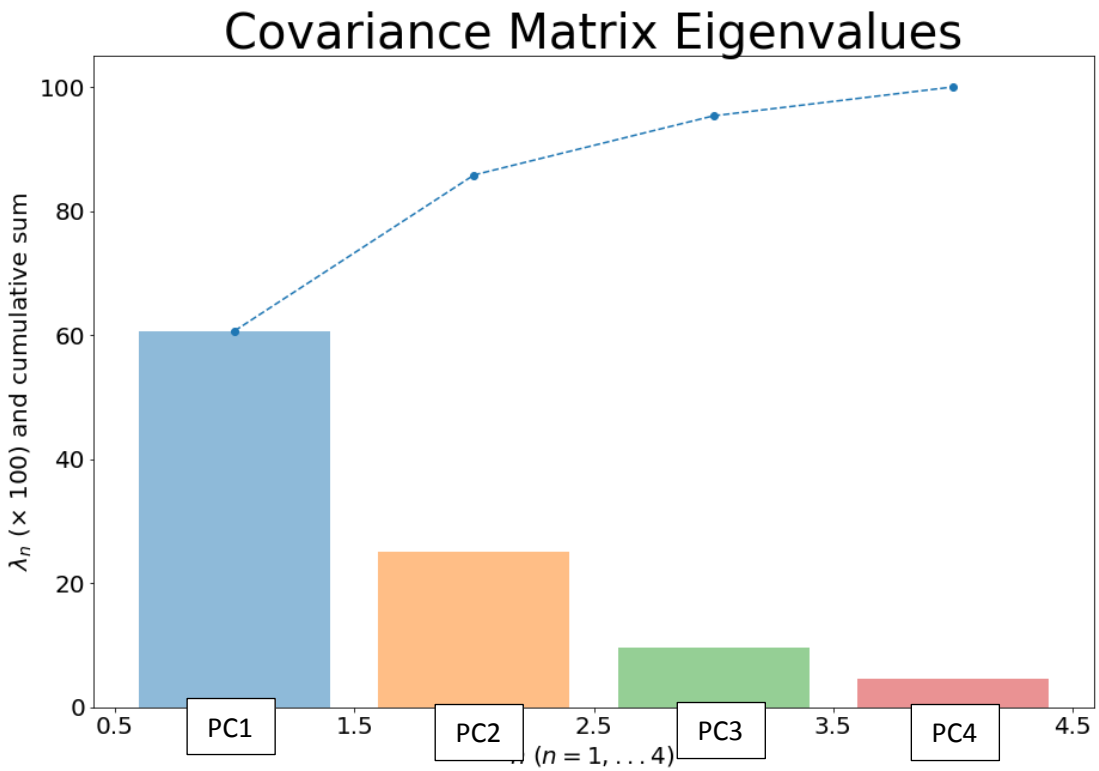

Importance of Components:				
	PC1	PC2	PC3	PC4
Standard Deviation	1.5452	1.0525	0.56823	0.42629
Proportion of Variance	0.5969	0.2769	0.08072	0.04543
Cumulative Proportion	0.5969	0.8739	0.95457	1

Figure 19: Covariance Matrix of the Principal Components

PC1 and PC2 account for the majority of the variance in the data set (87%). Most of the variance in the data set is accounted for by PC1 (59%), with PC2 accounting for 27% of the variance. PC1 and PC2 are most influenced by anther length and anther tip width.

2.4.4: Phylomorphospace

Phylomorphospace is a form of analysis that can be used to visualise how the species sampled occupy morphological space and how their occupation of morphological space is related to their phylogenetic position (based on the methodology used by Sakamoto and Ruta, 2012; Bookstein, 1985; Kimmel et al, 2017; Wilson et al, 2013). It provides a direct test of the null hypothesis that phylogeny constrains morphology. Species are represented by nodes, coloured by clade within the genus, and the shape of the node represents the anther cone shape present in that species. ● represents a 'pepper pot' anther cone, while □ represents a 'salt cellar' anther cone. For the definition of these cone types please refer to section **2.1.3.1.3**. Species nodes connected by a short line indicate species which are morphologically similar and with a high degree of relatedness. In these clusters morphology is constrained by phylogeny. Where species nodes are connected by long lines this indicates areas of divergence; a species occupies a distant area of morphological space relative to the species it is closely related to. This could be an indication of the action of selection driving a change in morphology.

The morphological space occupation was studied initially at the level of the entire genus, with all species sampled displayed at once, however due to the sheer number of species this is very difficult to examine. Therefore the phylomorphospace analysis was then split into the various clades within *Solanum* and where relevant/important this was further sub-divided. Whilst only species from a specific clade are shown for the phylomorphospaces divided by clade, these species are plotted with respect to the entire genus, not simply the species of that clade. Therefore their anther shape relative to the rest of the genus can be considered.

2.3.4.1: Entire genus *Solanum*

The phylomorphospace analysis used all 135 species for which measurement data were available and which were also included in the phylogeny of Särkinen et al. (2013). These species represent members of all the clades within *Solanum.* The nodes are colour coded by clade. Some clustering can be seen within clades and also within particular areas of morphological space. The majority of the species sit within particular areas of morphological space while other areas of space remain largely unoccupied. These unoccupied areas are generally areas that would represent 'extreme morphotypes' such as very long very thin anthers, or very thick and very short anthers.

There are some species which can be seen to diverge from the main species cluster. These all diverge in different ways and as a result of different anther dimensions. The phylomorphospace that uses the PCs can give an indication of species which diverge from the general morphological variation (Figure 20), the phylomorphospaces which use the standardised dimension measurement means can then be used to better understand where this divergence comes from (Figure 21).

Solanum uncinellum, a species in the Dulcamaroid clade, diverges from the main species cluster (Figure 20). From examining Figure 21, it can be concluded that *S.unicinellum* has large anther widths compared with the majority of species in *Solanum,* especially those species it is closely related to. *Solanum uncinellum* has wider anthers (in tip width, middle width and base width) than the other species in the Dulcamaroid clade.

Solanum lycocarpum, S. crinitum and S. *angustifolium* have longer anthers than those species in their clades which they are closely related to. *S.angustifolium* is a heterantherous species.

S. brownii (of Leptostemonum clade) and S. *pennellii* (tomato subclade) both have wider anther tips relative to those species closely related to them. *S.quitoense* (Leptostemonum) has a wider middle anther width.

S. wendlandii has in general larger anthers than would be expected relative to the species it is most closely related to. It has both a longer anther length and wider anther widths.

Due to the large number of species being examined this full phylomorphospace (Figure 20) is difficult to interpret with much clarity. The areas of morphological divergence are examined in more detail by dividing the phylomorphospace by main clade, allowing more careful examination of where species sit in morphological space relative to one another (Figures 22 to 31). This approach also allows other anther traits (cone type and epidermal cell outgrowth) to be examined alongside the anther dimensions. This first analysis allows us to conclude that phylogeny does not always constrain morphology within this genus and that there is variation between closely related species with regard to anther form.

Figure 20: Phylomorphospace for *Solanum* genus using principal components

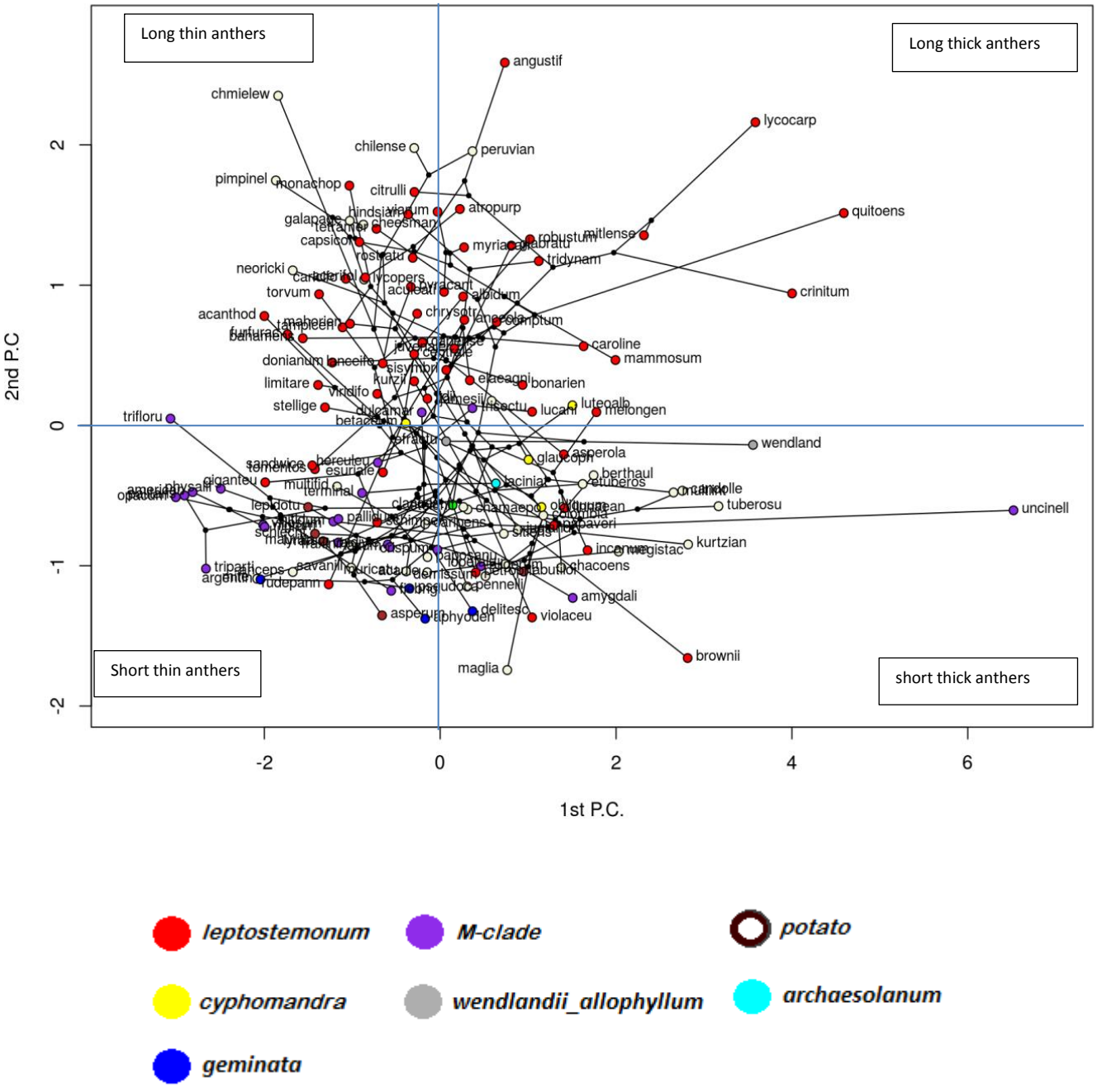

Figure 20: Phylomorphospace for *Solanum* genus using principal components

The above key shows the colour coding by clade used in the phylomorphospace to give a general idea of clade clustering/spread in morphological space.

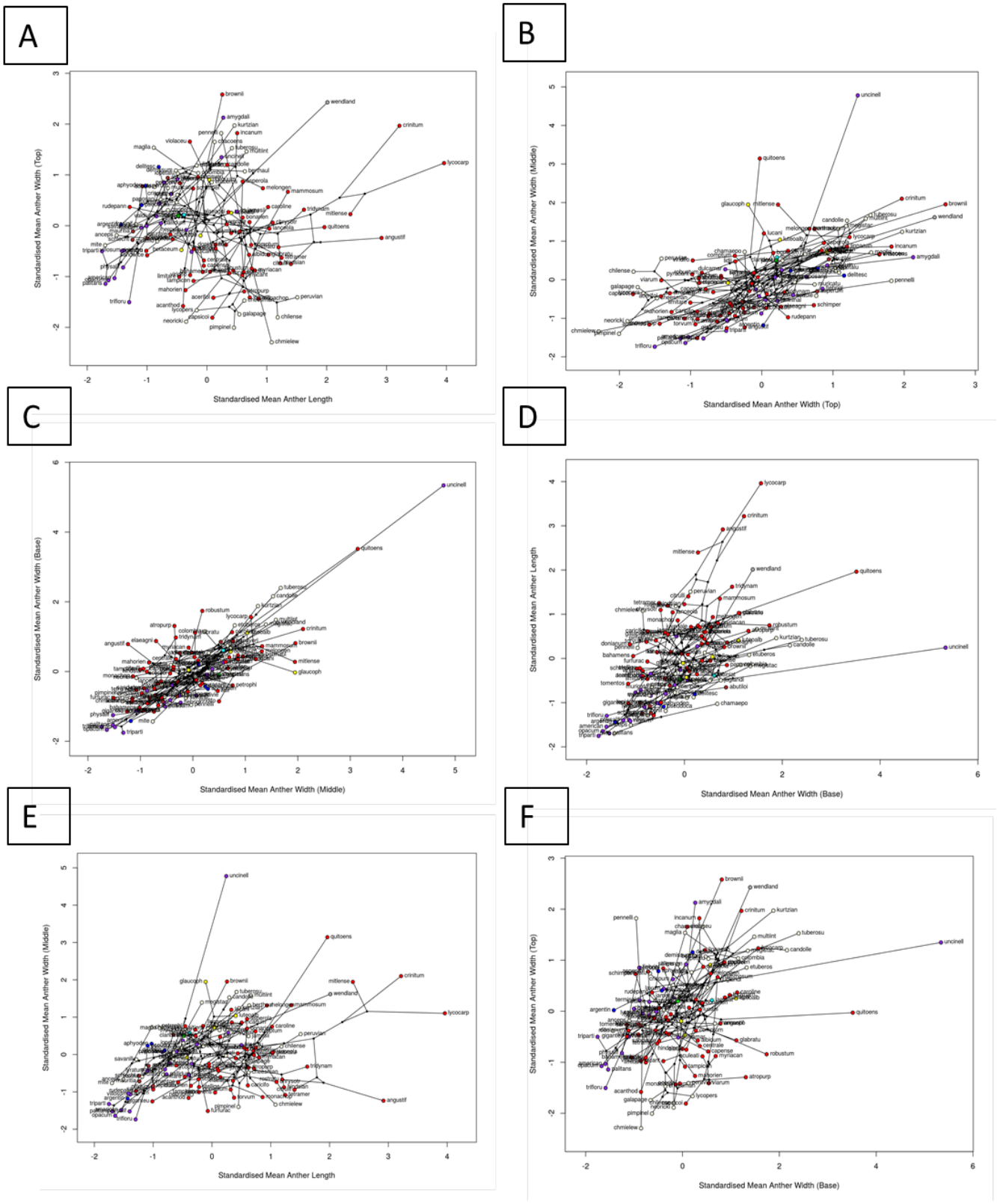

Figure 21: Phylomorphospaces for *Solanum* genus using standardised means of anther dimension measurements
A: Mean anther tip width and mean anther length plotted against one another in morphological space, with respect to the phylogeny. B: Mean anther tip width and mean anther middle width plotted against one another in morphological space, with respect to the phylogeny. C: Mean anther base width and mean anther middle width plotted against one another in morphological space, with respect to the phylogeny. D: Mean anther length and mean anther base width plotted against one another in morphological space, with respect to the phylogeny. E: Mean anther middle width and mean anther length plotted against one another in morphological space, with respect to the phylogeny. F: Mean anther tip width and mean anther base width plotted against one another in morphological space, with respect to the phylogeny.

2.3.4.2: Leptostemonum

The Leptostemonum clade occupies a large area of morphological space, representing the wide diversity of anther forms within this clade (Figure 22). In this case it is therefore more interesting to note which areas of the morphospace are unoccupied. Areas that are unoccupied in morphological space are those representing very extreme morphologies eg: very long thin anthers, or very short thin anthers (Figure 22). There are however some species which occupy extreme anther morphospace when the anther is thicker/wider. For example, *S. lycocarpum* and *S.quitoense* have very long thick anthers compared to the rest of the Leptostemonum clade (Figure 22) and also compared to the average anther dimension measurements for *Solanum* as a whole (Figure 23A, B, C and D). *Solanum quitoense* has an especially wide anther middle width and anther base width relative to the rest of *Solanum* and the Leptostemonum clade (Figure 23C and D). *S. brownii* occupies the area of very short but thick anthers (Figure 22) and also has a short anther length relative to Leptostemonum clade (Figure 22) and a slightly shorter than average anther length relative to the rest of *Solanum* (Figure 23A). *Solanum brownii* has a very wide anther relative to the rest of Leptostemonum (Figure 22) and also relative to the rest of *Solanum:* especially with regard to its anther tip width (Figure 23A and B) and anther middle width (Figure 23B). The anther base width of *S.brownii* is however only slightly thicker than average relative to the rest of *Solanum* (Figure 23C).

The species *S. angustifolium* diverges from the general morphological space occupied by Leptostemonum (Figure 22). The species has longer and thinner anthers than the majority of species in Leptostemonum (Figure 23A and E).

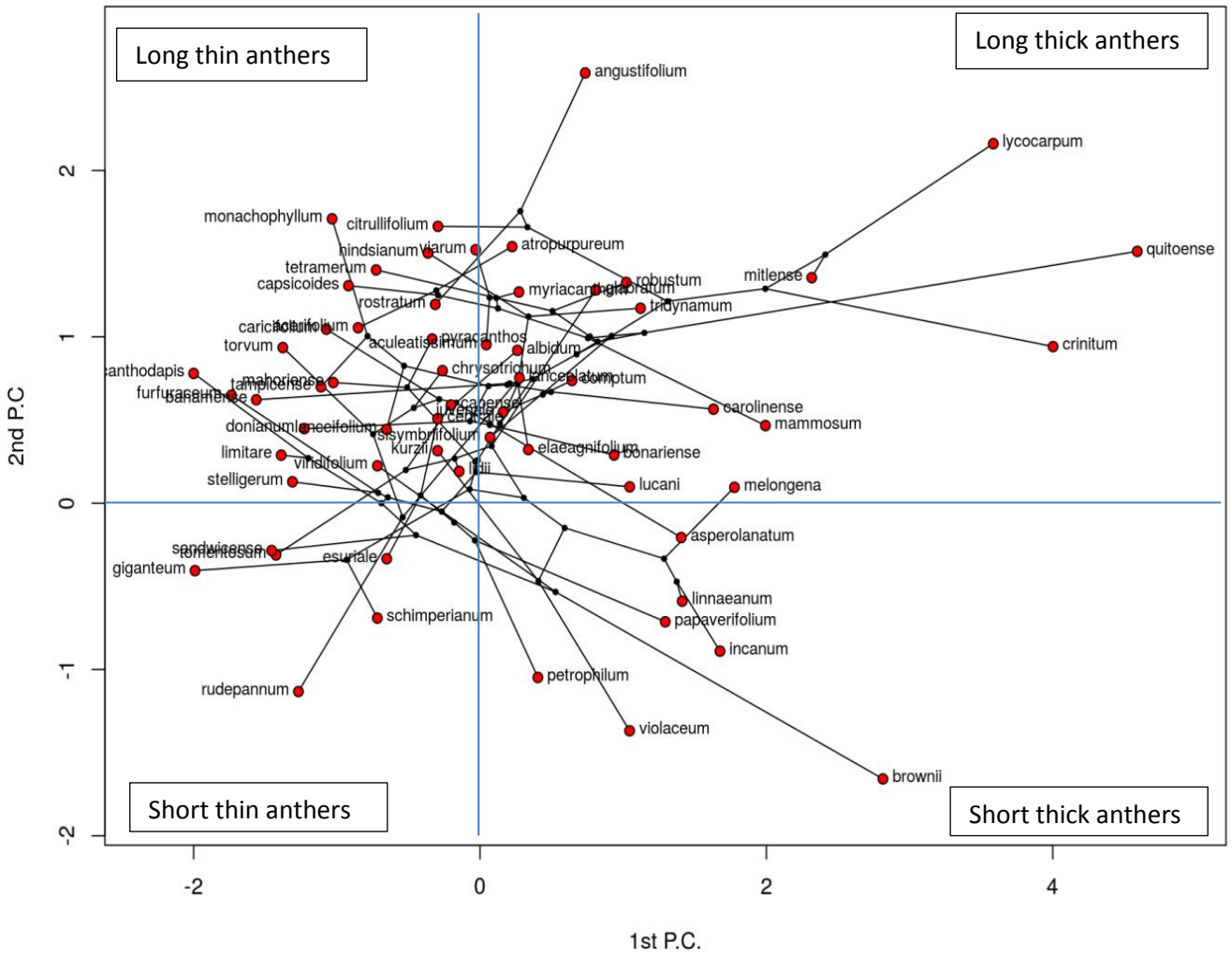

Figure 22: Phylomorphospace for the Leptostemonum clade of *Solanum*, using principal components 1 and 2.

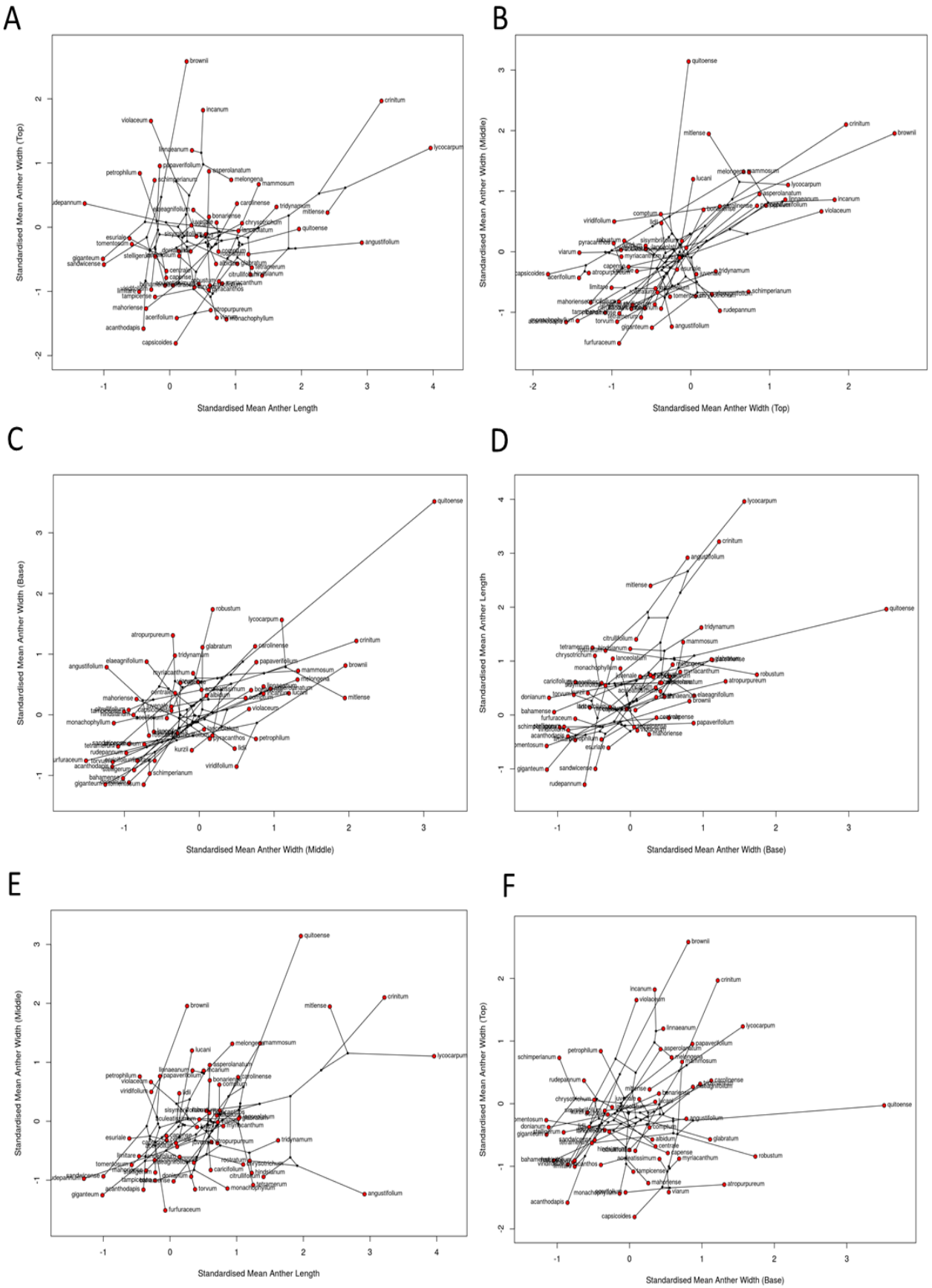

Figure 23: Phylomorphospaces for Leptostemonum clade using standardised means of anther dimension measurements

A: Mean anther tip width and mean anther length plotted against one another in morphological space, with respect to the phylogeny. B: Mean anther tip width and mean anther middle width plotted against one another in morphological space, with respect to the phylogeny. C: Mean anther base width and mean anther middle width plotted against one another in morphological space, with respect to the phylogeny. D: Mean anther length and mean anther base width plotted against one another in morphological space, with respect to the phylogeny. E: Mean anther middle width and mean anther length plotted against one another in morphological space, with respect to the phylogeny. F: Mean anther tip width and mean anther base width plotted against one another in morphological space, with respect to the phylogeny.

2.3.4.3: M-Clade.

The majority of the species of the M-Clade tend to have smaller anthers overall than the rest of *Solanum.* Most of the species in M-Clade occupy the 'short and thin' area of the phylomorphospace (Figure 24).

This skewing towards thin anther widths relative to the rest of *Solanum* is especially clear in Figure 25C. Overall M-Clade had generally small anthers in all anther dimension measurements relative to the rest of *Solanum,* but especially in terms of anther length (Figure 25A).

The subclades of M-Clade occupy different areas of morphological space (Figure 24). The Morelloid subclade tends to occupy the morphological space of most pronounced 'short and thin anthers' (Figure 24). An exception to this is the species *S. triflorum* (Figure 24), which has longer anthers than most of the Morelloid subclade. However the anthers of *S. triflorum* are still shorter than average for the rest of *Solanum* (Figure 25A). *Solanum fiebrigii* has even longer anthers than *S. triflorum* and as compared to the rest of the Morelloid subclade, but it still has shorter than average anther length for *Solanum*. This species has an anther tip width which is much thicker than the rest of the Morelloid subclade and which is slightly larger than average for *Solanum* (Figure 25A).

Species of the Dulcamaroid subclade have wider anthers than do species of the Morelloid group (Figure 24), however these species do not have wide anthers relative to the rest of *Solanum* but are merely average (Figure 24 and Figure 25B and C). The Dulcamaroid subclade have still shorter than average anther lengths (as is the case for the whole M-Clade) (Figure 24, Figure 25A) as compared to the rest of *Solanum*.

The species *S. uncinellum* occupies an area of morphological space distinct from the rest of the M-Clade (Figure 24). This species is also very distant from all the other species in the clade in Figures 25A-F, indicating that it diverges from the other species of M-Clade in all of its anther dimension measurements.

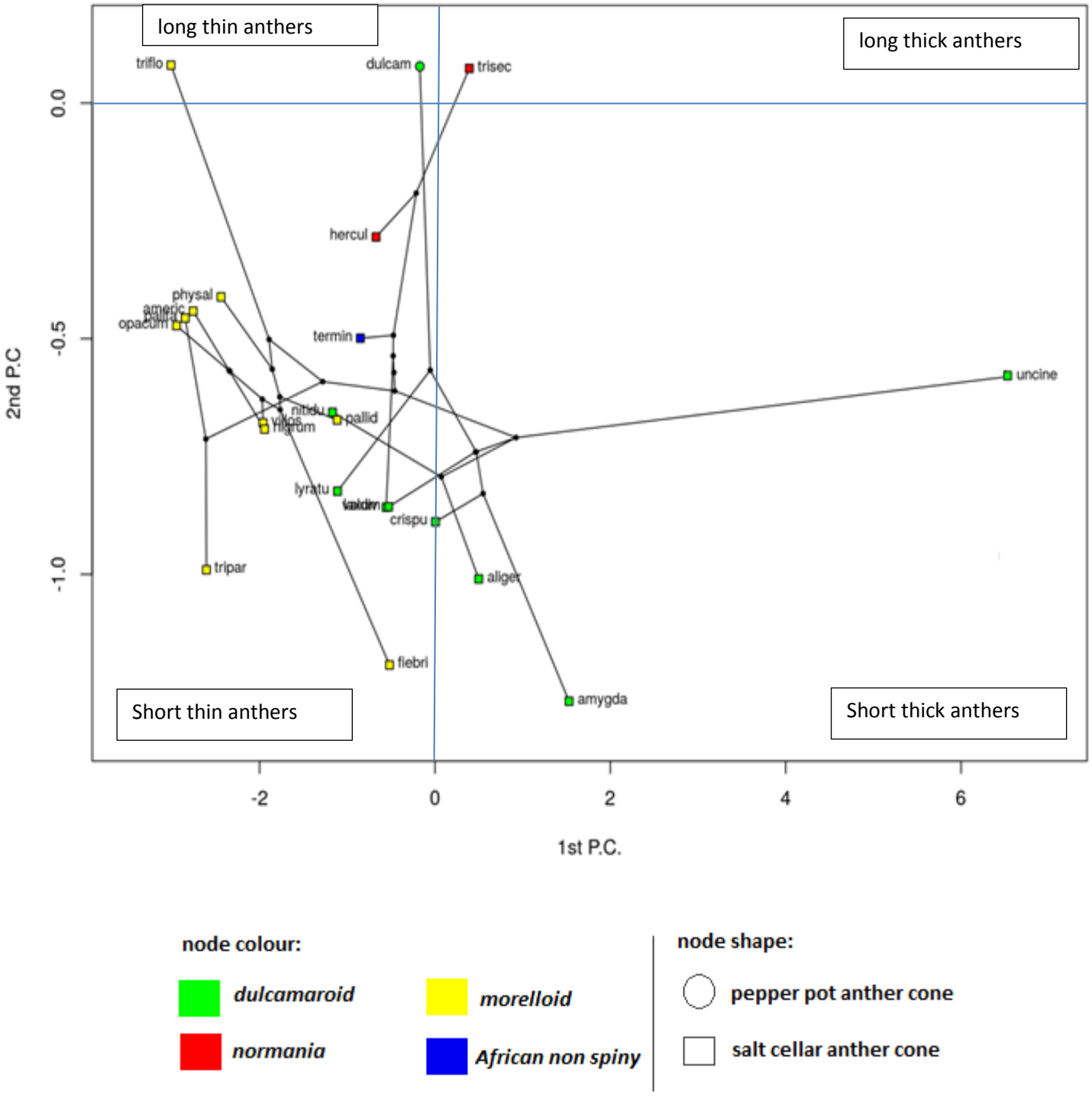

Figure 24: Phylomorphospace for M-clade of *Solanum* using principal components 1 and 2

The phylomorphospace for the *M-clade* is colour coded by subclade. The shape of the node indicates the cone shape.

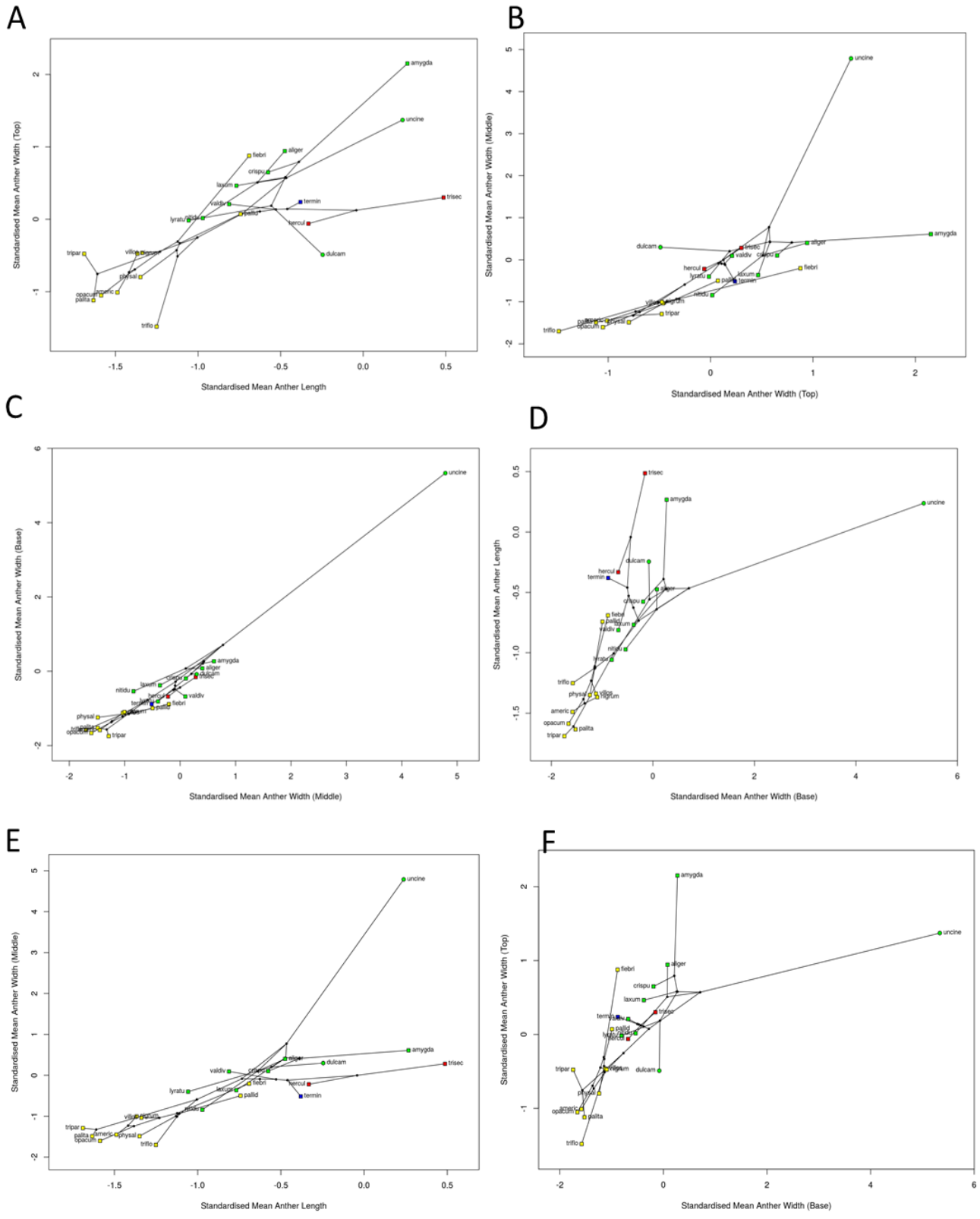

Figure 25. Phylomorphospace for M-clade of *Solanum* using standardised means of anther dimension measurements
A: Mean anther tip width and mean anther length plotted against one another in morphological space, with respect to the phylogeny. B: Mean anther tip width and mean anther middle width plotted against one another in morphological space, with respect to the phylogeny. C: Mean anther base width and mean anther middle width plotted against one another in morphological space, with respect to the phylogeny. D: Mean anther length and mean anther base width plotted against one another in morphological space, with respect to the phylogeny. E: Mean anther middle width and mean anther length plotted against one another in morphological space, with respect to the phylogeny. F: Mean anther tip width and mean anther base width plotted against one another in morphological space, with respect to the phylogeny.

2.3.4.3.1: Sub-clade Dulcamaroid

Species in the Dulcamaroid subclade tend to have slightly shorter anther lengths than the majority of species in *Solanum* (Figure 26A). Most of the Dulcamaroid clade occupy the area of morphological space of having short anthers with fairly average anther widths (Figure 25) for the genus *Solanum* (Figure 26B and C, where for the standardised anther width means, the species nodes tend to be close to the 0 value, which is the *Solanum* standardised mean average for that dimension).

S. amygdalifolium shows some divergence from the main species cluster for the Dulcamaroid subclade (Figure 26). Its anther length is longer than the rest of the species in Dulcamaroid (Figure 26A).

S. dulcamara is the only species included in this subclade which has a pepper pot anther cone. The species diverges in the morphological space it occupies compared to the rest of the Dulcamaroid subclade (Figure 26). It occupies an area of morphological space which represents longer and thinner anthers than the rest of the subclade. It is more similar to the Tomato subclade which also occupies this kind of morphological space relative to the rest of its clade and also has pepper pot anther cones (Figure 30). *S.dulcamara* has longer (Figure 26A) and thinner anthers (Figures 26A, B and C) than the rest of the species in its subclade.

The species *S. uncinellum* occupies different morphological space to the rest of its subclade (Figure 26). *S. uncinellum* has much thicker anthers than the rest of its subclade (Figure 26B and C). It also has a slightly longer anther length than the rest of the species in Dulcamaroid (except from *S. amygdalifolium*).

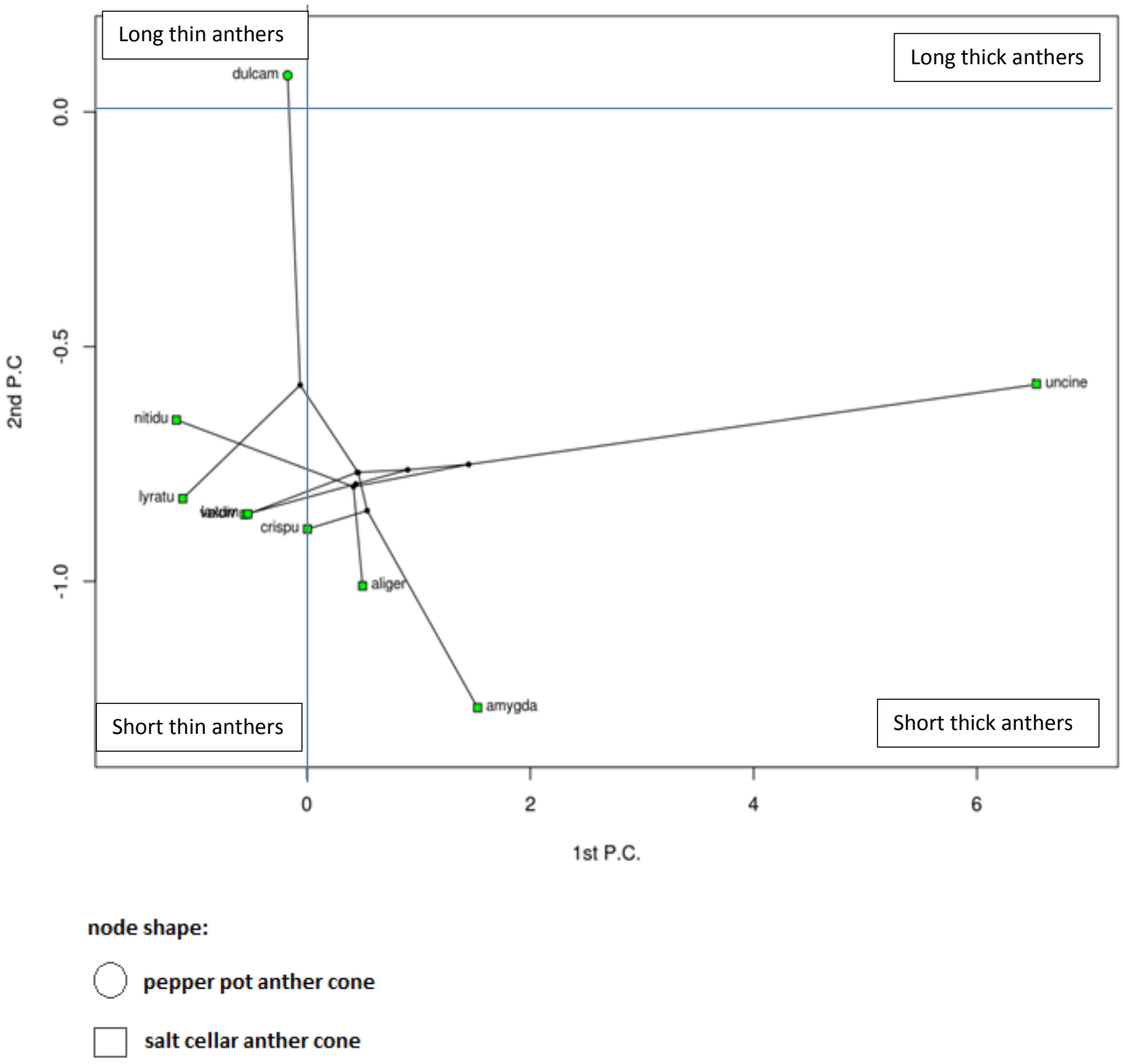

Figure 26: Phylomorphospace for Dulcamaroid clade of *Solanum* using principal components 1 and 2
Node shape indicates the anther cone type.

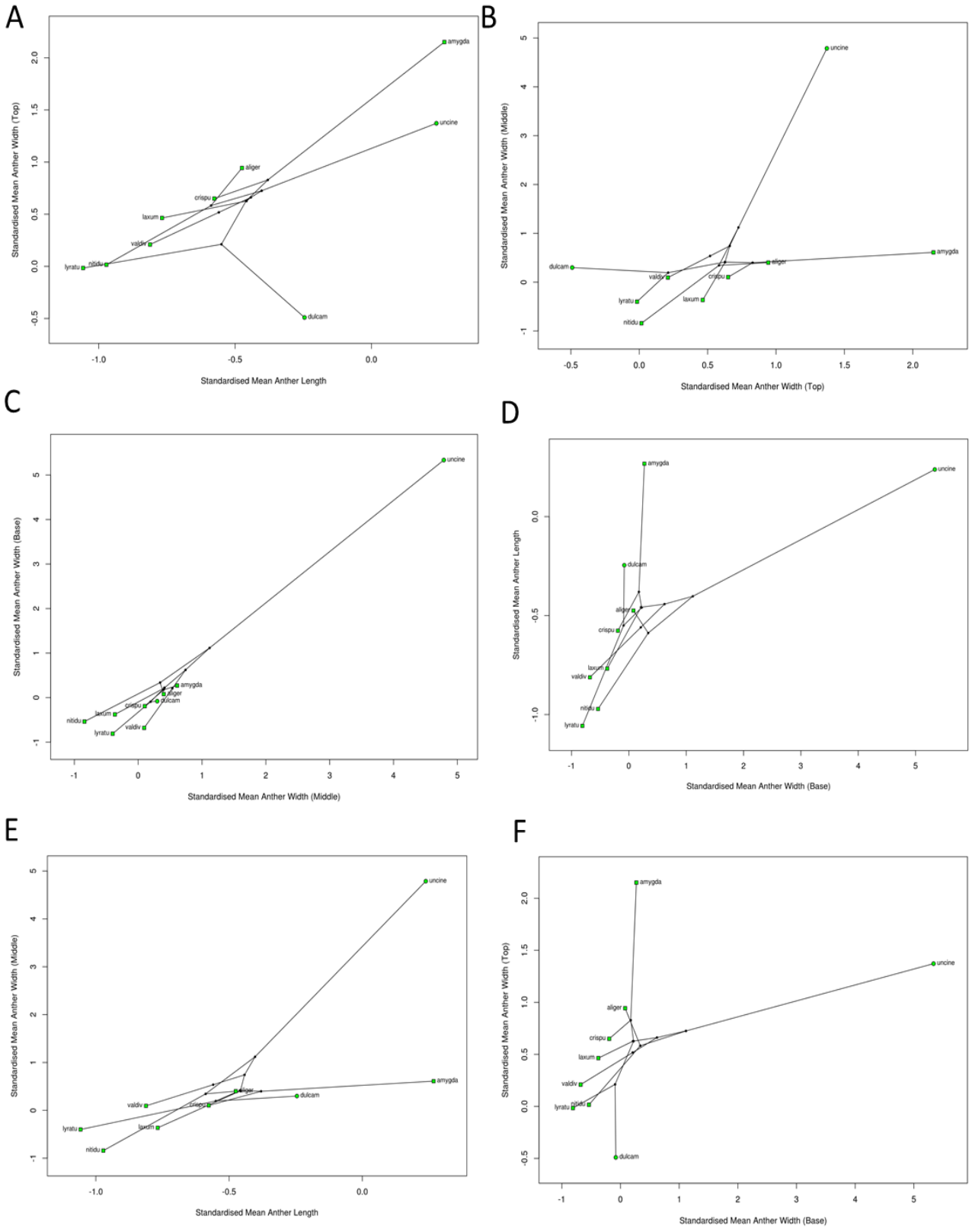

Figure 27: Phylomorphospace for Dulcamaroid clade of *Solanum* using principal components 1 and 2
A: Mean anther tip width and mean anther length plotted against one another in morphological space, with respect to the phylogeny. B: Mean anther tip width and mean anther middle width plotted against one another in morphological space, with respect to the phylogeny. C: Mean anther base width and mean anther middle width plotted against one another in morphological space, with respect to the phylogeny. D: Mean anther length and mean anther base width plotted against one another in morphological space, with respect to the phylogeny. E: Mean anther middle width and mean anther length plotted against one another in morphological space, with respect to the phylogeny. F: Mean anther tip width and mean anther base width plotted against one another in morphological space, with respect to the phylogeny.

2.3.4.4: Potato

The Potato clade occupies mainly these areas of morphological space: 'long thin anthers', 'short thin anthers' and 'short thick anthers' (Figure 28). The majority of the species in the clade sit within the 'short and thick anthers' section of the phylomorphospace.

There is a noticeable absence of species in the 'long and thick anthers' area of morphological space, which is almost entirely empty. Only *S. peruvianum* and *S. jamesii* are slightly in this morphological space, but remain very much on the edge and close to the other species of their respective subclades (Figure 28). It can be seen from Figure 29 that *S. peruvianum* has the longest anthers of the Tomato subclade (Figure 29A and E) and also the largest anther tip width (with the exception of *S. pennellii*) (Figure 29A). The anther middle width is also larger compared with the other species in its subclade (Figure 29B and E). However the anther base width of *S. peruvianum* is fairly similar to the rest of the Tomato subclade (Figure 29C). Therefore *S. peruvianum* has generally larger anthers than those species in the same subclade and these large values for especially its anther length and anther tip width are what contribute to the species position in the larger unoccupied 'long and thick anthers' area of morphological space. *Solanum jamesii* has a thinner anther middle width than the majority of species it is closely related to in the Petota subclade (Figure 29E). Otherwise the anther dimensions are fairly similar to the rest of the species in Petota subclade (Figure 29A-F). Therefore it is this thinner anther middle width which pulls the species node of *S. jamesii* away from the other species nodes in Petota and closer to the area of the phylomorphospace 'long and thin anthers' (Figure 28).

The subclades of the Potato clade occupy different areas of morphological space. Petota mainly occupies the 'short and thick anthers' area of morphological space. The Tomato subclade mainly occupies the 'long and thin anthers' area of the morphological space. The subclades Pteroidea-Herpystichum and Basarthrum mainly occupy the 'short and thin anthers' area of morphological space (Figure 28).

All pepper pot anther cone species in the Tomato subclade occupy the 'long thin anther' section of the phylomorphospace (Figure 28), except for *S. pennellii*, which instead is in the 'short and thick anther' section of morphological space with species which have salt cellar anther cones. *Solanum pennellii* occupies the same area of morphological space as most

members of the Petota subclade rather than the same area of morphological space as those species it is more closely related to: the species of the Tomato subclade.

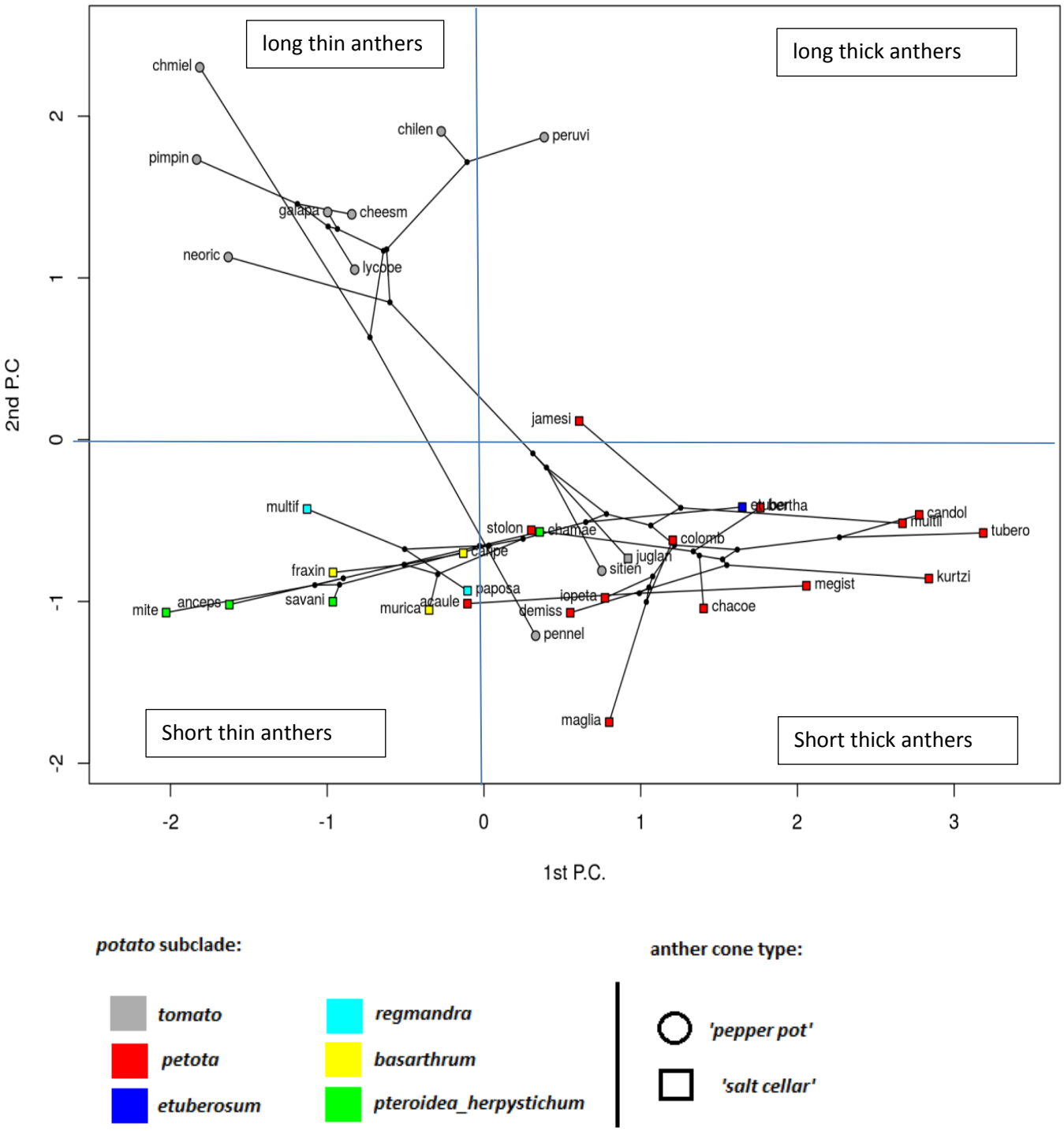

Figure 28: Phylomorphospace for Potato clade of *Solanum* using principal components 1 and 2

This Figure shows the species of the *Potato* clade of *Solanum* for which we have dimension measurements data, plotted in morphological space using principal component values for PC1 and PC2. The species nodes are colour coded by subclade and the node shape represents the cone shape of the anther cone.

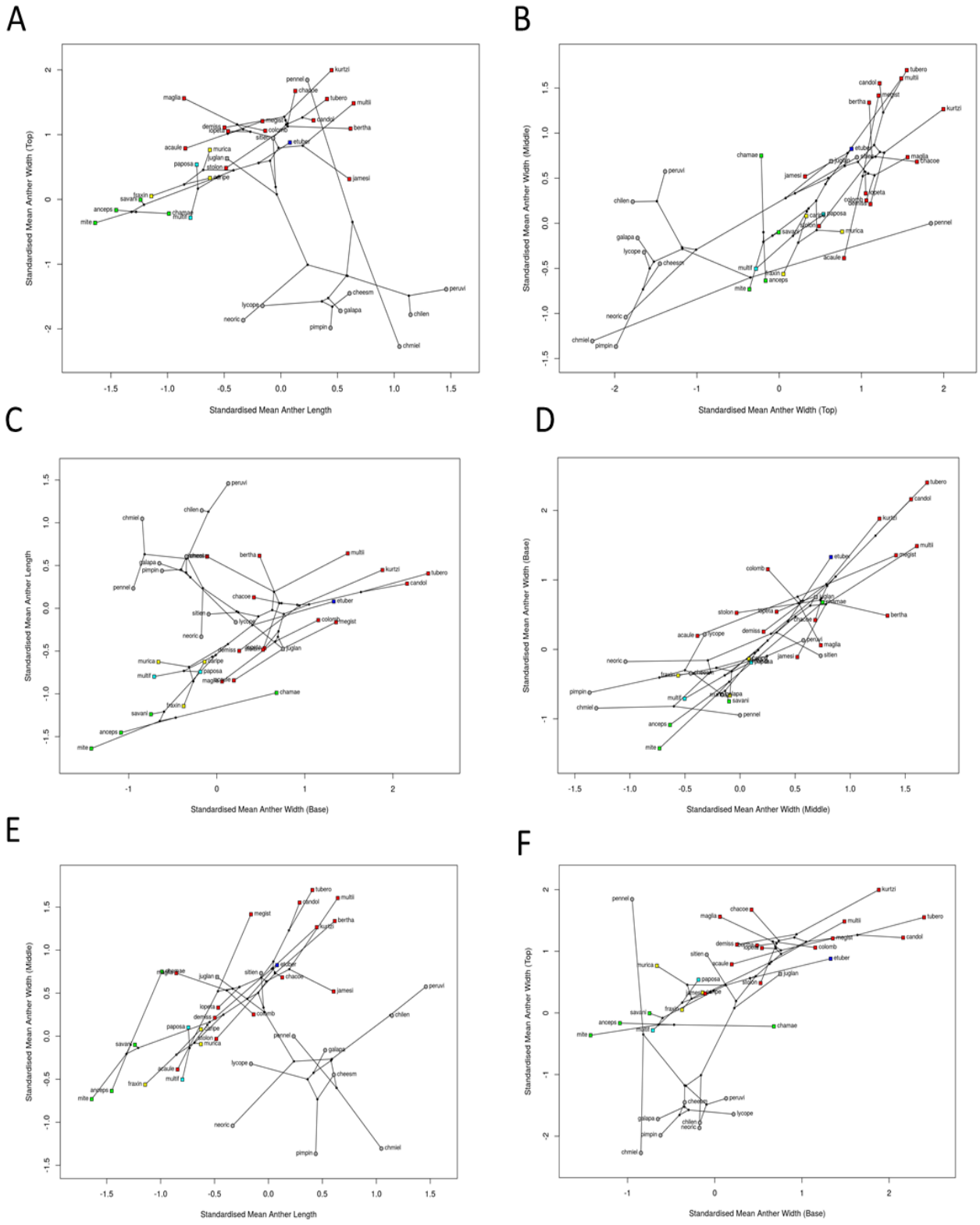

Figure 29: Phylomorphospace for potato clade of *Solanum* using standardised means of anther dimension measurements

A: Mean anther tip width and mean anther length plotted against one another in morphological space, with respect to the phylogeny. B: Mean anther tip width and mean anther middle width plotted against one another in morphological space, with respect to the phylogeny. C: Mean anther base width and mean anther middle width plotted against one another in morphological space, with respect to the phylogeny. D: Mean anther length and mean anther base width plotted against one another in morphological space, with respect to the phylogeny. E: Mean anther middle width and mean anther length plotted against one another in morphological space, with respect to the phylogeny. F: Mean anther tip width and mean anther base width plotted against one another in morphological space, with respect to the phylogeny.

2.3.4.4.1: Sub-clade Tomato

The anthers of some species of the Tomato subclade cluster very closely together in morphological space (S. *chilense, S. cheesmaniae, S. galapagense, S. chmielewski, S. peruvianum* and S. *pimpinellifolium*). All of these species occupy the area of morphological space 'long and thin anthers' (Figure 31) and have very similar anther shapes (Figure 31).

S. chmielewski has the most extreme anther shape, in the direction of 'long thin anthers' in the phylomorphospace (Figure 30). This is a result of *S. chmielewski* having very thin anthers, its anther tip width, middle width and base width are all very thin compared with the other members of the Tomato subclade (Figure 31A, B and C). However its anther length is very similar to the rest of the Tomato subclade (Figure 31A). *S. peruvianum* has thicker anthers than the rest of the Tomato subclade (Figure 31) and this is why it diverges into a slightly different area of morphological space compared with the rest of its subclade (Figure 30).

The species *S.juglandifolium* and *S.sitiens* are technically in the Tomato subclade however diverge morphologically from the rest of the subclade. These species are the members of the subclade which do not have a pepper pot anther cone. Their anthers are separate, yet connivent (the anthers are held close together but are not fused to one another in any way.) The species *S.pennellii* has a pepper pot anther cone, however its individual anther shape is more similar to that of *S.juglandifolium* and *S.sitiens* than to the other species of Tomato with which it shares the pepper pot anther cone trait (Figure 31). The area of morphological space occupied by these three species is 'short and thick anthers' compared with the majority of the Tomato subclade.

Figure 30: Phylomorphospace of Tomato subclade of Potato clade of *Solanum* using principal components 1 and 2

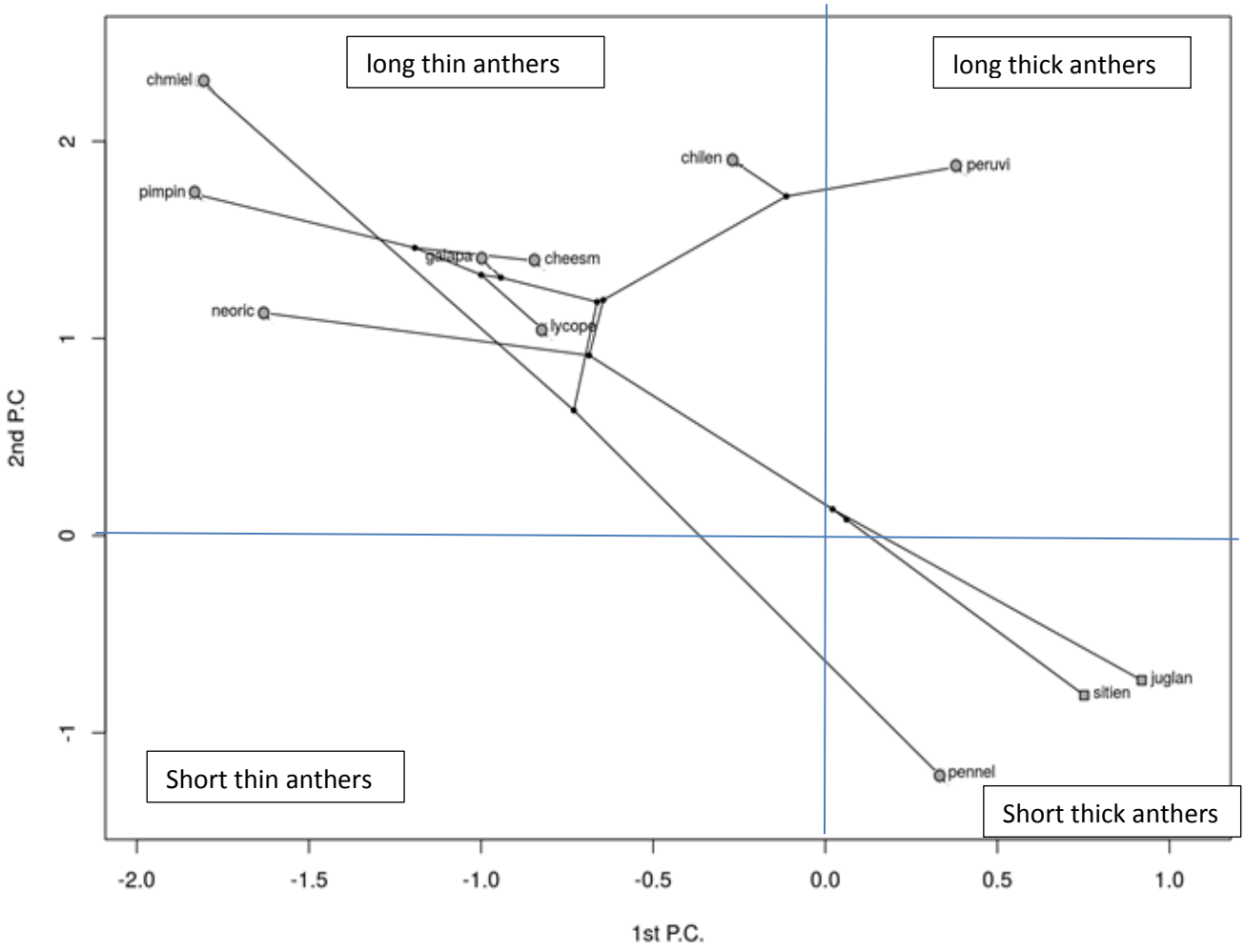

Figure 30: Phylomorphospace of Tomato subclade of potato clade of *Solanum* using principal components 1 and 2

Anther shape is marked on the main areas of morphological space. It should be noted that the scale is shifted towards the 'thinner' end of the overall morphospace, as anthers in the *tomato* subclade tend to be thinner than the rest of the genus *Solanum*.

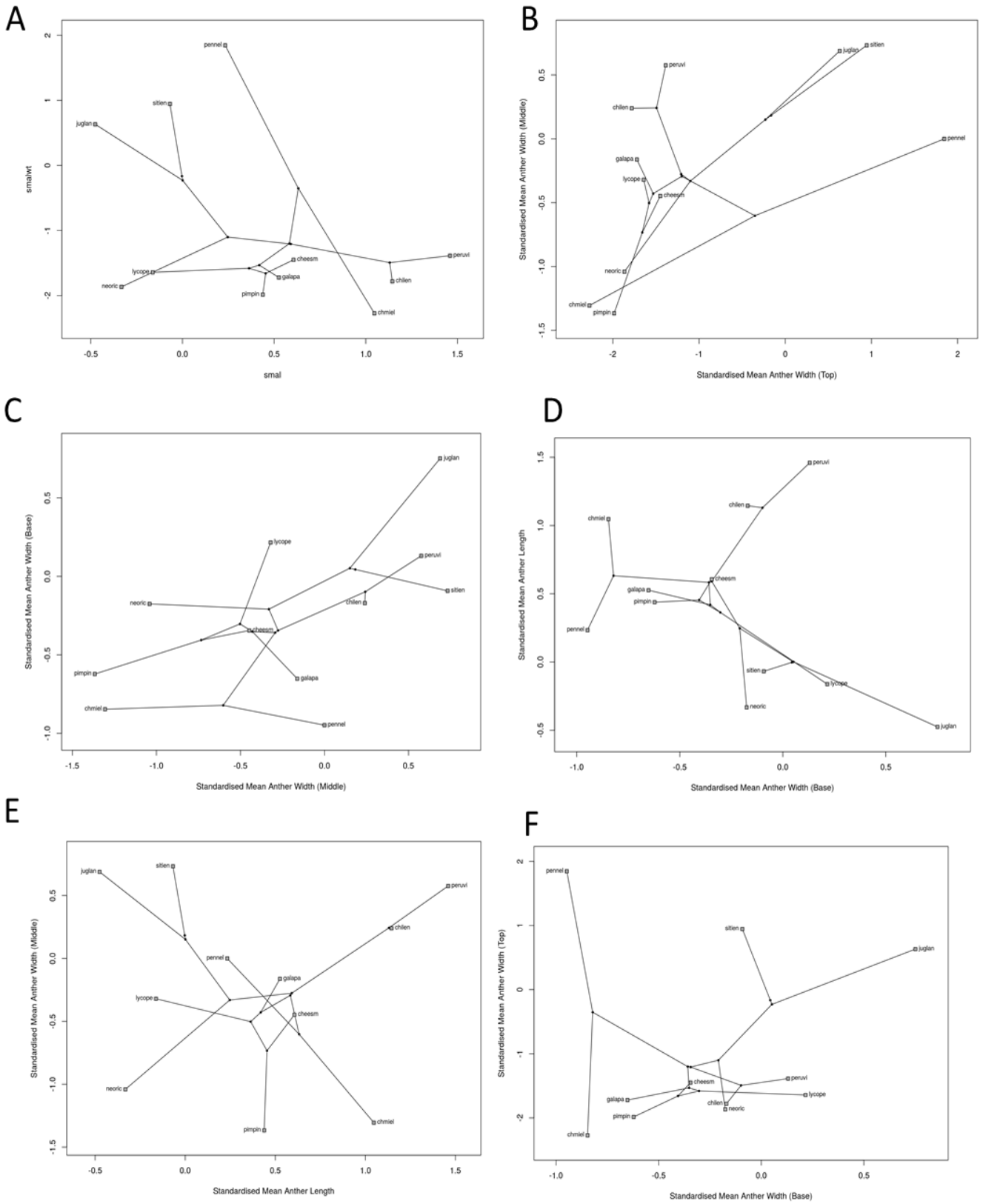

Figure 31: Phylomorphospace of Tomato subclade of Potato clade of *Solanum* using standardised means of anther dimension measurements

A: Mean anther tip width and mean anther length plotted against one another in morphological space, with respect to the phylogeny. B: Mean anther tip width and mean anther middle width plotted against one another in morphological space, with respect to the phylogeny. C: Mean anther base width and mean anther middle width plotted against one another in morphological space, with respect to the phylogeny. D: Mean anther length and mean anther base width plotted against one another in morphological space, with respect to the phylogeny. E: Mean anther middle width and mean anther length plotted against one another in morphological space, with respect to the phylogeny. F: Mean anther tip width and mean anther base width plotted against one another in morphological space, with respect to the phylogeny.

2.4.5: Epidermal outgrowths on anther surfaces of *Solanum*

There is variation in the epidermal cell outgrowths that are found on the surface of *Solanum* anthers. This study identifies a number of epidermal cell outgrowths which are present on the anthers of some species of *Solanum.* Some points of interest have been identified which could be subject to further study.

2.4.5.1: There is great variety in the epidermal cell outgrowths on the surface of *Solanum* anthers

There is variation in the proportion of the anther surface covered in papillae-type outgrowths. Some anthers were covered entirely in papillae, or entirely on the abaxial side of the anther, other species had anthers which had only some of their surface with epidermal cell outgrowths. Most commonly, species which had cell outgrowths on their anthers possessed them on only their abaxial side and only towards the base. Figure 32 illustrates the most commonly found arrangement of epidermal cell outgrowths found in this study.

Figure 32 A

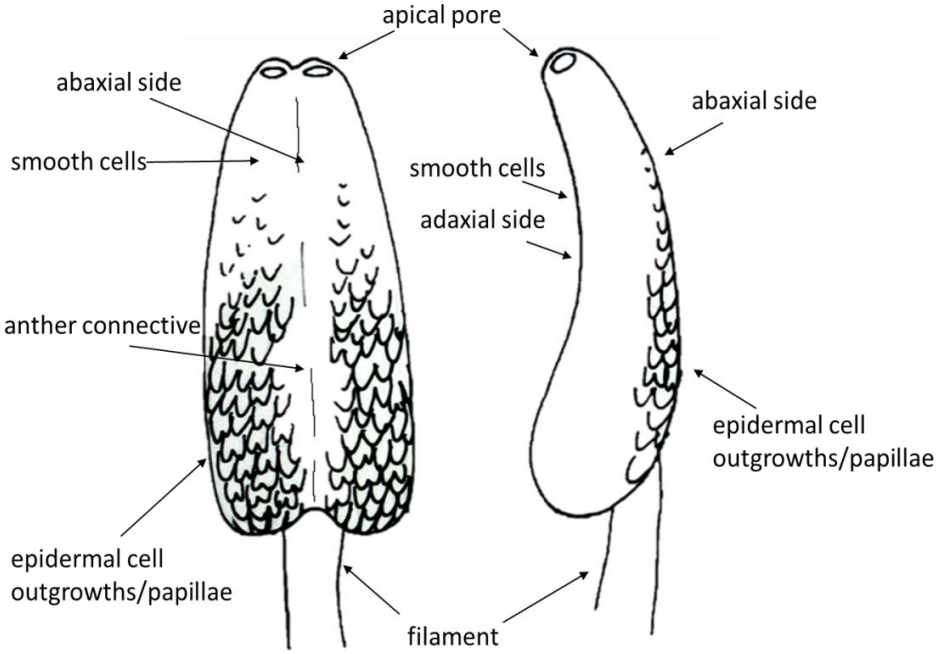

Figure 32: The most common arrangement of epidermal cell outgrowth coverage on the surface of an anther

This cartoon , figure 32 A is of a generic *Solanum* anther indicates where epidermal outgrowths are most commonly found on the anther surface. The outgrowths tend to be most numerous and most exaggerated at the base end of the anther and gradually fade from the base of the anther to the tip. At the tip of the anther the surface is generally smooth. This is the most common pattern of outgrowth coverage of the anther, however many different coverages were observed. This is also displayed in the SEM images of *S.aethiopicum* shown in figure 32 B. It can be seen in SEM I that the adaxial side of the anther has only smooth cells on the epidermal surface. SEM II shows the abaxial side of the anther, towards the base where the filament can be seen to attach: it can be seen here that there are epidermal cell outgrowths: papillae on the anther surface. SEM III shows these papillae extend up to the middle of the anther abaxial side but become less pronounced the nearer to the anther tip. SEM IIII shows the abaxial side of the anther tip, with the apical pores visible, it can be seen that the epidermal cell surface becomes smooth towards the anther tip and no more papillae can be seen. These SEM images were taken of herbarium specimens, so the papillae that are visible are collapsed.

Figure 32 B

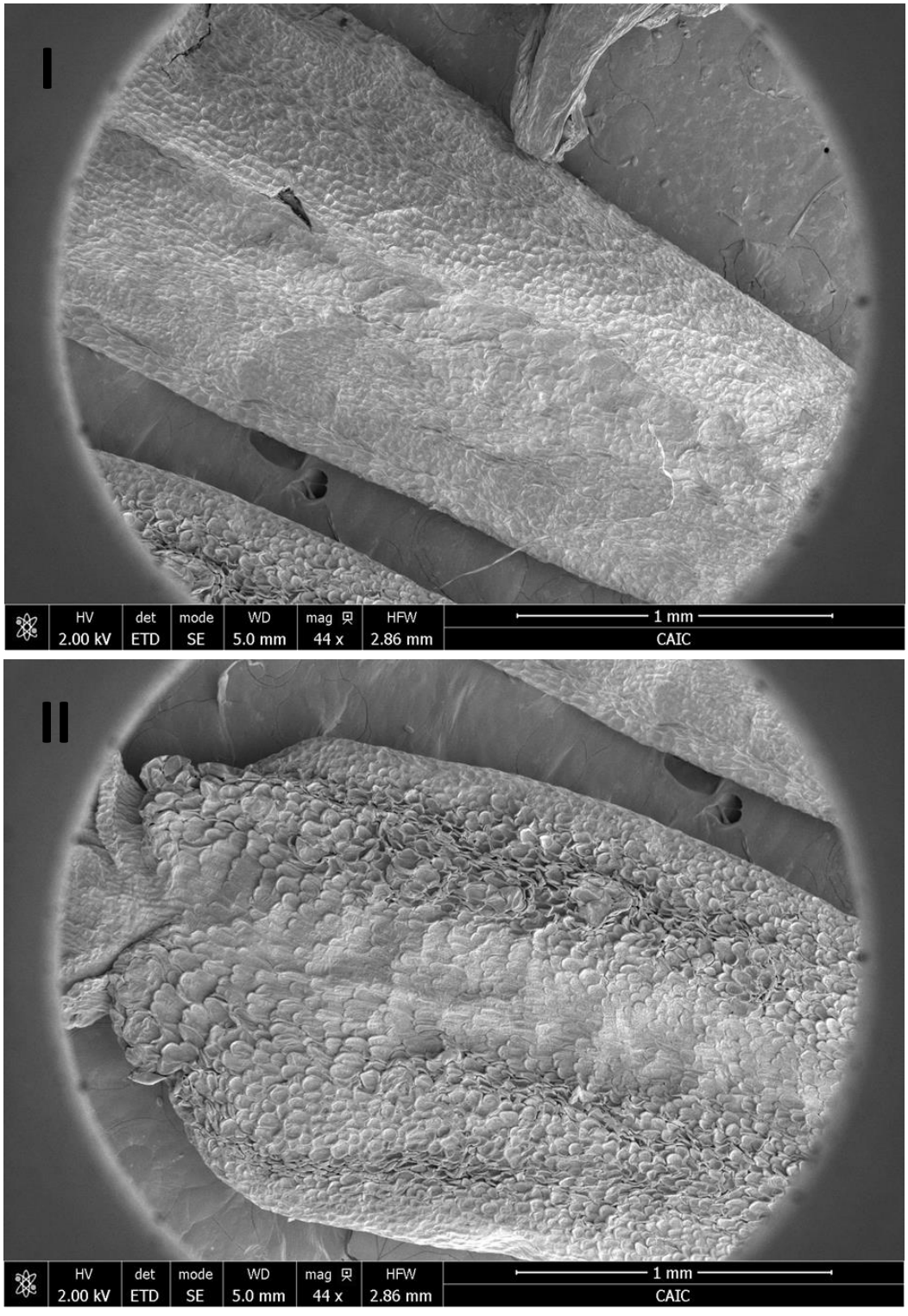
I
HV
2.00 kV
det
ETD
mode
SE
WD
5.0 mm
mag
44 x
HFW
2.86 mm
1 mm
CAIC
II
HV
2.00 kV
det
ETD
mode
SE
WD
5.0 mm
mag
44 x
HFW
2.86 mm
1 mm
CAIC

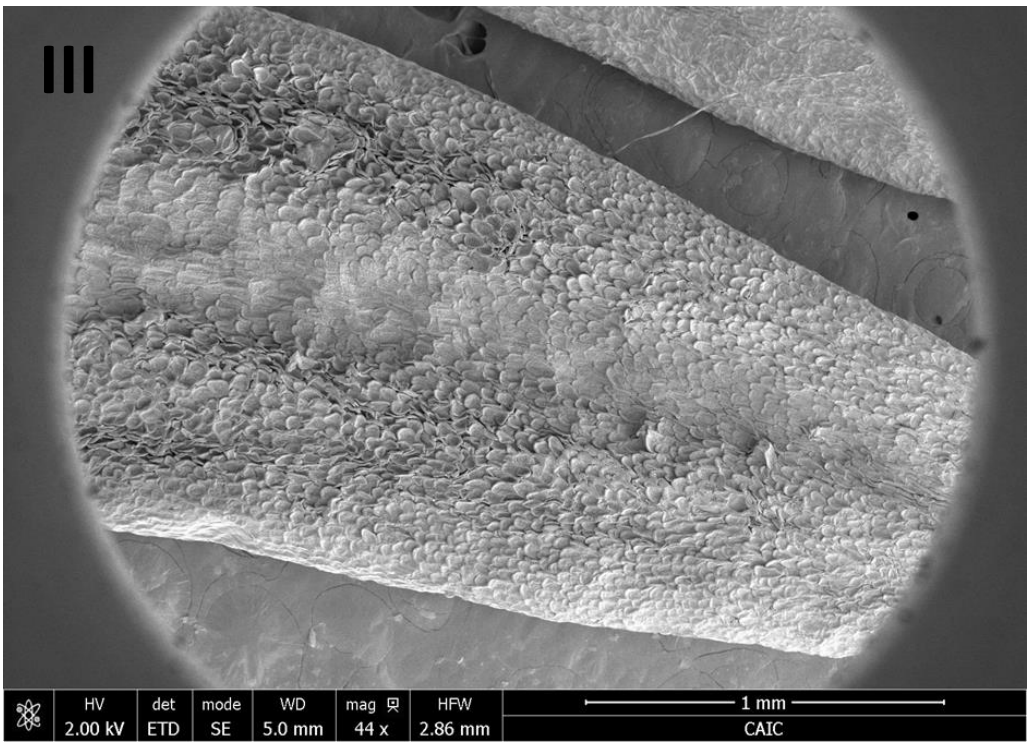
III
HV
2.00 kV
det
ETD
mode
SE
WD
5.0 mm
mag
44 x
HFW
2.86 mm
1 mm
CAIC

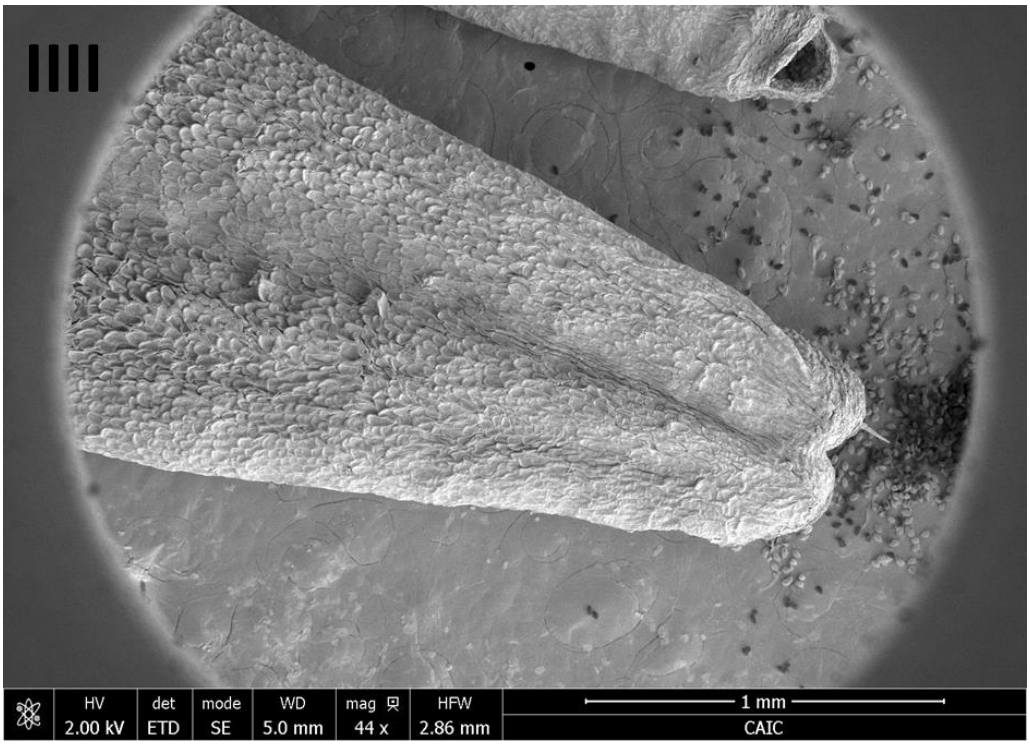
IIII
HV
2.00 kV
det
ETD
mode
SE
WD
5.0 mm
mag
44 x
HFW
2.86 mm
1 mm
CAIC

There appeared to be no correlation between anther size and the presence or type of epidermal cell outgrowth; anthers of various dimensions were examined under SEM and no pattern emerged as to which would have epidermal cell outgrowths and which would have flat anther surfaces (Appendix 8 contains an additional figure which displays this lack of correlation). Therefore we cannot predict what epidermal cell outgrowths a species will have based on anther size. There is variation in the 'extremeness' of outgrowth of the same kind between different species and between subclades. There was a great amount of variation observed in the epidermal cell outgrowths themselves. Outgrowths had different shapes and sizes, however were often oriented so that their 'point' faced towards the base of the anther, as demonstrated in Figure 32. Figure 33 Illustrates some of the diversity of outgrowths found on the anther surfaces of species of *Solanum* in this study. Appendix 5 gives details of what epidermal cell outgrowths were found on each specimen examined.

There was variation throughout *Solanum* in whether epidermal cell outgrowths of any kind were present and, if so, what kind of epidermal cell outgrowth was present. However it was more common for species to have some kind of epidermal cell outgrowth on the anther surface than to have an entirely flat/smooth anther surface. Of the species examined, 77 were scored as 'flat', 106 were scored as 'non-flat'. Where outgrowths were present it was more common for them to be non-trichome cell outgrowths/papillae than to be trichomes. It was least common for species to have only trichomes on their anther surface and no other kind of epidermal cell outgrowth/papillae. Eighty three species examined displayed cell outgrowths of some kind on their anther surface but no trichomes. Ten species examined had trichomes of some kind on their anther surface but no other kind of epidermal cell outgrowth. Twelve species had both trichomes on their anther surface and some other kind of cell outgrowth. The distribution of both the presence of cell outgrowths in general and the type of cell outgrowths present were explored by mapping the data to the phylogenetic tree of Särkinen et al (2013). This can be seen in Figure 34 which show the phylogeny with traits mapped to it, spread over multiple pages.

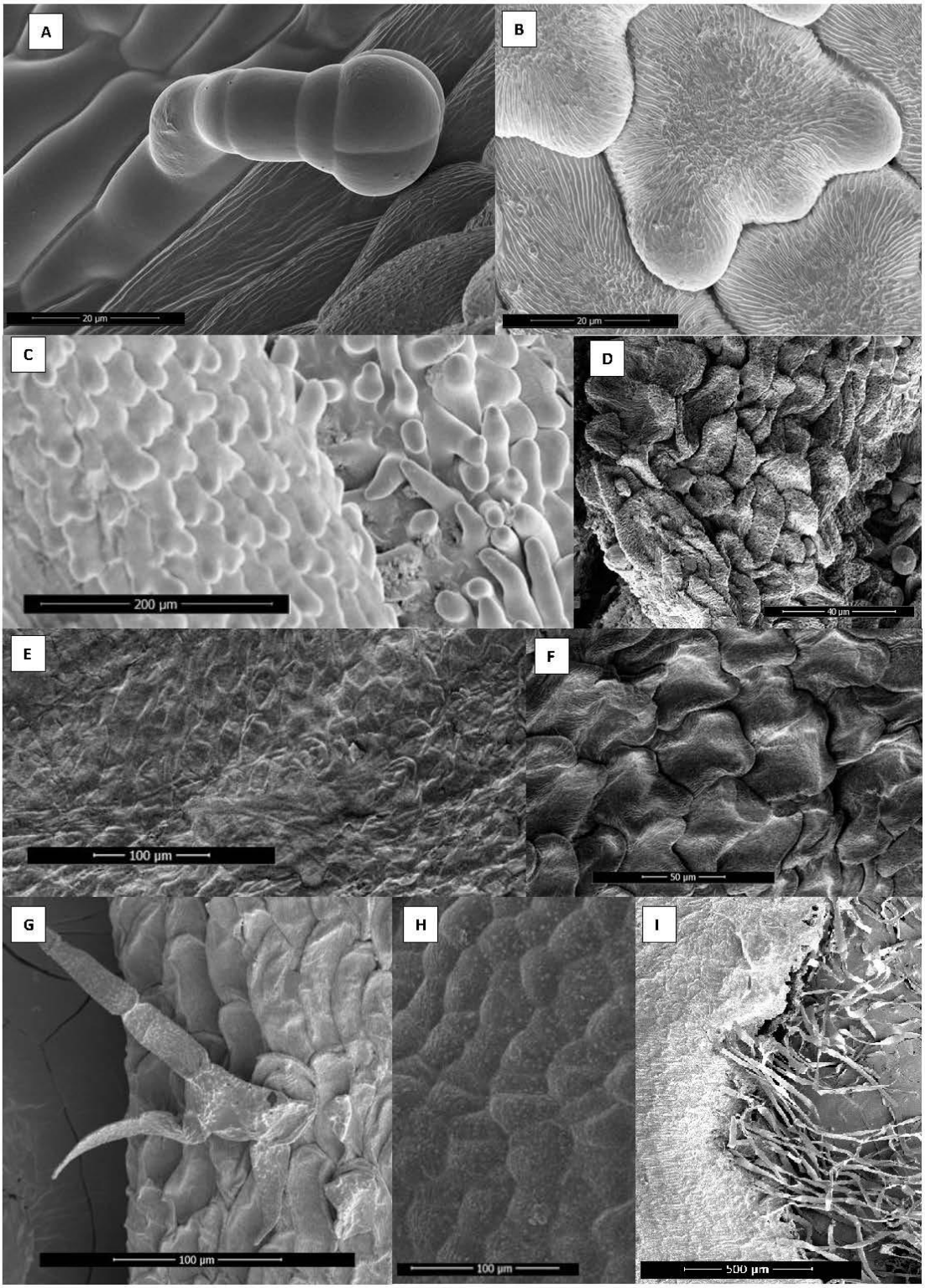

Figure 33: Epidermal cell outgrowth shapes found on the anthers of the genus *Solanum*

A great variety of epidermal cell outgrowths were found on the anthers of the genus *Solanum.* This Figure shows some of the variation seen. This Figure also showcases how cell shapes appear in herbarium specimens relative to casts from living specimens and how this affects the appearance of the same cell shape. A: A glandular trichome on the anther surface of *S. allophylum*. B: 'Glove-like' cell outgrowths on the anther surface of *S. pimpinellifolium*. C: Trichome outgrowths, forming a trichome mesh holding together the pepper pot anther cone of *S. pimpinellifolium*, as well as 'glove-like' cell outgrowths along the anther surface. D: Cell outgrowths of *S. morellifolium*, the cells are collapsed due to desiccation of the herbarium sample that was examined. E: Flat cells on the anther surface of a herbarium specimen of *S. oblongifolium*. F: Collapsed, desiccated 'glove-like' cell outgrowths on the anther surface of a herbarium specimen of *S.adscendens*. G: A branched trichome on the anther surface of *S. adscendens*. H: Flat cells on the anther surface of a cast of *S. melongena*. I: Long hairs on the base of the pollinating anther of *S. angustifolium*.

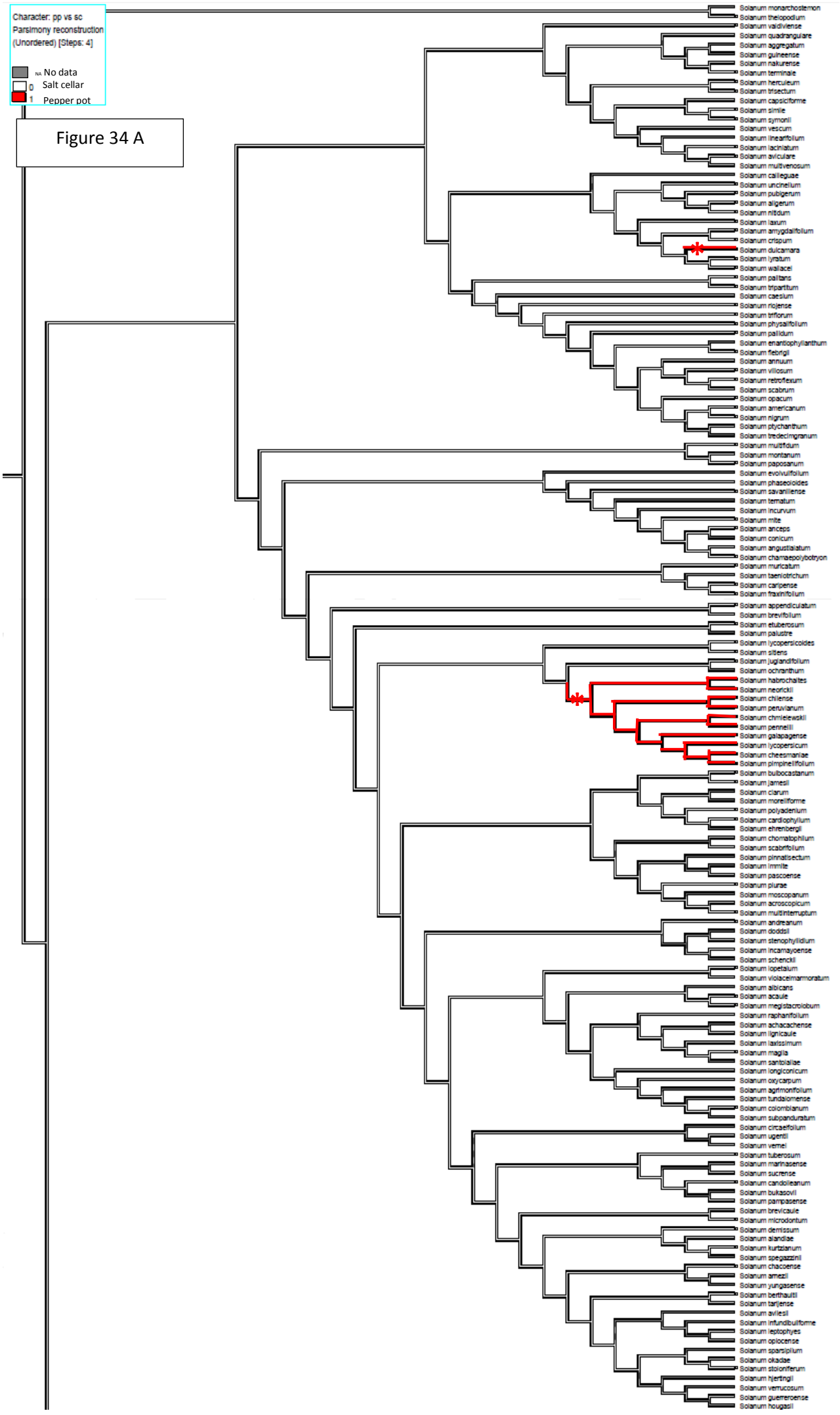
Character: pp vs sc
Parsimony reconstruction
(Unordered) [Steps: 4]
NA No data
0 Salt cellar
1 Pepper pot
Solanum monarchostemon
Solanum thelopodium
Solanum valdiviense
Solanum quadrangulare
Solanum aggregatum
Solanum guineense
Solanum nakurense
Solanum terminale
Solanum herculeum
Solanum trisectum
Solanum capsiciforme
Solanum simile
Solanum symonii
Solanum vescum
Solanum lineariifolium
Solanum laciniatum
Solanum aviculare
Solanum multivenosum
Solanum callieguae
Solanum uncinellum
Solanum pubigerum
Solanum aligerum
Solanum nitidum
Solanum laxum
Solanum amygdalifolium
Solanum crispum
Solanum dulcamara
Solanum lyratum
Solanum wallacei
Solanum palitans
Solanum tripartitum
Solanum caesium
Solanum riojense
Solanum triflorum
Solanum physalifolium
Solanum pallidum
Solanum enantiophyllanthum
Solanum febrigil
Solanum annuum
Solanum villosum
Solanum retroflexum
Solanum scabrum
Solanum opacum
Solanum americanum
Solanum nigrum
Solanum ptychanthum
Solanum tredecimgranum
Solanum multifidum
Solanum montanum
Solanum paposanum
Solanum evolvulifolium
Solanum phaseoloides
Solanum savanillense
Solanum ternatum
Solanum incurvum
Solanum mite
Solanum anceps
Solanum conicum
Solanum angustialatum
Solanum chamaepolybotryon
Solanum muricatum
Solanum taeniotrichum
Solanum caripense
Solanum fraxinifolium
Solanum appendiculiatum
Solanum brevifolium
Solanum etuberosum
Solanum palustre
Solanum lycopersicoides
Solanum sitiens
Solanum juglandifolium
Solanum ochranthum
Solanum habrochaites
Solanum neorickii
Solanum chilense
Solanum peruvianum
Solanum chmielewskii
Solanum pennellii
Solanum galapagense
Solanum lycopersicum
Solanum cheesmaniae
Solanum pimpinellifolium
Solanum bulbocastanum
Solanum jamesii
Solanum clarum
Solanum morelliforme
Solanum polyadenium
Solanum cardiophyllum
Solanum ehrenbergii
Solanum chomatophilum
Solanum scabrifolium
Solanum pinnatisectum
Solanum immite
Solanum pascoense
Solanum plurae
Solanum moscopanum
Solanum acroscopicum
Solanum multiinterruptum
Solanum andreanum
Solanum doddsii
Solanum stenophyllidium
Solanum incamayoense
Solanum schenckii
Solanum lopetalum
Solanum violaceimarmoratum
Solanum albicans
Solanum acaule
Solanum megistacroloburn
Solanum raphanifolium
Solanum achacachense
Solanum lignicaule
Solanum laxissimum
Solanum magdia
Solanum santolalae
Solanum longiconicum
Solanum oxycarpum
Solanum agrimonifolium
Solanum tundalomense
Solanum colombianum
Solanum subpanduratum
Solanum circaeifolium
Solanum ugentii
Solanum vernei
Solanum tuberosum
Solanum marinasense
Solanum sucrense
Solanum candolleanum
Solanum bukasovii
Solanum pampasense
Solanum brevicaule
Solanum microdontum
Solanum demissum
Solanum alandiae
Solanum kurtzianum
Solanum spegazzinii
Solanum chacoense
Solanum ameziI
Solanum yungasense
Solanum berthaultii
Solanum tarijense
Solanum aviles
Solanum infundibuliforme
Solanum leptophyes
Solanum oplocense
Solanum sparsipilum
Solanum okadae
Solanum stoloniferum
Solanum hjertingii
Solanum verrucosum
Solanum guerreroense
Solanum hougasii

Figure 34 A

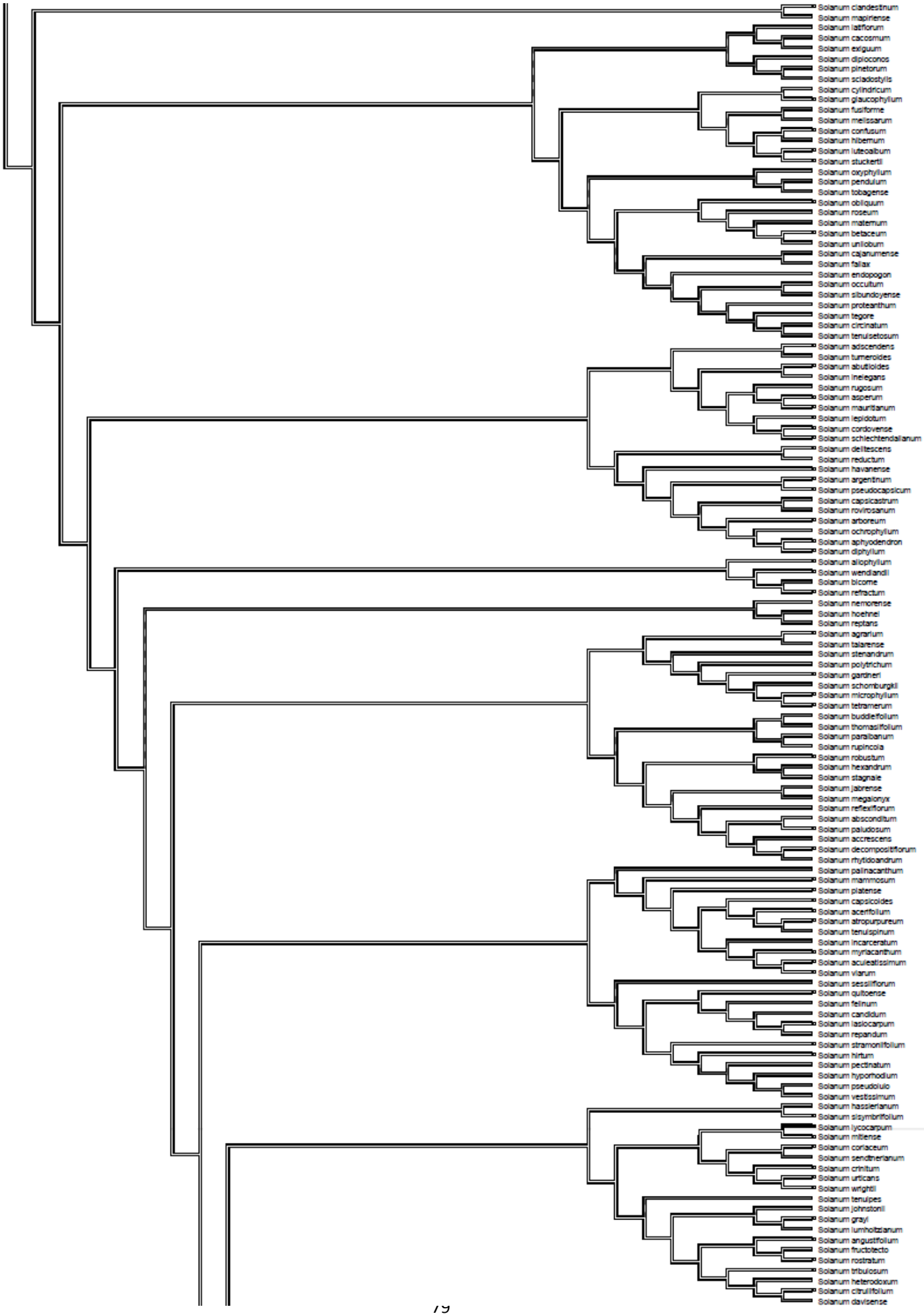
Solanum clandestinum
Solanum mapirense
Solanum latiflorum
Solanum cacosmum
Solanum exiguum
Solanum diploconos
Solanum pinetorum
Solanum sciadostylis
Solanum cylindricum
Solanum glaucophyllum
Solanum fusiforme
Solanum melissarum
Solanum confusum
Solanum hibernum
Solanum luteoalbum
Solanum stuckertii
Solanum oxyphyllum
Solanum pendulum
Solanum tobagense
Solanum obliquum
Solanum roseum
Solanum maternum
Solanum betaceum
Solanum uniflorum
Solanum cajanumense
Solanum fallax
Solanum endopogon
Solanum occultum
Solanum sibundoyense
Solanum proteanthum
Solanum tegore
Solanum circinatum
Solanum tenuisetosum
Solanum adscendens
Solanum turneroides
Solanum abutiloides
Solanum inelegans
Solanum rugosum
Solanum asperum
Solanum mauritianum
Solanum lepidotum
Solanum cordovense
Solanum schlechtendalianum
Solanum deltiscens
Solanum reductum
Solanum havanense
Solanum argentinum
Solanum pseudocapsicum
Solanum capsicastrum
Solanum rovirosanum
Solanum arboreum
Solanum ochrophyllum
Solanum aphyodendron
Solanum diphyllum
Solanum aliophyllum
Solanum wendlandii
Solanum bicome
Solanum refractum
Solanum nemorense
Solanum hoehnei
Solanum reptans
Solanum agrarium
Solanum talarense
Solanum stenandrum
Solanum polytrichum
Solanum gardneri
Solanum schomburgkii
Solanum microphyllum
Solanum tetramerum
Solanum buddleifolium
Solanum thomasiifolium
Solanum paraibanum
Solanum rupincola
Solanum robustum
Solanum hexandrum
Solanum stagnale
Solanum jabrense
Solanum megalonyx
Solanum reflexiflorum
Solanum absconditum
Solanum paludosum
Solanum accrescens
Solanum decompositiflorum
Solanum rhytidoandrum
Solanum palinacanthum
Solanum mammosum
Solanum platense
Solanum capsicoides
Solanum acerifolium
Solanum atropurpureum
Solanum tenuispinum
Solanum incarceratum
Solanum myriacanthum
Solanum aculeatissimum
Solanum viarum
Solanum sessiliflorum
Solanum quitoense
Solanum felinum
Solanum candidum
Solanum lasiocarpum
Solanum repandum
Solanum stramoniifolium
Solanum hirtum
Solanum pectinatum
Solanum hyporhodium
Solanum pseudoiuio
Solanum vestissimum
Solanum hasslerianum
Solanum sisymbriifolium
Solanum lycocarpum
Solanum mitlense
Solanum coriaceum
Solanum sendtnerianum
Solanum crinitum
Solanum urticans
Solanum wrightii
Solanum tenuipes
Solanum johnstonii
Solanum grayi
Solanum lumholtzianum
Solanum angustifolium
Solanum fructotecto
Solanum rostratum
Solanum tribulosum
Solanum heterodoxum
Solanum citrullifolium
Solanum davisense

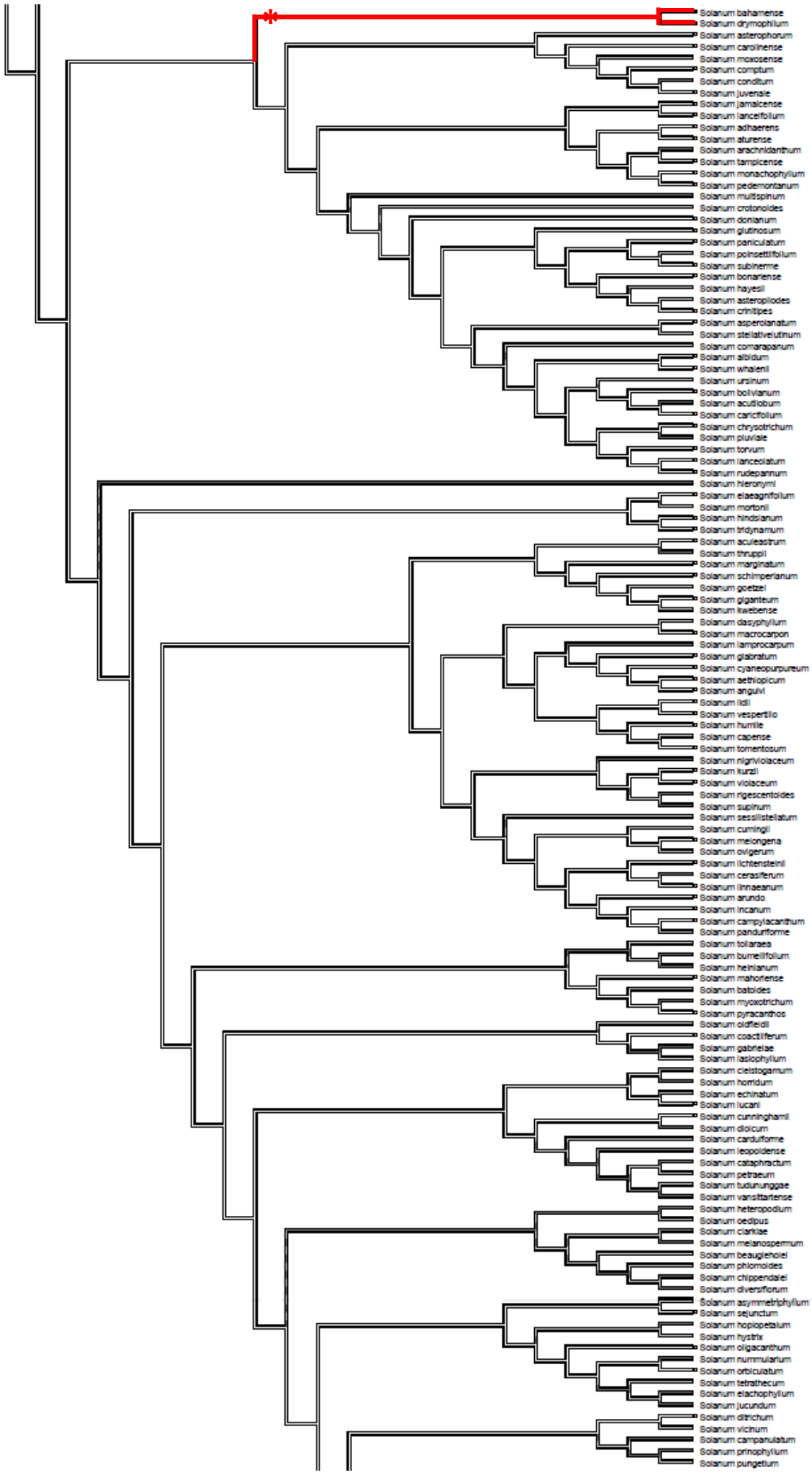
Solanum bahamense
Solanum drymophilum
Solanum asterophorum
Solanum carolinense
Solanum mixosense
Solanum comptum
Solanum condtum
Solanum juvenale
Solanum jamaicense
Solanum lanceifolium
Solanum adhaerens
Solanum aturense
Solanum arachnidanthum
Solanum tampicense
Solanum monachophyllum
Solanum pedemontanum
Solanum multispinum
Solanum crotonoides
Solanum donianum
Solanum glutinosum
Solanum paniculatum
Solanum poinsettiifolium
Solanum subinerme
Solanum bonariense
Solanum hayesii
Solanum asteropiloides
Solanum crinitipes
Solanum asperolanatum
Solanum stellativelutinum
Solanum comarapanum
Solanum albidum
Solanum whalenii
Solanum ursinum
Solanum bolivianum
Solanum acutilobum
Solanum caricifolium
Solanum chrysotrichum
Solanum pluviale
Solanum torvum
Solanum lanceolatum
Solanum rudepannum
Solanum hieronymi
Solanum elaeagnifolium
Solanum mortonii
Solanum hindsianum
Solanum tridynamum
Solanum aculeastrum
Solanum thruppii
Solanum marginatum
Solanum schimperianum
Solanum goetzei
Solanum giganteum
Solanum kwebense
Solanum dasyphyllum
Solanum macrocarpon
Solanum lamprocarpum
Solanum glabratum
Solanum cyaneopurpureum
Solanum aethiopicum
Solanum anguivi
Solanum lidii
Solanum vespertilio
Solanum humile
Solanum capense
Solanum tomentosum
Solanum nigrviolaceum
Solanum kurzii
Solanum violaceum
Solanum rigescentoides
Solanum supinum
Solanum sessilistellatum
Solanum cumingii
Solanum melongena
Solanum ovigerum
Solanum lichtensteinii
Solanum cerasiferum
Solanum linnaeanum
Solanum arundo
Solanum incanum
Solanum campylacanthum
Solanum pandurifome
Solanum tollaraea
Solanum burnellifolium
Solanum helmianum
Solanum mahoriense
Solanum batoides
Solanum myoxotrichum
Solanum pyracanthos
Solanum oldfieldii
Solanum coactiliferum
Solanum gabrielae
Solanum lasiophyllum
Solanum cleistogamum
Solanum horridum
Solanum echinatum
Solanum lucani
Solanum cunninghamii
Solanum diolicum
Solanum carduiforme
Solanum leopoldense
Solanum cataphractum
Solanum petraeum
Solanum tuduriunggae
Solanum vansittartense
Solanum heteropodium
Solanum oedipus
Solanum clarkiae
Solanum melanospermum
Solanum beaugleholei
Solanum phlomoides
Solanum chippendalei
Solanum diversiflorum
Solanum asymmetriphyllum
Solanum sejunctum
Solanum hoplopetalum
Solanum hystrix
Solanum oligacanthum
Solanum nummularium
Solanum orbiculatum
Solanum tetrathecum
Solanum elachophyllum
Solanum jucundum
Solanum dimorphum
Solanum vicinum
Solanum campanulatum
Solanum prinophyllum
Solanum pungetium

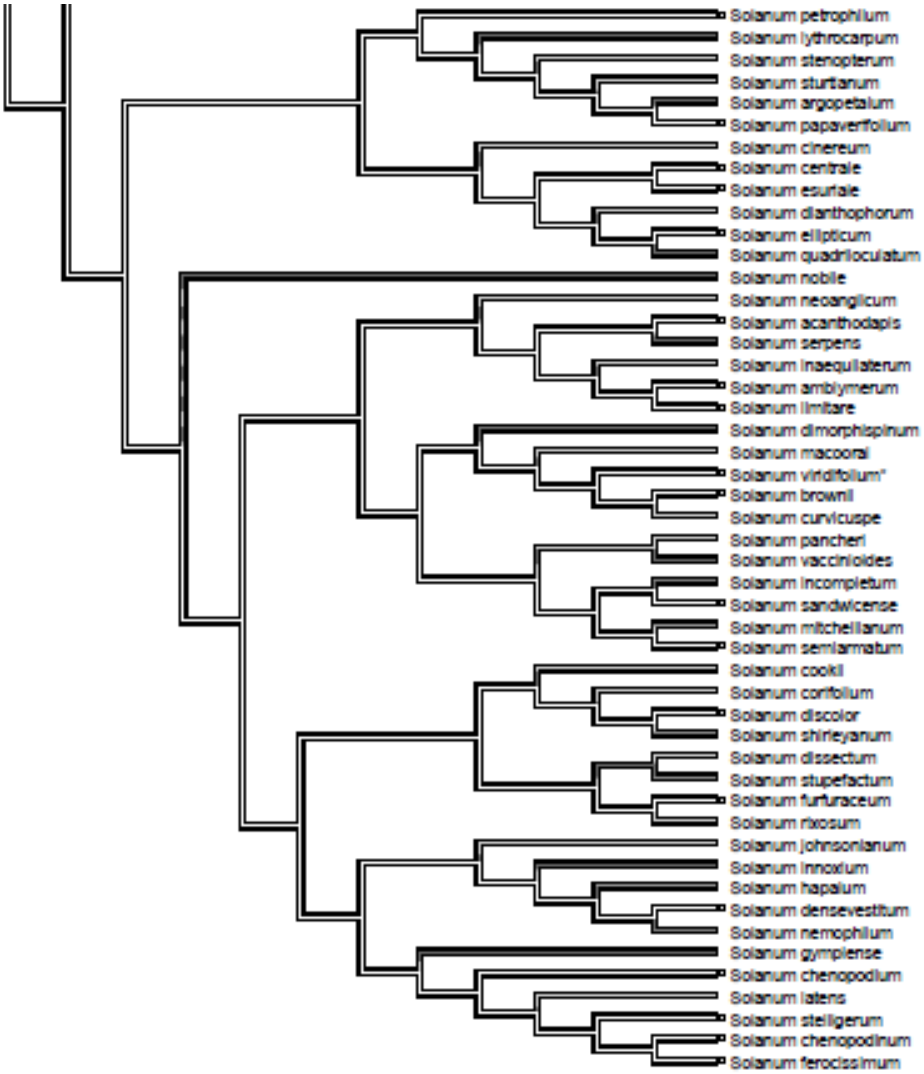

Figure 34 A: The 'anther cone type' mapped to the phylogeny of *Solanum*

The trait 'anther cone type' has been mapped to the phylogeny of *Solanum* (Särkinen et al, 2013). Black lines represent 1: pepper pot anther cone. White lines represent 0= salt cellar anther cone. Grey lines represent NA: no data for this species. The phylogeny is spread over multiple pages due to its large size and number of species.

Groups of pepper pot anther cone can be seen in the Tomato subclade, Dulcamaroid subclade and Bahamense subclade. A parsimony ancestral state reconstruction traces potential character history of the trait. According to this the ancestral state is salt cellar anther cone shape. There are three transitions from SC anther cone to PP cone that have occurred, shown in this phylogeny. These transitions to PP cone are noted on the phylogeny with a red star. Species with PP cones are indicated in red.

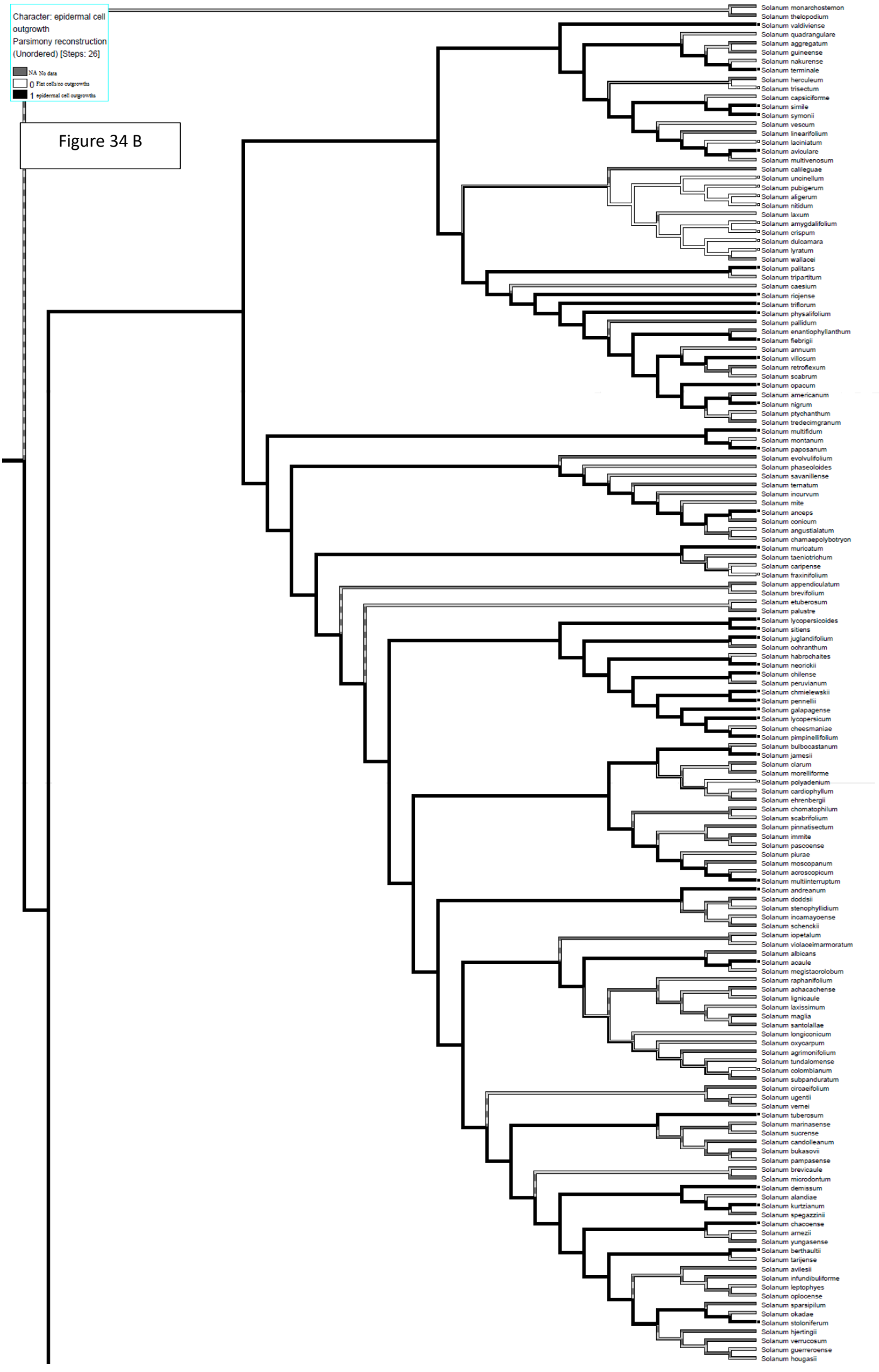
Character: epidermal cell outgrowth
Parsimony reconstruction (Unordered) [Steps: 26]
NA No data
0 Flat cells/so outgrowths
1 epidermal cell outgrowths
Figure 34 B
Solanum monarchostemon
Solanum thelopodium
Solanum valdiviense
Solanum quadrangulare
Solanum aggregatum
Solanum guineense
Solanum nakurense
Solanum terminale
Solanum herouleum
Solanum trisectum
Solanum capsiciforme
Solanum simile
Solanum symonii
Solanum vescum
Solanum linearifolium
Solanum laciniatum
Solanum aviculare
Solanum multivenosum
Solanum calileguae
Solanum uncinellum
Solanum pubigerum
Solanum aligerum
Solanum nitidum
Solanum laxum
Solanum amygdalifolium
Solanum crispum
Solanum dulcamara
Solanum lyratum
Solanum wallacei
Solanum palitans
Solanum tripartitum
Solanum caesium
Solanum riojense
Solanum triflorum
Solanum physalifolium
Solanum pallidum
Solanum enantiophyllanthum
Solanum fiebrigii
Solanum annuum
Solanum villosum
Solanum retroflexum
Solanum scabrum
Solanum opacum
Solanum americanum
Solanum nigrum
Solanum ptychanthum
Solanum tredecimgranum
Solanum multifidum
Solanum montanum
Solanum paposanum
Solanum evolvulifolium
Solanum phaseoloides
Solanum savanillense
Solanum ternatum
Solanum incurvum
Solanum mite
Solanum anceps
Solanum conicum
Solanum angustialatum
Solanum chamaepolybotryon
Solanum muricatum
Solanum taeniotrichum
Solanum caripense
Solanum fraxinifolium
Solanum appendiculatum
Solanum brevifolium
Solanum etuberosum
Solanum palustre
Solanum lycopersicoides
Solanum sitiens
Solanum juglandifolium
Solanum ochranthum
Solanum habrochaites
Solanum neorickii
Solanum chilense
Solanum peruvianum
Solanum chmielewskii
Solanum pennellii
Solanum galapagense
Solanum lycopersicum
Solanum cheesmaniae
Solanum pimpinellifolium
Solanum bulbocastanum
Solanum jamesii
Solanum clarum
Solanum morelliforme
Solanum polyadenium
Solanum cardiophyllum
Solanum ehrenbergii
Solanum chomatophilum
Solanum scabrifolium
Solanum pinnatisectum
Solanum immite
Solanum pascoense
Solanum piurae
Solanum moscopanum
Solanum acroscopicum
Solanum multiinterruptum
Solanum andreanum
Solanum doddsii
Solanum stenophyllidium
Solanum incamayoense
Solanum schenckii
Solanum iopetalum
Solanum violaceimarmoratum
Solanum albicans
Solanum acaule
Solanum megistacrolobum
Solanum raphanifolium
Solanum achacachense
Solanum lignicaule
Solanum laxissimum
Solanum maglia
Solanum santolallae
Solanum longiconicum
Solanum oxycarpum
Solanum agrimonifolium
Solanum tundalomense
Solanum colombianum
Solanum subpanduratum
Solanum circaeifolium
Solanum ugentii
Solanum vernei
Solanum tuberosum
Solanum marinasense
Solanum sucrense
Solanum candolleanum
Solanum bukasovii
Solanum pampasense
Solanum brevicaule
Solanum microdontum
Solanum demissum
Solanum alandiae
Solanum kurtzianum
Solanum spegazzinii
Solanum chacoense
Solanum arnezii
Solanum yungasense
Solanum berthaultii
Solanum tarijense
Solanum avilesii
Solanum infundibuliforme
Solanum leptophyes
Solanum oplocense
Solanum sparsipilum
Solanum okadae
Solanum stoloniferum
Solanum hjertingii
Solanum verrucosum
Solanum guerreroense
Solanum hougasii

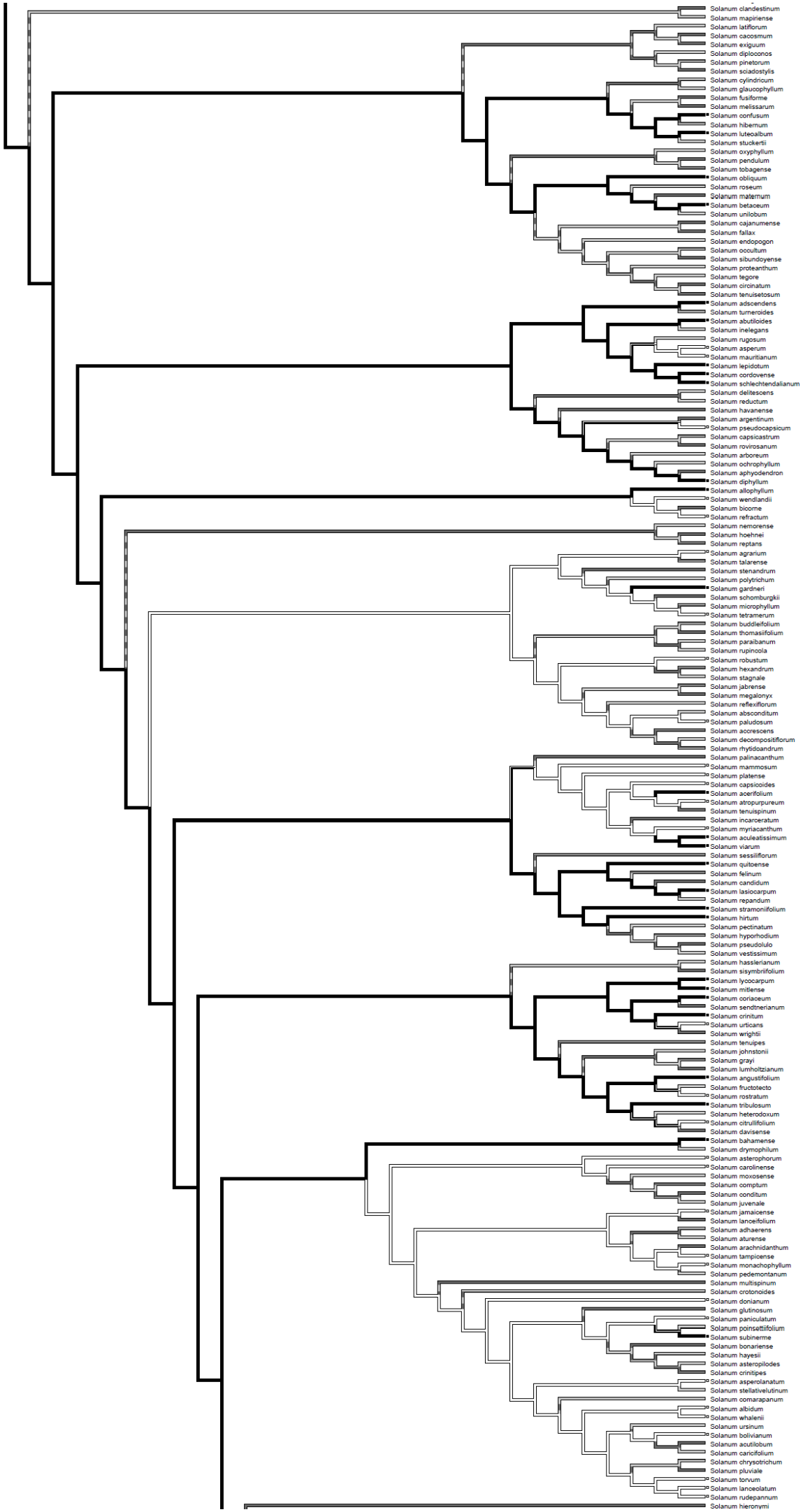
Solanum clandestinum
Solanum mapiriense
Solanum latiflorum
Solanum cacosmum
Solanum exiguum
Solanum diploconos
Solanum pinetorum
Solanum sciadostylis
Solanum cylindricum
Solanum glaucophyllum
Solanum fusiforme
Solanum melissarum
Solanum confusum
Solanum hibernum
Solanum luteoalbum
Solanum stuckertii
Solanum oxyphyllum
Solanum pendulum
Solanum tobagense
Solanum obliquum
Solanum roseum
Solanum maternum
Solanum betaceum
Solanum unilobum
Solanum cajanumense
Solanum fallax
Solanum endopogon
Solanum occultum
Solanum sibundoyense
Solanum proteanthum
Solanum tegore
Solanum circinatum
Solanum tenuisetosum
Solanum adscendens
Solanum turneroides
Solanum abutiloides
Solanum inelegans
Solanum rugosum
Solanum asperum
Solanum mauritianum
Solanum lepidotum
Solanum cordovense
Solanum schlechtendalianum
Solanum delitescens
Solanum reductum
Solanum havanense
Solanum argentinum
Solanum pseudocapsicum
Solanum capsicastrum
Solanum rovirosanum
Solanum arboreum
Solanum ochrophyllum
Solanum aphyodendron
Solanum diphyllum
Solanum allophyllum
Solanum wendlandii
Solanum bicorne
Solanum refractum
Solanum nemorense
Solanum hoehnei
Solanum reptans
Solanum agrarium
Solanum talarense
Solanum stenandrum
Solanum polytrichum
Solanum gardneri
Solanum schomburgkii
Solanum microphyllum
Solanum tetramerum
Solanum buddleifolium
Solanum thomasiifolium
Solanum paraibanum
Solanum rupincola
Solanum robustum
Solanum hexandrum
Solanum stagnale
Solanum jabrense
Solanum megalonyx
Solanum reflexiflorum
Solanum absconditum
Solanum paludosum
Solanum acrescens
Solanum decompositiflorum
Solanum rhytidoandrum
Solanum palinacanthum
Solanum mammosum
Solanum platense
Solanum capsicoides
Solanum aculeatum
Solanum atropurpureum
Solanum tenuispinum
Solanum incarceratum
Solanum myriacanthum
Solanum aculeatissimum
Solanum viarum
Solanum sessiliflorum
Solanum quitoense
Solanum felinum
Solanum candidum
Solanum lasiocarpum
Solanum repandum
Solanum stramonilifolium
Solanum hirtum
Solanum pectinatum
Solanum hyporhodium
Solanum pseudolulo
Solanum vestissimum
Solanum hasslerianum
Solanum sisymbriifolium
Solanum lycocarpum
Solanum mitlense
Solanum coriaceum
Solanum sendtnerianum
Solanum crinitum
Solanum urticans
Solanum wrightii
Solanum tenuipes
Solanum johnstonii
Solanum grayi
Solanum lumholtzianum
Solanum angustifolium
Solanum fructotecto
Solanum rostratum
Solanum tribulosum
Solanum heterodoxum
Solanum citrullifolium
Solanum davisense
Solanum bahamense
Solanum drymophilum
Solanum asterophorum
Solanum carolinense
Solanum moxosense
Solanum comptum
Solanum conditum
Solanum juvenale
Solanum jamaicense
Solanum lanceifolium
Solanum adhaerens
Solanum aturense
Solanum arachnidanthum
Solanum tampicense
Solanum monachophyllum
Solanum pedemontanum
Solanum multispinum
Solanum crotonoides
Solanum donianum
Solanum glutinosum
Solanum paniculatum
Solanum poinsettiifolium
Solanum subinerme
Solanum bonariense
Solanum hayesii
Solanum asteropilodes
Solanum crinitipes
Solanum asperolanatum
Solanum stellativelutinum
Solanum comarapanum
Solanum albidum
Solanum whalenii
Solanum ursinum
Solanum bolivianum
Solanum acutilobum
Solanum caricifolium
Solanum chrysotrichum
Solanum pluviale
Solanum torvum
Solanum lanceolatum
Solanum rudepannum
Solanum hieronymi

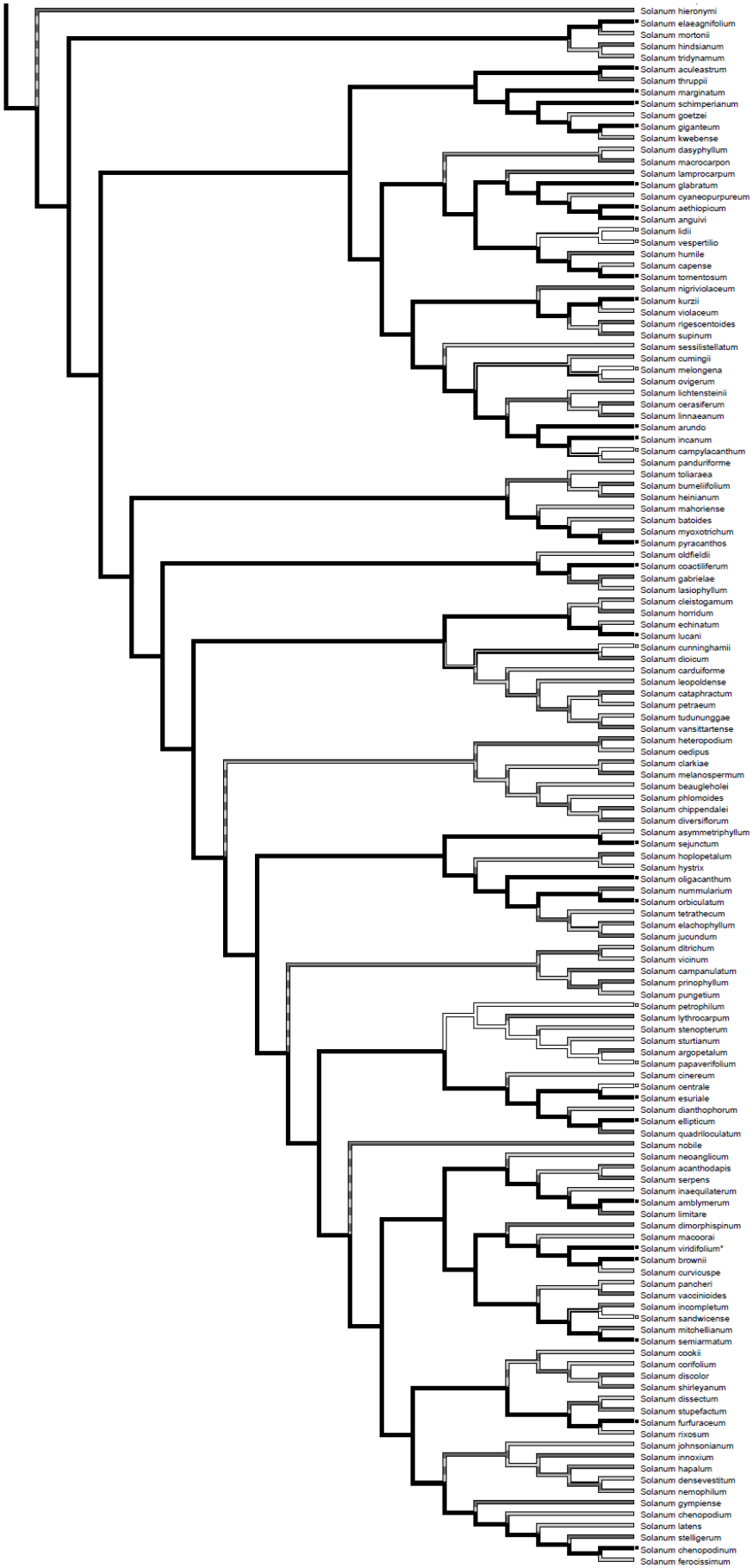

Figure 34 B: Anther trait 'epidermal cell outgrowths' mapped to the *Solanum* phylogeny.

The trait 'epidermal cell outgrowths' on the anther surface has been mapped to the phylogeny of *Solanum* (Särkinen et al, 2013). Black lines represent 1: epidermal cell outgrowths/papillae. White lines, 0: flat epidermal cell surface. Grey lines represent NA: no data for this species (the species was not examined under SEM). The phylogeny is spread over multiple pages due to its size/species number. Parsimony ancestral state reconstruction was conducted to trace the potential character history of the trait. According to this the ancestral state is for epidermal cell outgrowths/papillae of some kind to be present and then repeatedly lost.

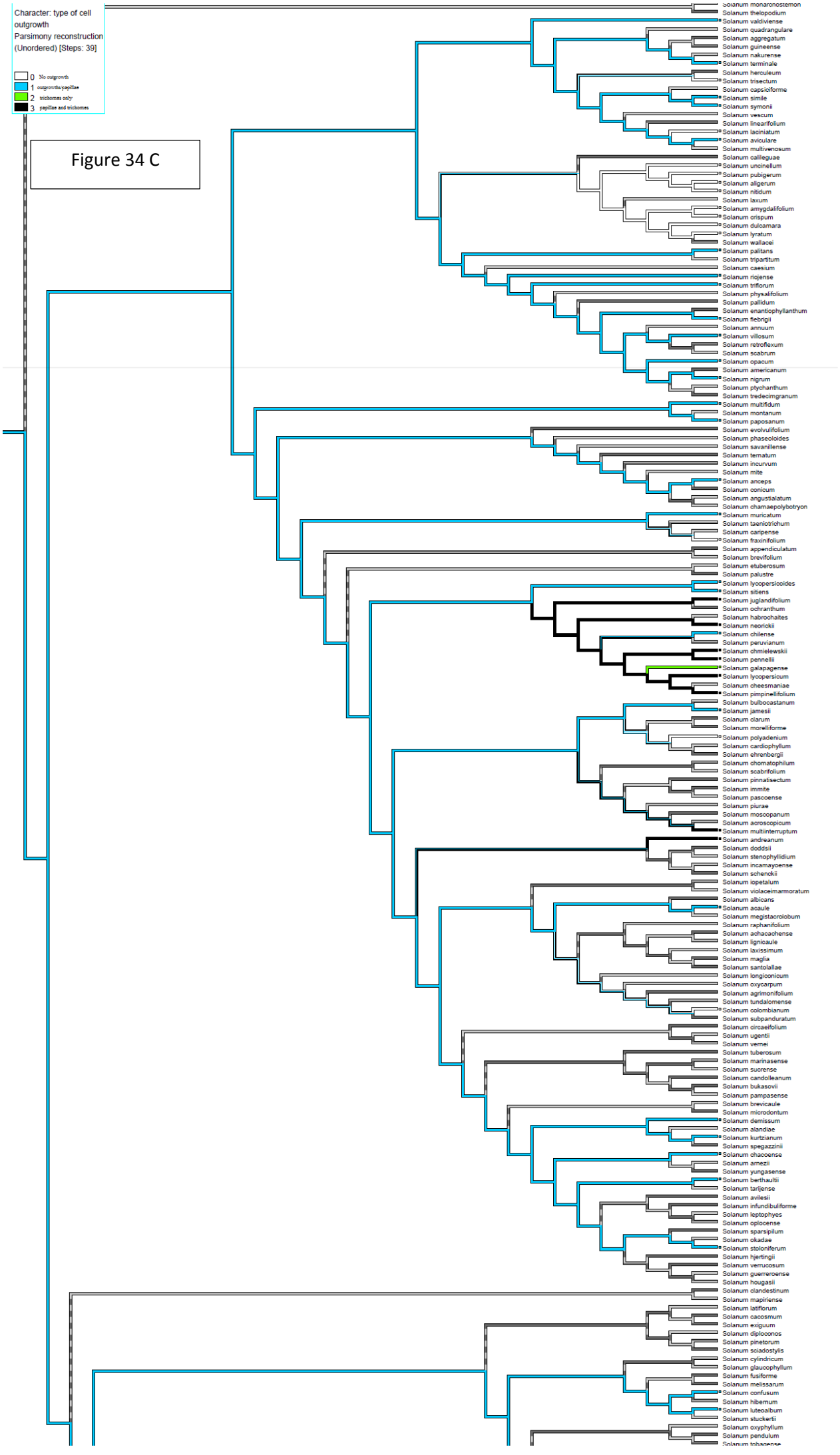
Character: type of cell outgrowth
Parsimony reconstruction (Unordered) [Steps: 39]
0 No outgrowth
1 outgrowths/papillae
2 trichomes only
3 papillae and trichomes
Solanum monanthemum
Solanum thelopodium
Solanum valdiviense
Solanum quadrangulare
Solanum aggregatum
Solanum guineense
Solanum nakurense
Solanum terminale
Solanum herculeum
Solanum trisectum
Solanum capsicoiforme
Solanum simile
Solanum symonii
Solanum vescum
Solanum linearifolium
Solanum laciniatum
Solanum aviculare
Solanum multivenosum
Solanum calleguae
Solanum uncinellum
Solanum pubigerum
Solanum aligerum
Solanum nitidum
Solanum laxum
Solanum amygdalifolium
Solanum crispum
Solanum dulcamara
Solanum lyratum
Solanum wallacei
Solanum palitans
Solanum tripartitum
Solanum caesium
Solanum riojense
Solanum triflorum
Solanum physalifolium
Solanum pallidum
Solanum enantiophyllanthum
Solanum fiebrigii
Solanum annuum
Solanum villosum
Solanum retroflexum
Solanum scabrum
Solanum opacum
Solanum americanum
Solanum nigrum
Solanum ptychanthum
Solanum tredecimgranum
Solanum multifidum
Solanum montanum
Solanum paposanum
Solanum evolvulifolium
Solanum phaseoloides
Solanum savanillense
Solanum tematum
Solanum incurvum
Solanum mite
Solanum anceps
Solanum conicum
Solanum angustialatum
Solanum chamaepolybotryon
Solanum muricatum
Solanum taeniotrichum
Solanum caripense
Solanum fraxinifolium
Solanum appendiculatum
Solanum brevifolium
Solanum etuberosum
Solanum palustre
Solanum lycopersicoides
Solanum sitiens
Solanum juglandifolium
Solanum ochranthum
Solanum habrochaites
Solanum neorickii
Solanum chilense
Solanum peruvianum
Solanum chmielewskii
Solanum pennellii
Solanum galapagense
Solanum lycopersicum
Solanum cheesmaniae
Solanum pimpinellifolium
Solanum bulbocastanum
Solanum jamesii
Solanum clarum
Solanum morelliforme
Solanum polyadenium
Solanum cardiophyllum
Solanum ehrenbergii
Solanum chomatophilum
Solanum scabrifolium
Solanum pinnatisectum
Solanum immite
Solanum pascoense
Solanum piurae
Solanum moscopanum
Solanum acroscopicum
Solanum multiinterruptum
Solanum andreanum
Solanum doddsii
Solanum stenophyllidium
Solanum incamayoense
Solanum schenckii
Solanum iopetalum
Solanum violaceimarmoratum
Solanum albicans
Solanum acaule
Solanum megistacrolobum
Solanum raphanifolium
Solanum achacachense
Solanum lignicaule
Solanum laxissimum
Solanum maglia
Solanum santolallae
Solanum longiconicum
Solanum oxycarpum
Solanum agrimonifolium
Solanum tundalomense
Solanum colombianum
Solanum subpanduratum
Solanum circaeifolium
Solanum ugentii
Solanum vernei
Solanum tuberosum
Solanum marinasense
Solanum sucrense
Solanum candolleanum
Solanum bukasovii
Solanum pampasense
Solanum brevicaule
Solanum microdontum
Solanum demissum
Solanum alandiae
Solanum kurtzianum
Solanum spegazzinii
Solanum chacoense
Solanum arnezii
Solanum yungasense
Solanum berthaultii
Solanum tarijense
Solanum avilesii
Solanum infundibuliforme
Solanum leptophyes
Solanum oplocense
Solanum sparsipilum
Solanum okadae
Solanum stoloniferum
Solanum hjertingii
Solanum verrucosum
Solanum guerreroense
Solanum hougasii
Solanum clandestinum
Solanum mapiriense
Solanum latiflorum
Solanum cacosmum
Solanum exiguum
Solanum diploconos
Solanum pinetorum
Solanum soladostylis
Solanum cylindricum
Solanum glaucophyllum
Solanum fusiforme
Solanum melissarum
Solanum confusum
Solanum hibernum
Solanum luteoalbum
Solanum stuckertii
Solanum oxyphyllum
Solanum pendulum
Solanum tobagense

Figure 34 C

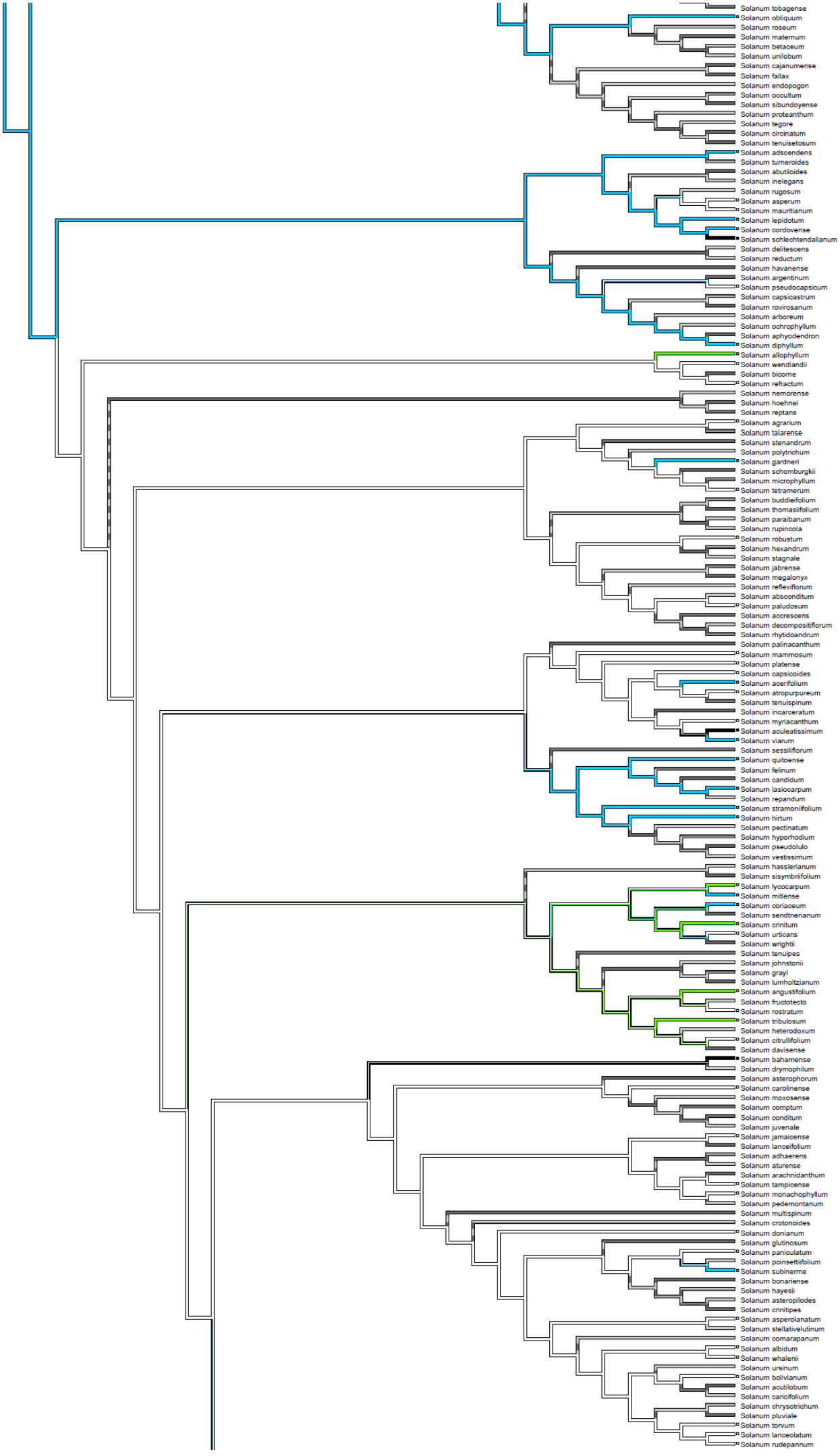
Solanum tobagense
Solanum obliquum
Solanum roseum
Solanum maternum
Solanum betaceum
Solanum unilobum
Solanum cajanumense
Solanum fallax
Solanum endopogon
Solanum occultum
Solanum sibundoyense
Solanum proteanthum
Solanum tegore
Solanum circinatum
Solanum tenuisetosum
Solanum adscendens
Solanum turneroides
Solanum abutiloides
Solanum inelegans
Solanum rugosum
Solanum asperum
Solanum mauritianum
Solanum lepidotum
Solanum cordovense
Solanum schlechtendalianum
Solanum delitescens
Solanum reductum
Solanum havanense
Solanum argentinum
Solanum pseudocapsicum
Solanum capsicoastrum
Solanum rovirosanum
Solanum arboreum
Solanum ochrophyllum
Solanum aphyodendron
Solanum diphyllum
Solanum allophyllum
Solanum wendlandii
Solanum bicorne
Solanum refractum
Solanum nemorense
Solanum hoehnei
Solanum reptans
Solanum agrarium
Solanum talarense
Solanum stenandrum
Solanum polytrichum
Solanum gardneri
Solanum schomburgkii
Solanum microphyllum
Solanum tetramerum
Solanum buddleifolium
Solanum thomasiifolium
Solanum paraibanum
Solanum rupincola
Solanum robustum
Solanum hexandrum
Solanum stagnale
Solanum jabrense
Solanum megalonyx
Solanum reflexiflorum
Solanum absconditum
Solanum paludosum
Solanum acrescens
Solanum decompositiflorum
Solanum rhytidoandrum
Solanum palinacanthum
Solanum mammosum
Solanum platense
Solanum capsicoides
Solanum acerifolium
Solanum atropurpureum
Solanum tenuispinum
Solanum incarceratum
Solanum myriacanthum
Solanum aculeatissimum
Solanum viarum
Solanum sessiliflorum
Solanum quitoense
Solanum felinum
Solanum candidum
Solanum lasiocarpum
Solanum repandum
Solanum stramoniifolium
Solanum hirtum
Solanum pectinatum
Solanum hyporhodium
Solanum pseudolulo
Solanum vestissimum
Solanum hasslerianum
Solanum sisymbriifolium
Solanum lycocarpum
Solanum mitlense
Solanum coriaceum
Solanum sendtnerianum
Solanum crinitum
Solanum urticans
Solanum wrightii
Solanum tenuipes
Solanum johnstonii
Solanum grayi
Solanum lumholtzianum
Solanum angustifolium
Solanum fructotecto
Solanum rostratum
Solanum tribulosum
Solanum heterodoxum
Solanum citrullifolium
Solanum davisense
Solanum bahamense
Solanum drymophilum
Solanum asterophorum
Solanum carolinense
Solanum moxosense
Solanum comptum
Solanum conditum
Solanum juvenale
Solanum jamaicense
Solanum lanceifolium
Solanum adhaerens
Solanum aturense
Solanum arachnidanthum
Solanum tampicense
Solanum monachophyllum
Solanum pedemontanum
Solanum multispinum
Solanum crotonoides
Solanum donianum
Solanum glutinosum
Solanum paniculatum
Solanum poinsettiifolium
Solanum subinerme
Solanum bonariense
Solanum hayesii
Solanum asteropilodes
Solanum crinitipes
Solanum asperolanatum
Solanum stellativelutinum
Solanum comarapanum
Solanum albidum
Solanum whalenii
Solanum ursinum
Solanum bolivianum
Solanum acutilobum
Solanum caricifolium
Solanum chrysotrichum
Solanum pluviale
Solanum torvum
Solanum lanceolatum
Solanum rudepannum

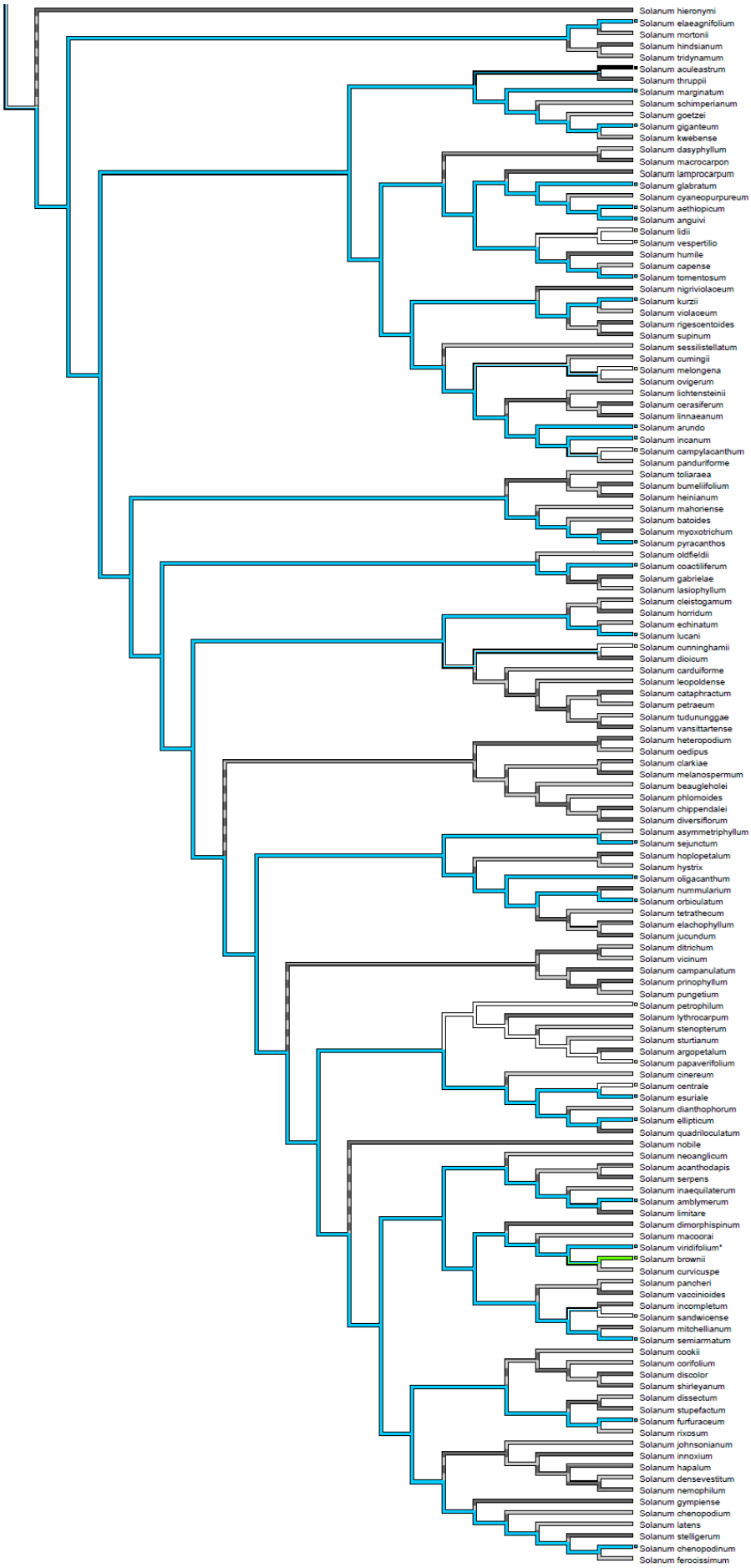

Figure 34 C: Type of epidermal cell outgrowth mapped to the *Solanum* phylogeny.

The type of epidermal cell outgrowth on the anther surface has been mapped to the phylogeny of *Solanum* (Särkinen et al, 2013). White represents o: no epidermal cell outgrowths, only a flat anther surface. Blue: 1: epidermal cell outgrowths/papillae only. Green: 2: trichomes only. Black: 3: both epidermal cell outgrowths/papillae and trichomes on the anther surface. Parsimony ancestral state reconstruction predicts the ancestral state of the character to be that there are epidermal cell outgrowths/papillae, which are then repeatedly lost or modified into other outgrowth forms throughout the phylogeny.

2.3.5.2: Different clades have different amounts of and types of epidermal cell outgrowths

The Leptostemonum clade contained some species with epidermal cell outgrowths and some without. More species had epidermal cell outgrowths of some kind than those species which were entirely flat-celled on their anther surface. However there were still a large number of species with only flat cells. 86 species from the Leptostemonum clade were examined using SEM and, of these, 48 species had some kind of cell outgrowth while 38 species had only flat epidermal cells on their anthers. There did not appear to be a pattern to where the epidermal cell outgrowths were found with regard to the subclades of Leptostemonum. Species with flat anther surfaces and species with epidermal cell outgrowths were found in all the Leptostemonum subclades, there was no one particular clade dominated by either morphology. The number of species with each morphology in each Leptostemonum subclade can be seen in the Appendix 5.

The M-clade had some species with epidermal cell outgrowths and some without. Of the 27 species examined using SEM, 18 had some kind of epidermal cell outgrowth, while 9 had only flat epidermal cells on their anther surface. The majority of the species examined from the M-clade were in the sub clade Dulcamaroid, of which all only had flat cells on the surface of their anthers. This accounts for the majority of the species with only flat cells exhibited by M-clade: only 2 species outside of Dulcamaroid were entirely flat-celled on their anther surface, one was in the Morelloid subclade the other was in the Normania subclade. The Morelloid subclade also contained species which had epidermal cell outgrowths. Only one species of Normania subclade was sampled, so no generalisations can be made about the rest of the subclade with regard to whether or not they have epidermal cell outgrowths.

Potato clade exhibits lots of epidermal cell outgrowths and some of the most extreme cell shapes. Of the 31 species of Potato examined 26 had epidermal cell outgrowths, only 5 had entirely flat anther surfaces. The Tomato subclade especially displayed lots of epidermal cell outgrowth on their anther surfaces. All 11 Tomato species examined had epidermal cell outgrowths of non-trichome/papillae on their anther surface and 8 species also had trichomes on their anther surface. Some species of the Tomato clade had very extreme

papillae: ‘glove like’ epidermal cell outgrowths on their anther surface towards the base of the anthers. These ‘glove like’ papillae are shown in Figure 36. This kind of cell outgrowth was observed on *S. lycopersicum* and *S. pimpinellifolium* which were both imaged with SEM from casts of living specimens. It is possible that more species had this kind of epidermal cell outgrowth, however it was hard to distinguish clearly from other kinds of non- trichome outgrowth when it was a herbarium specimen being examined as opposed to a cast from a living plant.

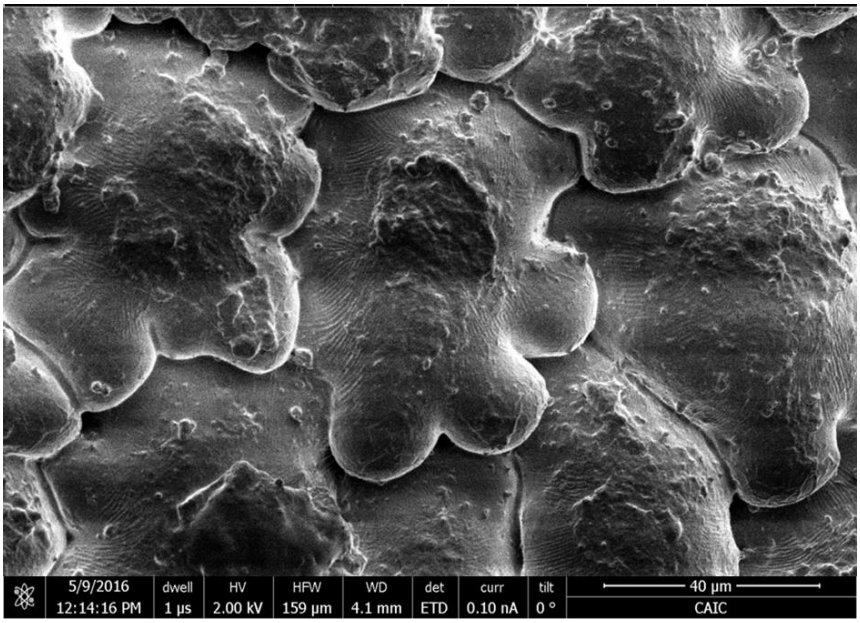

Figure 35: ‘Glove like’ papillate epidermal cell outgrowths
These ‘extreme’ appearing epidermal cell outgrowths are referred to here as ‘glove like’ papillae due to their multi-lobed appearance. This SEM image was of the species *S. lycopersicum,* from a cast of a living specimen. The ‘lobes’ or ‘points’ of the papillae were always found pointing towards the anther base.

Of 11 species which had both trichomes and non-trichome epidermal cell outgrowths/papillae, 8 of them belonged to the Potato clade (6 of these species were from the Tomato subclade). Of the remaining 3 species, 2 were from different subclades of the Leptostemonum clade: Bahamense (including *S. bahamense* which had stellate trichomes on the adaxial side of the anther and epidermal cell outgrowths/papillae on the abaxial side of the anther, shown in Figure 37). The other species was *S. aculeatissimum* which belongs to the Acanthophora sub clade of Leptostemonum. This species had papillae on its abaxial

surface but also had long thin trichomes towards the base of the anther. The final species with both trichomes and papillae was *S. schlechtendalianum* of the Brevantherum clade. Papillae covered the length of the anther on the abaxial side of the anther, whilst there were stellate trichomes on the adaxial side (it was unclear from this specimen whether the trichomes originated from the anther connective or the anther sac).

Of the 9 species that only had trichomes on their anther surface, 2 of the species belong to the Potato clade, 6 to Leptostemonum and 1 to Cyphomandra. Those species from the Potato clade were from the Tomato subclade and had trichome mesh. Those from the Leptostemonum clade were from a variety of subclades (1 species Bahamense, 1 species Old-world and 4 species of *Androceras-Crinitum*). 5 of those species had stellate trichomes on the adaxial anther surface (*S. polyacanthos, S. tribulosum, S. lycocarpum, S.crinitum* and *S. brownii*). *S. polyacanthos* is shown in Figure 36. The other had long hairs on the anther base (*S. angustifolium*). *S. crinitum* also had stellate hairs on the underside of its anther which appear to originate from the connective; however this species cannot be identified to clade level. Whether or not these trichomes originate from the tissue of the connective or the anther is not entirely clear, further examination of specimens, especially living specimens, could resolve this.

A species with particularly interesting epidermal cell outgrowth morphology is *S. juglandifolium*, which does not have a trichome mesh (like the Tomato clade species it is closely related to), but does have some outgrowths that are extended papillae which are almost trichomes. These are found at the base, on the side of the anther (Figure 38).

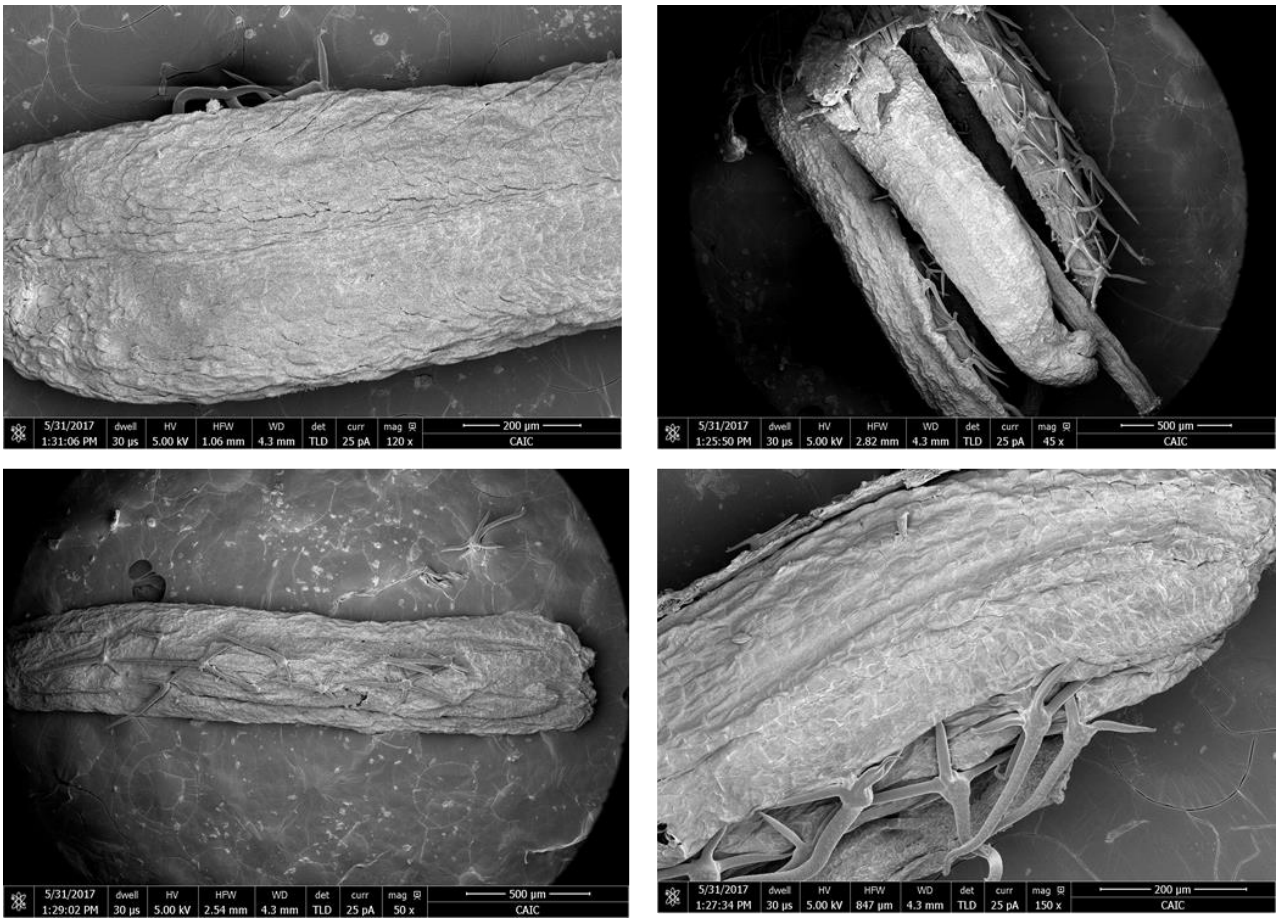

Figure 36: SEM of the anthers of *S. polyacanthos*, from the Bahamense clade.

It can be seen from this Figure that *S. polyacanthos* also exhibits stellate trichomes on its adaxial surface. The abaxial surface however appears to be smooth unlike *S. bahamense*. A: Abaxial surface of *S. polyacanthos* anther. B: Two anthers of *S. polyacanthos* in their arrangement in the flower. The style can be seen and part of a sepal. The abaxial surface can be seen to be smooth, but from the anther which is on its side stellate hairs can be seen protruding from the adaxial surface of the anther. C: Adaxial surface of *S. polyacanthos*, stellate hairs can be seen on the surface. D: An anther of *S. polyacanthos,* on its side. The adaxial side of the anther can be seen to have stellate hairs, while the abaxial side is smooth. The side between the two can also be seen to be smooth.

Figure 37: SEM and illustration of the anthers of *S. bahamense* displaying stellate trichomes on the adaxial side of the anthers and outgrowths/papillae on the abaxial side of the anther.

A: Adaxial side of the anther shown from the anther middle to towards the anther tip, showing stellate hairs. B: Side of the anther, part of the abaxial side can be seen: displaying epidermal cell outgrowths/papillae. Part of the adaxial side can also be seen showing stellate trichomes. C: The middle section of the adaxial side of the anther, stellate trichomes can be seen. D: Anther on its side, displaying part of the abaxial and part of the adaxial side of the middle section of the anther. E: The base section of the anther, shown from the side displaying some of the abaxial side of the anther and some of the adaxial side of the anther. F: The base section of the anther, showing where the filament meets the anther base. The image shows the adaxial side of the anther with stellate hairs. G: An illustration/cartoon showing observed locations of epidermal cell outgrowths on *S.bahamense*

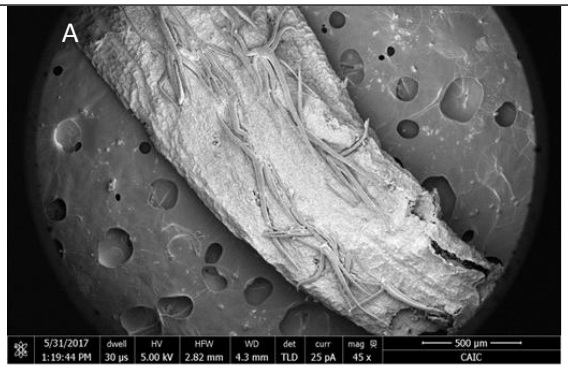

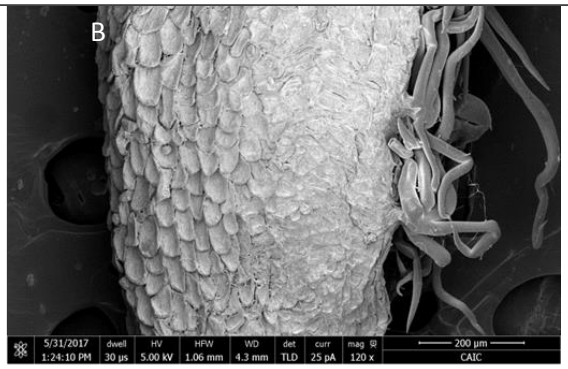

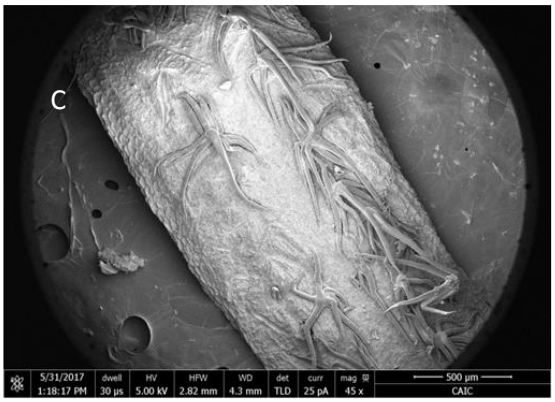

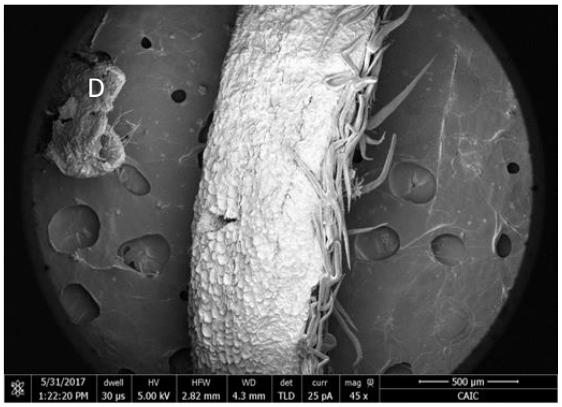

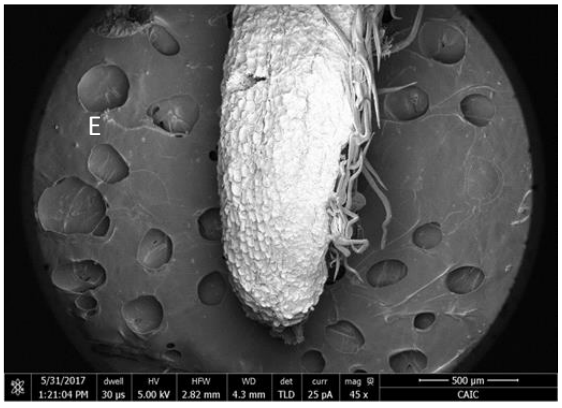

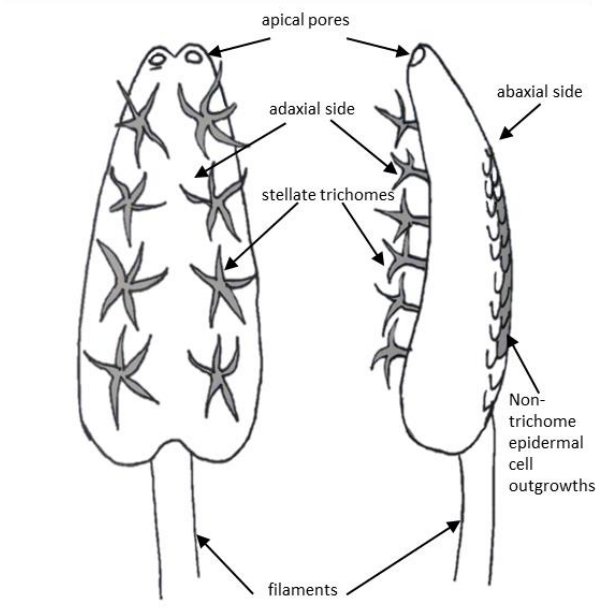

G

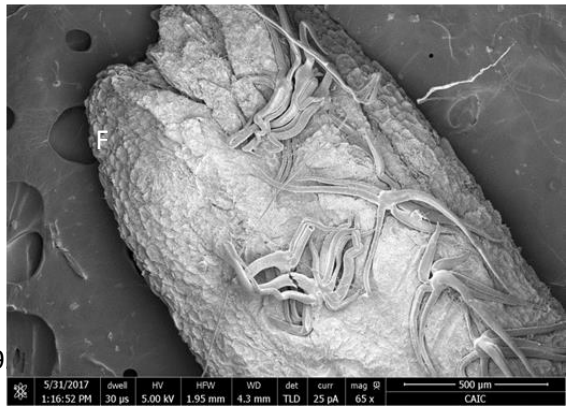

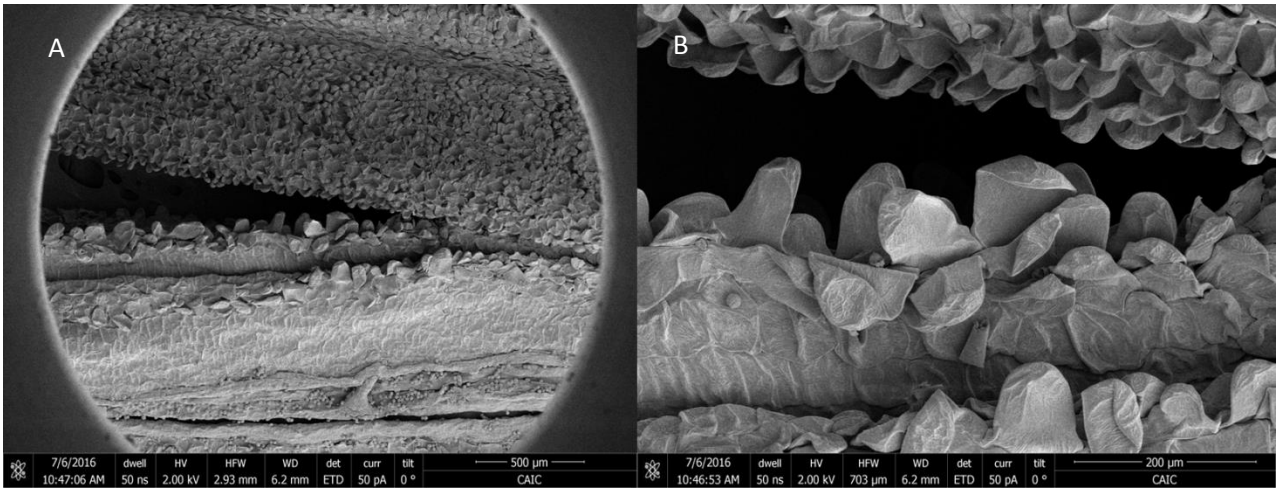

Figure 38: SEM of *S. juglandilifolium*

Trichome like outgrowths can be seen towards the base of the anther, growing out of the side of the anther. The abaxial side is also covered in non-trichome epidermal cell outgrowths/papillae. A: A section of two anthers of *S.juglandilifolium.* One anther is shown abaxial side up and the other is shown adaxial side up. The abaxial side is covered in epidermal cell outgrowths, whilst the adaxial side is flat. However, along the anther edge there are 'trichome-like' epidermal cell outgrowths which are more elongated than those found on the abaxial side of the anther. B: A closer image of the 'trichome-like' epidermal cell outgrowths found along the anther edge.

2.3.5.3 Anthers of heterantherous species of *Solanum* do not usually have epidermal cell outgrowths on their anther surface

In this study, 9 heterantherous species of *Solanum* were measured for the dimensions of both their pollinating and feeding anthers. Of these 9 species, 6 were examined under SEM (*S. lidii, S. citrullifolium, S. rostratum, S. trisectum, S. angustifolium* and *S. vespertilio*). All those examined possessed only smooth cells on the epidermal surfaces of both their feeding anthers and pollinating anthers. The only exception to this was *S. angustifolium* which displayed long hairs on the base of its pollinating anther (Figure 39).

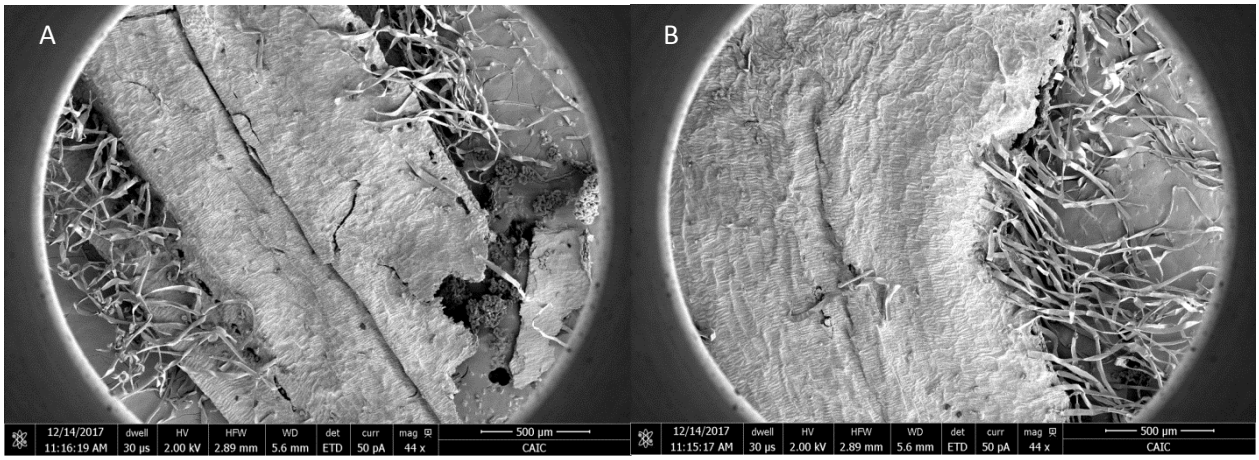

Figure 39: SEM of the base of the pollinating anther of *S. angustifolium*
At the base of the pollinating anthers of *S. angustifolium* long trichomes can be seen on the epidermal surface, growing from the sides of the anther. A and B show the anther base from two different angles, showing the hairs growing from the anther edge.

2.3.5.4: 'Pepper pot' anther cones in different parts of the phylogeny are held together in different ways and have different epidermal cell outgrowths on their anther surface

The species in the Tomato subclade within the Potato clade which possess pepper pot cones are all held together by means of a trichome mesh. It was known that the *S. lycopersicum* pepper pot cone was held together via trichome mesh (Glover et al, 2004) (Figure 40), but this study provides confirmation that all pepper pot anther cones in this part of the phylogenetic tree and in the wild tomato relatives are held together in the same way (Figure 41). The Tomato subclade species examined also had other epidermal cell outgrowths/papillae on the abaxial surface of the anthers in addition to the trichome mesh. It was also seen that there is variation in the papillae/outgrowth coverage of the anthers of different species in the Tomato subclade. Most of the Tomato subclade species had outgrowths/papillae towards the basal half of the anther, gradually fading to a smooth tip. The most exaggerated cell outgrowths were observed from the middle of the anther to the base of the anther. If 'glove-like' papillae were observed it was in this area of the anther. These were observed in *S. lycopersicum* and *S. pimpinellifolium*. It is possible that more of the species of the Tomato subclade possessed 'glove-like' papillae however only these two species were examined from casts of living tissue and the morphology of the cells clearly identified beyond simply being outgrowths. The top third of the anther of most of the Tomato subclade species was smooth and flat, with the bottom two thirds of the anther having papillae/outgrowths (the trichome mesh however would extend all the way to the anther tips, holding the anthers firmly pressed together in the pepper pot cone). This was seen for *S. lycopersicum, S. chmielewski, S. pimpinellifolium, S. neorickii, S. arcanum* and *S. galapagense.* For *S. pennellii,* however, the papillae/outgrowths ran the full length of the anther right to the tip.

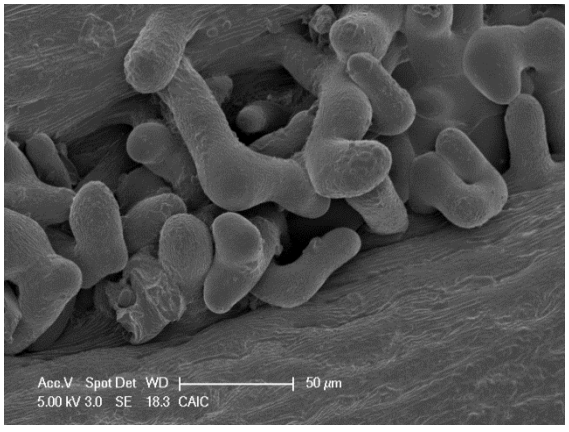

Figure 40: SEM of a section of the trichome mesh of *S. lycopersicum*
The trichomes can be seen tangled together between the two anthers, holding the anthers together into a tight cone.

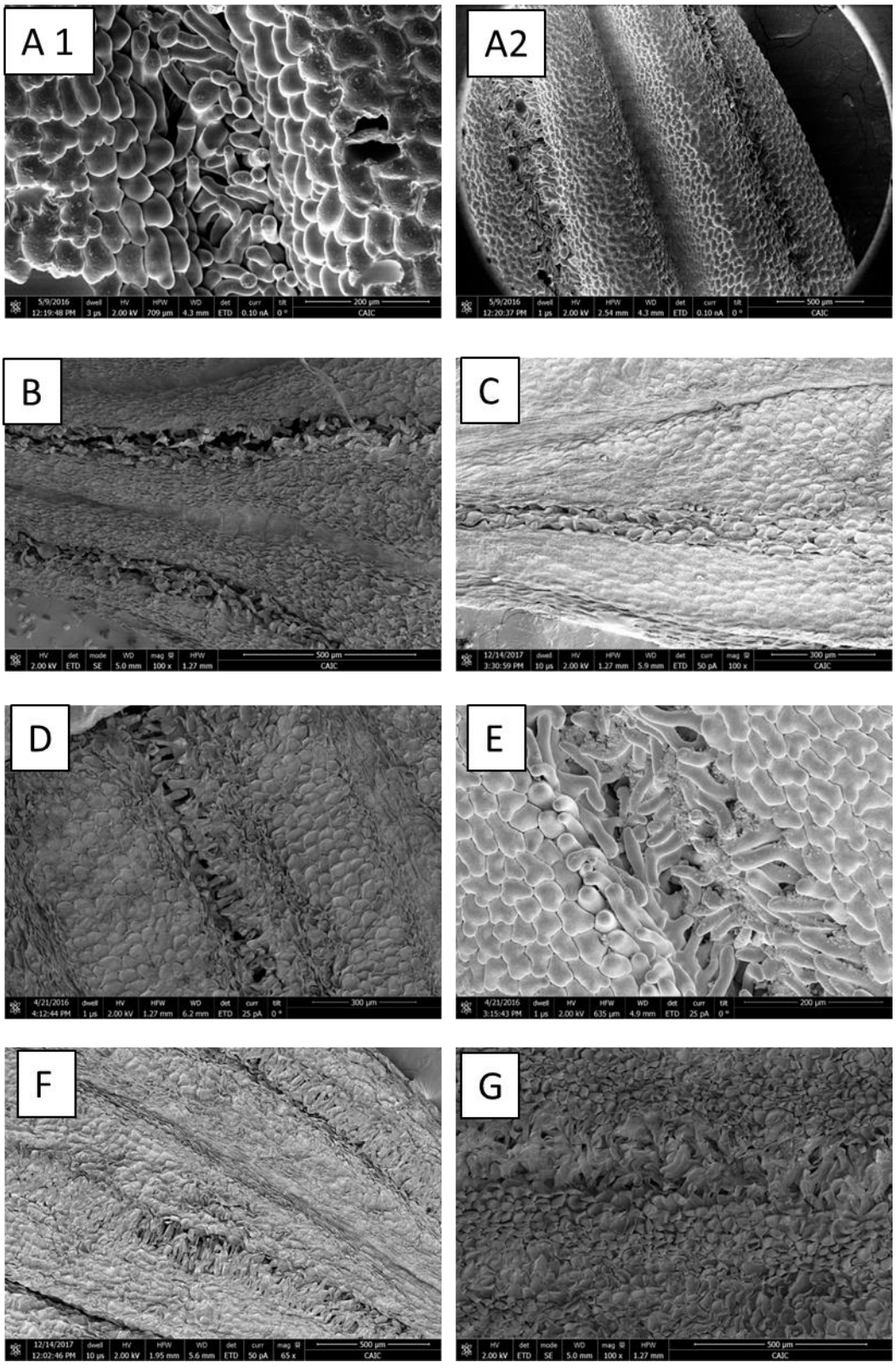

Figure 41: SEM of the trichome mesh of some *Tomato* subclade species.
Tomato subclade species, which have pepper pot cones held together with a trichome mesh. A1 and A2: *S. lycopersicum*. B: *S. chilense*. C: *S. chmielewski*. D: S*. neorickii.* E: *S. pimpinellifolium.* F: *S. galapagense*. G: *S. peruvianum.*

Only one species of the Dulcamaroid subclade sampled had a pepper pot cone. The species was *S. dulcamara.* In *S. dulcamara* it is known that the pepper pot cone is held together differently from the pepper pot cone of *S. lycopersicum*. It has been hypothesised that the anthers are held together by extracellular secretions gluing together the anthers (Glover et al, 2004). There are a number of species which were examined which had anthers that were tightly connivent, such as *S. uncinellum*, but *S. dulcamara* was the only true pepper pot cone species observed in the Dulcamaroid subclade. When examined under SEM, *S. dulcamara* also has no other epidermal cell outgrowths on its anthers at all. None of the species of Dulcamaroid subclade (including the tightly connivant species) examined under SEM had any cell outgrowths on the anther surface whatsoever.

In the *Bahamense* subclade, all three species of the subclade have pepper pot anther cones (*S. bahamense, S. ensifolium* and *S. polyacanthos*). *S. bahamense* and *S. polyacanthos* were examined with SEM. Neither possessed a trichome mesh, confirming that their pepper pot cone is not held together in the same way as in the Tomato subclade. However**,** epidermal cell outgrowths/papillae and stellate trichomes were observed on the anther surface and on the adaxial connective.

2.5 Discussion

2.5.1: There was variation in the anther dimension measurements

There is variation in the anther dimensions between the species in *Solanum.* For anther length, the largest anther length measured was 12.56mm largest than the smallest anther length measured. For anther tip width, the largest anther tip width was 1.02mm wider than the smallest anther tip width. For anther base width there was a difference of 2.13mm. For anther middle width there was a difference of 2.88mm.

It should be noted that this variation in anther dimension measurements is probably significantly correlated (not measured in this study) to flower size. However, the continuous nature of anther size is of interest. The anther sizes do not fall into distinct categories and instead form a continuous range from smallest to largest with all possible anther sizes in between represented.

It would be ideal to compare this variation in anther size to that found in other genera. However, there appear to be few studies addressing variation in anther or stamen dimensions within a genus. There are some studies which have examined variation in anther dimension measurements among different varieties within a single species, for instance between different varieties of wild barley (Giles and Bengtsson, 1988) and within different populations of sesame (of which significant differences were found between genotypes, but with no effect of environment on the variation observed) (Pfahler et al, 1996). There was a study that specifically examined variation in floral dimensions in *Solanum* section *Androceras* (Whalen, 1978). This study compared anther lengths of species from section *Androceras* with sections *Brevantherum* and *Tuberarium* and concluded that section *Androceras* had greater diversity in anther length, relative to the other sections of the genus (Whalen, 1978). However, this study mainly examined heterantherous species, only measured the pollinating anthers of section *Androceras*.

A study (Rick et al, 1978) investigated the relationship between the anther length of *S.pimpinellifolium* and cross pollination rates and concluded that with increased anther length there was a positive correlation with cross pollination (Rick et al, 1978). There was also observed to be a large range in anther lengths within this species: 5.4-10.5mm (Rick et al, 1978), this range of anther length was also observed in an earlier study (Rick et al, 1977).

Therefore there is a difference of 5.1mm within this single species. While the range seen in the whole of *Solanum* observed in this study was ~2.5x this, it is still a large amount of variation to observe within a single species. It should be noted that other species of *Solanum* may also have large ranges in their anther length measurements not necessarily captured by this study.

While there are some studies into the variation in anther dimensions in various species, rarely has it been considered in the context of an entire genus or on the scale of this study. This study was a first attempt to quantify the variation in anther dimensions within *Solanum* in a phylogenetic context and may provide an underpinning dataset from which further studies into *Solanum* anther variation may be conducted.

2.5.2: Different anther dimension measurements are uncorrelated to one another

The anther dimensions of the species analysed were not correlated with one another very strongly within a species. This was an unexpected result, as structural constraints of the anther might be expected to result in correlation. However, it can be seen from the results that, for example, an anther being large in one of its dimensions does not necessarily mean that the anther will also be large in its other dimensions. A long anther will not necessarily be a wide anther, nor is the reverse true: a small anther will not necessarily be wide or thin. It is apparent that almost every anther form or shape is possible within *Solanum*. This implies that anther shape can be highly varied, much more so than if the anther dimensions varied dependent on one another which would limit possible anther shapes. Therefore a much greater number of possible anther shapes may be produced. ((This may imply isolation/distinction between species/niches based on anther size and shape.)) ((This may imply that selection may act on individual aspects of anther shape: effecting different anther dimensions independently, therefore 'fine tuning' anther shape in response to selection.))

The anther dimensions which are most correlated to one another are the anther base and middle widths. This is perhaps unsurprising considering that the two measurements are close together along the anther length, and that the general shape and structure of the anther is a tube tapering towards the tip. This is likely to result in the middle and base width being fairly similar. This may be the best shape for grip and for structural strength of an

anther. A narrow base with a larger tip would be more easily damaged and might detach from the filament too easily when landed on by a pollinator.

Some anther forms, however, were not found very often. Anthers with very extreme morphologies were generally much rarer with fewer species occupying those areas of morphological space. This was especially true of anthers with small widths. There were more species with extreme morphologies when the anther was thicker ('thick and long anthers' and 'thick and short anthers' were areas of the morphological space more occupied by species of *Solanum* than 'short and thin anthers' or 'long and thin anthers'.) This is probably because of structural constraints to anther growth. Thin anthers may be weak and prone to breaking during the rough buzz pollination process, or difficult to support physically. They may also be restrained by the size of the pollinator: an anther which is overall very small (with a narrow width along its entire length and also a very short anther length) may be difficult to grip on by anything but an extremely small pollinator, which then may not be able to sonicate with a great enough amplitude. In turn, a pollinator landing on the end of a very long thin anther may be tipped off by the bending of the anther unable to sustain its weight.

Other anther shapes which were not observed in this study included anthers with a narrow middle but wider tip and base. Such an anther would potentially suffer from poor vibrational transfer (Buchmann, 1978; Harder and Barclay, 1994; King and Buchmann, 1995), be difficult to grip and pollen might become trapped by the narrow bottleneck in the middle, resulting in anther damage. This would result in reduced pollen transfer overall and therefore reduced fitness in the plant. This kind of anther shape may also be structurally more difficult to produce.

2.5.3: Anther shape varies throughout *Solanum* and different subclades occupy different areas of morphological space

There is a great diversity of anther shape within the genus *Solanum.* There is a great variety of morphological space occupied by *Solanum* anthers, despite the specialised pollination mechanism that they all share.

There are points where species diverge in their dimension values relative to the other species in the phylogeny and relative to species which they are more closely related to within their clade. This indicates an area in which phylogeny is not constraining morphology, and provides potential opportunities to study the selective pressures and developmental pathways which have driven anther morphological divergence.

Leptostemonum is a large diverse clade. It is the largest single clade within *Solanum*, occupying a diverse variety of habitats across the world. Therefore it is unsurprising that its anthers occupy a large and diverse area of morphological space; as illustrated by there being few areas of morphological space in the Leptostemonum diagram unoccupied. However, the 'short and thick anthers' area of morphological space was relatively unoccupied compared to the rest of the diagram. This area of morphological space was more occupied by the M-Clade species, showing different general anther forms within the different clades of *Solanum.* This may demonstrate specialisation towards different pollinators or pollen release strategies by the different clades within *Solanum. Solanum* as a whole occupies almost all possible morphological space in the phylomorphospace analyses, yet different clades occupy different sections of the morphological space. Perhaps diversification of anther shape is linked to species diversification and the diversity of anther form found in *Solanum* may help to explain the dramatic radiation of this genus.

A number of species were picked out from the phylomorphospace as in some way divergent in their anther shape from those species which were closely related to them, or relative to the rest of their clade/subclade.

In Leptostemonum the species *S.lycocarpum* and *S.quitoense* both had longer and thicker anthers than the rest of the Leptostemonum clade. *Solanum quitoense* had especially wide middle and base anther widths. S*olanum lycocarpum* is widely distributed in southeastern Brazil, often in the Brazillian savannah (http://solanaceaesource.org/; Lorenzi, 2002; Farruggia and Bohs, 2010). This species is often referred to as 'wolf fruit' or 'wolf apple' due to its large fleshy fruits being eaten by the maned wolf (Motta-Junior et al, 1996). Most of the research into this *Solanum* species has been into its potential for medicinal properties, (for example, Dall'Agnol and Poser, 2000; Vieira et al, 2003.) *Solanum lycocarpum* is part of the *Solanum* section *Crinitum*, which is mainly large trees and shrubs with generally large

flowers (Farruggia and Bohs, 2010). *S. lycocarpum* is an andromonoecious species (Martins et al, 2006; Oliveira-Filho and Oliveira, 1988). The anthers of *S.lycocarpum* produce large amounts of pollen (Oliveira-Filho and Oliveira, 1988) and the flowers are visited by centridini bees (Rabelo et al, 2014). These are oil collecting bees (Vilhena et al, 2012) but use *S.lycocarpum* as a pollen source (Rabelo et al, 2014). These bees are of medium-large size (~1.2cm or larger) (Frankie et al, 1983). Rabelo et al(2014) showed that it was usually the larger bee species which visited *Solanum* species. However the most efficient and frequent pollinator of *S.lycocarpum* is thought to be large *Xylocopa* bees (Oliveira-Filho and Oliveira, 1988). It is possible that the larger size of the *S.lycocarpum* anthers is a result of association with these large pollinators. However, there is nothing to indicate clearly why *S.lycocarpum* anther dimensions should diverge from the rest of the *Leptostemonum* clade. Perhaps the savannah habitat, the pollinator size or the requirements to produce the distinctive large fleshy fruit result in selection pressure in favour of large anthers, or perhaps the large anthers are simply due to the large size of the plant and flowers as a whole. *S.lycocarpum* is fairly closely related to *S.mitlense*, although not sister to it (Särkinen et al, 2013). *S.mitlense* has anthers which are much more similar in dimensions to the rest of the species in Leptostemonum. These species could be used as a study system for comparison to explore these anther dimensions changes further and gain a better understanding of anther morphology. However it should be noted that, while *S.lycocarpum* displayed epidermal cell outgrowths on its anther surface, *S.mitlense* did not display the same epidermal cell outgrowths (trichomes vs epidermal cell outgrowths/papillae). It is also worth noting that *S.crinitum* displayed the same epidermal cell outgrowths as *S.lycocarpum* (stellate trichomes) and also occupied a similar area of morphological space, however they are closely related which is the likely explanation. *S.quitoense,* while it occupies a similar morphological space to *S.lycocarpum and S.crinitum,* is instead found in the Lasiocarpa subclade of Leptostemonum. However *S.quitoense* is also strongly andromonoecious and also has generally large flowers (Diggle and Miller, 2004).

Also in *Leptostemonum,* but in the Old-World subclade, the species *Solanum brownii* occupied an area of morphological space which was divergent from the rest of its clade. The anthers were very short and thick, with an especially thick tip width and short anther lengths relative to both the rest of the Leptostemonum clade and also *Solanum* as a whole.

The species most closely related that was examined in this study was *S.viridifolium,* which has much more 'average' anther dimensions relative to the rest of *Solanum* and also Leptostemonum clade. These would make a good pair for studies examining the different anther dimensions, however the two species have different epidermal cell outgrowths. *S.brownii* has stellate trichomes on the anther connective whilst *S.viridifolium* has epidermal cell outgrowths/papillae. This perhaps highlights epidermal cell outgrowths combined with anther dimensions creating different specialisations.

S.angustifolium also has a long anther length relative to the rest of Leptostemonum, causing it to diverge in morphological space from the rest of its clade. This species is heterantherous and the anther which was measured in this study was the 'pollinating anther', therefore it is not possible to compare it to other anthers not performing this specialised function. These anthers tend to be longer due to their highly modified form (Luo et al, 2009; Vallejo-Marın et al 2009).

Solanum uncinellum of the Dulcamaroid subclade has larger anther widths than other species in the same clade. This species has been previously recorded to have one anther with a longer filament relative to the other anthers (Solanaceaesource.org/ Knapp). The apical pores lengthen to slits as the anthers age, but pollen is still accessed by sonication. The species has a wide distribution occupying a variety of habitats (Solanaceaesource.org/ Knapp). A search of the literature reveals very little about this species that might explain why it has unusual anthers. The anthers were smooth and flat when examined by SEM.

In the Tomato subclade of the Potato clade, *S.pennellii* was shown to occupy an area of morphological space different from the other Tomato subclade species with which it shared the pepper pot cone morphology, and to instead occupied a more similar area of morphological space to *S.juglandifolium* and *S.sitiens* which are Tomato subclade species which do not have a pepper pot anther cone. There are other aspects of *S.pennellii* which have been noted as unusual for the Tomato subclade, the flowers are slightly zygomorphic and have spathulate calyx lobes (http://solanaceaesource.org/taxonomy/term/108866/descriptions. Peralta, Knapp and Spooner). *Solanum pennellii* also lacks the sterile appendage on its anther that is present in the other species of Tomato (Bedinger et al, 2010). In this respect *S.pennellii* is more similar

to the Tomato clade allies *S.sitiens* and *S.juglandifolium,* yet it is otherwise considered like the rest of the Tomato clade (Bedinger et al, 2010). The differences between *S.pennellii* and the rest of the Tomato subclade were also recognised in a study investigating anther development within the subclade (Garcia and Barboza, 2006) and *S.pennellii* was consequently excluded from the investigation due to these differences. The species used to be excluded from the 'genus' Lycoperiscon, in which tomato used to placed, and has long been considered morphologically different from the rest of Tomato. Some differences cited include the greater anther curvature and dehiscence through both the apical pore and line (so that the species dehisces like *S.sitiens* and *S.juglandifolium*). Structural differences were also noted in the dehiscence zone and the distribution of thickened cells (Garcia and Barboza, 2006). Therefore it can be concluded that *S.pennellii* anthers are of interest due to their great morphological divergence from other species within the same subclade. However, an explanation for why the species diverges so strongly has yet to be gleaned, if there is an adaptive explanation for the observed changes rather than simply drift. It is possible that the shape somehow distinguishes *S.pennellii* from other species in the tomato subclade therefore making it markedly different in appearance for pollinators, in areas where the species may have geographical overlap. However considerable further study would be needed to explore these various possible explanations.

These species noted for their unusual anther dimensions measurements relative to the rest of their clade could be used as study systems for comparison with closely related species so as to explore particular changes in anther morphology and better understand these traits.

Changes in anther dimensions could alter vibrational energy transfer from sonication and therefore alter pollen release, or limit pollen release to only more effective pollinators. An increase in anther length would mean an increase in the number of collisions between pollen grains within the anther prior to release as a result of buzz pollination and may therefore produce a more explosive release, or one that requires less energy. More collisions would result in greater electrostatic charging of the pollen grains (Masuda et al, 1998; Corbert and Huang, 2014). Filament length has been proposed to have a dampening effect on the vibrations of sonication by altering the way the anthers resonate (Buchmann, 1978; Harder and Barclay, 1994; King and Buchmann, 1995). So anther dimension traits may dampen or enhance the transmission of vibrations and therefore can potentially affect

sonication positively or negatively (Passarelli and Cocucci, 2006; Harder and Barclay, 1994; King and Buchmann, 1995; King and Buchmann, 1996).

In *Solanum* it is possible that there is a selective pressure to reduce pollen wastage. As the pollen is used both for reproduction and for rewarding pollination services large amounts are required (Harder and Barclay, 1994). Yet using your own gametes (within the pollen) as a reward for pollination is potentially costly (De Luca and Vallejo-Marin, 2013). There is a conflict of interest between the pollinator and plant (Luo et al, 2018). The pollinator is under selective pressure to maximise pollen use for larval consumption and to reduce foraging distance, number of floral visits and other energetically costly behaviours (Rasheed and Harder, 1997). The plants, in contrast, are perhaps under selection for maximum pollen to be used for reproduction (Luo et al,2018; De Luca et al, 2013; Harder and Barclay, 1994; Harder and Thompson et al, 1989; Harder and Wilson, 1994). Therefore it is possible that there are adaptations of both the interacting plant and the pollinator associated with buzz pollination (Buchmann, 1983; Vogel, 1978). Poricidal anthers could be a strategy by which access to pollen could be limited by the plant (and some pollen thieves excluded) so as to reduce pollen waste and the cost to plant fitness (Harder and Barclay, 1994; De Luca and Vallejo-Marin, 2013), while modifying the anther dimensions could allow the modification of pollen release in response to sonication.

2.4.3.1: Species of *Solanum* with pepper pot anther cones share similar anther dimension measurements and occupy a similar area of morphospace

For the Tomato subclade of the Potato clade all species with a pepper pot anther cone occupied a different area of morphological space compared to the rest of the clade. All these pepper pot anther cone species occupied an area of morphological space which was for 'long and thin anthers' compared to the rest of their clade.

Solanum dulcamara, which has a pepper pot anther cone in the Dulcamaroid clade, also occupied the area of morphological space for 'long and thin anthers' relative to the rest of its clade. However, unlike the Tomato species, *S. dulcamara* does not hold its pepper pot anther cone together with a trichome mesh (Glover et al, 2004).

The species of the Bahamense subclade of Leptostemonum with pepper pot anther cones also occupied the 'long and thin anthers' area of morphological space. However this was not as marked a divergence from the rest of the Leptostemonum subclade, perhaps because of how much of the possible morphological space this clade occupied. There were species of the Leptostemonum clade with longer and thinner anthers than those of the *Bahamense* subclade. However it is still the case that all species with a pepper pot anther cone that were observed in this study, regardless of differences in the way in which the pepper pot anther cone was held together, occupied approximately the same area of morphological space.

It is possible that long, thin anthers is a specialisation in anther shape required to also allow for the formation of the pepper pot cone. It is possible that the formation of the pepper pot anther cone and the structural requirements to hold the anthers together by some means require a particular anther shape.

It is also possible that this long and thin anther shape morphology facilitates vibrational pollen release most effectively from a pepper anther pot cone. Greater anther length could reduce the amplitude of vibration required to cause pollen release as more pollen collisions occur within the anther therefore there is greater electrostatic charging of the pollen and easier pollen release (Masuda et al, 1998; Corbert and Huang, 2014). This would theoretically counteract the need for an increase in vibrational amplitude as a result of the anthers being attached together into a cone.

2.5.4: Characterisation and distribution of epidermal cell outgrowths on anther surfaces of *Solanum* and potential functions for these outgrowths

There is great variation in both type of epidermal cell outgrowth present on the surface of *Solanum* anthers and the amount of the anther which is covered by the epidermal cell outgrowths. However, outgrowths of some kind on the surface of the anthers was common, with the majority of species in *Solanum* having some form of outgrowth. Here the anther surface is treated as both the anther sacs and the connective, even though they are different tissues, because to a pollinator this distinction is unimportant and therefore outgrowths of both are worthwhile discussing as the pollinator will come in contact with both.

Outgrowths on the anther surface may be involved in a whole variety of roles: grip, scent production, protecting the anther during buzz pollination, physical guides for placing bees into the 'correct' orientation, altering vibrational transfer, and modifying gross-anther structuring by holding together an anther cone. Little data exist to support any of these roles, but there is considerable evidence to support a function of cellular outgrowths on petals in pollinator attraction (Whitney et al, 2009a; Whitney et al, 2009b; Alcorn et al, 2012).

It is possible that the epidermal cell outgrowths/papillae found on the majority of *Solanum* anthers have a role in facilitating improved pollinator grip on the anther during buzz pollination. On petals, epidermal cell outgrowths in the form of conical cells are present and have been shown to improve grip (Whitney et al, 2009a; Whitney et al, 2009b; Alcorn et al, 2012). However, in *Solanum* the bee does not interact with the petals but instead lands directly onto the anthers themselves. There have been repeated losses of conical cells on the petals of *Solanum* (Alcorn, 2013) and it was proposed that this was because of the lack of a need for them on a surface the pollinator did not directly interact with. This study concludes that there are epidermal cell outgrowths/papillae on the surface of many *Solanum* anthers and it is possible that they could serve this role in improving pollinator grip. The most common placement of epidermal cell outgrowths on the anther surface (as shown in Figure 32) is on the lower half of the anther where the bee grips during buzz

pollination. Therefore, having outgrowths at this position on the anther may improve or alter the way in which the bee grips the anther. The orientation of the papillae/cell outgrowths with their point towards the anther base as seen in Figure 35 possibly also supports this hypothesis. The point may be hooked from above by the claws of the pollinator, providing an improved and firmer grip when sonicating.

These epidermal cell outgrowths/papillae could also increase pollination efficiency by guiding a naïve bee by touch into the 'correct' position for effective buzz pollination. If an area of the anther is rougher, and therefore easier to grip than the rest of the anther, then the pollinator will naturally grip that area, especially if the rest of the anther is smooth and therefore slippery. So this would cause the pollinator to almost automatically slip into the correct position for most efficient buzz pollination, therefore facilitating the learning of the behaviour more easily (Kevan and Lane, 1985). This would be beneficial to both plant and pollinator.

However it should be noted that the conical cells on petals are a different shape to the epidermal cell outgrowths/papillae found on *Solanum* anthers. It is possible that the 'glove-like' epidermal cell outgrowths/papillae are specialised towards improved pollinator grip. Conical cells on petals balance a number of roles (Whitney et al, 2009a; Whitney et al, 2009b; Alcorn et al, 2012), whilst these outgrowths on anthers may not have to balance these various opposing functions and may merely be specialised towards bee grip.

It would make sense that the majority of the species examined have epidermal cell outgrowths if they have such an important role in grip. In this study, while not all the species examined had these epidermal cell outgrowths, a large number of them did (a larger number than were flat). It should also be noted that the data is artificially skewed to appear more even in the presence and absence of such outgrowths due to the inclusion of a disproportionate number of Dulcamaroid clade species. These were examined to try to ascertain whether the clade had any outgrowths at all: and all were found to be flat. Therefore epidermal cell outgrowths would be even more strongly in the majority of species examined had a representative number of species from other clades been examined. For the theory on grip to be proven or disproven, it should be tested through bee behavioural experiments in a flight arena, either using sister species of *Solanum* with similar anther

shapes but differences in epidermal cell outgrowth coverage or fake anthers with contrasting surfaces.

It should be noted that pollinators of various sizes may visit and sonicate any of the *Solanum* anthers regardless of the anther size, therefore the epidermal cell outgrowths/papillae may not always be in the place where the anther is gripped, merely where it is most commonly gripped.

The epidermal cell outgrowths/papillae could also have a role in protecting the anthers from damage during buzz pollination. During buzz pollination the pollinator may grip the anther roughly. Bruising is often observed on the surface of the anther from buzz pollination (Bin and Sorressi, 1973; Morandin et al, 2001). It is possible that the presence of cell outgrowths/papillae could help protect the anther from being pierced by the claws of the pollinator during handling and may keep the anther functional for longer. This hypothesis is also, like the grip hypothesis, supported by the common placement of the epidermal cell outgrowths/papillae in locations on the anther where the pollinator is likely to grip the anther.

Scent production by epidermal cell outgrowths/papillae was initially suggested by D'Arcy et al (1990). It has been recently demonstrated in *S. luridifuscescens* that epidermal cell outgrowths/papillae have secretory activity and produce lipophilic compounds (Falcão and Stehmann, 2018). These are proposed to be an evolutionary step in the direction of more specialised anther connectives such as those seen in other parts of the Cyphomandra clade (Falcão and Stehmann, 2018). In some species of Cyphomandra the anthers are visited in addition by male euglosine bees which 'milk' the secretory tissues (osmophores) at the swollen anther connective to collect scent (Sazima et al, 1993; Bohs, 2007). However other species in the clade are buzz pollinated and visited by female bees, and have papillate anthers (Bohs, 2001; Falcão and Stehmann, 2018). It has been proposed that such papillae, if producing scent, could act as a secondary or primary attractant for pollination, even if the scent is not being collected (Coccuci, 1996; Passarelli and Bruzzone,2004; Falcão and Stehmann, 2018). It is possible that the epidermal cell outgrowths/papillae on the anther surfaces of *Solanum* species have an attractive role to pollinators through scent production, however this would need to be examined and tested outside of the Cyphomandra clade.

There is an added layer of complexity to the understanding of epidermal cell outgrowths on the surface of the anther in a buzz pollinated species, as it is possible that any modification to the anther may or may not alter its vibrational properties and the way energy is transferred during sonication (Passarelli and Cocucci, 2006; Buchmann and Hurley, 1978; King, 1993; King and Buchmann, 1995; King and Buchmann, 1996; De Luca and Vallejo-Marín, 2013; Harder and Barclay, 1994). Anthers may be balancing multiple functions at the same time; traits which might improve pollinator grip or defend against 'pollen robbing' may also dampen the effect of sonication and reduce pollen release. Therefore the combination of anther traits may be a compromise between various factors.

The common placement of the epidermal cell outgrowths/papillae on the anthers of *Solanum* could be for any one of these explanations, or a combination of them. They could also be of no functional or adaptive significance at all. The epidermal cell outgrowths and how they affect grip, protect the anthers, whether they secret scent or alter vibrational transfer, all require further research to better understand them and their potential functions.

2.4.4.1: All heterantherous species examined had only smooth epidermal anther surfaces, except for *S.angustifolium*

Heterantherous species are found throughout the *Solanum* genus, although the anther morphology is rare. It is known to have independently evolved repeatedly throughout the genus (Bohs et al, 2007). All of the heterantherous species that were examined under SEM for this study showed no epidermal cell outgrowths (except for *S. angustifolium*). Heterantherous species were sampled from some parts of the genus where species in the same subclade have epidermal cell outgrowths yet only *S. angustifolium* has any form of epidermal cell outgrowth on the anthers at all. This could be for developmental reasons, adaptive reasons, as a bi-product of anther elongation or reduction associated with forming the feeding anthers and pollinating anthers, or through stochastic drift.

In heterantherous species the pollinator interacts largely with the feeding anthers (Mesquita-Neto et al, 2017), and so does not need to grip onto the pollinating anther. Therefore if epidermal cell outgrowths have a role in pollinator grip then there would be no selective pressure opposing the loss of these outgrowths from the pollinating anther. However, it would be expected that the feeding anthers would still possess these outgrowths as those are the anthers the pollinator directly handles. Yet the feeding anthers were also found to be entirely without epidermal cell outgrowths/papillae.

The only heterantherous species that showed anything other than complete flatness and smoothness along its entire anther length was *S. angustifolium* which had long thin hairs at the base of its pollinating anther. These hairs could be to modify the transfer of vibrations during sonication, perhaps to dampen the affect of sonication (however it should be noted that there are no studies which examine this specifically) on the long thin pollinating anther to make it less sensitive to vibrations and therefore reduce the amount of pollen release or the ease of pollen release (Passarelli and Cocucci, 2006; Buchmann and Hurley, 1978; King, 1993; King and Buchmann, 1995; King and Buchmann, 1996; De Luca and Vallejo-Marín, 2013; Harder and Barclay, 1994). Or in complete contrast, the hairs could act to increase vibrational transfer, acting as vibrational a receiver (Gagliano et al, 2012). However almost nothing is known about how such epidermal cell outgrowths might affect buzz pollination or

vibrational energy transfer in this context and further research would be required to understand if they do serve any purpose and what that might be. If they do serve a role in the control of pollen release in response to buzz pollination there could be adaptive benefits. Pollen wastage would be costly to the plant's fitness and by limiting pollen access, pollen transfer efficiency might be improved (Harder and Barclay, 1994). The hairs could also serve to protect the anther from pollen robbery, or make the flower generally less palatable and so less susceptible to herbivory as hairs have been shown to perform this role in other parts of the plant (Haberlandt, 1914; Woodman and Fernandes, 1991).

It should be noted that it is entirely possible that other heterantherous species in *Solanum* may also have hairs on their pollinating anthers and were merely not sampled by this study.

2.4.4.2: Pepper pot cones in species from different parts of the phylogeny are held together in different ways

The pepper pot cone anther morphology is rare but has evolved repeatedly in parts of the *Solanum* genus (Glover et al, 2004) (Figure 34 A).

It was found that all members of the Tomato subclade with pepper pot anther cones which were examined using SEM had trichome mesh to hold together their anther cone. Lots of members of the Tomato subclade also possessed substantial epidermal cell outgrowth/papillae in addition to the trichome mesh.

It is possible that the anthers of the Tomato subclade are held together in this way because epidermal cell outgrowths are so common in this part of the genus. The Potato clade species in general had both a large amount and variety of epidermal cell outgrowths/papillae on the anther surfaces. The prevalence of epidermal cell outgrowths in the Tomato subclade (and Potato clade as a whole) suggests a possibility that epidermal cell outgrowths are potentially easy to make in this clade. How epidermal cell outgrowths, and in turn the pepper pot cone, develop is a key question which will be examined in the second main part of this thesis, which analyses the trichome mesh of tomato (*Solanum lycopersicum)* from a developmental genetic perspective.

The pepper pot anther cone of *S. dulcamara* is held together using extracellular secretions (Glover et al, 2004). It is possible that this alternative solution to producing the pepper pot anther cone morphology is because species of the Dulcamaroid subclade have lost the ability to produce epidermal cell outgrowths on their anthers. No species examined as part of this study that was part of the Dulcamaroid subclade had any outgrowths on its anthers at all. There are suggestions from the thesis of Katrina Alcorn that the Dulcamaroid clade has lost the ability to make epidermal cell outgrowths on the petals (Alcorn, 2013), and this loss might extend to the anther epidermal surface as well. Therefore for a pepper pot cone to be formed, the anthers must be held together in some other way. It is possible that, as a result of this, forming a pepper pot cone is more difficult in this clade, therefore explaining why only *S. dulcamara* has this morphology out of all the species examined in this study. It is of course possible that there are other species in this clade, not identified in this study, which possess this pepper pot cone morphology in addition to *S.dulcamara*. It is possible that forming a pepper pot cone in the absence of the ability to produce epidermal cell outgrowths is more difficult due to the reduced number of possibilities by which attachment between the anthers could be formed. Therefore pepper pot cones would evolve less frequently (even in clades with highly connivant species such as *S. uncinellum*). However this in turn raises the question of why should *S.dulcamara* form a pepper pot cone if it is so difficult to in this clade?

The selective pressures underpinning pepper pot evolution remain to be explored. This is an area which could be further investigated with bee behavioural experiments to see what benefits to the fitness of a plant the pepper pot cone may produce. It is possible that the pepper pot anther cone improves handling efficiency during buzz pollination, or reduces handling time due to being a larger landing platform that is easier for the pollinator to grip. It would be interesting to investigate how the formation of a pepper pot anther cone could improve these factors relative to a tightly connivent anther cone.

In the Bahamense clade it was confirmed that there was no trichome mesh holding together the pepper pot anther cone. Therefore the pepper pot cone must be held together in some other way. It is possible that it could be held together in the same way as *S. dulcamara*, using extracellular secretions (Glover et al, 2004), but there is no evidence to suggest this is the case. The stellate trichomes on the adaxial side of the anthers of both *S. bahamense* and

S. polyacanthos suggest a possible mechanism by which the pepper pot cone may be held together: the stellate trichomes may become tangled or matted together on the inside of the anther cone. The anthers would thereby be held together from their adaxial sides. Figure 42 provides an illustration of a theoretical cross section showing how this might work. This idea would need to be thoroughly investigated using living specimens to test its likelihood. Only herbarium specimens of the *Bahamense* subclade species were available for use in this study. It is entirely possible that the stellate hairs have nothing at all to do with the pepper pot anther cone and may have another function, or no function at all.

The species of the Tomato subclade *S. juglandifolium* and *S. sitiens* are closely related (Peralta et al, 2008).They do not have the pepper pot morphology or a trichome mesh, but their anthers do have some outgrowths that are trichome-like at the base, on the side of the anther. These might suggest an evolutionary step towards specialisation towards the production of a pepper pot cone.

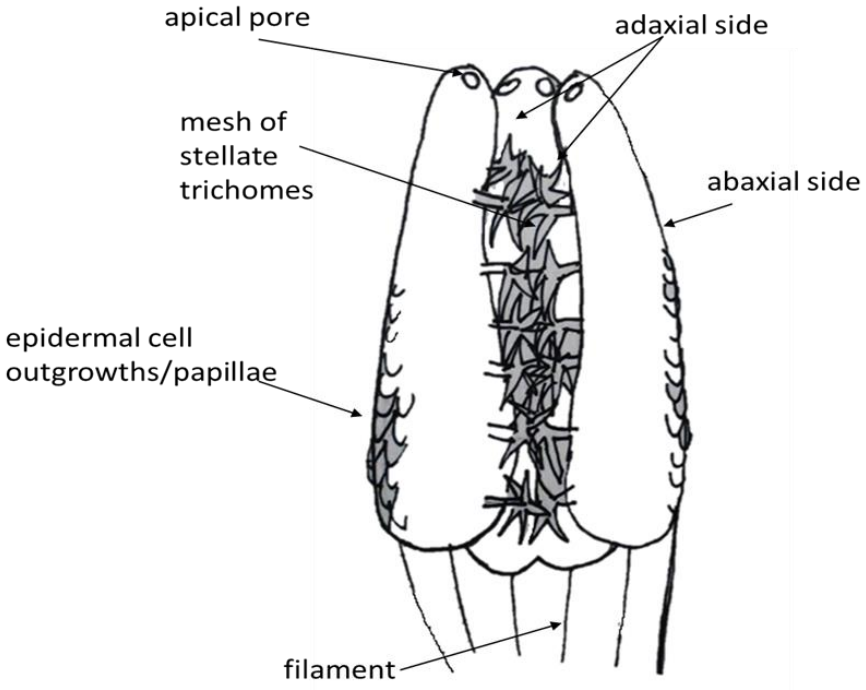

Figure 42. An illustration of a theoretical cross section of *S. bahamense*
This illustration of a theoretical cross section of *S. bahamense* shows a hypothetical mechanism by which the pepper pot anther cone might be held together by a mesh of interlocked/tangled stellate hairs on the adaxial sides of the anthers, thereby holding the cone together from within the centre of the cone. This is purely hypothetical and would need further study to confirm its possibility.

2.6: Conclusions

In conclusion the anthers of *Solanum* are highly variable. There is variation between species and between clades as well as within clades at both a macromorphological and a micromorphological level. This study provides a first examination on this scale of comparisons of morphological space occupation by the anthers of *Solanum.*

Key findings included that there was variation in anther dimension measurements and occupation of morphological space at all levels: between species within clades, between clades and within the genus as a Swhole. Anther dimensions were only weakly correlated with one another, allowing for greater variation in anther form. This may highlight potential explanations for the vast diversity seen in *Solanum*, with great variation in all anther dimensions allowing for distinction between species, isolation and speciation: especially if the anthers can be distinguished between by pollinators.

Epidermal cell outgrowths were both common on the anthers of species throughout *Solanum* and also highly varied in both how much of the anther they covered and in outgrowth form.

Pepper pot anther cones were held together in different ways in different parts of the phylogeny. In the Tomato subclade all pepper pot anther cones were held together by a mesh of interlocking trichomes. This particular trait is investigated from a developmental genetic perspective in *S.lycopersicum* in chapter 3 of this thesis.

Phylogeny was found to constrain morphology to some extent within the genus, but many exceptions were found for all anther traits studied. Particular traits and morphologies were found to evolve repeatedly across the genus.

This study highlighted closely related pairs of species for potential study systems to further investigate anther morphology. Functional and phylogenetic significance of differences in anther dimensions could be a worthwhile area for further study. Another area that would benefit from further research would be the vibrational properties of floral traits in *Solanum* so as to better understand how the anther traits highlighted here interact with buzz pollination from a biophysical perspective. Pollinator behavioural studies would be of great benefit to the understanding of potential significance of anther traits. These could

investigate handling efficiency, ability of pollinators to distinguish between variation in traits and pollen transfer efficiency.

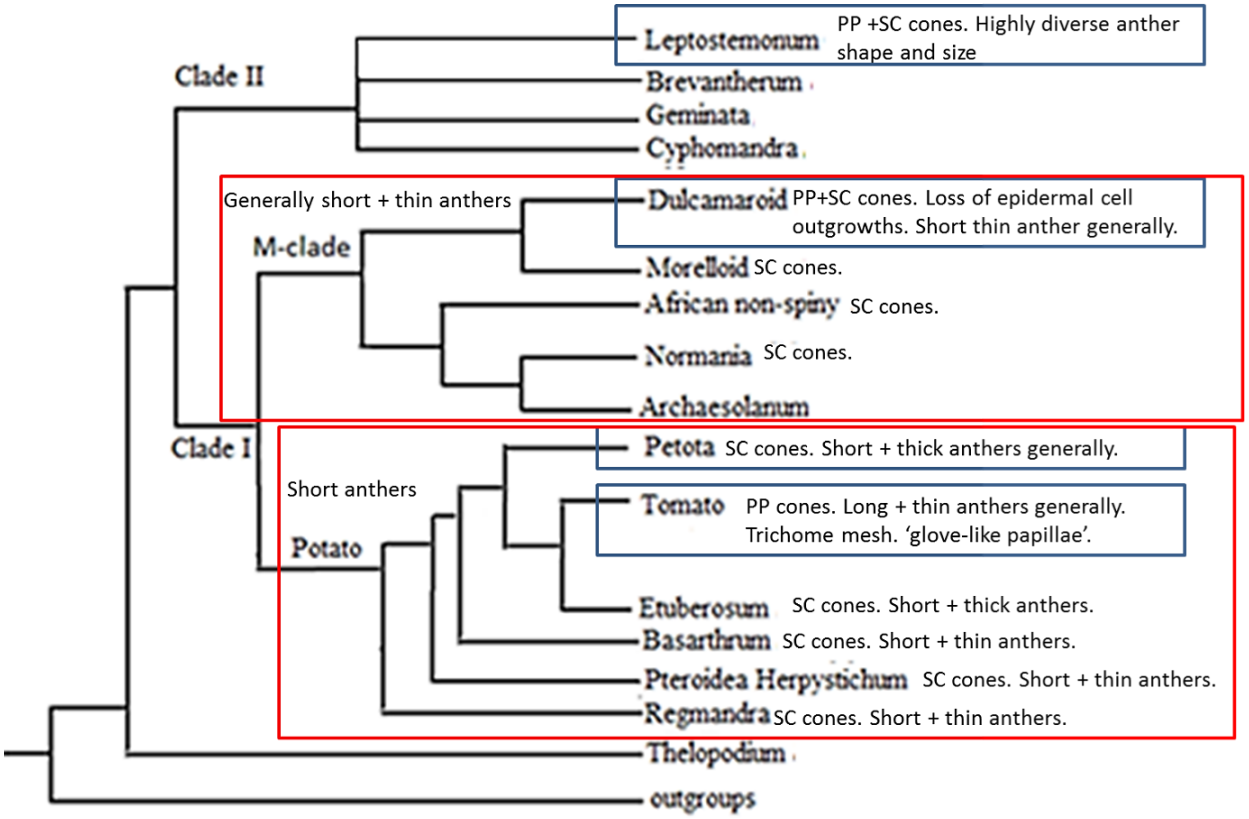

Figure 43 A summary cartoon of the variation of anther form throughout *Solanum.*
This cartoon phylogeny summarises the findings of the study in regards to variation in anther traits throughout the genus. Where Pepper pot (PP) and salt cellar (SC) anther cones are found is indicated to the side of each subclade as well as the general anther shape found in that clade or subclade (however there are important exceptions to this general trend and not all anthers are this shape or size, for example the PP species of the Duclamaroid subclade, *S.duclcamara* has long + thin anthers whilst the subclade generally has short thin anthers.) The loss of epidermal cell outgrowths on the anther surface is indicated in Dulcamaroid. In all other subclades there are epidermal cell outgrowths on some species and not on others and the type of outgrowths varies within the subclade.

Chapter 3: The R2R3 Subgroup 9 genes of *Solanum lycopersicum*

3.1 Overview

In order to better understand the function and evolution of a trait it is important to know how it is formed. This chapter explores the formation of the anther trichome mesh in *Solanum lycopersicum* from a developmental genetic perspective. This was done using a candidate gene approach. The MYB subgroup 9 family of transcription factors are known to be involved in the formation of epidermal cell outgrowths in a highly conserved manner throughout the Angiosperms. Therefore this gene family was explored as candidates for the regulators of the formation of the trichome mesh. The genome of *Solanum lycopersicum* has been sequenced, therefore the distinct motif defining this gene family can be searched for throughout the genome to identify candidate genes.

Once identified, the function of these candidate genes was investigated by ectopically expressing them in *Nicotiana tabacum* (tobacco) which is a model species for transgenic studies due to its ease of transformation and well characterised phenotype. A large number of previous studies have explored the function of MYB subgroup 9 proteins using ectopic expression in tobacco, and these studies allow functional comparison between genes from different species. A further investigation of the function of some of the candidate genes was attempted through CRISPR editing of genes in *Solanum lycopersicum,* albeit with limited success.

The expression of the candidate genes was investigated at different stages of floral development in *Solanum lycopersicum,* and at different stages of the formation of the trichome mesh, to provide correlative evidence about their likely involvement in trichome formation.

The trichome mesh that forms the pepper pot anther cone in *Solanum lycopersicum* is potentially important to the pollination of this economically important plant. An increased understanding of the developmental control of this trait could be used to investigate the way in which it influences pollination efficiency and handling time. Investigating it in *Solanum lycopersicum* creates a genetic toolbox which could be used to better understand the rest of the Tomato subclade of *Solanum* and the formation of the other anther trichome

meshes within this subclade. It could also provide a starting point for further investigation of epidermal cell outgrowth in the Potato clade as a whole and potentially the rest of *Solanum* since the previous chapter demonstrates that epidermal cell outgrowths are an important and varied trait throughout the family.

3.2 Introduction

3.2.1: Transcription factors control development

Transcription factors are found in all eukaryotes and are usually DNA binding proteins (Villar et al, 2014). Transcription factors are known to control gene expression at the level of transcription by binding to the regulatory elements of DNA (Cooper, 2000; Pabo and Sauer, 1992). They may act by blocking/stopping or by up-regulating/initiating transcription of the gene (Diamond et al, 1990; Endt et al, 2002). This modifies synthesis of mRNA by RNA polymerase II (Endt et al, 2002). This cellular function allows transcription factors to precisely regulate gene expression (Villar et al, 2014; Latchman, 1997) and developmental timing in a tissue specific manner, modified by external and internal signals such as hormones or the environment (Endt et al, 2002; Catchman, 1997).

Transcription factors bind to regulatory regions of DNA, singly or in groups, and form a transcription factor complex (Buchanan et al, 2000; Lelli et al, 2012). The regulatory region of a gene contains a promotor/initiation region, enhancer and/or silencer (reviewed Maniatis et al, 1987; Griffiths et al, 2000; Lelli et al, 2012). The regulatory region is usually located upstream of the gene of interest, in the 5' region. It is in the conserved non-coding sequences of DNA, and is not transcribed to RNA (Griffiths et al, 2000). It consists of a set of regulatory elements, of which the main components are transcription factor binding sites (TFBSs) (Griffiths et al, 2000; Lelli et al, 2012). When TFs bind to these sites the configuration of the DNA strand can be altered, along with the ability of the gene to be transcribed and the access that RNA polymerase has to it (Griffiths et al, 2000; Lelli et al, 2012). The core promoter of a gene is the minimum proportion of the regulatory region that needs to be involved for transcription to be initiated (Griffiths et al, 2000, Lelli et al, 2012).

The regulatory region of a gene can also contain enhancers, which, when bound by TFs, enhance transcription by increased recruitment of RNA polymerase to the TF complex (Griffiths et al, 2000; Spitz and Furlong, 2012; Lelli et al, 2012). Silencers may also be present

in the regulatory region, which prevent the interaction of RNA polymerase with the promoter sequence (Griffiths et al, 2000; Spitz and Furlong, 2012; Lelli et al, 2012). TFs that act as repressors bind to these silencers and this results in a reduction or even complete inhibition of transcription. TFs can also catalyse the activity of histone deacetylase, which makes DNA less accessible to transcription by increasing the strength of the association between DNA and histones (histones package and order DNA into nucleosomes). Transcription factors may also recruit corepressor proteins to the transcription factor DNA complex (Griffiths et al, 2000; Spitz and Furlong, 2012; Lelli et al, 2012).

Bound transcription factors can interact with one another, with non-DNA-binding cofactors and with the transcription machinery. TFs bound to enhancers or TFBSs in the regulatory region can affect the recruitment of transcriptional machinery to the core promoter, and the level of subsequent transcription (Griffiths et al, 2000; Spitz and Furlong, 2012; Lelli et al, 2012). Multiple transcription factors can act combinatorically, sometimes acting together to activate transcription, or to repress it or working in competition with each other (Griffiths et al, 2000; Spitz and Furlong, 2012; Lelli et al, 2012). Transcription factors can act antagonistically in the regulation of the same gene with one TF acting as a repressor and the other an activator (Griffiths et al, 2000; Spitz and Furlong, 2012).

RNA polymerase II binds to the TF complex, in the various forms described above, and thereby transcribes an mRNA copy of the DNA template – as a result the gene is expressed (Griffiths et al, 2000; Spitz and Furlong, 2012; Lelli et al, 2012). A combination of van der waals forces and hydrogen bonds allow the interaction and binding between the DNA binding domain of the TF and the corresponding complementary section of DNA (Liu and Bradley, 2012; Farrel et al, 2016; Lelli et al, 2012).

Transcription is one of the key points at which the expression of a gene may be altered and regulation occur (Spitz and Furlong, 2012; Griffiths et al, 2000; Lelli et al, 2012). Other points at which gene expression can be altered and regulated include at the point of translation (before the protein can be synthesised from the RNA template) (Brockmann et al, 2007), during RNA cleavage (Meister et al, 2004) and by RNA splicing (creating splice variants) (Amara et al, 1982).

Other proteins that modify gene expression but that lack DNA-binding domains are not classed as transcription factors but may be essential to gene regulation. Examples include coactivators and corepressors (Horwitz et al, 1996), histone acetyltransferases (Ogryzko et al, 1996) and histone deacetylases (Laherty et al, 1997). Such cofactors modulate the effect of transcription factors (Sande and Privalsky, 1996).

Transcription factors perform many important developmental roles including the regulation of gene expression, cell development, differentiation and growth (Pabo and Sauer, 1992; Lelli et al, 2012). The ability to control expression levels of a gene is extremely important. Differences in expression of the same sets of genes can lead to different phenotypes (Martin et al, 2010; Romero et al, 2014; Stern and Orgogozo, 2008).

Transcription factors are diverse and numerous (Pabo and Sauer, 1992). They comprise a significant proportion of the eukaryote genome (Cliften et al, 2003; Consortium, Mouse Genome Sequencing, 2002; Kellis et al, 2003; Harbison et al, 2004). In Arabidopsis there are over 2000 genes encoding transcription factors, in 60 different protein families. This represents nearly 8% of the genome and highlights the diversity of transcription factors found in plant species (Pérez-Rodríguez et al, 2010). By contrast, in the genome of *Drosophila* the number of transcription factor encoding genes is only 708, or 5% of the total (Hammonds et al, 2013). This demonstrates how much more numerous such genes are in plants as compared to animals. This is thought to be related to the great number of gene and whole genome duplications in the evolutionary history of plants (Cui et al, 2006). The frequency of genome duplication in plants can be partially attributed to their plastic development, which allows tolerance of polyploidy, genome duplication and hybridisation (Adams and Wendel, 2005). For example, the MYB family of transcription factors has only one member in *Drosophila*, three in vertebrate genomes, but two large plant-specific subfamilies including 126 members of the R2R3 MYB transcription factor group and 83 of the 1R group in the Arabidopsis genome (Bailey et al, 2008; Martin et al, 2010). Transcription factors are split into families based on the sequence and structure of their DNA binding domain, which is specific to the target sequences they regulate (Pabo and Sauer, 1992). The DNA binding domain is usually highly conserved, thereby acting as a family specific motif (Pabo and Sauer, 1992). Some examples of transcription factor families include helix-turn-helix (Brennan et al, 1989), steroid receptors (Umesono, and Evans,, 1989),

β-sheet DNA binding proteins (Breg et al, 1990) and zinc-fingers (Lee et al, 1989). Perhaps the most well studied family of plant transcription factors is the MADS box family, containing the ABC genes controlling floral organ development (Coen and Meyerowitz, 1991; Kramer and Hodges, 2010; Bowman et al, 2012). However, transcription factors play many important and varied roles in plant development (Singh, Foley and Onate-Sanchez, 2002; Hake et al, 2004; Dubos et al, 2010; Hay and Tsiantis, 2010; Shang et al, 2011; Bowman, Smyth and Meyerowitz, 2012).

3.2.2: Selection acting on transcription factors drives evolution

At any one time only some of the genes in the genome are expressed (Martin et al, 2010). Duplication of genes and genomes and subsequent sub-functionalisation are a key part of evolution in plants, and are associated with increased complexity (Martin et al, 2010). When a gene is duplicated, it allows an opportunity for directional selection to act on one of the copies whilst the other copy of the same gene maintains the original function: this can allow one of the copies to take on a novel function.

Gene duplication and sub-functionalisation can be especially important when this process acts upon transcription factors, because the control of gene expression is one of the most important points of regulation (Martin et al, 2010; Jacob et al, 1977; Akam, 1995). A single transcription factor can bind multiple target genes. Therefore a number of different genes can be controlled by a transcription factor which can cease or initiate transcription of collections of genes at the appropriate developmental stage. As a result, changes to a single transcription factor can change an entire genetic pathway, thereby altering expression timing, amount and tissue specific expression, as the transcription factor acts as a master regulator. Differences in gene expression of the same set of genes can lead to very different phenotypes (Martin et al, 2010; Doebley and Lukens, 1998, Weber et al, 2007). Many important evolutionary innovations are thought to have originated as a result of duplication and subsequent sub-functionalisaton of transcription factors eg: repeating body segments in arthropods (Jacob, Series and Jun, 1977; Akam, 1995).

3.2.3: A general introduction to plant development and the role of transcription factors.

Plant development and growth is controlled by a combination of hormonal and transcription factor regulation (Maughan et al, 2006; Rast and Simon, 2008; Galinha et al, 2009). In plants,

vegetative growth is both indeterminate and very plastic (Rast and Simon, 2008; Nieuwland et al, 2009). Growth is centred at the meristems: the root apical meristem and the shoot apical meristem (Nägeli, 1858; Steeves and Sussex, 1989). These apical meristems are maintained in an undifferentiated state by the action of homeobox transcription factors known as KNOX proteins (Braybrook and Kuhlemeier, 2010; Hay and Tsiantis, 2010), and a population of stem cells is maintained at the centre of the apical meristem through the action of the transcription factor WUSCHEL (Schoof et al, 2000). However, when switching to floral development, changes occur at the shoot apical meristem which switch development from plastic and indeterminate to deterministic; which ends with the production of a flower. WUSCHEL is first suppressed by the actions of the CLAVATA signalling cascade (reviewed in Somssich et al, 2016; Brand et al, 2000; Schoof et al, 2000), which allows for the differentiation of stem cells at the shoot apical meristem and deterministic growth begins. This cell differentiation is then guided by organ specific transcription factors of the MADS-box protein family (Coen and Meyerowitz, 1991; Kramer and Hodges, 2010; Bowman et al, 2012). The MADS-box family of transcription factors is highly expanded in flowering plants with many plant-unique functions and is particularly important in the development of the floral organs (Martin et al, 2010). *KNOX* expression is also suppressed by the plant growth hormone auxin, which results in the development of the organ primordia (Braybook and Kuhlemeier, 2010).

While floral development involves thousands of diverse genes, these are controlled by the smaller number of MADS-box transcription factors, which act as master regulators (Soltis et al, 2009) of the developmental processes involved in the creation of floral organs in successive whorls (Coen and Meyerowitz, 1991; reviewed in Ma, 1994; Weigel and Meyerowitz, 1994; Shore and Sharrocks, 1995; Irish, 2017). In the ABCDE model of floral development (Coen and Meyerowitz, 1991; Bowman et al, 2012; reviewed in Irish, 2017) these transcription factors act in combination with one another to specify organ identity of each whorl. A class genes expressed alone result in the formation of sepals, A and B combined result in petals, B and C combined result in anthers and C expressed alone results in carpels (Coen and Meyerowitz, 1991; Kramer and Hodges, 2010; Bowman et al, 2012; Irish, 2017). The D function genes are involved in the specification of ovule identity whilst E

function genes are required for the correct development of floral organs overall (Colombo et al, 1995; Pelaz et al, 2000; Theissen 2001; Soltis et al, 2009).

3.2.4 Stamen development.

Stamen development has been studied extensively in *Arabidopsis thaliana* (reviewed in Scott et al, 2004) and tobacco (Koltunow et al, 1990; Drews et al, 1992; reviewed in Goldberg et al, 1993).

Stamens develop in the third whorl of the flower and begin as a set of small bumps called the anther primordia (Coen et al 1991; Coen and Meyerowitz, 1991; reviewed Goldberg et al, 1993; reviewed in Scott et al, 2004). In tobacco this happens over ~two days (Koltunow et al, 1990). It occurs generally after the sepals and petals but before the carpel primordia have initiated (reviewed in Goldberg et al, 1993). The development of the stamen primordia from the floral meristem is specified by the combination of B and C function proteins. In *Arabidopsis* the genes that code for the transcription factors that control anther primordia specification are *PISTILLATA (PI), AGAMOUS (AG)* and *APETALA3* (AP3). Counterparts to these genes have been found in a number of species including tobacco (Hansen et al, 1993; reviewed in Goldberg et al, 1993), *Antirhinum majus* (Schwarz-Sommer et al, 1990; Coen 1991; Coen and Carpenter, 1993) and tomato (Pnueli et al, 1991). The proteins encoded by these genes contain a conserved MADS box region which acts as the DNA binding domain (Coen and Meyerowitz, 1991) and result in a transcriptional cascade which causes the differentiation of anther cell types in this whorl.

Once each stamen primordium has developed it differentiates into two compartments: one of which (the basal region) will become the filament and the other of which (the upper region) will become the anther (Goldberg et al, 1993; Scott et al, 2004). The locules are then established in the anther section (Goldberg et al, 1993; Scott et al, 2004). The B and C function genes will continue to be expressed throughout anther development. Activity of at least one of the *SEPALLATA* (*SEP*) genes (the E function genes) is also required and is necessary for correct organ formation (Bowman et al, 1991; Pelaz et al, 2000; Jack, 2001).

Next the major anther tissue and cell types form, including the microsporangium which ultimately produces the pollen grains (Goldberg et al, 1993; Scott et al, 2004). The anthers

will reach their full length and the filament elongates just before the flower opens. Once the flower has opened dehiscence will occur in most anthers.

A search of the literature found no papers that investigated the development of poricidal anthers specifically, although there have been some studies on aspects of anther development in tomato such as the role of jasmonate, auxin or various individual MADS-box genes (Ursin et al, 1989; Chmelnitsky et al, 2003; Dobritzsch et al, 2015; Cardarelli and Cerchettii, 2014; Guo et al, 2016).

3.2.5: R2R3 MYB transcription factors

The first Myb transcription factor that was identified and investigated was the *V-MYB* oncogene (Carr and Mott, 1991). This gene has a role in avain myeloblastosis (Carr and Mott, 1991; Oh and Reddy, 1999). It was then found that there were homologous genes to this across all main eukaryotic lineages and that this was an ancient and large family of transcription factors (Lipsick, 1996; Jiang et al, 2004; Yanhui et al, 2006).

There are four main groups of the plant MYB proteins, with many important functions including roles in regulating the control of secondary metabolites and cell fate determination. These groups of MYBs are determined by the number of repeats of the R motif (the DNA binding domain) they contain (Martin and Paz-Ares, 1997; Ares, 1997; Kranz et al, 1998; Dubos et al, 2010). MYB proteins contain a minimum of one copy of the R motif, an approximately 50 amino acid motif which is semi-conserved throughout the family of transcription factors (Lipsick 1996; Kranz et al, 1998; Romero et al, 1998; Jin and Martin, 1999; Dobos et al, 2010). The groups that the MYB proteins are separated into in this way are the 3RMYBs, the 4RMYBs, the heterogeneous MYB-related proteins and the R2R3 MYB proteins.

The R2R3 MYB proteins are a plant specific family of transcription factors which contain two copies of the MYB DNA binding domain (Meese et al, 1989) and carry out plant specific functions (Martin and Paz-Ares, 1997; Kranz et al, 1998; Dubos et al, 2010). They are one of the largest families of transcription factors (Stracke et al, 2001; Dubos et al, 2010). Each of these sequence-specific DNA binding domains forms a helix-turn-helix motif (Carr and Mott,

1991). In *Arabidopsis thaliana* there are 126 genes which code for R2R3 MYB transcription factors (Dubos et al, 2010).

The R2R3 MYB protein family can be further separated into subgroups based on other conserved motifs contained within them (Stracke et al 2001; Dubos et al, 2010). These separate subgroups often have functions specific to them (Stracke et al, 2001). For example, subgroup 15 has been demonstrated to be involved in epidermal patterning and the formation of root hairs and other trichomes (Dubos et al, 2010). Examples of such proteins include WEREWOLF/AtMyB66 and GLABROUS1/AtMYB0 (Dubos et al, 2010). Subgroup 12 R2R3 Myb proteins are involved in the control of glucosinolate metabolism (Dubos et al, 2010). Subgroup 9 proteins regulate epidermal cell outgrowths and projections such as conical cells or trichomes (summarised in Brockington et al, 2013.)

3.2.6: The R2R3 MYB transcription factor subgroup 9 proteins and their involvement in regulating epidermal cell outgrowth

The R2R3 MYB subgroup 9 subfamily of proteins is an ancient lineage (Brockington et al, 2013) that is especially important in the control of epidermal cell modifications. Members of this protein family have the R2R3 MYB DNA binding domain composed of the R2 and R3 repeats (Jin and Martin, 1999) and also share their own subgroup 9 domain which forms a conserved motif of amino acid sequence (Stracke, Weber and Weisshaar 2001). Duplication within this subfamily early in land plant evolution led to the creation of two lineages: 9A and 9B (Brockington et al, 2013). These lineages then each underwent further duplication and sub-functionalisation, leading to the R2R3 subgroup 9 family having four clades of genes in eudicots (Brockington et al, 2013), illustrated in Figure 44. These four sub-clades are (subgroup 9A) *MIXTA* and *MIXTA-like,* (subgroup 9B) *Myb17* and *Myb17-like.* Subgroup 9A and 9B proteins perform a range of functions in control of epidermal cell outgrowth development, but the roles of the subgroup 9B genes are less well understood than those of subgroup 9A.

The R2R3 MYB subgroup 9 proteins are involved in regulation of expression of genes involved in directional cell outgrowth, producing trichomes, conical cells and papillae. These epidermal cell outgrowths have been shown to follow the same developmental pathway, with differences in the timing of expression resulting in the different morphologies: if cell

division has finished when cell outgrowth occurs then expression will result in conical cells, however expression during cell division will result in the development of multicellular trichomes (Glover et al, 1998). This role has been demonstrated and functionally characterised in a variety of species and shown to be a conserved role throughout the angiosperms (reviewed in Brockington et al, 2013; Baumann et al, 2007; Noda et al, 1994; Jaffe et al, 2007; Machado et al, 2009; Walford et al, 2011). R2R3 subgroup 9 genes have been particularly well characterised in *Arabidopsis thaliana* (the *AtMYB16, AtMYB17* and *ATMYB106* genes) (Baumann et al, 2007; Gilding and Marks, 2010; Pastore et al, 2011), *Petunia hybrida* (the *PhMYB1* gene) (Baumann et al, 2007) and *Medicago truncatula* (the *MtMYBML3* gene). In cotton (*Gossypium hirsuta*) the genes *GhMYB25* and *GhMYB25-like* have been shown to be involved in trichome regulation. *GhMYB25* in the regulation of trichome density and also the elongation of cotton fibres (Machado et al, 2009) whilst GhMYB25-like is a regulator of cotton fibre development and initiation, (Walford et al, 2011).

R2R3 MYB subgroup 9 genes were first shown to be involved in epidermal cell outgrowth in *Antirhinum majus,* where the expression of the subgroup 9A gene *MIXTA* in the petal epidermis was found to result in the formation of conical cells (Noda et al, 1994). It was shown that the *MIXTA* gene was both sufficient and necessary for the production of conical cells (Noda et al, 1994; Glover et al, 1998; Martin et al, 2002). Four subgroup 9A genes have been described in *Antirrhinum majus* (Noda et al, 1994; Perez-Rodriguez et al, 2005; Jaffé et al, 2007; Baumann et al, 2007), all involved in epidermal cell outgrowth of some kind. *AmMYBMX (MIXTA)* (Glover et al, 1998; Noda et al, 1994) is required for conical cell development in the petal epidermis. *AmMYBML1 (Antirrhinum majus MYB MIXTA-LIKE1)* is involved in the differentiation of various types of petal epidermal cell including petal conical cell and trichome development, and ventral petal hinge formation (Glover et al, 1998; Perez-Rodriguez et al, 2005). This gene is also expressed earlier in floral development than *MIXTA* (Glover et al, 1998; Perez-Rodriguez et al, 2005.) *AmMYBML2* (*Antirrhinum majus MYB MIXTA-LIKE2*) (Perez-Rodriguez et al, 2005; Martin et al, 2002; Baumann et al, 2007) has also been shown to induce epidermal cell outgrowths in the form of conical cells when ectopically expressed in tobacco. It is expressed late in petal development in *A.majus* and is a positive regulator of conical cell development (Baumann et al, 2007). *AmMYBML3*

(*Antirrhinum majus MYB MIXTA-LIKE3*) is expressed only in outgrowing epidermal cells of all ariel organs, ectopically expressing it in tobacco results in the formation of conical cells on the usually flat tobacco carpel (Jaffé et al, 2007).

However, despite the wealth of studies examining members of this transcription factor family, it should be noted that there has not prior to this been a study which examined all members of the subgroup 9 family from a single species.

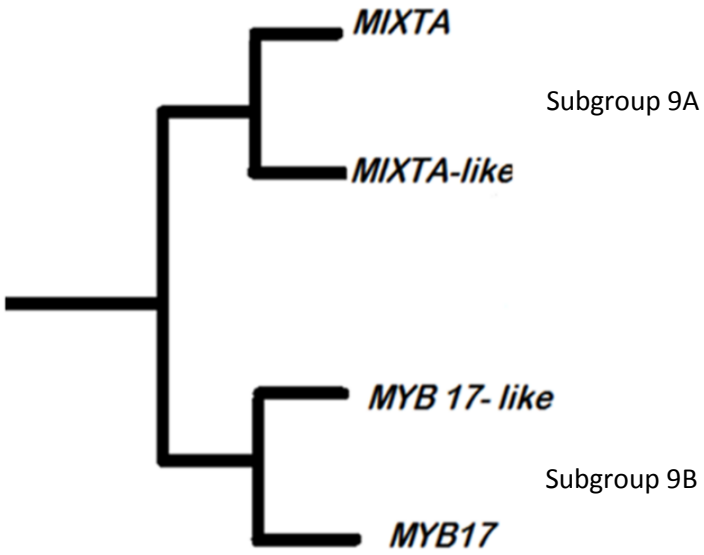

Figure 44: Cartoon of the phylogeny of R2R3 MYB subgroup 9 family of transcription factors
This cartoon phylogeny is based on (Brockington et al, 2013). The family is broken up into two subclades; Subgroup 9A and Subgroup 9B. These are then further subdivided into the following clades: subgroup 9A: *MIXTA* and *MIXTA-like* and subgroup 9B: *Myb17* and *Myb-17-like.*

3.2.7: The 'pepper pot' anther cone in *Solanum lycopersicum* is held together by a trichome mesh

In *Solanum lycopersicum* (tomato) the anthers are held together into a 'pepper pot' anther cone as defined in section **2.1.3.1.3**. The anthers in this pepper pot cone are held together by a mesh of trichomes (Figure 40 in section **2.3.5.4**).

It was concluded in section **2.3.5.4.** that all members of the Tomato subclade of the Potato clade of *Solanum* which have a pepper pot anther cone (and were examined as part of this

study) are held together in the same way: by a mesh of trichomes. It is likely that this mesh follows the same developmental control pathway in all species in this subclade.

It is unknown how the formation of this trichome mesh is controlled developmentally. This study aims to investigate this from a developmental genetic perspective to better understand how the trichome mesh forms and how its formation is controlled. It was hypothesised that the trichome mesh is regulated by Subgroup 9 R2R3 MYB proteins, since these are well characterised regulators of cellular outgrowth.

3.2.8: Trichome development in *Arabidopsis.*

The trichomes of Arabidopsis thaliana are unicellular, branched and regularly distributed on the epidermis (Pesch, 2004). The development of trichomes in Arabidopsis is regulated by a network of transcription factors from various TF families and has been well characterised (reviewed by Pattanaik et al, 2014; Uhrig and Hülskamp, 2010; summarised by Yang et al, 2011). Within the R2R3 MYB family, the gene GLABROUS1 (GL1) encodes a protein which acts as the key regulator in trichome formation (Marks and Feldmann, 1989; Oppenheimer et al, 1991). AtMYB23 (Oppenheimer et al, 1991; Kirik et al, 2001) and AtMYB82 (Liang et al, 2014) are also involved in the regulation of trichome development. The TESTA GLABRA1 (TTG1) gene (Walker, 1999), which encodes a WDR protein, is required for trichome formation to occur (Koornneef, 1981) and acts as a scaffold for the transcriptional complex. GLABRA3 (GL3) and ENHANCEROFGLABRA3 (EGL3) (Zhao et al, 2008) encode members of the bHLH family of transcription factors (Heim et al, 2003). Together these TFs form the MBW (MYB-bHLH-WDR) activation complex GL3/EGL3-GL1-TTG1. This complex results in the activation of trichome formation by regulating expression of various downstream targets. In particular, it activates expression of the genes GLABRA2 (GL2) (Rerie et al, 1994) and ENHANCEROFGLABRA2 (EGL2) (Larkin et al, 2003; Serna, 2004), whose protein products are necessary for trichome outgrowth. The complex also induces the expression of genes which encode repressors of trichome formation: TRIPTYCHON (TRY), CAPRICE (CPC) (Wada et al, 1997; Wada et al, 2002) and Trichomeless1(TCL1) (Wang et al, 2007). The proteins encoded by these genes move laterally in the epidermis, repressing trichome development in neighbouring cells and thereby forming the basis of the patterning system.

Whilst the trichome development of Arabidopsis is well understood and well described, the genetic module regulating Arabidopsis trichomes was not considered in this study. Both N.tabacum and Solanum are within the Asterid clade whilst Arabidopsis is within the Rosids. It has suggested that the Asterid and Rosid clades follow a different regulatory pathway for trichome development (Serna and Martin, 2006). Ectopic expression of the GL1 gene from Arabidopsis in N.tabacum did not result in ectopic trichome formation, nor did the ectopic expression of the A.majus MIXTA gene in Arabidopsis (Payne et al, 1999). Phylogenetic analyses suggest that the GL1 clade of MYB TFs arose within the Rosids, and since this is the key regulator of Arabidopsis trichomes it was considered unlikely that the Arabidopsis developmental programme would be similar to the tomato one.

3.2.9: The classic trichome mutants of *Solanum lycopersicum.*

There are a number of trichome mutants known in tomato, all identified in classical genetic screens.

The hairless (hl) mutant is a recessive mutation with a phenotype of abnormal trichome formation that results in trichomes which are distorted, bent, twisted and shortened on all tissues (Alvin and Reeves, 1977; Kang et al, 2010) and also has brittle easily broken stems (Dempsey and Sherif, 1987; Kang et al, 2010). There is also a reduction in the accumulation of polyphenolic compounds and sesquiterpenes in the glandular trichomes of this tomato mutant (Kang et al, 2010). The Hairless gene was recently cloned using a map-based approach (Kang et al, 2016) and found to encode a SRA1 subunit, which is involved in the control of actin filament nucleation. Normal trichome development was restored in the hl mutant when WT SRA1 cDNA was expressed (Kang et al, 2016).

The recessive dialytic mutant (dl) exhibits the loss of all trichome formation on the anthers. Therefore the anthers develop separately and are not fused (Rick, 1947; Glover et al, 2004). This lack of a trichome mesh attaching the anthers results in the anthers developing splayed in a star shape (Glover et al, 2004). There is also a reduced fruit set (Glover et al, 2004). The leaf trichomes are abnormal in this mutant phenotype, but still present (Glover et al, 2004).

The dominant Woolly (Wo) mutant is a naturally arising spontaneous tomato mutant. The phenotype involves excess trichome development which also results in a reduced number of

stomata (Glover et al, 2000). The Woolly (Wo) gene encodes a homeodomain protein which appears to interact with, and regulate the expression of, SlCycB2 which is necessary for cell division and therefore involved in the formation of trichomes (Yang et al, 2011).

The hair-absent (h) is a recessive mutation which results in a phenotype lacking in long trichomes except on the hypocotyl (Reeves, 1977). The Hair (H) gene has recently been shown to encode a C2H2 Zinc-finger protein which is involved in trichome formation in the same regulatory pathway as Wo and that knockdown of either H or Wo results in the hair-absent phenotype (Chang et al, 2018).

It is of interest that the only tomato trichome mutant in which the trichomes of the anthers are affected severely enough to result in the loss of the fused anther cone is the dialytic (dl) mutant. In hairless (hl) and hairs absent mutants, the trichome mesh of the anthers is unaffected. In the Woolly mutant the trichome mesh is also present, though the trichomes appear longer and more numerous in the trichome mesh than in WT, but the pepper pot anther cone is maintained.

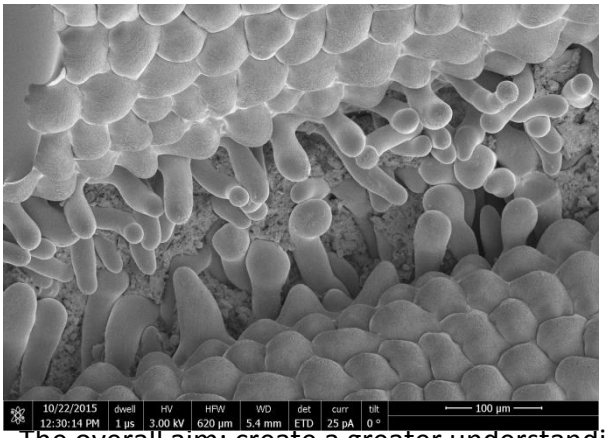

Figure 45: The trichome mesh of the hairless (hl) tomato mutant.

The trichome mesh is maintained even though trichome formation on other tissues is abnormal.

SEM taken with student Caroline Stone.

The overall aim: create a greater understanding of the development and control of the tomato trichome mesh from a developmental genetic perspective.

- Identify all R2R3 Myb Subgroup9 genes in *Solanum lycopersicum.*
- Explore the functionality of these proteins by ectopically expressing each candidate gene in tobacco.
- Analyse expression patterns of these genes in tomato using semi quantitative RT-PCR.
- Further examine gene functionality of some of these candidate genes, as determined by the results of the other aims, by using CRISPR gene editing in tomato.

3.3 Methods

3.3.1: Laboratory reagents and supplies.

Standard laboratory reagents and chemicals were supplied by the following: Fisher Scientific (Loughborough, UK), VWR (Leicestershire, UK), BDH Laboratory Supplies (Poole, UK), Sigma-Aldrich (Dorset, UK). Restriction endonucleases were from New England Biolabs (NEB, Hertfordshire, UK). EcoTaq DNA Polymerase was made in house. Phusion High Fidelity DNA Polymerase was purchased from Thermo Scientific (Paisley, UK). All oligononucleotide primers were ordered from Integrated DNA Technologies (IDT Primers, Leuven, Bulgaria). Antibiotics and Bacterial culture reagents were supplied by Becton, Dickinson and Co. (Sparks, MD, USA), Sigma-Aldrich (Dorset, UK), Oxoid, Ltd (Basingstoke, UK) and Melford Laboratories (Ipswich, UK). Kits and reagents not mentioned here are detailed in the text sections to which they are relevant. Recipes and protocols for media and solutions can be found in Appendix 6

3.3.2: General methods:

3.3.2.1: Preparation of plant tissue prior to DNA/RNA extraction.

For isolation of MYB Subgroup 9 genes from *Solanum lycopersicum*, tissue was harvested from flowers, young leaves, buds of various floral growth stages, cotyledons, young roots, hypocotyl (from seeds germinated hydroponically for a week: in an autoclaved conical flask, floating in MS (recipe in Appendix 6) on a shaker) and apical meristem. Plants were grown in the greenhouse at the Department of Plant Sciences, Cambridge and at the Cambridge University Botanic Garden greenhouses (for further details see **3.3.3:** on growth information). These plant tissue samples were flash frozen using liquid nitrogen. Pools were made from the various tissues to maximise ability to isolate all genes. Tissue selection for isolating of genes was guided by use of the Tomato efp Browser at Bar. UToronto.ca, Rose Lab Atlas, http://bar.utoronto.ca/efp_tomato/cgi-bin/efpWeb.cgi which provided predictions of expression profiles within different tissues of *Solanum lycopersicum*. Tissue was ground to a fine powder in liquid nitrogen in 1.5ml Eppendorf tubes using micropestles. Ground tissue was stored at -80˚C until use.

For genotyping of transgenic tobacco from the ectopic expression experiment, tissue from young leaves and buds was frozen in liquid nitrogen and ground to a fine powder using micropestles.

Material for sqRTPCR analysis of expression levels was collected from wildtype *Solanum lycopersicum* plants that were separated into three pools: A, B and C. These were frozen in liquid nitrogen. Within each of these pools, material was collected from various floral stages and treated separately. Leaf material of A, B and C was also collected to use as a background control. All pools and all floral stages were ground separately to a fine powder using micro-pestles in liquid nitrogen.

3.3.2.2: Nucleic acid extraction.

3.3.2.2.1: RNA/DNA extraction using CTAB buffer.

RNA was extracted by the CTAB buffer RNA extraction protocol method to confirm transgene expression in lines of transgenic tobacco. Tissue from young leaves and buds was collected, snap frozen in liquid nitrogen and ground to a fine powder. ~100mg of tissue was used for each extraction with 1500µl of CTAB extraction buffer per sample (recipe in Appendix 6). The extraction buffer was warmed to 55˚C. Once warmed, 300µl of 2-mercaptoethanol was added to inhibit RNAse by denaturation. This was mixed by inversion. 700µl of this combined extraction buffer was added to each sample tube and vortexed for 1 minute. 700µl of chlorophorm:isoamylalcohol (24:1) was added to each sample and vortexed for 1 minute. The mixture was then incubated at 55˚C for 15 minutes. After this the sample was centrifuged at 10,000rpm for 15 minutes at 4˚C. All steps from here on were conducted on ice, unless otherwise stated. The supernatant was transferred to a fresh tube to which an equal volume of chloroform:isoamylalcohol (24:1) was added. The tube was vortexed for 30 seconds and then centrifuged at 10,000rpm for 15 minutes at 4˚C. The supernatant was transferred to a fresh tube. 1/3 volume of 8M chilled LiCl (~200µl) was added to precipitate the RNA. The samples were incubated at 4˚C overnight. The following day the RNA was pelleted by centrifuge at 10,000rpm for 20 minutes at 4˚C. The supernatant was removed (and could be used for extraction of gDNA if required). 150µl of chilled 3M NaAc was added to the pellet of RNA. 2.5x volume (~500µl) of 100% ethanol was added. This was centrifuged at 13,000rpm for 20 minutes. The supernatant was discarded

and the pellet then washed with 70% ethanol. The pellet was air dried over ice. The RNA was dissolved in 25-30µl of autoclaved deionised water and stored at -80˚C.

3.3.2.2.2: RNA extraction using TRIZOL buffer.

RNA extraction for sqRTPCR and for some transgenic tobacco genotyping was done using the Trizol buffer protocol. Material was collected from various tissues (as outlined in section 2.8.1), snap frozen in liquid nitrogen and ground into a fine powder. 1000µl Trizol extraction buffer was added to 100mg of ground tissue. This was vortexed for 10 seconds. The mixture was centrifuged at 4˚C for 5 minutes at 1,000rpm to remove any unbroken lumps of tissue. The supernatant was transferred to a fresh tube and left to incubate at room temperature for 5 minutes. 200µl of 100% chloroform was added and mixed by inversion. This was incubated at room temperature for a further 5 minutes. The mixture was centrifuged at 12,000g for 15 minutes at 4˚C, 500µl of the upper phase was removed and transferred to a fresh tube. 200µl of 100% chloroform was added and incubated for 5 minutes before centrifugation for 15 minutes at 4˚C. 500µl of the upper phase was transferred to a fresh tube. 500µl of isopropanol was added to this supernatant and mixed by inversion. This was incubated for 10 minutes at room temperature to precipitate the RNA. This was pelleted by centrifuge at 12,000rpm for 10 minutes at 4˚C. The pellet was washed in 1ml 70% ethanol, centrifuged at 12,000rpm at 4˚C. The liquid was removed and the pellet air dried over ice. The RNA was re-suspended in 20-30µl of autoclaved deionised water. The recipe for the Trizol RNA extraction buffer can be seen in Appendix 6.

3.3.2.2.3: RNA extraction using Concert Plant™ RNA Reagent.

This RNA extraction method was used for isolation of all MYB Subgroup 9 coding sequences in *Solanum lycopersicum.* Fresh young tissue was collected from wild type *Solanum lycopersicum* and snap frozen in liquid nitrogen as described above. This material was ground to a fine powder in liquid nitrogen using micropestles. RNA was extracted from 100-200mg of the frozen tissue. 500µl of cold Concert™ Plant RNA Reagent (Invitrogen) was added to each Eppendorf of tissue. This was then incubated at room temperature for five minutes and then centrifuged at 12,500rpm for 2 minutes at 4˚C. The supernatant was transferred to a fresh tube containing 100µl of 5M sodium chloride and 300µl of 100%

chloroform and mixed by inversion. This tube was then centrifuged for 10 minutes at 12,500rpm at 4˚C. The supernatant was removed and added to a fresh tube containing an equal volume of 100% isopropanol, to precipitate the RNA for ten minutes at room temperature. The RNA was pelleted by centrifuge at 12,500rpm for 10 minutes at 4˚C. The pellet was washed with 1ml of 70% ethanol and centrifuged for 3 minutes at 12,500rpm. All liquid was removed and the pellet left to dry in air. The RNA was re-suspended in 25-30µl of sterile deionised water. RNA was stored at -80˚C.

3.3.2.2.4: DNase treatment for removal of gDNA contamination in RNA.

DNase treatment was conducted using DNase I and RNase free 'homemade' buffer (Ambion DNase enzyme 10x, 100mM Tris HCl pH7.5, 1mM $CaCl_2$, 25mM $MgCl_2$). This could be done straight after RNA extraction by any of the methods.

DNase treatment using 'homemade buffer' method	
RNA	10µg
homemade buffer'	10µl
Dnase I	1.5µl
H2O	vary to make up to total
total	**100µl**
incubate 1 hour 37˚C	
note: if insufficient RNA then use all there is extracted.	

Figure 46: Reaction conditions for DNase treatment of RNA using 'homemade buffer' method.

After DNase treatment, the RNA must undergo Phenol:Chloroform purification.

3.3.2.2.5: Phenol:Chloroform purification of DNase treated RNA.

One volume (usually 100µl) of chilled phenol:chloroform isoamyl alcohol (24:1) was added to the RNA. This was mixed by vortex for 10 seconds. The mixture was centrifuged for 5 minutes at 13,000rpm at 4˚C. The upper phase was transferred to a fresh tube to which 3 volumes of chilled 100% ethanol was added (usually ~300µl). 1/10 x volume (~30µl) of chilled 3M NaAc pH5.5 was added and mixed by inversion. The mixture was incubated for 15 minutes at -20˚C, before being centrifuged for 20 minutes at 13,000rpm at 4˚C. All the liquid was removed and the pellet washed in 1ml 70% ethanol. This was centrifuged for 5 minutes

at 13,000rpm at 4˚C. The ethanol was removed and the pellet air dried over ice. The pellet was re-suspended in 20-30µl of autoclaved de-ionised water.

3.3.2.2.6: cDNA synthesis.

cDNA was synthesised for general use using BioScript™ (Bioline) following manufacturer's instructions. For each sample, ~1µg of DNase treated-purified RNA was put into a PCR tube. This was made up to 11µl with autoclaved diH2O. This mixture was incubated for 5 minutes at 70˚C in a thermocycler, after which it was immediately transferred to ice. In a second tube the following was mixed together (multiplied by the number of samples) 1µl oligo dT (10µM), 1µl 40mM dNTP mix (10mM each), 4µl BioScript reaction buffer (5x), 1µl autoclaved diH2O, 1µl BioScript reverse transcriptase, 1µl RNase inhibitor. Then 9µl of this mixture was added to each tube of RNA. This was incubated at 42˚C for 40 minutes. The reaction was stopped by heating the mixture to 85˚C for 5 minutes. cDNA was then stored at -20˚C until use.

cDNA was synthesised for semi-qRTPCR using Superscript II retrotranscription kit (Invitrogen), following the manufacturer's instructions. ~1.5µg of RNA was transcribed for each tissue. cDNA amount used for each tissue in each semi-qPCR reaction was adjusted so that PCR amplification of the housekeeping gene in each tissue appeared approximately the same. The housekeeping gene/reference gene used for the semi-qPCR was the tomato CAC gene (SGN-U314153, clathrin adaptor complex subunit), which was shown to have consistent and stable expression levels in tomato and therefore was selected as the housekeeping gene, as it was especially recommended for use in studies using floral tissue (Expósito-Rodríguez et al, 2008). The primers used were those described in (Expósito-Rodríguez et al, 2008).

3.3.2.3: Standard Gel Electrophoresis using TBE buffer for visualisation of nucleic acids.

0.8% w/v electrophoresis grade agarose was dissolved in 0.5 x TBE (see Appendix 6 for recipe) by heating for 2 minutes in the microwave. This molten gel was cooled and then poured into a 200ml, 100ml or 50ml gel tray as required. 1-2µl of ethidium bromide was added (to create a final concentration of ~0.1µgml^{-1}) and mixed into the molten gel before it cooled to the point of solidifying. A plastic comb was added to create the required

size/number of wells. The gel was left to set for 20-30 minutes. The gel was placed in an electrophoresis tank and submerged in 0.5xTBE. 2µl of loading buffer (see Appendix 6 for recipe) was added to 5-12µl of sample and was transferred into the gel's wells alongside 1kb ladder (Bioline) or 100bp ladder (Bioline) depending on predicted band size. For RNA, 3-6µl of RNA was added to 2µl of loading buffer and made up to 10µl with autoclaved DI water. An electric current was applied at 111V using a Consort $E8_{35}$ powerpack (Sigma-Aldrich) until the dye neared the end of the gel. The gel was then removed and photographed under UV light.

3.3.2.4: Gel extraction.

Bands of desired DNA were cut from the gel using a scalpel. These were purified using PureLink™ Quick Gel Extraction Kit K210012, Invitrogen (Thermo Fisher Scientific) according to the manufacturer's instructions.

3.3.2.5: Nucleic acid quantification.

Nucleic acids were quantified using a NanoDrop ND-1000 spectrophotometer (Thermo Scientific, Wilmington, USA). A blank reading was taken using 1µl of water or elution buffer. 1µl of undiluted nucleic acid solution was measured using either the RNA or DNA setting of the NanoDrop spectrophotometer.

3.3.2.6: Sequencing.

All sequencing was conducted by the University of Cambridge Department of Biochemistry sequencing facility.

Sequences of tomato *MYB Subgroup9* genes were confirmed by alignment using ClustalOmega, against the sequenced tomato genome as viewed on PhytozomeV12.1 (JGI Phytozome v12.1, The Plant Genomics Resource) and Sol Genomics Network (Current Tomato Genome version SL3.0 and Annotation ITAG3.10).

3.3.2.7: Polymerase chain reaction (PCR)

3.3.2.7.1: PCR primer design.

Primers were designed to amplify the full length of each gene from start codon to stop codon, for each potential *MYB Subgroup 9* gene sequence identified in the *Solanum lycopersicum* genome. Genes were found from the genome through a Blast search (NCBI) for

the conserved motif of the subgroup9A and subgroup 9B transcription factor families. Primers were designed to be ~20-25bp long and to be gene specific. Oligo Calc (http://www.basic.northwestern.edu/biotools/oligocalc.html) was used to predict melting temperatures and primers adjusted so that all melting temperatures were ~60˚C and to make sure that annealing temperatures would be similar enough and that primers would not self-anneal. Primers were checked to predict hair-pins, primer dimer and non-target specificity. For a full list of primers used please see Appendix 7

3.3.2.7.2: Isolation of *MYB subgroup 9* genes from *Solanum lycopersicum* (tomato).

Coding sequences of the *MYB subgroup 9* genes of tomato were isolated by RTPCR using Phusion High Fidelity DNA Polymerase. This polymerase was chosen for its proof-reading function. Gene specific primers were used to amplify from tomato cDNA. General reaction conditions are shown in the table below, for specific annealing temperatures for each primer set see primer list in Appendix 7 The following PCR machines were used; 3Prime thermocycler (TECHNE), TC-3000G thermocycler (TECHNE), TC-412 thermocycler (TECHNE), Flexigene Thermocycler (TECHNE) and the PCR conditions are shown in the table below.

Phusion PCR for *Myb subgroup 9* gene isolation.	
cDNA template	1-2µl
dntps	0.4µl
Forward primer	1µl
Reverse primer	1µl
phusion DNA polymerase	0.2µl
GC phusion buffer	4µl
H2O	12.4µl
Total	**20µl**

Reaction Phase:	**Temperature/ ˚C**	**Time:**	
Initial Denaturation:	95	30 seconds	
Denaturation:	95	10 seconds	
Primer annealing:	60-75	30 seconds	**35 cycles**
Extension:	72	15sec-1min	
Final Extension:	72	30sec-2min	
Final Hold:	10	~	

3.3.2.7.3: EcoTaq DNA Polymerase for colony PCR and genotyping.

EcoTaq DNA polymerase was used for colony PCR to identify successfully transformed

Figure 47: The mixture and thermocycler conditions for amplification of R2R3 subgroup 9 genes using RT PCR with Phusion DNA polymerase.

the primer library in Appendix 7 For genotyping, the forward gene specific primer was used with 35SReverse primer. The PCR conditions can be seen in the table below.

EcoTaq PCR for showing transgene is expressed	
cDNA	1µl of a 1/25 dilution
dntps	0.5µl
EcoTaq polymerase	0.05µl
Forward primer	1µl
Reverse primer	1µl
EcoTaq buffer	2.5µl
H2O	18.95µl
Total	**25µl**

EcoTaq PCR for genotyping GDNA	
GDNA	100ng
dntps	0.5µl
EcoTaq polymerase	0.05µl
Forward primer	1µl
Reverse primer	1µl
EcoTaq buffer	2.5µl
H2O	vary with gDNA conc
Total	**25µl**

EcoTaq PCR for colony PCR	
Denatured cells	5µl
dntps	0.5µl
EcoTaq polymerase	0.05µl
Forward primer	1µl
Reverse primer	1µl
EcoTaq buffer	2.5µl
H2O	14.5µl
Total	**25µl**

Reaction Phase:	**Temperature/ ˚C**	**Time:**	
Initial Denaturation:	95	60 seconds	
Denaturation:	95	30 seconds	
Primer annealing:	50-60	10-30 seconds	**25-30cycles**
Extension:	72	15-60seconds	
Final Extension:	72	30-60 seconds	
Final Hold:	10	~	

Figure 48: PCR reaction mixture for RT-PCR using EcoTaq polymerase and corresponding thermocycler conditions.

3.3.2.7.4: Colony screening by colony PCR (cPCR)

Bacterial colonies were screened for the desired plasmid or insert by cPCR.

For *E.coli,* white colonies were selected for screening. The colony was pricked and a small amount transferred to 5µl sterile water. A PCR reaction was set up using the conditions described in **3.3.2.7.3** and using primers designed to produce a band in correspondence with the desired insert or plasmid.

For *Agrobacterium*, a single colony was pricked and transferred to 20µl of 20mM NaOH. This was incubated at 37˚C for 10 minutes before being denatured at 98˚C for 5 minutes (using a PCR machine). 2µl of this mixture was used as the template for PCR using Ecotaq (Department of Plant Sciences, Cambridge) and PCR reaction was set up as described in **3.3.2.7.3**. The primers 35S forward and reverse were used to amplify a band the length of the transgene.

The PCR products were separated using gel electrophoresis as described in **3.3.2.3.**

Successful transformation of the plasmid was confirmed by a band of the correct size. Orientation of the gene was checked by sequencing where required.

Once a successful transformation was identified the colony would be used to purify the plasmid.

3.3.2.7.5: Thermocycling conditions for semi-quantitative RT-PCR and PCR Bio conditions.

PCR Bio was used for the semi-qRTPCR. 5µl of the PCR was removed from the reaction after 30, 35 and 40 cycles. These PCR reactions were then run on a gel of 1.5g/100ml agar for 30 minutes.

The positive control was the plasmid containing the gene. The negative control was water.

Thermocycler conditions for Semi-qRTPCR		
Initial denatature	98˚C	1 min
samples taken after	**98˚C**	**15 sec**
30, 35 and 40 cycles	**55˚C**	**15 sec**
	72˚C	**15 sec**
Final extension	72˚C	15 sec
final hold	10˚C	

PCR Bio PCR for Semi-qRTPCR	
cDNA	0.25-1µl
Forward primer	1µl
Reverse primer	1µl
5X PCR Bio buffer	5µl
PCR Bio Taq	0.25µl
H2O	16.75-17.5µl
Total	**25µl**

Figure 49: Thermocycler conditions for Semi-qRTPCR and reaction mixture for PCR Bio.

3.3.2.8: Preparation of chemically competent *E.coli* strain DH5α

Cells of *E.coli* line DH5α were streaked onto an LB plate (recipe in Appendix 6 from a glycerol stock and grown overnight at 37˚C. A single colony was obtained and used to start a culture, by pricking the colony and adding it to 10ml of LB and grown overnight at 37˚C shaking at 180rpm. The following day 4ml of this culture was added to 120ml LB in a 500ml

conical flask or 1ml added to 4 x 30ml LB in 50ml falcon tubes. This was incubated for 3 hours at 37˚C, shaking at 180rpm. After this incubation period the cultures were pelleted using a cold centrifuge set to 4˚C for 5 minutes at 4000rpm. All subsequent steps were conducted in the cold room, at 4˚C. The supernatant was discarded. The pellets were re-suspended in 10ml of 100mM MgCl2 and left to rest for 5 minutes. The cultures were then pelleted by centrifuge for 5 minutes at 4000rpm, the supernatant was discarded. The pellet was gently re-suspended in 2ml *E.coli* freezing solution (60mM CaCl2, 15% glycerol, 10mM PIPES pH7, filter sterilised). The solution was separated into 50µl aliquots in 1.5ml autoclaved Eppendorf tubes. These were snap frozen using liquid nitrogen and then stored at -80˚C until use.

3.3.2.9: Transfer of PCR products to a plasmid vector.

3.3.9.1: Ligation of PCR product into pBlue plasmid.

pBlue is a version of pBluescript, restriction digested to produce blunt ends and stored as a lab stock for cloning. The PCR product was combined with pBlue plasmid, T4 ligase and T4 ligation buffer in the mixture outlined by the below table. This was incubated overnight at 16˚C.

Ligation of PCR products into pBlue	
PCR product	1-4µl depending on product conc
pBlue plasmid	0.5µl
T4 ligation buffer	0.5µl
T4 ligase	1µl
H2O	0-3µl to make up to total
Total	**5µl**
incubated overnight 16˚C	

Figure 50: Reaction conditions for ligation of PCR products into pBlue.

3.3.9.2: Transfer of PCR product from pBlue into pGreen by restriction digestion followed by ligation.

pGreen is a binary vector for plant transformation (Hellens et al, 2000). The lab's version of pGreen contains two copies of the CaMV 35S promoter and the 35S terminator, allowing strong constitutive expression in plant tissue (thesis of C.Wilkins, 2004).

Restriction digest to remove insert from pBlue	
Plamid containing insert	1µg
SalI HF	2µl
BamHI HF	2µl
Cutsmart buffer	5µl
H2O	make up to total
Total	**50µl**
2 hours 37˚C	

Figure 51: Reaction conditions for restriction digest of pBlue.

The insert was then ligated into the pGreen vector under the reaction conditions shown in (Figure 52).

ligation of insert into pGreen	
Insert	10µl
pGreen	2µl
H2O	5µl
T4 buffer	2µl
T4 ligase	1µl
total	**20µl**
incubated overnight at 16˚C	

Figure 52: Reaction conditions for ligation of insert into pGreen.

3.3.2.10: Transformation of *DH5α E.coli.*

5µl of the construct or ligation was added to 25-50µl of competent cells before being left on ice for 15-30 minutes. This was followed by a 1 minute heat shock at 42˚C. The cells were left to recover for 1 minute on ice. 1ml LB was added to the mix which was then incubated for 30minutes-1hour at 37˚C. Following this, cells were centrifuged for 1 minute at 5000rpm. 900µl of the supernatant was discarded and the remaining bacterial pellet was gently re-suspended and plated out on LB+ appropriate antibiotics for the plasmid (recipe see Appendix 6 along with 100µl of IPTG (100µM) and 20µl of XGAL (40µg/ml) for plasmids with blue/white selection. The mixture was spread across the plate using sterile beads. The plates were incubated at 37 ˚C overnight.

pBluescript plasmids contain the β-lactamase gene and the lacZ gene. β-lactamase confers resistance to ampicillin. The cloning site of the plasmid is located over the lacZ gene so that its coding region is split by a successful insertion event. The lacZ gene codes for the enzyme β-galactosidase which metabolises X-gal to produce a blue coloured product. However β-galactosidase will not be synthesised and so blue coloration will be absent if the lacZ gene is split due to a successful ligation into the plasmid. Therefore successful colonies can be identified easily by eye as they will be white. Blue colonies indicate the ligation was unsuccessful, while a lack of colonies indicates an unsuccessful transformation of any plasmid into *E.coli*.

3.3.2.11: Transformation of *Agrobacterium tumefaciens*

3.3.2.11.1: Transformation of *Agrobacterium tumefaciens* strain GV3101.

An electroporation cuvette was chilled on ice. 1µl of purified plasmid (of about 100ng) was added to a 50µl aliquot of GV3101 strain *Agrobacterium tumefaciens* and mixed gently before being transferred to the chilled BioRad electroporation cuvette (Hertfordshire, UK). A Biorad electroporation machine (BioRad Micropulser electroporator) at 2.5kV was used to electroporate the cuvette and cause the cells to take up the plasmid. 1ml of LB was added to the cuvette. The LB and cells were then transferred to an Eppendorf and left to recover for 3-4 hours in a 30˚C shaking incubator (~180rpm). This *Agrobacterium* was then plated out on LB plates with Kanamycin (50mg/L) (for selection of the pGreen vector) and Gentamycin (25mg/L) (for selection for virulence plasmid in the *Agrobacterium* to allow for successful transformation). The plates grew for 48 hours, incubated at 30˚C (no shaking).

Bacterial cells were checked for the transgene plasmid by colony PCR (as in section **3.3.2.7.4**).

Once a positive colony was identified, a culture was started using 50ml LB with Kanamycin (50mg/L) and Gentamycin (25mg/L) and the pricked colony. This colony was selected to grow as a culture and used to create a glycerol stock which was stored at -80˚C until use. Glycerol stock was created by adding 500µl of the miniculture to 500µl of 50% glycerol in a 1.5ml screw cap tube. This was mixed by inversion and then frozen in liquid nitrogen.

3.3.2.11.2: Transformation of *Agrobacterium tumefaciens* strain AGL1.

Transformation of constructs was conducted as outlined in section **3.3.2.11.1** using *A. tumefaciens* strain AGL1 and selection with 50µg/ml Carbenicillin (that AGL1 is resistant to and so selects for this strain) and 50µg/ml Kanamycin (selects for the plasmid construct).

3.3.2.12: Growth of cells for plasmid purification.

Liquid LB media containing antibiotics appropriate to the plasmid was used as the growth medium for selected bacterial cells. *E.coli* were grown at 37˚C, 180rpm overnight (~18 hours), in 3ml of LB media and antibiotics appropriate to the plasmid. *Agrobacterium* was grown at 28-30˚C for ~36 hours in 10ml of LB media and appropriate antibiotics.

3.3.2.13: Plasmid purification

3.3.2.13.1: Plasmid purification by plasmid purification kit.

Plasmid purification for use in construction of CRISPR vectors was conducted using QIAprep® Spin miniprep kit (cat.No. 27104, QIAGEN) following the manufacturer's instructions. Yield was quantified using a Nanodrop ND-1000 spectrophotometer.

3.3.2.13.2: Plasmid purification by 'miniprep plasmid purification alkaline lysis' method.

Plasmid purification for general use was conducted using the miniprep plasmid purification alkaline lysis method as follows.

A 3ml liquid culture was grown overnight at 37˚C with the appropriate antibiotic. In the morning 1.5ml of this culture was transferred to an Eppendorf tube. This was centrifuged for one minute at maximum speed, 14,000rpm. All LB was removed. 300µl of SOL1 and 5µl of RNAseA (10mg/ml) was added to the pellet which was then re-suspended by vortexing. 300µl of SOL2 was then added and the tube mixed by inversion. Next 300 µl of SOL3 was added and the tube mixed by inversion. The mixture was then left on ice for 5 minutes after which it was centrifuged for 10 minutes at maximum speed, 14,000rpm. 800 µl of the liquid was collected by pipetting without disturbing the cell debris. 640 µl of isopropanol was added to this collected liquid to precipitate the DNA. The DNA was spun down into a pellet by centrifuge for 20 minutes at maximum speed, 14,000rpm. All liquid was removed and the pellet was washed with 1ml of 70% ethanol. The pellet was then dried and re-suspended in 20-25µl of sterile water.

SOL1, SOL2 and SOL3 were made using the recipes in Appendix 6

3.3.2.14: Transformation of tobacco leaf discs by *Agrobacterium tumefaciens.*

The *Agrobacterium* containing the transgene-plasmid stock was streaked out onto an LB plate containing 50mg/L Kanamycin and 25mg/L Gentamycin (for selection for the pGREENII and Ti Plasmid respectively). This was grown for 48 hours at 30˚C incubation (no shaking) to obtain a single colony. On the third day this colony was pricked and transferred to 50ml LB in a falcon tube with 25mg/L Gentamycin and 50mg/L Kanamycin. This culture was incubated at 28˚C for 24 hours with shaking (180rpm). After this 1ml of the culture was transferred to 200ml fresh LB (with 25mg/L Gentamycin and 50mg/L Kanamycin) in a sterilised conical flask with bung. This was incubated for 24 hours at 28˚C with shaking (180rpm). This was then sub-cultured again in the same way the following day and incubated for 24 hours. On day 6, the OD600 of the *Agrobacterium* culture was calculated against an LB blank using a SANYO SP75UV/Vis Spectrophotometer (GALLENKAMP). The *Agrobacterium* culture was transferred to 4 x 50ml falcon tubes and spun down by centrifuge for 5 minutes, 5000rpm at 10˚C. The supernatant was discarded and the pellets re-suspended in 25ml half MS, the recipe for this can be found in Appendix 6

Young green tobacco leaves (*Nicotiana tabacum* Samsun) were sterilised using 10% domestic bleach for 15 minutes. They were then washed with autoclaved DI water five times. Sterile scalpel blades were used to cut the tobacco leaves into ~1cm^2 fragments submerged in the *Agrobacterium* culture in a petri dish. The leaf fragments were blotted dry with autoclaved filter paper and placed onto MS plates (Appendix 6 with no antibiotics. These were incubated at room temperature for 48 hours in the dark. The leaf fragments were then transferred to MS9 plates (Appendix 6 for recipe) containing antibiotics (500mg/ml Cefotaxime, 200mg/ml Ampicillin and 100mg/ml Kanamycin) and hormones (0.5mg/ml IAA: auxin and 1mg/ml BAP: cytokinin). The antibiotics were used to kill the *Agrobacterium* (cefotaxime), select for transformed tobacco cells (Kanamycin) and help keep the plates from becoming infected (Ampicillin). The hormones were to stimulate regeneration of the tobacco leaf fragments. These explants were grown at 23˚C with 16 hours light and 8 hours dark in a controlled growth room. Fragments were transferred to fresh plates every week for the first month and then every 2 weeks thereafter until shoot formation. Once a shoot had formed, this was cut and transferred to a Hamilton jar

containing MS9 with antibiotics (100mg/ml Kanamycin, 50mg/ml Cefotaxime, 200mg/ml Ampicillin) but without the hormones so that the plantlet could grow roots. Once roots had grown the plantlet could be transferred to soil. Rooted shoots grown in soil were tested for the presence and expression of the transgene using PCR BIO as described in 3.3.2.7.5, with a cycle length of 35 cycles. Successfully transformed plants were grown to maturity under the growth conditions described in 3.3.3.

3.3.2.15: Genotyping of tobacco expression lines (gDNA and cDNA).

Lines were initially genotyped from the gDNA. gDNA was extracted using the following 'quick method for genotyping' protocol.

A small piece of leaf tissue was ground at room temperature using a plastic micropestle in an Eppendorf tube. 400µl of extraction buffer (recipe in Appendix 6 was added to this and grinding continued for another 15 seconds. The tube was vortexed for 5 seconds then centrifuged at room temperature for 10 minutes at maximum speed. The supernatant was transferred to a clean Eppendorf tube to which 320µl of 100% isopropanol was added. This was mixed by inversion and centrifuged at maximum speed, 14,000rpm for 30 minutes at room temperature. The supernatant was discarded. The pellet was washed using 1ml of 70% ethanol and then air dried at room temperature before being re-suspended in 25-30 µl of sterile DI water. The gDNA was quantified by nanodrop and then stored at -20˚C.

PCR was then conducted using the gene specific primers or the gene specific forward primer with the 35S Reverse primer. Once the presence of the transgene was confirmed its expression was analysed. RNA was extracted using the CTAB protocol (3.3.2.2.1)or TRIZOL protocol (3.3.2.2.2). Both protocols are outlined in section 3.3.2.2. RNA was cleaned using a phenol chloroform purification before undergoing DNase treatment to remove any gDNA that may confound the result with a false positive. The RNA was then purified again using phenol chloroform purification to remove any DNase prior to cDNA synthesis. PCR was conducted on the RNA to check all gDNA had been removed. This PCR was conducted using Ecotaq and the gene specific primer set and conditions were as described in section 3.3.2.7.3. cDNA was synthesised from the RNA as described in section 3.3.2.2.6.

PCR was conducted using gene specific primers (Appendix 7) and conditions as described in section 3.3.2.7.3 Ubiquitin primers were used as a positive control to confirm quality of cDNA. Wild type tobacco gDNA was used as a negative control.

5 lines per transgene constructs were examined and confirmed to have transgene both present and expressed. The phenotype of these lines was examined.

3.3.2.16: Phenotypic characterisation of tobacco overexpression lines.

Transgenic lines were photographed using Samsung camera WB550 and the camera of a phone (Sony Xperia, 4.4.4 Android). Flowers at several stages from bud to fully open were photographed from above and the side. Leaves of various stages were photographed and the full plant was photographed at maturity. All plant tissue was photographed against black velvet.

Microscopic phenotype was preliminarily examined using the Keyence light microscope VHX-5000 at the Department of Plant Sciences (University of Cambridge). The adaxial and abaxial sides of leaves were examined for abnormal trichome growth and epidermal cell outgrowths. The following floral organs were dissected out of the flowers; anthers, stigma and ovary, and were examined for abnormal cell outgrowths on their surface.

3.3.2.17: Cryo SEM analysis.

Characterisation of transgenic line phenotypes was conducted using the Zeiss EVO HD15 Cryo-Scanning Electron Microscope at the Sainsbury Laboratory University of Cambridge. The following tissues were examined; mature leaf abaxial surface, mature leaf adaxial surface, mature stigma, corolla tube inner surface, surface ofpetal lobe, mature ovary surface, anther surface (for lines where anthers dehisced immature anthers were examined; for lines where anthers did not dehisce anthers from mature flowers were examined). Tissues were dissected and mounted on metal stubs. Tissue was mounted using a mix of collodial graphite (G303, Agar Scientific.ltd. unit 7) and O.C.T compound (Scigen Tissue-Plus®, O.C.T. Scigen Scientific Gardena, LA90248USA). This glue was mixed in a ratio of 1/3 collodial graphite to 2/3 O.C.T. The samples were cryogenically frozen and then underwent a sublimation of 5-9 minutes at -90˚C to remove any excess moisture from the tissue surface which would cause ice crystals and potentially obscure the tissue surface. They were sputter coated with 5nm of platinum.

3.3.2.18: CRISPR genome editing in tomato.

3.3.2.18.1: Choice of genes for further functional analysis by CRISPR genome editing.

A subset of *MYB Subgroup 9* genes were chosen for further analysis using CRISPR-Cas9 genome editing. This was done by examining the Tomato efp Browser at Bar. UToronto.ca, Rose Lab Atlas, http://bar.utoronto.ca/efp_tomato/cgi-bin/efpWeb.cgi. Only those genes with predicted expression profiles in buds and young flowers were selected for further analysis. The ectopic expression phenotypes in tobacco were also considered, as was the information that a collaborating lab was generating CRISPR-Cas9 lines with one of the genes. This experiment was therefore conducted with only Solyc05g048830.2.1 (*MYB17-2*) and Solyc05g007690.1 (*MIXTA-4*).

3.3.2.18.2: Primer design for CRISPR.

20bp target sequences were identified within the coding region of the target gene. Potential target sequences were identified using Zifit (http://zifit.partners.org/ZiFiT/CSquare9Nuclease.aspx). Two target sequences were selected per target gene, designed to cause a frame shift between the two target sequences where possible. Target sequences were selected for maximum specificity. Target sequences were examined using BLAST and any non-target matches identified from this were checked for a minimum of 5bp mismatches for the primer to be considered specific to the desired target. Any potential off target sites were noted. Target sequences were designed not to contain the restriction sites BsaI and BpiI as this would interfere with plasmid construction during cut-ligation steps. Once target sequences were selected primers were designed as indicated in Appendix 7

3.3.2.18.3: Construct assembly for CRISPR.

The sgRNA was amplified by conducting a PCR with the primers designed as described in section 3.3.2.18.2 The construct pICH86966:AtU6p::sgRNA_PDS (Addgene plasmid 46966) was used as the template for this PCR . This was done using Phusion as outlined in section **3.3.2.7.2** with an annealing temperature of 72˚C (Appendix 6).

The PCR product for each individual gene was checked by sequencing before the next step. It was desalted using a QIAquick PCR purification kit (QUIAGEN) as per the manufacturer's instructions. Once de-salted, the PCR product was used in a golden gate cloning as

summarised in the table below. This was based on the cut ligation described in Weber et al (2011). This cut ligation produced a Level 1 vector. This level 1 vector used pICH47751 or pICH47761 as the backbone and incorporated the AtU6 promoter from pICSL01009::AtU6p (level 0) and the PCR product (which contained the guide sequence). The level 1 vector used for the backbone was chosen so that pICH47751 was used for one of the guides for a particular gene and then pICH47761 was used for the other guide from the same gene. These allowed multiple guides to be assembled within one final level 2 vector.

Once the level 1 was assembled it was transformed into *E.coli* as described in section **3.3.2.10.** Colonies were chosen by blue-white selection. Correctly constructed vectors were checked by restriction digestion as described in section **3.3.2.18.4**. The selected colony was grown up as a miniculture and plasmid purification was conducted using the kit as described in section **3.3.2.13.1.**

The purified Level 1 vectors were used in a golden gate cloning reaction as summarised in the table below, to form a final Level 2 vector which contained both of the guides for a single gene. This cut ligation was transformed into *E. coli* and red-white selection was used to indicate successful transformations. White colonies contained an insert which interrupted the ability of the backbone vector to produce the red colour. The red colouration results from a selectable marker cRed which is an artificial bacterial operon that results in the biosynthesis of canthaxanthin. The final construct was confirmed by restriction digestion as described in **3.3.2.18.4** and by sequencing.

Level 0 → Level 1 vector		**reaction conditions**
pICSL01009::AtU6P	40fmol	5 hours 37˚C
sgRNA PCR product	40fmol	5 minutes 50˚C
pICH47751	40fmol	10 minutes 80˚C
ensyme BsaI	1µl (10U)	
T4 ligase	1µl (10U)	
T4 ligation buffer	1µl	
H2O	vary to make up to total	
total	**10µl**	

Level 1 vector → Level 2 vector		**reaction conditions**
pICH47732::NOSp::NPTII-OCST	40fmol	5 hours 37˚C
pICH47742::35Sp::Cas9-NOST	40fmol	5 minutes 50˚C
pICH47751: AtU6p::sgRNA1	40fmol	10 minutes 80˚C
pICH47761:: AtU6p::sgRNA2	40fmol	
pICH41780:: linker	40fmol	
pICSL4723 level2 vector	40fmol	
BSA (10x dilution)	1.5µl	
enzyme BpiI	0.5µl (10U)	
T4 ligase	0.5µl (10U)	
T4 ligation buffer	1.5µl	
H2O	vary to make up to total	
total	**15µl**	

Figure: 53 Reaction conditions for CRISPR construct cut-ligations.

3.3.2.18.4: Confirmation of CRISPR constructs by restriction digestion.

The Level 1 constructs were checked by restriction digestion with the enzyme BpiI as follows:

plasmid	4µl
buffer G	2µl
enzyme BpiI	0.6µl
H2O	13.4µl
total	**20µl**
2hrs 37˚C	
expected bands:	
1	4352bp
2	226bp

The Level 2 final constructs were checked by restriction digestion with the enzyme PstI as follows:

plasmid	4µl
buffer 3.1	2µl
enzyme PstI	0.6µl
H2O	13.4µl
total	**20µl**
2hrs 37˚C	
expected bands:	
1	6338bp
2	2457bp
3	1968bp
4	1212bp
5	304bp
6	234bp

Figure 54: Restriction digestion conditions of CRISPR constructs to confirm structure.

Once a plasmid purification containing a successfully formed construct was identified, this was sent to sequencing to confirm the presence of both sgRNA guides. For details of primers used see primer list in Appendix 7.

3.3.2.18.5: Transformation of tomato cotyledons.

Tomato seeds were soaked in 70% EtOH for 2 minutes to loosen the seed coat and then rinsed with sterile water. The seeds were then sterilised in 10% bleach for 15 minutes. The seeds were washed 4 times with sterile water. Seeds were placed on MS agar plates and stored in the fridge at 4˚C for two days, and then germinated and seedlings grown in the growth room for seven days. The conditions of the growth room were 16h/8h light/dark, at 21˚C, 60% humidity. For transformation, the cotyledons must be still young and expanding with no true leaf formation visible.

On the day of transformation the cotyledons were cut underwater (using sterile water and a sterilised scalpel). These explants were stored in sterile water, abaxial surface facing upwards until they were transferred into the *Agrobacterium* culture.

The AGL1 strain of *Agrobacterium tumefaciens* containing the CRISPR construct was cultured overnight at 28˚C with appropriate antibiotics. The culture was spun down and resuspended in MS medium with 3% sucrose to an OD_{600} of 0.4-0.5. This bacterial suspension was placed in a petri dish and the explants immersed for ~2minutes. The explants were removed and blotted on sterile filter paper. The explants were left for two days in the dark, in the culture room on MS plates. After these two days the explants were transferred from the plates to tomato regeneration plates (see Appendix 6). The explants were transferred to fresh regeneration plates every week. After ~3-4 weeks the explants were transferred to tomato regeneration media in aseptically produced 250ml jars to allow more room for the growth of the explants, with ~3 explants per jar. Once the explants were large enough that they required more growth room, they were each placed in their own jar of tomato regeneration media (recipe in Appendix 6. Once shoot formation occurs, the shoot is cut and placed into rooting medium (recipe in the Appendix 6), however no rooting occurred in this study.

3.3.3: Plant growth conditions for wild type tomato, wild type tobacco and transgenic tobacco growth conditions.

Wild type (WT) plants grown for molecular analysis by quantitative PCR were the cultivar "Moneymaker" of *S. lycopersicum* and were grown under controlled conditions at the University of Cambridge Plant Growth Facility. Light levels were 150µmol for a 16 h day. The temperature was maintained at 21˚C and the humidity at 60%. Watering was carried out

daily. Feeding (of tomatoes) was with Levington's Tomorite liquid plant fertiliser, 5ml/L of water, once a week after fruiting was initiated. Transgenic tobacco plants were grown at the Plant Growth Facility of the University of Cambridge, also under these controlled conditions.

Wild type tobacco (Samsun variety) was grown for transformation using *Agrobacterium*, in the glasshouse of the Department of Plant Sciences. Day length was 16h day/8h night, with temperature maintained at 21˚C and humidity at 60%. Watering was carried out daily and the plants were fed once a week with Levington's Tomorite liquid plant food, 5ml/L.

3.4: Results

3.4.1: R2R3 MYB Subgroup 9 genes in *Solanum lycopersicum*

A search of the tomato genome for the *MYB subgroup 9* motif revealed the presence of seven genes in this family in *Solanum lycopersicum.* These seven genes can be divided into the subclades of Subgroup 9A and Subgroup 9B by the presence of a further motif, shown in Figure 56 and 57 (summarised in Figure 55). The subgroup membership was also confirmed by phylogenetic analysis using the phylogeny of (Brockington et al, 2013) as a framework. The phylogenetic placement of the 7 tomato genes examined in this study can be seen in Figure 56 and Figure 57. There are four genes which belong to the *MIXTA* subclade of *MYB subgroup 9A*, while one gene belongs to the *MIXTA-like* subclade. In *subgroup 9B* there ae only two genes and both are part of the *Myb17* subclade. There are no members of the *Myb17*.

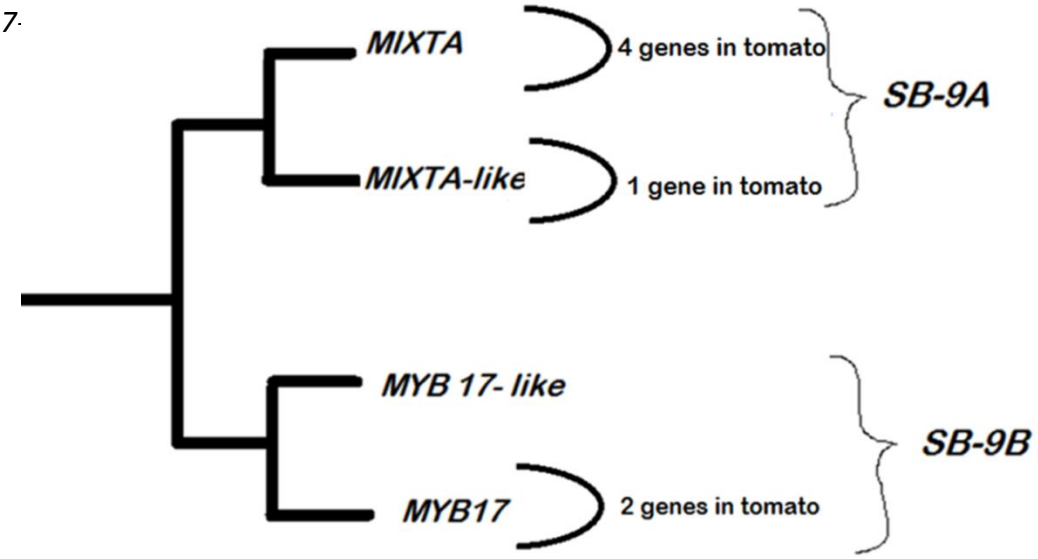

Figure 55: A cartoon phylogeny of the *Myb subgroup 9* family of transcription factors showing numbers in tomato.
This cartoon phylogeny is based on the phylogenetic analysis of (Brockington et al, 2013). This cartoon shows the *Myb subgroup 9* family of transcription factors and its division into subgroup 9A and subgroup 9B. These in turn are subdivided into SB-9A: *MIXTA* and *MIXTA-like,* and SB-9B: *Myb17-like* and *Myb-17*. In *Solanum lycopersicum* there are 7 genes in the *Myb subgroup 9* family of transcription factors. 5 of these genes are in SB-9A (with 4 genes in *MIXTA* subclade and 1 in the *MIXTA-like* subclade). In SB-9B there are 2 genes in *Solanum lycopersicum,* both of these are in the *Myb17* subclade.

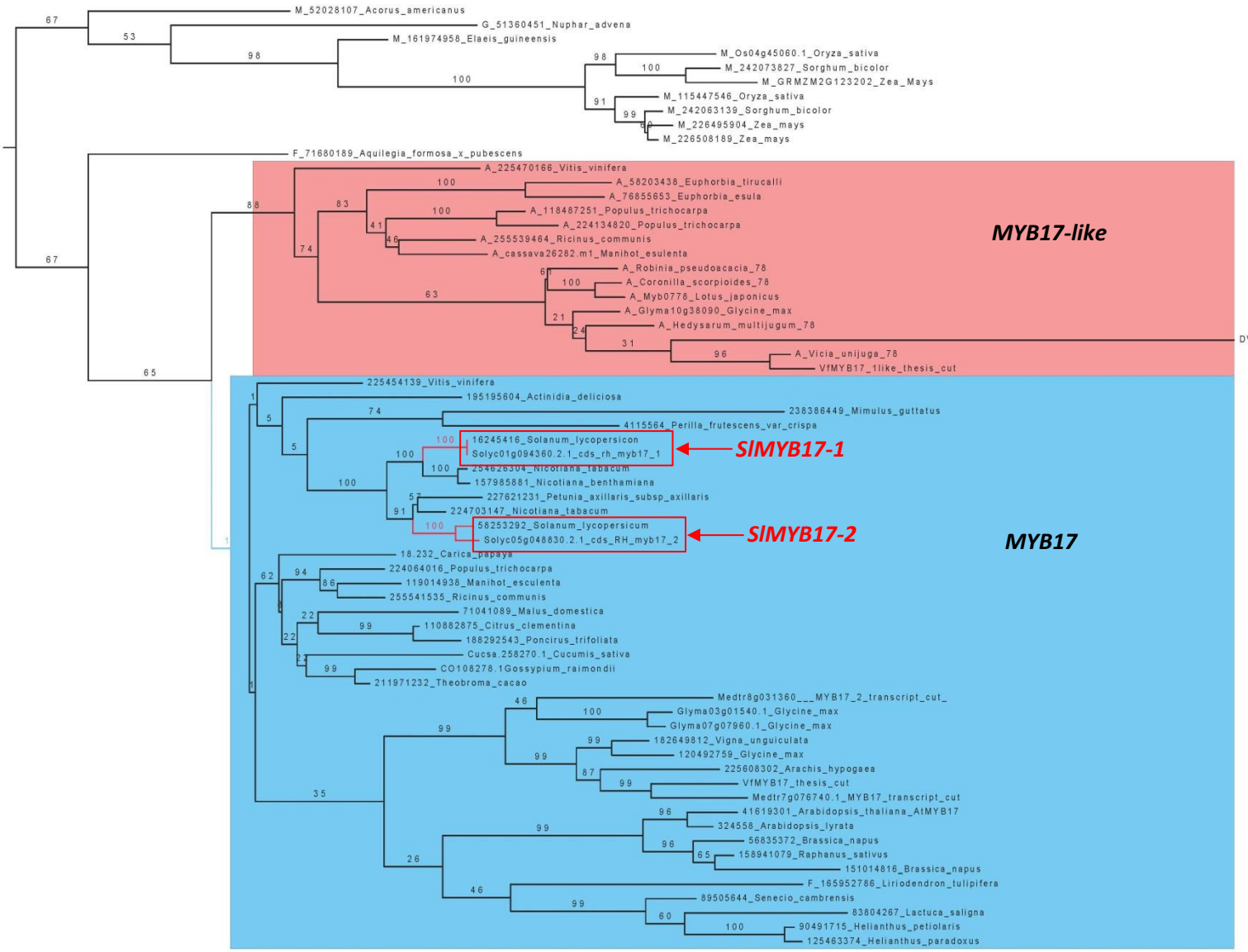

Figure 56 Tomato genes that fall within R2R3 MYB subgroup 9B

Alignments of candidate genes were used to include them in the alignment and phylogenetic analysis of R2R3 MYB subgroup 9B genes in (Brockington et al, 2013). Conserved motif image taken from (Brockington et al, 2013). GARLI maximum likelihood phylogram of 220 members of the subgroup 9 R2R3 MYB genes, the candidate genes were manually aligned with the phylogram at the level of amino acids.

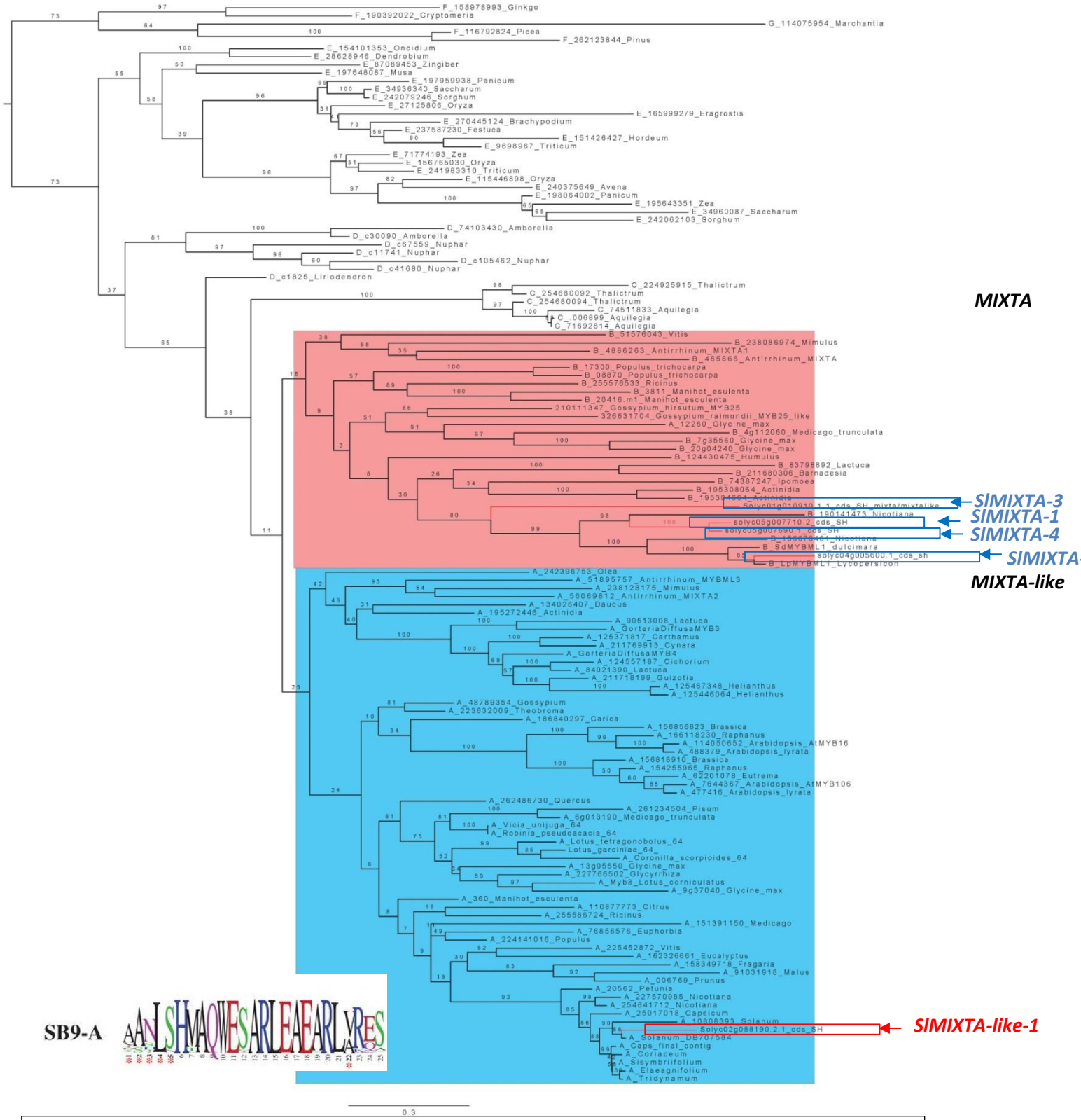

Figure 57: Tomato genes that fall within R2R3 MYB subgroup 9A

Alignments of candidate genes were used to include them in the alignment and phylogenetic analysis of R2R3 MYB subgroup 9A genes in (Brockington et al, 2013). Conserved motif image taken from (Brockington et al, 2013). GARLI maximum likelihood phylogram of 220 members of the subgroup 9 R2R3 MYB genes, the candidate genes were manually aligned with the phylogram at the level of amino acids.

The sequences of the proteins encoded by the candidate genes were aligned to previously studied members of the R2R3MYB subgroup 9 lineages to assess whether there were any marked differences such as frame-shifts or deletions. However all of the candidate genes have a fairly high degree of similarity with the representative genes from other species.

From the alignment seen in Figure 58, it can be seen that the *SlMIXTA-like-1* protein greatly resembles the previously studied *MIXTA-like* proteins of *Antirrhinum majus. SlMIXTA-like-1* has a 74.2 percent identity to *AmMYBMl3* (*AmMIXTA-like-3*) which it overall most greatly resembles structurally. (*AmMYBMl2* (*AmMIXTA-like-2*) has a very similar percentage identity when compared to *AmMYBMl3* (*AmMIXTA-like-3*) of 75%). The sequences all match near completely to one another for the first ~180 amino acids, after which they begin to diverge. Up until ~180 amino acids *SlMIXTA-like-1* matches *AmMYBMl2* (*AmMIXTA-like-2*) nearly perfectly. After this point, *the SlMIXTA-like-1* protein has a number of insertions and overall is a longer sequence than those found in *A.majus.*

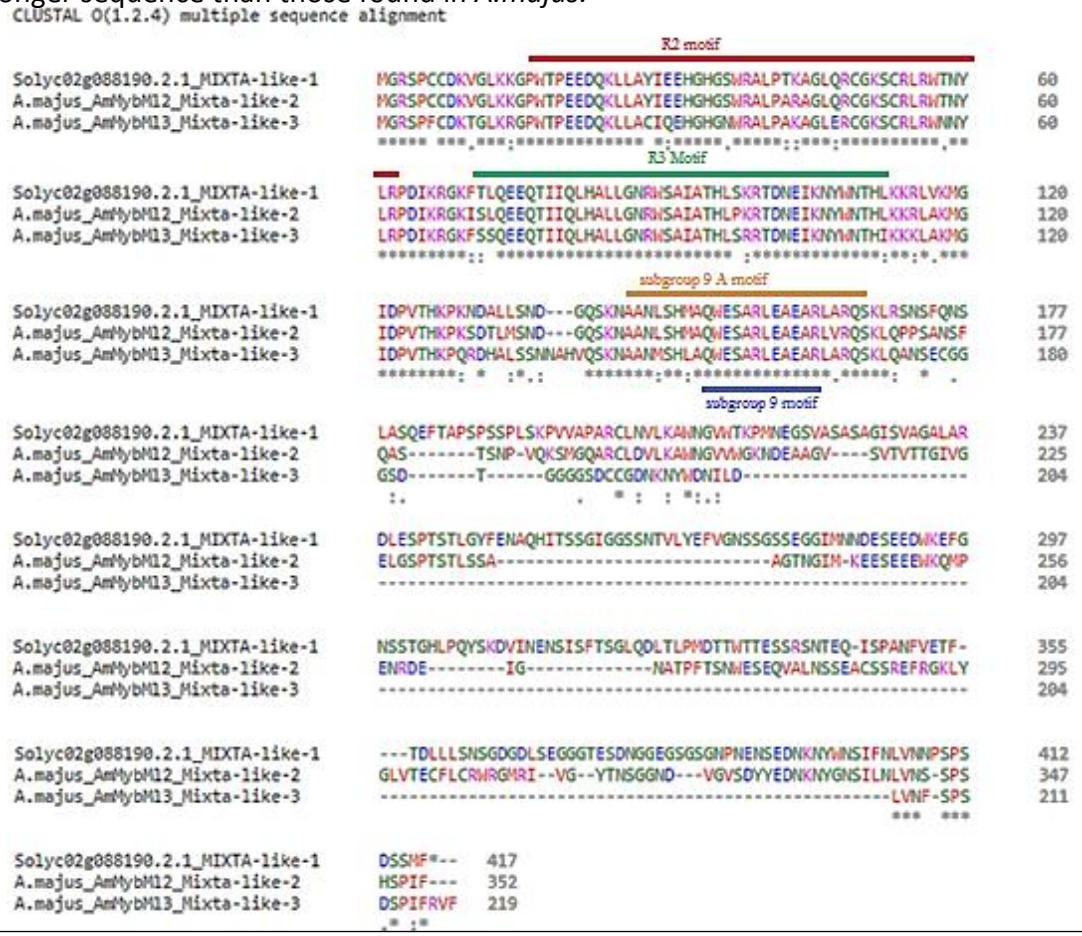

Figure 58: The *MIXTA-like* protein of tomato aligned against previously studied *MIXTA-like* proteins from *Antirrhinum majus.*

These proteins from *Antirrhinum majus* have been shown to regulate cell outgrowths previously, therefore it is of interest to compare their sequence structure to that of the *MIXTA-like* protein of *Solanum lycopersicum*. *AmMYBMl2* (*AmMIXTA-like-2*) (Genbank:AY821655. Baumann et al, 2007). *AmMYBMl3* (*AmMIXTA-like-3*) (Genbank: AY661654. Jaffe et al, 2007).

From the alignment of the *SlMIXTA* proteins with the previously studied *MIXTA* proteins of *A.majus* (Figure 59) it can be seen that the peptide sequences begin almost identical, as to be expected as this area of the sequence contains the conserved DNA binding motif. After this the sequences begin to diverge from one another. All the peptide sequences are of similar length, with *AmMybMX* being the shortest and *AmMYBMl1* being the longest, with the *SlMIXTA* proteins all sitting somewhere in between. However there is not a enormous degree of sequence similarity. All the *SlMIXTA* proteins only have a percentage identity of ~52% with one another and with the *A.majus* sequences. *AmMybMX* had a 62.5% percent identity to *AmMYBMl1*, the other *A.majus* sequence. The *SlMIXTA* proteins do not resemble either of the *A.majus* proteins more than the other: when compared to *AmMybMX* the percentage identities are: *SlMIXTA-1* 51%, *SlMIXTA-2* 52%, *SlMIXTA-3* 56%, *SlMIXTA-4* 52%. Similarly, when compared to AmMYBMl1 the percentage identities are: *SlMIXTA-1* 50%, *SlMIXTA-2* 50%, *SlMIXTA-3* 57%, *SlMIXTA-4* 52%. The sequences that most resembled one another are that of *SlMIXTA-1* and *SlMIXTA-4* with a percentage identity of 90%. The remaining *SlMIXTA* proteins do not resemble each other with a greater than 56% percentage identity.

Figure 59: The *MIXTA* proteins of tomato aligned against previously studied *MIXTA* proteins from *Antirrhinum majus.*

These proteins from *Antirrhinum majus* have been shown to regulate cell outgrowths previously, and provided the classic phenotypic studies for understanding the regulation of epidermal cell outgrowths and conical cells. Therefore it is of interest to compare their sequence structure to that of the *MIXTA* proteins of *Solanum lycopersicum*.

AmMYBMX MIXTA (Genbamk: X79108. Noda et al, 1994). *AmMYBMl1* (*AmMIXTA-like-1*) (Genbank: AJ006292. Perez-Rodriguez, 2005).

The *SlMYB17* proteins were aligned with those of the previously studied *MYB17* protein of *Arabidopsis thaliana* (Figure 59). The *SlMYB17* proteins resembled one another with a fairly high percentage identity of 79%. *SlMyb17-1* resembles the *A.thaliana MYB17* sequence slightly more than *MYB17-2* does, with percentage identities of 65.3% and 64% to *AtMYB17* respectively. The *SlMYB17* proteins have a similar length to one another (308 vs 319 aas) and both are longer sequences than that of *AtMYB17* (299). This appears to be largely due to an insert of ~21 amino acids at around the 200 mark relative to *AtMYB17.*

Figure 60: The *MYB17* proteins of tomato aligned against the previously studied *MYB17* protein from *Arabidopsis thaliana*.

This gene from *Arabidopsis* has been previously studied and shown to be involved in flowering, however it has not be shown to be involved in the formation of outgrowths (Pastore et al, 2011.) This gene was used in the construction of the phylogeny across plant families for the *R2R3 MYB subgroup 9* genes in (Brockington et al, 2013).

AtMYB17 (Genbank: 295743.1. Pastore et al, 2011).

3.4.2: Genotyping of tobacco with ectopically expressed *Solanum lycopersicum R2R3 Myb Subgroup 9* genes.

Plants from a minimum of four independent lines for each gene were genotyped by checking for transgene expression using RT-PCR with gene specific primers. DNA bands after gel electrophoresis for tobacco lines expressing the individual genes ectopically can be seen in Figure 61.

Callus formation was induced in over 90% of the transformed explant disks which then resulted in an average of 20 plantlets being transferred to soil and grown to maturity for each gene.

Of those plants grown to maturity, for tobacco plants transformed with *SlMYB17-1* 90% of the lines had a transgenic phenotype that could be identified without the use of microscopy (because the anthers did not dehisce). 7 lines were genotyped, 5 lines were shown to be expressing the transgene.

For *SlMyb17-2,* 11 of the lines that grew to maturity were examined, of which 9 had a similar and clear phenotype (with anthers that did not dehisce and when examined by light microscope had large numbers of trichomes on the anthers). 5 lines were genotyped and all of them shown to be expressing the transgene. A small number of lines did not set any seed and an even smaller number of lines never flowered.

There were 10 lines of *SlMIXTA-like-1* that were examined at maturity, of which 4 were shown to be expressing the transgene. A further two were also found to express the transgene however did not set seed. The phenotype was not so clear that plants could be assessed as transgenic without genotyping, but it is likely that the transformation efficiency was high.

For *SlMIXTA-1* 10 lines were examined at maturity of the 20 that grew in soil. Of these 10, 8 plants had anthers that did not dehisce and under a light microscope could be seen to be covered in trichomes. 5 lines were genotyped at cDNA level to show expression of the transgene.

For *SlMIXTA-2* 13 lines were examined. 5 lines were genotyped from cDNA and shown to be expressing the transgene, with a sixth line not expressing.

Of the 11 *SlMIXTA-3* transformed tobacco lines grown to maturity, 5 were shown by genotyping to be expressing the transgene.

For *SlMIXTA-4* 11 lines were grown to maturity, 2 of which did not set any seed. 7 lines were shown to be expressing the transgene.

All genotyping gels can be seen in Figure 61.

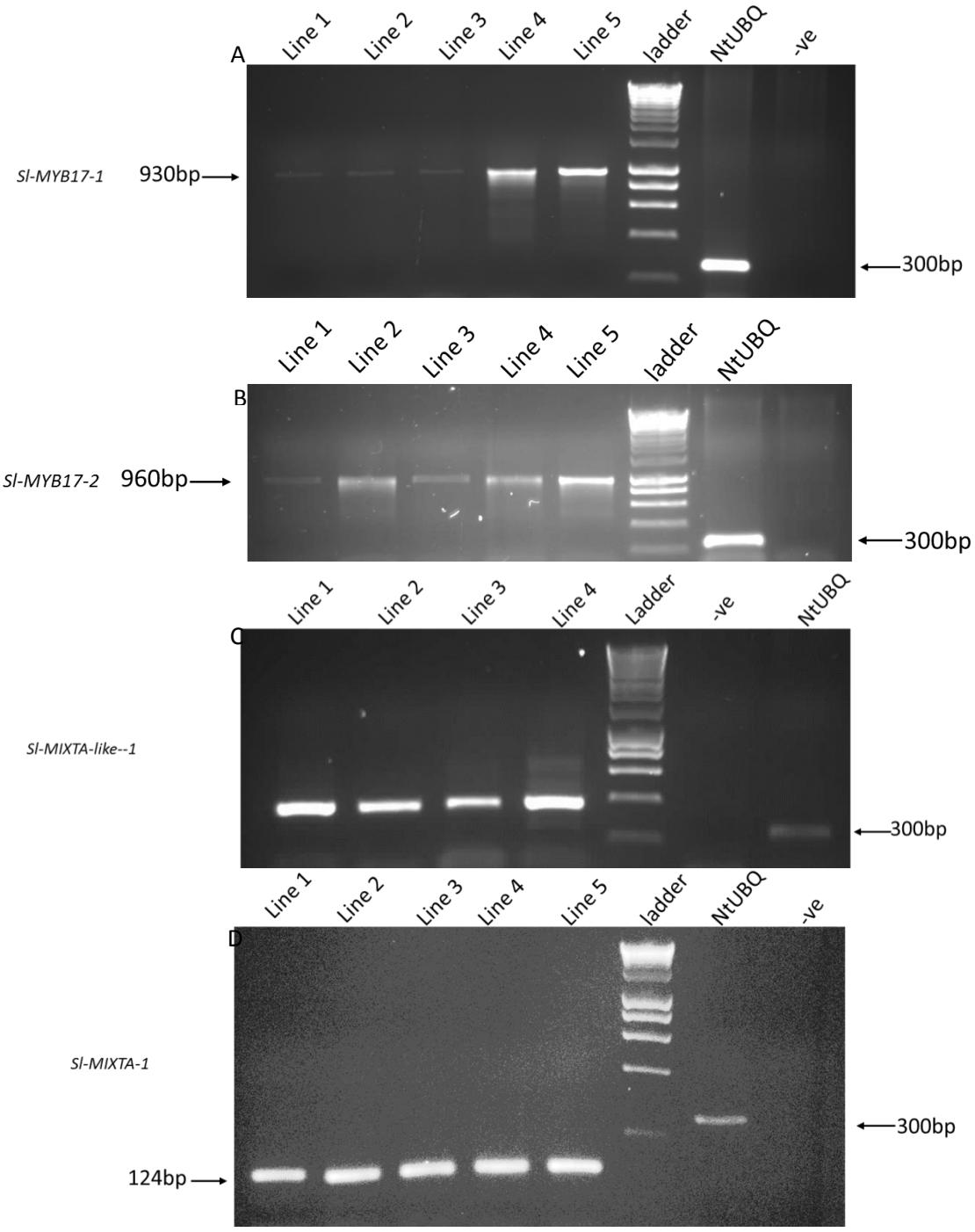
A
Line 1
Line 2
Line 3
Line 4
Line 5
ladder
NtUBQ
-ve
Sl-MYB17-1
930bp
300bp
B
Line 1
Line 2
Line 3
Line 4
Line 5
ladder
NtUBQ
Sl-MYB17-2
960bp
300bp
C
Line 1
Line 2
Line 3
Line 4
Ladder
-ve
NtUBQ
Sl-MIXTA-like--1
300bp
D
Line 1
Line 2
Line 3
Line 4
Line 5
ladder
NtUBQ
-ve
Sl-MIXTA-1
300bp
124bp

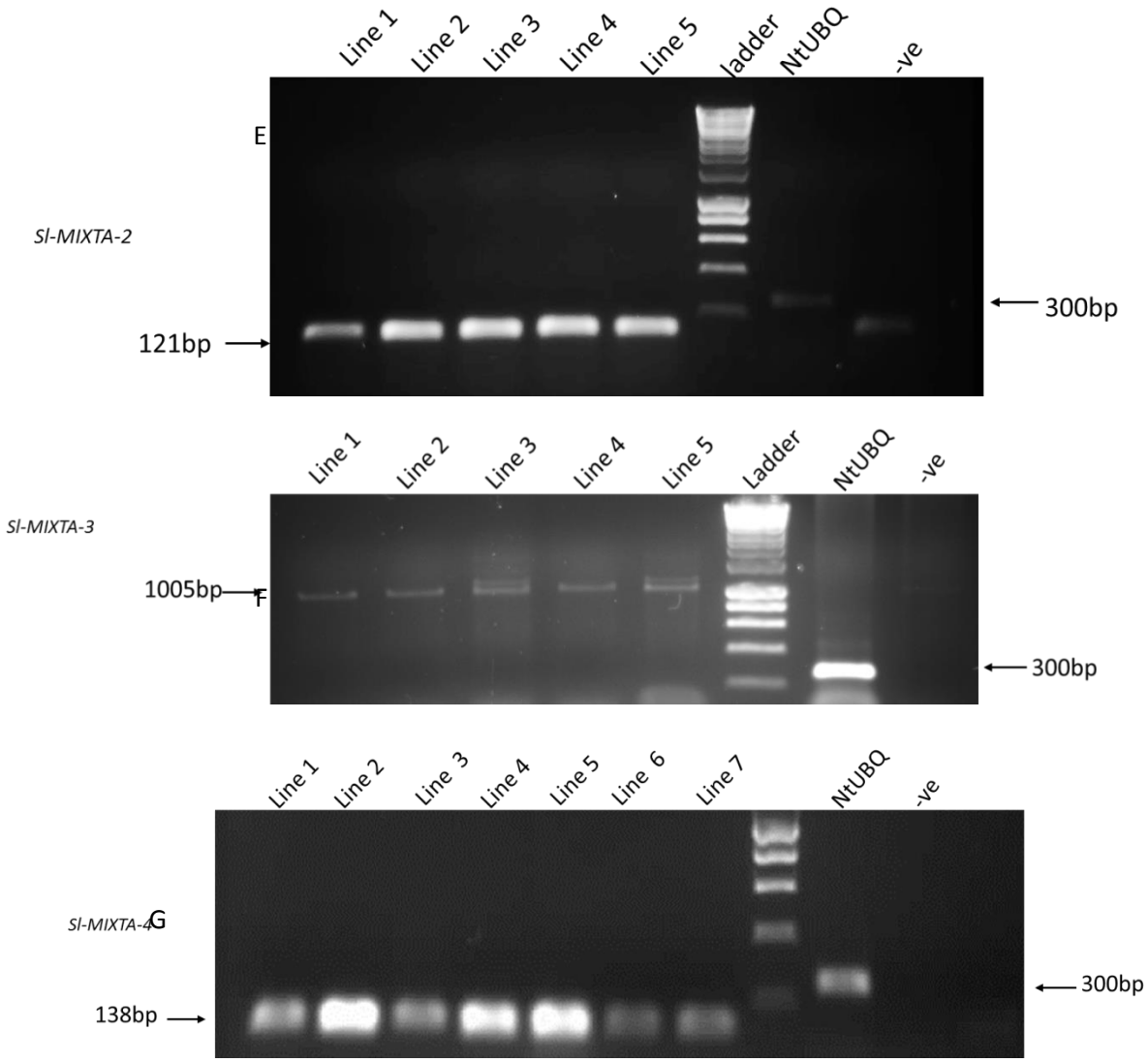

Figure 61: Analysis of transgene expression in transgenic tobacco lines.

All gels show RT-PCR products from tobacco leaf cDNA, using transgene specific primers. Negative control contains wild type tobacco leaf cDNA with the same primers. Positive control lanes show amplified tobacco ubiquitin from the same wild type sample.

A: PCR bands confirming that transgenic tobacco lines contained ectopically expressed *SlMYB17-1*. B: PCR bands confirming that transgenic tobacco lines contained ectopically expressed *SlMYB17-2*.C: PCR bands confirming that transgenic tobacco lines contained ectopically expressed *SlMIXTA-like-1*.D: PCR bands confirming that transgenic tobacco lines contained ectopically expressed *SlMIXTA-1.* E: PCR bands confirming that transgenic tobacco lines contained ectopically expressed *SlMIXTA-2*. F: PCR bands confirming that transgenic tobacco lines contained ectopically expressed *SlMIXTA-3.* G: PCR bands confirming that transgenic tobacco lines contained ectopically expressed *SlMIXTA-4.*

All primers used were gene specific, some produced a band that was the full length of the gene; however other primer sets produced a band that was only a small section of the expressed gene.

3.4.3: Phenotypes of tobacco with ectopically expressed *Solanum lycopersicum R2R3 Myb Subgroup 9* genes.

3.4.3.1: Phenotypes of *Solanum lycopersicum MIXTA* genes expressed in tobacco.

The lines of transformed tobacco shown to be expressing the transgene were phenotyped by cryoSEM. 5 lines were phenotyped for each gene, even if more lines were confirmed to be expressing than 5. Where only 4 lines were expressing only 4 lines were examined by cryoSEM. Each Figure displaying the phenotype of the lines containing the ectopically expressed gene is of a single line, however one that is representative of the phenotype of the other lines. For comparison and to better understand the effect of the gene on the tobacco phenotype, WT tobacco was also examined by cryoSEM as seen in Figure 63.

For each line, the following organs are imaged in the same order each time, and in the same order as for WT for ease of comparison: A: Closeup of the anther, focussed on the anther connective. B: The whole anther. C: Ovary tissue. D: Stigma. E: White section of corolla tube. F: Petal lobes. G: Leaf adaxial surface. H: Leaf abaxial surface.

In those lines where the anther was able to dehisce, the anther was imaged when immature, so as to examine the epidermal cell surface. Where the anther did not dehisce, the anther was imaged at maturity.

Photographs are also shown of the whole tobacco flower at various stages of opening (Figure 62 shows representative wild type (WT) tobacco flowers). Flowers from only one line are shown, but a line that is representative of the phenotype of the other lines.

Figure 62: Photo of WT tobacco flowers

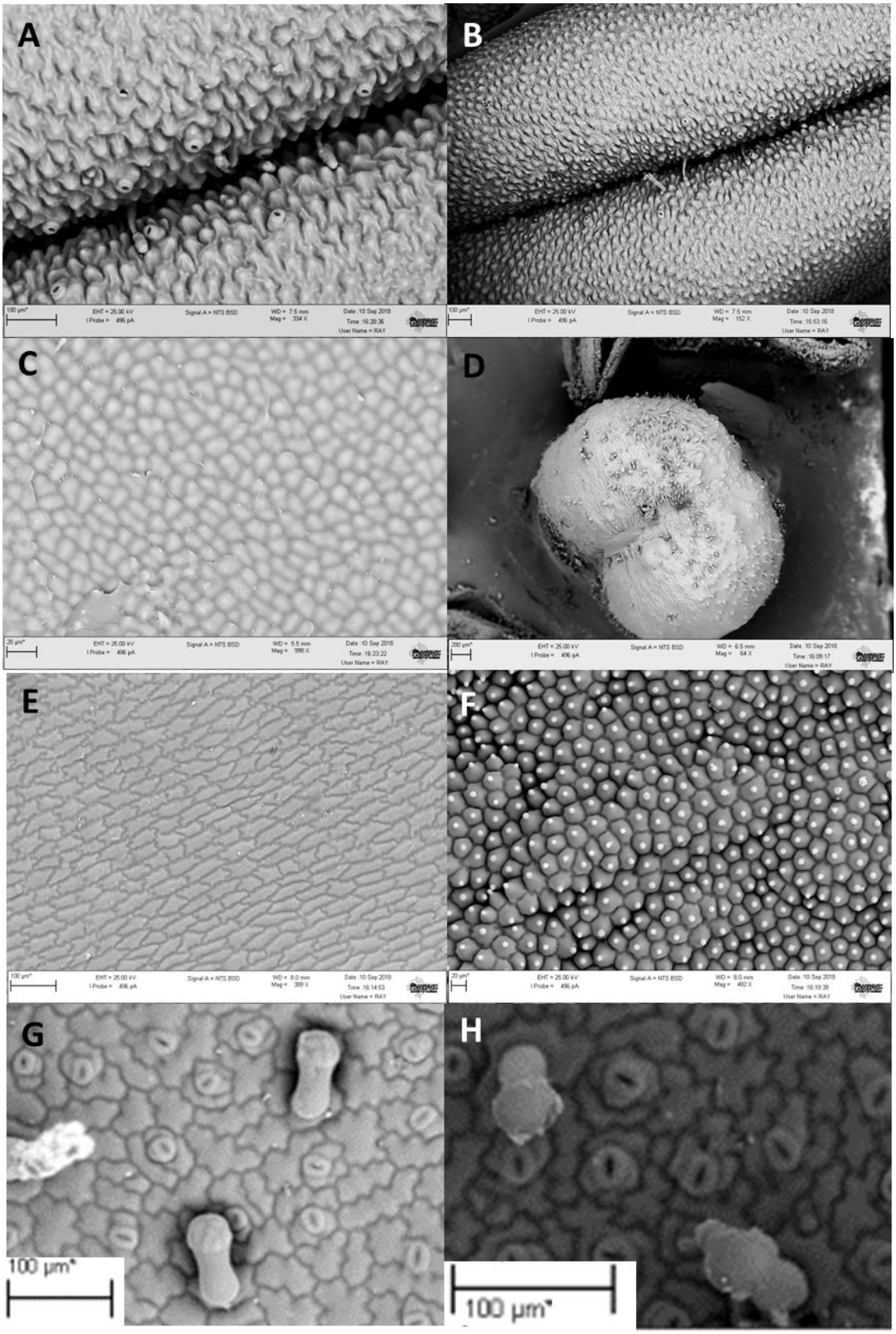

Figure 63: CryoSEM images of WT tobacco organ surfaces for comparison with transgenic lines.
A: Closeup of immature anther surface B: Full immature anther. C: Ovary surface D: Stigma.
E: Corolla tube. F: Petal lobe G: Adaxial leaf surface H: Abaxial leaf surface

3.4.3.1.1: Phenotype of *Solanum lycopersicum MIXTA-1* gene expressed in tobacco.

Tobacco plants expressing *Solanum lycopersicum MIXTA-1* showed normal growth habit and normal leaves, and the gross flower morphology appeared normal. However, the anthers did not dehisce even when the flower was mature. The flowers also appeared more rounded, with petals that had less of a point to their tip than in WT (Figure 64). The anther surfaces of the transgenic lines were covered in trichome-like epidermal cell outgrowths and conical cells (Figure 65 A and B). Some of the trichomes observed on the anther surface were branched. Some stomata were also observed on the anther surface, which was not unusual compared to WT; however sometimes these stomata were observed on the end of trichomes, which was unusual compared to WT. As the anthers did not dehisce these transgenic lines had to be hand pollinated.

The ovaries of the transgenic plants had very unusual epidermal surfaces. The ovary was covered in many trichome-like outgrowths which were more elongated, and in places 'multi-lobed' where in WT the ovary cells are flat (Figure 65 C)

The petal epidermal surfaces appeared normal in both the lobe and corolla tube sections (Figure 65 E and F).

Branching trichomes were observed on the leaf epidermal surface on both sides (Figure 65 G and H). Conical cells were also observed developing on the leaf epidermal surface especially on the adaxial side (Figure 65 G).

Figure 64 Photos of line of transgenic tobacco ectopically expressing *SlMIXTA-1*

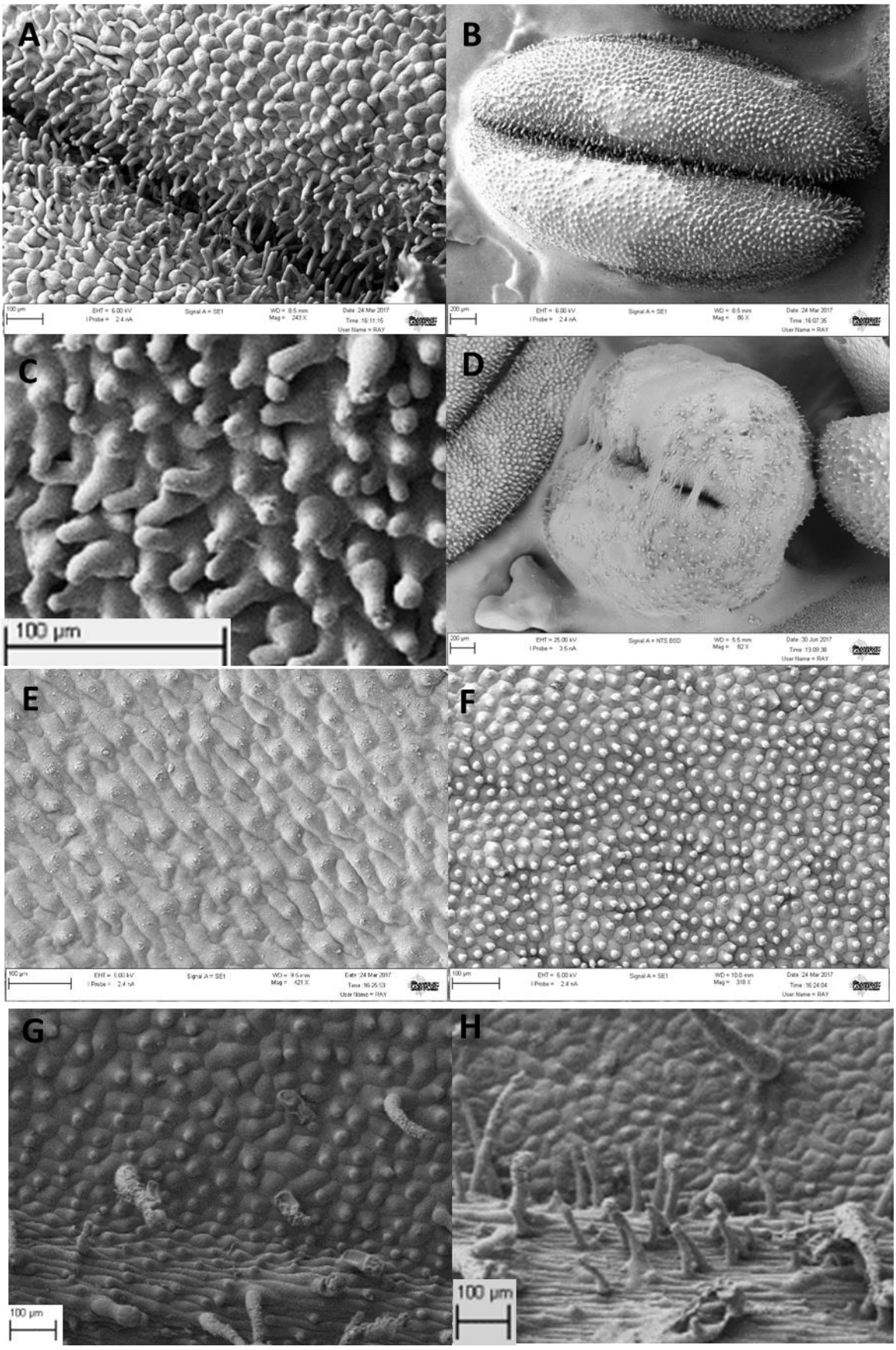

Figure 65: CryoSEM images of epidermal surfaces of organs of a line of transgenic tobacco ectopically expressing *SlMIXTA-1*

CryoSEM images of various transgenic tobacco tissues of a single line representative of the other lines containing this ectopically expressed gene: A: Anther connective. B: Full anther. C: Ovary D: Stigma. E: Corolla tube. F: Petal lobe. G: Leaf adaxial side. H: Leaf abaxial side.

3.4.3.1.2: Phenotype of *Solanum lycopersicum SlMIXTA-2 gene* expressed in tobacco.

Tobacco plants expressing *Solanum lycopersicum MIXTA-2* showed normal growth habit and normal leaves, and the gross flower morphology appeared normal (Figure 66).

The anther epidermal surface had a few glandular trichomes on it. Non glandular trichome-like outgrowths were also observed along the anther connective and along the sides of the anther; however none of this differed markedly from the WT (Figure 67 A and B). The anthers were able to dehisce normally and so these transgenic lines could self to produce a good seed set. The filament was smooth with no epidermal cell outgrowths (Figure 67 B).

The ovary was smooth and did not differ markedly from WT tobacco (Figure 67 C), although occasionally stomata were seen on the ovary epidermal surface. The stigma also appeared normal (Figure 67 D).

Both petal lobe and corolla tube were normal (Figure 67 E and F), however occasional stomata were observed in the corolla tube.

The leaves had some branched trichomes on the adaxial side of the leaf, but otherwise resembled WT (Figure 67G). The abaxial sides of the leaf resembled WT (Figure 67 H). The overall phenotype of these transgenic lines was extremely weak.

Figure 66: Photos of tobacco ectopically expressing *SlMIXTA-2.*
On a macro-scale the transgenic tobacco plants appear fairly normal. There is some curling to the leaves which is usual in plants that have undergone transformation and regeneration. Flowers appear generally fairly normal and dehisce normally.

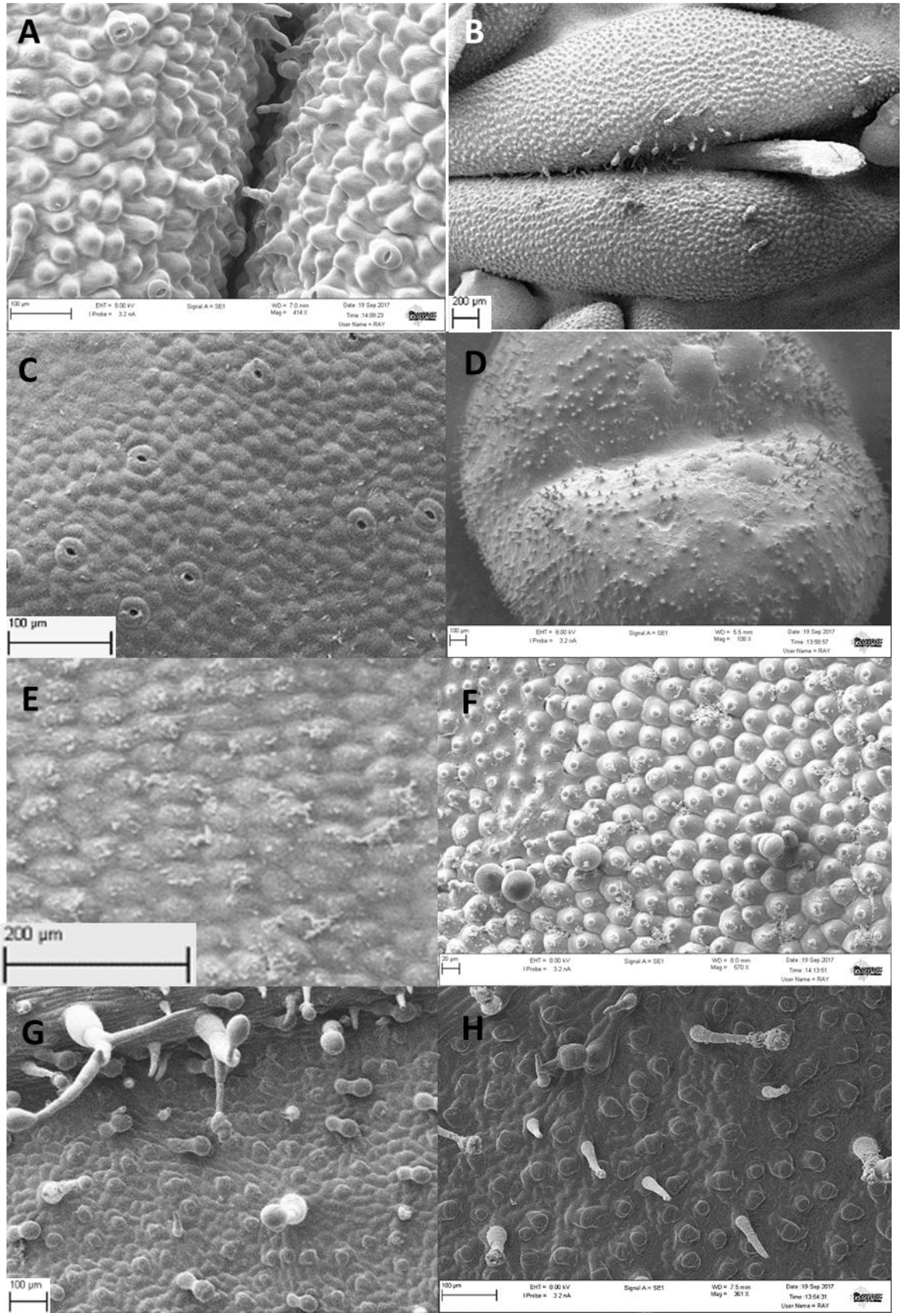

Figure 67: CryoSEM images of epidermal surfaces of organs of a line of transgenic tobacco ectopically expressing *SlMIXTA-2*

CryoSEM images of various transgenic tobacco tissues: A: Anther connective. B: Full anther. C: Ovary D: Stigma. E: White section of the corolla tube. F: Petal lobe. G: Leaf adaxial side. H: Leaf abaxial side.

3.4.3.1.3: Phenotype of *Solanum lycopersicum SLMIXTA-3 gene* expressed in tobacco.

Tobacco plants expressing *Solanum lycopersicum SLMIXTA-3* showed normal growth habit and normal leaves, and the gross flower morphology appeared normal. Anthers dehisced normally (Figure 68).

Glandular trichomes were observed on the anther epidermal surface. Some non-glandular trichomes were also observed along the anther connective. There were also stomata, most pronounced at the anther connective, however none of this differed significantly from the WT anther surface (Figure 69 A and B).

The ovary surface appeared almost normal, with very small outgrowths from the cells (Figure 69 C). Stomata were occasionally observed on the ovary surface, but not consistently between lines so cannot be considered a reliable, true phenotype. The stigma appeared normal (Figure 69 D).

The epidermal surfaces of the corolla tube resembled WT (Figure 69 E) The surface of the petal lobe also resembled WT (Figure 69 F).

The epidermal cell surface of the leaves had branched trichomes, both glandular and non-glandular on the adaxial surface of the leaf (Figure 69 G .) The abaxial side of the leaf resembled WT. Overall the phenotype of this gene expressed ectopically in tobacco was very weak and the plants largely resembled WT.

Figure 68: Photos of tobacco ectopically expressing *SlMIXTA-3*
On a macro-scale the transgenic plants appeared fairly normal. Flower shape was generally normal. Anthers dehisced normally.

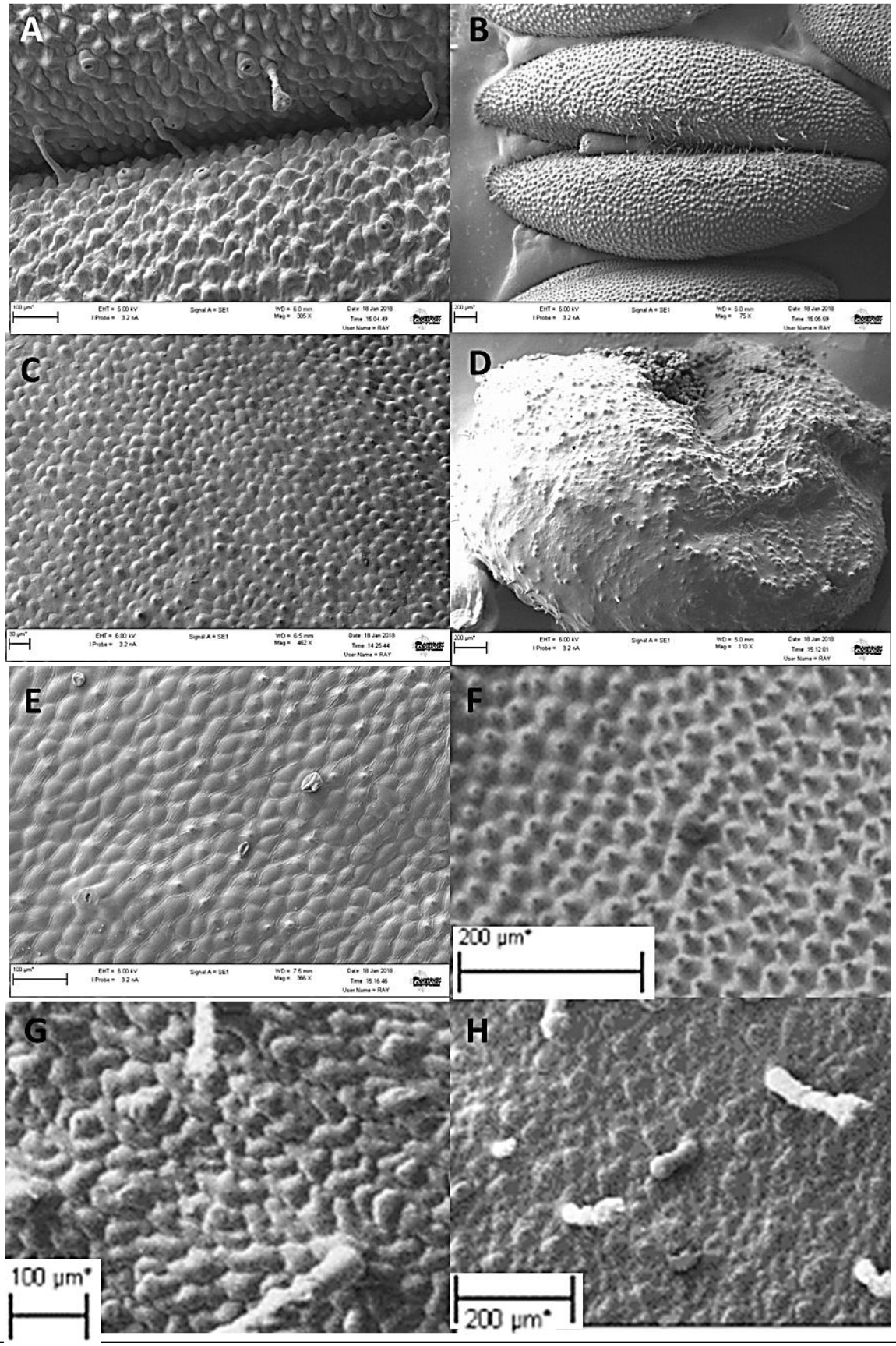

Figure 69: CryoSEM images of epidermal surfaces of organs of a line of transgenic tobacco ectopically expressing *SlMIXTA-3*

CryoSEM images of various transgenic tobacco tissues: A: Anther connective. B: Full anther. C: Ovary D: Stigma. E: White section of the corollatube. F: Petal lobe. G: Leaf adaxial side. H: Leaf abaxial side. All images except for C were from a single line. C is imaged from another line due to being a clearer image, however the image is representative of all of the lines ectopically expressing this gene.

3.4.3.1.4: Phenotype of *Solanum lycopersicum SlMIXTA-4* gene expressed in tobacco.

Tobacco plants expressing *Solanum lycopersicum SlMIXTA-4* showed normal growth habit and normal leaves, and the gross flower morphology appeared normal (Figure 70).

Epidermal surface cells of the anther were slightly conical. Glandular trichomes were also observed on the anther surface along with non-glandular trichomes and stomata, however this did not differ significantly from WT (Figure 71 A and B). The conical shape of the epidermal surface cells of the anther became more pronounced as the anther reached maturity and began to dehisce, non-glandular trichomes were also more exaggerated and numerous on the anther connective (Figure 72 A and B). The anthers dehisced, but not so completely as in WT, allowing them to be imaged when partially dehisced to show these more pronounced conical cell shapes on the anther surface (Figure 72 B). Trichomes were observed on the filaments of mature anthers, but not on immature anthers (Figure 72 A).

The ovary of the transgenic lines had conical cells towards the base of the ovary and some trichome like outgrowths were also observed (Figure 71C and I). The extent of the ovary phenotype varied between the transgenic lines, perhaps indicating different levels of expression of the transgene, however all of these traits were observed on all of the lines to some degree or another on the ovary epidermal surface. The stigma appeared to be normal (Figure 71 D).

The corolla tube surface resembled WT (Figure 70G) and the petal lobe resembled WT (Figure 71H).

Branched trichomes were observed occasionally on the leaf epidermal surface on both sides of the leaf, however the surfaces were overall very similar to WT (Figure 71 G and H).

Figure 70. Photos of tobacco ectopically expressing *SlMIXTA-4*
Plants appeared normal on a macroscale. Anthers dehisced normally.

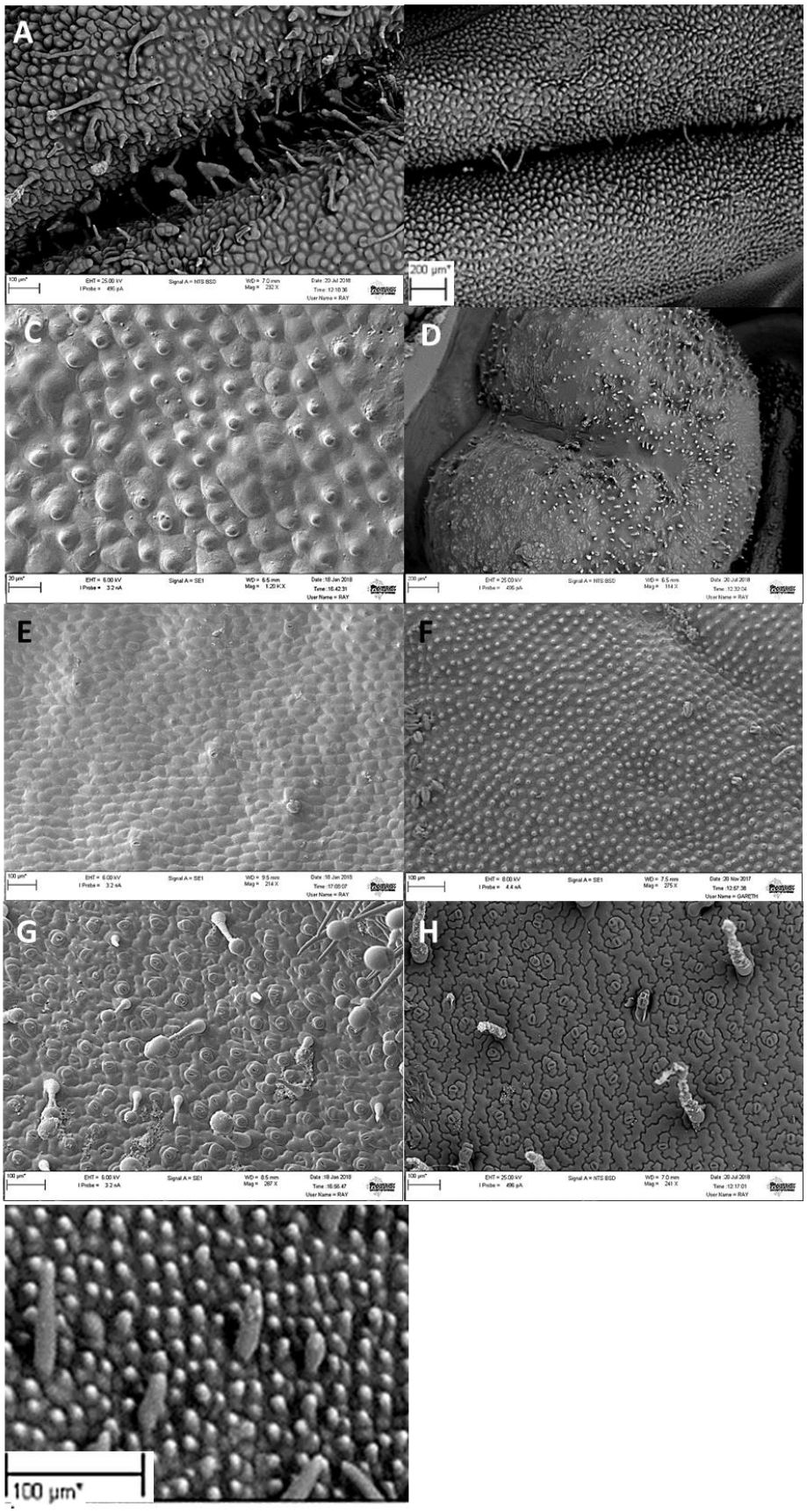

Figure 71: CryoSEM images of epidermal surfaces of organs of a line of transgenic tobacco ectopically expressing *SlMIXTA-4*

CryoSEM images of various transgenic tobacco tissues: A: Anther connective. B: Full anther. C: Ovary D: Stigma. E: White section of the corolla tube. F: Petal lobe. G: Leaf adaxial side. H: Leaf abaxial side. I: Additional image of ovary surface from same line as anthers, as this image displays more clearly the trichome outgrowths in addition to the altered epidermal cell shape. It should be noted that the images of the petal and ovary in these Figures are from a different line ectopically expressing the same gene, as the images are clearer than for the line used for the rest of the floral organs. The line however is also representative of the phenotype of all the lines ectopically expressing this gene, there is also no difference between the appearances of the petal surface in these lines compared to WT.

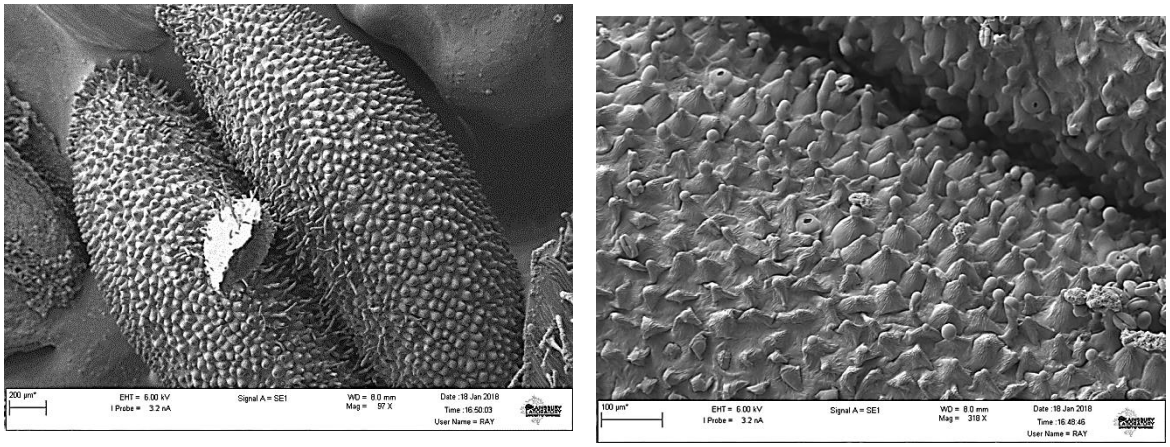

Figure 72: Additional CryoSEM images of mature anthers, partially dehisced, of tobacco expressing the *SlMIXTA-4* gene.

Anthers that were partially dehisced when imaged displayed more exaggerated epidermal cell outgrowths on the anther surface.

3.4.3.2: Phenotype of *Solanum lycopersicum SlMIXTA-like* gene expressed in tobacco

The *MIXTA-like* clade of the Subgroup 9A genes contains only a single member in tomato. Tobacco plants expressing *Solanum lycopersicum MIXTA-like-1* showed normal growth habit and normal leaves, and the gross flower morphology appeared normal (Figure 73).

The anther, when examined with cryo-SEM, had glandular trichomes on the epidermal surface. There were also a number of stomata on the anther surface. However both of these things can sometimes be seen in WT tobacco. The rest of the anther surface was covered in conical cells, which do not resemble WT (Figure 74 A and B). The filament, however, is normal and smooth with no epidermal cell outgrowths (Figure 74 B).

The ovary has some conical-like cells on the surface; however the phenotype is not very strong (Figure 74 C). The stigma appears normal (Figure 74 D).

The surface of the corolla tube has smooth flat cells as is observed in wild type tobacco, however there are occasionally a few more conical cells on the surface (Figure 74E). The petal lobe has the conical cells on its epidermal surface which are seen in WT tobacco (Figure 74 F).

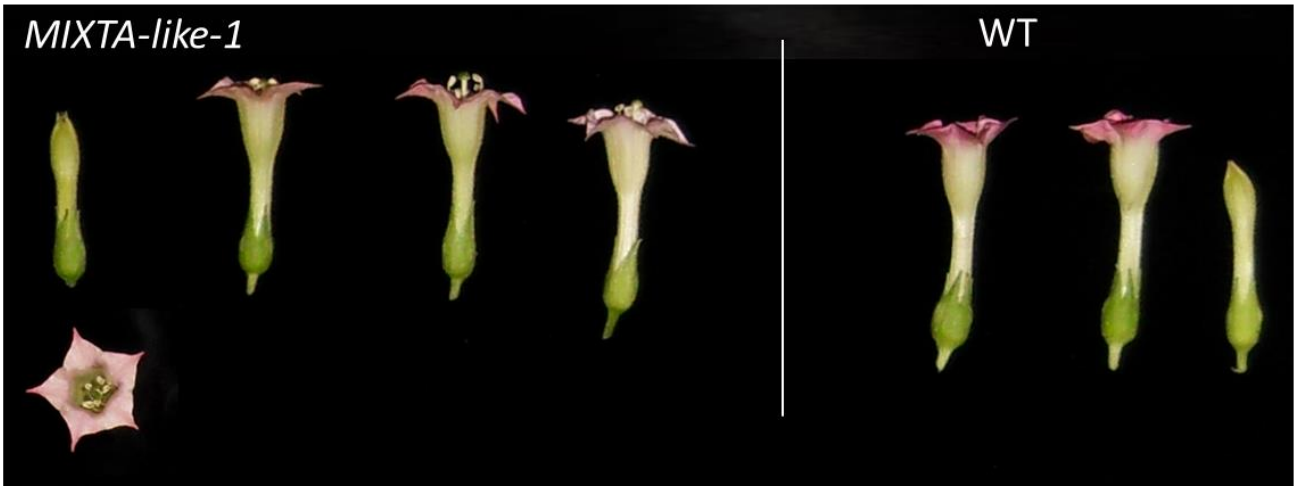

Figure 73: Photos of tobacco ectopically expressing *SlMIXTA-like-1*
The flowers are normal compared to wild type and anthers dehisce normally.

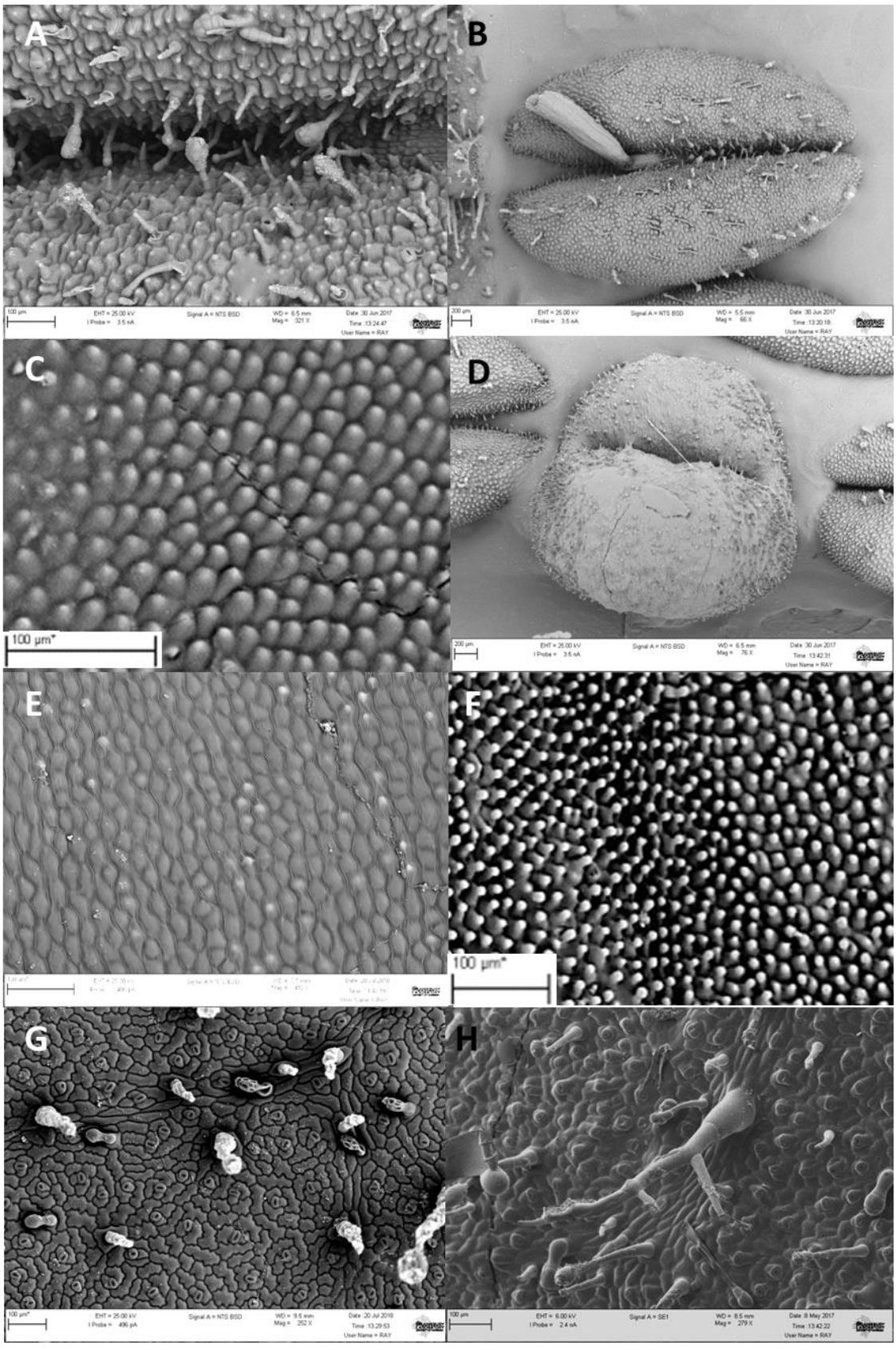

Figure 74. CryoSEM images of epidermal surfaces of organs of a line of transgenic tobacco ectopically expressing Sl*MIXTA-like-1*

CryoSEM images of various transgenic tobacco tissues: A: Anther connective. B: Full anther. C: Ovary D: Stigma. E: Surface of corolla tube. F: Surface of petal lobe G: Leaf adaxial side. H: Leaf abaxial side. It should be noted that the petal images are from a second line ectopically expressing the same gene, which has the same phenotype on the other floral organs.

3.4.3.3: Phenotypes of *Solanum lycopersicum MYB17* genes expressed in tobacco

3.4.3.3.1: Phenotype of *Solanum lycopersicum SlMyb17-1* gene expressed in Tobacco.

Tobacco plants expressing *Solanum lycopersicum SlMyb17-1* showed normal growth habit and normal leaves, and the gross flower morphology appeared normal. However, the anthers did not dehisce even when flowers were past full maturity (Figure 75).

Parts of the plants were examined by cryo-SEM. This showed that the anthers were covered in trichome like outgrowths and conical cells (Figure 76 A and B). This is most pronounced along the anther connective (Figure 76A). Trichome-like outgrowths were also present on the filament (Figure 76B). Along with trichomes on the anthers, stomata were also observed, and while this is sometimes seen in WT, these stomata were often formed on the end of a trichome, which is not normal. Anthers were unable to dehisce, presumably due to the outgrowths preventing them from doing so. Therefore the flowers had to be pollinated by hand. The ovaries of these plant lines had many epidermal cell outgrowths which were trichome-like, with a mixture of long and shorter trichomes and some conical cells. These outgrowths were most exaggerated towards the base of the ovary. Some of these cell outgrowths were multi-lobed (Figure 76C). The stigma appeared normal, however was drier than usual (Figure 76 D). This presented a problem for pollination as the liquid on the stigma surface is required for pollen germination. Therefore for pollination to occur, wild type pollen had to be germinated on wild type stigma and then transferred to the transgenic stigma. Seed set for these transgenic lines was relatively small. Both the corolla tube and petal lobe were examined on their inner surface. The surface of the corolla tube (which is normally flat-celled) exhibited conical cells and trichomes of varied sizes (Figure 76 E). The petal lobe exhibited both the conical cells usually found on this section of the petals and also occasionally larger trichomes (Figure 76 F). The adaxial leaf surface also had branching trichomes and conical cells (Figure 76 G). The adaxial leaf surface had large numbers of branching trichomes, the majority of trichomes on the leaf surface were branched, whilst some of the epidermal surface cells had conical cell outgrowths, but not the majority (Figure 76 G). The abaxial surface of the leaves had large numbers of branched trichomes as well as many conical cells, yet not all the epidermal surface cells were conical in shape, some remained flat and normal (Figure 76 H). The transgenic plants were generally unhealthy, with leaves that frequently turned brown and died. Five independent transgenic lines were

phenotypically characterised by cryo SEM, all of which had the same phenotype and were shown to be expressing the transgene by RT-PCR using gene-specific primers. The line shown in Figure 76 is representative of the others.

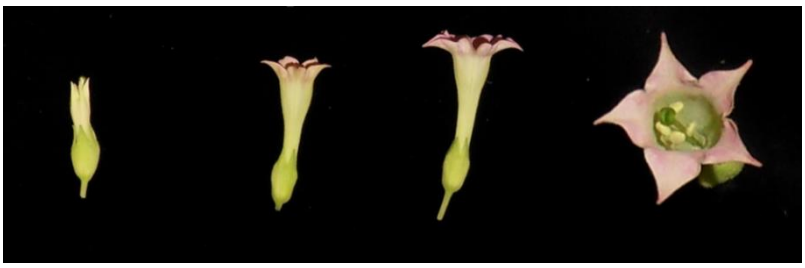

Figure 75: Photos of the flowers of Tobacco expressing *SlMyb17-1.*
Flowers are normal aside from non-dehiscing anthers.

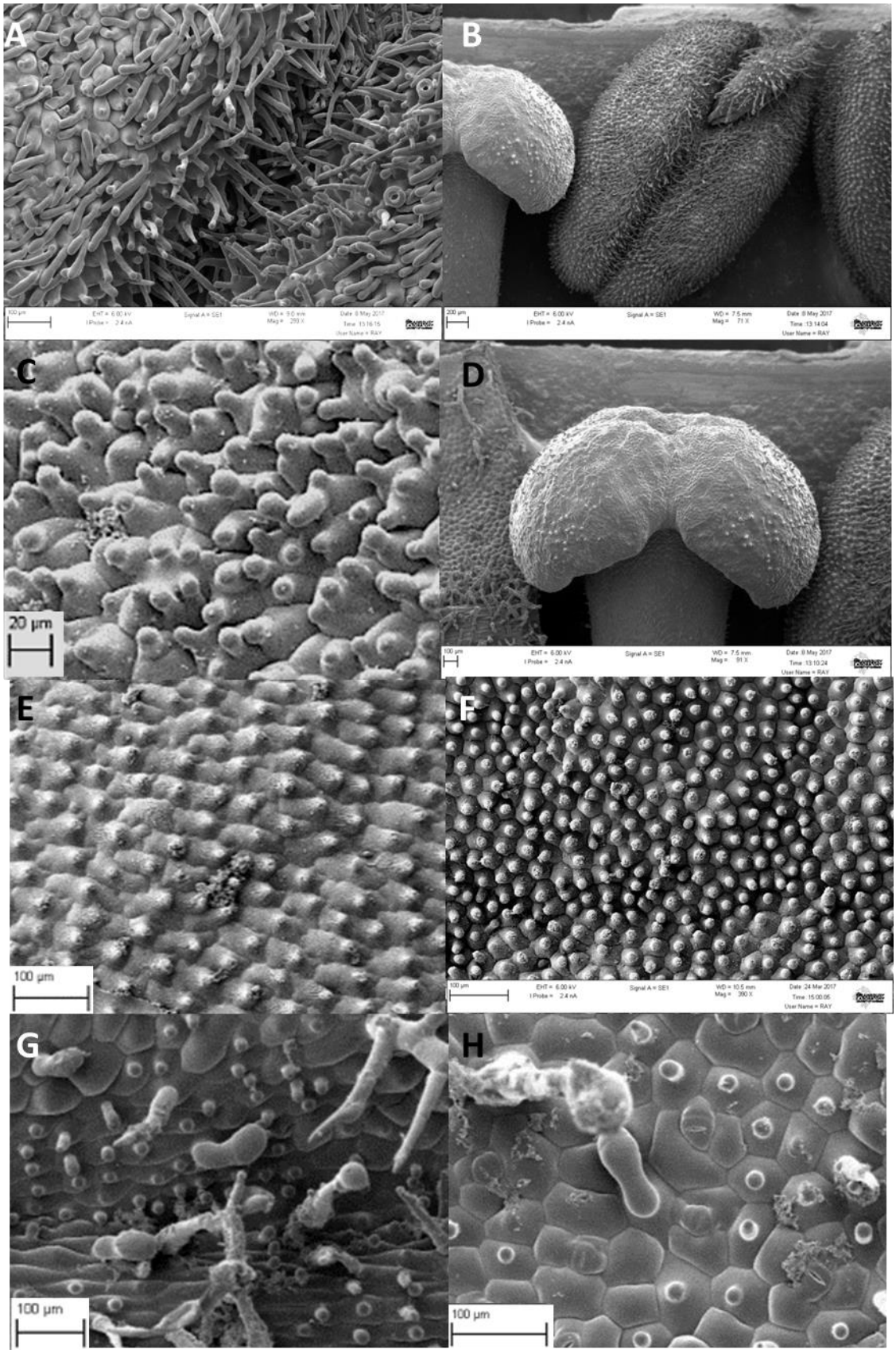

Figure 76: CryoSEM images of epidermal surfaces of organs of a line of transgenic tobacco ectopically expressing *SlMYB17-1*

CryoSEM images of various transgenic tobacco tissues: A: Anther connective. B: Full anther. C: Ovary D: Stigma. E: White section of the corolla tube. F: Petal lobe. G: Leaf adaxial side. H: Leaf abaxial side. It should be noted that all the images are from the same transgenic line except for E, F and C which are from a second transgenic line due to these images being clearer, but all are representative of all of the lines.

3.4.3.3.2: Phenotype of *Solanum lycopersicum SlMyb17-2* gene expressed in Tobacco.

Tobacco plants expressing *Solanum lycopersicum Myb17-2* showed normal growth habit and normal leaves, and the gross flower morphology appeared normal, yet with petal lobes which appeared pointy compared to WT. The anthers did not dehisce even in fully mature flowers (Figure 77).

The anther surfaces of the transgenic lines were covered in epidermal cell outgrowths. Trichomes and conical cells covered the anther surface and stomata were observed on the ends of trichomes on the anther surface (Figure 78 A). Longer glandular trichomes were also sometimes observed at the anther connective (Figure 78 A). Outgrowths were generally most exaggerated at the anther connective (Figure 78 B). The filament also had trichomes on its surface. This can be seen in Figure 78 B. The ovary epidermal surface was covered in outgrowths. The outgrowths were trichome like and were most exaggerated at the base of the ovary (Figure 78 C) .The surface of the petal lobes appeared normal, with only the usually observed conical cells (Figure 78 F). The surface of the corolla tube did not appear as flat as on the WT, with some more conical shape to the epidermal cells and with some development of trichomes (Figure 78 E). In some flowers and some lines these trichomes became more exaggerated, resulting in an extreme number of trichomes causing deformities on the corolla tube (shown and discussed later in Figure 88). The surface of the stigma was dry and so the pollen had to be germinated on a wildtype stigma for pollination by hand to occur, as described for *SlMyb17-1* in section 3.4.3.3.1. The surface otherwise resembled WT (Figure 78 D). The abaxial and adaxial surfaces of the leaves exhibited branched glandular and non- glandular trichomes. No conical cells were observed on the abaxial surface, however some conical cells were occasionally observed on the adaxial leaf surface, most often on and around the leaf vein (Figure 78 G and H).

Five independent transgenic lines were phenotypically characterised by cryo-SEM, all of which had the same phenotype and were shown to be expressing the transgene by RT-PCR using gene-specific primers. The line shown in Figure 78 is representative of the other lines.

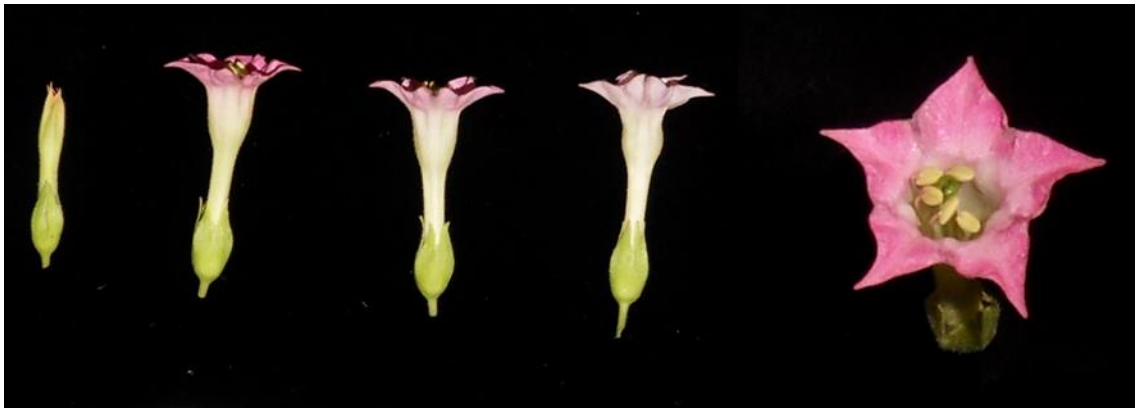

Figure 77: Photos of the flowers of Tobacco expressing *SlMyb17-2*.

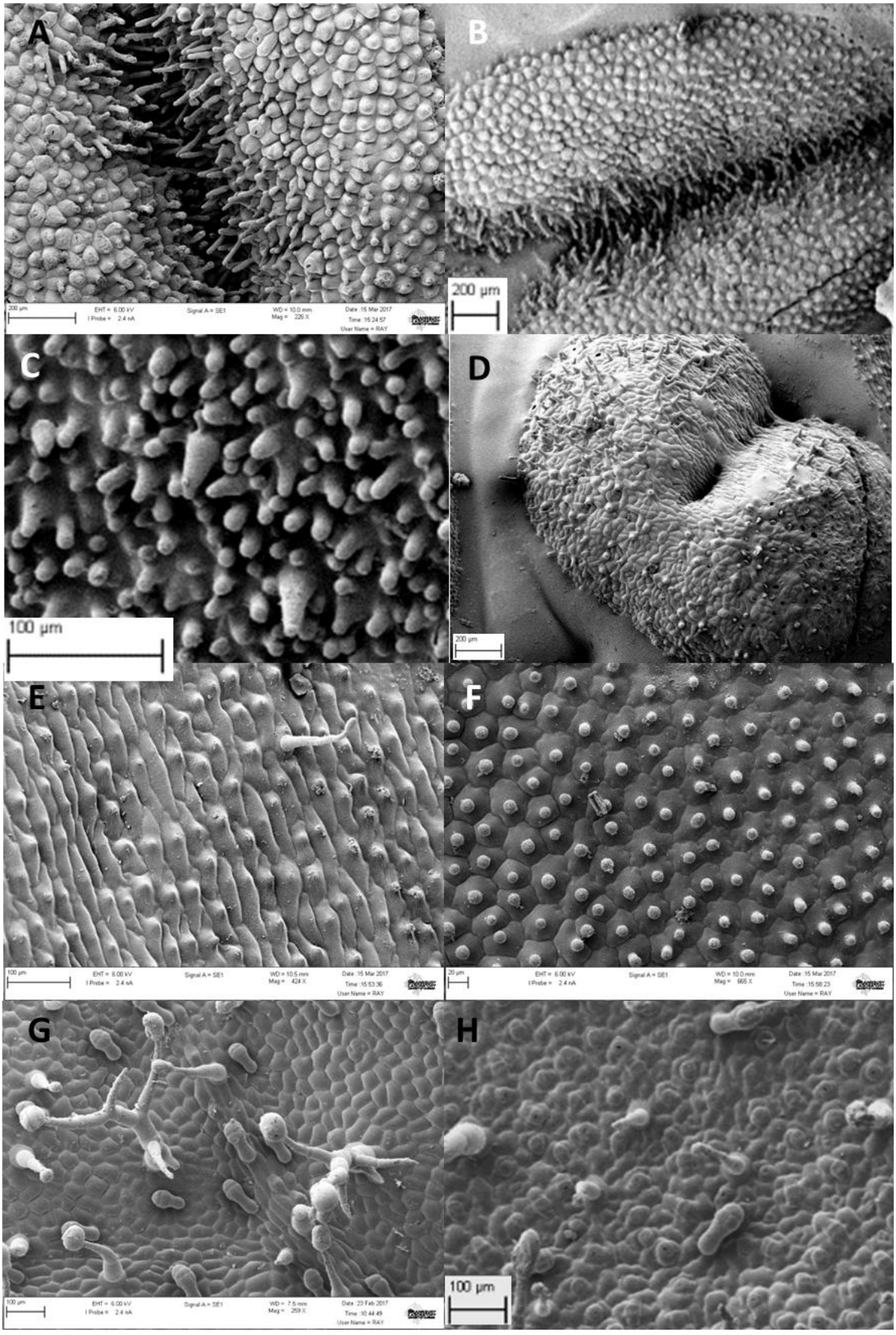

Figure 78: CryoSEM images of epidermal surfaces of organs of a line of transgenic tobacco ectopically expressing *SlMYB17-2*

CryoSEM images of various transgenic tobacco tissues: A: Anther connective. B: Full anther. C: Ovary D: Stigma. E: Corolla tube. F: Petal lobe. G: Leaf adaxial side. H: Leaf abaxial side.

3.4.3: CRISPR genome editing in *Solanum lycopersicum*

3.4.3.1: Selection of genes for further analysis through knockout

Based on predicted expression patterns of the *R2R3 MYB subgroup9* genes of tomato from the tomato eFP browser (http://bar.utoronto.ca/efp_tomato/cgi-bin/efpWeb.cgi), some genes were selected for further investigation of their function by mutation using CRISPR. The genes chosen were those that were expressed in unopened buds, as at this stage the trichome mesh of the anthers is forming. The genes selected were: *MYB17-2, MIXTA-4* and *MIXTA-like-1*. Constructs were built for *MIXTA-4* and *MIXTA-like-1*. The *MYB17-2* construct proved difficult to build and had to be abandoned due to time constraints. The *MIXTA-like-1* construct was not used to transform tomato as, after the completion of the construct, it was found that another team had conducted a CRISPR knockout of this gene. The other team offered access to flowers from their lines, but unfortunately their plants died without flowering. Therefore only the *MIXTA-4* CRISPR construct was used to transform tomato. The protein encoded by this gene did demonstrate the ability to induce cellular outgrowth on the tobacco ovary, making it a good candidate for control of the tomato anther trichome mesh.

3.4.3.2: CRISPR knockout of *MIXTA-4* gene in *Solanum lycopersicum*

The *MIXTA-4* CRISPR construct was used to transform tomato cotyledon fragments. Calli were formed by ~80% of the fragments. These calli reached a considerable size, and were moved into 250ml jars. At this stage leaf formation was evident and calli began to form shoots and take on a tomato-like appearance. However once shoot formation occurred the plantlets began to die and became highly susceptible to infection. Once moved onto rooting media, the plantlets became even less healthy and no root formation occurred. At the point of thesis submission a number of calli and plantlets remain but none have rooted. This may be a problem with the protocol, or might suggest that the knockout of the *MIXTA-4* gene badly affects the health of the plant (perhaps by interfering with stomatal development). For further study of the function of these genes a different gene knockout approach could be used and would provide useful information as to the importance of these genes.

3.4.4: Expression analysis by semi quantitative RTPCR in tomato flowers at different developmental stages

3.4.4.1: Choice of tissues for expression analysis

During the development of the tomato flower from bud to mature open flower the anthers develop separately and then the trichomes begin to develop on the anther surface, slowly knitting the anthers together as the trichome mesh forms between the different anthers' cellular outgrowths. Flower stages were determined according to macroscopic features of organ position (Figure 79) and trichome mesh development defined at each stage. During stage 2 the epidermal cell outgrowths for the trichome mesh begin to develop. By stage 3 the trichome mesh has developed mostly but the anthers are not yet fully held together and the epidermal cell outgrowths other than the trichome mesh have not yet developed. The bud begins to open slightly, with the trichome mesh fully formed, and the anthers held together, by stage 4. At this stage the epidermal cell outgrowths on the anther surface in addition to the trichome mesh have begun to develop. At stage 5 the anther cone protrudes from the end of the bud and the petals begin to open more fully. By stage 6 the flower is fully open and the anthers completely exposed.

These stages were chosen as they show the stages during which the trichome mesh develops and so allow us to see which genes are highly expressed during this process. The floral stages can be seen in Figure 79, and the corresponding micro-morphology of the epidermal surface of the anther for each stage is shown.

Tissue for expression analysis was separated into 3 pools: A, B and C; which contained tissue from separate individuals. Each pool contained multiple individuals, but approximately the same number of individuals were in each pool.

Tissue for each pool was collected from:

Stage 1 and stage 2 buds: growth stages were pooled due to small size of material. Whole bud was collected

Stage 3: whole bud

Stage 4: anthers

Stage 5: anthers

Stage 6: anthers

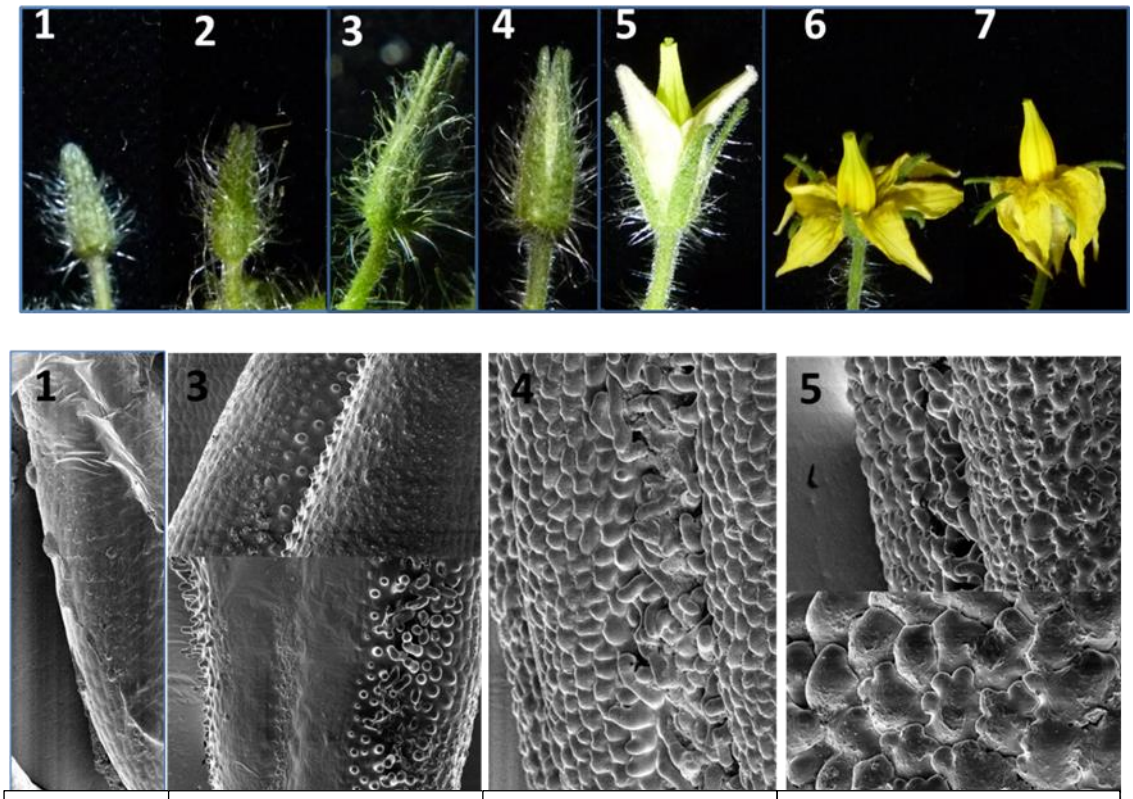

Figure 79: Tomato floral stages for semi-qRTPCR

The photographs and corresponding SEM images show stages in the growth of the flower of *Solanum lycopersicum.* 1: The bud is at its smallest and is completely sealed at its tip, the anther cone has not yet formed, neither have 'glove-like' papillae on the anther surface. The anther surface is smooth. 2: The tip of the bud has split slightly and bud size has increased only a small amount. 3: Bud size has increased further, the bud has elongated and there is a clear split at the bud tip. The pepper pot cone has not yet formed, but there is initial growth of trichome like outgrowths along the sides of the anther which will form the basis of the trichome mesh. 4: The bud has begun to split open revealing the petals within, at this point the pepper pot anther cone is almost formed completely, the anthers have become fused and the 'glove-like' papillae have begun to develop. 5: The flower has begun to open and the anther cone can be seen. At this stage the pepper-pot cone is completely formed and the 'glove-like' papillae have taken on their distinctive shape. 6: The flower is fully open. 7: The petals have become reflexed back away from the anther cone.

3.4.4.2: Semi Quantitative RT-PCR expression analysis of *Solanum lycopersicum* subgroup 9 genes

The transcription of the tomato R2R3 MYB subgroup 9 genes was analysed using semi-quantitative RT-PCR and comparing activity against that of *CAC* as a reference gene. Floral buds were collected at different stages of development, and consequently at different stages of the formation of the trichome mesh and anther cone development. At stage 1+2 and stage 3 the flower buds were too small for the anthers to be dissected out, however in later stages the anther cone was dissected out and only tissue from this was used. Stage 1 and stage 2 were pooled due to the buds being so tiny and a large amount of tissue required for RNA extraction. There is very little change between stage 1 and 2 with regards to the development of the trichome mesh and the anthers, the two stages only being distinguished by a slight change in the size of the bud. Stage 5 and stage 6 were also pooled into one stage 5+6 as at this point the anther cone is formed, the trichome mesh has finished development and the epidermal cell outgrowths on the anther surface are also fully formed.

The *SlMYB17-1* gene is expressed in the floral tissue stages 1+2 and 3 and then expression level drops in stage 4. By stage 5+6 the band is only visible at 40 cycles and is very faint and expression has further faded. The gene is expressed most strongly early in the development of the buds, when the trichome mesh of the anthers is forming. At stage 3 the band is especially bright compared to the housekeeping gene. By stage 4 the trichome mesh is completely formed and the anther cone is formed, the epidermal cell outgrowths on the rest of the anther surface have begun developing. It should however be noted that the tissue pools 1+2 and 3 contain entire buds, while 4 and 5+6 contain only the anthers, which were dissected from the buds. Therefore it is possible that the expression here reflects a steady low expression in the anthers, with the brightness of the bands in 1+2 and 3 representing an expression in petals, sepals, and other non-anther tissues in the bud. So while the sqRTPCR result may reflect a peak of gene expression in the anthers early in development, it may also be that expression in other floral tissues is confusing the picture.

The *SlMYB17-2* gene is expressed in all floral stages. The bands are brightest and most visible in stages 1+2 and stage 3. Stage 3 is especially bright compared to the housekeeping gene. This gene is expressed in a near identical pattern to *SlMYB17-1*, and the data should be interpreted with the same caution.

SlMIXTA-like-1 is not expressed very strongly in any of the floral tissues. A band is visible only at cycle 40, however this faint band is visible in tissues for all floral stages.

SlMIXTA-1 is expressed in stage 1+2 and stage 3. The bands are most visible in stage 1+2. The expression fades in stage 4 and stage 5+6, however a very faint band can be seen at cycle 40 of stage 4 and 5+6. *SlMIXTA-2* is not expressed in any of these tissues, or is expressed at such a low level that it cannot really be detected here. *SlMIXTA-3* is also expressed at an extremely low level in all four stages. *SlMIXTA-4* also has very low level expression - the bands are only very faint and can only be seen at cycle 40 for each of the tissue stages. The bands are most visible, and the expression highest, in stage 4 and stage 5+6. This expression pattern is the opposite of that expected from a gene controlling trichome mesh development.

These data were compared to the expression patterns predicted by the tomato eFP browser (http://bar.utoronto.ca/efp_tomato/cgi-bin/efpWeb.cgi). It should be noted that this facility does not separate out floral organs or floral developmental stages, so can only give an indication of expression in our tissues. According to this facility *MYB17-1* is only expressed in green fruit, and even then at very low levels, in contrast to what was found in the semi-qPCR conducted here. *MYB17-2* is predicted to be expressed most highly in unopened buds and in fully opened flowers, but also at low levels throughout the leaves of the plant. The results of the sqRTPCR agree with this, showing the gene to be expressed throughout each of the floral stages. *MIXTA-like-1* was predicted to be expressed in unopened flower buds, leaves and fruit, and the sqRTPCR results also show the gene to be expressed, at low levels, in the flower at all stages of anther cone development. *MIXTA-1* was predicted by the eFP browser to be expressed in unopened flower buds, and the data here also agree with this prediction. *MIXTA-2* was predicted by the eFP browser to be expressed only in the tomato leaves, so its lack of expression in the tissues examined here agrees with this prediction. *MIXTA-3* was predicted to be expressed in unopened flower buds whereas here it is expressed at a very low level in all stages. *MIXTA-4* was predicted to be expressed in unopened flower buds and fully open flowers, while the sqRTPCR results suggest slightly later expression. However it is perhaps not too great a concern that the sqRTPCR results and that of the eFP browser do not completely agree. The eFP browser uses a bulk tissue pool: in this case the entire flower (including anthers, carpel, petals, sepals etc) whilst in my

later floral stages only anthers were sampled. Therefore why my results differ from the eFP browser may reflect the different tissues investigated. Also, the EFP browser does not distinguish between different stages of floral development: it only separates between 'open flower' and 'bud'. Buds of differing sizes are at very different developmental stages with regards to the formation of the trichome mesh. It is possible that the genes involved with the production of the trichome mesh are only active for a very short window of time and expressed only at low levels, therefore it is possible that gene expression could be missed by the EFP browser. A literature search was conducted to find any other sources of expression data for these genes which could be compared to this study's findings, however none was found.

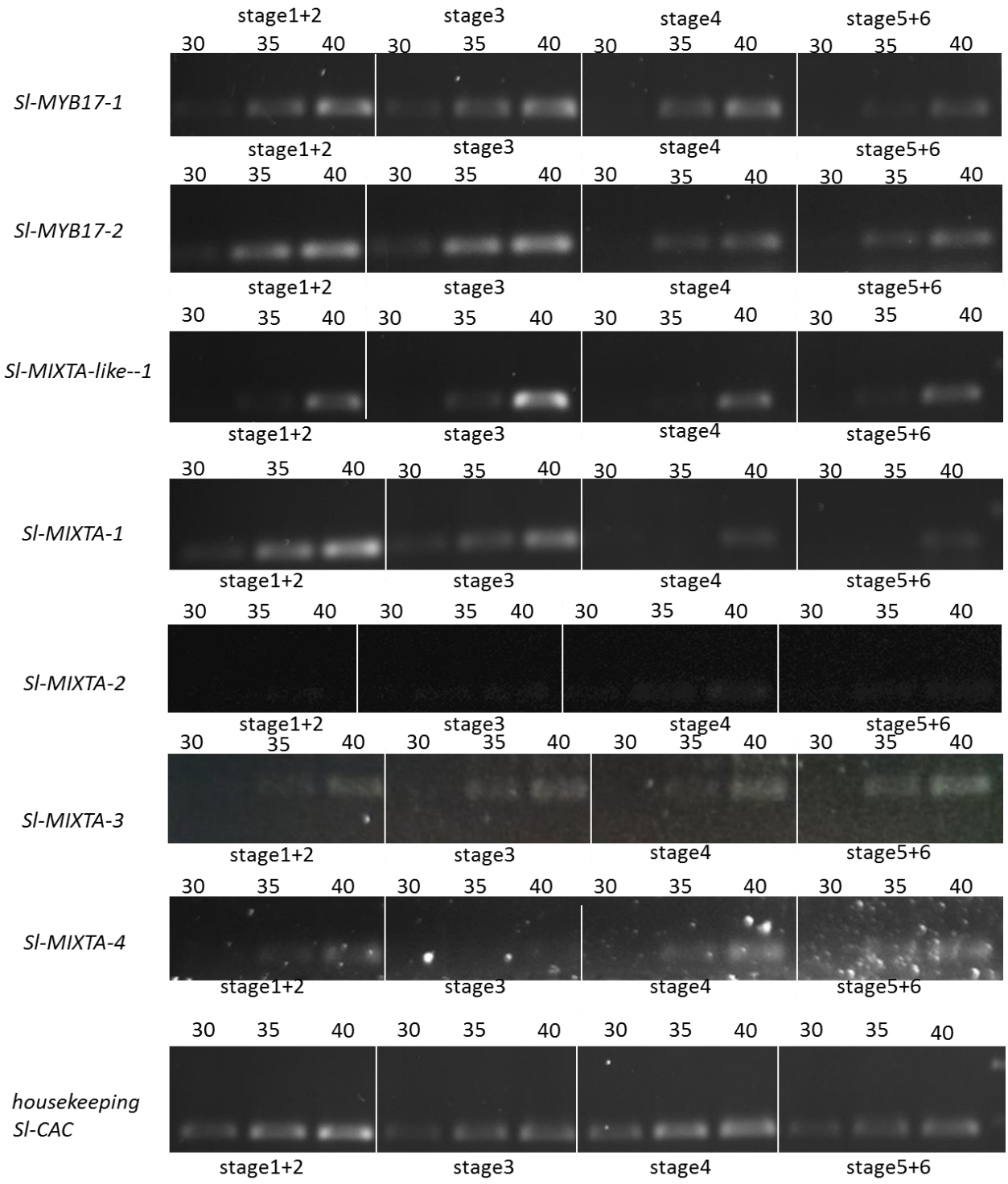

Figure 80: Semi quantitative RT PCR of all Solanum lycopersicum R2R3 MYB subgroup 9 genes during development of the flower.

Four tissue stages are shown, these stages refer to those in Figure 78 above each lane, the number of cycles is indicated. Positive and negative controls were conducted for each primer set, with the positive control being the same primers amplifying from a plasmid containing the sequenced gene. The negative control was the same primers with only water.

3.4.4: R2R3 MYB Subgroup 9 genes in other sequenced Solanum species compared to candidate genes.

It was investigated how the candidate R2R3 subgroup 9 genes varied between species of Solanum which have been sequenced; it is of interest to see the level of conservation of these genes. Genes that corresponded to the candidate genes from tomato were searched for within the genomes of other sequenced species: this was done using the candidate genes in a BLAST search in sol genomics (https://solgenomics.net/tools/blast/). The peptide sequence of the tomato candidate genes was used as the basis for a protein to protein blast, where peptide sequence was possible for other Solanum species. This way highly similar peptide sequences to that of the R2R3 Myb subgroup 9 candidate genes could be found. Once found these sequences were compared by alignment using Clustal Omega (https://www.ebi.ac.uk/Tools/msa/clustalo/). This allows us to see the amount of conservation at the protein level. S.pennellii and S.peruvianum are both species which are closely related to S.lycopersicum and sit within the Tomato subclade of the potato clade. S. tuberosum (potato), is within the Petota subclade of the Potato clade so whilst still fairly closely related to S.lycopersicum it is more distantly related than the 'wild tomato species'. S.melongena (aubergine/eggplant), is within the Old World subclade of Leptostemonum clade and so is more distantly related to tomato.

For *S.penellii* seven R2R2 MYB Subgroup 9 genes were found. For *S.pimpinellifolium,* seven genes were found in the family of transcription factors and each was completely identical in peptide sequence to those from *S.lycopersicum.* For *S.tuberosum* nine sequences were identified. For *S.melongena* only five sequences were identified.

The allignments shown in figures 81-87 were conducted for each *S.lycopersicum* candidate gene in turn aligned against the most similar gene/genes from each of the species.

The alignment in figure 81 is of most similar sequences found from each of the species to the peptide sequence of *SlMIXTA-1*. The peptide sequence from *S.pimpinellifolium* is completely identical that that of *SLMIXTA-1.* The peptide sequence from *S.penellii* is also highly similar: 97.57%ID according to Sol genomics, with the majority of peptides aligning exactly with that of *S.lycopersicum*. The most notable difference between the peptide sequence from *S.pennellii* and that of *S.lycopersicum* is that the *S.penellii* sequence is shorter, missing 75 peptides from the end of the sequence compared to tomato. In *S.tuberosum* the peptide shown had a 91.72%ID with *SlMIXTA-1* and so was still highly similar but more different than that of *S.pennellii.* There was no equivalent gene in *S.melongena.*

```
Solanum_tuberosum_PGSC0003DMP400032077              MGRFDKEGLKKGPWTPEEDQKLLSFIDKHGCGSWRALPAKAGLQRCGKSCRLRWINYLRP   60
Solanum_lycopersicum_SlMIXTA-1_Solyc05g007710.2.1   MGRFDKEGLKKGPWTPEEDQKLLSFIDTYGCGSWRALPAKAGLQRCGKSCRLRWINYLRP   60
Solanum_pimpinellifolium_Sopim05g007710             MGRFDKEGLKKGPWTPEEDQKLLSFIDTYGCGSWRALPAKAGLQRCGKSCRLRWINYLRP   60
Solanum_pennellii_Sopen05g003580                    MGKFDKEGLKKGPWTPEEDQKLLSFIDTYGCGSWRALPAKAGLQRCGKSCRLRWINYLRP   60
                                                    **:**********************.:****************************

Solanum_tuberosum_PGSC0003DMP400032077              DIKRGKFSLQEERTIIQLHALLGNRWSAIAAYLPSRTDNEIKNYWNSRLKKRLTKMGIDP   120
Solanum_lycopersicum_SlMIXTA-1_Solyc05g007710.2.1   DIKRGKFSLQEERTIIQLHALLGNRWSAIATYLPSRTDNEIKNYWNSRLKKRLTKMGIDP   120
Solanum_pimpinellifolium_Sopim05g007710             DIKRGKFSLQEERTIIQLHALLGNRWSAIATYLPSRTDNEIKNYWNSRLKKRLTKMGIDP   120
Solanum_pennellii_Sopen05g003580                    DIKRGKFSLQEERTIIQLHALLGNRWSAIATYLPSRTDNEIKNYWNSRLKKRLTKMGIDP   120
                                                    ****************************:****************************

Solanum_tuberosum_PGSC0003DMP400032077              MTHKPNGEGSSKYVANLSHMAEWESARLEAEARLVQKSKIFFNNNNNSHNYNINPSTISQ   180
Solanum_lycopersicum_SlMIXTA-1_Solyc05g007710.2.1   MTHKPNGAGSSKYVANLSHMAEWESARLEAEARLVRKSKILFNNNNNSHNYNINPSTISQ   180
Solanum_pimpinellifolium_Sopim05g007710             MTHKPNGAGSSKYVANLSHMAEWESARLEAEARLVRKSKILFNNNNNSHNYNINPSTISQ   180
Solanum_pennellii_Sopen05g003580                    MTHKPNGAGSSKYVANLSHMAEWESARLEAEARLVRKSKILFNNNNNSHNYNINPSTISQ   180
                                                    ******* ***************************:****:******************

Solanum_tuberosum_PGSC0003DMP400032077              QLPY-YQQLPCLDILKAWQMTSTKLPTINDISHAILRNNSKNKKLDSSIPSST----TNI   235
Solanum_lycopersicum_SlMIXTA-1_Solyc05g007710.2.1   QLPY-YQQLPCLDRLKAWQIASTKLPTINDISHAILRNNSKNKKLDSSIPSSSLNSSENI   239
Solanum_pimpinellifolium_Sopim05g007710             QLPY-YQQLPCLDRLKAWQIASTKLPTINDISHAILRNNSKNKKLDSSIPSSSLNSSENI   239
Solanum_pennellii_Sopen05g003580                    QLPYHYQQLPCLDILKAWQIASTKLPTINDISHAILRNNSKNKKLDSSIPSSTLNSSENI   240
                                                    **** ******** *****::*******************************:     **

Solanum_tuberosum_PGSC0003DMP400032077              FANNAPTTTKVG-DDHQNLHDLSTINSCFEDDHL-QTELPSFMQEFSGLFPEYTQNSTNG   293
Solanum_lycopersicum_SlMIXTA-1_Solyc05g007710.2.1   FANNAPTTTKVDDDDHQNLQNLSTINSCFEDDQLLQTELPSFMQEFSGVFPEYAQNSTNG   299
Solanum_pimpinellifolium_Sopim05g007710             FANNAPTTTKVDDDDHQNLQNLSTINSCFEDDQLLQTELPSFMQEFSGVFPEYAQNSTNG   299
Solanum_pennellii_Sopen05g003580                    FANNAPTTTKVDDDDHQNLHNLSTINSCFEDDQL-HTELPSFMQEFSGDSCGPY------   293
                                                    **********. ******::**********:* :************

Solanum_tuberosum_PGSC0003DMP400032077              LQVDNTMGSCSGDFEDNKLLINWNDFPNYMVNSPIDCIN-  332
Solanum_lycopersicum_SlMIXTA-1_Solyc05g007710.2.1   LQVDNFMGSYSEDFEDNKLLINWNNFPNYLVNSPIDCIN*  338
Solanum_pimpinellifolium_Sopim05g007710             LQVDNFMGSYSEDFEDNKLLINWNNFPNYLVNSPIDCIN-  338
Solanum_pennellii_Sopen05g003580                    ------------------------------------- 293
```

Figure 81: *SlMIXTA-1* aligned against most similar genes from other Solanum species.
An alignment using Clustal Omega with potential *MIXTA* genes found from a blast search in other Solanum species using the tomato candidate genes. Only those most similar in peptide sequence to *SLMIXTA-1* are shown here.

The alignment in figure 82 is of most similar sequences found from each of the species to the peptide sequence of *SlMIXTA-2*. The peptide sequence from *S.pimpinellifolium* is completely identical that that of *SLMIXTA-2.* For *S.pennellii* the peptide sequence is the most different from that of *SLMIXTA-2* out of all of the sequences found. The peptide sequence is shorter: it misses the first 118 peptides of the *SLMIXTA-2* sequence and then has an additional 38 peptides on the end of the sequence instead that does not correspond to the *SLMIXTA-2* sequence. There is also a small gap in the peptide sequence after about 53 peptides compared to *S.lycopersicum.* All these changes may change the structure and function of the protein in *S.pennellii* or may not. For *S.tuberosum* the peptide sequence is highly similar to that of *SlMIXTA-2* with a 92.15% ID and 305/331 alignment of peptides. There was no similar gene found in *S.melongena.*

```
Solanum_penellii_Sopen04g001640                 ------------------------------------------------------------  0
Solanum_lycopersicum_SlMIXTA-2_Solyc04g005600.1.1  MGRSPCLDKDGLKKGPWTHDEDQKLLAYVDEHGYGSWSDLPLRAGLQRCGRSCRLRWINY  60
Solanum_pimpinellifolium_Sopim04g005600         MGRSPCLDKDGLKKGPWTHDEDQKLLAYVDEHGYGSWSDLPLRAGLQRCGRSCRLRWINY  60
Solanum_tuberosum_PGSC0003DMP400005110          MGRSPCLDKEGLKKGPWTHDEDQKLLAYVEEHGYGSWSDLPLRAGLQRCGRSCRLRWINY  60

Solanum_penellii_Sopen04g001640                 ------------------------------------------------------MG  2
Solanum_lycopersicum_SlMIXTA-2_Solyc04g005600.1.1  LRPNIKRGKFSSEEERTIFQLHALLGNRWSIIASHLPNRSDNEIKNYWNTRLKKRLINMG  120
Solanum_pimpinellifolium_Sopim04g005600         LRPNIKRGKFSSEEERTIFQLHALLGNRWSIIASHLPNRSDNEIKNYWNTRLKKRLINMG  120
Solanum_tuberosum_PGSC0003DMP400005110          LRPNIKRGKFSSEEERTIFKLHALLGNRWSTIASHLPNRSDNEIKNYWNTHLKKRLINMG  120
                                                                                                            **

Solanum_penellii_Sopen04g001640                 IDPMNHQPKRDGSNYKSIASLSHMAEWETARLEAEARLVRNKSTYNNNNN---------N  53
Solanum_lycopersicum_SlMIXTA-2_Solyc04g005600.1.1  IDPMTHQPKRDGSNYKSIASLSHMAEWETARLEAEARLVRNKSTYNNNNNNNNNNNNNNN  180
Solanum_pimpinellifolium_Sopim04g005600         IDPMTHQPKRDGSNYKSIASLSHMAEWETARLEAEARLVRNKSTYNNNNNNNNNNNNNNN  180
Solanum_tuberosum_PGSC0003DMP400005110          IDPMTHQPKRDGSDYKSIASLSHMAEWETARLEAEARLVRNRSTYNNNNNNN----NDNN  176
                                                ****.********:*************************:********       *

Solanum_penellii_Sopen04g001640                 NNPYRRPYNNLHRIPCLNILKAWQMSRTNVPTINDISAVLLDGFIKNTRTKICDSTTRST  113
Solanum_lycopersicum_SlMIXTA-2_Solyc04g005600.1.1  NNLYRRPHNTLHRIPCLDILKAWQMSRTNVPTINDISAILLDGFIKNTRTKICDSTTRST  240
Solanum_pimpinellifolium_Sopim04g005600         NNLYRRPHNTLHRIPCLDILKAWQMSRTNVPTINDISAILLDGFIKNTRTKICDSTTRST  240
Solanum_tuberosum_PGSC0003DMP400005110          NNPYHRPHNNLQRIPCLDILKAWQMSRTNVLTLNDISAILLDGFIKNTRTKICDSTTRST  236
                                                ** *:**:*.*:*****:*********** *:*****:*********************

Solanum_penellii_Sopen04g001640                 FNNIEENVEVGEDICIFEDTITKDNDIQTEFSIIEGLDELFPEYGYSQNPGNYSSEVQMD  173
Solanum_lycopersicum_SlMIXTA-2_Solyc04g005600.1.1  FNNIEENVEVGEDLCIFEDTITKDNDIQTEFSIIEGLDELFPEYGYSQNPGNYSSEVQMD  300
Solanum_pimpinellifolium_Sopim04g005600         FNNIEENVEVGEDLCIFEDTITKDNDIQTEFSIIEGLDELFPEYGYSQNPGNYSSEVQMD  300
Solanum_tuberosum_PGSC0003DMP400005110          FNNIEENVEVGEDLCIFEDTMRKDNDIQTEFSIIEDLDELFPEYGCSQNPGNYSSEVQID  296
                                                ************:******: ************.******** ************:*

Solanum_penellii_Sopen04g001640                 SCFGNFEDNKSTNWNNIAHLVMTSTNWISIILSIHDSFGLFCMHFFPFLIPVVVNWMRSL  233
Solanum_lycopersicum_SlMIXTA-2_Solyc04g005600.1.1  GCFGNFEDNKSTNWNNIAHLVMTSPIGSPLL*---------------------------  331
Solanum_pimpinellifolium_Sopim04g005600         GCFGNFEDNKSTNWNNIAHLVMTSPIGSPLL---------------------------  331
Solanum_tuberosum_PGSC0003DMP400005110          SCFGNFEDNKSTNWNNIAHVVMTSPIGSPLF---------------------------  327
                                                .*****************:****     ::

Solanum_penellii_Sopen04g001640                 RTPNKKYLV       242
Solanum_lycopersicum_SlMIXTA-2_Solyc04g005600.1.1  ---------       331
Solanum_pimpinellifolium_Sopim04g005600         ---------       331
Solanum_tuberosum_PGSC0003DMP400005110          ---------       327
```

Figure 82: SlMIXTA-2 aligned against most similar genes from other Solanum species.
An alignment using Clustal Omega with potential *MIXTA* genes found from a blast search in other Solanum species using the tomato candidate genes. Only those most similar in peptide sequence to *SLMIXTA-2* are shown here.

The alignment in figure 83 is of most similar sequences found from each of the species to the peptide sequence of *SlMIXTA-3*. A highly similar peptide sequence was found in all of the species examined. The peptide sequence was most similar in *S.pimpinellifolium,* where it was completely identical. The second most similar peptide sequence was from *S.pennellii* which had a 95.01% ID and 324/341 alignment. The peptide sequence from *S.tuberosum* had a 90%ID and 306/340 alligment, there was a little bit of difference in the peptide sequence just after the diagnostic motif for the family of transcription factors. The peptide sequence from *S.melongena* was the most different from that of *SlMIXTA-3* but still highly similar with a 80.12%ID and 274/342 alignment. Overall the peptide sequence of *SlMIXTA-3* seems to be fairly conserved throughout the species examined.

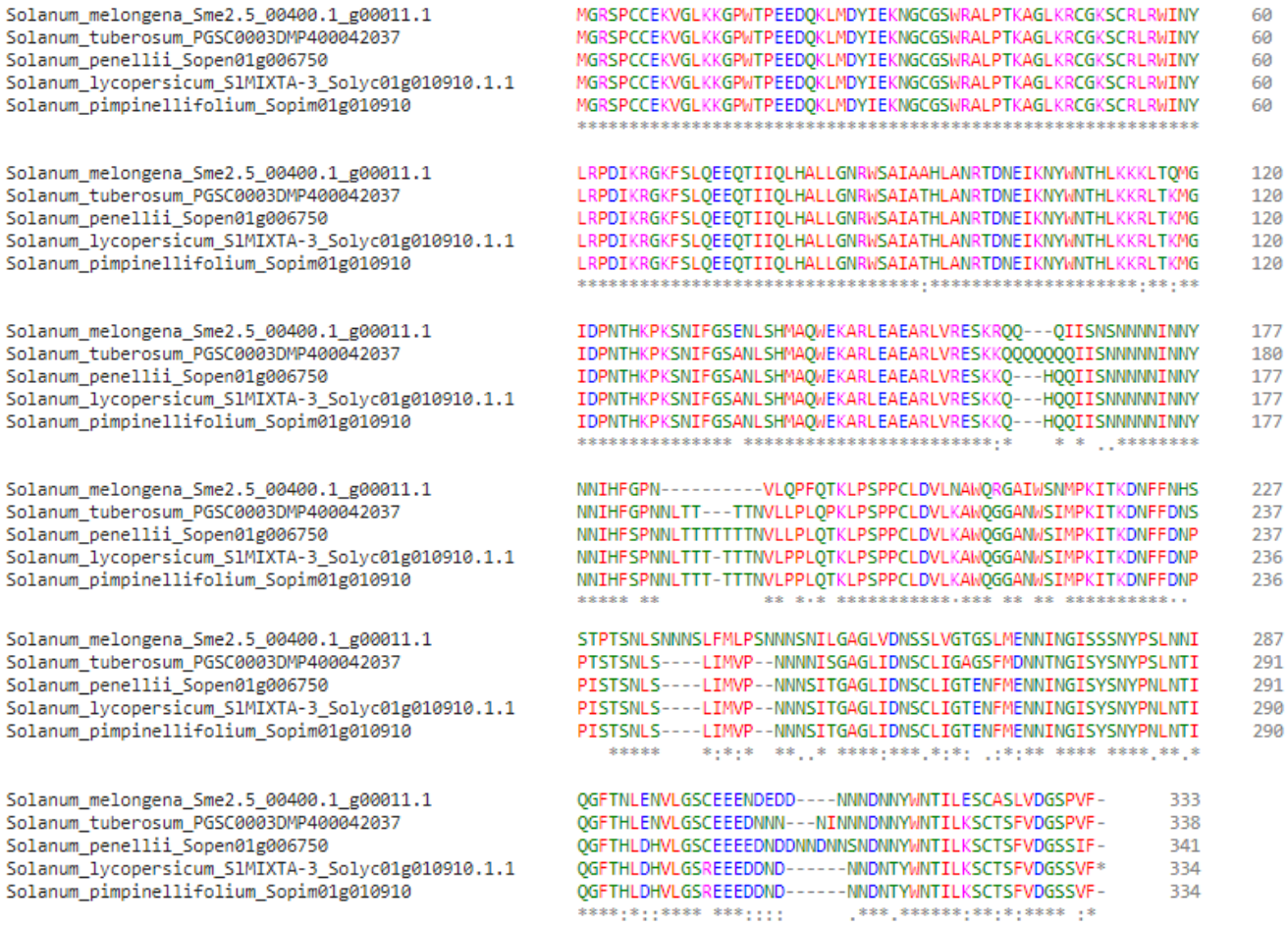

Figure 83: SlMIXTA-3 aligned against most similar genes from other Solanum species.
An alignment using Clustal Omega with potential *MIXTA* genes found from a blast search in other Solanum species using the tomato candidate genes. Only those most similar in peptide sequence to *SLMIXTA-3* are shown here.

The alignment in figure 84 is of most similar sequences found from each of the species to the peptide sequence of *SlMIXTA-4*. The peptide sequence from *S.pimpinellifolium* was completely identical to that of *SlMIXTA-4.* The peptide sequence from *S.tuberosum* was also highly similar to that of *SlMIXTA-4* with a 91.8% ID. There was no similar peptide sequence to *SlMIXTA-4* in *S.pennellii* or *S.melongena.*

Figure 84: SlMIXTA-4 aligned against most similar genes from other Solanum species.
An alignment using Clustal Omega with potential *MIXTA* genes found from a blast search in other Solanum species using the tomato candidate genes. Only those most similar in peptide sequence to *SLMIXTA-4* are shown here.

The alignment in figure 85 is of most similar sequences found from each of the species to the peptide sequence of *SlMIXTA-like-1.* Highly similar peptide sequences were found in all of the species examined. The sequence was highly conserved. *S.pimpinellifolium* had a sequence which was completely identical to that of *SlMIXTA-like-1. S.pennellii* had a sequence with a 98.56% ID. *S.tuberosum* had a peptide sequence with a 95.92%ID compared to *SlMIXTA-like-1. S.melongena* had a peptide sequence with a 92.34%ID, and whilst having the most different peptide sequence from *SlMIXTA-like-1* it was still highly similar differing in only a small number of peptides.

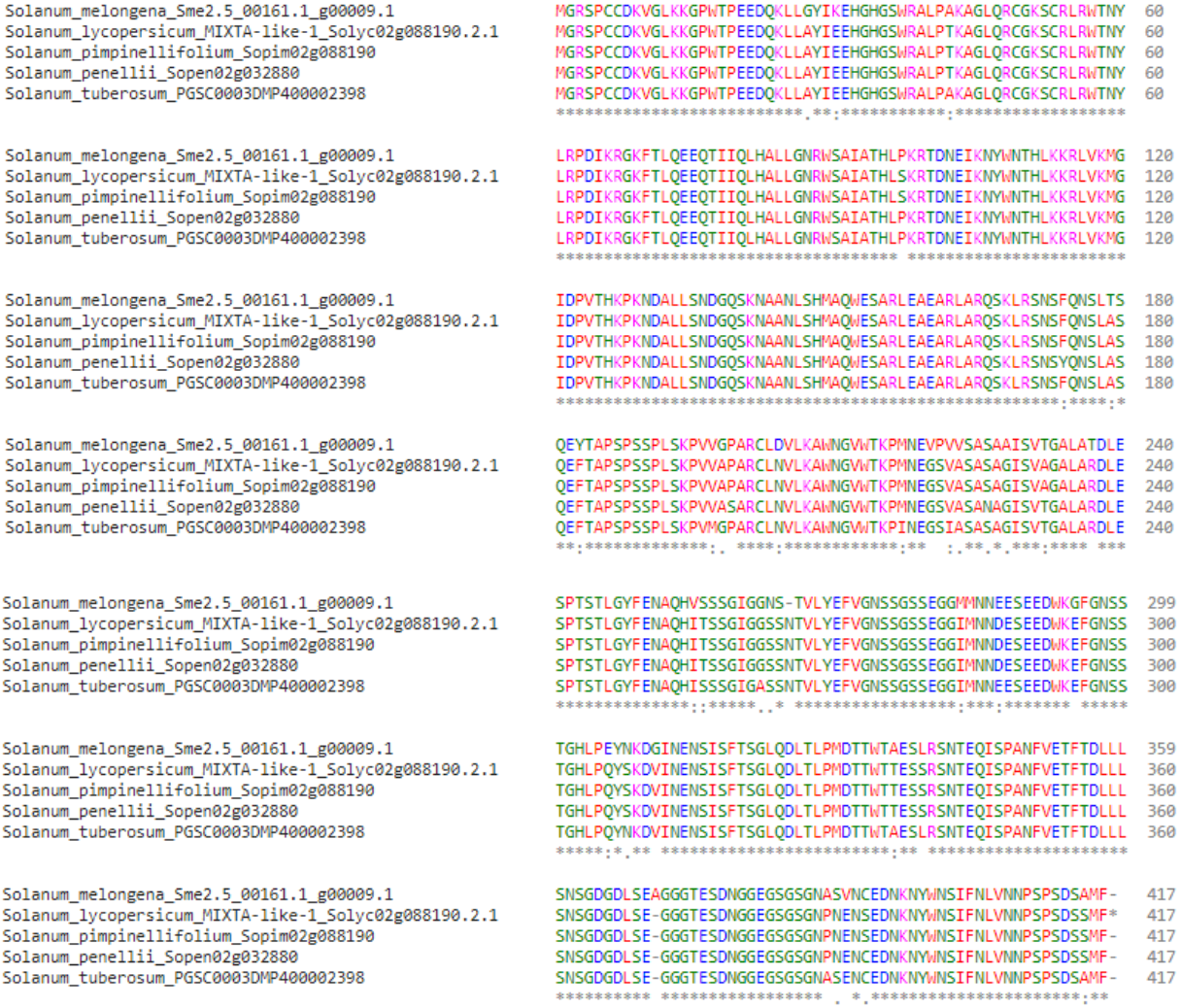

Figure 85: *SlMIXTA-like-1* aligned against most similar genes from other Solanum species.
An alignment using Clustal Omega with potential *MIXTA-like* genes found from a blast search in other Solanum species using the tomato candidate genes. Only those most similar in peptide sequence to *SLMIXTA-like-1* are shown here.

The alignment in figure 86 is of most similar sequences found from each of the species to the peptide sequence of *SlMYB17-1.* A highly similar peptide sequence to *SlMYB17-1* was found in all of the species examined. The peptide sequence from *S.pimpinellifolium* was completely identical to that of *SlMYB17-1.* The peptide sequence from *S.pennellii* was nearly completely identical to that of *SlMYB17-1* with a 99.48%ID, but was missing 118 peptides from the beginning of the sequence, which may alter the protein structure. The peptide sequence of *S.tuberosum* was more similar in length to that of *SlMYB17-1* but had some peptide changes here and there, and resulted in a lower but still %ID of 97.41. The sequence for *S.melongena* was also still highly similar in both length and peptide sequence with a 92.81%ID.

```
Solanum_melongena_Sme2.5_00166.1_g00017.1              MGRTPCCDKNGLTRGPWTAEEDDKLIQFIKKNGHGSWRSLPKLAGLRRCGKSCRLRWTNY     60
Solanum_tuberosum_PGSC0003DMP400000076                 MGRTPCCDKNGLTRGPWTPEEDEKLIQFINKNGHGSWRSLPKLAGLLRCGKSCRLRWTNY     60
Solanum_lycopersicum_SlMyb17-1_Solyc01g094360.2.1      MGRTPCCDKNGLTRGPWTPEEDEKLVQFINKNGHGSWRSLPKLAGLLRCGKSCRLRWTNY     60
Solanum_pimpinellifolium_Sopim01g094360                MGRTPCCDKNGLTRGPWTPEEDEKLVQFINKNGHGSWRSLPKLAGLLRCGKSCRLRWTNY     60
Solanum_penellii_Sopen01g038150                        ------------------------------------------------------------      0

Solanum_melongena_Sme2.5_00166.1_g00017.1              LRPDIIRGPFSPEEQKLVIQLHGILGNRWAAIASQLPGRTDNEIKNLWNTHLKKRLLSMG     120
Solanum_tuberosum_PGSC0003DMP400000076                 LRPNIIRGPFSPEEQKLVIQLHGILGNRWAAIASQLPGRTDNEIKNLWNTHLKKRLLSMG     120
Solanum_lycopersicum_SlMyb17-1_Solyc01g094360.2.1      LRPDIIRGPFSPEEQKLVIQLHGILGNRWAAIASQLPGRTDNEIKNLWNTHLKKRLLSMG     120
Solanum_pimpinellifolium_Sopim01g094360                LRPDIIRGPFSPEEQKLVIQLHGILGNRWAAIASQLPGRTDNEIKNLWNTHLKKRLLSMG     120
Solanum_penellii_Sopen01g038150                        ------------------------------------------------------------MG       2
                                                                                                                         **

Solanum_melongena_Sme2.5_00166.1_g00017.1              IDPQTHEQCSDPNGLLRRPATSPSTRHLAQWESARLEAEARLSRESQFLVPSSVGRSETD     180
Solanum_tuberosum_PGSC0003DMP400000076                 IDPQTHEQYSDPNGLLRRPATSPSARHLAQWESARLEAEARLSRESQFLVPSSVGRSETD     180
Solanum_lycopersicum_SlMyb17-1_Solyc01g094360.2.1      IDPQTHEQYSDPNGLLRRPATSPSARHLAQWESARLEAEARLSRESQFLVPSSVGRSETD     180
Solanum_pimpinellifolium_Sopim01g094360                IDPQTHEQYSDPNGLLRRPATSPSARHLAQWESARLEAEARLSRESQFLVPSSVGRSETD     180
Solanum_penellii_Sopen01g038150                        IDPQTHEQYSDPNGLLRRPATSPSARHLAQWESARLEAEARLSRESQFLVPSSVGRSETD      62
                                                       ******** **************:**********************************

Solanum_melongena_Sme2.5_00166.1_g00017.1              YFLRIWNSEIGEAFRNFKKGEKPACQSPASQASSCTKYGSASGITTEVELGAAGSPVTGS     240
Solanum_tuberosum_PGSC0003DMP400000076                 YFLRIWNSEIGDSFRKFKKGEKNACQSPASQASSCTKYGSASGITTEVELGVAGSPVTGS     240
Solanum_lycopersicum_SlMyb17-1_Solyc01g094360.2.1      YFLRIWNSEIGESFRKFKKGEKNACQSPTSQASTCTKYGSASGITTEFELGVAGSPVTGS     240
Solanum_pimpinellifolium_Sopim01g094360                YFLRIWNSEIGESFRKFKKGEKNACQSPTSQASTCTKYGSASGITTEFELGVAGSPVTGS     240
Solanum_penellii_Sopen01g038150                        YFLRIWNSEIGESFRKFKKGEKNACQSPTSQASSCTKYGSASGITTEFELGVAGSPVTGS     122
                                                       **********::**:****** *****:****:************.***.********

Solanum_melongena_Sme2.5_00166.1_g00017.1              NQNEYTEWNIGQPYTEDFLKGSDTSSSNAMEEDSSESALQLLLDFPSNNDMSFLGHGDSY     300
Solanum_tuberosum_PGSC0003DMP400000076                 NQNEYKEWKIGQPYTEDFLQGSDTSSSNAME-DSSESALQLLLDFPSNNDMSFLGHGDSY     299
Solanum_lycopersicum_SlMyb17-1_Solyc01g094360.2.1      NQHEYKEWKIGQPYTEDFLQGSDTSSSNAME-DSSESALQLLLDFPSNNDMSFLGHSDSY     299
Solanum_pimpinellifolium_Sopim01g094360                NQHEYKEWKIGQPYTEDFLQGSDTSSSNAME-DSSESALQLLLDFPSNNDMSFLGHSDSY     299
Solanum_penellii_Sopen01g038150                        NQHEYKEWKIGQPYTEDFLQGSDTSSSNAME-DSSESALQLLLDFPSNNDMSFLGHSDSY     181
                                                       **:**.**:**********:********** **********************.***

Solanum_melongena_Sme2.5_00166.1_g00017.1              SLDPFFD----      307
Solanum_tuberosum_PGSC0003DMP400000076                 SLYPFLSESS-      309
Solanum_lycopersicum_SlMyb17-1_Solyc01g094360.2.1      SLYPFLSESS*      309
Solanum_pimpinellifolium_Sopim01g094360                SLYPFLSESS-      309
Solanum_penellii_Sopen01g038150                        SLYPFLSESS-      191
                                                       ** **:.
```

Figure 86: *SlMYB17-1* aligned against most similar genes from other Solanum species.
An alignment using Clustal Omega with potential *MYB17* genes found from a blast search in other Solanum species using the tomato candidate genes. Only those most similar in peptide sequence to *SLMYB17-1* are shown here.

The alignment in figure 87 is of most similar sequences found from each of the species to the peptide sequence of *SlMYB17-2.* The peptide sequence from *S.pimpinellifolium* is completely identical to that of *SlMYB17-2.* The peptide sequence from *S>pennellii* is also highly similar with a 98.75% ID, the sequence is the same length but with an occasional peptide substitution within the sequence. In *S.tuberosum* there was a highly similar peptide sequence to that of *SlMYB17-2* with a 97.18% ID to *SlMYB17-2* and the same length with only a few different peptides within the sequence. However there were also two additional highly similar peptide sequences. These sequences however are missing the first 119 peptides, but then are largely identical to *SlMYB17-2* after that point. The *S.melongena* peptide sequence had 88.75%ID to *SlMYB17-2.*

```
Solanum_melongena_Sme2.5_04124.1_g00002.1                MGRTPCCDKKGLKKGPWTPEEDEKLVEYIKNNHGHGSWRSLPHLAGLARCGKSCRLRWTN   60
Solanum_tuberosum_PGSC0003DMP400037546                   MGRTPCCEKKGLKKGPWTPEEDEKLVEYIK-NHGHGSWRSLPHLAGLARCGKSCRLRWTN   59
Solanum_tuberosum_PGSC0003DMP400037545                   ------------------------------------------------------------   0
Solanum_tuberosum_PGSC0003DMP400037547                   ------------------------------------------------------------   0
Solanum_lycopersicum_SLMYB17-2_Solyc05g048830.2.1        MGRTPCCDKKGLKKGPWTPEEDEKLVEYIK-NHGHGSWRSLPHLAGLARCGKSCRLRWTN   59
Solanum_pimpinellifoloum_Sopim05g048830                  MGRTPCCDKKGLKKGPWTPEEDEKLVEYIK-NHGHGSWRSLPHLAGLARCGKSCRLRWTN   59
Solanum_penellii_Sopen05g028160                          MGRTPCCDKKGLKKGPWTPEEDEKLVEYIK-NHGHGSWRSLPHLAGLARCGKSCRLRWTN   59

Solanum_melongena_Sme2.5_04124.1_g00002.1                YLRPDIKRGPFSHEEEKLVIQLHGILGNRWAAIASQLPGRTDNEIKNLWNTHLKKRLLSM   120
Solanum_tuberosum_PGSC0003DMP400037546                   YLRPDIKRGPFSHDEEKLVIQLHGILGNRWAAIASQLPGRTDNEIKNLWNTHLKKRLLSM   119
Solanum_tuberosum_PGSC0003DMP400037545                   ------------------------------------------------------------M   1
Solanum_tuberosum_PGSC0003DMP400037547                   ------------------------------------------------------------M   1
Solanum_lycopersicum_SLMYB17-2_Solyc05g048830.2.1        YLRPDIKRGPFSHDEEKLVIQLHGILGNRWAAIASQLPGRTDNEIKNLWNTHLKKRLLSM   119
Solanum_pimpinellifoloum_Sopim05g048830                  YLRPDIKRGPFSHDEEKLVIQLHGILGNRWAAIASQLPGRTDNEIKNLWNTHLKKRLLSM   119
Solanum_penellii_Sopen05g028160                          YLRPDIKRGPFSHDEEKLVIQLHGILGNRWAAIASQLPGRTDNEIKNLWNTHLKKRLLSM   119
                                                                                                                        *

Solanum_melongena_Sme2.5_04124.1_g00002.1                GIDPQTNEPNSAPDGVLISPPTSLASRHMAQWESARLEAEARLSRGSKLLVPSSVGRSGT   180
Solanum_tuberosum_PGSC0003DMP400037546                   GVDPQTHEPSSAPNGLMITPPTSLAARHMAQWESARLEAEARLSRESQPLVPSSVGRSGT   179
Solanum_tuberosum_PGSC0003DMP400037545                   GVDPQTHEPSSAPNGLMITPPTSLAARHMAQWESARLEAEARLSRESQPLVPSSVGRSGT   61
Solanum_tuberosum_PGSC0003DMP400037547                   GVDPQTHEPSSAPNGLMITPPTSLAARHMAQWESARLEAEARLSRESQPLVPSSVGRSGT   61
Solanum_lycopersicum_SLMYB17-2_Solyc05g048830.2.1        GVDPQTHEPSSAPNGQMITPPTSLAARHMAQWESARLEAEARLSRESQPLVPSSVGRSGT   179
Solanum_pimpinellifoloum_Sopim05g048830                  GVDPQTHEPSSAPNGQMITPPTSLAARHMAQWESARLEAEARLSRESQPLVPSSVGRSGT   179
Solanum_penellii_Sopen05g028160                          GVDPQTHEPSSAPNGQMITPPTSLAARHMAQWESARLEAEARLSRESQPLVPSSVGRSGT   179
                                                         *:****:**.***:* :*:******:****************** *: **********

Solanum_melongena_Sme2.5_04124.1_g00002.1                DCFLRIWNSEVGEAFRKFNKKEGRTTCESSASQASSSTKYGSVSGITTEIDLSFAANQND   240
Solanum_tuberosum_PGSC0003DMP400037546                   DYFLRIWNSEVGEAFRKLNKKEGRTTCESSASQASSSTKFGSTSGVTTEMDVSFAAYQNE   239
Solanum_tuberosum_PGSC0003DMP400037545                   DYFLRIWNSEVGEAFRKLNKKEGRTTCESSASQASSSTKFGSTSGVTTEMDVSFAAYQNE   121
Solanum_tuberosum_PGSC0003DMP400037547                   DYFLRIWNSEVGEAFRKLNKKEGRTTCESSASQASSSTKFGSTSGVTTEMDVSFAAYQNE   121
Solanum_lycopersicum_SLMYB17-2_Solyc05g048830.2.1        DYFLRIWNSEVGESFRKFNKKEGRTTCESPASQASSSTKFGSTSGVTTEMDVSFAAYQNE   239
Solanum_pimpinellifoloum_Sopim05g048830                  DYFLRIWNSEVGESFRKFNKKEGRTTCESPASQASSSTKFGSTSGVTTEMDVSFAAYQNE   239
Solanum_penellii_Sopen05g028160                          DYFLRIWNSEVGESFRKLDKKEGRTTCESPASQASSSTKFGSTSGVTTEMDVSFAAYQNE   239
                                                         * ***********.***.*********** ********.** **.***.*.**** **.

Solanum_melongena_Sme2.5_04124.1_g00002.1                DTEWKKSQPWMEDVLKGYEDTCSSSGLEDSSESALQLLLDFPSNNDLSFLGQSDTYSLYP   300
Solanum_tuberosum_PGSC0003DMP400037546                   DTEWKNSQPYTEDVLQGYDDTSSSSGLEDSSESALQLLLDFPSNNDMSFLEHSDTYSLYP   299
Solanum_tuberosum_PGSC0003DMP400037545                   DTEWKNSQPYTEDVLQGYDDTSSSSGLEDSSESALQLLLDFPSNNDMSFLEHSDTYSLYP   181
Solanum_tuberosum_PGSC0003DMP400037547                   DTEWKNSQPYTEDVLQGYDDTSSSSGLEDSSESALQLLLDFPSNNDMSFLEHSDTYSLYP   181
Solanum_lycopersicum_SLMYB17-2_Solyc05g048830.2.1        ETEWKNSQPYTEDVLQGYDDTSSSSGLEDSSESALQLLLDFPSNNDMSFLGHSDTYSLYP   299
Solanum_pimpinellifoloum_Sopim05g048830                  ETEWKNSQPYTEDVLQGYDDTSSSSGLEDSSESALQLLLDFPSNNDMSFLGHSDTYSLYP   299
Solanum_penellii_Sopen05g028160                          DTEWKNSQPYTEDVLQGYDDTSSSSGLEDSSESALQLLLDFPSNNDMSFLGHSDTYSLYP   299
                                                         :****:***: ****:**:**.**********************:*** :********

Solanum_melongena_Sme2.5_04124.1_g00002.1                EFLSESSFKCSPAEHELGFV-    320
Solanum_tuberosum_PGSC0003DMP400037546                   EFLSERSFKCSSAEHEVGFL-    319
Solanum_tuberosum_PGSC0003DMP400037545                   EFLSERSFKCSSAEHEVGFL-    201
Solanum_tuberosum_PGSC0003DMP400037547                   EFLSERSFKCSSAEHEVGFL-    201
Solanum_lycopersicum_SLMYB17-2_Solyc05g048830.2.1        EFLSESSFKCSSAQHEVGFL*    319
Solanum_pimpinellifoloum_Sopim05g048830                  EFLSESSFKCSSAQHEVGFL-    319
Solanum_penellii_Sopen05g028160                          EFLSESSFKCSSAEHEVGFL-    319
                                                         ***** ***** *:**:**:
```

Figure 87: *SlMYB17-2* aligned against most similar genes from other Solanum species.
An alignment using Clustal Omega with potential *MYB17* genes found from a blast search in other Solanum species using the tomato candidate genes. Only those most similar in peptide sequence to *SLMYB17-2* are shown here.

3.5: Discussion

The R2R3 MYB subgroup 9 transcription factors of *Solanum lycopersicum* that were investigated in this study were shown, to various degrees, to be capable of inducing outgrowth of cells when they were ectopically expressed in tobacco. This indicates that these genes have the potential to be able to initiate such epidermal cell outgrowths as conical cells and trichomes in *Solanum lycopersicum.* However, the degree to which epidermal cell outgrowths were induced and the number of tissues in which they were observed to act, varied from gene to gene. The genes seem to be fairly well conserved in Solanum, with similar peptide sequences found in all the species examined.

This range of phenotypes resembles that reported in a classic set of studies in which the R2R3 subgroup 9A genes of *Antirrhinum majus* were ectopically expressed in tobacco. The strongest phenotype in these studies was that of tobacco lines containing ectopically expressed *AmMIXTA* (Glover et al, 1998) in which trichomes were observed covering most tissues and with an especially large amount of epidermal cell outgrowth observed on the surface of the ovary. These outgrowths included branched and glandular trichomes on the ovary and the production of conical cell protrusions on the epidermal leaf surface on both sides of the leaf (some lines even produced trichomes from the centre of these conical protrusions). On the petals of the *AmMIXTA* lines all the cells were converted into conical cells and they were longer than those observed in WT tobacco. None of the *R2R3 subgroup 9* genes of *Solanum lycopersicum* produced phenotypes as extreme as this when ectopically expressed in tobacco, but the strongest phenotypes were seen in the lines expressing *SlMYB17-1* and *SlMYB17-2*. The phenotype was reminiscent of that of *AmMIXTA* expressing tobacco: the majority of tissues exhibited epidermal cell outgrowths with the ovary and anthers especially covered in trichomes of varying types. However no branched or glandular trichomes were observed on the epidermal surface of the ovary, only single celled trichomes of a variety of lengths and sizes. The trichomes on the anthers also sometimes had stomata on the end of them. Conical protrusions were not observed on the leaf surfaces for *SlMYB17-2*, only for *SlMYB17-1,* but branched trichomes were observed in all the lines (where they were only observed in some of the lines expressing *AmMIXTA*). There were a number of lines where some flowers displayed ‘lumps’ on the petals, however when

examined using cryo-SEM this was shown to be a result of large numbers of trichomes developing on the inner-side of the corolla petal, creating a 'hair-ball' which resulted in a bump on the outside of the petal. This can be seen in Figure 88.

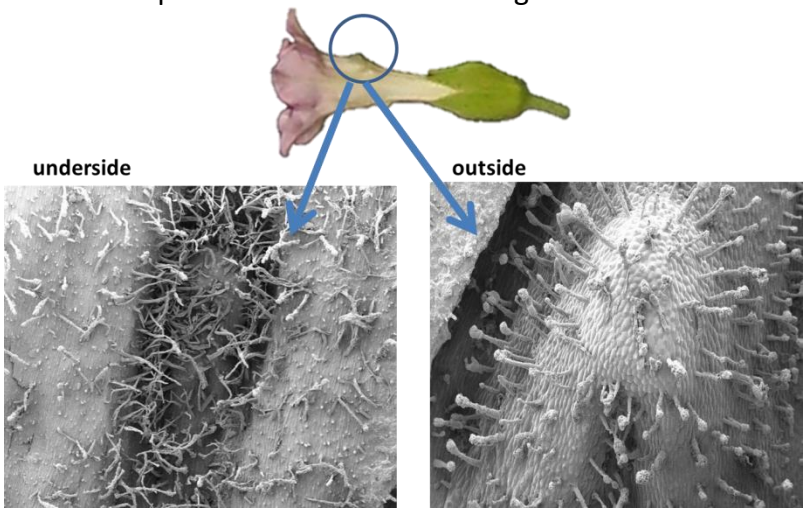

Figure 88: Trichome 'protrusions' on the corolla petal surface of some tobacco lines expressing *SlMYB17-2*
Protrusions that deformed the corolla tube of lines expressing *SlMYB17-2* were occasionally observed. These resulted from parts of the corolla petal being so covered in trichomes that they buckled into 'hair balls'.

The second most extreme phenotype observed was that resulting from expression of *SlMYB17-1,* which was very similar phenotypically to the ectopically expressing lines of *SlMYB17-2*, except lacking in the trichomes on the petals. However, in contrast to the *SlMYB17-1* expressing tobacco phenotype, and more reminiscent of the *AmMIXTA* expressing tobacco phenotype, these lines did sometimes have conical protrusions on the epidermal surface of the leaves. *SlMYB17-1* and *SlMYB17-2* have near identical expression patterns in the tomato flower, as seen in the results of the sqRTPCR, which is interesting considering that our prediction based on the efp browser was that *SlMYB17-2* would be expressed but not *SlMYB17-1*. The phenotype of *SlMyb17-1* the outgrowths on the ovary are multi-lobed and resemble to an extent the 'glove-like papillae' on the epidermal abaxial surface of the tomato. The outgrowths on the anther surface of the *SlMyb17-1* transgenic lines are very like the trichomes which make up the trichome mesh. Therefore based on the phenotype of the transgenic this gene is a good candidate both for the control of the formation of the trichome mesh and for the 'glove-like' papillae on the anther surface.

SlMyb17-2 also created trichomes on the anthers of the transgenic which resemble those of the trichome mesh. The outgrowths on the ovary surface also resemble the trichome mesh trichomes making this also another good candidate gene based on the phenotype of the transgenic lines.

Based on these data, the two *SlMYB17* genes are considered the most likely candidates for the control of the development of the trichome mesh. They are both expressed most strongly in the tissue stages 1+2 and 3, where the trichome mesh is developing, and are capable of inducing cellular outgrowth very strongly when expressed in novel tissues. The two genes may function together or simply be redundant.

This conclusion is surprising because previously studied representatives of the *MYB17* subgroup of genes have not shown an involvement in epidermal cell outgrowth. *AtMYB17* (Pastore et al, 2011) has been shown to be involved in flowering commitment based on examination of mutant plants, but no epidermal phenotype was seen. AtMYB17 has also been shown to be involved in the regulation of the activity of *APETALA1* in the flowers of *Arabidopsis thaliana* and is thought to act together with LEAFY (Zhang et al, 2009) but again no epidermal cell outgrowth function was suggested. However, it has been argued previously that with so much paralogy in the MYB subgroup 9 lineages it is possible that the *ATMYB17* gene of *Arabidopsis thaliana* may have acquired a different role to other *MYB17* representatives and that a possible role for *MYB17* genes in the regulation of epidermal outgrowth should not be dismissed entirely (Brockington et al, 2013.) The Brockington et al (2013) study also implicated *MYB17* lineage genes in epidermal outgrowth regulation as the *Nicotiana* EST-derived fragments that nested within the *MYB17* subgroup were those derived from trichome-specific transcriptomes. Therefore the marked phenotypes with regards to epidermal cell outgrowth resulting from the ectopic expression of both of the *SlMYB17* genes are perhaps not wholly unexpected. The expression patterns of the two *SlMYB17* genes, as indicated by sqRTPCR, also support a potential role in trichome mesh development.

A *MYB17-like* gene (*LjMYB17-like)* from *Lotus japonicus* was examined by (Brockington et al, 2013) and when it was ectopically expressed in tobacco it produced a very strong phenotypic effect. The epidermal cells on the adaxial and abaxial leaf surfaces had become conical in shape and there was a reduced number of stomata. The filament of the stamen had also gained trichomes and conical cells on its epidermal surface. The ovary surface was covered in long conical cells and the cells on the petal lobe had become elongated and glandular trichomes were found in addition (Brockington et al, 2013). Whilst this *LjMYB17-like* gene is not a *MYB17* gene, it is still in the R2R3 MYB subgroup 9B where fewer genes have been characterised and is worth comparing to the *SlMYB17* genes. The *SlMYB17* genes phenotype is reminiscent of the *LjMYB17-like* phenotype when ectopically expressed in tobacco.

Expression patterns of these genes should be further investigated by quantitative RT-PCR and their functions confirmed by downregulation or genome editing.

The *A.majus* subgroup 9 gene with the second strongest phenotype when expressed in tobacco was *AmMYBML-1*, another *MIXTA* gene (Perez-Rodriguez et al, 2005). The anthers of these lines were covered in conical cells and failed to dehisce as a result. The ovary surface was covered in a mixture of conical cells and trichomes. The corolla petals also displayed glandular trichomes. However the epidermal surface of the leaves was considered to be the same as WT in appearance. The phenotype of lines expressing *SlMIXTA-1* was highly reminiscent of this and could be considered the third strongest phenotype observed in this study. A mixture of conical cells and trichomes were observed on the ovary surface and trichomes were also found on the anther surface and consequently the anthers did not dehisce. The corolla tube however did not exhibit any glandular trichomes and the cells were only slightly conical in shape. Branched trichomes were also observed on the leaf surface and occasional conical protrusions on the leaf surface, however in general the phenotype was weaker than that observed in *AmMIXTA* lines and closer in resemblance to those of *AmMYBML-1.* The phenotype of the transgenic lines of *SlMIXTA-1* trichome outgrowths on the anther surface resemble the trichomes of the trichome mesh found in tomato, however are not so outgrown as those found in the SlMYB17-1 and SlMYB17-2 transgenic lines and are not as outgrown as those in the trichome mesh. The ovary

outgrowths are trichome like, but the trichomes don't look like those in the trichome mesh of tomato nor the glove like papillae found on the tomato anther surface.

SlMIXTA-1 is expressed in stages 1+2 and stage 3 whilst the trichome mesh is developing. However the expression is strongest in stage 1+2, with the expression fading in stage 3 and expression falling away entirely in later stages. The gene is not expressed as strongly in stage 3, and less so than the *SlMYB17* genes. However the gene appears to be more expressed in stage 1+2 than the *SlMYB17 genes*.

The *SlMIXTA-4* lines were also reminiscent in phenotype of the *AmMYBML-1* study. However the phenotype was less strong than observed in *SlMIXTA-1* lines. The ovary still exhibited both conical cells and trichomes, but the proportion of conical cells relative to trichomes was increased. The number of trichome outgrowths observed on the anther surface was less than that observed in *SlMIXTA-1* lines and the anthers were able to dehisce as a result of only slightly conical shaped cells and some glandular trichomes rather than large numbers of simple trichome like outgrowths. The petal epidermis did not have any conical like cells and resembled WT tobacco, as did the leaves. The *SlMIXTA-4* transgenic line phenotype did not resemble the trichome mesh of tomato. The ovary cell are slightly outgrown like conical cells, this however does not resemble the trichome mesh of tomato nor the 'glove-like papillae' on the anther surface. Many of the outgrowths seen on the *SlMIXTA-4* transgenic lines were glandular trichomes, however the trichome mesh of tomato is non-glandular.

The *SlMIXTA-4* gene was expressed slightly more strongly in the later stages of the development of the flower, as seen from the semi-qRTPCR which could indicate an involvement in the development of the trichome mesh because of the anther-specific nature of these tissue pools, or could suggest an involvement in later stage developmental processes such as the development of the glove-like papillae. The *MIXTA* genes of *Gossypium hirsuta* that have been characterised, *GhMYB25,* and *GhMYB25-like,* have been shown to be involved in trichome and fibre development (Walford et al, 2011; Machado et al,2009). This reinforces the role of genes from this subgroup in trichome development.

The remaining *A.majus* genes expressed in tobacco, *AmMYBML2* and *AmMYBL3,* had the weakest phenotypes of those studied (Jaffe et al, 2007). These genes belong to the *MIXTA*-

like clade of Brockington et al (2013). These transgenic lines had a WT appearance in most of their tissues. However the petal surface, where conical cells are observed in WT tobacco, appeared to have longer cell outgrowths in these transgenic lines. The ovary also still possessed conical cells on its epidermal surface (Jaffe et al, 2007). The *MIXTA-like* genes (Brockington et al, 2013) from *Arabidopsis thaliana* (*AtMYB16)* and *Petunia hybrida (PhMYB1)* when ectopically expressed in tobacco produced near identical phenotypes to that produced by ectopic expression of *AmMYBML2* (Baumann et al, 2007). The *TtMYBML2* gene of *Thalictrum thalictroides* also induces conical cells on the ovary and carpel and elongates those of the petal lobe (Di Stilio et al, 2009). The lines expressing *SlMIXTA-like-1* in this study were reminiscent of this phenotype, yet slightly stronger. The ovary surface exhibited only conical cells and no trichomes, like the *AmMYBML2* and *AmMYBML3* phenotypes, yet conical cell-like protrusions were also observed on the anther surface (although they did not affect dehiscence) and on the surface of some cells of the white sections of the corolla tube. The conical cells on the petal lobe, where conical cells are observed in WT tobacco, also appeared longer in the *SLMIXTA-like* expressing lines. The leaves were WT in appearance. The trichomes of the *Sl-MIXTA-like* transgenic lines largely did not resemble those of the tomato trichome mesh. The trichome mesh does not contain glandular trichomes like were found on the transgenic lines. Conical cells were more outgrown on the petals of the transgenic lines, however they do not resemble the trichome mesh of tomato nor the 'glove-like papillae' found on the tomato anther surface.

The *SlMIXTA-like* gene was however not really expressed during the development of the flower, apart from at a very low level in all the tissues, only observed as a very faint band after 40 cycles. Therefore it is unlikely to be involved in the formation of the trichome mesh.

The weakest phenotypes observed in this study from *Solanum lycopersicum* R2R3MYB subgroup 9 genes were those of *SlMIXTA-2* and *SlMIXTA-3,* which had an even weaker phenotype than the weakest of the *A.majus* phenotypes in tobacco. Lines expressing *SlMIXTA-2* and *Sl-MIXTA-3* greatly resembled WT tobacco plants and had the least extreme phenotypes of all the genes examined. The only phenotypic trait which is reminiscent of the *A.majus* subgroup 9 genes was that of branched trichomes on the epidermal leaf surface, which were observed in some lines of *AmMIXTA* (Glover et al, 1998), the phenotypes in every other regard do not resemble *AmMIXTA* at all, however. The *SlMIXTA-2* and *SlMIXTA-*

3 plants showed even weaker phenotypes than the weakest *A.majus* subgroup 9 gene expression phenotype, that of *AmMYBML3*, which was WT in appearance aside for the appearance of shallow conical cells on the ovary surface. The *SlMIXTA-2* and *SlMIXTA-3* lines were lacking more than a few shallow conical cells on the ovary surface. The phenotypes of the transgenic lines of *SlMIXTA-2* and *SlMIXTA-3* did not resemble the cell outgrowths of the tomato trichome mesh. The outgrowths were not exaggerated enough and did not form the same kind or size of trichomes found in the tomato trichome mesh.

The expression levels in the tomato flowers of these genes during floral development were also extremely low, and they could be considered to be not expressed during the development of the tomato flower. Therefore these two candidates, while they cannot be entirely ruled out, are highly unlikely to be involved in the development of the trichome mesh in *Solanum lycopersicum,* displaying neither the capacity for the production of epidermal cell outgrowths, nor the expression in the correct tissues. The almost absence of outgrowths on the carpel/ovary was highly unusual as all other studies of such genes prior to this have displayed outgrowths on this floral organ.

To fully understand the function of these genes, knockout or silencing of each gene should be investigated. The failure of the CRISPR knockout lines was a disappointment as this experiment had the potential to provide vital further information on the genes and on the control of the development of the trichome mesh. Other potential silencing/knockout methods could be attempted, or the same experiment repeated with more time to trouble shoot the transformation protocol. It may be that knockout of these genes is lethal to the plant, in which case reducing expression may be an alternative option to genome editing. Methods such as silencing using RNA interference may be a solution (Ossowski et al, 2008).

A number of classical genetic mutants with lesions in trichome development have been described in tomato. These tomato trichome mutants should be investigated to understand further how tomato trichomes, including those regulating the anther trichome mesh, develop. The *hairless (hl)* tomato mutant has defects in trichome production, where the trichomes that form are shortened and bent, whilst the glandular trichomes do not properly accumulate secondary compounds (Rick and Butler, 1956; Reeves, 1977; Kang et al, 2016; Kang et al, 2010B). The other known trichome mutants such a *hairless (hl),* (Rick and Butler,

1956; Reeves, 1977) *hair-absent (h)* (Reeves, 1977; Chang et al, 2018) and *Woolly (Wo)* (Glover et al, 2000; Yang et al, 2011)would also be of interest for investigation due to the altered trichome phenotype they produce. The *dialytic (dl)* mutant is of particular interest for further investigation from a developmental genetic perspective, as in this mutant the trichome mesh of the anthers is absent (Glover et al, 2004; Rick 1947). Any differences in expression of the MYB subgroup 9 genes or in the structure of those genes in these trichome mutants as opposed to WT, might help further elucidate the function of these genes in WT tomato.

Further investigation into the expression levels of the MYB subgroup 9 genes using quantitative RTPCR could give a clearer understanding of the expression levels of these genes and clarify in more detail how they are expressed in the different stages of the development of the trichome mesh.

It is difficult from these results to determine which gene or genes could be responsible for the development of the trichome mesh. However it can be seen that *SlMIXTA-4* and *SlMIXTA-like-1* are not expressed in the stages during which the trichome mesh is developing and therefore are unlikely to be involved. *SlMIXTA-4* however does become more strongly expressed in the later tissue stages 4 and 5+6, which may indicate an involvement in the development of the epidermal cell outgrowths/ 'glove' like papillae. However it should be noted that the expression level is still very low. It should also be noted that the expression of all the candidate genes was rather low in general, with bands only truly visible after 35 or 40 cycles.

From their expression patterns alone, the involvement of *SlMYB17-2*, *SlMYB17-2* and *SlMIXTA-1* cannot be ruled out. All three of these genes are expressed most strongly in the stages of the floral development where the trichome mesh is developing. There are also genes which are expressed in all of the tissue stages at a background level such as *SlMIXTA-3,* which is more likely to perform some other background role/function needed in all of the stages of the floral development at some low level. It is possible that the *MIXTA* genes of tomato represent a degree of redundancy due to multiple duplications.

It should also be noted that whilst the phenotypes observed when these genes were expressed ectopically in tobacco may indicate an ability to induce the production of

trichomes, this does not necessarily mean that this is the function of the genes in *Solanum lycopersicum*. For example, the *AmMIXTA* gene resulted in extensive trichome production when expressed in tobacco, however has been shown to not be involved in trichome production in *A.majus* and instead is responsible for conical cell production on petals (Noda et al, 1994). Transgenic phenotypes must always be interpreted with caution, because phenotype of the transgenic doesn't necessarily mean that this is the role of the gene in the plant. However, of the various phenotypes shown here the ones that make outgrowths that most resemble the anther trichomes in the tomato trichome mesh are SlMyb17-1 followed by SlMyb17-2 and SlMIXTA-1.

3.6: Overall conclusions.

From the results described in this chapter a number of candidate genes can be potentially dismissed from having a role in the development of the trichome mesh: *SlMIXTA-2, SlMIXTA-3* and *SlMIXTA-like-1.* The most likely candidates for the control of the trichome mesh development are *SlMYB17-1, SlMYB17-2* and *SlMIXTA-1.* At this stage it is not possible to determine which of these genes is the more likely candidate without further genetic/transgenic work in tomato or more detailed expression analysis. However, this study presents the first analysis of the complete set of MYB subgroup 9 transcription factors in a single species, and it has been interesting and informative to compare the different expression profiles and protein capabilities of the seven genes.

Chapter 4: Discussion.

4.1 Summary

This PhD project focussed on the evolution of male form and function in nightshade flowers, more specifically on understanding diversity of anther form within the entirely buzz pollinated genus *Solanum*. The work took a multidisciplinary approach which examined the anthers of the genus *Solanum* from a morphological perspective and also from a developmental genetic perspective.

The morphological section of this project investigated key anther traits at both a macro- and microscopic level. Anther dimensions were measured for ~300 species from herbarium specimens and some living material, with a focus on anther length and width at the anther tip, base and middle. These measurements could be taken together to produce an approximation of anther shape. The measurements underwent principal component analysis to summarise them, resulting in the identification of two principal components which accounted for approximately 95% of the variation seen in these measurements. These principal components were plotted in morphological space with respect to the phylogenetic tree of *Solanum*, creating a phylomorphospace analysis which allowed patterns in anther shape within and between clades to be highlighted. This also allowed species which diverged strongly in their anther morphology from those closely related to them to be highlighted for further investigation. These analyses led to some key findings: first, there appears to be an anther morphological shape specific to forming a pepper pot anther cone. Second, clades of *Solanum* usually cluster in different areas of anther morphological space relative to one another. Third, anther shape was found not to be correlated with the presence or absence of epidermal outgrowths on the anther surface. The anther surface was characterised with SEM for 180 species, to better understand the range of anther epidermal cell traits within the genus. Trichomes of various kinds and other types of epidermal outgrowths such as papillae or conical cells may affect the way in which pollinators interact with the flower during buzz pollination and also may affect the way in which vibrations are received by the flower and hence the transfer of energy to the pollen

and resulting pollen release. The location of epidermal cell outgrowths on the anthers was found to generally be towards the base end of the anther, fading towards smooth cells at the top. The base is where the bee grips during pollination and so suggests a possible function in aiding pollinator grip, or in protecting the anthers during the rough action of buzz pollination or in providing texture-based guides to the bees as to where to grip the anther.

This study has contributed to our understanding of the evolution within a buzz pollination genus. This study has furthered our understanding of traits associated with this pollination method. It was found that anther shape can be highly variable; each dimension is able to vary independently from one another which may allow selection to act on each aspect of anther shape individually creating a great diversity of possible anther shapes. This has allowed for the possibility of niche division between clades through anther dimensions: clades were shown to generally occupy different areas of morphological space. However there were species which diverged from the general anther shape of their clade, demonstrating the action of selection on anther shape to create new morphologies. It is possible that selection on anther size and shape may drive some aspects of evolution and diversity in Solanum. More research into the vibrational properties of different anther shapes and experiments investigating pollinator interactions with anthers with respect to size and shape would be needed however to fully understand and prove this. Anther shape and the presence and type of epidermal cell outgrowths vary independently from one another and irrespective of one another: therefore selection can act on both together and separately. This study shows at least 3 independent evolutions of the pepper pot cone, each held together in different ways. In the tomato subclade, examination of *S.juglandifolium* provides a possible suggestion for how the trichome mesh and pepper pot cone may have evolved.

The study could also contribute to our understanding of the evolution of buzz pollination overall once the traits studied here are further examined from a pollinator interactions perspective. Studies which investigated pollinator interactions with key traits allow understanding of how such traits may affect the plant-pollinator interactions in buzz

pollination and potential selective pressures that may help enhance knowledge of the evolution of Poricidal anthers and buzz pollination as well as speciation in Solanum. How the anther traits affect vibrational energy transfer to the pollen would be a highly important next investigation that could allow an increased understanding of the evolution of buzz pollination. The question of how anther traits in buzz pollinated species, both inside and outside of the genus Solanum affect vibrational energy transfer is the upcoming topic of research of Dr Vallejo Marin at the University of Stirling and this project will likely when combined with the findings of this study provide much information about the evolution of buzz pollination overall.

The developmental genetic section of this project focussed on understanding the developmental regulation of the pepper pot anther cone, as found in the tomato. The pepper pot cone is held together by a trichome mesh. A candidate gene approach was taken using the R2R3 Myb sub group 9 family of transcription factors. 7 candidate genes were identified and functionally characterised by ectopically expressing them in tobacco. The strongest phenotypes were seen for the tobacco lines ectopically expressing *SlMYB17-1, SlMYB17-2* and *SlMIXTA-1,* with the weakest phenotypes resulting from ectopic expression of *SlMIXTA-2* and *SlMIXTA-3*. The expression levels of these 7 genes was investigated at different points of floral development and consequently at different stages of development of the trichome mesh. From this it was seen that the genes expressed most strongly at early points of flower development (and when the trichome mesh was developing) were *SlMYB17-1, SlMYB17-2* and *SlMIXTA-1.* From these investigations it is most likely that the development of the trichome mesh is controlled by one or more of these three genes, but no firm conclusion can be reached without further investigation of these genes using a gene downregulation or knock out approach.

Overall, this study provided a large scale survey of anther traits throughout the genus *Solanum,* providing a database of morphological analyses which can be used in future studies. It identified key anther traits and quantified them throughout the genus, providing information on trends in anther morphology at a macro- and micro-scale. These data provide insights on anther shape variation throughout the genus and on evolutionary transitions within and between clades. This project has also shed light on the functionality of a family of transcription factors in tomato.

4.2 Further work: morphological analysis

The absence of flower size measurements to compare to the anther dimensions is a major limiting factor of this study. If flower size had been measured from each sample, a flower size:anther size ratio could have been created. This ratio might have allowed us to exclude individual species whose anther size was contingent on a particularly large or particularly small flower, and could potentially give more meaningful insight into the causes and consequences of anther size variation. Such measurements would not have been possible for all species sampled in this study, because not all herbarium specimens preserve the flower in a way which would allow meaningful size measurement. However, these data would be useful even for a subset of the species analysed.

It was originally planned that anther filament length would also be measured in this study. However, in many of the herbarium specimens the filament was obscured and could not be measured reliably. This limiting factor could potentially be overcome with destructive sampling and manipulation of the herbarium specimens using water and forceps. However, not all herbaria are willing to grant permission for this sort of work, and therefore this approach would not be possible on the genus-wide scale of this project. Filament length variation is one the key traits for taxonomic identification of *Solanum* species, so the variation is large. The consequences of filament length are most likely related to anther vibration and pollen release, so identifying species with unusual lengths would be potentially very informative.

The initial aim of this project was to sample as broadly as possible across the genus. However, since not all species have been included in molecular phylogenetic analyses, this meant that some of the measurements or traits recorded could not be plotted with respect to the phylogenetic tree. While these data did still provide some insight, a sampling strategy focussed on those species with confirmed phylogenetic position might have been more informative. Sampling could also have been tailored to specific clades or subclades for a more in depth understanding. The wide survey conducted here could allow broad trends to be identified, and gives insight into the breadth of anther morphology throughout the genus. However, a more focussed study could have allowed for more detailed and thorough analysis, for example a focus on the Potato clade would have allowed for a more in-depth understanding of the evolution of epidermal cell outgrowths throughout that clade. One of

the main limiting factors with any study of this kind is the availability of material. Herbarium collections are varied in both quality and in availability of species. Cultivated species tend to be represented at a greater frequency, naturally, and so the study will always be biased by the material that is available. The use of a greater number of living species would have been interesting to see how greatly the drying process of creating herbarium specimens altered the anther dimensions. Some traits could also have been more easily identified by examination of living specimens. However, it is clear that without the use of herbarium specimens a study of this scale would not be possible.

4.3 Further work: functional analysis

The morphological analyses described in this thesis allow the generation of hypotheses concerning the functional significance of various anther traits. One key future direction this research could take is to investigate the importance of the anther traits to the interaction with pollinators. This could allow a greater understanding of ways these traits could evolve as a result of the pollinator interactions and also how such traits may modify and interact with buzz pollination.

Epidermal cell outgrowths were found on the anthers of species belonging to almost all clades. The position of these outgrowths on the parts of the anther surface which are likely to come into contact with a pollinator during buzz pollination suggests a potential role in aiding or altering grip. Improved grip could reduce pollinator handling time and improve ease and efficiency of pollination. Anther dimensions may also affect the way in which the pollinators handle the anther, with some anther shapes being easier to grip onto than others. These ideas could be investigated using behavioural experiments with laboratory bumblebees in a flight arena. Handling time could be directly recorded for sister species with differing anther morphologies, and choice experiments between different anther surfaces could also be conducted. Pairs of species could be chosen based on the anther epidermal surface morphology but with otherwise similar overall morphologies. For example, *S.dulcamara* and *S.lycopersicum* would be an interesting pair of species to use. While they are not closely related, they are very similar morphologically, both possessing a similarly shaped and sized pepper pot anther cone. However *S.dulcamara* has no epidermal cell outgrowths on the anther surface: they are entirely smooth. *S.lycopersicum* has 'glove-like papillae' on the anther surface as well as other epidermal cell outgrowths on the anther,

namely the trichome mesh. Differences in the ways in which bees handle these different, yet similar, flowers could allow for a greater understanding of the way epidermal cell outgrowths affect grip. However any such experiment is at risk from confounding variables such as scent or pollen amount, which may affect the results. Most notably, these two species have flowers of very different colours (yellow for *S. lycopersicum*, purple for *S. dulcamara*) so any experimental design would need to incorporate a strategy to prevent colour preferences influencing the result.

An experimental option which would avoid the difficulties of confounding variables between species would be to use WT tomato compared to transgenic lines in which the trait of interest had been perturbed. The characterisation of the *R2R3 Myb Subgroup 9* genes presented in this study could aid with the design of such transgenic plants. However, it is always difficult to predict the phenotype that will result from overexpression or silencing of a gene, and lines would have to be carefully analysed to ensure they were useful for comparison with WT in bee choice experiments. It would be ideal to generate transgenic tomato plants which maintained the pepper pot anther cone, but lost the 'glove-like papillae' on the anther surface. It would then also be interesting to generate a phenotype where the trichome mesh is lost, and therefore the anther cone is no longer fused, yet the anthers retain the 'glove-like papillae'. This method has the advantage that it would mean working within a single species and therefore minimising confounding variables which may occur.

Another way in which pollinator interaction with anther traits could be investigated would be through the use of artificial flowers. This may be quicker and would minimise the effect of the different scents of sister species, or unrelated species with differing traits. It would also allow traits to be precisely modified. This could be achieved through casts using epoxy resin or silicon. 3D printing could also be employed in the creation of artificial flowers and anthers. However reproduction of the epidermal surface of the anther may be limited, as 3D printing is not yet able to produce such precision at such a small scale generally. A combination of both casts and 3D printing may allow for the generation of ideal and easily modified artificial flowers and anthers for pollinator behaviour studies, as casts could allow for different epidermal cell surfaces to be recreated while 3D printing could allow for

different anther dimensions to be produced, with different internal anther layering structures.

The 'glove-like papillae' observed on a number of species differ from the more classic shape of the conical cells on petals. It would be of interest to investigate how the two cell types differ in the effect on pollinator grip. An attempt was made to investigate this question during this study using claw drag experiments, in which the force required to drag a mounted bee claw along a rough surface can be accurately measured. Such an investigation would be worth continuing. Initial difficulties encountered were that the curvature of the anther casts affected the drag force required and this would need to be modified in some way to produce flatter casts for the effect of just the epidermal cell outgrowths to be investigated.

Another important aspect of anther traits which could be further investigated is the vibrational properties of the anthers. Buzz pollination involves the transfer of vibrational energy from the bee's muscles to the anther and then to the pollen held within the anther. This then results in pollen release. The structural properties of the anther could greatly affect the way in which this energy is transferred or how much of this energy is transferred. Anther internal layering may be especially important, but anther dimensions and epidermal surface traits could certainly modify vibrational transfer to some degree by dampening or enhancing vibrational transfer. It has been suggested previously that filament length may have a dampening effect on the vibrational energy transfer. This could be investigated through a combination of bee behavioural experiments and observations and laser vibrometry which can measure the vibration of a flower through the use of a laser and Doppler displacement of the laser as a result of the effect of the flower surface oscillations. Previous studies have investigated this briefly in the heterantherous species *S.rostratum* (De Luca et al, 2012). However, heterantherous species are unlikely to be representative of the vibrational energy transfer in *Solanum* as a whole. Vibrational measurements of buzz pollination of species with a variety of anther morphologies could greatly enhance our understanding of how the traits effect buzz pollination and the resulting pollen release.

A related question to be investigated would be the importance of the pepper pot anther cone. This trait has evolved multiple times independently throughout the *Solanum* genus,

yet the evolutionary path to this trait is still unclear. Why do certain species evolve this trait and not others? The case of *S.dulcamara* is especially interesting due to it being the only pepper pot anther cone species in the Dulcamaroid clade and it is the only cone not held together through the use of epidermal cell outgrowths. The loss of epidermal cell outgrowths in the Dulcamaroid clade would also be worth investigating. An investigation searching for the *S.dulcamara R2R3 subgroup 9* genes and examining them from a structural and functional perspective may allow for a greater understanding of the Dulcamaroid clade and their lack of epidermal cell outgrowths.

4.4 Further work: developmental genetic analysis

The formation of the pepper pot cone from a developmental genetic perspective in tomato still requires further investigation. Genome editing via an optimised tomato transformation protocol or knockout via RNAi instead of CRISPR are alternatives that could be considered. Alternatively, if it proves that the knockout of these genes is indeed lethal to the transformants, then creating transgenic plants with an inducibly reduced level of expression of these genes could also result in phenotypes that would help understand the function of these genes. The classic tomato trichome mutants could also be investigated: the cause of the mutant phenotypes, if it is found to be connected with *the R2R3 MYB subgroup 9* genes, would allow better understanding of the function of those genes. The expression patterns and sequences of the *R2R3 MYB subgroup 9* genes in species related to tomato but lacking the pepper pot anther cone, such as *S.juglandilifolium,* could be investigated. *S.juglandilifolium* does not have a pepper pot cone yet has epidermal cell outgrowths all over the anther surface, and most interestingly extended trichome-like outgrowths towards the base of the anthers which could represent a step in the direction of the production of the pepper pot cone. Other species in the tomato clade such as *S.pimpinellifolium* are likely to form their pepper pot anther cone in the same way as tomato, however where there is variation, for example in the coverage of epidermal cell outgrowths over the length of the anther, and where they are more ‘glove-like’ in shape or ‘scale shape’, could be interesting to investigate from the perspective of expression patterns of the *R2R3 MYB subgroup 9* genes.

The pepper pot anther cone of *S.bahamense* could benefit greatly from a more detailed morphological investigation. It has not been fully established how this anther cone is held

together, although this study has made suggestions. Live specimens would need to be located and investigated morphologically, through careful examination using microscopy and sectioning of the anthers to find exactly where the stellate trichomes originate (the anther connective or the anthers themselves) and if the anther cone is held together by the stellate hairs matting together. This could then lead to further developmental genetic studies to explore whether the method of cone formation resembles that of tomato. Are there equivalent genes in *S.bahamense* to those in tomato? Seeing a trait evolve independently via convergent evolution through a similar morphological route and also seeing what that means from a genetic perspective, would be interesting from an evolutionary point of view.

4.5 Conclusions

Overall, this project enhances the understanding of the anthers of the genus *Solanum* from a morphological, evolutionary and developmental genetic perspective and paves the way for further studies which investigate the importance of these anther traits to the interactions of buzz-pollinating insects with these plants. Further studies into the vibrational properties of these traits, the ways in which they affect handling time, efficiency and pollinator choice, and further investigation into the function, development and evolution of the pepper pot anther cone would be an ideal series of next steps.

Ackerman, JD. (2000) Abiotic pollen and pollination: ecological, functional, and evolutionary perspectives. Plant Syst. Evol. 222 (1/4) 167-185

Adedeji, O; Ajuwon, OY; Babawale, OO. (2007) Foliar Epidermal Studies, Organographic Distribution and Taxonomic Importance of Trichomes in the Family Solanacae. Int. J. Bot. 3 (3) 276-283

Aflitos, S; Schijlen, Elio et al. (2014) Exploring genetic variation in the tomato (Solanum section Lycopersicon) clade by whole-genome sequencing. Plant J. 80 136-148

Ai, Y; Singh, A; Coleman, Craig E et al. (1990) Self-incompatibility in Petunia inflata: isolation and characterization of cDNAs encoding three S-allele-associated proteins. Sex. Plant Reprod. 3 (2) 130-138

Akam, M. (1995) Hox genes and the evolution of diverse body plans. Philos. Trans. R. Soc. Lond. B. Biol. Sci. 349 (1329) 313-319

Alcorn, K; Whitney, H; Glover, B. (2012) Flower movement increases pollinator preference for flowers with better grip. Funct. Ecol. 26 (4) 941-947

Alcorn, K. (2013) Pollinator behaviour and the evolutionary genetics of petal surface texture in the Solanacae.

Amara, SG; Jonas, V; Rosenfeld, MG et al. (1982) Alternative RNA processing in calcitonin gene expression generates mRNAs encoding different polypeptide products. Nature 298 240

Baker, HG. (1959) Reproductive methods as factors in speciation in flowering plants. Cold Spring Harb. Symp. Quant. 24 177-191

Bartkowska, MP; Johnston, MO. (2012) Pollinators cause stronger selection than herbivores on floral traits in Lobelia cardinalis (Lobeliaceae). New Phytol. 193 (4) 1039-1048

Batterman, MRW; Lammers, T. (2004) Branched Foliar Trichomes of Lobelioideae (Campanulaceae) and the Infrageneric Classification of Centropogon. 29 Syst. Bot. 448-458

Baumann, K; Perez-Rodriguez, M; Bradley, D et al. (2007) Control of cell and petal morphogenesis by R2R3 MYB transcription factors. Development 134 (9) 1691-1701

Bedinger, PA; Chetelat, RT; McClure, B et al. (2011) Interspecific reproductive barriers in the tomato clade: opportunities to decipher mechanisms of reproductive isolation. Sex. Plant Reprod. 24 (3) 171-187

Behnke, HD. (1984) Plant trichomes: structure and ultrastructure: general terminology, taxonomic applications, and aspects of trichome-bacteria interaction in leaf tips on Dioscorea. Plenum Press New York, etc. 1-21

Bin, F; Sorressi, GP. (1973) Pollinating insects and the production of hybrid tomato seed. Genet. Agrar. 27 35-74

Bohs, L; Olmstead, G. (1999) Solanum Phylogeny Inferred From Chloroplast Dna Sequence Data. Solanaceae IV 97-110

Bohs, L; Olmstead, RG. (1997) Phylogenetic Relationships in Solanum (Solanaceae) Based on ndhF Sequences. Syst. Bot. 22 (1) 5-17

Bohs, L; Weese, T; Myers, N et al. (2007) Zygomorphy and heteranthery in solanum in aphylogenetic context. Acta Hortic. 745 201-223

Bohs, L. (2001) Revision of Solanum Section Cyphomandropsis (Solanaceae). Syst. Bot. Monogr. 61 1-85

Bohs, L. (2005) Major clades in Solanum based on ndhF sequence data. Monogr. Syst. Bot.

Bohs, L. (2007) Phylogeny of the Cyphomandra Clade of the Genus Solanum (Solanaceae) Based on ITS Sequence Data. Taxon 56 (4) 1012-1026

Bombarely, A; Moser, M; Amrad, A et al. (2016) Insight into the evolution of the Solanaceae from the parental genomes of Petunia hybrida. Nat. Plants 2 (May) 1-9

Bombarely, A; Rosli, HG; Vrebalov, J et al. (2012) A Draft Genome Sequence of Nicotiana benthamiana to Enhance Molecular Plant-Microbe Biology Research. Mol. Plant-Microbe Interact. 25 (12) 1523-1530

Bookstein, FL. (1985) Morphometrics in Evolutionary Biology: the Geometry of Size and Shape Change, with Examples from Fishes.

Bowman, JL; Smyth, DR; Meyerowitz, EM. (2012) The ABC model of flower development: then and now. Development 139 (22) 4095-4098

Boyden, A. (1935) Genetics and Homology. Q. Rev. Biol. 10 (4) 448-451

Boyden, A. (1943) Homology and Analogy: A Century After the Definitions of “Homologue” and “Analogue” of Richard Owen. Q. Rev. Biol. 18 (3) 228-241

Brand, U; Fletcher, JC; Hobe, M et al. (2000) Dependence of Stem Cell Fate in Arabidopsis on a Feedback Loop Regulated by CLV3 Activity. Science (80-.). 289 (July) 617-620

Braybrook, SA; Kuhlemeier, C. (2010) How a Plant Builds Leaves. Plant Cell 22 (4) 1006 LP —- 1018

Breg, JN; van Opheusden, JHJ; Burgering, MJM et al. (1990) Structure of Arc repressor in solution: evidence for afamily of beta-sheet DMA-binding proteins. Nature 346 586-589

Brennan, RG; Matthews, W. (1989) The Helix-Turn-Helix DNA Binding Motif. J. Biol. Chem. 264 (4) 22-25

Brockington, SF; Alvarez-Fernandez, R; Landis, JB et al. (2013) Evolutionary Analysis of the MIXTA Gene Family Highlights Potential Targets for the Study of Cellular Differentiation. Mol. Biol. Evol. 30 (3) 526-540

Brockmann, R; Beyer, A; Heinisch, JJ et al. (2007) Posttranscriptional Expression Regulation: What Determines Translation Rates?. PLoS Comput. Biol. 3 (3) e57

Buchmann, SL; Cane, JH. (1989) Bees assess pollen returns while sonicating Solanum flowers. Oecologia 81 (3) 289-294

Buchmann, SL; Hurley, JP. (1978) A biophysical model for buzz pollination in angiosperms. J. Theor. Biol. 72 (4) 639-657

Buchmann, SL; Jones, CE; Colin, LJ. (1978) Vibratile pollination of Solanum douglasii and S. xanti (Solanaceae) in southern California. Wasmann J. Biol. 35 (1) 1-25

Buchmann, SL. (1885) Bees Use Vibration to Aid Pollen Collection from Non-Poricidal Flowers. J. Kansas Entomol. Soc. 58 (3) 517-525

Buchmann, SL. (1983) Buzz pollination in angiosperms. Handb. Exp. Pollinat. Biol. Van Nostrand Reinhold Company 73-113

Cannon, WA. (1909) Studies in heredity as illustrated by the trichomes of species and hybrids of Juglans, Oenothera, Papaver, and Solanum.

Cardarelli, M; Cecchetti, V. (2014) Auxin polar transport in stamen formation and development : how many actors? Front. Plant Sci. 5 (July) 1-13

Carr, MD; Mott, RF. (1991) The transcriptional control proteins c-Myb and v-Myb contain a basic region DNA binding motif. FEBS Lett. 282 (2) 293-294

Caruso, CM; Scott, SL; Wray, JC et al. (2010) Pollinators, Herbivores, and the Maintenance of Flower Color Variation: A Case Study with Lobelia siphilitica. Int. J. Plant Sci. 171 (9) 1020-1028

Chanderbali, AS; Berger, BA; Howarth, DG et al. (2017) Evolution of floral diversity: genomics, genes and gamma. Philos. Trans. R. Soc. BBiol. Sci. 372 (1713)

Chang, J; Yu, T; Gao, S et al. (2016). Fine mapping of the dialytic gene that controls multicellular trichome formation and stamen development in tomato. Theoretical and Applied Genetics 129 1531-1539

Chang, J; Yu, T; Yang, Q et al. (2018). Hair, encoding a single C2H2 zinc-finger protein, regulates multicellular trichome formation in tomato. Plant Journal 96 90-102

Charlesworth, D; Charlesworth, B. (1987) Inbreeding Depression and its Evolutionary Consequences. Annu. Rev. Ecol. Syst. 18 (1) 237-268

Chinwalla, AT; Cook, Lisa L et al. (2002) Initial sequencing and comparative analysis of the mouse genome. Nature 420 520

Chittka, L; Waser, NM. (1997) Why red flowers are not invisible to bees. Isr. J. Plant Sci. 45 (2-3) 169-183

Clark, KR; Okuley, JJ; Collins, PD et al. (1990) Sequence variability and developmental expression of S-alleles in self-incompatible and pseudo-self-compatible petunia. Plant Cell 2 (8) 815 LP —- 826

Cliften, P; Sudarsanam, P; Desikan, A et al. (2003) Finding Functional Features in Saccharomyces Genomes by Phylogenetic Footprinting. Science (80-.). 301 (July) 71-77

Cocucci, AA. (1996) El osmoforo de Cyphomandra (Solanaceae): estudio con microscopio electronicode barrido. Darwiniana 34 (1/4) 145-150

Coen, ES; Meyerowitz, EM. (1991) The war of the whorls: genetic interactions controlling flower development. Nature 353 31

Colombo, L; Franken, J; Koetje, E et al. (1995) The petunia MADS box gene FBP11 determines ovule identity. Plant Cell 7 (11) 1859-1868

Corbet, SA; Huang, SQ. (2014) Buzz pollination in eight bumblebee-pollinated Pedicularis species: Does it involve vibration-induced triboelectric charging of pollen grains?. Ann. Bot. 114 (8) 1665-1674

Corsi, G; Bottega, S. (1999) Glandular Hairs of Salvia officinalis: New Data on Morphology, Localization and Histochemistry in Relation to Function. Ann. Bot. 84 (5) 657-664

Costa, BKP; Schlindwein, C. (2017) Heteranthery as asolution to the demand for pollen as food and for pollination – Legitimate flower visitors reject flowers without feeding anthers. Plant Biol. 19 942-950

Cox, PA. (1988) Hydrophilous Pollination. Annu. Rev. Ecol. Syst. 19 (1) 261-279

Crepet, WL; Niklas,KJ. (2009) Darwin's second "abominable mystery": Why are there so many angiosperm species?. Am. J. Bot. 96 (1) 366-381

Cui, L; Wall, PK Leebens-Mack, JH et al. (2006) Widespread genome duplications throughout the history of flowering plants. Genome Res. (814) 738-749

D'Arcy, WG; D'Arcy, NS; Keating, RC. (1990) Scented anthers in the Solanaceae. Rhodora 92 (870) 50-53

D'Arcy, WG. (1986) Vibratile pollination in Solanum and Lycopersicon: alook at pollen chemistry. Solanaceae Biol. Syst. Columbia Univ. Press. New York, 237-252

Dall'Agnol, R; Lino von Poser, G. (2000) The use of complex polysaccharides in the management of metabolic diseases: the case of Solanum lycocarpum fruits. J. Ethnopharmacol. 71 (1-2) 337-341

Darwin, C. (1859) On the Origin of selection. Murray, London.

Darwin, C. (1976) The effects of cross and self fertilisation in the vegetable kingdom. London John Murray.

Darwin, F. (1899) The botanical work of Darwin. Ann. Bot. 13 ix—-xix

Dassanayake, M; Larkin, JC. (2017) Making Plants Break a Sweat: the Structure, Function, and Evolution of Plant Salt Glands. Front. Plant Sci. 8 406

de Luca, PA; Bussiere, LF; Souto-Vilaros, D et al. (2013) Variability in bumblebee pollination buzzes affects the quantity of pollen released from flowers. Oecologia 172 (3) 805-816

De Luca, PA; Vallejo-Mari, M. (2013) What's the 'buzz' about ? The ecology and evolutionary significance of buzz-pollination. Curr. Opin. Plant Biol. 16 1-7

Dell B, McComb JA. (1978) Plant resins-their formation, secretion and possible functions. Adv Bot Res 6 276-316

Dempsey, WH; Sherif, THI. (1987). Brittleness in the stem of the seven 'hairless' mutants. Report of the Tomato Genetics Cooperative 37

Di Stilio, VS; Martin, C; Schulfer, AF et al. (2009) An ortholog of MIXTA-like2 controls epidermal cell shape in flowers of Thalictrum. New Phytol. 183 (3) 718-728

Diamond, MI; Miner, JN; Yoshinaga, SK et al. (1990) Transcription Factor Interactions : Selectors of Positive or Negative Regulation from aSingle DNA Element. Science (80-.). 249 (6) 1266-1272

Diaz-Castelazo, C; Rico-Gray, V; Ortega, F et al. (2005) Morphological and secretory characterization of extrafloral nectaries in plants of coastal Veracruz, Mexico. Ann. Bot. 96 (7) 1175-1189

Diggle, PK; Miller, JS. (2004) Architectural effects mimic floral sexual dimorphism in Solanum (Solanaceae). Am. J. Bot. 91 (12) 2030-2040

Dobritzsch, S; Weyhe, M; Schubert, R et al. (2015) Dissection of jasmonate functions in tomato stamen development by transcriptome and metabolome analyses. BMC Biol. 1-18

Dobson, HEM. (1994) Floral volatiles in insect biology. Insect–Plant Interact. (ed. E. A. Bernays), CRC Press. BocaRafton, FL. 47—-81.

Dubos, C; Stracke, R; Grotewold, R et al. (2010) MYB transcription factors in Arabidopsis. Trends Plant Sci. 15 (10) 573-581

Dudareva, N; Pichersky, E; Gershenzon, J. (2004) Biochemistry of Plant Volatiles. Plant Physiol. 135 (4) 1893 LP —- 1902

Dunal, MF. (1852) Solanaceae. AP DeCandolle, Prodromus Syst. Nat. regni Veg. 3 Victoris Masson, Paris. 1-690

Ehleringer, J. (1984) Ecology and ecophysiology of leaf pubescence in North American desert plants. Biol. Chem. Plant Trichomes (E. Rodrigues, P. L. Heal. I. Mehta, eds), Plenum, New York. 113-132

Endress, PK. (1996) Diversity in Angiosperm anthers: 'Solanum-type' flowers, buzz pollination and poricidal anthers, heteranthery and synanthery. Anther Form, Funct. Phylogeny. Ed. by WG, D'Arcy. Keating, RC

Entani, T; Iwano, M; Shiba, H et al. (1999) Centromeric localization of an S-RNase gene in Petunia hybrida Vilm. Theor. Appl. Genet. 99 (3-4) 391-397

Esau, K. (1965) Plant Anatomy. 767

Esau, K. (1977) Anatomy of Seed Plants.

Escaravage, N; Flubacker, E; Pornon, A et al. (2001) Stamen Dimorphism in Rhododendron ferrugineum (Ericaceae): Development and Function. Am. J. Bot. 88 (1) 68-75

Evans, RM. (1988) The steroid and thyroid hormone receptor superfamily. Science (80). 240 889-895

Faegri, K; van der Pijl, L. (1972) The Principles of Pollination Ecology. J. Ecol. 60 (3)

Faegri, K. (1986) The solanoid flower. Trans. Bot. Soc. Edinburgh, 150th Anniv. Suppl. 51-59

Fahn, A. (1988) Secretory tissues in vascular plants. New Phytol. 108 (3) 229-257

Falcao, BF; Stehmann, JR. (2018) Functional anatomy reveals secretory activity in papillose anthers of abuzz-pollinated Solanum species (Cyphomandra clade - Solanaceae). Plant Biol. 20 (4) 654-661

Farrel, A; Murphy, J; Guo, J-T. (2016) Structure-based prediction of transcription factor binding specificity using an integrative energy function. Bioinformatics 32 306-313

Farruggia, FT; Bohs, L. (2010) Two new South American species of Solanum section Crinitum (Solanaceae). PhytoKeys (1) 67-77

Fenster, CB; Armbruster, WS; Wilson, P et al. (2004) Pollination Syndromes and Floral Specialization. Annu. Rev. Ecol. Evol. Syst. 35 (1) 375-403

Fiz-Palacios, O; Schneider, H; Heinrichs, J et al. (2011) Diversification of land plants: insights from a family-level phylogenetic analysis. BMC Evol. Biol. 201111:341

Francis, JS; Muth, F; Papaj, DR et al. (2016) Nutritional complexity and the structure of bee foraging bouts. Behav. Ecol. 27 (3) 903-911

Frankie, GW; Haber, WA; Opler, PA et al. (1983) Characterstics and organization of the large bee pollination system in the Costa Rican dry forest. Handb. Exp. Pollinat. Biol. Van Nostrand Reinhold Company 411-447

Frodin, DG. (2004) History and Concepts of Big Plant Genera. Taxon 53 (3) 753-776

Gagliano, M; Mancuso, S; Robert, D. (2012) Towards understanding plant bioacoustics. Trends Plant Sci. 17 (6) 323-325

Galinha, C; Bilsborough, G; Tsiantis, M. (2009) Hormonal input in plant meristems: A balancing act. Semin. Cell Dev. Biol. 20 (9) 1149-1156

Garcia, CC; Barboza, GE. (2006) Anther wall development and structure in wild tomatoes (Solanum sect . Lycopersicon): functional inferences. Aust. J. Bot. 54 83-89

Gebhardt, C. (2016) The historical role of species from the Solanaceae plant family in genetic research. Theor. Appl. Genet. 129 (12) 2281-2294

Gerats, T; Vandenbussche, M. (2005) A model system for comparative research: Petunia. Trends Plant Sci. 10 (5) 251-256

Gilbert, LE. (1971) Butterfly-Plant Coevolution: Has Passiflora adenopoda Won the Selectional Race with Heliconiine Butterflies?. Science 172 (3983) 585-586

Giles, BE. (1988) Variation in anther size in wild barley (Hordeum vulgare ssp. spontaneum). Hereditas 205 199-205

Glover, BJ; Bunnewell, S; Martin, C. (2004) Convergent evolution within the genus Solanum: The specialised anther cone develops through alternative pathways. Gene 331 (1-2) 1-7

Glover, BJ; Perez-Rodriguez, M; Martin, C. (1998) Development of several epidermal cell types can be specified by the same MYB-related plant transcription factor. Development 125 3497-3508

Glover, BJ. (2000). Differentiation in plant epidermal cells. Journal of Evolutionary Biology 51 497-505

Goodin, MM; Zaitlin, D; Naidu, RA et al. (2008) Nicotiana benthamiana: its history and future as a model for plant-pathogen interactions. Mol. Plant. Microbe. Interact. 21 (8) 1015-1026

Grant, V. (1949) Pollination Systems as Isolating Mechanisms in Angiosperms Author(s): Verne Grant Source:. Evolution (N. Y). 3 (1) 82-97

Griffiths, AJF; Miller, JH; Suzuki, DT et al. (2000) Transcription: an overview of gene regulation in eukaryotes. An Introd. to Genet. Anal. 7th Ed. New York W. H. Free.

Griffiths, AJF; Miller, JH; Suzuki, DT. (2000) An Introduction to Genetic Analysis.

Guo, X; Hu, Z; Yin, W et al. (2016) The tomato floral homeotic protein key roles in petal and stamen development. Nat. Publ. Gr. (October 2015) 1-13

Haberlandt, G. (1914) Physiological plant anatomy.

Hake, S; Smith, HMS; Holtan, H et al. (2004) The role of knox genes in plant development. Annu. Rev. Cell Dev. Biol. 20 125-151

Hammonds, AS; Bristow, CA; Fisher, WW et al. (2013) Spatial expression of transcription factors in Drosophila embryonic organ development. Genome Biol. 14 1-15

Harbison, CT; Gordon, DB; Lee, TI et al. (2004) Transcriptional regulatory code of a eukaryotic genome. Nature 431 99

Harder, LD; Barclay, RMR. (1994) The functional significance of poricidal anthers and buzz pollination: controlled pollen removal from Dodecatheon. Funct. Ecol. 8 509-517

Harder, LD; Thomson, JD. (1989) Evolutionary options for maximizing pollen dispersal of animal-pollinated plants. Am. Nat. 133 323-344

Hawkes, JG; Nee, M; Symon, DE et al. (1999) The economic importance of the family Solanaceae. Solanaceae IV Adv. Biol. Util. Eds; R. Bot. Gard. Kew, UK; 1—-8.

Hay, A; Tsiantis, M. (2010) KNOX genes: versatile regulators of plant development and diversity. Development 137 (19) 3153-3165

Heim, MA; Jakoby, M; Werber, M et al (2003). The basic helix-loop-helix transcription factor family in plants: a genome-wide study of protein structure and functional diversity. Molecular biology and evolution 20 735-747

Hellens, RP; Edwards, EA; Leyland, NR et al. (2000) pGreen: a versatile and flexible binary Ti vector for Agrobacterium-mediated plant transformation. Plant Mol. Biol. 42 (6) 819-832

Hileman, LC; Baum, DA. (2003) Why Do Paralogs Persist? Molecular Evolution of CYCLOIDEA and Related Floral Symmetry Genes in Antirrhineae (Veronicaceae). Mol. Biol. Evol. 20 (4) 591-600

Hileman, LC; Kramer, EM; Baum, DA. (2003) Differential regulation of symmetry genes and the evolution of floral morphologies. Proc. Natl. Acad. Sci. U. S. A. 2003

Horwitz, KB; Jackson, TA; Bain, DL et al. (1996) Nuclear Receptor Corepressors Coactivators. Mol. Endocrinol. 10 (10) 1167-1177

Hubbs, CL. (1944) Concepts of Homology and Analogy. Am. Nat. 78 (777) 289-307

Hunziker, AT. (1979) South American Solanaceae: a synoptic survey. 49-85

Ioerger, TR; Gohlke, JR; Xu, B et al. (1991) Primary structural features of the self-incompatibility protein in solanaceae. Sex. Plant Reprod. 4 (2) 81-87

Irish, V. (2017) The ABC model of floral development. Curr. Biol. 27 (17) R887—-R890

Irwin, RE; Adler, LS; Agrawal, AA. (2004) Community and Evolutionary Ecology of Nectar1. Ecology 85 (6) 1477-1478

Jacob, F. (1977) Evolution and tinkering. Science (80-.). 196 (4295) 1161 LP —- 1166

Jesson, LK; Barrett, SCH. (2003) The Comparative Biology of Mirror-Image Flowers. Int. J. Plant Sci. 164 (S5) S237—-S249

Jin, H; Martin, C. (1999) Multifunctionality and diversity within the plant MYB-gene family. Plant Mol. Biol. 577-585

Johnson, B. (1953) The injurious Effects of the Hooked Epidermal Hairs of French Beans (Phaseolus vulgaris L.) on Aphis craccivora Koch. Bull. Entomol. Res. 44 (4) 779-788

Johnson, HB. (1975) Plant Pubescence: An ecological perspective. Bot. Rev. Vol.41. No.3. 233-258

Jolliffe, IT; Cadima, J. (2016) Principal component analysis: a review and recent developments. Philos. Trans. A. Math. Phys. Eng. Sci. 374 (2065) 20150202

Kang, JH; Campos, ML; Zemelis-Durfee, S et al. (2016) Molecular cloning of the tomato Hairless gene implicates actin dynamics in trichome-mediated defense and mechanical properties of stem tissue. J. Exp. Bot. 67 (18) 5313-5324

Kang, JH; Shi, F; Jones, AD et al. (2010) Distortion of trichome morphology by the hairless mutation of tomato affects leaf surface chemistry. J. Exp. Bot. Bot. 61 1053-1064

Kao, TH; McCubbin, AG. (1996) How flowering plants discriminate between self and non-self pollen to prevent inbreeding. Proc. Natl. Acad. Sci. U. S. A. 93 (22) 12059-12065

Kao, TH; McCubbin, AG. (1997) Molecular and biochemical bases of gametophytic self-incompatibility in solanaceae'. Plant Physiol. Biochem. 35 (3) pp. 171—-176

Kao, TH; Tsukamoto, T. (2004) The Molecular and Genetic Bases of S-RNase-Based Self-Incompatibility. Plant Cell 16 (suppl 1) S72 LP —- S83

Karabourniotis, G; Kotsabassidis, DY; Manetas, Y. (1995) Trichome density and its protective potential against ultraviolet-B radiation damage during leaf development. Can. J. Bot. 73 (3) 376-383

Kariyat, RR; Smith, JD; Stephenson, AG et al. (2017) Non-glandular trichomes of Solanum carolinense deter feeding by Manduca sexta caterpillars and cause damage to the gut peritrophic matrix. Proceedings. Biol. Sci. 284 (1849)

Kay, QON; Daoud, HS; Stirton, CH. (2018) Pigment distribution, light reflection and cell structure in petals. Bot. J. Linn. Soc. 83 (1) 57-83

Kellis, M; Patterson, N; Endrizzi, M et al. (2003) Sequencing and comparison of yeast species to identify genes and regulatory elements. Nature 423 241

Kevan, PG; Baker, HG. (1983) Insects as Flower Visitors and Pollinators. Annu. Rev. Entomol. 28 (1) 407-453

Kevan, PG; Lane, MA. (1985) Flower petal microtexture is atactile cue for bees. Proc. Natl. Acad. Sci. U. S. A. 82 (14) 4750-4752

Kim, S; Park, M; Yeom, SI et al. (2014) Genome sequence of the hot pepper provides insights into the evolution of pungency in Capsicum species. Nat. Genet. 46 (3) 270-278

Kimmel, CB; Small, CM; Knope, ML. (2017) A rich diversity of opercle bone shape among teleost fishes. PLoS One 12 (12) e0188888

Kimura, S; Sinha, N. (2008) Tomato (Solanum lycopersicum): A Model Fruit-Bearing Crop. CSH Protoc. 2008 pdb.emo105

King MJ, Buchmann S. (1996) Sonication dispensing of pollen from Solanum laciniatum flowers. Funct. Ecol. 10 (4) 449-456

King MJ, Buchmann SL. (2003) Floral sonication by bees: mesosomal vibration by Bombus and Xylocopa, but not Apis (Hymenoptera: Apidae), ejects pollen from poricidal anthers. J. Kansas Ento- mological Soc. 76 295-305

King, MJ; Buchmann, SL. (1995) Bumble Bee-Initiated Vibration Release Mechanism of Rhododendron Pollen. Am. J. Bot. 82 (11) 1407-1411

King, MJ. (1993) Buzz foraging mechanism of bumble bees. J. Apic. Res. 32 41-49

Kirik, V; Schnittger, A; Radchuk, V et al. (2001). Ectopic expression of the Arabidopsis AtMYB23 gene induces differentiation of trichome cells. Developmental biology 235 366-377

Knapp, S; Bohs, L; Nee, M et al. (2004) Solanaceae-a model for linking genomics with biodiversity. Comp. Funct. Genomics 5 (3) 285-291

Knapp, S. (2002) Tobacco to tomatoes: a phylogenetic perspective on fruit diversity in the Solanaceae. J. Exp. Bot. 53 (377) 2001-2022

Knapp, S. (2004) Floral Diversity and evolution in Solanaceae. Cronk, Q. (Ed.), Bateman, R. (Ed.), Hawkins, J. (Ed.), Warren, A. (2002). Dev. Genet. Plant Evol. London CRC Press. 267—- 297.

Knapp, S. (2010) On 'various contrivances': pollination, phylogeny and flower form in the Solanaceae. Philos. Trans. R. Soc. BBiol. Sci. 449-460

Koornneef M. (1981). The complex syndrome of ttg mutants Arabidopsis. Inf Serv 18 45-51

Kramer, EM; Hodges, SA. (2010) Aquilegia as a model system for the evolution and ecology of petals. Philos. Trans. R. Soc. Lond. B. Biol. Sci. 365 (1539) 477-490

Kranz, HD; Denekamp, M; Greco, R et al. (1998) Towards functional characterisation of the members of the R2R3-MYB gene family from Arabidopsis thaliana. Plant J. 16 (May) 263-276

Laherty, CD; Yang, W-M; Sun, J-M et al. (1997) Histone deacetylases associated with with the mSin3 Corepressor Mediate Mad Transcriptional Repression. Cell 89 (3) 349-356

Larkin, JC; Brown, ML; Schiefelbein, J. (2003). How do cells know what they want to be when they grow up? Lessons from epidermal patterning in Arabidopsis. Annual review of plant biology 54 403-430

Lee, MINS; Gippert, GP; Soman, KV et al. (1989) Three-Dimensional Solution Structure of a Single Zinc Finger DNA-Binding Domain. Science (80-.). 245 (4918) 635-637

Leitch, IJ; Hanson, L; Lim, KY et al. (2008) The ups and downs of genome size evolution in polyploid species of Nicotiana (Solanaceae). Ann. Bot. 101 (6) 805-814

Lelli, KM; Slattery, M; Mann, RS. (2012) Disentangling the Many Layers of Eukaryotic Transcriptional Regulation. Annu. Rev. Genet. 46 43-68

Levin, DA. (1973) The Role of Trichomes in Plant Defense. Q. Rev. Biol. 48 (1, Part 1) 3-15

Li, G; Ruan, X; Auerbach, RK et al. (2012) Extensive Promoter-Centered Chromatin Interactions Provide aTopological Basis for Transcription Regulation. Cell 148 (1-2) 84-98

Liakoura, V; Stefanou, M; Manetas, Y et al. (1997) Trichome density and its UV-B protective potential are affected by shading and leaf position on the canopy. Environ. Exp. Bot. 38 (3) 223-229

Liang, G; He, H; Li, Y et al. (2014). MYB82 functions in regulation of trichome development in Arabidopsis. Journal of experimental botany 65 3215-3223

Liu, LA; Bradley, P. (2012) Atomistic modeling of protein-DNA interaction specificity: progress and applications. Curr. Opin. Struct. Biol. 22 (4) 397-405

Lopes, AV; Vogel, S; Machado, IC. (2002) Secretory trichomes, a substitutive floral nectar source in Lundia A. DC. (Bignoniaceae), a genus lacking afunctional disc. Ann. Bot. 90 (2) 169-174

Lord, EM; Russell, SD. (2002) The Mechanisms of Pollination and Fertilization in Plants. Annu. Rev. Cell Dev. Biol. 18 (1) 81-105

Lorenzi, H. (1978) Brazilian Trees: A Guide to the Identification and Cultivation of Brazilian Native Trees.

Lorenzi, H. (2002) {Arvores Brasileiras: Manual de Identificaçao eCultivo das Plantas Arboreas do Brasil}. 369

Luo, Z-L; Gu, L; Zhang, D. (2009) Intrafloral differentiation of stamens in heterantherous flowers. 47 J. Syst. Evol. 43-56

Machado, A; Wu, Y; Yang, Youming et al. (2009) The MYB transcription factor GhMYB25 regulates early fibre and trichome development. Plant J. 59 52-62

Maniatis, T; Goodbourn, S; Fischer, JA. (1987) Regulation of Inducible and Tissue-specific gene expression. Science (80-.). 236 1237-1244

Marks, MD; Feldmann, KA. (1989). Trichome Development in Arabidopsis thaliana. I. T-DNA Tagging of the GLABROUS1 Gene. The Plant Cell 1 1043 LP-1050

Martin, C; Bhatt, K; Baumann, K et al. (2002) The mechanics of cell fate determination in petals. Philos. Trans. R. Soc. Biol. Sci. (May) 809-813

Martin, C; Ellis, N; Rook, F. (2010) Do Transcription Factors Play Special Roles in Adaptive Variation?. Plant Physiol. 154 (October) 506-511

Martin, C; Glover BJ. (2007). Functional aspects of cell patterning in aerial epidermis. Current Opinion in Plant Biology 10 70-82

Martins, K., Chaves, L. J., Buso, GSC, Kageyama, PY. (2006) Mating system and fine-scale spatial genetic structure of Solanum lycocarpum St.Hil. (Solanaceae) in the Brazilian Cerrado. Conserv. Genet. 7 (6) 957-969

Masuda, H; Matsusaka, S; Shimomura, H. (1998) Measurement of mass flow rate of polymer powder based on static electrification of particles. Adv. Powder Technol. 9 (2) 169-179

Matsusaka, S; Maruyaa, H; Matsuyama, T et al. (2010) Triboelectric charging of powders: A review. Chem. Eng. Sci. 65 (22) 5781-5807

Maughan, SC; Murray, JAH; Bogre, L. (2006) A greenprint for growth: signalling the pattern of proliferation. Curr. Opin. Plant Biol. 9 (5) 490-495

McCaskill, D; Gershenzon, J; Croteau, R. (1992) Morphology and monoterpene biosynthetic capabilities of secretory cell clusters isolated from glandular trichomes of peppermint (Mentha piperita L.). Planta 187 (4) 445-454

Meister, G; Landthaler, M; Patkaniowska, A et al. (2004) Human Argonaute2 Mediates RNA Cleavage Targeted by miRNAs and siRNAs. Mol. Cell 15 (2) 185-197

Michener, CD. (1962) An interesting method of pollen collecting by bees from flowers with tubular anthers. Rev. Biol. Trop. 10 167-175

Michener, CD. (2007) The Bees of the World.

Mione, T; Anderson, GJ. (1992) Pollen-ovule ratios and breeding system evolution in Solanum section Basarthrum (Solanaceae). Am. J. Bot. 79 (3) 279-287

Misra, SK; Wang, C; Han, S et al. (1987) EPR of CO2+-doped NiSO47H2O and MgSO47H2O: Co2+-Ni2+ exchange interaction. Phys. Rev. B 36 (7) 3542-3547

Mitchell, RJ; Shaw, RG; Waser, NM. (1998) Pollinator Selection, Quantitative Genetics, and Predicted Evolutionary Responses of Floral Traits in Penstemon centranthifolius (Scrophulariaceae). Int. J. Plant Sci. 159 (2) 331-337

Mitchell, RJ; Waser, NM. (1992) Adaptive Significance of Ipomopsis Aggregata Nectar Production: Pollination Success of Single Flowers. Ecology 73 (2) 633-638

Morandin, LA; Laverty, TM. (2001) Effect of Bumble Bee (Hymenoptera : Apidae) Pollination Intensity on the Quality of Greenhouse Tomatoes. J. Econ. Entomol. 94 (1) 172-179

Motta-Junior, JC; Talamoni, SA; Lombardi, JA et al. (1996) Diet of the maned wolf, Chrysocyon brachyurus, in central Brazil. J. Zool. 240 (2) 277-284

Mueller, LA; Solow, TH; Taylor, N et al. (2005) The SOL Genomics Network: acomparative resource for Solanaceae biology and beyond. Plant Physiol. 138 (3) 1310-1317

Muller, Hermann. (1881) Two Kinds of Stamens with Different Functions in the same Flower. Nature 24 307

Muller, Hermann. (1882) Y iiber die Farben- liebhaberei der Honigbiene. Kosmos 12 273-299

Nägeli, C. (1958) {Uber das Wachstum des Stammes und der Wurzel bei den Gefäss pflanzen}. Beiträ ge zur Wissenschaftlichen Bot. Wilhelm Engelmann 1-11

Nicolson, SW. (2011) Bee food: the chemistry and nutritional value of nectar, pollen and mixtures of the two. African Zool. 46 (2) 197-204

Nieuwland, J; Scofield, S; Murray, JAH. (2009) Control of division and differentiation of plant stem cells and their derivatives. Semin. Cell Dev. Biol. 20 (9) 1134-1142

Noda, K; Glover, BJ; Linstead, P et al. (1994) Flower colour intensity depends on specialized cell shape controlled by aMyb-related transcription factor. Nature 369 (6482) 661-664

Ogryzko, VV; Schiltz, RL; Russanova, V et al. (1996) The Transcriptional Coactivators p300 and CBP Are Histone Acetyltransferases. Cell 87 (5) 953-959

Oh, IH; Reddy, EP. (1999) The MYB gene family in cell growth, differentiation and apoptosis. Oncogene 18 (19) 3017-3033

Oliveira-Filho, AT; Oliveira, LCA. (1988) Biologia floral de uma populac¸ a˜ ode Solanum lycocarpum St Hil (Solanaceae) em Lavras. MG. Rev. Bras. Bot.,

Olmstead, RG. (2013) Phylogeny and biogeography in Solanaceae, Verbenaceae and Bignoniaceae: acomparison of continental and intercontinental diversification patterns. Bot. J. Linn. Soc. 171 (1) 80-102

Oney, MA; Bingham, R. (2014) Effects of simulated and natural herbivory on tomato (Solanum lycopersicum var. esculentum) leaf trichomes. Bios 85 (4) 192-198

Oppenheimer, DG; Herman, PL; Sivakumaran, S et al. (1991). A myb gene required for leaf trichome differentiation in Arabidopsis is expressed in stipules. Cell 67 483-493

Ossowski, S; Schwab, R; Weigel, D. (2008) Gene silencing in plants using artificial microRNAs and other small RNAs. Plant J. 53 (4) 674-690

Pabo, C; Sauer, RT. (1992) Transcription Factors: Structural Families and Principles of DNA Recognition. Annu. Rev. Biochem. 61 1053-1095

Parachnowitsch, AL; Kessler, A. (2010) Pollinators exert natural selection on flower size and floral display in Penstemon digitalis. New Phytol. 188 (2) 393-402

Parachnowitsch, AL; Manson, JS; Sletvold, N. (2018) Evolutionary ecology of nectar. Ann. Bot.

Parachnowitsch, AL; Raguso, RA; Kessler, A. (2012) Phenotypic selection to increase floral scent emission, but not flower size or colour in bee-pollinated Penstemon digitalis. New Phytol. 195 (3) 667-675

Passarelli, L; Bruzzone, L. (2004) Significance of floral colour and scent in three Solanum sect. Cyphomandropis species (Solanaceae) with different floral rewards. Aust. J. Bot. 52 659-667

Passarelli, L; Cocucci, A. (2006) Dynamics of pollen release in relation to anther-wall structure among species of Solanum (Solanaceae). 54 Aust. J. Bot. - AUST JBOT

Pastore, JJ; Limpuangthip, A; Yamaguchi, N et al. (2011) LATE MERISTEM IDENTITY2 acts together with LEAFY to activate APETALA1. Development 138 (15) 3189-3198

Pattanaik, S; Patra, B; Singh, SK et al. (2014). An overview of the gene regulatory network controlling trichome development in the model plant, Arabidopsis. Frontiers in plant science 5 259

Payne, T; Clement, J; Arnold, D et al. (1999). Heterologous myb genes distinct from GL1 enhance trichome production when overexpressed in Nicotiana tabacum. Development 126 671 LP-682

Pelaz, S; Ditta, GS; Baumann, E et al. (2000) Band Cfloral organ identity functions require SEPALLATA MADS-box genes. Nature 405 (6783) 200-203

Peralta, IE; Spooner, DM; Knapp, S. (2008) Taxonomy of Wild Tomatoes and Their Relatives (Solanum sect. Lycopersicoides, sect. Juglandifolia, sect. Lycopersicon; Solanaceae). 84 Syst. Bot. Monogr. 1-186

Perez-Rodriguez, M; Jaffe, FW; Butelli, Eugenio et al. (2005) Development of three different cell types is associated with the activity of aspecific MYB transcription factor in the ventral petal of Antirrhinum majus flowers. Development 132 (2) 359-370

Perret, M; Chautems, A; Spichiger, R et al. (2001) Nectar Sugar Composition in Relation to Pollination Syndromes in Sinningieae (Gesneriaceae). Ann. Bot. 87 (2) 267-273

Pesch, M; Hulskamp, M. (2004). Creating a two-dimensional pattern de novo during Arabidopsis trichome and root hair initiation. Current opinion in genetics & development 14 422-427

Pfahler, PL; Pereira, MJ; Barnett, RD. (1996) Genetic and environmental variation in anther, pollen and pistil dimensions in sesame. Sex. Plant Reprod. 9 228-232

Pollard, AH, Briggs, D. (1984) Genecological studies of Urtica dioica.L. III. Stinging hairs and plant-herbivore interactions. New Phytol. 97 507—-522.

Proenqa, CEB. (1992) Buzz pollination - older and more widespread than we think ?. J. Trop. 8 115-120

Puttick, MN; Morris, JL; Williams, TA et al. (2018) The Interrelationships of Land Plants and the Nature of the Ancestral Embryophyte Article The Interrelationships of Land Plants and the Nature of the Ancestral Embryophyte. Curr. Biol. 28 (5) 733—-745.e2

Rabelo, LS; Vilhena, AMGF; Bastos, EMAF et al. (2014) Differentiated use of pollen sources by two sympatric species of oil-collecting bees (Hymenoptera: Apidae). J. Nat. Hist. 48 (25-26) 1595-1609

Rabelo, LS; Vilhena, AMGF; Bastos, EMAF et al. (2015) Oil-collecting bee–flower interaction network: do bee size and anther type influence the use of pollen sources?. Apidologie 46 (4) 465-477

Ramesar-Fortner, NS, Aiken, SG, Dengler, NG. (1995) Phenotypic plasticity in leaves of four species of Arctic Festuca (Poacaeae). Can. J. Bot 73 1810 1823

Rasheed, S; Harder, L. (1997) Economic motivation for plant species preferences of pollen-collecting bumble bees. Ecol. Entomol. 22 (2) 209-219

Rast, MI; Simon, Rudiger. (2008) The meristem-to-organ boundary: more than an extremity of anything. Curr. Opin. Genet. Dev. 18 (4) 287-294

Reeves, AF. (1977) Tomato trichomes and mutations affecting their development. Am. J. Bot. 64 (2) 186-189

Rerie, WG; Feldmann, KA; Marks, MD. (1994). The GLABRA2 gene encodes a homeo domain protein required for normal trichome development in Arabidopsis. Genes & development 8 1388-1399

Richardson, HH. (1943) The action of bean leaves against the bedbug. J. Econ. Entom. 36 543-545

Rick CM, Butler L. (1956) Cytogenetics of the tomato. Adv. Genet. (8) 267-282

Rick, CM; Fobes, JF; Holle, M. (1977) Genetic variation inLycopersicon pimpinellifolium: Evidence of evolutionary change in mating systems. Plant Syst. Evol. 127 (2) 139-170

Rick, CM. (1947). Partial Suppression of Hair Development Indirectly Affecting Fruitfulness and the Proportion of Cross-Pollination in a Tomato Mutant. The American Naturalist 81 185-202

Rick, M; Thorp, Robbin W. (1978) Rates of cross-pollination in Lycopersicon pimpinellifolium impact of genetic variation in floral characters. Plant Syst. Evol. 129 31-44

Robertson, C. (1928) Flowers and insects; lists of visitors of four hundred and fifty-three flowers.

Robertson, K; Goldberg, EE; Igic, B. (2011) Comparative evidence for the correlated evolution of polyploidy and self-compatibility in Solanaceae. Evolution 65 (1) 139-155

Rodriguez, E; Healy, PL; Mehta, I. (1984) Biology and Chemistry of Plant Trichomes.

Roe, KE. (1967) A revision of Solanum, Section Brevantherum in North and Central America. Brittonia 19

Roe, KE. (1971) Terminology of Hairs in the Genus Solanum. Taxon 20 (4) 501-508

Romero, IG; Ruvinsky, I; Gilad, Y. (2014) Comparative studies of gene expression and the evolution of gene regulation. Nat. Rev. Genet. 13 (7) 505-516

Roy, BA; Stanton, ML; Eppley, SM. (2001) Effects of environmental stress on leaf hair density and consequences for selection. J. Evol. Biol. 12 (6) 1089-1103

Roy, BA; Stanton, ML. (1999) Asymmetry in wild mustard, Sinapis arvensis (Brassicaceae), in response to severe physiological stresses. J. Evol. Biol. 12 (3) 440-449

Russell, AL; Morrison, SJ; Moschonas, EH et al. (2017) Patterns of pollen and nectar foraging specialization by bumblebees over multiple timescales using RFID. Sci. Rep. 7 42448

Saedler, H; Huijser, P. (1993) Molecular biology of flower development in Antirrhinum majus (snapdragon). Gene 135 (1-2) 239-243

Sakamoto, M; Ruta, M. (2012) Convergence and Divergence in the Evolution of Cat Skulls: Temporal and Spatial Patterns of Morphological Diversity. PLoS One 7 (7) e39752

Samuels, J. (2009) The Solanaceae-novel crops with high potential. Org. Grow. 9 32-34

Samuels, J. (2015) Biodiversity of Food Species of the Solanaceae Family: APreliminary Taxonomic Inventory of Subfamily Solanoideae. 4 (2) Resources 277-322

Sande, S; Privalsky, ML. (1996) Identification of TRACs (T3 receptor-associating cofactors), afamily of cofactors that associate with, and modulate the activity of, nuclear hormone receptors. Mol. Endocrinol. 10 (7) 813-818

Sanders, LC; Lord, EM. (1989) Directed movement of latex particles in the gynoecia of three species of flowering plants. Science (80-.). 243 (4898) 1606-1608

Sangwan, NS; Farooqi, AHA; Shabih, F et al. (2001) Regulation of essential oil production in plants. Plant Growth Regul. 34 (1) 3-21

Sarkinen, T; Bohs, L; Olmstead, RG et al. (2013) Aphylogenetic framework for evolutionary study of the nightshades (Solanaceae): adated 1000-tip tree. BMC Evol. Biol. 13 214

Sazima, M; Vogel, S; Cocucci, A et al. (1993) The perfume flowers ofCyphomandra (Solanaceae): Pollination by euglossine bees, bellows mechanism, osmophores, and volatiles. Plant Syst. Evol. 187 (1) 51-88

Schiestl, FP; Johnson, SD. (2013) Pollinator-mediated evolution of floral signals. Trends Ecol. Evol. 28 (5) 307-315

Schoof, H; Lenhard, M; Haecker, A et al. (2000) The Stem Cell Population of Arabidopsis Shoot Meristems Is Maintained by aRegulatory Loop between the CLAVATA and WUSCHEL Genes. Cell 100 (6) 635-644

Schwinn, K; Venail, J; Shang, Y et al. (2006) ASmall Family of MYB-Regulatory Genes Controls Floral Pigmentation Intensity and Patterning in the Genus Antirrhinum. Plant Cell 18 (April) 831-851

Scott, RJ; Spielman, M; Dickinson, HG. (2004) Stamen Structure and Function. Plant Cell 16 46-61

Seithe, A. (1962) Die Haararten der Gattung Solanum L. und ihre taxonomische Ve wertung. Bot. Jb. 81 (3) 233-261

Serna, L; Martin, C. (2006). Trichomes: different regulatory networks lead to convergent structures. Trends in plant science 11 274-280

Serna, L. (2004). A Network of Interacting Factors Triggering Different Cell Fates. The Plant Cell 16 2258 LP-2263

Shang, Y; Venail, J; Mackay, S et al. (2011) The molecular basis for venation patterning of pigmentation and its effect on pollinator attraction in flowers of Antirrhinum. New Phytol. 189 (2) 602-615

Sierro, N; Battey, JND; Ouadi, S et al. (2014) The tobacco genome sequence and its comparison with those of tomato and potato. Nat. Commun. 5 3833

Singh, K; Foley, RC; Onate-Sanchez, L. (2002) Transcription factors in plant defense and stress responses. Curr. Opin. Plant Biol. 5 (5) 430-436

Skaltsa, H; Verykokidou, E; Harvala, C et al. (1994) UV-B protective potential and flavonoid content of leaf hairs of Quercus ilex. Phytochemistry 37 (4) 987-990

Solanaceaesource.org.

Soltis, DE; Albert, VA; Leebens-Mack, J et al. (2009) Polyploidy and angiosperm diversification. Am. J. Bot. 96 (1) 336-348

Soltis, PS; Brockington, SF; Yoo, M-J et al. (2009) Floral variation and floral genetics in basal angiosperms. Am. J. Bot. 96 (1) 110-128

Somssich, M; Je, BI. (2016) CLAVATA-WUSCHEL signaling in the shoot meristem. Development 143 3238-3248

Spaethe, J; Tautz, J; Chittka, L. (2001) Visual constraints in foraging bumblebees: Flower size and color affect search time and flight behavior. Proc. Natl. Acad. Sci. 98 (7) 3898 LP —- 3903

Spitz, F; Furlong, EE. (2012) Transcription factors: from enhancer binding to developmental control. Nat. Rev. Genet. 13 (9) 613-626

Stebbins, GL. (1970) Adaptive Radiation of Reproductive Characteristics in Angiosperms, I: Pollination Mechanisms. Annu. Rev. Ecol. Syst. 1 (1) 307-326

Steeves, TA; Sussex, IM. (1989) Patterns in Plant Development.

Stern, DL; Orgogozo, V. (2008) The loci of evolution: how predictable is genetic evolution?. Evolution (N. Y). 62 (9) 2155-2177

Stracke, R; Werber, M; Weisshaar, B. (2001) The R2R3-MYB gene family in Arabidopsis thaliana. Curr. Opin. Plant Biol. 4 (5) 447-56

Symon, DE. (1979) Sex forms in Solanum (Solanaceae) and the role of pollen collecting insects. Hawkes, JG, Lester, RN, Skelding, AD (Eds.), Biol. Taxon. Solanaceae. Acad. Press. London.

Tattersall, A; Glover, BJ; Jaffe, FW. (2007) Atruncated MYB transcription factor from Antirrhinum majus regulates epidermal cell outgrowth. J. Exp. Bot. 58 (6) 1515-1524

The Eggplant Genome Consortium. (2016) The Eggplant Genome Reveals Key Events in Solanaceae Evolution. Final Annu. Conf. COST FA1106 "Quality Fruit"

The Tomato Genome Consortium. (2012) The tomato genome sequence provides insights into fleshy fruit evolution. Nature 485 635-641

Theissen, G; Melzer, R; Rumpler, F. (2016) MADS-domain transcription factors and the floral quartet model of flower development: linking plant development and evolution. Development 143 (18) 3259-3271

Thorp, RW. (1979) Structural, Behavioral, and Physiological Adaptations of Bees (Apoidea) for Collecting Pollen. Ann. Missouri Bot. Gard. 66 (4) 788-812

Thorp, RW. (2000) The collection of pollen by bees. Plant Syst. Evol. 222 (1/4) 211-223

Thurston, R. (1970) Toxicity of Trichome Exudates of Nicotiana and Petunia Species to Tobacco Hornworm Larvae. J. Econ. Entomol. 63 (11) 272-274

Tominaga-Wada, R; Nukumizu, Y; Sato, S et al. (2013) Control of Plant Trichome and Root-Hair Development by aTomato (Solanum lycopersicum) R3 MYB Transcription Factor. PLoS One 8 (1) e54019

Uhrig, JF; Hulskamp, M. (2010). Trichome development in Arabidopsis. Methods in molecular biology (Clifton, N.J.) 655 77-88

Upadhyaya, MK; Furness, NH. (1994) Influence of light intensity and water stress on leaf surface characteristics of Cynoglossum officinale, Centaurea spp., and Tragopogon spp. Can. J. Bot. 72 (9) 1379-1386

Uphof, JCT. (1962) Plant hairs. Handb. der Pflanz. Anat. 4.

Vallejo-Marin, M; Da Silva, EM; Sargent, RD et al. (2010) Trait correlates and functional significance of heteranthery in flowering plants. New Phytol. 188 (2) 418-425

Vallejo-Marin, M; Dorken, ME; Barrett, SCH. (2010) The Ecological and Evolutionary Consequences of Clonality for Plant Mating. Annu. Rev. Ecol. Evol. Syst. 41 (1) 193-213

Vallejo-Marin, M; Manson, JS; Thomson, JD et al. (2009) Division of labour within flowers: Heteranthery, afloral strategy to reconcile contrasting pollen fates. J. Evol. Biol. 22 (4) 828-839

Vallejo-Marin, M; Walker, C; Friston-Reilly, P et al. (2014) Recurrent modification of floral morphology in heterantherous Solanum reveals aparallel shift in reproductive strategy. Philos. Trans. R. Soc. Lond. B. Biol. Sci. 369 (1649) 20130256

Vieira, GJr; Ferreira, PM; Matos, LG et al. (2003) Anti-inflammatory effect of Solanum lycocarpum fruits. Phytother. Res. 17 (8) 892-896

Vilhena, AMGF; Bastos, EMAF; Rabelo, LS et al. (2012) Acerola pollinators in the savanna of Central Brazil: Temporal variations in oil-collecting bee richness and amutualistic network. Apidologie 43 (1) 51-62

Vogel, S. (1978) Evolutionary shifts from reward to deception in pollen flowers. RICHARDS, A., Pollinat. flowers by insects. - Linn. Soc. Syrup. Bot. - London Acad. Press. Ser. 6: 89-96.

Vom Endt, D; Kijne, JW; Memelink, J. (2002) Transcription factors controlling plant secondary metabolism: what regulates the regulators?. Phytochemistry 61 (2) 107-114

Wada, T; Kurata, T; Tominaga, R et al. (2002). Role of a positive regulator of root hair development, CAPRICE, in Arabidopsis root epidermal cell differentiation. Development 129 5409 LP-5419

Wada, T; Tachibana, T; Shimura, Y et al. (1997). Epidermal Cell Differentiation in Arabidopsis Determined by a Myb Homolog, CPC. Science 277 1113 LP-1116

Wagner, GJ; Wang, E; Shepherd, RW. (2004) New approaches for studying and exploiting an old protuberance, the plant trichome. Ann. Bot. 93 (1) 3-11

Walford, S; Wu, Y; Llewellyn, DJ et al. (2011) GhMYB25-like : akey factor in early cotton fibre development. Plant J. 65 785-797

Walker, AR; Davison, PA; Bolognesi-Winfield, AC et al. (1999). The TRANSPARENT TESTA GLABRA1 Locus, Which Regulates Trichome Differentiation and Anthocyanin Biosynthesis in Arabidopsis, Encodes a WD40 Repeat Protein. The Plant Cell 11 1337 LP-1349

Walter Macior, L. (1964) An Experimental Study of the Floral Ecology of Dodecatheon meadia. 51 Am. J. Bot. 96-108

Wang, L; Li, J; Zhao, J et al. (2015) Evolutionary developmental genetics of fruit morphological variation within the Solanaceae. Front. Plant Sci. 6 248

Wang, S; Kwak, S-H; Zeng, Q et al. (2007). TRICHOMELESS1 regulates trichome patterning by suppressing GLABRA1 in Arabidopsis. Development 134 3873 LP-3882

Waser, NM; Chittka, L; Price, MV et al. (1996) Generalization in pollination systems, and why it matters. Ecology 77 (4) 1043-1060

Weese, TL; Bohs, L. (2007) AThree-Gene Phylogeny of the Genus Solanum (Solanaceae). Syst. Bot. 32 (2) 445-463

Weiss, Martha R. (1991) Floral colour changes as cues for pollinators. Nature 354 227

Weiss, Martha R. (1995) Floral color change: awidespread functional convergence. Am. J. Bot. 82 (2) 167-185

Whalen, Michael D. (1978) Reproductive Character Displacement and Floral Diversity in Solanum Section Androceras. Syst. Bot. 3 (1) 77-86

Whitney, HM; Bennett, KMV; Dorling, M et al. (2011) Why do so many petals have conical epidermal cells?. Ann. Bot. 108 (4) 609-616

Whitney, HM; Chittka, L; Bruce, TJA et al. (2009) Report Conical Epidermal Cells Allow Bees to Grip Flowers and Increase Foraging Efficiency. Curr. Biol. 19 (11) 948-953

Whitney, HM; Kolle, M; Andrew, P et al. (2009) Floral iridescence, produced by diffractive optics, acts as acue for animal pollinators. Science 323 (5910) 130-133

Wilkens, RT; Shea, GO; Halbreich, S et al. (1996) Resource availability and the trichome defenses of tomato plants. Oecologia 106 (2) 181-191

Willmer, P. (2011) Pollination and Floral Ecology.

Wilson, LAB; Colombo, M; Hanel, R et al. (2013) Ecomorphological disparity in an adaptive radiation: opercular bone shape and stable isotopes in Antarctic icefishes. Ecol. Evol. 3 (9) 3166-3182

Woodman, RL; Fernandes, GW. (1991) Differential Mechanical Defense: Herbivory, Evapotranspiration, and Leaf-Hairs. Oikos 60 (1) 11-19

Woodman, RL; Fernandes, GW. (1991) Nordic Society Oikos Differential Mechanical Defense : Herbivory , Evapotranspiration , and Leaf-Hairs Author (s): Robert L . Woodman and G . Wilson Fernandes Published by : Wiley on behalf of Nordic Society Oikos Stable URL : https://www.jstor.org/stab. Nord. Soc. Oikos 60 (1) 11-19

Wright, GA; Schiestl, FP. (2009) The evolution of floral scent: the influence of olfactory learning by insect pollinators on the honest signalling of floral rewards. Funct. Ecol. 23 (5) 841-851

Xu, X; Pan, S et al. (2011) Genome sequence and analysis of the tuber crop potato. Nature 475 189

Yang, C; Li, H; Zhang, J et al (2011). A regulatory gene induces trichome formation and embryo lethality in tomato. PNAS 108 11836-11841

Zhao, M; Morohashi, K; Hatlestad, G et al. (2008). The TTG1-bHLH-MYB complex controls trichome cell fate and patterning through direct targeting of regulatory loci. Development 135 1991 LP-1999

Appendix 1. List of all species studied, with authorities

***Solanum* species**	**Authority**
abitaguense	S.Knapp.
abutiloides	Griseb.
acanthodapis	A.R.Bean.
acanthodes	Hook. f.
acaule	Bitter.
acerifolium	Dunal.
actaeabotrys	Rusby.
aculeatissimum	Jacq.
acuminatum	Ruiz & Pav.
adenobasis	M.Nee & Farruggia.
adoense	Hochst. ex A.Rich.
adscendens	Sendtn.
aethiopicum	L.
africanum	Mill.
agrarium	Sendtn.
albidum	Dunal.
aligerum	Schltdl.
allophyllum	Standl.
aloysiifolium	Dunal.
alphonsei	Dunal.
alpinum	Zoll. & Moritzi
altissimum	Benitez.
amblophyllum	Hook.
amblymerum	Dunal.
americanum	Mill.
amnicola	S.Knapp
amotapense	Svenson
amygdalifolium	Steud.
anceps	Ruiz & Pav.
andreanum	Baker.
anguivi	Lam.
angustifolium	Mill.
anomalostemon	S.Knapp & M.Nee
antisuyo	Särkinen & S.Knapp
aphyodendron	S.Knapp
appressum	K.E.Roe.
arcanum	Peralta.
argenteum	Dunal.
argentinum	Bitter & Lillo.
aridum	Morong.
arundo	Mattei.
asperolanatum	Ruiz & Pav.
asperrimum	Bitter & Moritz.
asperum	Rich.
athroanthum	Dunal.
atropurpureum	Schrank.
aturense	Dunal.
aureum	Dunal.
aviculare	G.Forst.

***Solanum* species**	**Authority**
bahamense	L.
barbeyanum	Huber.
barbulatum	Zahlbr.
baretiae	Tepe.
basendopogon	Bitter.
bauerianum	Endl.
berthaultii	Hawkes.
betaceum	Cav.
betroka	D'Arcy & Rakot.
bicolor	Willd.
bolivianum	Britton ex Rusby
bonariense	Bukasov.
brachyantherum	Phil.
brevipedicellatum	K.E.Roe
brownii	Dunal.
campylacanthum	Hochst. ex A.Rich.
candolleanum	Berthault
canense	Rydb.
capense	L.
capsicoides	All.
carense	Dunal.
caricaefolium	Rusby
caripense	Dunal
carolinense	L.
catilliflorum	G.J.Anderson, Martine, Prohens & Nuez
centrale	J.M.Black
chacoense	Bitter
chalmersii	S.Knapp
chamaepolybotryon	Bitter
cheesmaniae	(L.Riley) Fosberg
chenopodinum	F.Muell.
chenopodioides	Lam.
chilense	(Dunal) Reiche
Chimborazense	Bitter & Sodiro
chmielewskii	(C.M.Rick, Kesicki, Fobes & M.Holle) D.M.Spooner, G.J.A
chrysotrichum	Schltdl.
citrullifolium	A.Braun
clandestinum	Bohs
clathratum	Sendtn.
clivorum	S.Knapp
coactiliferum	J.M.Black
coagulans	Jacq.
coalitum	S.Knapp
cochoae	G.J.Anderson & Bernardello
colombianum	Dunal
comptum	C.V.Morton
confine	Dunal
confusum	C.V.Morton
conglobatum	Dunal
consimile	C.V.Morton

***Solanum* species**	**Authority**	***Solanum* species**	**Authority**
cordatum	Forssk.	*incanum*	L.
cordovense	Sessé & Moc.	*iopetalum*	(Bitter) Hawkes
coriaceum	Dunal	*ivohibe*	D'Arcy & Rakot.
crinitipes	Dunal	*jamaicense*	Mill.
crinitum	Lam.	*jamesii*	Torr.
crispum	Ruiz & Pav.	*juglandifolium*	Dunal
cunninghamii	Benth.	*junctum*	S.Stern & M.Nee
dammerianum	Lauterb. & K.Schum.	*juninense*	Bitter
delitescens	C.V.Morton	*juvenale*	Thell.
demissum	Lindl.	*kulliwaita*	S.Knapp
denticulatum	Nees	*kurtzianum*	Bitter & Wittm.
diphyllum	Osbeck	*kurzii*	Brace ex Prain
discolor	R.Br.	*laciniatum*	Aiton
diversifolium	Dunal	*lanceifolium*	Jacq.
donianum	Walp.	*lanceolatum*	Cav.
douglasii	Dunal	*lasiocarpum*	Dunal
dulcamara	Hill.	*laxum*	Spreng.
echegarayi	Hieron.	*lepidotum*	Dunal
elaeagnifolium	Cav.	*leptocaulon*	Van Heurck & Müll.Arg.
ellipticum	R.Br.	*leucocarpon*	Dunal
ensifolium	Dunal	*lidii*	Sunding
erianthum	D.Don	*limitare*	A.R.Bean
esuriale	Lindl.	*lindenii*	Rusby
etuberosum	Lindl.	*linnaeanum*	Hepper & P.-M.L. Jaeger
excisirhombeum	Bitter	*longifilamentum*	Särkinen & P.Gonzáles
fernandezianum	Phil.	*lucani*	Mueller
ferocissimum	Lindl.	*luteoalbum*	Pers.
fiebrigii	Bitter	*lycocarpum*	A.St.-Hil.
forskalii	Dunal	*lycopersicoides*	Dunal
fraxinifolium	Dunal	*lycopersicum*	Hill
furcatum	Dunal	*lyratum*	Thunb.
furfuraceum	R.Br.	*macbridei*	Hunz. & Lallana
galapagense	S.C.Darwin & Peralta	*macrocarpon*	L.
gardneri	Sendtn.	*macrothyrsum*	Dammer
giganteum	Jacq.	*macrotonum*	Bitter
glabratum	Dunal	*madagascariense*	Dunal
glaucophyllum	Desf.	*ferrugineum*	Jacq.
gonocladum	Dunal	*maglia*	Schltdl..
gracile	Otto ex W.Baxter	*mahoriense*	D'Arcy & Rakot.
grandiflorum	Ruiz & Pav.	*malletii*	S.Knapp
grayi	Rose	*mammosum*	L.
habrochaites	S.Knapp & D.M.Spooner	*marginatum*	L.f.
herbabona	Reiche	*mariae*	Särkinen & S. Knapp
herculeum	Bohs	*maturecalvans*	Bitter
hindsianum	Benth.	*mauritianum*	Scop.
hirtum	Vahl	*medians*	Bitter
hispidum	Pers.	*megistacrolobum*	Bitter.
houstonii	Martyn	*melongena*	L.
humblotii	Dammer	*memphiticum*	J.F.Gmel.
imamense	Dunal	*microdontum*	Bitter.

Solanum species	Authority
mite	Ruiz & Pav.
mitlense	Dunal
monachophyllum	Dunal
morellifolium	Bohs
multifidum	Lam.
multiinterruptum	Bitter.
muricatum	Aiton Hort.
myriacanthum	Dunal
myrsinoides	D'Arcy & Rakot.
nava	Webb & Berthel.
neorickii	D.M.Spooner,G.J.Anderson & R.K.Jansen
nigrescens	M.Martens & Galeotti
nigrum	L.
nitidibaccatum	Bitter
nitidum	Ruiz & Pav.
nudum	Dunal
nutans	Ruiz & Pav.
obliquum	Ruiz & Pav.
oblongifolium	Dunal
oligacanthum	Mueller
opacum	A.Braun & Bouché .
orbiculatum	Dunal
oxycoccoides	Bitter
palitans	C.V.Morton
pallidum	Rusby
paludosum	Moric.
paniculatum	L.
papaverifolium	Symon
paposanum	Phil.
papuanum	Symon
peekelii	Bitter
pennellii	Correll
pentlandii	Dunal
peruvianum	L.
petrophilum	Mueller
physalifolium	Rusby
pimpinellifolium	L.
pinnatum	Cav.
pittosporifolium	Hemsl.
platacanthum	Dunal
platense	Diekm.
polyacanthos	Lam.
polyadenium	Greenm.
polygamum	Vahl
polytrichostylum	Bitter
praetermissum	Kerr ex Barnett
premnifolium	(Miers) Bohs
procumbens	Lour.
pseudocapsicum	L.
pubescens	Willd.
pubigerum	Dunal
pygmaeum	Cav.
pyracanthos	Lam.
quitoense	Lam.
radicans	L.f.
refractum	Hook. & Arn.
remyanum	Phil.
restrictum	C.V.Morton
richardii	Dunal
riojense	Bitter
robustum	H.L.Wendl.
rostratum	Dunal
rudepannum	Dunal
runsoriense	C.H.Wright
salicifolium	Phil.
sambiranense	D'Arcy & Rakot.
sanchez-vegae	S.Knapp
sandwicense	Hook. & Arn.
saponaceum	Dunal
sarrachoides	Sendtn.
saturatum	M.Nee
savanillense	Bitter
schimperianum	Hochst. ex A.Rich.
schlechtendalianum	Walp.
scuticum	M.Nee.
seaforthianum	Andrews
selachophyllum	Bitter
semiarmatum	Mueller
septemlobum	Bunge
sieberi	Van Heurck & Müll.Arg.
simile	Mueller
sinuatirecurvum	Bitter
sisymbriifolium	Lam.
sitiens	I.M.Johnst.
spirale	Roxb.
stelligerum	Sm.
stoloniferum	Schltdl.
stramoniifolium	Jacq.
stuckertii	Bitter
subinerme	Jacq.
cordifolium	Dunal
symonii	H.Eichler
tampicense	Dunal
terminale	Forssk.
tetramerum	Dunal
tomentosum	L.
torvum	Sw.
tribulosum	Schauer
trichopetiolatum	D'Arcy & Rakot.
triflorum	Nutt.

***Solanum* species**	**Authority**
trinominum	J.R.Benn.
tripartitum	Dunal
triquetrum	Cav.
trisectum	Dunal
humblotii	Dammer
tuberosum	L.
tweedianum	Hook.
uncinellum	Lindl.
urticans	Dunal
vaillantii	Dunal
valdiviense	Dunal
vespertilio	Aiton
viarum	Dunal
villosum	Mill.
violaceum	Ortega
virginianum	L.
viridifolium	Dunal
volubile	Sw.
wendlandii	Hook.f.
whalenii	M.Nee
woodii	Särkinen & S. Knapp
wrightii	Benth.
zanzibarense	Vatke.

Appendix 2: Full raw data set for anther dimensions (in mm)

major_clade	clade	sample_name	species	herbarium code	anther length/mm	tip width/mm	base width/mm	middle width/mm
Geminata	Geminata	abitaguense_1	abitaguense	bm_000943650	6.936	1.469	1.093	1.377
Geminata	Geminata	abitaguense_2	abitaguense	bm_000943644	6.474	1.6	1.204	1.455
Geminata	Geminata	abitaguense_3	abitaguense	bm_000943650	6.991	0.946	1.129	1.605
Brevantherum	Brevantherum	abutiloides_1	abutiloides	bm_000935352	4.485	0.937	1.342	1.402
Brevantherum	Brevantherum	abutiloides_2	abutiloides	e00112788	3.123	0.778	1.068	1.428
Brevantherum	Brevantherum	abutiloides_3	abutiloides	e00112788	3.289	0.941	1.078	1.391
Leptostemonum	old_world	acanthodapis_1	acanthodapis	L0281392	4.18	0.36	0.65	0.78
Potato	Petota	acaule_2	acaule	bm_000887234	2.573	0.752	0.714	0.972
Potato	Petota	acaule_3	acaule	bm_000887234	5.931	0.896	1.076	1.454
Potato	Petota	acaule_4	acaule	bm_001134709	2.778	0.981	1.083	1.05
Potato	Petota	acaule_5	acaule	bm_001134709	2.357	0.792	0.936	0.949
Potato	Petota	acaule_6	acaule	bm_001134709	3.058	0.816	1.009	1.022
Leptostemonum	Acanthophora	acerifolium_1	acerifolium	bm_000887254	5.171	0.37	0.8	1.096
Leptostemonum	Acanthophora	acerifolium_11	acerifolium	bm_000846605	4.355	0.342	0.803	0.911
Leptostemonum	Acanthophora	acerifolium_12	acerifolium	bm_000072667	4.213	0.386	0.813	0.847
Leptostemonum	Acanthophora	acerifolium_13	acerifolium	bm_000072667	5.643	0.412	0.843	0.965
Leptostemonum	Acanthophora	acerifolium_14	acerifolium	bm_000849469	5.317	0.396	1.041	1.045
Leptostemonum	Acanthophora	acerifolium_15	acerifolium	bm_000849469	5.334	0.518	0.615	1.367
Leptostemonum	Acanthophora	acerifolium_2	acerifolium	bm_000887254	4.931	0.253	1.195	1.331
Leptostemonum	Acanthophora	acerifolium_3	acerifolium	bm_000887254	5.186	0.262	1.022	1.174
Leptostemonum	Acanthophora	acerifolium_6	acerifolium	bm_001070034	5.976	0.481	0.944	0.896
Leptostemonum	Acanthophora	acerifolium_8	acerifolium	bm_000934880	6.179	0.438	0.83	1.058
Leptostemonum	Torva	actaeibotrys_4	actaeibotrys	bm_001114711	9.258	0.661	1.381	1.637
Leptostemonum	Acanthophora	aculeatissimum_1	aculeatissimum	e00057515	7.076	0.389	1.168	1.257
Leptostemonum	Acanthophora	aculeatissimum_2	aculeatissimum	e00057515	7.098	0.373	0.766	1.137
Leptostemonum	Acanthophora	aculeatissimum_3	aculeatissimum	e00057515	5.783	0.238	0.895	1.353
Leptostemonum	Acanthophora	aculeatissimum_6	aculeatissimum	e00112791	4.849	0.645	0.775	1.077
Leptostemonum	Acanthophora	aculeatissimum_7	aculeatissimum	e00112745	5.4	0.577	1.024	1.274
Leptostemonum	Acanthophora	aculeatissimum_8	aculeatissimum	e00112745	5.184	0.614	1.205	1.058
Geminata	Geminata	acuminatum_1	acuminatum	bm_000848354	3.301	0.979	0.628	1.478
Geminata	Geminata	acuminatum_2	acuminatum	bm_000848354	2.71	1.345	0.64	1.755
Geminata	Geminata	acuminatum_6	acuminatum	bm_000848456	3.242	0.908	0.716	1.523
Geminata	Geminata	acuminatum_7	acuminatum	bm_001114713	3.013	0.851	1.045	1.746
Geminata	Geminata	acuminatum_8	acuminatum	bm_001114713	3.601	1.174	0.935	1.754
Geminata	Geminata	acuminatum_9	acuminatum	bm_001114713	3.677	1.091	0.966	1.806
m_clade	African_non_spiny	africanum_11	africanum	g00443467	2.791	0.7	0.99	1.195
m_clade	African_non_spiny	africanum_3	africanum	g00443468	2.76	0.832	0.955	1.581
m_clade	African_non_spiny	africanum_6	africanum	g00443466	3.318	0.586	0.739	1.199
m_clade	African_non_spiny	africanum_7	africanum	g00443466	2.789	0.52	0.885	1.145
m_clade	African_non_spiny	africanum_8	africanum	g00443466	2.329	0.558	0.577	1.233
m_clade	African_non_spiny	africanum_9	africanum	g00443467	2.779	0.716	0.885	1.52
Leptostemonum	Torva	albidum_1	albidum	bm_000934946	4.228	0.496	0.935	0.95
Leptostemonum	Torva	albidum_11	albidum	bm_001120308	5.661	0.425	1.1	1.199
Leptostemonum	Torva	albidum_12	albidum	bm_000934943	5.944	0.589	1.129	1.143
Leptostemonum	Torva	albidum_13	albidum	bm_000849352	6.596	0.704	0.735	1.077
Leptostemonum	Torva	albidum_14	albidum	bm_000849352	7.409	0.614	1	1.058
Leptostemonum	Torva	albidum_15	albidum	bm_000849353	6.914	0.512	0.518	1.308
Leptostemonum	Torva	albidum_17	albidum	bm_000849353	6.616	0.425	1.154	1.461
Leptostemonum	Torva	albidum_18	albidum	bm_000815967	7.305	0.667	0.854	1.291
Leptostemonum	Torva	albidum_19	albidum	bm_000815967	7.622	0.547	1.135	1.423
Leptostemonum	Torva	albidum_2	albidum	bm_000815966	7.397	0.603	1.338	1.558
Leptostemonum	Torva	albidum_20	albidum	bm_000815967	7.229	0.645	1.195	1.6
Leptostemonum	Torva	albidum_21	albidum	bm_000815964	6.737	0.53	0.858	1.675
Leptostemonum	Torva	albidum_23	albidum	bm_000815964	6.838	0.503	0.802	1.123
Leptostemonum	Torva	albidum_4	albidum	bm_000887270	6.201	0.747	1.271	1.381
Leptostemonum	Torva	albidum_8	albidum	bm_000887270	6.997	0.544	0.944	1.179
Leptostemonum	Torva	albidum_9	albidum	bm_000887270	6.338	0.62	0.904	1.342
m_clade	Dulcamaroid	aligerum_5	aligerum	bm_000942221	3.718	0.905	0.858	1.503
m_clade	Dulcamaroid	aligerum_8	aligerum	bm_000887276	3.988	0.805	1	0.947
m_clade	Morelloid	aloysiifolium_1	aloysiifolium	bm_000887461	3.519	0.743	0.654	1.015
m_clade	Morelloid	aloysiifolium_10	aloysiifolium	bm_000887464	3.935	0.854	0.603	1.394
m_clade	Morelloid	aloysiifolium_11	aloysiifolium	bm_000887464	3.991	0.699	0.752	1.313
m_clade	Morelloid	aloysiifolium_12	aloysiifolium	bm_000887461	3.442	0.886	0.671	0.682
m_clade	Morelloid	aloysiifolium_14	aloysiifolium	bm_001134562	5.923	0.578	0.984	0.803
m_clade	Morelloid	aloysiifolium_2	aloysiifolium	bm_001070378	4.848	0.53	0.628	1.007
m_clade	Morelloid	aloysiifolium_4	aloysiifolium	bm_001070378	4.15	0.516	0.536	0.809
m_clade	Morelloid	aloysiifolium_9	aloysiifolium	bm_000887464	4	0.737	0.482	0.865
m_clade	Dulcamaroid	alphonsei_1	alphonsei	e00125348	2.91	0.98	0.816	1.183

major_clade	clade	sample_name	species	herbarium code	anther length/mm	tip width/mm	base width/mm	middle width/mm
m_clade	Dulcamaroid	alphonsei_2	alphonsei	e00125348	2.856	0.677	0.72	1.083
m_clade	Dulcamaroid	alphonsei_3	alphonsei	e00125348	2.544	0.807	0.687	1.07
m_clade	Morelloid	alpinum_1	alpinum	bm000886120	1.952	0.819	0.499	0.906
m_clade	Morelloid	alpinum_1	alpinum	bm000886230	2.203	0.572	0.925	1.224
m_clade	Morelloid	alpinum_4	alpinum	bm000886230	2.571	0.332	0.511	0.482
m_clade	Morelloid	alpinum_5	alpinum	bm000886230	2.244	0.347	0.695	0.914
Leptostemonum	Crinitum	altissimum_1	altissimum	bm_0000887284	10.566	0.751	1.471	2.034
Geminata	Geminata	amblophyllum_1	amblophyllum	bm_001134798	3.457	1.506	0.712	1.553
Geminata	Geminata	amblophyllum_2	amblophyllum	bm_001134798	3.542	1.247	0.529	1.521
Geminata	Geminata	amblophyllum_3	amblophyllum	bm_001134798	3.842	1.232	0.835	1.117
m_clade	Morelloid	americanum_11	americanum	bm000886029	1.625	0.501	0.456	0.766
m_clade	Morelloid	americanum_12	americanum	bm000886029	1.654	0.427	0.404	0.539
m_clade	Morelloid	americanum_13	americanum	bm000886029	1.631	0.508	0.449	0.613
m_clade	Morelloid	americanum_14	americanum	bm000886029	1.735	0.516	0.499	0.651
m_clade	Morelloid	americanum_15	americanum	bm000886025	1.408	0.518	0.396	0.645
m_clade	Morelloid	americanum_16	americanum	bh000040570	3.203	0.462	0.294	0.462
m_clade	Morelloid	americanum_2	americanum	bm000886019	1.412	0.597	0.34	0.635
m_clade	Morelloid	americanum_3	americanum	bm000886019	1.211	0.468	0.434	0.525
m_clade	Morelloid	americanum_4	americanum	bm000886019	1.472	0.396	0.369	0.62
m_clade	Morelloid	americanum_6	americanum	bm000886028	1.407	0.457	0.404	0.569
m_clade	Morelloid	americanum_7	americanum	bm000886028	1.382	0.451	0.465	0.656
Geminata	Geminata	amnicola_1	amnicola	bm_001017360	4.812	0.462	0.81	1.142
Geminata	Geminata	amnicola_1	amnicola	bm_001017360	5.545	0.726	1.162	1.135
Geminata	Geminata	amnicola_2	amnicola	bm_001017360	4.52	0.768	0.912	1.443
Cyphomandra	Pachyphylla	amotapense_1	amotapense	e00045257	4.642	0.83	1.441	2.373
Cyphomandra	Cyphomandra	amotapense_4	amotapense	e00045257	4.001	0.803	0.962	1.246
m_clade	Dulcamaroid	amygdalifolium_1	amygdalifolium	e00045265	5.689	1.004	0.925	1.361
m_clade	Dulcamaroid	amygdalifolium_2	amygdalifolium	e00045265	5.926	1.201	0.385	1.28
m_clade	Dulcamaroid	amygdalifolium_3	amygdalifolium	e00045265	5.73	1.083	1.353	1.717
m_clade	Dulcamaroid	amygdalifolium_4	amygdalifolium	e00045265	5.114	1.241	1.283	1.346
na	na	anamala_1	anamala	24223_plantae_colombianae	3.371	0.707	0.731	1.137
Potato	Pteroidea_Herpysti	anceps_13	anceps	bm_000848401	2.255	0.649	0.578	0.968
na	incertaeNAsedis	anomalostemon_1	anomalostemon	uni_of_calafornia_n'9611	2.693	0.972	1.419	2.167
na	incertaeNAsedis	anomalostemon_2	anomalostemon	uni_of_calafornia_n'9611	2.426	0.924	1.146	1.973
m_clade	Morelloid	antisuyo_10	antisuyo	bm_001114944	2.536	0.539	0.539	0.827
m_clade	Morelloid	antisuyo_12	antisuyo	bm_001120238	3.804	0.423	0.716	1.164
m_clade	Morelloid	antisuyo_13	antisuyo	bm_001120238	3.746	0.666	0.68	0.735
m_clade	Morelloid	antisuyo_14	antisuyo	bm_001070130	2.974	0.59	0.561	0.846
m_clade	Morelloid	antisuyo_16	antisuyo	bm_001114944	3.172	0.347	0.626	0.841
m_clade	Morelloid	antisuyo_19	antisuyo	bm_001114944	3.552	0.654	0.801	1.109
m_clade	Morelloid	antisuyo_2	antisuyo	bm_001034686	3.102	0.621	0.523	0.98
m_clade	Morelloid	antisuyo_3	antisuyo	bm_001070370	3.765	0.536	0.699	0.956
m_clade	Morelloid	antisuyo_4	antisuyo	bm_000887720	2.374	0.272	0.409	0.608
m_clade	Morelloid	antisuyo_5	antisuyo	bm_000887720	3.038	0.675	0.752	1.212
m_clade	Morelloid	antisuyo_6	antisuyo	bm_00546702	3.335	0.572	0.404	0.785
m_clade	Morelloid	antisuyo_7	antisuyo	bm_001070369	3.213	0.5	0.673	1.077
m_clade	Morelloid	antisuyo_8	antisuyo	bm_001070369	3.115	0.822	0.592	0.999
m_clade	Morelloid	antisuyo_9	antisuyo	bm_001070130	2.964	0.7	0.621	0.816
Geminata	Geminata	aphyodendron_1	aphyodendron	bm_000848345	2.433	0.412	0.481	1.115
Geminata	Geminata	aphyodendron_10	aphyodendron	bm_00101035223	2.549	0.612	0.818	1.364
Geminata	Geminata	aphyodendron_11	aphyodendron	bm_000848462	3.156	1.291	1.135	1.508
Geminata	Geminata	aphyodendron_12	aphyodendron	bm_000848462	4.059	1.442	1.105	1.754
Geminata	Geminata	aphyodendron_13	aphyodendron	bm_000848417	3.943	1.038	1.039	1.827
Geminata	Geminata	aphyodendron_14	aphyodendron	bm_000848417	2.893	0.77	0.518	1.23
Geminata	Geminata	aphyodendron_15	aphyodendron	bm_000848408	2.916	0.708	0.612	1.541
Geminata	Geminata	aphyodendron_2	aphyodendron	bm_000810007	2.77	0.936	0.882	1.441
Geminata	Geminata	aphyodendron_3	aphyodendron	bm_000810007	2.72	0.783	0.749	1.428
Geminata	Geminata	aphyodendron_5	aphyodendron	bm_001134666	2.536	0.645	0.674	1.17
Geminata	Geminata	aphyodendron_7	aphyodendron	bm_001120269	2.315	0.8	0.512	0.673
Geminata	Geminata	aphyodendron_8	aphyodendron	bm_001120269	2.028	0.776	0.572	0.926
Brevantherum	Brevantherum	appressum_10	appressum	bm_000887330	3.746	1.329	0.966	1.355
Brevantherum	Brevantherum	appressum_11	appressum	bm_00120354	3.093	0.916	0.875	1.231
Brevantherum	Brevantherum	appressum_2	appressum	bm_000849428	3.865	0.536	0.912	1.299
Brevantherum	Brevantherum	appressum_6	appressum	bm_000636406	3.18	0.822	0.724	1.42
Brevantherum	Brevantherum	appressum_7	appressum	bm_000849428	3.736	0.77	1.037	1.385
Brevantherum	Brevantherum	appressum_8	appressum	bm_000849428	4.097	0.861	0.873	1.265
Potato	Tomato	arcanum_anther_1	arcanum	bm_001120719	8.206	0.267	0.775	1.105

major_clade	clade	sample_name	species	herbarium code	anther length/mm	tip width/mm	base width/mm	middle width/mm
Potato	Tomato	arcanum_anther_1	arcanum	bm_001120786	8.013	0.407	1.328	1.132
Potato	Tomato	arcanum_anther_1	arcanum	bm_001120786	8.583	0.34	1.027	1.216
Potato	Tomato	arcanum_anther_1	arcanum	bm_000778164	6.581	0.37	0.783	1.268
Potato	Tomato	arcanum_anther_1	arcanum	bm_000778164	6.477	0.361	0.838	1.385
Potato	Tomato	arcanum_anther_1	arcanum	bm_000778164	5.417	0.828	0.828	1.12
Potato	Tomato	arcanum_anther_2	arcanum	bm_001134691	8.944	0.347	1.05	1.363
Potato	Tomato	arcanum_anther_2	arcanum	bm_001134722	6.875	0.155	0.494	1.139
Potato	Tomato	arcanum_anther_2	arcanum	bm_001134722	6.932	0.268	0.566	0.973
Potato	Tomato	arcanum_anther_2	arcanum	bm_001120719	7.393	0.359	0.709	1.034
Potato	Tomato	arcanum_anther_5	arcanum	bm_001120684	9.967	0.308	0.962	1.501
Potato	Tomato	arcanum_anther_8	arcanum	bm_001120797	7.905	0.404	1.041	1.455
Brevantherum	Brevantherum	argenteum_1	argenteum	bm_000849446	9.152	1	1.71	1.672
Brevantherum	Brevantherum	argentinum_1	argentinum	bm_000849446	2.306	0.626	0.5	0.743
Brevantherum	Brevantherum	argentinum_10	argentinum	bm_000849446	2.304	0.751	0.551	0.84
Brevantherum	Brevantherum	argentinum_11	argentinum	bm_000849194	1.948	0.83	0.695	0.941
Brevantherum	Brevantherum	argentinum_12	argentinum	bm_000849194	2.121	0.785	0.422	0.803
Brevantherum	Brevantherum	argentinum_2	argentinum	bm_000849036	2.1	0.695	0.31	0.705
Brevantherum	Brevantherum	argentinum_3	argentinum	bm_000849036	2.203	0.709	0.367	0.789
Brevantherum	Brevantherum	argentinum_5	argentinum	bm_000849035	1.596	0.577	0.577	0.828
Brevantherum	Brevantherum	argentinum_6	argentinum	bm_000849194	2.058	0.74	0.485	0.886
Brevantherum	Brevantherum	argentinum_8	argentinum	bm_001016948	1.446	0.637	0.52	0.699
Brevantherum	Brevantherum	argentinum_9	argentinum	bm_000849446	2.485	0.826	0.389	0.881
Leptostemonum	Carolinense	aridum_1	aridum	NY00139054	6.18	0.38	0.74	0.72
Leptostemonum	Carolinense	aridum_2	aridum	bm_000778105	8.138	0.601	0.923	1.241
Leptostemonum	Carolinense	aridum_3	aridum	bm_000778105	8.405	0.853	1.056	1.196
Leptostemonum	Torva	asperolanatum_10	asperolanatum	bm_000887338	6.034	0.598	0.931	1.342
Leptostemonum	Torva	asperolanatum_11	asperolanatum	bm_000887338	5.606	0.985	0.801	1.781
Leptostemonum	Torva	asperolanatum_13	asperolanatum	bm_001120474	5.977	0.929	0.955	1.978
Leptostemonum	Torva	asperolanatum_15	asperolanatum	bm_00076166	5.807	1.327	1.288	1.273
Leptostemonum	Torva	asperolanatum_17	asperolanatum	bm_001120516	5.341	1.26	1.351	1.603
Leptostemonum	Torva	asperolanatum_18	asperolanatum	bm_001120516	7.409	0.965	1.237	1.793
Leptostemonum	Torva	asperolanatum_2	asperolanatum	bm_000887340	5.441	0.692	1.11	1.407
Leptostemonum	Torva	asperolanatum_4	asperolanatum	bm_000887338	5.737	0.768	0.99	1.686
Leptostemonum	Torva	asperolanatum_5	asperolanatum	bm_001120862	8.753	1.162	1.351	2.135
Leptostemonum	Torva	asperolanatum_7	asperolanatum	bm_000849439	8.638	0.907	0.891	1.726
Leptostemonum	Micracantha	asperrimum_2	asperrimum	bm_000887358	9.355	0.52	0.993	1.464
Brevantherum	Brevantherum	asperum_1	asperum	bm_001120533	2.897	0.662	0.616	1.216
Brevantherum	Brevantherum	asperum_1	asperum	bm_001120533	2.601	0.766	0.616	1.328
Brevantherum	Brevantherum	asperum_12	asperum	bm_000887348	2.752	1.026	0.516	1.067
Brevantherum	Brevantherum	asperum_2	asperum	bm_000887347	2.492	0.83	0.751	1.008
Brevantherum	Brevantherum	asperum_3	asperum	bm_001016930	3.123	1.109	0.742	0.94
Brevantherum	Brevantherum	asperum_4	asperum	bm_000887346	2.776	0.868	0.759	1.347
Brevantherum	Brevantherum	asperum_5	asperum	bm_001016933	2.168	0.74	0.667	0.871
Brevantherum	Brevantherum	asperum_6	asperum	bm_001016930	3.158	0.828	0.664	0.74
Brevantherum	Brevantherum	asperum_7	asperum	bm_001120533	2.778	0.929	0.572	1.193
Brevantherum	Brevantherum	asperum_8	asperum	bm_001120533	2.933	0.955	1.024	1.419
Brevantherum	Brevantherum	asperum_9	asperum	bm_000887347	2.335	0.697	0.716	0.955
na	na	athroanthum_1	athroanthum	bm000778325	3.419	0.284	0.516	0.631
na	na	athroanthum_2	athroanthum	bm000778325	4.558	0.192	0.355	0.558
na	na	athroanthum_3	athroanthum	bm000778325	4.601	0.182	0.31	0.617
Leptostemonum	Acanthophora	atropurpureum_1	atropurpureum	MPU012682	6.36	0.42	1.3	1.08
Leptostemonum	Torva	auctosepalum_1	auctosepalum	bm_000815960	5.824	0.489	0.926	0.843
m_clade	Dulcamaroid	aureum_1	aureum	bm_000072654	4.029	0.864	0.989	1.728
m_clade	Dulcamaroid	aureum_11	aureum	bm_000072654	3.568	0.871	0.714	1.195
m_clade	Dulcamaroid	aureum_12	aureum	bm_000072656	3.655	1.152	1.035	1.446
m_clade	Dulcamaroid	aureum_13	aureum	bm_000072656	3.825	1.091	0.906	1.324
m_clade	Dulcamaroid	aureum_15	aureum	bm_000072657	3.038	1.078	0.712	1.27
m_clade	Dulcamaroid	aureum_16	aureum	bm_000072657	3.792	0.838	0.712	1.328
m_clade	Dulcamaroid	aureum_19	aureum	bm_000887373	3.727	1.344	1.393	1.855
m_clade	Dulcamaroid	aureum_2	aureum	bm_000072654	3.739	0.929	0.725	1.414
m_clade	Dulcamaroid	aureum_20	aureum	bm_000887372	4.674	0.614	1.143	1.405
m_clade	Dulcamaroid	aureum_21	aureum	bm_000072654	3.957	0.865	0.888	1.45
m_clade	Dulcamaroid	aureum_22	aureum	bm_000887373	3.969	1.252	1.019	1.293
m_clade	Dulcamaroid	aureum_3	aureum	bm_000072656	3.892	1.069	0.914	1.129
m_clade	Dulcamaroid	aureum_5	aureum	bm_00072659	4.042	0.931	0.586	1.376
m_clade	Dulcamaroid	aureum_6	aureum	bm_00072659	3.385	1.019	0.637	1.404
m_clade	Dulcamaroid	aureum_7	aureum	bm_00076109	3.674	1.021	1.757	1.489
m_clade	Dulcamaroid	aureum_8	aureum	bm_000072655	3.011	0.894	0.792	1.17
m_clade	Dulcamaroid	aureum_9	aureum	bm_000072655	3.466	0.723	0.501	1.243
Leptostemonum	Bahamense	bahamense_1	bahamense	e00112786	5.01	0.692	0.731	0.86
Leptostemonum	Bahamense	bahamense_4	bahamense	e00112793	4.161	0.407	0.336	0.736
Leptostemonum	Bahamense	bahamense_5	bahamense	e00112792	6.355	0.551	0.803	1.192
Leptostemonum	Bahamense	bahamense_6	bahamense	e00112792	5.865	0.5	0.604	0.871
Leptostemonum	Bahamense	bahamense_8	bahamense	e00112786	5.173	0.423	0.49	0.904
Wendlandii_Allophy	Wendlandii_Allopl	barbeyanum_2	barbeyanum	bm_0011120434	8.241	0.594	1.877	1.708
Geminata	Geminata	barbulatum_1	barbulatum	bm_000072691	2.843	0.935	0.555	1.254
Geminata	Geminata	barbulatum_10	barbulatum	bm_000559408	3.825	1.157	0.5	1.018
Geminata	Geminata	barbulatum_11	barbulatum	bm_000072693	2.596	0.722	0.773	0.872
Geminata	Geminata	barbulatum_12	barbulatum	bm_000072693	2.775	0.662	0.726	1.111

major_clade	clade	sample_name	species	herbarium code	anther length/mm	tip width/mm	base width/mm	middle width/mm
Geminata	Geminata	barbulatum_14	barbulatum	bm_000072691	2.916	0.677	0.624	1.349
Geminata	Geminata	barbulatum_16	barbulatum	bm_000849369	2.59	0.601	0.286	0.797
Geminata	Geminata	barbulatum_17	barbulatum	bm_000849369	2.642	0.689	0.402	0.736
Geminata	Geminata	barbulatum_18	barbulatum	bm_000849369	2.795	0.758	0.475	0.832
Geminata	Geminata	barbulatum_19	barbulatum	bm_000887393	2.853	0.457	0.512	0.62
Geminata	Geminata	barbulatum_2	barbulatum	bm_000072691	3.134	1.099	0.617	1.758
Geminata	Geminata	barbulatum_20	barbulatum	bm_000887393	2.969	0.72	0.427	1.024
Geminata	Geminata	barbulatum_21	barbulatum	bm_000887393	3.365	0.662	0.578	1.144
Geminata	Geminata	barbulatum_22	barbulatum	bm_000887391	2.649	0.793	0.693	1.207
Geminata	Geminata	barbulatum_3	barbulatum	bm_000095976	2.539	0.886	0.5	1.034
Geminata	Geminata	barbulatum_4	barbulatum	bm_000095976	2.279	0.878	0.761	1.239
Geminata	Geminata	barbulatum_7	barbulatum	bm_000887385	3.843	0.869	1.404	1.847
Geminata	Geminata	barbulatum_8	barbulatum	bm_000887385	3.571	0.637	0.496	0.983
Geminata	Geminata	barbulatum_9	barbulatum	bm_000887385	3.519	0.886	1.131	1.608
Potato	Anarrhichomenum	baretiae_1	baretiae	bm_001115161	3.655	0.731	1.007	1.404
Potato	Anarrhichomenum	baretiae_2	baretiae	bm_001115161	3.342	1.059	0.964	1.392
Potato	Anarrhichomenum	baretiae_3	baretiae	bm_001115161	3.454	0.68	1.101	1.147
Potato	Basarthrum	basendopogon_1	basendopogon	bm_001120729	4.368	0.885	1.374	1.648
Potato	Basarthrum	basendopogon_3	basendopogon	bm_001114799	3.921	0.604	0.775	0.989
Potato	Basarthrum	basendopogon_4	basendopogon	bm_001120729	3.006	1.101	0.909	1.381
Potato	Basarthrum	basendopogon_7	basendopogon	bm_001134755	3.193	0.798	0.692	0.846
Potato	Petota	berthaultii_1	berthaultii	bm001211391	6.382	0.912	1.051	1.697
Cyphomandra	Cyphomandra	betaceum_1	betaceum	G00343174	4.12	0.59	0.92	1.18
m_clade	African_non_spiny	betroka_10	betroka	newyork_00827723	4.76	0.778	1.226	1.537
m_clade	African_non_spiny	betroka_11	betroka	newyork_00827723	4.455	0.682	1.287	2.063
m_clade	African_non_spiny	betroka_13	betroka	p00349318	4.658	0.785	1.095	1.877
m_clade	African_non_spiny	betroka_14	betroka	p00349318	4.264	0.724	1.446	1.916
m_clade	African_non_spiny	betroka_15	betroka	p00349318	4.656	0.875	0.86	1.76
m_clade	African_non_spiny	betroka_16	betroka	p00349318	5.242	0.759	1.661	2.253
m_clade	African_non_spiny	betroka_2	betroka	p00349299	4.071	1.127	1.264	2.111
m_clade	African_non_spiny	betroka_3	betroka	p00349299	4.325	0.827	1.54	1.824
m_clade	African_non_spiny	betroka_8	betroka	n'3033182	3.358	0.778	0.946	1.934
m_clade	African_non_spiny	betroka_9	betroka	newyork_00827723	4.22	0.803	0.916	1.074
Brevantherum	Brevantherum	bicolor_2	bicolor	bm_000887404	1.58	0.389	0.482	0.835
Brevantherum	Brevantherum	bicolor_3	bicolor	e00249706	1.746	0.664	0.663	0.891
Leptostemonum	Torva	bonariense_1	bonariense	bm000846142	6.372	0.768	0.966	1.488
Leptostemonum	Torva	bonariense_10	bonariense	bm000846142	5.715	0.68	1.004	1.281
Leptostemonum	Torva	bonariense_11	bonariense	e00112757	6.134	0.535	1.101	1.366
Leptostemonum	Torva	bonariense_12	bonariense	e00112757	5.399	0.525	0.944	1.212
Leptostemonum	Torva	bonariense_13	bonariense	e00112758	6.215	1.077	0.547	1.637
Leptostemonum	Torva	bonariense_14	bonariense	e00112758	6.054	0.846	0.981	1.562
Leptostemonum	Torva	bonariense_15	bonariense	e00112761	6	0.781	1.25	1.751
Leptostemonum	Torva	bonariense_16	bonariense	e00112761	6.425	0.816	1.256	1.797
Leptostemonum	Torva	bonariense_17	bonariense	e00112761	6.816	0.773	1.238	1.664
Leptostemonum	Torva	bonariense_18	bonariense	e00112760	7.234	0.82	1.093	1.616
Leptostemonum	Torva	bonariense_19	bonariense	e00112760	7.296	0.619	0.748	1.462
Leptostemonum	Torva	bonariense_2	bonariense	e00112759	6.373	0.791	1.027	1.523
Leptostemonum	Torva	bonariense_20	bonariense	e00112759	5.004	0.859	1.355	1.574
Leptostemonum	Torva	bonariense_21	bonariense	e00112759	5.905	0.732	1.24	1.32
Leptostemonum	Torva	bonariense_22	bonariense	e00112811	6.52	0.751	1.017	1.717
Leptostemonum	Torva	bonariense_23	bonariense	e00112811	6.619	0.808	1.041	1.216
Leptostemonum	Torva	bonariense_3	bonariense	e00114900	6.065	0.67	1.225	1.17
Leptostemonum	Torva	bonariense_5	bonariense	e0045260	6.828	0.585	0.83	1.168
Leptostemonum	Torva	bonariense_6	bonariense	e0045261	6.421	0.699	0.851	1.615
Leptostemonum	Torva	bonariense_7	bonariense	bm001207505	6.804	0.663	0.748	1.12
Leptostemonum	Torva	bonariense_8	bonariense	bm000846142	5.719	0.672	0.955	1.162
Leptostemonum	Torva	bonariense_9	bonariense	bm000846142	6.768	0.705	1.227	1.832
Brevantherum	Brevantherum	brevipedicellatum	brevipedicellatur	bm_000815941	5.091	0.973	0.907	1.539
Leptostemonum	old_world	brownii_1	brownii	bm000846808	5.578	1.227	1.151	1.934
Potato	Petota	candolleanum_1	candolleanum	bm_001114877	4.973	1.046	1.339	1.8
Potato	Petota	candolleanum_11	candolleanum	bm_001134803	6.544	1.115	1.577	1.995
Potato	Petota	candolleanum_12	candolleanum	bm_001134797	5.842	0.884	1.68	2.036
Potato	Petota	candolleanum_13	candolleanum	bm_001134797	6.113	0.851	1.514	1.746
Potato	Petota	candolleanum_14	candolleanum	bm_001114877	5.68	1.177	1.279	1.588
Potato	Petota	candolleanum_2	candolleanum	bm_001114791	4.808	0.933	1.428	1.374
Potato	Petota	candolleanum_4	candolleanum	bm_001114882	5.397	1.058	1.947	2.141
Potato	Petota	candolleanum_5	candolleanum	bm_001114742	4.75	0.848	1.481	1.503
Potato	Petota	candolleanum_6	candolleanum	bm_001114742	5.309	0.582	1.654	1.928
Potato	Petota	candolleanum_8	candolleanum	bm_0011134708	6.236	0.851	1.652	1.759
Potato	Basarthrum	canense_3	canense	bm_001034732	5.682	0.987	1.366	1.646
na	na	carense_1	carense	bm000942269	3.91	0.554	0.547	0.955
na	na	carense_10	carense	bm000942267	3.571	0.619	0.726	1.128
na	na	carense_11	carense	bm000942267	3.741	0.541	0.676	1.095
na	na	carense_12	carense	bm000942266	4.355	0.768	0.63	0.791

major_clade	clade	sample_name	species	herbarium code	anther length/mm	tip width/mm	base width/mm	middle width/mm
na	na	carense_13	carense	bm000942266	3.967	0.709	0.637	0.793
na	na	carense_15	carense	bm000942271	4.2	0.709	0.572	1.198
na	na	carense_2	carense	bm000942269	3.681	0.656	0.52	0.912
na	na	carense_5	carense	bm000942269	4.503	0.697	0.56	0.714
na	na	carense_9	carense	bm000942268	3.576	0.735	0.462	0.673
Leptostemonum	Torva	caricaefolium_1	caricaefolium	bm_000887423	6.586	0.327	0.491	0.768
Leptostemonum	Torva	caricaefolium_10	caricaefolium	bm_00063409	7.135	0.482	0.752	0.788
Leptostemonum	Torva	caricaefolium_11	caricaefolium	bm_00063409	8.121	0.576	0.74	0.966
Leptostemonum	Torva	caricaefolium_12	caricaefolium	bm_000887423	5.712	0.406	0.693	0.778
Leptostemonum	Torva	caricaefolium_14	caricaefolium	bm_000887422	4.633	0.547	0.653	0.899
Leptostemonum	Torva	caricaefolium_15	caricaefolium	bm_001016915	6.01	0.508	0.656	0.93
Leptostemonum	Torva	caricaefolium_16	caricaefolium	bm_000777279	7.233	0.68	0.808	1.142
Leptostemonum	Torva	caricaefolium_2	caricaefolium	bm_000887422	4.308	0.604	0.682	1.073
Leptostemonum	Torva	caricaefolium_20	caricaefolium	bm_000934950	6.695	0.598	0.783	1.227
Leptostemonum	Torva	caricaefolium_4	caricaefolium	bm_0000887428	5.226	0.257	0.832	1.043
Leptostemonum	Torva	caricaefolium_7	caricaefolium	bm_0000887425	7.093	0.463	0.693	1.024
Leptostemonum	Torva	caricaefolium_8	caricaefolium	bm_000934950	6.839	0.453	0.582	0.83
Leptostemonum	Torva	caricaefolium_9	caricaefolium	bm_000934950	7.007	0.602	0.566	0.835
Potato	Basarthrum	caripense_1	caripense	bm_000887439	4.645	0.993	1.169	1.554
Potato	Basarthrum	caripense_2	caripense	bm_000887447	4.025	0.667	1.067	1.142
Potato	Basarthrum	caripense_3	caripense	bm_000072680	4.09	0.68	0.789	1.021
Potato	Basarthrum	caripense_5	caripense	bm_000887433	4.273	0.858	0.929	1.795
Potato	Basarthrum	caripense_6	caripense	e00112764	2.693	0.731	0.773	1.096
Potato	Basarthrum	caripense_7	caripense	e00112764	3	0.645	0.683	0.993
Potato	Basarthrum	caripense_8	caripense	e00112764	2.644	0.723	0.636	0.962
Leptostemonum	Carolinense	carolinense_1	carolinense	e00112910	6.487	0.834	1.471	1.479
Leptostemonum	Carolinense	carolinense_10	carolinense	e00112910	7.79	0.646	0.895	1.49
Leptostemonum	Carolinense	carolinense_5	carolinense	e00112908	5.634	0.773	1.159	1.442
Leptostemonum	Carolinense	carolinense_6	carolinense	e00112909	6.785	0.939	1.158	1.319
Leptostemonum	Carolinense	carolinense_7	carolinense	e00112910	10.578	0.578	1.511	1.103
Leptostemonum	Carolinense	carolinense_9	carolinense	e00112910	8.106	0.916	1.199	1.741
Potato	Basarthrum	catilliflorum_1	catilliflorum	bm_001114765	2.85	0.699	0.558	1.173
Potato	Basarthrum	catilliflorum_3	catilliflorum	bm_001114765	2.611	0.762	0.914	1.251
Leptostemonum	old_world	centrale_1	centrale	bm001070002	4.923	0.547	1.015	1.091
Potato	Petota	chacoenseNA_1	chacoenseNA	BM001034787	5.306	1.033	1.032	1.453
Geminata	Geminata	chalmersii_1	chalmersii	bm_000849114	3.424	0.889	1.015	1.74
Geminata	Geminata	chalmersii_3	chalmersii	bm_000849116	3.149	0.748	0.847	1.075
Potato	Pteroidea_Herpysti	chamaepolybotryo	chamaepolybotry	bm_000887454	2.84	0.639	1.109	1.478
Potato	Tomato	cheesmaniae_antl	cheesmaniae	bm_001115038	6.043	0.371	0.614	0.803
Potato	Tomato	cheesmaniae_antl	cheesmaniae	bm_001115088	7.439	0.382	0.655	0.976
Potato	Tomato	cheesmaniae_antl	cheesmaniae	bm_001115035	7.046	0.386	0.971	0.952
Potato	Tomato	cheesmaniae_antl	cheesmaniae	bm_001115133	5.862	0.404	0.536	0.989
na	na	chenopoides_1	chenopoides	16188CGE	2.53	0.396	0.551	0.775
na	na	chenopoides_10	chenopoides	cambridge_herbariun	2.318	0.588	0.563	0.756
na	na	chenopoides_11	chenopoides	cambridge_herbariun	2.199	0.52	0.443	0.756
na	na	chenopoides_12	chenopoides	cambridge_herbariun	2.606	0.434	0.462	0.761
na	na	chenopoides_13	chenopoides	cambridge_herbariun	2.474	0.572	0.43	0.611
na	na	chenopoides_14	chenopoides	cambridge_herbariun	2.582	0.629	0.528	0.673
na	na	chenopoides_15	chenopoides	cambridge_herbariun	2.471	0.541	0.681	0.809
na	na	chenopoides_3	chenopoides	e00057521	1.827	0.299	0.208	0.465
na	na	chenopoides_4	chenopoides	e00057521	2.167	0.426	0.513	0.697
na	na	chenopoides_5	chenopoides	e00057521	1.539	0.402	0.5	0.505
na	na	chenopoides_6	chenopoides	e00057521	1.582	0.189	0.28	0.414
na	na	chenopoides_7	chenopoides	e00057551	2.074	0.5	0.525	0.645
na	na	chenopoides_8	chenopoides	e00057551	2.406	0.544	0.519	0.596
na	na	chenopoides_9	chenopoides	e00057551	1.931	0.432	0.301	0.313
Potato	Tomato	chilense_anther_1	chilense	e00131891	7.277	0.288	0.972	2.671
Potato	Tomato	chilense_anther_1	chilense	E00621882	5.963	0.219	0.724	1.019
Potato	Tomato	chilense_anther_1	chilense	e00621882	6.169	0.136	0.551	1.21
Potato	Tomato	chilense_anther_2	chilense	e00131891	6.392	0.308	0.716	0.906
Potato	Tomato	chilense_anther_3	chilense	e00131891	7.439	0.313	0.795	1.306
Potato	Tomato	chilense_anther_5	chilense	e00230420	9.843	0.496	1.402	1.292
Potato	Tomato	chilense_anther_8	chilense	e00143503	8.19	0.499	0.955	1.054
Potato	Tomato	chilense_anther_9	chilense	e00143503	9.159	0.273	0.716	1.192
Potato	Anarrhicomenum	chimboragense_(C	Chimborazense	field_museum_of_na	2.147	0.525	0.432	0.766
Potato	Anarrhicomenum	chimboragense_(C	Chimborazense	field_museum_of_na	2.429	0.572	0.516	0.922
Potato	Anarrhicomenum	chimboragense_(C	Chimborazense	1345767_chicago_nat	4.4	0.776	0.671	1.261
Potato	Anarrhicomenum	chimboragense_(C	NAChimborazens	1345766_chicago_nat	3.656	0.688	0.886	1.259
Potato	Anarrhicomenum	chimboragense_(C	NAChimborazens	1345766_chicago_nat	3.968	0.715	0.928	1.664
Potato	Anarrhicomenum	chimboragense_(C	NAChimborazens	1345766_chicago_nat	3.467	0.561	0.932	1.308
Potato	Anarrhicomenum	Chimborazense	Chimborazense	field_museum_of_na	2.58	0.73	0.626	1.096
Potato	Anarrhicomenum	Chimborozense	Chimborazense	1345767_chicago_nat	3.86	0.692	0.756	1.174
Potato	Tomato	chmielewskii_antl	chmielewskii	bm000778180	7.11	0.177	0.716	0.897
Potato	Tomato	chmielewskii_antl	chmielewskii	bm000778181	7.566	0.246	0.585	0.53
Leptostemonum	Torva	chrysotrichum_1	chrysotrichum	bm00942323	7.182	0.578	0.761	0.819
Leptostemonum	Androceras_Crinitu	citrullifolium	citrullifolium	F0073082F	7.58	0.59	0.67	0.7
Leptostemonum	Androceras_Crinitu	citrullifolium	citrullifolium	live	8.468	0.475	1.192	1.022
Leptostemonum	Androceras_Crinitu	citrullifolium_pol_	citrullifolium_po	live	11.988	0.373	1.423	0.898
mapiriense_clandes	mapiriense_clande	clandestinum_1	clandestinum	n'5799156_missouri	3.969	0.731	0.879	1.395
Brevantherum	Brevantherum	clathratum_1	clathratum	bm_000846535	2.675	0.716	0.566	1.049
Brevantherum	Brevantherum	clathratum_2	clathratum	bm_000072713	2.725	0.67	0.724	0.95
Brevantherum	Brevantherum	clathratum_3	clathratum	bm_000072713	2.271	0.612	0.52	0.993
Brevantherum	Brevantherum	clathratum_4	clathratum	bm_001016890	4.07	0.943	0.7	1.26
Geminata	Geminata	clivorum_1	clivorum	bm_000849373	3.021	0.942	0.69	1.256
Geminata	Geminata	clivorum_10	pyracanthos	e00112848	6.01	0.451	0.774	1.346
Geminata	Geminata	clivorum_4	clivorum	bm_001120642	2.182	0.881	0.731	1.105

major_clade	clade	sample_name	species	herbarium code	anther length/mm	tip width/mm	base width/mm	middle width/mm
Geminata	Geminata	clivorum_5	clivorum	bm_001120642	2.874	0.857	0.739	1.631
Geminata	Geminata	clivorum_6	clivorum	bm_001120642	2.641	0.832	0.816	1.327
Geminata	Geminata	clivorum_7	clivorum	bm_001120830	2.111	0.712	0.574	0.935
Geminata	Geminata	clivorum_8	clivorum	bm_001120830	2.114	0.949	0.786	1.028
Geminata	Geminata	clivorum_9	clivorum	bm_001120830	1.926	0.705	0.561	1.067
Leptostemonum	old_world	coagulans_1	coagulans	bm000942276	4.714	0.9	1.007	1.347
Leptostemonum	old_world	coagulans_10	coagulans	bm000942277	5.035	0.882	0.885	1.327
Leptostemonum	old_world	coagulans_11	coagulans	bm000942280	5.705	0.878	0.912	1.611
Leptostemonum	old_world	coagulans_14	coagulans	bm000942732	5.969	0.619	1.012	1.511
Leptostemonum	old_world	coagulans_2	coagulans	bm000942276	4.337	0.854	0.723	1.336
Leptostemonum	old_world	coagulans_4	coagulans	bm000942276	5.198	0.818	0.711	1.21
Leptostemonum	old_world	coagulans_5	coagulans	bm000942279	4.657	0.885	0.8	1.164
Leptostemonum	old_world	coagulans_6	coagulans	bm000942279	4.979	0.929	0.682	1.154
Leptostemonum	old_world	coagulans_7	coagulans	bm000942279	4.568	0.997	1.165	1.379
Leptostemonum	old_world	coagulans_8	coagulans	bm000942277	5	0.827	0.587	1.121
Leptostemonum	old_world	coagulans_9	coagulans	bm000942277	4.958	1.048	0.87	1.331
Potato	Basarthrum	cochoae_1	cochoae	bm001134702	4.407	0.939	1.169	1.835
Potato	Basarthrum	cochoae_2	cochoae	bm001134702	4.464	0.956	1.232	1.533
Potato	Basarthrum	cochoae_3	cochoae	bm001134702	4.074	0.815	1.254	1.521
Potato	Petota	colombianum_1	colombianum	bm000849473	4.719	0.905	1.252	1.293
Leptostemonum	Carolinense	comptum_1	comptum	NY00139104	6.61	0.61	0.99	1.44
na	na	cordatum_2	cordatum	bm000942303	4.422	0.797	0.689	1.425
na	na	cordatum_5	cordatum	bm000942301	5.36	0.658	0.572	1.17
Leptostemonum	Torva	crinitipes_1	crinitipes	P00325676	3.68	0.51	0.91	0.43
Leptostemonum	Androceras_Crinitu	crinitum_1	crinitum	bm000849358	11.894	1.099	1.273	1.988
m_clade	Dulcamaroid	crispum_10	crispum	e00182312	4.087	0.845	0.827	1.291
m_clade	Dulcamaroid	crispum_11	crispum	e00182312	4.312	0.993	1.25	1.909
m_clade	Dulcamaroid	crispum_12	crispum	e00182313	4.911	0.711	0.866	1.634
m_clade	Dulcamaroid	crispum_13	crispum	e00182312	4.431	1.012	1.452	1.763
m_clade	Dulcamaroid	crispum_14	crispum	e00182312	3.858	1.414	1.395	1.822
m_clade	Dulcamaroid	crispum_15	crispum	e00182313	5.19	0.574	0.793	0.938
m_clade	Dulcamaroid	crispum_16	crispum	e00182724	2.677	0.923	0.736	1.376
m_clade	Dulcamaroid	crispum_17	crispum	e00200836	3.4	0.778	0.462	1.035
m_clade	Dulcamaroid	crispum_18	crispum	e00031958	2.981	0.848	0.712	1.288
m_clade	Dulcamaroid	crispum_19	crispum	e00031958	3.535	0.614	0.535	1.054
m_clade	Dulcamaroid	crispum_2	crispum	e00182309	3.195	0.512	1.133	1.825
m_clade	Dulcamaroid	crispum_20	crispum	e00031958	3.253	0.758	0.653	0.779
m_clade	Dulcamaroid	crispum_21	crispum	e00014582	3.709	0.839	0.643	1.252
m_clade	Dulcamaroid	crispum_22	crispum	e00014582	3.901	0.775	0.642	0.964
m_clade	Dulcamaroid	crispum_23	crispum	e00057487	4.157	0.819	0.894	1.214
m_clade	Dulcamaroid	crispum_24	crispum	e00057487	3.616	0.379	0.56	1.154
m_clade	Dulcamaroid	crispum_25	crispum	e00224040	3.166	0.816	0.943	1.1
m_clade	Dulcamaroid	crispum_26	crispum	e00224040	3.346	1.009	1.469	1.808
m_clade	Dulcamaroid	crispum_27	crispum	e00224040	3.522	0.832	1.038	1.538
m_clade	Dulcamaroid	crispum_28	crispum	e00224040	3.048	0.912	0.867	1.091
m_clade	Dulcamaroid	crispum_29	crispum	e00282782	4.253	1.178	0.896	1.332
m_clade	Dulcamaroid	crispum_3	crispum	e00241919	2.75	0.566	0.793	1.147
m_clade	Dulcamaroid	crispum_30	crispum	e00282782	4.438	1.113	0.845	1.219
m_clade	Dulcamaroid	crispum_31	crispum	e00282782	4.601	1.043	0.664	1.139
m_clade	Dulcamaroid	crispum_32	crispum	e00114932	4.188	1.17	0.968	1.81
m_clade	Dulcamaroid	crispum_33	crispum	e00125356	2.969	0.964	1.136	1.423
m_clade	Dulcamaroid	crispum_34	crispum	e00420874	3.577	0.711	0.675	1.096
m_clade	Dulcamaroid	crispum_35	crispum	e00057520	4.28	0.518	1.144	1.436
m_clade	Dulcamaroid	crispum_36	crispum	e00125357	4.053	0.797	1.003	1.186
m_clade	Dulcamaroid	crispum_37	crispum	e00125358	4.42	0.697	0.895	1.067
m_clade	Dulcamaroid	crispum_38	crispum	e00125358	5.216	0.724	0.59	1.002
m_clade	Dulcamaroid	crispum_39	crispum	e00125359	3.086	0.958	0.677	0.928
m_clade	Dulcamaroid	crispum_4	crispum	e00241919	2.923	0.501	0.661	1.039
m_clade	Dulcamaroid	crispum_40	crispum	e00057513	3.304	0.707	0.864	1.185
m_clade	Dulcamaroid	crispum_41	crispum	e00057569	4.116	0.733	0.949	1.173
m_clade	Dulcamaroid	crispum_42	crispum	e00045259	4.326	1.078	0.905	0.984
m_clade	Dulcamaroid	crispum_43	crispum	e00057560	3.608	0.943	0.693	1.344
m_clade	Dulcamaroid	crispum_44	crispum	e00114917	4.025	0.574	0.74	1.371
m_clade	Dulcamaroid	crispum_45	crispum	e00114921	4.398	1.104	0.885	1.074
m_clade	Dulcamaroid	crispum_46	crispum	e00112767	3.473	0.79	0.798	0.962
m_clade	Dulcamaroid	crispum_49	crispum	e00112769	4.297	0.821	0.779	1.204
m_clade	Dulcamaroid	crispum_5	crispum	e00251354	1.035	0.616	0.619	1.035
m_clade	Dulcamaroid	crispum_50	crispum	e00112769	3.93	0.871	0.866	1.297
m_clade	Dulcamaroid	crispum_51	crispum	e00112771	4.135	0.827	0.658	1.019
m_clade	Dulcamaroid	crispum_52	crispum	e00112771	4.328	1.015	0.912	1.114
m_clade	Dulcamaroid	crispum_53	crispum	e00112777	3.482	0.901	0.848	1.266
m_clade	Dulcamaroid	crispum_54	crispum	e00112804	3.828	0.928	0.881	1.334
m_clade	Dulcamaroid	crispum_55	crispum	e00112804	3.865	0.909	0.692	1.137
m_clade	Dulcamaroid	crispum_6	crispum	e00251354	3.541	0.671	0.635	1.243
m_clade	Dulcamaroid	crispum_7	crispum	e00251354	3.74	0.667	0.971	1.72
m_clade	Dulcamaroid	crispum_8	crispum	e00251354	3.127	0.803	0.908	1.23
m_clade	Dulcamaroid	crispum_9	crispum	e00251354	3.415	0.677	0.646	0.939
Geminata	Geminata	delitescens_1	delitescens	F0073252F	3.31	0.93	0.97	1.25
Potato	Petota	demissum_1	demissum	E00129589	5.185	0.906	0.981	1.468
Potato	Petota	demissum_1	demissum	e00129589	4.766	0.956	1.107	1.493
Potato	Petota	demissum_2	demissum	e00129589	4.109	0.847	0.997	1.258
Potato	Petota	demissum_4	demissum	e00129572	2.859	0.759	1.007	1.417
Potato	Petota	demissum_6	demissum	_e00129572	3.091	0.95	1.211	1.346
Cyphomandra	Cyphomandra	diversifolium_1	diversifolium	BM000602761	3.685	0.353	0.505	0.874
Leptostemonum	Torva	donianum_1	donianum	e00526586	6.153	0.604	0.55	0.832
Leptostemonum	Torva	donianum_4	donianum	e00526586	5.264	0.611	0.594	0.869
m_clade	Morelloid	douglasii_1	douglasii	e00526506	2.624	0.582	0.721	0.939

major_clade	clade	sample_name	species	herbarium code	anther length/mm	tip width/mm	base width/mm	middle width/mm
m_clade	Morelloid	douglasii_2	douglasii	e00526505	2.63	0.673	0.718	1.088
m_clade	Morelloid	douglasii_3	douglasii	e00526505	2.615	0.761	0.547	0.821
m_clade	Dulcamaroid	dulcamara_anther	dulcamara	e00112774	5.086	0.468	0.696	0.728
m_clade	Dulcamaroid	dulcamara_anther	dulcamara	bm000942577	4.981	0.748	0.779	1.527
m_clade	Dulcamaroid	dulcamara_anther	dulcamara	bm000942577	4.846	0.486	0.791	1.132
m_clade	Dulcamaroid	dulcamara_anther	dulcamara	bm000942577	5.004	0.383	0.739	0.683
m_clade	Dulcamaroid	dulcamara_anther	dulcamara	e00291774	3.978	0.395	0.572	0.603
m_clade	Dulcamaroid	dulcamara_anther	dulcamara	e00289535	4.048	0.585	0.792	1.222
m_clade	Dulcamaroid	dulcamara_anther	dulcamara	e00112773	4.458	0.491	0.634	0.993
m_clade	Dulcamaroid	dulcamara_anther	dulcamara	bm000942558	5.77	0.663	1.283	1.408
m_clade	Morelloid	echegarayi	echegarayi	e00114935	4.081	0.871	0.981	1.347
Leptostemonum	Elaeagnifolium	elaeagnifolium_1	elaeagnifolium	US01178087	4.36	0.85	1.02	1.03
Leptostemonum	Elaeagnifolium	elaeagnifolium_12	elaegnifolium	e00114569	7.313	0.547	1.227	1.493
Leptostemonum	Elaeagnifolium	elaeagnifolium_13	elaegnifolium	e00057519	7.469	0.924	0.974	1.147
Leptostemonum	Elaeagnifolium	elaeagnifolium_14	elaegnifolium	e00057519	0.997	0.454	0.523	0.997
Leptostemonum	Elaeagnifolium	elaeagnifolium_17	elaegnifolium	e00118841	6.027	0.489	1.292	1.158
Leptostemonum	Elaeagnifolium	elaeagnifolium_18	elaegnifolium	e00118839	7.811	0.492	0.536	0.908
Leptostemonum	Elaeagnifolium	elaeagnifolium_19	elaegnifolium	e00118837	8.067	0.588	0.749	1.081
Leptostemonum	Elaeagnifolium	elaeagnifolium_2	elaeagnifolium	US01178088	7.23	0.64	1.32	0.87
Leptostemonum	Elaeagnifolium	elaeagnifolium_21	elaegnifolium	e00118836	10.298	0.673	1.022	1.637
Leptostemonum	Elaeagnifolium	elaeagnifolium_22	elaegnifolium	e00118836	10.737	0.626	1.241	1.435
Leptostemonum	Elaeagnifolium	elaeagnifolium_23	elaegnifolium	e00009916	7.119	0.484	0.898	1.301
Leptostemonum	Elaeagnifolium	elaeagnifolium_24	elaegnifolium	e00057563	9.348	0.616	1.231	1.311
Leptostemonum	Elaeagnifolium	elaeagnifolium_26	elaegnifolium	e00118856	9.228	0.616	1.212	2.051
Leptostemonum	Elaeagnifolium	elaeagnifolium_29	elaegnifolium	e00118854	6.847	0.465	0.423	0.82
Leptostemonum	Elaeagnifolium	elaeagnifolium_3	elaegnifolium	e00180243	9.008	0.378	0.673	0.673
Leptostemonum	Elaeagnifolium	elaeagnifolium_30	elaegnifolium	e00118851	5.903	0.578	0.904	1.135
Leptostemonum	Elaeagnifolium	elaeagnifolium_4	elaegnifolium	e00118851	7.22	0.697	0.801	1.024
Leptostemonum	Elaeagnifolium	elaeagnifolium_5	elaegnifolium	e00118851	6.744	0.64	0.871	1.115
Leptostemonum	Elaeagnifolium	elaeagnifolium_6	elaegnifolium	e00118851	7.535	0.832	0.905	1.252
Leptostemonum	Bahamense	ensifolium_2	ensifolium	e00249862	4.939	1.698	1.565	1.763
Leptostemonum	Bahamense	ensifolium_3	ensifolium	e00249862	4.939	0.639	0.578	0.792
Leptostemonum	Bahamense	ensifolium_4	ensifolium	e00249862	5.382	1.533	1.404	1.591
Leptostemonum	Bahamense	ensifolium_5	ensifolium	e00249862	5.382	0.547	0.551	0.762
Brevantherum	Brevantherum	erianthum_10	erianthum	e00112902	2.005	0.413	0.416	0.581
Brevantherum	Brevantherum	erianthum_11	erianthum	bm00942400	3.032	0.723	0.811	1.285
Brevantherum	Brevantherum	erianthum_13	erianthum	bm00942400	2.91	0.623	0.558	1.001
Brevantherum	Brevantherum	erianthum_14	erianthum	bm00942401	3.4	0.807	0.758	1.105
Brevantherum	Brevantherum	erianthum_17	erianthum	bm00942402	2.577	0.618	0.822	1.043
Brevantherum	Brevantherum	erianthum_19	erianthum	bm00942402	2.27	0.7	0.897	1.032
Brevantherum	Brevantherum	erianthum_25	erianthum	bm000847029	2.866	0.908	0.639	1.069
Brevantherum	Brevantherum	erianthum_28	erianthum	bm000900083	2.924	0.702	0.731	1.123
Brevantherum	Brevantherum	erianthum_3	erianthum	bm001034933	3.359	0.979	0.892	1.251
Brevantherum	Brevantherum	erianthum_32	erianthum	bm000942389	2.836	0.8	0.901	1.195
Brevantherum	Brevantherum	erianthum_38	erianthum	bm000900090	2.512	0.473	0.503	0.925
Brevantherum	Brevantherum	erianthum_39	erianthum	e000526447	2.596	0.712	0.673	1.135
Brevantherum	Brevantherum	erianthum_4	erianthum	bm000847029	2.818	0.793	0.885	0.958
Brevantherum	Brevantherum	erianthum_40	erianthum	e000526447	2.487	0.775	0.543	0.936
Brevantherum	Brevantherum	erianthum_41	erianthum	bm001034930	2.891	0.749	0.492	0.97
Brevantherum	Brevantherum	erianthum_7	erianthum	bm000847026	2.361	0.715	0.754	1.04
Leptostemonum	old_world	esuriale_1	esuriale	1794CGE	3.728	0.653	0.817	1.102
Potato	Etuberosum	etuberosum	etuberosum	e00621247	5.105	0.968	1.126	1.527
Potato	Etuberosum	etuberosum	etuberosum	e00158633	5.686	0.827	1.173	1.784
Potato	Etuberosum	etuberosum	etuberosum	e00621247	4.947	0.98	1.454	1.568
Potato	Etuberosum	etuberosum	etuberosum	e006211247	5.065	0.801	1.466	1.182
na	na	excisirhornbeum_1	excisirhornbeum	e00182133	2.166	0.574	0.538	0.885
na	na	excisirhornbeum_2	excisirhornbeum	e00182133	2.116	0.63	0.457	0.947
na	na	excisirhornbeum_3	excisirhornbeum	e00182133	1.962	0.786	0.493	0.993
m_clade	Morelloid	fiebrigii	fiebrigii	e00114912	3.498	0.508	0.639	1.058
Leptostemonum	old_world	forskali_1	forskalii	BM000942261	5.08	0.732	0.879	1.3
Leptostemonum	old_world	forskalii_1	forskalii	bm000942261	5.667	0.594	0.7	0.986
Potato	Basarthrum	fraxinifolium_1	fraxinifolium	live	2.497	0.695	0.792	0.99
m_clade	Morelloid	furcatum_1	furcatum	e00649054	2.911	0.582	0.58	1.077
m_clade	Morelloid	furcatum_10	furcatum	e00282740	2.269	0.521	0.54	0.809
m_clade	Morelloid	furcatum_11	furcatum	e00106310	3.189	0.721	0.993	1.266
m_clade	Morelloid	furcatum_12	furcatum	e000399929	2.701	0.716	0.562	0.716
m_clade	Morelloid	furcatum_14	furcatum	e000399930	2.703	0.568	0.485	0.726
m_clade	Morelloid	furcatum_15	furcatum	e00057566	3.228	0.912	0.584	1.155
m_clade	Morelloid	furcatum_16	furcatum	e00057566	3.236	0.724	0.714	0.933
m_clade	Morelloid	furcatum_18	furcatum	e00593070	3.046	0.867	0.427	0.779
m_clade	Morelloid	furcatum_20	furcatum	e00125339	3.393	0.569	1.181	1.199
m_clade	Morelloid	furcatum_21	furcatum	e00125339	3.574	0.758	0.674	0.975
m_clade	Morelloid	furcatum_22	furcatum	e00282665	2.501	0.853	0.636	1.002
m_clade	Morelloid	furcatum_23	furcatum	e00282665	2.259	0.551	0.626	0.807
m_clade	Morelloid	furcatum_3	furcatum	e00158644	3.359	0.724	0.512	0.612
m_clade	Morelloid	furcatum_4	furcatum	e00158644	3.061	0.705	0.442	0.586
m_clade	Morelloid	furcatum_6	furcatum	e00182308	2.32	0.728	0.544	0.857
m_clade	Morelloid	furcatum_7	furcatum	e00182308	2.144	0.682	0.603	0.912
m_clade	Morelloid	furcatum_8	furcatum	e00182333	3.257	0.508	0.538	0.793
m_clade	Morelloid	furcatum_9	furcatum	e00030038	2.818	0.683	0.73	1.107
Leptostemonum	old_world	furfuraceum	furfuraceum	BM000596883	4.88	0.5	0.68	0.65
Potato	Tomato	galapagense_anth	galapagense	bm001120067	5.778	0.407	0.536	1.022
Potato	Tomato	galapagense_anth	galapagense	bm001120067	5.916	0.243	0.92	1.286
Potato	Tomato	galapagense_anth	galapagense	bm001120067	6.121	0.313	0.802	1.115
Potato	Tomato	galapagense_anth	galapagense	bm001120062	6.931	0.341	0.578	1.132
Leptostemonum	old_world	giganteum_2	giganteum	bm000900136	2.867	0.501	0.563	0.865

major_clade	clade	sample_name	species	herbarium code	anther length/mm	tip width/mm	base width/mm	middle width/mm
Leptostemonum	old_world	glabratum_1	glabratum	e00617990	7.641	0.603	2.729	1.206
Leptostemonum	old_world	glabratum_11	glarbatum	bm000942620	5.847	0.539	0.694	1.36
Leptostemonum	old_world	glabratum_12	glarbatum	bm000942629	6.959	0.693	0.672	1.436
Leptostemonum	old_world	glabratum_14	glarbatum	bm000942627	5.405	0.501	0.603	0.977
Leptostemonum	old_world	glabratum_16	glarbatum	bm000942610_	5.508	0.608	0.541	1.222
Leptostemonum	old_world	glabratum_17	glarbatum	bm000942610_	5.501	0.5	0.373	1.007
Leptostemonum	old_world	glabratum_21	glarbatum	bm000942619	7.155	0.651	0.79	1.497
Leptostemonum	old_world	glabratum_3	glabratum	bm000942602	6.234	0.517	0.81	1.094
Leptostemonum	old_world	glabratum_4	glabratum	bm000942602	6.388	0.611	0.704	0.966
Leptostemonum	old_world	glabratum_6	glabratum	bm000942602	8.637	0.574	0.722	1.388
Leptostemonum	old_world	glabratum_7	glarbatum	bm000943054	6.353	0.619	1.015	1.547
Leptostemonum	old_world	glabratum_8	glarbatum	bm000943054	6.673	0.673	0.769	1.45
Cyphomandra	Cyphomandra	glaucophyllum_1	glaucophyllum	e00057571	4.751	0.616	0.966	2.066
Cyphomandra	Cyphomandra	glaucophyllum_2	glaucophyllum	e00057571	4.849	0.682	0.832	1.797
na	na	habrochaites_anth	habrochaites	e00160277	12.902	0.273	1.257	1.687
na	na	habrochaites_anth	habrochaites	e00700632	9.403	0.367	1.392	1.777
na	na	habrochaites_anth	habrochaites	e00700632	10.56	0.212	1.271	1.366
na	na	habrochaites_anth	habrochaites	e00700814	9.647	0.45	1.172	1.842
m_clade	Normania	herculeum_2	herculeum	bm_000849101	4.29	0.651	0.7	0.997
Leptostemonum	Elaeagnifolium	hindsianum_1	hindsianum	K000063726	5.95	0.51	0.88	0.52
Leptostemonum	Elaeagnifolium	hindsianum_2	hindsianum	e00526534	9.345	0.561	0.933	1.25
Leptostemonum	Torva	hispidum_1	hispidum	17206CGE	6.974	0.481	1.273	1.166
na	na	humblotii	humblotii	new_york_2013-8366	5.951	0.693	0.555	1.428
na	na	humblotii	humblotii	new_york_botanical_	4.583	0.673	1.196	1.837
m_clade	African_non_spiny	humblotii _1	humblotii	bm000797934	3.916	0.523	0.752	1.093
m_clade	African_non_spiny	humblotii_2	humblotii	wag0341669_	4.774	0.762	1.007	1.96
m_clade	African_non_spiny	imamense_2	imamense	p00349057	4.141	0.901	1.791	2.65
m_clade	African_non_spiny	imamense_6	imamense	p00349078	4.231	0.901	1.24	2.078
m_clade	African_non_spiny	imamense_7	imamense	p00349078	4.254	0.822	1.385	2.081
m_clade	African_non_spiny	imamense_9	imamense	n04672966	4.608	0.982	1.009	1.585
Leptostemonum	old_world	incanum_1	incanum	E00112795	8.128	0.712	1.171	1.605
Leptostemonum	old_world	incanum_1	incanum	bm_000847637	5.977	1.247	1.256	1.859
Leptostemonum	old_world	incanum_10	incanum	bm000942655	6.496	1.04	1.078	2.023
Leptostemonum	old_world	incanum_12	incanum	bm000942654	5.535	1.137	0.901	1.689
Leptostemonum	old_world	incanum_14	incanum	bm000942664	5.548	0.677	0.911	1.7
Leptostemonum	old_world	incanum_17	incanum	bm000942596	4.871	0.597	0.49	0.981
Leptostemonum	old_world	incanum_18	incanum	bm000942596	4.541	0.505	0.735	1.138
Leptostemonum	old_world	incanum_2	incanum	e00621003	5.214	0.63	0.778	1.097
Leptostemonum	old_world	incanum_20	incanum	bm000942633	6.579	1.059	1.145	1.68
Leptostemonum	old_world	incanum_24	incanum	bm_000847637	5.987	0.803	1.058	1.962
Leptostemonum	old_world	incanum_25	incanum	e00112795	7.467	0.55	1.027	1.603
Leptostemonum	old_world	incanum_3	incanum	e00112795	6.916	0.851	1.307	1.878
Leptostemonum	old_world	incanum_4	incanum	e00621009	6.24	0.711	1.035	1.643
Leptostemonum	old_world	incanum_5	incanum	e00621009	7.449	1.102	0.896	1.066
Leptostemonum	old_world	incanum_6	incanum	e00112796	6.859	1.479	1.256	2.031
Leptostemonum	old_world	incanum_7	incanum	e00112796	6.617	1.104	1.508	1.788
Leptostemonum	old_world	incanum_9	incanum	bm000942699	5.053	0.775	0.646	1.502
Potato	Petota	iopetalum_1	iopetalum	e00129582	3.993	0.749	0.938	1.121
Potato	Petota	iopetalum_2	iopetalum	e00129582	3.848	0.914	1.037	1.23
Potato	Petota	iopetalum_4	iopetalum	e00129582	4.061	0.885	1.096	1.425
Potato	Petota	iopetalum_5	iopetalum	e00129582	4.283	1.265	0.971	1.541
Potato	Petota	iopetalum_6	iopetalum	e00129583	3.815	0.846	1.11	1.271
Potato	Petota	iopetalum_7	iopetalum	e00129583	4.152	0.75	1.256	1.179
m_clade	African_non_spiny	ivohibe_1	ivohibe	p00349079	4.247	0.803	0.816	1.931
m_clade	African_non_spiny	ivohibe_3	ivohibe	p00349079	4.156	0.984	0.674	1.788
m_clade	African_non_spiny	ivohibe_5	ivohibe	p00352690	3.12	0.724	0.761	1.393
m_clade	African_non_spiny	ivohibe_6	ivohibe	p00352690_	2.78	0.707	0.707	1.357
Potato	Petota	jamesii_1	jamesii	E00129564	5.262	0.826	1.109	1.722
Potato	Petota	jamesii_4	jamesii	e00129563	7.457	0.551	0.635	0.982
Potato	Tomato	juglandifolium	juglandifolium	bm000778149	3.973	0.816	1.131	1.455
m_clade	Morelloid	juninense_1	juninense	bm001134588	2.892	0.581	0.639	0.943
m_clade	Morelloid	juninense_4	juninense	bm001134588	2.834	0.491	0.508	0.785
m_clade	Morelloid	juninense_5	juninense	bm001134588	2.828	0.506	0.617	0.962
Leptostemonum	Carolinense	juvenale_1	juvenale	e00114936	5.382	0.894	1.058	1.008
Leptostemonum	Carolinense	juvenale_2	juvenale	e00114936	6.844	0.714	1.05	1.101
Leptostemonum	Carolinense	juvenale_3	juvenale	e00114936	6.774	0.646	0.697	1.018

major_clade	clade	sample_name	species	herbarium code	anther length/mm	tip width/mm	base width/mm	middle width/mm
Leptostemonum	Carolinense	juvenale_5	juvenale	e00114936	7.196	0.566	0.985	1.211
m_clade	Dulcamaroid	kulliwaita_1	kulliwaita	stockholm_herb_n'_s	3.339	0.925	1.121	1.611
m_clade	Dulcamaroid	kulliwaita_2	kulliwaita	stockholm_herb_n'_s	4.664	0.914	1.411	1.636
Potato	Petota	kurtzianum_1	kurtzianum	bm001035312	6.013	1.1	1.471	1.67
Leptostemonum	old_world	kurzii_2	violaceum	bm000900299	5.974	0.687	0.732	1.218
Archaesolanum	Archaesolanum	laciniatum_1	laciniatum	E00610031	4.644	0.69	0.683	0.699
Archaesolanum	Archaesolanum	laciniatum_2	laciniatum	e0112803	3.786	0.778	1.497	2.151
na	na	lanatum_1	asperolanatum	bm000887649	6.833	0.966	2.034	2.619
Leptostemonum	Micracantha	lanceifolium_1	lanceifolium	bm000887652	7.116	0.632	1.616	1.252
Leptostemonum	Micracantha	lanceifolium_2	lanceifolium	bm000887652	4.621	0.688	0.637	0.929
Leptostemonum	Micracantha	lanceifolium_3	lanceifolium	bm000887652	4.57	0.462	0.423	0.778
Leptostemonum	Micracantha	lanceifolium_4	lanceifolium	bm000887652	5.037	0.602	0.616	0.984
Leptostemonum	Torva	lanceolatum_1	lanceolatum	E00526544	7.758	0.664	0.877	1.233
Leptostemonum	Torva	lanceolatum_1	lanceolatum	e00526541	7.56	0.628	0.988	1.084
Leptostemonum	Torva	lanceolatum_2	lanceolatum	e00526542	8.199	0.585	0.62	0.989
Leptostemonum	Torva	lanceolatum_4	lanceolatum	e00526528	7.25	0.662	0.809	1.531
Leptostemonum	Torva	lanceolatum_5	lanceolatum	e00526528	7.372	0.827	0.775	1.435
Leptostemonum	Torva	lanceolatum_6	lanceolatum	e00526529	5.496	0.809	0.94	1.12
m_clade	Dulcamaroid	laxum	laxum	bm000900297	3.721	0.816	0.894	1.193
m_clade	Dulcamaroid	laxum	laxum	bm000900297	3.727	0.925	0.905	1.227
m_clade	Dulcamaroid	laxum	laxum	bm000900297	3.623	1.035	0.952	1.283
m_clade	Dulcamaroid	laxum_1	laxum	BM000935924	2.18	0.48	0.73	0.87
m_clade	Dulcamaroid	laxum_3	laxum	e0112799	3.776	0.838	0.672	1.041
m_clade	Dulcamaroid	laxum_4	laxum	e00112799	3.406	0.646	0.747	1.138
m_clade	Dulcamaroid	laxum_5	laxum	e00112800	3.46	0.59	0.788	1.068
m_clade	Dulcamaroid	laxum_6	laxum	e00112798	2.057	0.587	0.897	1.108
m_clade	Dulcamaroid	laxum_7	laxum	e00112798	2.231	0.635	0.828	0.942
m_clade	Dulcamaroid	laxum_8	laxum	e00112801	3.769	0.904	0.68	0.838
m_clade	Dulcamaroid	laxum_9	laxum	e00112801	3.84	0.993	0.613	0.871
m_clade	Morelloid	leonii_1	macrotonum	bm000058811	2.707	0.709	0.586	0.982
m_clade	Morelloid	leonii_10	macrotonum	bm000849249	4.212	0.618	0.808	1.348
m_clade	Morelloid	leonii_11	macrotonum	bm000058811	1.947	0.547	0.475	0.758
m_clade	Morelloid	leonii_12	macrotonum	bm000058811	2.585	0.614	0.508	0.761
m_clade	Morelloid	leonii_13	macrotonum	bm001070105	2.394	0.7	0.711	0.75
m_clade	Morelloid	leonii_15	macrotonum	bm001070105	2.375	0.658	0.505	0.653
m_clade	Morelloid	leonii_16	macrotonum	bm001070385	2.279	0.783	0.773	0.853
m_clade	Morelloid	leonii_17	macrotonum	bm001070385	2.1	0.518	0.559	0.847
m_clade	Morelloid	leonii_18	macrotonum	bm000943648	2.733	0.439	0.784	0.97
m_clade	Morelloid	leonii_2	macrotonum	bm001070111	2.704	0.736	0.52	0.699
m_clade	Morelloid	leonii_5	macrotonum	bm001070132	2.449	0.453	0.462	0.762
m_clade	Morelloid	leonii_6	macrotonum	bm000943648	2.763	0.661	0.686	0.819
m_clade	Morelloid	leonii_7	macrotonum	bm000943648	2.596	0.42	0.523	0.894
m_clade	Morelloid	leonii_8	macrotonum	bm000849249	3.95	0.766	0.518	0.979
Brevantherum	Brevantherum	lepidotum_1	lepidotum	bm_00887663	2.673	0.643	0.523	0.859
Brevantherum	Brevantherum	lepidotum_2	lepidotum	bm_00887663	2.838	0.586	0.516	0.752
Brevantherum	Brevantherum	lepidotum_3	lepidotum	bm_00849368	3.139	0.758	0.993	1.225
Brevantherum	Brevantherum	lepidotum_5	lepidotum	bm_00887663	3.243	0.695	0.621	1.049
Brevantherum	Brevantherum	lepidotum_6	lepidotum	bm_00887660	2.866	0.671	0.596	0.758
Brevantherum	Brevantherum	lepidotum_7	lepidotum	bm_00887660	2.589	0.645	0.56	0.813
m_clade	Morelloid	leptocaulon_1	leptocaulon	bm_00849349	3.648	0.626	0.865	1.569
m_clade	Morelloid	leptocaulon_3	leptocaulon	bm_00849349	3.326	0.543	0.642	0.798
Geminata	Geminata	leucocarpon_4	leucocarpon	bm_001120603	3.941	1.058	1.222	1.629
Geminata	Geminata	leucocarpon_5	leucocarpon	bm_000887685	5.742	1.371	1.445	2.097
Geminata	Geminata	leucocarpon_6	leucocarpon	bm_000887693	4.963	1.283	1.502	2.056
Leptostemonum	old_world	lidii_feeding_anth	lidii	bm000847707	5.328	0.631	0.74	1.415
Leptostemonum	old_world	limitare_1	limitare	NSW522346	4.04	0.48	0.68	0.99
Leptostemonum	na	linnaeanum	linnaeanum	e00112866	6.635	0.97	1.102	1.591
Leptostemonum	na	linnaeanum	linnaeanum	e00112866	6.302	0.735	1.212	1.319
Leptostemonum	old_world	linnaeanum_1	linnaeanum	e00112866	4.305	1.009	1.124	1.392
m_clade	Morelloid	longifilamentum_	longifilamentum	bm_001070089	2.964	0.602	0.574	0.977
m_clade	Morelloid	longifilamentum_	longifilamentum	_bm_001120296	1.77	0.438	0.543	0.667
m_clade	Morelloid	longifilamentum_	longifilamentum	bm_001134662	1.939	0.491	0.586	0.74
m_clade	Morelloid	longifilamentum_	longifilamentum	bm_001034687	2.528	0.404	0.311	0.667
m_clade	Morelloid	longifilamentum_	longifilamentum	bm_001134662	1.914	0.457	0.561	0.662
m_clade	Morelloid	longifilamentum_	longifilamentum	bm_001134662	1.648	0.411	0.468	0.721
m_clade	Morelloid	longifilamentum_	longifilamentum	bm_001114796	2.055	0.534	0.578	0.86
m_clade	Morelloid	longifilamentum_	longifilamentum	bm_000849216	1.837	0.173	0.49	0.521
m_clade	Morelloid	longifilamentum_	longifilamentum	bm_000849216	1.935	0.284	0.505	0.599
m_clade	Morelloid	longifilamentum_	longifilamentum	bm_001120295	1.485	0.518	0.486	0.621
m_clade	Morelloid	longifilamentum_	longifilamentum	bm_001120296	1.829	0.396	0.481	0.751
m_clade	Morelloid	longifilamentum_	longifilamentum	bm_001070089	2.369	0.541	0.423	0.442
m_clade	Morelloid	longifilamentum_	longifilamentum	bm_001120039	2.439	0.525	0.551	0.795
m_clade	Morelloid	longifilamentum_	longifilamentum	bm_001120039	2.592	0.396	0.423	0.785
m_clade	Morelloid	longifilamentum_	longifilamentum	bm_001034687	2.565	0.422	0.423	0.82
m_clade	Morelloid	longifilamentum_	longifilamentum	bm_001034687	2.365	0.577	0.585	0.843
m_clade	Morelloid	longifilamentum_	longifilamentum	bm_0010346552	1.826	0.275	0.31	0.427
m_clade	Morelloid	longifilamentum_	longifilamentum	_bm_001120039	2.671	0.528	0.628	0.805
na	na	lorentzii_1	aloysiifolium	e00106312	3.883	0.723	0.68	0.882
na	na	lucannii_1	lucani	live	6.592	0.555	1.004	1.664
na	na	lucannii_2	lucani	live	6.4	0.597	0.92	1.523
na	na	lucannii_3	lucani	live	6.298	0.693	0.943	1.622
na	na	lucannii_4	lucani	live	4.613	0.637	0.907	1.547
na	na	lucannii_5	lucani	live	4.702	0.639	1.009	1.569
na	na	lucannii_6	lucani	live	5.565	0.826	0.977	1.548
na	na	lucannii_7	lucani	live	6.097	0.835	1.158	1.904
na	na	lucannii_8	lucani	live	5.758	0.771	1.077	1.661
na	na	lucannii_9	lucani	live	5.584	0.705	1.129	1.849
Cyphomandra	Cyphomandra	luteoalbum_1	luteoalbum	NA	5.613	0.851	1.207	1.45
Cyphomandra	Cyphomandra	luteoalbum_1	luteoalbum	bm_001035112	6.352	0.617	1.392	1.816
Cyphomandra	Cyphomandra	luteoalbum_2	luteoalbum	bm_000887708	5.631	0.925	0.972	1.423
Cyphomandra	Cyphomandra	luteoalbum_3	luteoalbum	bm_000887708	5.336	0.882	1.355	1.684
Cyphomandra	Cyphomandra	luteoalbum_6	luteoalbum	bm_001035112	6.53	0.594	1.274	1.598
OUT	out	lycianthes_1	genus Lycianthes	newyork_00852820	3.26	0.585	0.581	1.039
Potato	Tomato	lycopersicum	lycopersicum	e00143536	5.941	0.174	0.675	0.697
NA	NA	lyococarpum_1	lyococarpum	bm000935470	13.484	0.946	1.377	1.619
m_clade	Dulcamaroid	lyratum_1	lyratum	bm000900348	3.147	0.67	0.789	1.187
m_clade	Dulcamaroid	lyratum_11	lyratum	bm00942427	3.153	0.79	0.699	1.058
m_clade	Dulcamaroid	lyratum_12	lyratum	bm00942427	3.015	0.63	0.683	1.069

major_clade	clade	sample_name	species	herbarium code	anther length/mm	tip width/mm	base width/mm	middle width/mm
m_clade	Dulcamaroid	lyratum_13	lyratum	bm00942421	1.952	0.785	0.651	1.096
m_clade	Dulcamaroid	lyratum_14	lyratum	bm00942437	3.004	0.775	0.611	1.077
m_clade	Dulcamaroid	lyratum_15	lyratum	bm00942437	2.525	0.499	0.569	1.04
m_clade	Dulcamaroid	lyratum_16	lyratum	bm00942437	2.717	0.62	0.68	1.007
m_clade	Dulcamaroid	lyratum_17	lyratum	bm00942437	2.405	0.692	0.658	0.846
m_clade	Dulcamaroid	lyratum_18	lyratum	bm00942421	2.238	0.578	0.786	1.152
m_clade	Dulcamaroid	lyratum_2	lyratum	bm000900348	3.079	0.712	0.563	1.003
m_clade	Dulcamaroid	lyratum_3	lyratum	bm000900348	2.696	0.616	0.962	1.192
m_clade	Dulcamaroid	lyratum_4	lyratum	e00291803	2.345	0.567	0.664	0.718
m_clade	Dulcamaroid	lyratum_5	lyratum	e00291804	2.555	0.593	0.523	0.793
m_clade	Dulcamaroid	lyratum_6	lyratum	bm00942415	2.555	0.594	0.32	0.971
m_clade	Dulcamaroid	lyratum_8	lyratum	bm00942417	2.747	0.864	0.748	1.189
m_clade	Dulcamaroid	lyratum_9	lyratum	bm00942417	2.597	0.949	0.673	1.408
na	na	macrothyrsum	macrothyrsum	bm000887183	3.654	0.981	0.77	1.692
m_clade	African_non_spiny	macrothyrsum_1	macrothyrsum	n'5730088	3.576	1.184	1	1.919
m_clade	African_non_spiny	macrothyrsum_2	macrothyrsum	n'5730088	3.404	1.097	1.173	1.884
m_clade	African_non_spiny	macrothyrsum_3	macrothyrsum	n'5730088	3.645	1.103	1.261	2.53
m_clade	African_non_spiny	macrothyrsum_4	macrothyrsum	n'5730088	3.593	1.131	1.088	1.79
m_clade	African_non_spiny	macrothyrsum_6	macrothyrsum	n'5730088	3.723	1.345	1.447	2.503
m_clade	Morelloid	macrotonum_1	macrotonum	bm_000887725	3.104	0.561	0.592	0.789
m_clade	Morelloid	macrotonum_10	macrotonum	bm_001070367	3.186	0.55	0.714	0.752
m_clade	Morelloid	macrotonum_11	macrotonum	bm_001134581	3.061	0.637	0.601	0.742
m_clade	Morelloid	macrotonum_12	macrotonum	bm_001134581	3.267	0.596	0.632	0.743
m_clade	Morelloid	macrotonum_13	macrotonum	bm_001134579	3.147	0.545	0.697	0.973
m_clade	Morelloid	macrotonum_15	macrotonum	bm_000887725	3.376	0.569	0.585	0.811
m_clade	Morelloid	macrotonum_16	macrotonum	e00526507	2.434	0.465	0.779	0.881
m_clade	Morelloid	macrotonum_19	macrotonum	bm_001070386	2.679	0.601	0.517	0.979
m_clade	Morelloid	macrotonum_2	macrotonum	bm_001120211	2.15	0.355	0.355	0.49
m_clade	Morelloid	macrotonum_21	macrotonum	bm_001134579	3.595	0.449	0.68	0.832
m_clade	Morelloid	macrotonum_5	macrotonum	bm_000943660	3.163	0.443	0.539	0.779
m_clade	Morelloid	macrotonum_7	macrotonum	bm_001070386	2.86	0.551	0.602	0.793
m_clade	Morelloid	macrotonum_9	macrotonum	bm_001070367	3.372	0.521	0.574	0.656
m_clade	African_non_spiny	madagascariense_	madagascariense	p00349373	3.819	0.816	1.089	1.179
m_clade	African_non_spiny	madagascariense_	madagascariense	new_york_00853207	4.441	1.404	1.356	1.758
m_clade	African_non_spiny	madagascariense_	madagascariense	new_york_00853207	4.021	1.123	1.105	1.61
m_clade	African_non_spiny	madagascariense_	madagascariense	p00352679	4.422	1.069	1.189	1.605
m_clade	African_non_spiny	madagascariense_	madagascariense	p00352679	4.877	0.936	0.974	1.661
m_clade	African_non_spiny	madagascariense_	madagascariense	p00352679	4.777	1.019	1.025	1.408
m_clade	African_non_spiny	madagascariense_	madagascariense	new_york_00827818	4.108	0.699	1.385	1.579
m_clade	African_non_spiny	madagascariense_	madagascariense	p00853209	5.235	1.046	0.656	1.867
m_clade	African_non_spiny	madagascariense_	madagascariense	p00853209	5.188	1.16	1.17	2.08
m_clade	African_non_spiny	madagascariense_	madagascariense	new_york_00827818	4.115	0.596	1.099	1.481
m_clade	African_non_spiny	madagascariense_	madagascariense	missouri_n'3033183	2.212	0.396	0.518	1.011
m_clade	African_non_spiny	madagascariense_	madagascariense	missouri_n'3033183	2.331	0.547	0.508	0.809
m_clade	African_non_spiny	madagascariense_	madagascariense	missouri_n'3491983	2.477	0.568	0.639	0.835
m_clade	African_non_spiny	madagascariense_	madagascariense	missouri_n'3491983	2.177	0.639	0.677	0.993
m_clade	African_non_spiny	madagascariense_	madagascariense	missouri_n'5748875	3.454	0.675	0.79	1.493
na	na	madrense_1	madrense	e00177489	8.217	0.448	1.101	0.74
Potato	Petota	maglia_1	maglia	e00125312	2.997	0.901	0.635	1.118
Potato	Petota	maglia_11	maglia	e00420403	3.25	1.031	0.865	1.676
Potato	Petota	maglia_3	maglia	e00125312	2.589	0.905	0.949	1.408
Potato	Petota	maglia_4	maglia	e00125312	2.491	0.953	1.009	1.456
Potato	Petota	maglia_5	maglia	e00125312	3.655	1.065	0.929	1.441
Potato	Petota	maglia_9	maglia	e00420403	3.828	0.956	1.152	1.646
Leptostemonum	na	mahoriense	mahoriense	P00586384	4.36	0.42	0.7	1.02
Leptostemonum	na	mahoriense	mahoriense	BR0000005912643	4.17	0.43	1.27	0.78
Geminata	Geminata	malletii_1	malletii	bm_000849220	2.21	0.805	0.688	1.153
Leptostemonum	Acanthophora	mammosum_1	mammosum	17214CGE	7.477	0.836	1.39	1.496
Leptostemonum	Acanthophora	mammosum_2	mammosum	bm_000072915	6.222	0.972	0.732	1.669
Leptostemonum	Acanthophora	mammosum_3	mammosum	bm_000072915	10.048	0.677	1.253	1.934
Potato	Basarthrum	mariae_1	mariae	bm_001034676	2.71	0.756	0.37	1.157
Potato	Basarthrum	mariae_2	mariae	bm_001034676	2.608	0.871	0.832	1.373
Potato	Basarthrum	mariae_3	mariae	bm_001034677	2.299	0.574	0.632	1.338
Potato	Basarthrum	mariae_4	mariae	bm_001034676	2.942	0.743	0.594	1.35
Geminata	Geminata	maturecalvans_1	maturecalvans	bm_000943106	4.484	1.022	0.731	1.865
Geminata	Geminata	maturecalvans_11	maturecalvans	bm_000848450	5.553	1.324	1.041	2.432
Geminata	Geminata	maturecalvans_13	maturecalvans	bm_000887740	4.002	0.962	0.762	1.66
Geminata	Geminata	maturecalvans_14	maturecalvans	bm_000887740	4.654	0.654	0.869	1.788
Geminata	Geminata	maturecalvans_16	maturecalvans	bm_000887745	5.177	1.129	1.223	1.515
Geminata	Geminata	maturecalvans_18	maturecalvans	bm_001120208	4.083	0.926	0.892	1.624
Geminata	Geminata	maturecalvans_2	maturecalvans	bm_000943106	4.011	1.166	0.904	1.983
Geminata	Geminata	maturecalvans_4	maturecalvans	bm_001114930	5.547	1.475	0.808	1.936
Geminata	Geminata	maturecalvans_6	maturecalvans	bm_001114884	5.457	1.719	1.007	2.354
Geminata	Geminata	maturecalvans_8	maturecalvans	bm_001120757	4.341	1.173	1.287	2.384
na	na	mauitianum_1	mauritianum	e00668557	2.661	0.592	0.727	1.048
na	na	mauitianum_2	mauritianum	e00668559	2.855	0.577	0.541	0.943
na	na	mauitianum_3	mauritianum	e00668557	2.815	0.779	0.742	1.121
na	na	mauitianum_4	mauritianum	e00112904	2.359	0.578	0.689	0.967
Brevantherum	Brevantherum	mauritianum_1	mauritianum	bm_000847720	2.427	0.49	0.749	0.983
Brevantherum	Brevantherum	mauritianum_2	mauritianum	bm_000847720	2.855	0.639	0.754	1.007
Brevantherum	Brevantherum	mauritianum_3	mauritianum	bm_000847720	2.58	0.493	0.966	1.177
Brevantherum	Brevantherum	mauritianum_4	mauritianum	bm_000847621	2.822	0.639	0.522	0.809
Brevantherum	Brevantherum	mauritianum_5	mauritianum	bm_000847621	2.779	0.85	0.768	1.035
Brevantherum	Brevantherum	mauritianum_6	mauritianum	bm_000847620	1.748	0.359	0.49	0.62
Brevantherum	Brevantherum	mauritianum_7	mauritianum	bm_000847620	2.339	0.8	0.506	0.998
Brevantherum	Brevantherum	mauritianum_8	mauritianum	bm_000847620	1.281	0.508	0.643	0.67
Brevantherum	Brevantherum	mauritianum_9	mauritianum	bm000900303	2.725	0.604	0.92	0.947
na	na	mautianum_6	mauritianum	e00112904	2.415	0.876	0.711	0.93
na	na	mautianum_7	mauritianum	e00112904	2.382	0.672	0.748	0.98
Dulcamaroid	Dulcamaroid	maximowiczii_1	dulcamara	bm00847001	2.312	0.781	0.662	0.97
Potato	Petota	medians_1	medians	bm_001134766	6.42	1.098	1.111	1.686
Potato	Petota	medians_2	medians	bm_001134766	5.234	0.962	1.183	1.884
Potato	Petota	medians_3	medians	bm_001134792	4.283	0.905	1.273	1.56
Potato	Petota	medians_4	medians	bm_001134789	5.106	1.084	1.982	2.075
Potato	Petota	medians_5	medians	bm_001134750	4.913	0.907	1.528	1.782
Potato	Petota	medians_6	medians	bm_001134789	4.219	1.136	1.557	1.931
Potato	Petota	megistacrolobum_	megistacrolobum	bm_000516962	4.667	0.732	1.385	1.654
Potato	Petota	megistacrolobum_	megistacrolobum	bm_000516962	4.739	0.93	1.518	2.118
Potato	Petota	megistacrolobum_	megistacrolobum	bm_000516962	4.79	1.045	1.012	1.867

major_clade	clade	sample_name	species	herbarium code	anther length/mm	tip width/mm	base width/mm	middle width/mm
Potato	Petota	megistacrolobum_	megistacrolobum	bm_000887756	4.66	1.177	1.335	1.996
Leptostemonum	old_world	melongena-_1	melongena	living	6.348	0.504	0.615	0.96
Leptostemonum	old_world	melongena-_10	melongena	e00112818	7.787	0.783	1.295	1.708
Leptostemonum	old_world	melongena-_11	melongena	e00112818	8.075	0.821	1.963	2.432
Leptostemonum	old_world	melongena-_12	melongena	e00112818	8.433	0.776	1.82	2.475
Leptostemonum	old_world	melongena-_2	melongena	e00112818	4.179	0.683	0.636	1.336
Leptostemonum	old_world	melongena-_3	melongena	bm00847000	6.186	0.705	0.623	1.217
Leptostemonum	old_world	melongena-_4	melongena	bm00847000	6.415	0.751	0.632	1.336
Leptostemonum	old_world	melongena-_6	melongena	bm000942854	8.153	1.035	1.073	1.746
Leptostemonum	old_world	melongena-_7	melongena	bm000942854	6.241	1.174	0.892	1.498
Leptostemonum	old_world	melongena-_8	melongena	e00112818	7.465	0.854	1.268	1.646
m_clade	Morelloid	memphiticium_2	memphiticum	e00112820	1.811	0.586	0.385	0.754
m_clade	Morelloid	memphiticium_3	memphiticum	e00112820	1.433	0.451	0.449	0.626
m_clade	Morelloid	memphiticium_4	memphiticum	e00320656	1.713	0.423	0.396	0.532
m_clade	Morelloid	memphiticium_6	memphiticum	e00320656	1.794	0.576	0.284	0.511
na	na	metarsium_1	sinuatirecurvum	e00182716	4.157	0.798	0.539	1.121
na	na	metarsium_2	sinuatirecurvum	e00182716	3.509	0.869	0.835	1.255
m_clade	Morelloid	michaelneei_1	michaelneei	missouri__3414739	2.486	0.318	0.795	0.93
m_clade	Morelloid	michaelneei_10	michaelneei	new_york_00852718	2.439	0.422	0.601	0.585
m_clade	Morelloid	michaelneei_3	michaelneei	missouri__3414739	3.158	0.661	1.053	1.389
m_clade	Morelloid	michaelneei_6	michaelneei	missouri__3414737	2.571	0.496	0.482	0.645
m_clade	Morelloid	michaelneei_7	michaelneei	missouri__3414737	2.598	0.459	0.857	0.911
m_clade	Morelloid	michaelneei_8	michaelneei	new_york_00852718	2.166	0.658	0.809	0.939
m_clade	Morelloid	michaelneei_9	michaelneei	new_york_00852718	2.595	0.566	0.532	0.686
Potato	Pteroidea_Herpysti	mite_1	mite	bm_000935136	1.4	0.586	0.422	0.975
Potato	Pteroidea_Herpysti	mite_4	mite	bm_000887771	1.077	0.616	0.5	0.673
Potato	Pteroidea_Herpysti	mite_5	mite	bm_000887771	0.93	0.496	0.508	0.68
Leptostemonum	Androceras_Crinitu	mitlense_1	mitlense	e00526500	9.286	0.693	1.115	1.995
Leptostemonum	Androceras_Crinitu	mitlense_1	mitlense	BM00848378	10.924	0.774	1.216	2.221
Leptostemonum	Androceras_Crinitu	mitlense_2	mitlense	e00526500	10.224	0.743	0.64	1.577
Leptostemonum	Micracantha	monachophyllum_	monachophyllum	bm_000887772	6.869	0.416	0.866	0.971
na	na	mscrothyrsum_(sp	macrothyrsum	bm000887183	3.268	0.858	0.846	1.942
Potato	Regmandra	multifidum_2	multifidum	bm_000886399	2.842	0.619	0.539	0.832
Potato	Regmandra	multifidum_3	multifidum	bm_000886287	2.972	0.742	0.766	1.115
Potato	Regmandra	multifidum_4	multifidum	bm_000886287	3.179	0.789	1.006	1.316
Potato	Regmandra	multifidum_5	multifidum	bm_001070246	3.838	0.639	0.658	1.054
Potato	Regmandra	multifidum_7	multifidum	bm_001070246	3.786	0.379	0.559	0.628
Potato	Petota	multiinterruptum_	multiinterruptum	bm_000887779	4.621	1.032	1.012	1.546
Potato	Petota	multiinterruptum_	multiinterruptum	bm_001134746	6.071	1.083	1.463	2.19
Potato	Petota	multiinterruptum_	multiinterruptum	bm_001134748	6.445	0.854	0.956	1.584
Potato	Petota	multiinterruptum_	multiinterruptum	bm_001134748	5.826	1.087	1.021	1.047
Potato	Petota	multiinterruptum_	multiinterruptum	bm_001134807	7.294	0.611	1.603	1.886
Potato	Petota	multiinterruptum_	multiinterruptum	bm_001134807	6.185	0.794	1.129	1.435
Potato	Petota	multiinterruptum_	multiinterruptum	bm_000887779	5.177	1.058	1.142	1.571
Potato	Petota	multiinterruptum_	multiinterruptum	bm_001134796	6.401	1.125	1.508	1.656
Potato	Petota	multiinterruptum_	multiinterruptum	bm_001034728	7.443	1.179	1.558	2.204
Potato	Petota	multiinterruptum_	multiinterruptum	bm_001034728	6.348	1.076	1.455	2.196
Potato	Petota	multiinterruptum_	multiinterruptum	bm_001134687	7.817	0.851	1.81	1.654
Potato	Petota	multiinterruptum_	multiinterruptum	bm_001134747	6.56	1.124	1.408	2.001
Potato	Petota	multiinterruptum_	multiinterruptum	bm_001134746	6.926	0.938	1.257	2.063
Potato	Basarthrum	muricatum_1	muricatum	bm_000887780	3.492	0.896	0.803	1.073
Potato	Basarthrum	muricatum_2	muricatum	bm_00072743	4.175	0.731	0.596	1.477
Potato	Basarthrum	muricatum_3	muricatum	bm_000795843	3.251	0.904	0.718	0.944
m_clade	African_non_spiny	myrsinoides_1	myrsinoides	missouri_n'4367010	6.324	0.742	1.162	1.694
Leptostemonum	Anguivi	NAcapense	NAcapense	e00621053	4.918	0.525	1.066	1.118
na	na	NAterminale	terminale	bm000847803	4.381	0.705	0.523	0.977
m_clade	Normania	nava_feeding_antl	nava	bm000070494	3.167	0.439	0.224	0.715
m_clade	Normania	nava_pollinating_	nava_pollinating	bm000070494	6.615	0.503	0.63	0.821
m_clade	Normania	nava_pollinating_	nava_pollinating	bm000070492	9.578	0.471	1.212	1.415
Potato	Tomato	neorickii_anther_1	neorickii	bm_000848324	3.933	0.286	0.732	0.74
m_clade	Morelloid	nigrescens_1	nigrescens	e00106080	2.501	0.907	0.621	0.673
m_clade	Morelloid	nigrescens_2	nigrescens	e00106080	2.427	0.827	0.308	0.654
m_clade	Morelloid	nigrescens_3	nigrescens	e00125318	2.621	0.539	0.367	0.865
m_clade	Morelloid	nigrescens_4	nigrescens	e00125318	3.319	0.503	0.465	0.796
m_clade	Morelloid	nigrum_1	nigrum	bm000900347	2.05	0.645	0.541	0.664
m_clade	Morelloid	nigrum_10	nigrum	bm000900039	2.444	0.561	0.494	0.83
m_clade	Morelloid	nigrum_11	nigrum	bm000900039	2.263	0.654	0.457	0.756
m_clade	Morelloid	nigrum_12	nigrum	bm000900036	1.711	0.608	0.559	0.731
m_clade	Morelloid	nigrum_13	nigrum	bm000900026	1.931	0.603	0.523	0.758
m_clade	Morelloid	nigrum_15	nigrum	bm000900033	1.808	0.508	0.476	0.643
m_clade	Morelloid	nigrum_17	nigrum	bm000900056	2.533	0.624	0.49	0.844
m_clade	Morelloid	nigrum_18	nigrum	bm000900301	2.05	0.347	0.326	0.449
m_clade	Morelloid	nigrum_19	nigrum	bm000900301	2.211	0.551	0.351	0.611
m_clade	Morelloid	nigrum_20	nigrum	bm000900054	1.954	0.586	0.423	0.785
m_clade	Morelloid	nigrum_21	nigrum	bm000900054	1.967	0.566	0.422	0.82
m_clade	Morelloid	nigrum_22	nigrum	bm000900054	2.06	0.547	0.536	0.705
m_clade	Morelloid	nigrum_23	nigrum	bm000900044	1.401	0.588	0.468	0.778
m_clade	Morelloid	nigrum_24	nigrum	bm000900044	1.539	0.439	0.468	0.7
m_clade	Morelloid	nigrum_25	nigrum	bm000900347	2.189	0.704	0.64	0.885
m_clade	Morelloid	nigrum_26	nigrum	live	2.446	0.594	0.766	0.881
m_clade	Morelloid	nigrum_27	nigrum	live	2.597	0.655	0.604	0.871
m_clade	Morelloid	nigrum_28	nigrum	live	2.455	0.559	0.763	0.928
m_clade	Morelloid	nigrum_29	nigrum	e00112826	1.66	0.539	0.389	0.677
m_clade	Morelloid	nigrum_30	nigrum	e00112825	1.884	0.443	0.439	0.654
m_clade	Morelloid	nigrum_31	nigrum	e00112825	1.72	0.611	0.5	0.8
m_clade	Morelloid	nigrum_32	nigrum	e00112824	1.328	0.413	0.387	0.723
m_clade	Morelloid	nigrum_33	nigrum	e00112823	1.229	0.608	0.336	0.558
m_clade	Morelloid	nigrum_4	nigrum	bm000900050	1.789	0.54	0.446	0.636
m_clade	Morelloid	nigrum_6	nigrum	bm000900050	1.837	0.535	0.718	0.748
m_clade	Morelloid	nigrum_7	nigrum	e00593504	2.536	1.154	1.37	1.538
m_clade	Morelloid	nigrum_8	nigrum	e00593504	3.025	0.754	0.905	1.695
m_clade	Morelloid	nigrum_9	nigrum	e00593516	2.187	0.577	1.321	1.699
m_clade	Morelloid	nitidibaccatum	nitidibaccatum	e00593447	1.931	0.558	0.869	0.82
m_clade	Morelloid	nitidibaccatum	nitidibaccatum	e00593447	2.04	0.288	0.886	0.964
m_clade	Morelloid	nitidibaccatum	nitidibaccatum	e00593447	2.077	0.411	1	1.825
m_clade	Morelloid	nitidibaccatum_bi	nitidibaccatum	bm001207447	1.654	0.416	0.355	0.438
m_clade	Morelloid	nitidibaccatum_bi	nitidibaccatum	bm001207447	1.719	0.382	0.267	0.53
m_clade	Morelloid	nitidibaccatum_bi	nitidibaccatum	bm001207447	1.861	0.432	0.422	0.586

major_clade	clade	sample_name	species	herbarium code	anther length/mm	tip width/mm	base width/mm	middle width/mm
m_clade	Morelloid	nitidibaccatum_bi	nitidibaccatum	bm001207447	1.682	0.275	0.551	0.677
m_clade	Morelloid	nitidibaccatum_bi	nitidibaccatum	bm001207446	2.062	0.42	0.407	0.645
m_clade	Morelloid	nitidibaccatum_bi	nitidibaccatum	bm001207446	1.996	0.465	0.304	0.566
m_clade	Morelloid	nitidibaccatum_bi	nitidibaccatum	bm001207448	1.455	0.246	0.389	0.608
m_clade	Morelloid	nitidibaccatum_bi	nitidibaccatum	bm001207448	1.954	0.366	0.308	0.566
m_clade	Morelloid	nitidibaccatum_bi	nitidibaccatum	bm001207448	1.619	0.301	0.251	0.585
m_clade	Morelloid	nitidibaccatum_bi	nitidibaccatum	bm001207450	1.654	0.366	0.329	0.482
m_clade	Morelloid	nitidibaccatum_bi	nitidibaccatum	bm001207447	2.071	0.447	0.475	0.547
m_clade	Dulcamaroid	nitidum_1	nitidum	P00366844	3.08	0.67	0.67	0.62
m_clade	Dulcamaroid	nitidum_3	nitidum	e00096028	2.658	0.715	0.818	0.998
m_clade	Dulcamaroid	nitidum_4	nitidum	e00096028	2.891	0.671	0.742	1.04
Geminata	Geminata	nudum_1	nudum	bm_846627	2.269	0.733	0.979	1.287
Geminata	Geminata	nudum_2	nudum	bm_000887833	3.171	1.067	1.033	1.393
Geminata	Geminata	nudum_3	nudum	bm_000795401	2.187	0.885	0.827	1.115
Geminata	Geminata	nudum_4	nudum	bm_000547015	2.795	0.894	0.955	1.308
Geminata	Geminata	nudum_6	nudum	bm_000072664	4.494	0.886	1.468	1.849
Geminata	Geminata	nudum_7	nudum	bm_000072664	4.154	1.054	0.958	1.875
Geminata	Geminata	nudum_8	nudum	bm_000072666	4.619	0.816	1.334	2.333
Geminata	Geminata	nudum_9	nudum	bm_000058817	5.537	1.182	0.718	1.596
Geminata	Geminata	nutans_1	nutans	bm_000887836	3.192	0.835	0.697	1.078
Geminata	Geminata	nutans_11	nutans	bm_000934882	4.602	0.887	0.656	1.446
Geminata	Geminata	nutans_13	nutans	bm_001120829	4.416	1.012	1.818	2.492
Geminata	Geminata	nutans_2	nutans	bm_000887836	3.504	0.874	0.818	1.201
Geminata	Geminata	nutans_5	nutans	bm_000849192	4.155	0.963	0.876	1.543
Geminata	Geminata	nutans_8	nutans	bm_000795405	4.862	1.249	0.939	1.366
Cyphomandra	Cyphomandra	obliquum_1	obliquum	bm_000777990	4.929	0.773	1.152	1.585
Cyphomandra	Cyphomandra	obliquum_2	obliquum	bm_000839471	5.295	0.983	1.006	1.369
Geminata	Geminata	oblongifolium_1	oblongifolium	bm_000887843	4.858	1.278	0.853	1.961
Geminata	Geminata	oblongifolium_10	oblongifolium	bm_00072789	3.678	0.773	0.993	1.833
Geminata	Geminata	oblongifolium_11	oblongifolium	bm_00072789	3.778	1.158	0.929	2.142
Geminata	Geminata	oblongifolium_12	oblongifolium	bm_000846628	3.659	1.035	0.881	1.61
Geminata	Geminata	oblongifolium_2	oblongifolium	bm_000887843	5.21	1.075	0.997	1.926
Geminata	Geminata	oblongifolium_4	oblongifolium	bm_000887855	5.352	1.207	1.694	2.2
Geminata	Geminata	oblongifolium_5	oblongifolium	bm_000887855	4.595	1.319	1.076	1.647
Geminata	Geminata	oblongifolium_7	oblongifolium	bm_000887856	3.601	1.208	1.36	1.988
Geminata	Geminata	oblongifolium_8	oblongifolium	bm_00072732	3.018	0.743	0.894	1.646
Geminata	Geminata	oblongifolium_9	oblongifolium	bm_00072789	3.863	0.747	0.83	1.493
m_clade	Morelloid	opacum_1	opacum	bm000886117	1.174	0.465	0.396	0.501
m_clade	Morelloid	opacum_2	opacum	bm000886117	1.469	0.53	0.382	0.616
m_clade	Morelloid	opacum_3	opacum	bm000886117	1.144	0.465	0.277	0.501
m_clade	Morelloid	opacum_4	opacum	bm000886229	1.808	0.473	0.406	0.594
m_clade	Morelloid	opacum_5	opacum	bm000886229	1.418	0.355	0.404	0.355
m_clade	Morelloid	opacum_7	opacum	bm000886229	1.616	0.454	0.577	0.811
m_clade	Morelloid	opacum_8	opacum	bm000886229	1.805	0.535	0.396	0.712
na	incertaeNAsedis	orbignyianum	orbignianum	duke10005052	3.352	0.775	0.924	1.058
Potato	Anarrhichomenum	oxycoccoides_3	oxycoccoides	field_museum_of_na	4.316	0.559	0.811	1.158
m_clade	Morelloid	palitans_1	palitans	e00125340	1.32	0.508	0.369	0.517
m_clade	Morelloid	palitans_2	palitans	e00125341	1.406	0.404	0.503	0.733
m_clade	Morelloid	palitans_6	palitans	e00125340	1.515	0.494	0.468	0.664
m_clade	Morelloid	pallidum_2	pallidum	e00526047	3.114	0.561	0.581	0.838
m_clade	Morelloid	pallidum_3	pallidum	e00526047	3.652	0.754	0.632	1.015
Leptostemonum	old_world	papaverifolium_1	papaverifolium	bm001035312	4.708	0.888	1.168	1.493
Potato	Regmandra	paposanum	paposanum	e00096029	4.218	0.737	0.853	1.208
Potato	Regmandra	paposanum	paposanum	e00096029	4.357	0.907	0.955	1.36
Potato	Regmandra	paposanum_1	paposanum	calafornia_n'18113	1.97	0.766	0.861	1.229
Potato	Regmandra	paposanum_3	paposanum	e00230406	3.219	0.75	0.599	1.309
Potato	Regmandra	paposanum_5	paposanum	e00230406	3.743	0.85	0.727	1.137
na	na	pedunculare_1	Lycianthes pedur	e0112829	3.131	0.547	1.323	1.366
Leptostemonum	old_world	peekelii_1	peekelii	bm000886237	3.687	0.522	0.494	0.683
Potato	Tomato	penellii_1	penelliiNA	bm001120801	5.765	1.181	0.682	0.798
Potato	Tomato	penellii_2	penelliiNA	bm000848321	5.314	0.956	0.558	1.6
m_clade	Morelloid	pentlandii_1	pentlandii	e00106313	1.737	0.637	0.448	0.821
m_clade	Morelloid	pentlandii_2	pentlandii	e00106313	2.056	0.651	0.543	0.815
m_clade	Morelloid	pentlandii_4	pentlandii	e00106313	1.667	0.676	0.509	0.827
Potato	Tomato	peruvianum_anthe	peruvianum	bm000777770	9.893	0.512	0.917	1.404
Potato	Tomato	peruvianum_anthe	peruvianum	bm000943215	7.407	0.427	0.786	1.358
Potato	Tomato	peruvianum_anthe	peruvianum	bm000943215	7.347	0.402	0.985	1.078
Potato	Tomato	peruvianum_anthe	peruvianum	bm000943399	7.472	0.361	0.808	1.205
Potato	Tomato	peruvianum_anthe	peruvianum	bm000943399	7.405	0.468	0.997	1.131
Potato	Tomato	peruvianum_anthe	peruvianum	bm000943400	9.27	0.159	0.997	1.322
Potato	Tomato	peruvianum_anthe	peruvianum	bm000943400	9.818	0.344	1.065	1.63
Potato	Tomato	peruvianum_anthe	peruvianum	bm000943215	7.385	0.434	1	1.91
Leptostemonum	old_world	petrophilum_1	petrophilum	bm000846827	4.062	0.864	0.788	1.491
m_clade	Morelloid	physalifolium_1	physalifolium	cambridge_herbariun	2.093	0.459	0.413	0.463
m_clade	Morelloid	physalifolium_2	physalifolium	cambridge_herbariun	1.825	0.471	0.45	0.555
m_clade	Morelloid	physalifolium_3	physalifolium	cambridge_herbariun	2.057	0.547	0.735	0.813
m_clade	Morelloid	physalifolium_4	physalifolium	cambridge_herbariun	2.192	0.596	0.529	0.754
Potato	Tomato	pimpinellifolium_	pimpinellifolium	bm0000849171	6.166	0.346	0.718	0.677
Potato	Regmandra	pinnatum_1	pinnatum	e00125324	3.629	0.694	0.871	1.006
Potato	Regmandra	pinnatum_11	pinnatum	e00182426	2.204	0.611	0.778	1.214
Potato	Regmandra	pinnatum_12	pinnatum	e00182426	3.046	0.957	0.566	1.419
Potato	Regmandra	pinnatum_13	pinnatum	e00182426	3.121	0.977	0.774	1.27
Potato	Regmandra	pinnatum_15	pinnatum	e00183656	3.714	1.002	0.898	1.349
Potato	Regmandra	pinnatum_16	pinnatum	e00183656	4.086	0.811	0.714	1.514
Potato	Regmandra	pinnatum_17	pinnatum	e00125324	4.438	0.775	0.805	0.982
Potato	Regmandra	pinnatum_18	pinnatum	e00125324	4.602	0.694	0.597	1.062
Potato	Regmandra	pinnatum_19	pinnatum	e00125328	2.839	0.624	0.568	0.828
Potato	Regmandra	pinnatum_2	pinnatum	e00027328	3.239	0.843	1.089	1.466
Potato	Regmandra	pinnatum_21	pinnatum	e00125328	3.287	0.823	0.743	1.007
Potato	Regmandra	pinnatum_22	pinnatum	e00125328	3.575	0.705	0.841	1.015
Potato	Regmandra	pinnatum_23	pinnatum	e00125328	3.068	0.795	0.643	1.1
Potato	Regmandra	pinnatum_24	pinnatum	e00125328	3.199	0.616	0.696	0.847
Potato	Regmandra	pinnatum_25	pinnatum	e00125328	3.21	0.654	0.687	0.947
Potato	Regmandra	pinnatum_26	pinnatum	e00125328	2.895	0.608	0.628	0.952
Potato	Regmandra	pinnatum_28	pinnatum	e00125321	4.673	0.77	0.53	1.069
Potato	Regmandra	pinnatum_29	pinnatum	e00125321	3.819	0.887	0.724	1.371
Potato	Regmandra	pinnatum_31	pinnatum	e00125321	3.67	0.711	0.632	1.414
Potato	Regmandra	pinnatum_33	pinnatum	e00212843	3.682	0.83	0.604	1.372
Potato	Regmandra	pinnatum_34	pinnatum	e00212843	3.228	0.572	0.724	1.322
Potato	Regmandra	pinnatum_36	pinnatum	e00212843	3.684	0.99	0.711	1.299

major_clade	clade	sample_name	species	herbarium code	anther length/mm	tip width/mm	base width/mm	middle width/mm
Potato	Regmandra	pinnatum_37	pinnatum	e00212843	3.107	0.803	0.457	1.133
Potato	Regmandra	pinnatum_38	pinnatum	e00212843	3.918	0.732	0.775	1.694
Potato	Regmandra	pinnatum_40	pinnatum	e00212817	3.657	0.766	1.062	1.575
Potato	Regmandra	pinnatum_41	pinnatum	e00212817	3.924	0.544	0.98	1.708
Potato	Regmandra	pinnatum_43	pinnatum	e00212817	3.045	0.523	0.592	1.258
Potato	Regmandra	pinnatum_44	pinnatum	e00212817	3.597	0.676	0.547	1.117
Potato	Regmandra	pinnatum_45	pinnatum	e00112919	3.357	0.608	0.697	1.139
Potato	Regmandra	pinnatum_46	pinnatum	e00112919	3.809	0.578	0.769	1.21
Potato	Regmandra	pinnatum_47	pinnatum	e00057564	3.725	0.594	0.83	1.015
Potato	Regmandra	pinnatum_48	pinnatum	e00057564	3.8	0.634	0.645	1.385
Potato	Regmandra	pinnatum_49	pinnatum	e00057564	3.443	0.711	0.687	1.376
Potato	Regmandra	pinnatum_50	pinnatum	e00125325	3.577	0.947	0.892	1.319
Potato	Regmandra	pinnatum_51	pinnatum	e00125325	3.232	0.819	0.879	0.873
Potato	Regmandra	pinnatum_53	pinnatum	e00125326	3.476	0.563	0.769	1.223
Potato	Regmandra	pinnatum_54	pinnatum	e00125326	3.366	0.667	0.586	1.227
Potato	Regmandra	pinnatum_55	pinnatum	e00125326	3.727	0.756	0.695	1.297
Potato	Regmandra	pinnatum_56	pinnatum	e00125326	3.862	0.751	0.761	1.179
Potato	Regmandra	pinnatum_58	pinnatum	e00125327	3.62	0.726	0.726	1.29
Potato	Regmandra	pinnatum_7	pinnatum	e00125322	3.524	0.829	0.673	1.097
Potato	Regmandra	pinnatum_8	pinnatum	e00125322	3.642	0.721	0.559	1.212
m_clade	Dulcamaroid	pittosporifolium_1	pittosporifolium	bm00942325	2.858	0.584	0.383	0.664
m_clade	Dulcamaroid	pittosporifolium_2	pittosporifolium	bm000943412	2.824	0.832	0.45	0.923
m_clade	Dulcamaroid	pittosporifolium_3	pittosporifolium	bm00942325_	2.876	0.558	0.522	1.077
m_clade	Dulcamaroid	pittosporifolium_4	pittosporifolium	bm000943412	2.714	0.885	0.396	0.877
m_clade	Dulcamaroid	pittosporifolium_5	pittosporifolium	bm000943412	2.712	0.639	0.816	1.046
m_clade	Dulcamaroid	pittosporifolium_7	pittosporifolium	bm000943412	2.766	0.694	0.79	1.169
Leptostemonum	old_world	platacanthum_1	platacanthum	e00144736	4.203	0.558	0.385	0.642
Leptostemonum	old_world	platacanthum_2	platacanthum	e00044084	4.052	0.481	1.299	1.665
Leptostemonum	old_world	platacanthum_5	platacanthum	bm000942675	5.001	0.444	0.554	0.947
Leptostemonum	old_world	platacanthum_6	platacanthum	bm000942253	4.544	0.484	0.541	0.993
na	na	polygamum_1	polygamum	e00112832	1.717	0.582	0.838	0.809
na	na	polygamum_2	polygamum	e00112832	2.409	1.071	0.811	1.282
m_clade	Morelloid	polytrichostylum	polytrichostylum	bm_000887287	2.991	0.547	0.506	0.917
m_clade	Morelloid	polytrichostylum	polytrichostylum	bm_000887287	3.221	0.536	0.682	0.743
m_clade	Morelloid	polytrichostylum	polytrichostylum	bm_000887287	3.05	0.5	0.695	1.003
Leptostemonum	old_world	praetermissum_1	praetermissum	bm000886099	8.025	0.577	0.848	1.088
Leptostemonum	old_world	praetermissum_2	praetermissum	bm000886099	7.159	0.574	0.732	1.023
Leptostemonum	old_world	praetermissum_3	praetermissum	bm000886099	8.029	0.476	1.156	1.387
Leptostemonum	old_world	procumbens	procumbens	bm00942492	3.123	0.55	0.726	1.467
Leptostemonum	old_world	procumbens_1	procumbens	bm00942492	5.12	0.699	0.616	1.065
Leptostemonum	old_world	procumbens_2	procumbens	bm00942492	4.743	0.602	0.686	1.031
Leptostemonum	old_world	procumbens_3	procumbens	bm00942492	4.936	0.478	0.481	1.008
Geminata	Geminata	pseudocapsicum_	pseudocapsicum	16198CGE	2.997	0.751	0.794	1.076
Geminata	Geminata	pseudocapsicum_	pseudocapsicum	e00112837	2.878	0.597	0.516	1.332
Geminata	Geminata	pseudocapsicum_	pseudocapsicum	e00112834	3.114	0.83	0.599	1.348
Geminata	Geminata	pseudocapsicum_	pseudocapsicum	bm000900307	2.646	0.852	0.775	1.381
Geminata	Geminata	pseudocapsicum_	pseudocapsicum	bm000900307	3	1.083	0.963	1.548
Geminata	Geminata	pseudocapsicum_	pseudocapsicum	e00262013	2.729	0.777	1.616	1.89
Geminata	Geminata	pseudocapsicum_	pseudocapsicum	e00057531	2.517	0.985	0.457	1.07
Geminata	Geminata	pseudocapsicum_	pseudocapsicum	e00057531	2.189	0.888	0.766	1.197
Geminata	Geminata	pseudocapsicum_	pseudocapsicum	bm000900307	2.761	0.886	0.779	1.417
Geminata	Geminata	pseudocapsicum_	pseudocapsicum	e00114909	2.563	0.907	0.711	1.426
Geminata	Geminata	pseudocapsicum_	pseudocapsicum	e00112833	2.284	0.793	1.073	1.321
Geminata	Geminata	pseudocapsicum_	pseudocapsicum	e00112835	2.972	0.816	0.735	1.5
Geminata	Geminata	pseudocapsicum_	pseudocapsicum	e00112836	2.224	0.532	0.594	0.939
Geminata	Geminata	pseudocapsicum_	pseudocapsicum	e00112833	2.576	0.955	0.619	1.127
Geminata	Geminata	pseudocapsicum_	pseudocapsicum	e00112837	3.128	0.854	0.803	1.171
Geminata	Geminata	pseudocapsicum_	pseudocapsicum	e00112837	2.988	0.684	0.533	1.193
Geminata	Geminata	pseudocapsicum_	pseudocapsicum	e00112833	2.695	0.623	0.731	1.2
Leptostemonum	old_world	pubescens_3	pubescens	bm000942689	5.461	1.164	1.17	1.942
m_clade	Morelloid	pygmaeum_1	pygmaeum	e00057539	2.807	0.86	0.602	1.321
m_clade	Morelloid	pygmaeum_10	pygmaeum	e00057539	3.612	0.587	0.53	1.091
m_clade	Morelloid	pygmaeum_2	pygmaeum	e00057538	2.774	0.571	0.597	0.843
m_clade	Morelloid	pygmaeum_3	pygmaeum	e00057502	3.575	0.673	0.547	0.861
m_clade	Morelloid	pygmaeum_5	pygmaeum	e00057539	3.523	0.958	0.55	1.278
m_clade	Morelloid	pygmaeum_6	pygmaeum	e00057538	2.662	1.082	0.773	1.287
m_clade	Morelloid	pygmaeum_7	pygmaeum	e00057502	3.23	0.536	0.499	0.63
m_clade	Morelloid	pygmaeum_8	pygmaeum	e00057505	2.295	0.639	0.566	0.683
m_clade	Morelloid	pygmaeum_9	pygmaeum	e00057508	2.963	0.712	0.529	1.045
Leptostemonum	old_world	pyracanthos_3	pyracanthos	e00112849	6.575	0.475	0.803	1.179
na	na	pyracanthum_1	pyracanthos	E00112848	7.917	0.36	0.594	0.979
Leptostemonum	Lasiocarpa	quitoense_2	quitoense	bm000942883	9.22	0.544	1.963	2.03
m_clade	Morelloid	radicans_1	radicans	bm000846516	1.861	0.413	0.365	0.619
m_clade	Morelloid	radicans_3	radicans	bm000846174	2.012	0.612	0.505	0.789
m_clade	Morelloid	radicans_5	radicans	bm000846174	2.159	0.749	0.465	0.935
Wendlandii_Allophy	Wendlandii_Allopl	refractum_1	refractum	e00526484	3.986	0.766	0.756	1.35
Wendlandii_Allophy	Wendlandii_Allopl	refractum_1	refractum	E00526484	4.888	0.561	1.196	1.192
Potato	Regmandra	remyanum_1	remyanum	e00230430	3.75	0.578	0.673	1.288
Potato	Regmandra	remyanum_10	remyanum	e00014515	1.992	0.816	0.499	0.914
Potato	Regmandra	remyanum_11	remyanum	e00014515	1.794	0.742	0.587	0.973
Potato	Regmandra	remyanum_12	remyanum	e00014515	1.817	0.816	0.532	0.931
Potato	Regmandra	remyanum_13	remyanum	e00114931	2.765	0.769	0.406	0.906
Potato	Regmandra	remyanum_14	remyanum	e00114931	3.117	0.736	0.518	1.037
Potato	Regmandra	remyanum_15	remyanum	e00125343	2.72	0.895	0.97	1.254
Potato	Regmandra	remyanum_16	remyanum	e00125343	3.116	0.864	0.637	1.257
Potato	Regmandra	remyanum_4	remyanum	e00057548	3.308	0.658	0.607	1.012
Potato	Regmandra	remyanum_5	remyanum	e00057548	2.989	0.946	0.566	1.169
Potato	Regmandra	remyanum_6	remyanum	e00057548	2.951	0.843	0.599	1.564
Potato	Regmandra	remyanum_7	remyanum	e00112921	4.163	0.611	0.721	1.129
Potato	Regmandra	remyanum_8	remyanum	e00112921	3.878	0.624	1.035	1.231
Potato	Regmandra	remyanum_9	remyanum	e00112921	3.929	0.619	0.908	1.223
Leptostemonum	Erythrotrichum	robustum_1	robustum	bm000847032	6.624	0.616	1.429	1.41
Leptostemonum	Androceras_Crinitu	rostratum_dunal_2	rostratum	GH00077533	5.66	0.45	0.51	0.45
Leptostemonum	Androceras_Crinitu	rostratum_dunal_3	rostratum	16190CGE	8.222	0.49	1.127	0.714
Leptostemonum	Androceras_Crinitu	rostratum_dunal_7	rostratum	bm000846177	8.861	0.555	0.731	1.336
Leptostemonum	Torva	rudepannum_1	rudepannum	e00526493	2.152	0.878	0.646	0.809
Leptostemonum	Torva	rudepannum_1	rudepannum	E00526493	2.396	0.936	0.791	1.065
m_clade	African_non_spiny	runsoriense_1	runsoriense	bm000847515	3.284	0.7	0.481	1.125

major_clade	clade	sample_name	species	herbarium code	anther length/mm	tip width/mm	base width/mm	middle width/mm
m_clade	African_non_spiny	runsoriense_2	runsoriense	bm000847515	3.394	0.639	0.935	1.141
m_clade	African_non_spiny	runsoriense_3	runsoriense	bm000847515	2.614	0.508	0.5	1.018
m_clade	Morelloid	salicifolium_11	salicifolium	e00057554	3.644	0.478	0.896	0.912
m_clade	Morelloid	salicifolium_14	salicifolium	n'2137529	4.345	0.758	0.821	1.363
m_clade	Morelloid	salicifolium_2	salicifolium	e00057510	3.909	0.952	0.711	1.234
m_clade	Morelloid	salicifolium_3	salicifolium	e00057510	3.862	0.779	0.571	0.805
m_clade	Morelloid	salicifolium_4	salicifolium	e00057510	4.427	0.737	0.779	0.841
m_clade	Morelloid	salicifolium_6	salicifolium	e00057537	3.769	0.709	0.517	0.843
m_clade	Morelloid	salicifolium_7	salicifolium	e00057537	3.531	0.731	0.751	1.135
m_clade	Morelloid	salicifolium_8	salicifolium	e00057537	4.508	0.723	0.93	1.307
m_clade	Morelloid	salicifolium_9	salicifolium	e00057554	3.812	0.723	1.034	1.225
m_clade	African_non_spiny	sambiranense_10	sambiranense	p00352337	4.909	0.739	0.754	1.251
m_clade	African_non_spiny	sambiranense_11	sambiranense	g00006890	4.853	0.75	0.779	1.418
m_clade	African_non_spiny	sambiranense_12	sambiranense	g00006890	5.542	0.658	1.052	1.824
m_clade	African_non_spiny	sambiranense_13	sambiranense	g00006890	4.465	0.7	0.928	1.637
m_clade	African_non_spiny	sambiranense_15	sambiranense	g00090461	4.043	0.687	1.077	1.979
m_clade	African_non_spiny	sambiranense_16	sambiranense	g00090461	4.434	0.603	1.136	1.801
m_clade	African_non_spiny	sambiranense_17	sambiranense	g00376126	5.28	0.993	0.715	1.849
m_clade	African_non_spiny	sambiranense_18	sambiranense	g00376126	4.947	0.821	0.826	1.938
m_clade	African_non_spiny	sambiranense_19	sambiranense	g00376126	4.935	0.714	0.754	1.785
m_clade	African_non_spiny	sambiranense_5	sambiranense	p00352326	3.488	0.876	0.866	1.754
m_clade	African_non_spiny	sambiranense_6	sambiranense	p00352326	3.465	0.882	0.952	1.594
m_clade	African_non_spiny	sambiranense_7	sambiranense	missouri_n'3033184	3.703	0.654	0.762	1.259
m_clade	African_non_spiny	sambiranense_8	sambiranense	missouri_n'3033184	4.053	0.517	0.599	1.172
m_clade	African_non_spiny	sambiranense_9	sambiranense	p00352337	4.235	0.351	0.754	1.435
m_clade	African_non_spiny	sambiranense_ma	macrothyrsum	g00443673	3.539	0.756	1.059	2.039
m_clade	African_non_spiny	sambiranense_ma	macrothyrsum	g00443673	3.702	1.148	0.928	2.592
m_clade	African_non_spiny	sambiranense_ma	macrothyrsum	g00443673	3.581	1.138	0.993	2.305
m_clade	African_non_spiny	sambiranense_ma	madagascariens	g00443670	3.792	0.972	0.923	1.419
m_clade	African_non_spiny	sambiranense_ma	madagascariens	g00443637	2.778	0.673	1.016	1.5
m_clade	African_non_spiny	sambiranense_ma	madagascariens	g00443641	2.144	0.726	0.646	1.066
m_clade	African_non_spiny	sambiranense_ma	madagascariens	g00443430	2.837	0.862	1.226	1.36
m_clade	African_non_spiny	sambiranense_ma	madagascariens	g00075357	3.495	0.907	0.827	1.355
m_clade	African_non_spiny	sambiranense_ma	madagascariens	g00075358	2.442	0.667	0.673	1.098
m_clade	African_non_spiny	sambiranense_ma	madagascariens	g00075358	3.143	0.664	0.663	1.214
m_clade	African_non_spiny	sambiranense_ma	madagascariens	g00443664	2.318	0.779	0.654	1.135
m_clade	African_non_spiny	sambiranense_ma	madagascariens	g00443664	2.45	0.839	0.845	1.089
m_clade	African_non_spiny	sambiranense_ma	madagascariens	g00443670	4.133	0.624	0.601	1.276
m_clade	African_non_spiny	sambiranense_ma	madagascariens	g00443670	3.609	0.541	0.816	1.36
m_clade	Dulcamaroid	sanchez-vegae_10	sanchez-vegae	bm001034720	4.241	0.737	1.081	1.441
m_clade	Dulcamaroid	sanchez-vegae_11	sanchez-vegae	bm001034720	4.603	0.751	0.95	1.232
m_clade	Dulcamaroid	sanchez-vegae_20	sanchez-vegae	bm000849364	3.815	1.013	1.174	1.297
m_clade	Dulcamaroid	sanchez-vegae_22	sanchez-vegae	bm000849364	4.126	1.033	1.12	1.169
m_clade	Dulcamaroid	sanchez-vegae_24	sanchez-vegae	bm000849364	4.074	0.877	1.037	1.162
m_clade	Dulcamaroid	sanchez-vegae_25	sanchez-vegae	bm000849364	4.389	0.865	0.955	1.181
m_clade	Dulcamaroid	sanchez-vegae_26	sanchez-vegae	bm000849364	4.427	1.059	1.223	1.666
m_clade	Dulcamaroid	sanchez-vegae_27	sanchez-vegae	bm000939134	5.257	0.977	0.997	1.601
m_clade	Dulcamaroid	sanchez-vegae_28	sanchez-vegae	bm000939134	5.974	0.693	0.828	1.66
m_clade	Dulcamaroid	sanchez-vegae_29	sanchez-vegae	bm000939134	5.443	1.039	1.236	1.568
m_clade	Dulcamaroid	sanchez-vegae_3	sanchez-vegae	bm000939131	4.555	1.049	1.11	1.558
m_clade	Dulcamaroid	sanchez-vegae_5	sanchez-vegae	bm000939131	4.612	0.966	0.907	1.515
m_clade	Dulcamaroid	sanchez-vegae_7	sanchez-vegae	bm001134315	5.192	0.811	1.374	1.92
m_clade	Dulcamaroid	sanchez-vegae_9	sanchez-vegae	bm001134315	4.951	0.736	1.458	1.606
NA	NA	sandwichense_1	sandwichense	BM000846696	2.898	0.568	0.763	0.864
Leptostemonum	Torva	saponaceum_1	saponaceum	bm001120983	8.259	0.781	1.076	1.296
Leptostemonum	Torva	saponaceum_10	saponaceum	bm001114764	10.082	0.499	0.879	1.033
Leptostemonum	Torva	saponaceum_13	saponaceum	bm001114764	10.543	0.462	1.154	1.292
Leptostemonum	Torva	saponaceum_14	saponaceum	bm001114763	8.825	0.438	0.83	1.131
Leptostemonum	Torva	saponaceum_16	saponaceum	bm001114763	9.416	0.436	1.028	1.284
Leptostemonum	Torva	saponaceum_17	saponaceum	bm001070162	7.81	0.539	1.23	1.313
Leptostemonum	Torva	saponaceum_20	saponaceum	bm000846247	8.508	0.427	1.016	1.251
Leptostemonum	Torva	saponaceum_23	saponaceum	bm000934944	7.078	0.382	1.075	1.133
Leptostemonum	Torva	saponaceum_24	saponaceum	bm000934944	5.014	0.358	0.916	0.854
Leptostemonum	Torva	saponaceum_25	saponaceum	bm000934945	5.858	0.427	1.283	1.131
Leptostemonum	Torva	saponaceum_26	saponaceum	bm000934945	5.832	0.608	1.297	1.395
Leptostemonum	Torva	saponaceum_27	saponaceum	bm000934945	6.64	0.697	1.189	1.46
Leptostemonum	Torva	saponaceum_28	saponaceum	bm000846536	6.444	0.576	0.594	0.904
Leptostemonum	Torva	saponaceum_4	saponaceum	bm001134665	7.061	0.5	1.211	1.423
Leptostemonum	Torva	saponaceum_5	saponaceum	bm000849371	9.513	0.585	1.022	1.214
Leptostemonum	Torva	saponaceum_6	saponaceum	bm000849371	9.648	0.576	1.148	1.488
m_clade	Morelloid	sarrachoides_1	sarrachoides	e00057527	1.896	0.365	0.327	0.481
m_clade	Morelloid	sarrachoides_2	sarrachoides	e00057527	1.256	0.487	0.408	0.438
m_clade	Morelloid	sarrachoides_3	sarrachoides	e00057527	1.659	0.414	0.34	0.603
m_clade	Morelloid	sarrachoides_7	sarrachoides	bm000942888	2.094	0.471	0.681	0.747
m_clade	Morelloid	sarrachoides_8	sarrachoides	bm000942888	2.181	0.577	0.72	0.993
m_clade	Morelloid	sarrachoides_9	sarrachoides	bm000942143	1.78	0.766	0.581	0.766
Leptostemonum	Torva	saturatum_m.nee_	saturatum	bm000849326	9.376	0.651	1.352	1.6
Potato	Pteroidea_Herpysti	savanillense_bitte	savanillense	bm000943661	2.097	0.439	0.63	1.147
Potato	Pteroidea_Herpysti	savanillense_bitte	savanillense	bm000943661	2.174	0.562	0.667	1.115
Potato	Pteroidea_Herpysti	savanillense_bitte	savanillense	bm000943661	2.288	0.653	0.651	1.115
Potato	Pteroidea_Herpysti	savanillense_bitte	savanillense	bm000887976	2.49	0.779	0.773	1.265
Leptostemonum	old_world	schimperianum_1	schimperianum	P00341767	3.96	1.17	0.82	0.9
Leptostemonum	old_world	schimperianum_1	schimperianum	bm000942695	4.801	0.749	0.628	1.035
Leptostemonum	old_world	schimperianum_1	schimperianum	bm000942695	4.859	0.861	0.781	1.109
Leptostemonum	old_world	schimperianum_2	schimperianum	e00621036	4.733	0.811	0.904	1.144
Leptostemonum	old_world	schimperianum_3	schimperianum	e00621038	4.19	0.675	0.313	0.422
Leptostemonum	old_world	schimperianum_4	schimperianum	e00621037	4.692	0.697	0.25	0.404
Brevantherum	Brevantherum	schlechtendalianu	schlechtendaliar	bm000887984	2.448	0.697	0.653	1.147
Brevantherum	Brevantherum	schlechtendalianu	schlechtendaliar	bm000887984	2.331	0.482	0.637	0.887
Brevantherum	Brevantherum	schlechtendalianu	schlechtendaliar	bm000943655	2.354	0.682	0.653	0.845
m_clade	Dulcamaroid	seaforthianum_10	seaforthianum	bm000887926	2.771	0.803	1.08	1.531
m_clade	Dulcamaroid	seaforthianum_12	seaforthianum	bm000887926	2.718	0.888	1.135	1.475
m_clade	Dulcamaroid	seaforthianum_13	seaforthianum	bm000887989	2.676	0.964	0.987	1.329
m_clade	Dulcamaroid	seaforthianum_14	seaforthianum	bm000887989	2.984	1.069	0.749	1.147
m_clade	Dulcamaroid	seaforthianum_15	seaforthianum	bm000887989	2.619	1.046	0.706	1.24
m_clade	Dulcamaroid	seaforthianum_16	seaforthianum	bm000887997	2.919	1.103	0.818	1.511
m_clade	Dulcamaroid	seaforthianum_17	seaforthianum	bm000887997	2.877	0.811	0.79	0.882
m_clade	Dulcamaroid	seaforthianum_18	seaforthianum	bm000887997	2.805	0.955	0.708	1.169
m_clade	Dulcamaroid	seaforthianum_19	seaforthianum	bm000887997	2.628	1.163	0.789	1.292

major_clade	clade	sample_name	species	herbarium code	anther length	tip width	base width	middle width
m_clade	Dulcamaroid	seaforthianum_2	seaforthianum	NY00689169	2.91	1.09	0.86	1.38
m_clade	Dulcamaroid	seaforthianum_20	seaforthianum	bm000887997	2.641	0.629	0.536	1.17
m_clade	Dulcamaroid	seaforthianum_21	seaforthianum	bm000887995	2.483	1.004	0.919	0.858
m_clade	Dulcamaroid	seaforthianum_22	seaforthianum	bm000900331	2.785	0.774	0.937	1.236
m_clade	Dulcamaroid	seaforthianum_23	seaforthianum	bm000900331	2.821	0.669	0.882	1.247
m_clade	Dulcamaroid	seaforthianum_25	seaforthianum	bm000900331	3.207	0.922	0.785	1.326
m_clade	Dulcamaroid	seaforthianum_26	seaforthianum	bm000847036	3.019	0.811	0.981	1.5
m_clade	Dulcamaroid	seaforthianum_27	seaforthianum	bm000847036	3.124	0.858	0.914	1.455
m_clade	Dulcamaroid	seaforthianum_28	seaforthianum	bm000847036	3.39	1.066	0.864	1.283
m_clade	Dulcamaroid	seaforthianum_29	seaforthianum	bm000847036	3.314	0.997	1.119	1.301
m_clade	Dulcamaroid	seaforthianum_4	seaforthianum	bm000887993	1.929	0.998	0.801	1.2
m_clade	Dulcamaroid	seaforthianum_6	seaforthianum	bm000887993	2.215	1.195	0.905	1.582
m_clade	Dulcamaroid	seaforthianum_7	seaforthianum	bm000887926	2.907	0.953	0.871	1.211
m_clade	Dulcamaroid	seaforthianum_8	seaforthianum	bm000887926	2.714	0.97	0.917	1.587
m_clade	Dulcamaroid	seaforthianum_9	seaforthianum	bm000887926	2.086	0.851	1.24	1.374
Brevantherum	Brevantherum	selachophyllum_1	selachophyllum	bm000846473	2.692	0.752	0.783	1.107
Brevantherum	Brevantherum	selachophyllum_2	selachophyllum	bm000846473	2.678	0.846	0.651	0.967
Brevantherum	Brevantherum	selachophyllum_4	selachophyllum	bm000846473	2.838	0.832	0.602	0.715
Brevantherum	Brevantherum	selachophyllum_6	selachophyllum	bm000888000	2.299	0.793	0.626	1.06
Brevantherum	Brevantherum	selachophyllum_7	selachophyllum	bm000888000	2.442	0.645	0.79	1.009
Brevantherum	Brevantherum	selachophyllum_8	selachophyllum	bm000846472	4.241	1.386	1.737	1.656
Brevantherum	Brevantherum	selachophyllum_9	selachophyllum	bm000846472	3.429	1.195	1.154	1.588
m_clade	Dulcamaroid	septemlobum_11	septemlobum	bm00942505	2.748	0.938	0.68	1.288
m_clade	Dulcamaroid	septemlobum_12	septemlobum	bm00942508	2.48	1.003	0.788	1.077
m_clade	Dulcamaroid	septemlobum_16	septemlobum	bm00942505	2.458	0.651	0.728	0.751
m_clade	Dulcamaroid	septemlobum_18	septemlobum	bm00942502	3.196	0.748	0.629	0.964
m_clade	Dulcamaroid	septemlobum_2	septemlobum	bm00942508	2.779	0.864	0.463	1.009
m_clade	Dulcamaroid	septemlobum_20	septemlobum	bm00942502	3.222	0.712	0.484	1.08
m_clade	Dulcamaroid	septemlobum_22	septemlobum	bm00942509	3.527	0.672	0.596	0.964
m_clade	Dulcamaroid	septemlobum_27	septemlobum	bm00942498	3.102	0.301	0.676	0.835
m_clade	Dulcamaroid	septemlobum_29	septemlobum	bm00942500	2.64	0.779	0.869	1.326
m_clade	Dulcamaroid	septemlobum_31	septemlobum	bm00942511	2.88	0.64	0.385	0.968
m_clade	Dulcamaroid	septemlobum_32	septemlobum	bm00942511	2.632	0.68	0.587	0.921
m_clade	Dulcamaroid	septemlobum_33	septemlobum	bm00942511	2.382	0.559	0.7	0.689
m_clade	Dulcamaroid	septemlobum_4	septemlobum	bm00942509	2.292	0.816	0.643	1.091
m_clade	Dulcamaroid	septemlobum_5	septemlobum	bm00942506	3.251	0.259	0.547	1.088
m_clade	Dulcamaroid	septemlobum_9	septemlobum	bm00942505	2.91	1.02	0.731	1.579
Geminata	Geminata	sieberi_1	sieberi	e00249864	2.665	0.838	0.685	1.25
Geminata	Geminata	sieberi_2	sieberi	e00249864	2.773	0.708	0.663	1.204
m_clade	Morelloid	sinuatirecurvum	sinuatirecurvum	e00125349	2.086	0.62	0.49	0.754
m_clade	Morelloid	sinuatirecurvum	sinuatirecurvum	e00125349	2.517	0.599	0.626	1.204
m_clade	Morelloid	sinuatirecurvum	sinuatirecurvum	e00125349	2.328	0.86	0.655	1.058
Leptostemonum	sisymbriifolium	sisymbriifolium	sisymbriifolium	live	2.067	0.342	0.346	0.368
Leptostemonum	sisymbriifolium	sisymbriifolium	sisymbriifolium	live	2.26	0.492	0.409	0.476
Leptostemonum	sisymbriifolium	sisymbriifolium	sisymbriifolium	live	2.501	0.585	0.43	0.661
Leptostemonum	sisymbriifolium	sisymbriifolium	sisymbriifolium	e00125352	2.388	0.534	0.439	0.501
Leptostemonum	sisymbriifolium	sisymbriifolium	sisymbriifolium	e00125352	2.253	0.525	0.443	0.551
Leptostemonum	sisymbriifolium	sisymbriifolium	sisymbriifolium	e00125352	2.128	0.626	0.449	0.411
Leptostemonum	sisymbriifolium	sisymbriifolium	sisymbriifolium	e00125352	2.147	0.505	0.469	0.539
Leptostemonum	Sisymbriifolium	sisymbriifolium_1	sisymbriifolium	e00125352	6.383	0.655	0.658	1.227
Leptostemonum	Sisymbriifolium	sisymbriifolium_1	sisymbriifolium	bm000847027	9.169	0.547	0.803	1.309
Leptostemonum	Sisymbriifolium	sisymbriifolium_1	sisymbriifolium	bm000900328	7.019	0.89	0.732	1.591
Leptostemonum	Sisymbriifolium	sisymbriifolium_1	sisymbriifolium	bm000900327	7.188	0.83	1.251	1.971
Leptostemonum	Sisymbriifolium	sisymbriifolium_2	sisymbriifolium	e00426649	7.875	0.682	0.734	1.401
Leptostemonum	Sisymbriifolium	sisymbriifolium_3	sisymbriifolium	e00125351	8.345	0.569	1.156	1.897
Leptostemonum	Sisymbriifolium	sisymbriifolium_4	sisymbriifolium	e00112913	9.389	0.938	1.231	1.866
Leptostemonum	Sisymbriifolium	sisymbriifolium_5	sisymbriifolium	e00112913	9.824	0.811	1.138	1.563
Leptostemonum	Sisymbriifolium	sisymbriifolium_6	sisymbriifolium	e00112913	9.824	0.811	1.138	1.563
Leptostemonum	Sisymbriifolium	sisymbriifolium_7	sisymbriifolium	e00112913	9.588	0.866	1.047	1.675
Leptostemonum	Sisymbriifolium	sisymbriifolium_8	sisymbriifolium	e00125350	7.13	0.867	1.139	1.86
Leptostemonum	Sisymbriifolium	sisymbriifolium_9	sisymbriifolium	bm000900329	10.257	0.709	1.275	1.565
Potato	Tomato	sitiens_2	sitiens	e00230407	4.914	0.827	0.732	1.45
Geminata	Geminata	spirale_1	spirale	bm000900073	3.914	1.265	0.766	1.557
Geminata	Geminata	spirale_12	spirale	bm000942517	2.85	0.891	0.72	1.531
Geminata	Geminata	spirale_13	spirale	bm000942517_	2.965	0.676	0.626	1.336
Geminata	Geminata	spirale_5	spirale	bm000900072	3.262	1.138	0.816	1.404
Geminata	Geminata	spirale_7	spirale	bm000942518	3.899	0.92	0.828	1.105
Geminata	Geminata	spirale_9	spirale	bm000942518	3.673	0.821	0.75	1.219
Potato	Petota	stoloniferum_1	stoloniferum	E00129601	3.999	0.826	0.752	1.019
Potato	Petota	stoloniferum_1	stoloniferum	E00129601	5.174	0.879	2.084	1.707
Potato	Petota	stoloniferum_2	stoloniferum	e00129579	3.639	0.827	0.838	1.301
Potato	Petota	stoloniferum_4	stoloniferum	e00129601	3.363	0.792	0.748	0.955
Potato	Petota	stoloniferum_5	stoloniferum	e00129601	4.001	0.672	0.949	1.076
Potato	Petota	stoloniferum_6	stoloniferum	e00129601	4.235	0.789	1.008	1.214
Leptostemonum	Micracantha	tampicense_1	tampicense	E00526138	4.554	0.463	0.923	0.838
na	na	terminale	terminale	bm000847803	3.965	0.761	0.757	0.937
m_clade	African_non_spiny	terminale_1	terminale	g00443458	4.479	1.4	0.797	1.508
m_clade	African_non_spiny	terminale_11	terminale	g00386367	4.326	2.411	1.698	2.292
m_clade	African_non_spiny	terminale_12	terminale	g00386367	4.326	0.74	0.821	1.029
m_clade	African_non_spiny	terminale_13	terminale	g00386367	4.234	0.904	0.519	0.846
m_clade	African_non_spiny	terminale_14	terminale	g00443445	4.604	0.608	0.646	1.158
m_clade	African_non_spiny	terminale_2	terminale	g00443458	4.231	1.328	0.79	1.508
m_clade	African_non_spiny	terminale_8	terminale	g00443455	2.803	1.304	0.779	1.319
Leptostemonum	Gardneri	tetramerum_1	tetramerum	E00526139	7.692	0.558	0.751	0.809
Leptostemonum	old_world	tomentosum_1	tomentosum	17197CGE	3.792	0.748	0.709	1.293
Leptostemonum	old_world	tomentosum_2	tomentosum	17197CGE	3.788	0.482	0.448	0.666
Leptostemonum	old_world	tomentosum_3	tomentosum	17197CGE	3.829	0.673	0.529	0.847
Leptostemonum	Torva	torvum_1	torvum	17209CGE	6.189	0.518	0.62	0.861
Leptostemonum	Torva	torvum_10	torvum	bm001034945	4.301	0.487	0.626	0.676
Leptostemonum	Torva	torvum_11	torvum	bm001034944	7.169	0.462	0.692	0.766
Leptostemonum	Torva	torvum_16	torvum	bm001034941	5.917	0.543	0.795	1.145
Leptostemonum	Torva	torvum_19	torvum	bm000900158	5.789	0.547	0.586	0.725
Leptostemonum	Torva	torvum_2	torvum	bm000900158	5.826	0.635	0.952	0.864
Leptostemonum	Torva	torvum_22	torvum	bm000900160	5.547	0.469	0.735	0.763
Leptostemonum	Torva	torvum_23	torvum	bm000900160	6.289	0.468	0.723	0.805
Leptostemonum	Torva	torvum_24	torvum	bm000900160	5.642	0.508	0.857	1.049
Leptostemonum	Torva	torvum_28	torvum	bm000900180	6.527	0.545	0.786	0.966
Leptostemonum	Torva	torvum_29	torvum	bm000900180	6.535	0.49	0.705	0.686

major_clade	clade	sample_name	species	herbarium code	anther length/mm	tip width/mm	base width/mm	middle width/mm
Leptostemonum	Torva	torvum_3	torvum	bm000900173	6.325	0.651	0.764	0.898
Leptostemonum	Torva	torvum_31	torvum	bm000900173	5.727	0.49	0.637	0.847
Leptostemonum	Torva	torvum_32	torvum	bm000900173	4.782	0.542	0.603	0.711
Leptostemonum	Torva	torvum_33	torvum	bm000900173	5.103	0.432	0.5	0.663
Leptostemonum	Torva	torvum_4	torvum	bm001034945	5.559	0.366	0.434	0.532
Leptostemonum	Torva	torvum_5	torvum	bm001034945	5.041	0.409	0.597	0.621
Leptostemonum	Torva	torvum_6	torvum	bm001034945	5.722	0.361	0.454	0.571
Leptostemonum	Torva	torvum_7	torvum	bm001034945	5.703	0.585	0.581	0.637
Leptostemonum	Torva	torvum_8	torvum	bm001034945	5.636	0.516	0.732	0.654
Leptostemonum	Torva	torvum_9	torvum	bm001034945	6.502	0.422	0.775	0.881
m_clade	African_non_spiny	trichopetiolatum_	trichopetiolatum	p00343459	4.213	0.868	1.372	1.983
m_clade	African_non_spiny	trichopetiolatum_	trichopetiolatum	p00352291	3.132	0.821	0.578	1.175
m_clade	African_non_spiny	trichopetiolatum_	trichopetiolatum	missouri_n'04870184	4.285	0.811	0.637	1.533
m_clade	African_non_spiny	trichopetiolatum_	trichopetiolatum	g00443614	3.61	0.547	0.584	1.113
m_clade	African_non_spiny	trichopetiolatum_	trichopetiolatum	missouri_n'5895760	3.511	0.53	0.68	1.364
m_clade	African_non_spiny	trichopetiolatum_	trichopetiolatum	missouri_n'3684562	3.969	0.69	0.991	1.698
m_clade	African_non_spiny	trichopetiolatum_	trichopetiolatum	missouri_n'3684562	3.573	0.329	1	1.441
m_clade	African_non_spiny	trichopetiolatum_	trichopetiolatum	p00343459	3.907	0.925	1.335	1.919
Leptostemonum	Elaeagnifolium	tridynamum_1	houstonii	G00343357	8.65	0.54	1.2	1.03
Leptostemonum	Elaeagnifolium	tridynamum_2	houstonii	MA604687	8.33	0.97	1.2	1.15
m_clade	Morelloid	triflorum_nutt_1	triflorum	bm001207453	2.031	0.465	0.459	0.535
m_clade	Morelloid	triflorum_nutt_2	triflorum	bm001207453	2.259	0.204	0.409	0.423
m_clade	Morelloid	triflorum_nutt_3	triflorum	bm001207454	2.488	0.379	0.423	0.541
Potato	Regmandra	trinominum_1	trinominum	e00114933	6.346	0.545	0.724	1.109
Potato	Regmandra	trinominum_1	trinominum	e00114933	5.243	0.721	0.778	1.007
Potato	Regmandra	trinominum_3	trinominum	e00114934	5.14	0.653	0.961	1.184
Potato	Regmandra	trinominum_4	trinominum	e00114934	5.942	0.539	0.775	0.981
Potato	Regmandra	trinominum_5	trinominum	e00114933	6.324	0.628	0.544	1.199
na	na	trinum_1	trinominum	e00114933	5.018	0.639	0.925	1.197
m_clade	Morelloid	tripartitum_1	tripartitum	e00094838	1.248	0.619	0.331	0.725
m_clade	Morelloid	tripartitum_2	tripartitum	e00094838	1.332	0.551	0.43	0.714
m_clade	Normania	trisectum_1	trisectum	bm_000072291	7.606	0.654	0.756	1.428
m_clade	Normania	trisectum_2	trisectum	bm_000641870	4.591	0.84	0.961	1.18
Potato	Petota	tuberosum_1	tuberosum	bm000942524	5.914	0.75	1.385	1.673
Potato	Petota	tuberosum_11	tuberosum	bm001207464	6.538	0.987	1.351	1.673
Potato	Petota	tuberosum_4	tuberosum	bm001207463	5.332	1.543	2.024	2.103
Potato	Petota	tuberosum_5	tuberosum	bm001207463	5.508	1.047	1.945	2.088
Potato	Petota	tuberosum_6	tuberosum	bm001207462	6.044	0.739	1.448	1.661
Potato	Petota	tuberosum_7	tuberosum	bm001207462	6.207	1.018	1.241	1.642
Potato	Petota	tuberosum_9	tuberosum	bm001207462	5.922	0.973	1.997	2.342
m_clade	Morelloid	tweedianum_10	tweedianum	e00057533	3.433	0.692	0.808	1.009
m_clade	Morelloid	tweedianum_11	tweedianum	e00057533	4.568	0.404	0.731	1.098
m_clade	Morelloid	tweedianum_12	tweedianum	e00057574	4	0.771	0.778	1.121
m_clade	Morelloid	tweedianum_13	tweedianum	e00057574	4.541	0.929	0.693	0.878
m_clade	Morelloid	tweedianum_14	tweedianum	e00057574	4.096	0.75	0.348	0.888
m_clade	Morelloid	tweedianum_15	tweedianum	e00057530	4.707	0.766	0.695	0.793
m_clade	Morelloid	tweedianum_18	tweedianum	e00057545	4.485	0.697	0.646	0.961
m_clade	Morelloid	tweedianum_19	tweedianum	e00057545	4.014	0.748	0.645	0.993
m_clade	Morelloid	tweedianum_2	tweedianum	e00057540	3.661	0.813	0.792	1.056
m_clade	Morelloid	tweedianum_3	tweedianum	e00057540	4.639	0.898	0.661	0.924
m_clade	Morelloid	tweedianum_5	tweedianum	e00057540	3.818	0.551	0.886	0.912
m_clade	Morelloid	tweedianum_7	tweedianum	e00057540	4.421	0.811	0.899	1.128
m_clade	Morelloid	tweedianum_8	tweedianum	e00057540	4.715	0.786	0.877	1.115
m_clade	Morelloid	tweedianum_9	tweedianum	e00057540	4.052	0.525	0.887	0.769
m_clade	Dulcamaroid	uncinellum_1	uncinellum	P00335286	5.55	0.97	2.51	2.98
m_clade	Dulcamaroid	valdiviense_1	valdiviense	e00114930	2.876	0.653	0.533	1.072
m_clade	Dulcamaroid	valdiviense_10	valdiviense	e00158598	3.121	0.74	0.654	1.321
m_clade	Dulcamaroid	valdiviense_11	valdiviense	e00158598	3	0.539	0.711	1.308
m_clade	Dulcamaroid	valdiviense_12	valdiviense	e00182609	3.219	0.676	0.754	1.326
m_clade	Dulcamaroid	valdiviense_13	valdiviense	e00182609	3.511	0.979	0.608	1.302
m_clade	Dulcamaroid	valdiviense_14	valdiviense	e00182609	3.061	0.827	0.615	1.214
m_clade	Dulcamaroid	valdiviense_15	valdiviense	e00182609	3.685	0.844	0.877	1.257
m_clade	Dulcamaroid	valdiviense_16	valdiviense	e00182609	3.667	0.886	0.808	1.487
m_clade	Dulcamaroid	valdiviense_17	valdiviense	e00182424	3.101	0.712	0.751	1.195
m_clade	Dulcamaroid	valdiviense_18	valdiviense	e00166172	2.876	0.654	0.683	1.309
m_clade	Dulcamaroid	valdiviense_19	valdiviense	e00166172	3.223	0.614	0.597	0.928
m_clade	Dulcamaroid	valdiviense_2	valdiviense	e00114930	2.741	0.654	0.55	0.878
m_clade	Dulcamaroid	valdiviense_20	valdiviense	e00166172	3.1	0.582	0.733	1.463
m_clade	Dulcamaroid	valdiviense_22	valdiviense	e00096093	2.734	0.518	0.494	0.853
m_clade	Dulcamaroid	valdiviense_23	valdiviense	e00125362	3.055	0.792	0.707	1.223
m_clade	Dulcamaroid	valdiviense_24	valdiviense	e00125362	3.152	0.818	0.62	1.062
m_clade	Dulcamaroid	valdiviense_25	valdiviense	e00125362	3.519	0.85	0.619	1.042
m_clade	Dulcamaroid	valdiviense_26	valdiviense	e00125360	3.855	0.865	0.925	1.731
m_clade	Dulcamaroid	valdiviense_27	valdiviense	e00125360	4.403	0.818	0.98	1.408
m_clade	Dulcamaroid	valdiviense_29	valdiviense	e00125360	3.706	0.631	0.566	1.008
m_clade	Dulcamaroid	valdiviense_3	valdiviense	e00167232	3.113	0.74	0.547	1.214
m_clade	Dulcamaroid	valdiviense_30	valdiviense	e00125361	3.826	0.592	0.74	1.056
m_clade	Dulcamaroid	valdiviense_4	valdiviense	e00167232	2.88	0.693	0.667	1.158
m_clade	Dulcamaroid	valdiviense_5	valdiviense	e00167232	2.919	0.603	0.732	1.096
m_clade	Dulcamaroid	valdiviense_6	valdiviense	e00114903	2.893	0.811	0.862	1.237
m_clade	Dulcamaroid	valdiviense_7	valdiviense	e00114903	3.041	0.709	0.706	1.425
m_clade	Dulcamaroid	valdiviense_8	valdiviense	e00158598	3.161	0.751	0.742	1.27
m_clade	Dulcamaroid	valdiviense_9	valdiviense	e00158598	2.996	0.731	0.838	1.432
Leptostemonum	Acanthophora	viarum_1	viarum	bm000942527_	5.028	0.69	1.332	1.553
Leptostemonum	Acanthophora	viarum_11	viarum	bm000900339	6.788	0.462	1.569	1.213
Leptostemonum	Acanthophora	viarum_13	viarum	bm000942525	6.29	0.336	0.947	1.006
Leptostemonum	Acanthophora	viarum_2	viarum	bm001019375	6.626	0.327	0.912	1.237
Leptostemonum	Acanthophora	viarum_5	viarum	bm001034963	8.023	0.413	1.257	1.823
Leptostemonum	Acanthophora	viarum_6	viarum	bm001034965	6.772	0.365	0.966	1.091
Leptostemonum	Acanthophora	viarum_8	viarum	bm001034965	6.738	0.4	0.835	0.988
Leptostemonum	Acanthophora	viarum_9	viarum	bm000847013	6.424	0.402	0.743	1.172
m_clade	Morelloid	villosum	villosum	e00593455	2.679	0.813	0.66	0.952
m_clade	Morelloid	villosum_1	villosum	16187CGE	1.422	0.446	0.742	1.07
m_clade	Morelloid	villosum_10	villosum	bm000900048	1.403	0.535	0.416	0.613
m_clade	Morelloid	villosum_11	villosum	bm000900062	1.29	0.482	0.366	0.577
m_clade	Morelloid	villosum_15	villosum	bm000943784	1.972	0.645	0.37	0.711
m_clade	Morelloid	villosum_2	villosum	e00621078	2.408	0.596	0.992	1.189
m_clade	Morelloid	villosum_22	villosum	bm000942739	1.99	0.577	0.522	0.712

major_clade	clade	sample_name	species	herbarium code	anther length/mm	tip width/mm	base width/mm	middle width/mm
m_clade	Morelloid	villosum_23	villosum	bm000942777	2.402	0.533	0.453	0.682
m_clade	Morelloid	villosum_25	villosum	bm000943785	1.808	0.624	0.385	0.643
m_clade	Morelloid	villosum_27	villosum	bm000943789	2.364	0.528	0.578	0.86
m_clade	Morelloid	villosum_28	villosum	bm000943789	2.368	0.697	0.586	0.853
m_clade	Morelloid	villosum_29	villosum	bm000943762	1.847	0.594	0.534	0.667
m_clade	Morelloid	villosum_3	villosum	e00621076	2.656	0.64	0.689	1.623
m_clade	Morelloid	villosum_31	villosum	bm000943764	3.915	0.731	0.758	1.377
m_clade	Morelloid	villosum_4	villosum	e00621077	2.588	0.632	0.714	1.211
m_clade	Morelloid	villosum_5	villosum	bm000900003	1.75	0.581	0.554	1.058
m_clade	Morelloid	villosum_7	villosum	bm000900027	1.352	0.663	0.457	0.603
m_clade	Morelloid	villosum_8	villosum	bm000900027	1.695	0.592	0.443	0.637
Leptostemonum	Anguivi	virginianum	virginianum	China, unbarcoded NHM	4.871	0.543	0.832	0.957
Leptostemonum	Anguivi	virginianum	virginianum	China, unbarcoded NHM	9.046	0.821	0.838	1.529
Leptostemonum	Anguivi	virginianum	virginianum	China, unbarcoded NHM	4.949	0.307	0.912	1.024
Leptostemonum	Anguivi	virginianum	virginianum	China, unbarcoded NHM	5.933	0.936	1.054	1.345
Leptostemonum	Anguivi	virginianum	virginianum	China, unbarcoded NHM	7.329	1.053	1.351	1.887
Leptostemonum	Anguivi	virginianum	virginianum	China, unbarcoded NHM	7.185	0.87	1.601	2.213
Leptostemonum	old_world	viridifolium_1	viridifolium	bm000900427	4.431	0.487	0.651	1.395
m_clade	Dulcamaroid	viscidissimum	alpinum	bm000778312	2.885	0.715	0.395	0.697
m_clade	Dulcamaroid	viscidissimum	alpinum	bm000778312	2.924	0.848	0.481	1.039
m_clade	Dulcamaroid	viscidissimum	alpinum	bm000778312	2.801	0.635	0.714	1.1
Wendlandii_Allophy	Wendlandii_Allopl	wendlandii_1	wendlandii	bm000900351	9.327	1.205	1.327	1.673
m_clade	Morelloid	woodii_11	woodii	missouri_6203805	2.441	0.607	1.035	1.218
m_clade	Morelloid	woodii_2	woodii	kew_k000788099	3.648	0.631	1.219	1.682
m_clade	Morelloid	woodii_3	woodii	kew_k000788099	2.679	0.68	0.894	1.36
m_clade	Morelloid	woodii_4	woodii	kew_k000788099	3.005	0.423	0.762	1.078
m_clade	Morelloid	woodii_7	woodii	missouri_6203805	2.613	0.653	0.736	0.988
m_clade	Morelloid	woodii_8	woodii	missouri_6203805	2.962	0.574	0.67	0.985
m_clade	Morelloid	woodii_9	woodii	missouri_6203805	2.91	0.521	1.02	1.231
Leptostemonum	old_world	zanzibarense_1	zanzibarense	new_york_00827938	6.107	0.505	0.604	0.862

Appendix 3: Plasmid maps

LV2 CRISPR *MIXTA-4* Knockout.

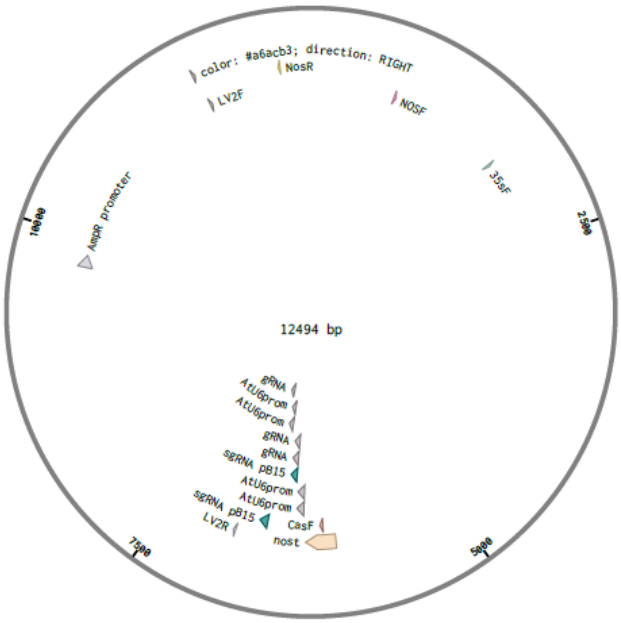

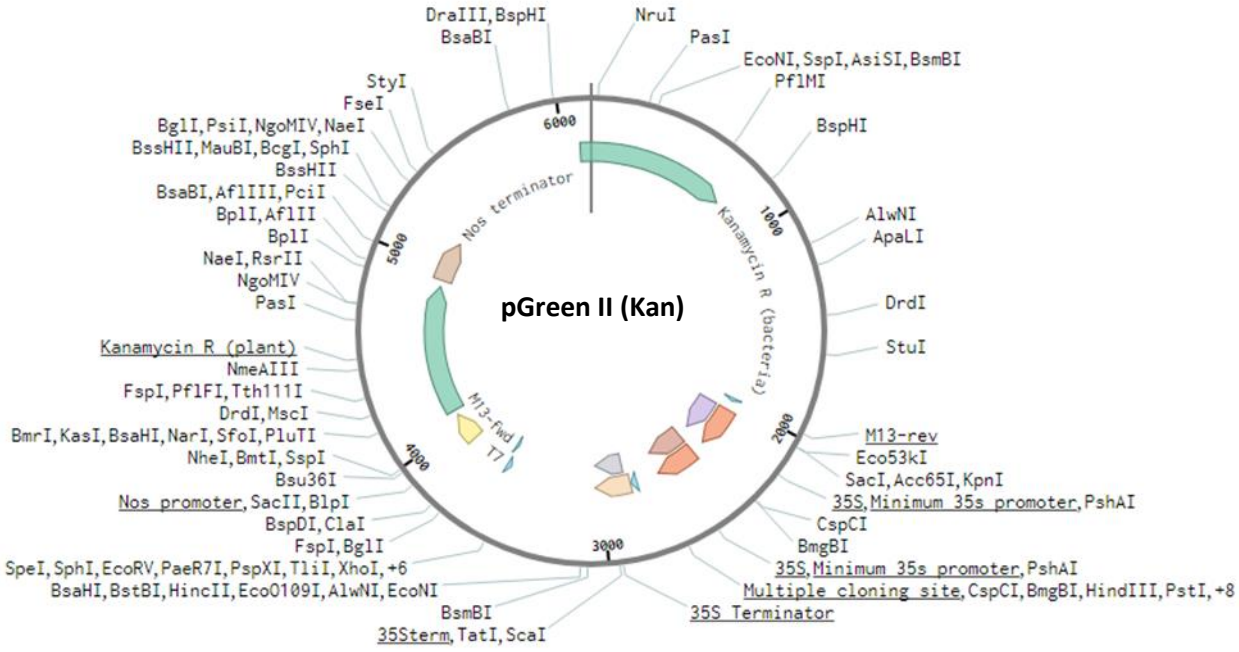

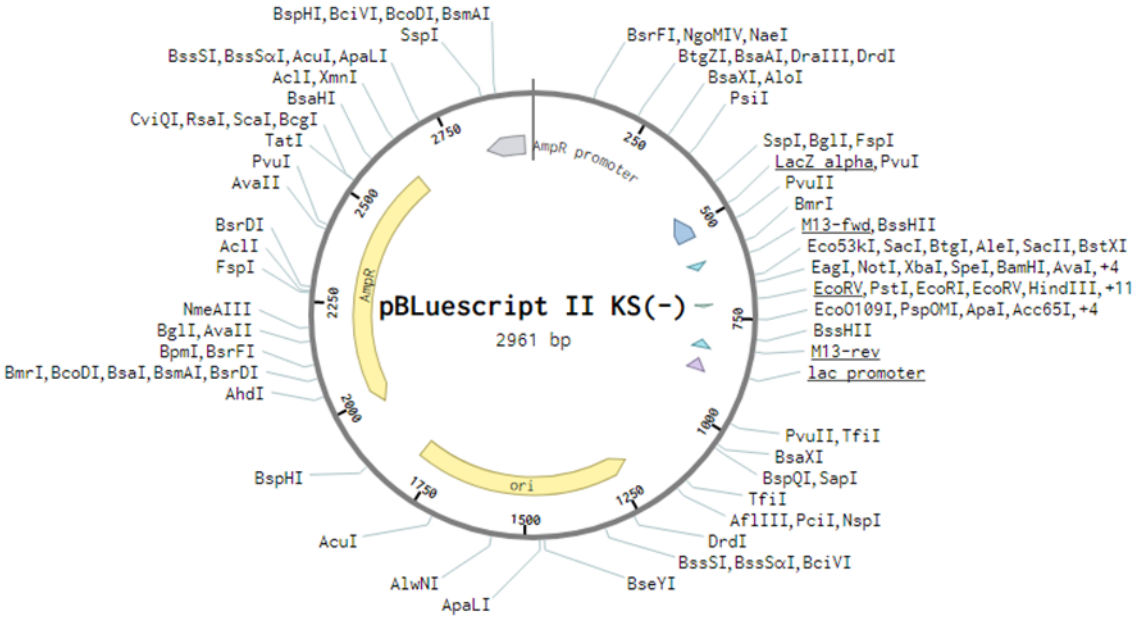
pBLuescript II KS(-)
2961 bp
AmpR promoter
AmpR
ori
250
500
750
1000
1250
1500
1750
2000
2250
2500
2750
BspHI, BciVI, BcoDI, BsmAI
SspI
BssSI, BssSαI, AcuI, ApaLI
AclI, XmnI
BsaHI
CviQI, RsaI, ScaI, BcgI
TatI
PvuI
AvaII
BsrDI
AclI
FspI
NmeAIII
BglI, AvaII
BpmI, BsrFI
BmrI, BcoDI, BsaI, BsmAI, BsrDI
AhdI
BspHI
AcuI
AlwNI
ApaLI
BseYI
BssSI, BssSαI, BciVI
DrdI
AflIII, PciI, NspI
TfiI
BspQI, SapI
BsaXI
PvuII, TfiI
BsrFI, NgoMIV, NaeI
BtgZI, BsaAI, DraIII, DrdI
BsaXI, AloI
PsiI
SspI, BglI, FspI
LacZ alpha, PvuI
PvuII
BmrI
M13-fwd, BssHII
Eco53kI, SacI, BtgI, AleI, SacII, BstXI
EagI, NotI, XbaI, SpeI, BamHI, AvaI, +4
EcoRV, PstI, EcoRI, EcoRV, HindIII, +11
Eco0109I, PspOMI, ApaI, Acc65I, +4
BssHII
M13-rev
lac promoter

Appendix 4: Phylomorphospaces using PC3 and PC4

Solanum:

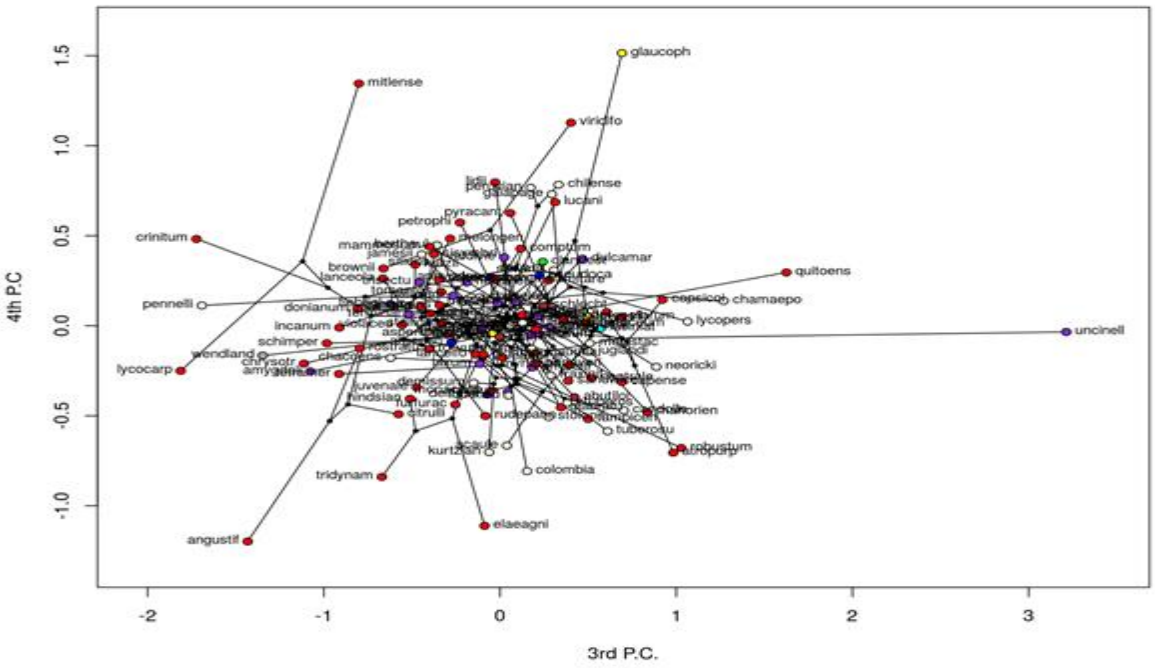

Dulcamaroid clade:

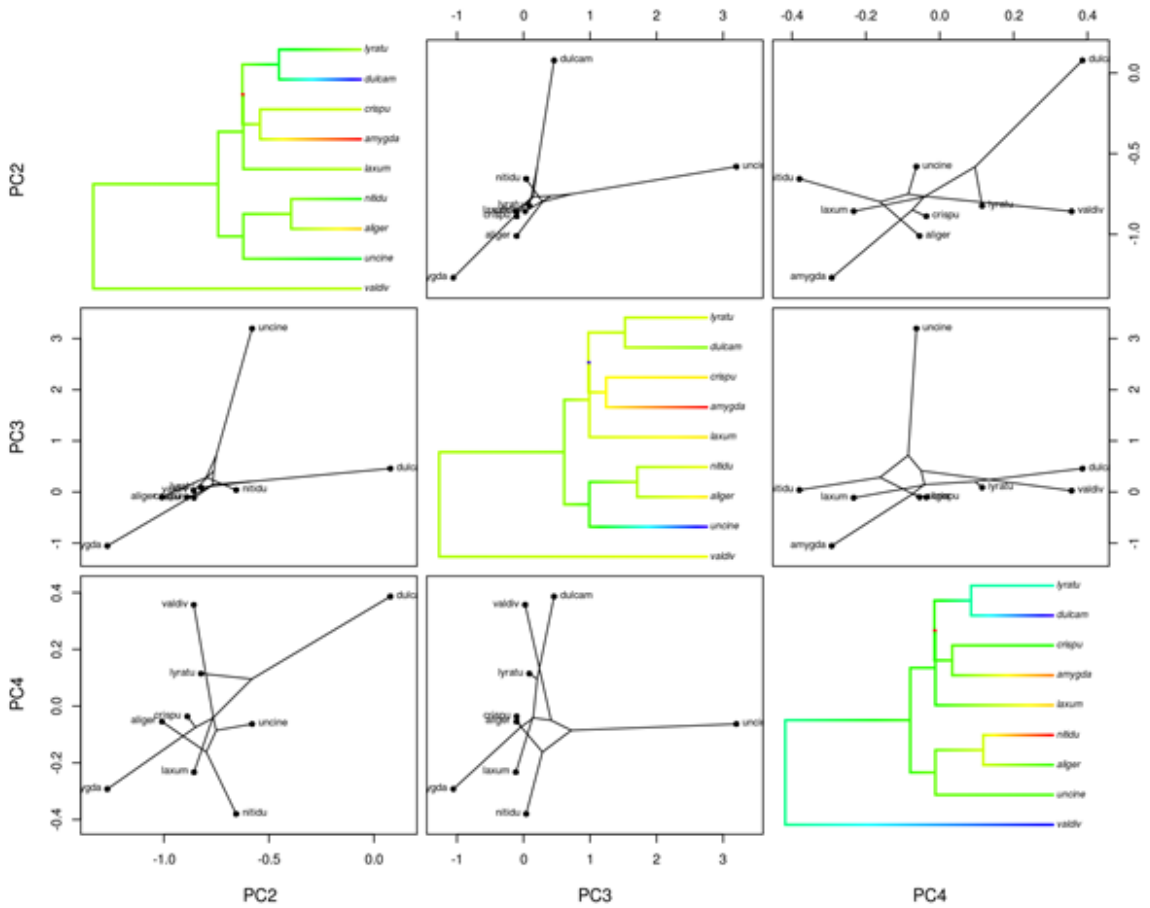

Leptostemonum clade:

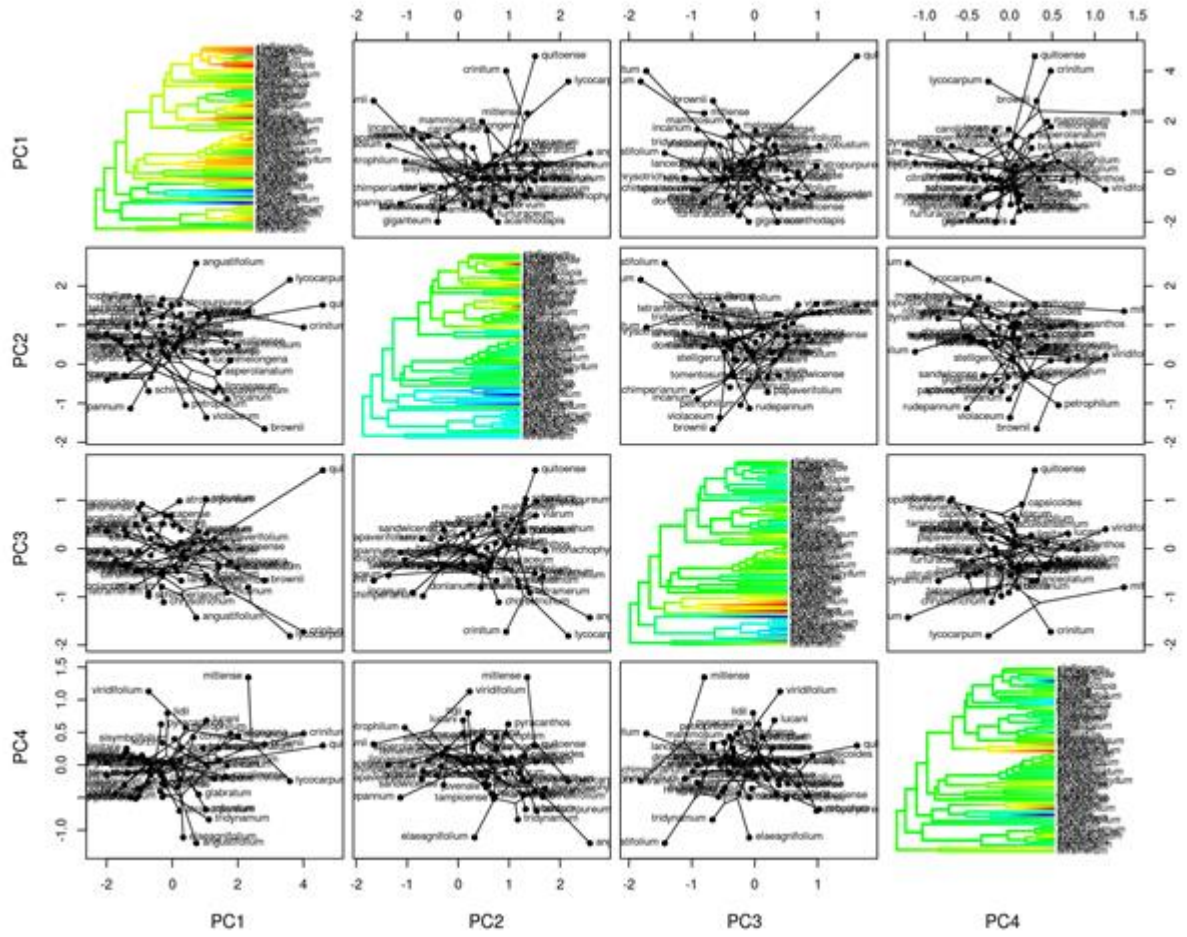

M-Clade

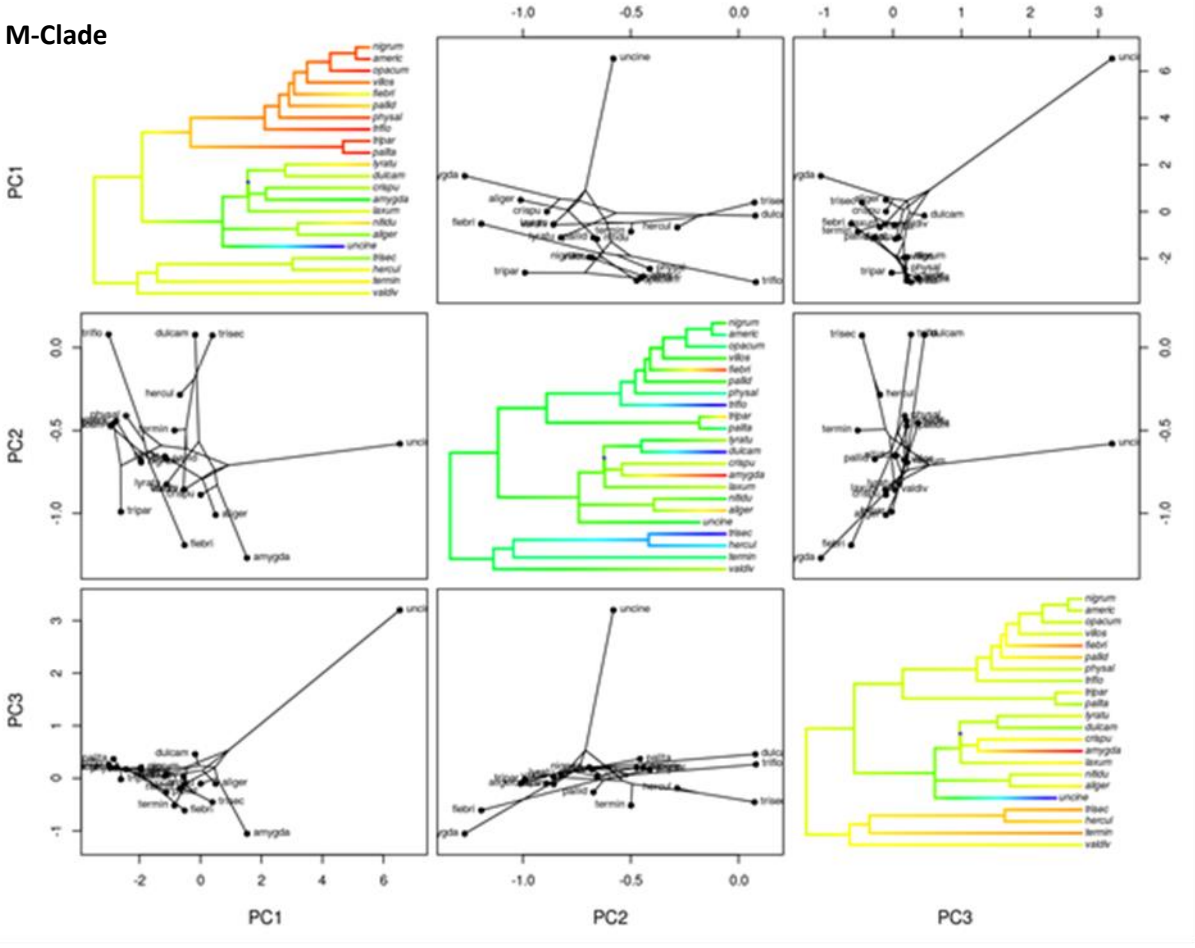

Tomato subclade:

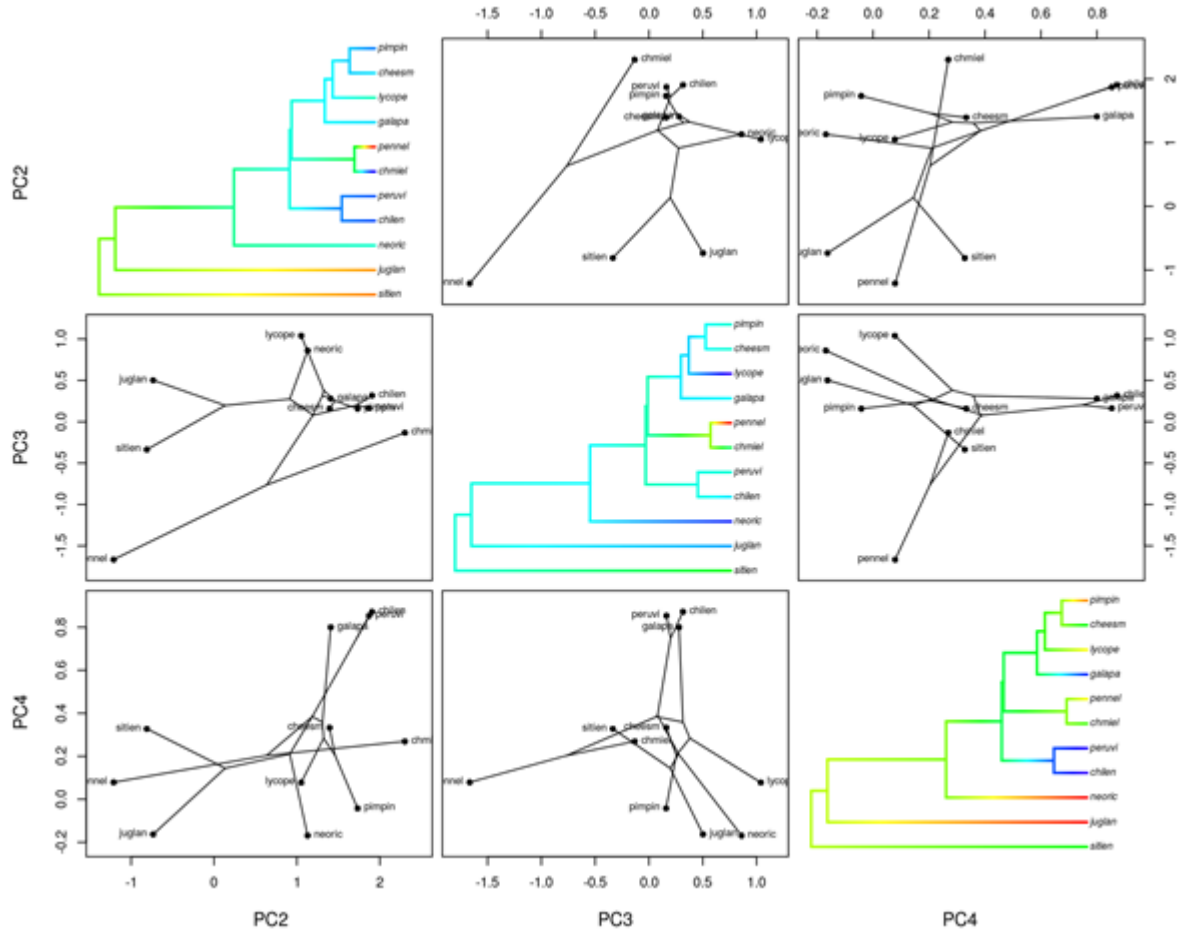

Potato Clade:

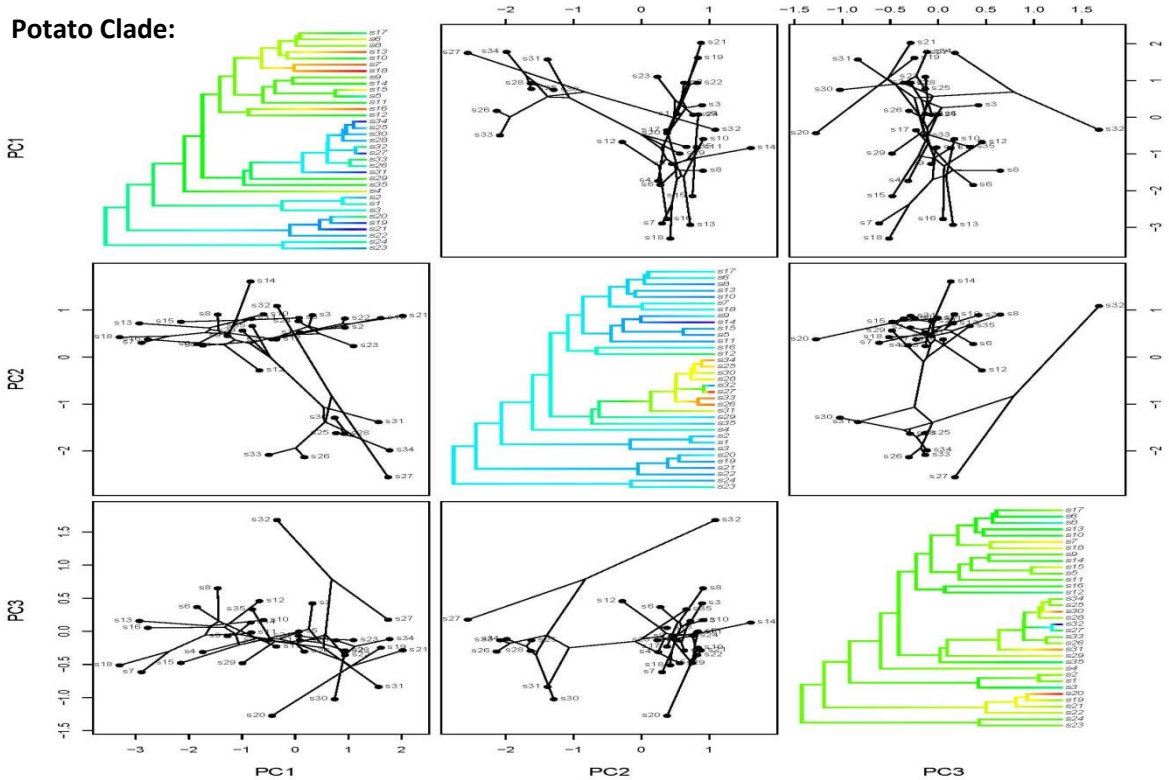

Appendix 5: All species examined using SEM

clade	species	herbarium barcode	epidermal cell outgrowth	outgrowth type	description of outgrowths
Morelloid	palitans	cast and E00125341	yes	Papillae	na
Acanthophora	acerifolium	17210CGE	yes	Papillae	glove-like' papillae, point towards base.
Acanthophora	vaillantii	17222CGE	yes	Papillae	glove-like' papillae, point towards base
Acanthophora	viarum	17223CGE	yes	Papillae	na
African_non_spiny	terminale	BM000942704	yes	Papillae	outgrowths all along length
Androceras_Crinitum	coriaceum	BM001016940	yes	Papillae	outgrowths exaggerated at base along full length
Androceras_Crinitum	mitlense	E00526500 and BM00848378	yes	Papillae	outgrowths only towards base, fade to flat at tip
Archaesolanum	aviculare	E00426870 and cast	yes	Papillae	bubble shaped cell outgrowths
Archaesolanum	simile	E00426896	yes	Papillae	outgrowths at base fade to tip
Basarthrum	muricatum	cast and BM000072743	yes	Papillae	bubble shaped cell outgrowths
Basarthrum	catilliflorum	BM001114765	yes	Papillae	bubble shaped cell outgrowths, full length from base to tip, only on outside
Brevantherum	adscendens	E0019089065	yes	Papillae	na
Brevantherum	cordovens	BM000887459	yes	Papillae	papillae along length
Brevantherum	lepidotum	BM000072713	yes	Papillae	na
Cyphomandra	confusum	BM000887477	yes	Papillae	na
Cyphomandra	luteoalbum	BM000887708	yes	Papillae	papillae fade to tip, more exaggerated towards base and side
Cyphomandra	morellifolium	bm000046748	yes	Papillae	na
Elaeagnifolium	elaeagnifolium	16197CGE	yes	Papillae	na
Gardneri	gardneri	17213CGE	yes	Papillae	na
Geminata	diphyllum	E00112784	yes	Papillae	bubble shaped cell outgrowths
Lasiocarpa	hirtum	E00526405	yes	Papillae	outgrowths at base, fade to tip
Lasiocarpa	lasiocarpum	E00061975	yes	Papillae	outgrowths at base, fade to tip
Lasiocarpa	quitoense	E00112850	yes	Papillae	outgrowths at base only
Lasiocarpa	stoloniferum	E00129601	yes	Papillae	outgrowths on full length
Lasiocarpa	stramoniifolium	E00700933	yes	Papillae	na
Morelloid	fiebrigii	E00269992	yes	Papillae	na
Morelloid	nigrum	cast	yes	Papillae	na
Morelloid	nitidibaccatum	16194CGE	yes	Papillae	bubble shaped cell outgrowths
Morelloid	opacum	E00426993	yes	Papillae	na
Morelloid	riojense	cast	yes	Papillae	na
Morelloid	triflorum	E00057525	yes	Papillae	na
Morelloid	villosum	16187CGE and cast	yes	Papillae	bubble shaped cell outgrowths
old_world	aethiopicum	E00112783	yes	Papillae	outgrowths at base, fade to tip
old_world	anguivi	not barcoded, Edinburgh	yes	Papillae	na
old_world	arundo	E00426739	yes	Papillae	glove-like' papillae
old_world	chenopodinum	E00526985	yes	Papillae	na
old_world	coactiliferum	E00526989	yes	Papillae	na
old_world	coagulans	16202CGE	yes	Papillae	outgrowths at base, fade to tip
old_world	ellipticum	E00610005	yes	Papillae	na
old_world	esuriale	1794CGE	yes	Papillae	bubble shaped cell outgrowths
old_world	furfuraceum	E00610012	yes	Papillae	na
old_world	giganteum	E00705825	yes	Papillae	na
old_world	glabratum	BM000942603	yes	Papillae	na
old_world	kurzii	E00705823	yes	Papillae	na
old_world	lucani	cast	yes	Papillae	na
old_world	oligacanthum	E00610063	yes	Papillae	na
old_world	orbiculatum	E00610067	yes	Papillae	glove-like' papillae, point towards base, fade to flat tip
old_world	papuanum	E00426994	yes	Papillae	na
old_world	pyracanthos	E00112848	yes	Papillae	na

clade	species	herbarium barcode	epidermal cell outgrowth	outgrowth type	description of outgrowths
old_world	semiarmatum	E00426894	yes	Papillae	bubble shaped cell outgrowths
old_world	tomentosum	17197CGE	yes	Papillae	na
old_world	viridifolium	BM000900427	yes	Papillae	slight bubble towards base, facing towards base
old_world	forskali	BM000942261	yes	Papillae	glove shaped. Most exaggerated at base
old_world	incanum	E00112795	yes	Papillae	glove shaped. Most exaggerated at base
old_world	amblymerum	e00526972	yes	Papillae	slight at base, fade to tip, turns flat about half way up the length
Petota	chacoense	BM001034787	yes	Papillae	bubbly cells full anther length
Petota	demissum	E00129589	yes	Papillae	bubbly cells along entire length
Petota	jamesii	E00129564	yes	Papillae	blobby cells
Petota	kurtzianum	bm001115326	yes	Papillae	bubbly cells full length
Petota	medians	BM001134766	yes	Papillae	bubble
Petota	berthaultii	BM001211391	yes	Papillae	bubbly cells
Petota	acaule	BM001114735	yes	Papillae	bubble shaped cell outgrowths, full length from base to tip (not on underside)
Petota	tuberosum	16193CGE	yes	Papillae	full length of upper side of anther
Pteroidea_Herpystichu	anceps	BM000887320	yes	Papillae	bubble full length of anther
Regmandra	multifidum	BM000886398	yes	Papillae	na
Regmandra	paposanum	E00230406	yes	Papillae	na
Regmandra	trinominum	BM000887066	yes	Papillae	bubble cells pointing towards base
Tomato	chilense	E00621882	yes	Papillae	na
Tomato	sitiens	E00230407	yes	Papillae	na
Torva	hispidum	17206CGE	yes	Papillae	na
Torva	junctum	BM0094356	yes	Papillae	glove-like, pointing down to base. Flatter at tip, most exaggerated towards base
Torva	subinerme	17208CGE	yes	Papillae	point to base.
Torva	ochraceo- ferrugineum	17204cge	yes	Papillae	fade to tip, point of Papillae towards base
Torva	dammerianum	e00426977	yes	Papillae	only very slight conical cell outgrowth at side of base
Valdiviense	valdiviense	E00112900	yes	Papillae	all along length
Morelloid	juninense	possibly junananense bm001134588	yes	Papillae	along length, exaggerated almost glove-like towards base
NA	subscandens	17220CGE	yes	Papillae	towards base with point to base, flat at tip, fades along the length
Brevantherum	erianthum	e00426662	yes	Papillae	na
Morelloid	palitans	16203CGE	yes	Papillae	na
Morelloid	chenopodioides	16188CGE	yes	Papillae	fade to tip
Archaesolanum	symonii	E00426914	yes	Papillae	bubble at base fade to tip
Cyphomandra	obliquum	BM000777990	yes	Papillae	bubble cells (and trichome long thin at base? Or dirty?)
old_world	marginatum	E00125315	yes	Papillae	na
Acanthophora	aculeatissimum	E00112791	yes	Papillae and trichomes	bubbly-cells, long thin hairs at base
Bahamense	bahamense	E00112792	yes	Papillae and trichomes	glove-like point towards base on upper side. Stellate trichomes on underside of anther
Brevantherum	schlechtendalianum	E00700796	yes	Papillae and trichomes	Papillae over full length of top of anther. Bottom of anther covered in stellate trichomes
Petota	andreanum	BM0011203	yes	Papillae and trichomes	bubble and trichome like extensions along base side
Petota	multiinterruptum	BM000887779	yes	Papillae and trichomes	bubbles and a bit hairy long thin at base (or dirty?)
Tomato	chmielewski	BM000778180	yes	Papillae and trichomes	bubbly cells on base, pp held together by trichome mesh
Tomato	juglandifolium	BM000887640	yes	Papillae and trichomes	cell outgrowths along length, trichome like outgrowths at side of base
Tomato	lycopersicum	E00143527 and cast	yes	Papillae and trichomes	trichome mesh, cell outgrowth glove along length, fade to tip
Tomato	pennellii	bm001120801	yes	Papillae and trichomes	trichome mesh. Bubbly Papillae all along length
Tomato	pimpinellifolium	cast and E00160256	yes	Papillae and trichomes	trichome mesh pp with outgrowths at base
Tomato	neorickii	BM001114762	yes	Papillae and trichomes	outgrowths at base cells bubble fade to flat at tip, trichome mesh to hold together pp
NA	carpensis	E00112764	yes	Papillae and trichomes	bubbly cells all-over, elongates trichome like Papillae along underside
Acanthophora	atropurpureum	17212CGE	no	na	na
Acanthophora	capsicoides	cast	no	na	na
Acanthophora	mammosum	17214CGE	no	na	na

clade	species	herbarium barcode	epidermal cell outgrowth	outgrowth type	description of outgrowths
Acanthophora	platense	17217CGE	no	na	na
Androceras_Crinitum	citrullifolium	cast	no	na	na
Androceras_Crinitum	grandiflorum	16207cge	no	na	na
Androceras_Crinitum	rostratum	E00593454	no	na	na
Androceras_Crinitum	tribulosum	17201cge	no	na	na
Androceras_Crinitum	urticans	e00426430	no	na	looks flat but whole sample covered in mess, so unclear
Archaesolanum	laciniatum	E00610031	no	na	na
Basarthrum	muriacatum	bm000072743	no	na	na
Basarthrum	fraxinifolium	cast	no	na	flat I think, but with jigsaw type shapes to the cells
Brevantherum	asperum	E00426576	no	na	na
Brevantherum	bicolor	E00426582	no	na	na
Brevantherum	conglobatum	BM001114718	no	na	na
Brevantherum	mauritianum	E00426838	no	na	na
Brevantherum	erianthum	e00426982	no	na	na
Carolinense	carolinense	BM000778105 and cast	no	na	na
Cyphomandra	diversifolium	BM000602761	no	na	na
Dulcamaroid	aligerum	BM000942221	no	na	na
Dulcamaroid	alphonsei	E00224037	no	na	na
Dulcamaroid	amygdalifolium	E00114895	no	na	na
Dulcamaroid	aureum	BM000072654	no	na	na
Dulcamaroid	coalitum	BM000848290	no	na	na
Dulcamaroid	crispum	E00112769	no	na	na
Dulcamaroid	dulcamara	16195CGE and cast	no	na	pepper pot but no outgrowths.
Dulcamaroid	nitidum	E00096028	no	na	na
Dulcamaroid	pittosporifolium	BM000942324	no	na	na
Dulcamaroid	sanchez-vegae	E00700858	no	na	na
Dulcamaroid	seaforthianum	E00112901	no	na	na
Dulcamaroid	triquetrum	E00112894	no	na	na
Dulcamaroid	uncinellum	E00112831	no	na	na
Dulcamaroid	lyratum	e00320693	no	na	na
Dulcamaroid	pubigerum	E00112842	no	na	na
Erythrotrichum	paludosum	17215CGE	no	na	na
Erythrotrichum	robustum	BM000847032	no	na	na
Gardneri	agrarium	17211cge	no	na	na
Gardneri	tetramerum	E00526139	no	na	na
Geminata	amnicola	BM001017360	no	na	na
Geminata	confine	BM001207620	no	na	na
Geminata	nutans	BM00887836	no	na	na
Geminata	oblongifolium	BM000887847	no	na	na
Geminata	pseudocapsicum	16198CGE	no	na	na
Micracantha	jamaicense	17207CGE and cast	no	na	na
Micracantha	monachophyllum	BM000887772	no	na	na
Micracantha	tampicense	E00526138	no	na	na
Morelloid	juninense	BM001134588	no	na	na
Normania	trisectum	BM000072291	no	na	na
old_world	campylacanthum	E00426766	no	na	na
old_world	centrale	BM001070002	no	na	na
old_world	cunninghamii	E00526991	no	na	na

clade	species	herbarium barcode	epidermal cell outgrowth	outgrowth type	description of outgrowths
old_world	lidii	16199CGE	no	na	na
old_world	lucanni	cast	no	na	na
old_world	melongena	cast	no	na	na
old_world	papaverifolium	BM001035312	no	na	na
old_world	petrophilum	BM000846827	no	na	na
old_world	sandwicense	BM000846696	no	na	na
old_world	vespertilio	16201CGE	no	na	na
old_world	bauerianum	e00526978	no	na	na
Petota	colombianum	BM000849473	no	na	na
Petota	polyadenium	E00129585	no	na	na
Tomato	lycopersicoides	BM000848332	yes	na	na
Torva	albidum	E00507783 and BM000887268	no	na	na
Torva	asperolanatum	BM000887340	no	na	na
Torva	bolivianum	bm001016952	no	na	na
Torva	consimile	BM000887480	no	na	na
Torva	donianum	E00526586	no	na	na
Torva	lanceolatum	E00526544	no	na	na
Torva	paniculatum	17216CGE	no	na	na
Torva	rudepannum	E00526493	no	na	na
Torva	torvum	17209CGE	no	na	na
Torva	whalenii	E00426431	no	na	na
Wendlandii_Allophyllu	refractum	E00526484	no	na	na
Wendlandii_Allophyllu	wendlandii	E00112872	no	na	na
Dulcamaroid	dulcamaraceum		no	na	na
Geminata	nudum Dunal	BM000887833	no	na	na
Torva	scuticum M.Nee	17221CGE	no	na	na
Androceras_Crinitum	rostratum	16190CGE	no	na	na
Androceras_Crinitum	angustifolium-pollinating	E00526597	yes	trichomes	long thin hairs along base side
Androceras_Crinitum	tribulosum	17201CGE	yes	trichomes	stellate trichome on underside
Cyphomandra	allophyllum	cast	yes	trichomes	glandular/oil secreting trichome, otherwise entirely flat
Androceras_Crinitum	lycocarpum	BM000935470	yes	trichomes	stellate trichomes underside
Bahamense	polyacanthos	BM000888769	yes	trichomes	stellate trichomes on anther underside
old_world	brownii	BM000846808	yes	trichomes	stellate trichomes along underside middle line
Tomato	arcanum	BM00112068	yes	trichomes	trichome mesh
Tomato	galapagense	BM001120067	yes	trichomes	trichome mesh to hold together pepper pot cone
NA	crinitum	BM000849358	yes	trichomes	stellate trichomes and long branched big trichomes along side and underside.

Epidermal cell outgrowth data by clade and subclade:

main clade	clade	number of species sampled	number flat	number with outgrowths
Archaesolanum	Archaesolanum	4	1	3
Brevantherum	Brevantherum	9	5	4
Cyphomandra	Cyphomandra	6	1	5
Geminata	Geminata	6	5	1
Leptostemonur	Acanthophora	8	4	4
Leptostemonur	Androceras_Crinitum	10	5	5
Leptostemonur	Bahamense	2	0	2
Leptostemonur	Carolinense	1	1	0
Leptostemonur	Elaeagnifolium	1	0	1
Leptostemonur	Erythrotrichum	2	2	0
Leptostemonur	Gardneri	3	2	1
Leptostemonur	Lasiocarpa	5	0	5
Leptostemonur	Micracantha	3	3	0
Leptostemonur	old_world	36	11	25
Leptostemonur	Torva	15	10	5
M-clade	African_non_spiny	1	0	1
M-clade	Dulcamaroid	16	16	0
M-clade	Morelloid	9	1	8
M-clade	Normania	1	1	0
Potato	Basarthrum	4	2	2
Potato	Petota	12	2	10
Potato	Pteroidea_Herpystichu	1	0	1
Potato	Regmandra	3	0	3
Potato	Tomato	11	0	11
Wendlandii_All	Wendlandii_Allophyllu	2	2	0
	unkown	12	5	7

Epidermal cell outgrowth data summarised by clade:

main clade	number of species sampled	number flat	number with outgrowths
Archaesolanum	4	1	3
Brevantherum	9	5	4
Cyphomandra	6	1	5
Geminata	6	5	1
Leptostemonum	86	38	48
M-clade	27	18	9
Potato	31	4	27
Wendlandii_Allophyllum	2	2	0

Appendix 6: Solutions and recipes

CTAB extraction buffer recipe:

CTAB RNA extraction buffer		
solution/reagent	**final concentration**	**for 100ml**
CTAB	2%	2g
PVP (MW 40,000)	2%	2g
5M NaCl	1.4M	28mL
0.5M EDTA pH8	20mM	4mL
1M TrisHCL pH8	100mM	10mL
2-Mercaptoethanol	2%	2mL
(note: 2-Mercaptoethanol added just prior to use.)		
(PVP= polyvinylpyrrolidone)		
(CTAB= hexadecyltrimethylammonium bromide)		

Trizol extraction buffer recipe:

Trizol RNA extraction buffer:		
solution/reagent	**final concentration**	**amount for 1 sample**
solution D:		
guanidine isothiocyanate	4M	
sodium citrate pH7	25mM	
sarkosyl	0.50%	
		500µl of 'solution D'
phenol		500µl
2M sodium acetate pH4		50µl
Phenol and sodium acetate added just prior to use.		
1000µl of final Trizol solution per sample.		

Loading buffer recipe for gels: 30% glycerol, 0.25% bromophenol blue, 0.25% xylene cyanol, 10mM Tris HCl pH7.6

Plasmid purification by 'miniprep plasmid purification alkaline' method solution recipes:

SOL1	**SOL2**	**SOL3**
500mM glucose	0.2M NaOH	5M potassium acetate 60ml
25mM TrisHCL (pH8)	1% SDS	glacial acetic acid 11.5ml
10mM EDTA (pH8)		H2O 28.5ml
autoclaved		(final solution is 3MK and 5M acetate)
stored at 4˚C	made fresh each time	store at 4˚C

MS recipe: 4.4g/L Murashige-Skoog Medium with vitamins (Duchefa); 35g/L Sucrose. For solid media: 4g/L Agar (Sigma-Aldrich)

LB Recipe: 10g/L Tryptone, 10g/L Sodium Chloride, 5g/L; Yeast Extract. For solid media: 6g/L Bacto-agar (Sigma-Aldrich)

MS9 Recipe: 4.4g/L Murashige-Skoog Medium (with vitamins), 20g/L Sucrose, 1ml BAP (1mg/ml), 0.5ml IAA (1mg/ml) 8g Agar.

Half-MS: 2.2g Murashige-Skoog Medium (with vitamins), 20g/L Sucrose.

GDNA extraction buffer recipe:

extraction buffer for gDNA extraction for genotyping:	
TRIS HCl pH7.5	250mM
EDTA	25mM
NaCl	250mM
SDS	1%

Regeneration media and rooting media recipes for tomato transformation:

Tomato regeneration medium	
	/Litre
MS salts (without vitamins)	1x/4.3g
myo-inositol	0.1g
Nitsch's vitamins	0.1g
Sucrose	20g
phytogel	4g
pH 6.0 (KOH)	
Autoclave	
Timentin (100mg/ml)	3.2ml
Zeatin (2mg/ml)	1ml
Cefotaxim (250mg/ml)	0.5ml
Kanamycin (50mg/ml)	2ml

Tomato rooting medium	
	/Litre
MS salts (with vitamins)	2.2g
Sucrose	5g
Gelrite	2.25g
pH 6.0 (KOH)	
Autoclave	
Kanamycin (50mg/ml)	1ml
Timentin (100mg/ml)	3.2ml

10X TBE recipe: 108g Tris-base, 55g Boric Acid, 40ml 0.5M EDTA (pH8.0) in 1L of DI water. (For solid gels TBE was microwaved with agar. The most common concentration used was 0.5g agar/50ml TBE. For semi-qRTPCR gels used were 0.75g/50ml TBE)

Appendix 7: Primer sequences

Primer Name	Sequence	tm phusion	Tm kapa	Purpose	Bp product	Bp product
oGVD001-F	ATGGGGAGAACACCATGTTGTG	70	57.6	RV primer to clone full length version of *Solyc01g094360 SlMYB17-1*		
oGVD002-R	TCA TGA GCT TTC ACT CAA AAA GGG	70	55.7	RV primer to clone full length version of *Solyc01g094360 SlMYB17-1*	930	2,230
oGVD003-F	ATG GGG AGA ACA CCG TGT TG	65	57.6	FW primer to clone full length version of *>Solyc05g048830.2.1 SlMYB17-2*		
oGVD004-R	TCA GAG AAA GCC AAC TTC ATG TTG	65	55.6	RV primer to clone full length version of *>Solyc05g048830.2.1 SlMYB17-2*	960	2223
oGVD005-F	ATGGGAAGGTTTGATAAAGAGGGA	62	55.9	FW primer to clone full length version of *>Solyc05g007710.2.1 SlMIXTA-1*		
o-GVD006-R	TTA GTT AAT ACA ATC AAT AGG TGA ATT AAC	62	50.7	RV primer to clone full length version of *>Solyc05g007710.2.1 SlMIXTA-1*	1017	2113
o-GVD007-F	ATG GGT CGA TCT CCG TGT TG	62	57	FW primer to clone full length version of *>Solyc02g088190.2.1 SlMIXTA-like-1*		
o-GVD008-R	TTAGAACATAGATGAATCAGATGGAG	62	52.2	RV primer to clone full length version of *>Solyc02g088190.2.1 SlMIXTA-like-1*	1254	2350
o-GVD009-F	ATG GGA AGA TCA CCA TGT TTA GAT	65	54	FW primer to clone full length version of *>Solyc04g005600.1.1 SlMIXTA-2*		
o-GVD010-R	TTA GAG TAA TGG AGA TCC AAT TGG	65	52.2	RV primer to clone full length version of *>Solyc04g005600.1.1 SlMIXTA-2*	995	1283
o-GVD011-F	CCT CCG TTG TGA TGT AAC TGG		55.5	FW primer reference genes using CAC gene in tomato for use as positive control in Semi-qRTPCR		
o-GVD012-R	ATT GGT GGA AAG TAA CAT CAT CG		53.3	RV primer reference genes using CAC gene in tomato for use as positive control in Semi-qRTPCR	173	610
TIUBQ-F (13F primer)	CCAACATCCAGGACAGGAA		54.4	shis positive control reference genes tomato Ubiquitin, from Kaz		
TIUBQ-R (14R primer)	TAAAATCAATCGCCTCCAGC		54.4	shis positive control reference genes tomato Ubiquitin, from Kaz	300	
o-GVD015-F	ATGGGAAGATCACCATGTTGTG	65	58	FW primer to clone full length version of tomato myb geneSolyc01g010910.1 *MIXTA-3*		
o-GVD016-R	TTA AAA TAC TGA TGA ACC ATC AAC AA	65	55	RV primer to clone full length version of tomato myb geneSolyc01g010910.1 *MIXTA-3*	1005	3220
o-GVD017-F	ATGGGAAGATCCAAATATTGTGAT	62/61	55.8	FW primer to clone full length version of tomato myb gene Solyc05g007690.1 *MIXTA-4*		
o-GVD018-R	TTA AAA TAC TGG AGA ACC AAT AGG	62/61	55.8	RV primer to clone full length version of tomato myb gene Solyc05g007690.1 *MIXTA-4*		2185
GVD-CRISPR-p1A-F	tgtggtctcaATTGAAGAAGCGCCTGCTTTCCAgttttagagctagaaatagcaag	72		target sequence for CRISPR knockout of gene *Solyc01g094360 SlMYB17-1*	164	
GVD-CRISPR-p2B-F	tgtggtctcaATT**GAGTTTGAACTCGGTGTTGC**gttttagagctagaaatagcaag	72		target sequence for CRISPR knockout of gene *Solyc01g094360 SlMYB17-1*	164	
GVD-CRISPR-p3A-F	tgtggtctcaATT**GAACCCTCTTCAGCACCTAA**gttttagagctagaaatagcaag	72		target sequence for CRISPR knockout of gene *Solyc05g048830.2.1 SlMYB17-2*	164	
GVD-CRISPR-p4B-F	tgtggtctcaATT**GACGATACCTCTAGCTCTAG**gttttagagctagaaatagcaag	72		target sequence for CRISPR knockout of gene *Solyc05g048830.2.1 SlMYB17-2*	164	
GVD-CRISPR-p5A-F	tgtggtctcaATT**GGAACTCACGTCTGAAAAAG**gttttagagctagaaatagcaag	72		target sequence for CRISPR knockout of gene *Solyc05g007710.2.1 SlMIXTA-1*	164	
GVD-CRISPR-p6B-F	tgtggtctcaATT**GACACACAAACCAAATGGTG**gttttagagctagaaatagcaag	72		target sequence for CRISPR knockout of gene *Solyc05g007710.2.1 SlMIXTA-1*	164	
GVD-CRISPR-p7A-F	tgtggtctcaATT**GTCTCAACGTGCTGAAAGCC**gttttagagctagaaatagcaag	72		target sequence for CRISPR knockout of gene *Solyc02g088190.2.1 SlMIXTA-like-1*	164	
GVD-CRISPR-p8B-F	tgtggtctcaATTGGTGGCACGGAATCCGATAAgttttagagctagaaatagcaag	72		target sequence for CRISPR knockout of gene *Solyc02g088190.2.1 SlMIXTA-like-1*	164	
GVD-CRISPR-p9A-F	tgtggtctcaATTGTACAAATGGATGGTTGCTTgttttagagctagaaatagcaag	72		target sequence for CRISPR knockout of gene *Solyc04g005600.1.1 SlMIXTA-2*	164	
GVD-CRISPR-p10B-F	tgtggtctcaATT**GTCTTGACATACTAAAAGCT**gttttagagctagaaatagcaag	72		target sequence for CRISPR knockout of gene *Solyc04g005600.1.1 SlMIXTA-2*	164	
GVD-CRISPR-p15A-F	tgtggtctcaATT**GTCAGCTATTGCGACTCATT**gttttagagctagaaatagcaag	72		target sequence for CRISPR knockout of gene *Solyc01g010910.1 Sl-MIXTA-3*	164	
GVD-CRISPR-p16B-F	tgtggtctcaATT**GATGTGTTAAAAGCATGGCA**gttttagagctagaaatagcaag	72		target sequence for CRISPR knockout of gene *Solyc01g010910.1 Sl-MIXTA-3*	164	
GVD-CRISPR-p17A-F	tgtggtctcaATTGTCTAGACATATTGAAAGCAgttttagagctagaaatagcaag	72		target sequence for CRISPR knockout of gene *Solyc05g007690.1 SlMIXTA-4*	164	
GVD-CRISPR-p18B-F	tgtggtctcaATT**GACACACAAACCAAGTGATG**gttttagagctagaaatagcaag	72		target sequence for CRISPR knockout of gene *Solyc05g007690.1 SlMIXTA-4*	164	
35sF	CTTCGCAAGACCCTTCCTCT		53			
35sR	CGGGAAACTACTCACAC		53			
GVD-CRISPR-LV2F	CTTAATAACACATTGCGGACG		56	located in the pAGM4723 backbone vector, used to pcr/sequence the located in the KAN resistance within the NOS promoter	~650bp	
GVD-CRISPR-LV2-NOSR	AGCTGCGCAAGGAACGC		57	section of the Lv2 vector for CRISPR containing RNAguides+promoters and linker		
GVD-CRISPR-LV2-NOSF	AGCGGCGAACTAATAACGC		53	located in the NOS promoter insert, used to sequence towards Cas9	~728bp	
GVD-CRISPR-LV2-CasR	TGTTGAAAAGTCTCAATAGC		51	located In the CAS9 used to sequence towards the NOSp to verify insert for CRISPR LV2 vector		
GVD-CRISPR-LV2-CasF	ATGTAATAATTAACATGTAATGCATGACG		58	located in the CAS9 insert, used to sequnce towards the backbone, verifying insert of RNAguides+promoters and linker	~790bp	
GVD-CRISPR-LV2R	AAATGGACGAACGGATAAACC		56	located in the PAGM4723 backbone vector, used to verify insert of RNAguides+promoters and linker into LV2CRISPR vector		
CRISPR-LV1-R	TTAATAACACATTGCGGACG		53	sequencing primers for CRISPR Lv1 vectors. When used in colony pcr, use 52 annealing temperature		
CRISPR-LV1-F	ATGCACATACAAATGGACG		52	sequencing primers for CRISPR Lv1 vectors. When used in colony pcr, use 52 annealing temperature		
GVD-linkerF	gattaagttgggtaacgccag		58	for sequcing the linker insert section of the linker vector component for use in assembling the lv2 construct for crispr		
GVD-CasRnew	gaatccgaggaggtttccc		59	for sequencing the cas9 vector being used for assmbling the lv2 construct for crispr		
CS1	TTGGAAGGAATTTGGGAACTC		55	Forward primer for Semi quantiative RTPCR of *Solyc02g088190.2.1 SlMIXTA-like-1*	133	
CS2	TCTGTTGTCCATGTTGTGTC		55	reverse primer for Semi quantiative RTPCR of *Solyc02g088190.2.1 SlMIXTA-like-1*	133	
CS3	CCCTGGAAACTACTCAAGTG		55	forward primer for semi quantitative RTPCR of *Solyc04g005600.1.1 SlMIXTA-2*	121	
CS4	ATGGAGATCCAATTGGTGAAG		55	reverse primer for semi quantitative RTPCR of *Solyc04g005600.1.1 SlMIXTA-2*	121	
CS9	TTAAAAGCATGGCAAGGAGG		55	forward primer for semi qunatitative RTPCT of *Solyc01g010910.1 SlMIXTA-3*	150	
CS10	ATCAATTAATCCAGCCCCTG		55	reverse primer for semi qunatitative RTPCT of *Solyc01g010910.1 SlMIXTA-3*	150	
CS11	GCATGGCAAATAGCTAGCAC		55	forward primer for semi quantitative RTPCR of *Solyc05g007710.2.1 SlMIXTA-1*	124	
CS12	CTCCGAGGAATTCAACGATG		55	Reverse primer for semi quantitative RTPCR of *Solyc05g007710.2.1 SlMIXTA-1*	124	
CS13	**AAGATCCAAATATTGTGATGAAGAG**		55	forward primer for semi quantitative RTPCR of *Solyc05g007690.1 SlMIXTA-4*	138	
CS14	TTGCAGACCAGCTTTAGCAG		55	reverse primer for semi quantitative RTPCR of *Solyc05g007690.1 SlMIXTA-4*	138	

Appendix 8: The presence of epidermal cell outgrowths displayed against anther shape ratio.

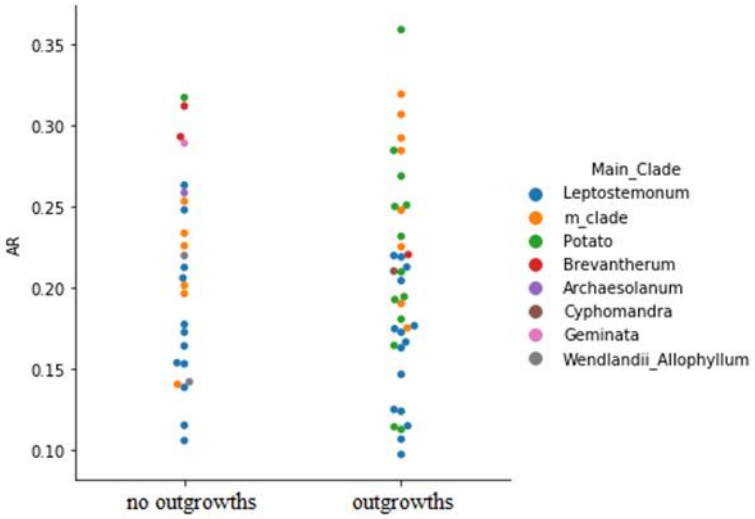

Presence of epidermal cell outgrowths displayed against aspect ratio (AR).

Here the anther shape is represented aspect ratio, which was calculated for each species by (tip width X middle width X base width)/anther length. This is plotted against the presence or absence of outgrowths of some kind. It can be seen that the presence and absence of epidermal cell outgrowths is distributed evenly at all anther shapes.